Technological change and innovation: Ausewell Wood, Dartmoor – an early industrial metallurgical ‘laboratory’

Volume 1 of 2

Submitted by Carlotta Farci,

To the University of Exeter

as a thesis for the degree of

Doctor of Philosophy in Archaeology,

April 2022.

I certify that all material in this thesis which is not my own work has been identified and that any material that has previously been submitted and approved for the award of a degree by this or any other University has been acknowledged.

Signature……

Abstract

From the early Medieval period onwards, the iron industry in Europe experienced important technological changes that transformed the scale and nature of production and organization of ironmaking, ultimately leading to the Industrial Revolution of the 18th century. The use of water power to drive mechanical processes such as grinding, crushing, hammering and powering bellows, developed into the blast furnace and finery forge, which were introduced around the 12th century in Europe and 15th century in England. Ausewell Wood, a post-medieval iron-working site in Devon, South West England, is characterised by the presence of a blast furnace, areas of charcoal-processing, slag heaps, a long leat providing water to various channels and wheel pits, and further along the same river, an area dedicated to post-smelting operations. It is in this area that over twenty years ago a team from the University of Exeter and Dartmoor National Park carried out excavations; the excavated assemblage is the object of this study. Archaeometallurgical studies are employed here in combination with historical research with the aim to gain insight into the innovations and changes that occurred in the iron industry during the post-medieval period. To this end, over 2,750kg of slags and metal scraps were first subjected to macro-morphological investigation: the aims were to identify distinctive typologies and features peculiar to the technology represented on site and to link identified morphological traits of waste material to the spatial organisation of the ironworking area. The study of the assemblage in its entirety provided the first link between the remote part of the site where the blast furnace is situated and the excavated slag heap. The following chemical analysis campaign was then designed to investigate the connection between the two areas of the site and to reconstruct the metallurgical practices that generated the excavated slag heap. The selection of samples was devised accordingly: 56 between slag and metal pieces were studied using optical microscopy and SEM-EDS. The results of this research revealed that at the iron-working complex iron was smelted in the blast furnace and then carried over to the finery forge to be refined. This study not only provides the first secure evidence for this technology in the South West of England but also sheds new light on the artisanal origins and methods of fining pig iron.

Table of Contents

List of Figures

CHAPTER 5

List of Tables

CHAPTER 4

CHAPTER 5

Glossary

Alloy: a combination of two or more metals, or of a metal with a non-metal, for the purpose of producing a material with specific characteristics or properties.

Ancony: a flat, thick bar of wrought iron, with a knob on each end.

Bar Iron: the final product of the finery forge, made of wrought iron.

Bloom: the lump of iron that forms inside a bloomery furnace. The bloom forms below the melting point of iron and is a mixture of metal and slag.

Buddle: pits of circular form used in mineral mining industries to separate by sedimentation minerals from lighter rock dust in crushed ore.

Cast Iron: an alloy of iron that contains between 2 and 5% carbon, along with varying amounts of silicon, manganese, sulphur and phosphorus. It is made by reducing iron ore in a blast furnace.

Cementite: a hard brittle iron carbide Fe3C that occurs in steel, cast iron and iron-carbon alloys.

Cold short: a metal that is brittle at low temperatures.

Ferrite: a form of pure iron with a body-centred cubic crystal structure.

Fining: the process of removing carbon by re-melting pig iron in an open charcoal-fired hearth (the finery). See refining.

Hambone: term used in the Midlands to indicate chafery hearth slag. See Mosser.

Hearth: a structure, usually made from clay, used to work metals. Depending on the metal being worked, and on the process used, different temperatures could be obtained inside these installations.

Hot short: a metal that is brittle at high temperatures.

Leat: an artificial watercourse that conveys water to a mill wheel.

Loop: from the French loupe, is the mass of metal and slag obtained from fining pig iron.

Mosser: northern British term for chafery hearth slag. Rounded mass of slag of high density.

Ore: A natural rock or sediment which contains a combination of minerals from which one or more metals can be economically extracted.

Pearlite: a two-phased, lamellar structure composed of alternating layers of ferrite and cementite, present in cast iron and steel.

Pig Iron: the intermediate product obtained from smelting iron ore in the blast furnace. It is cast iron (white, grey or mottled) cast in oblong moulds.

Refining: the process of removing impurities from a smelted metal. The term is also used to describe the fining process and it also refers to the 19th century refining process, which was performed before puddling to remove silicon from pig iron (see chapter 6). Refining is also used in non-ferrous metallurgy, and it generally refers to the removal of impurities.

Roasting: a metallurgical process in which sulphide ores are converted to oxides, prior to smelting, by heating them to high temperatures in the presence of air.

Slag: waste products of metalworking activities. Slags can be produced during smelting, refining, smithing, refining and casting of metals.

Sluice: an artificial channel for carrying water, with an opening to control the flow of the water.

Steadite: a eutectic of iron phosphide Fe3P and iron that occurs as a microconstituent of high-phosphorus cast iron.

Tailings: the waste materials left after the target mineral is extracted from the ore. They consist of crushed rocks, water and trace quantities of metals.

Tailrace: a channel that carries away water from a water wheel.

Acknowledgments

First and foremost I would like to thank my two supervisors, Gillian Juleff and Fiona Brock, for their support and guidance over the past few years. Working with you on this project has been a very formative experience and I am very grateful for all your comments and help during the writing process. Gill, thank you for giving me the opportunity to teach in your modules, this has been the most rewarding experience for me. Fiona, thank you for your constant interest in the project and for checking on me when I needed it.

I would also like to thank Lee Bray for helping me move very heavy bags of iron slags from Dartmoor to Exeter, and back, and for sharing his knowledge of the archaeology of Dartmoor while he drove me to the site of Ausewell Wood.

In the laboratories of Shrivenham, I would like to thank Adrian Mustey and Jonathan Painter for their help, especially during the last months of my analytical work when COVID-19 had already made things complicated.

In Exeter, I want to thank my kind neighbour Melek for being there in a difficult period of my life in the city and for adopting my plants when I left. The house at the Iron Bridge is the most beautiful memory of my time there and I will always be grateful for meeting you. I also wish to thank Francesco Orlandi for his friendship and passion for his work, it has been a real inspiration sharing time and thoughts with you.

To my UCL friends, Frederik, Umberto and Agnese, thank you for your support when I was away from London, and for not giving up on our friendship.

To my Sardinian brothers and sisters, I always miss you when we are not together. If there is a place where I always want to return to, it is you.

Finally, to my family for always supporting and believing in me. These have been difficult years, and without your love I would not be the person I am today. To Irene, for bringing so much joy to our lives.

To my grandmother, Delia

‘There’s beauty in completion. And always faith in the unknown.’

Kendrick Lamar

CHAPTER 1 INTRODUCTION

Figure 1.1. Landscape with a foundry. Herri met de Bles (1525-1550).

1.1 THE BACKGROUND: CHANGE AND INNOVATION IN POST-MEDIEVAL IRON PRODUCTION

The introduction of the blast furnace to the iron industry is generally associated with the Industrial Revolution of the 18th century. Virtually any reader picturing tall furnaces flaring smoke and fire, working day and night would associate this image with modern days industries. Indeed, the new technology brought about enormous changes, revolutionising not only the iron industry itself, but equally people's lives and landscapes. However, the way to the Industrial Revolution was a long one. Introduced to Europe from at least the 12th century, the new iron smelting method spread at different speeds across the Continent, coexisting for a long time with the previous iron smelting method, the bloomery technology. By the 15th century, blast furnaces were being employed in most part of Europe, including England, but only in the form of sparse enterprises; meanwhile, most iron was still produced in bloomery furnaces within a small-scale production system tending to local needs. Over the course of the following centuries, the new technology inexorably progressed as the advantages of large-scale production responded more and more to the needs of an increasing population with growing iron demand. Thus, between the 15th and 17th centuries the industry progressively developed and adapted itself alongside important social, economic, cultural and historical changes that both caused and generated technological innovations.

Historically the two centuries between 1400 and 1600 are characterised by a sense of rebirth following the crisis of the late Middle Ages, during which the Black Death (1346 – 1353), famines and wars reduced the population of Europe and halted growth and prosperity (Brady *et al*. 1994). Hence, the *Renaissance* – a term coined in the 19th century after the French historian Jules Michelet used the term in the title of a volume on sixteenth century France (Campbell 2019) – saw the recovery of economy and population and witnessed profound changes in the context of artisanal crafts and technology. Additionally, during these centuries the European states emerged – against the religious-dominated world of the Medieval period – and started their oversea expansions establishing large colonial empires through which trade and cultural exchanges flourished (Brady *et al.* 1994). In the arts there was a return to classic antiquity, while the realms of craft and technology entered a new dimension where learning and making,

scholars and artisans came together in a concerted effort to produce and understand the natural world (Dupré 2014, Long and Morrall 2019). This is evidence by the numerous treatises on arts and technologies and by the numerous paintings depicting workshops and laboratories, as these were equally perceived as places of learning and manufacturing (figure 1.1). The Renaissance courts and wealthy individuals played a fundamental role in bringing together artisans and scholars and creating places where knowledge could be shared, exchanged and improved (Dupré 2014, xi).

It is within this context of artisanal and technological interplay that the present study is situated. In fact, similarly to other metal industries, glass and ceramic, the iron trade developed as a consequence of cultural and historical drives of the period. Indeed, the large structures and machines employed in iron production, with water wheels powering huge bellows fascinated craftsmen and intellectuals. Iron was employed in many sectors, and the introduction of the blast furnace expanded its use, as iron could now be cast directly into moulds to (mass) produce objects. Navigation and sea explorations, together with the production of ordnance with which the new European states armed and defended themselves, were important driving forces behind the technological innovations of the iron industry. The principal product of the charcoal blast furnace, however, was a metal (pig or cast iron, a high-carbon iron alloy) destined to the forge. Indeed, the demand at the time was for a metal that could be forged into shape, which was not possible with the brittle cast iron only suitable for casting. The solution was to introduce a further stage in iron making, which through the decarburisation of cast iron, produced a low carbon iron that could be hammered and shaped in a smithing workshop. The process of decarburisation, termed fining, was conducted in the finery forge. Thus, the iron trade now consisted of two elements, a smelting furnace where iron ore was smelted to cast iron, and a finery forge where cast iron was converted into wrought iron.

The conversion process came to be a fundamental step in the iron industry. From this moment onwards, more emphasis and resources will be directed towards the practice and improvement of post-smelting operations, which produced the final metal. In fact, there were many versions of fining all over Europe, albeit the principle behind all of them was to remove carbon from cast

iron and obtain a mass of iron that could be worked by a blacksmith. In England, the method employed was the so-called Walloon method. The Walloon finery forge was introduced to England, together with the blast furnace, by French workers, who from Normandy moved to the Weald in South East England bringing the new technology with them (Awty 1981).

While the history of the introduction of the blast furnace and finery forge is historically well established, little work has been done on the archaeology and physical evidence of the finery technology. The innovations and technological development that took place in the iron industry during the post-medieval period are still poorly understood as the study of this period has made much less use of archaeological excavations and archaeometry (Cranstone 2004b, Bayley *et al.* 2008). Traditionally the domain of historians, the investigation of post-medieval technologies has focused on historical sources rather than archaeological techniques (Bayley and Crossley 2004, 17); consequently, their material remains are poorly understood. The very same transition from bloomery smelting technology to blast furnace production is still debated and is a subject that needs further investigation. The adoption of the blast furnace in Western Europe was a slow and diverse process which evolved differently and at different times in the various regions of Europe. The overall distribution of early blast furnaces in Europe is still unclear (Geddes 1991) and the technology and development of the finery forge between the 15th and 18th centuries requires further research (Bayley *et al.* 2008, 69).

This thesis deals with the archaeometallurgical study of metallurgical debris excavated from a finery forge discovered in Devon, South West England. The area historically associated with non-ferrous production (tin and copper), is not the expected venue for the study of early industrial iron production, but excavations conducted in 1999 and 2000 have revealed a well-preserved metal-working complex, which is taken as a case study to investigate change and innovations in post-medieval iron production.

1.2 THE CASE STUDY: AUSEWELL WOOD

Ausewell Wood, within Dartmoor National Park, is a well-preserved site in a large area of woodland on the banks of the river Dart, near Ashburton in Devon. The site, extending for about 600m along the river, is characterised by the presence of at least one, possibly two, blast furnaces, areas for charcoal-

processing, a long leat providing water to various channels and wheel pits, buildings and two slag deposits. One, near the blast furnace, consists of typical glassy blast furnace slag, while the second, located to the north of the blast furnace at a distance of about 475m, is characterised by iron-rich slag of the type normally associated with bloomery smelting. Moreover, the site contains ore-processing features, such as crushing and dressing floors for copper ore, dated to the 18th and 19th century (Crombie 1982, Juleff 2000, Cranstone 2001a).

The site of Ausewell Wood was first mentioned by Amery in 1924 when he described the remains of a blast furnace near the River Dart to the Devonshire Association (Amery 1924), correlating the furnace with a map of 1605 which marks an iron mill and two buildings. In addition, documentary evidence attests that the land belonged to Adrian Gilbert, half-brother to Sir Walter Raleigh, an Elizabethan entrepreneur with an interest in developing new metal technologies and exploiting the mineral resources of his own personal landholdings (Greeve 1987, Phillpotts 2001). In 1982, Crombie reviewed the documentary evidence and physical details of the site. Two slag samples collected by Crombie from the two different slag deposits were analysed at University College London by Blick in 1984. The results of this analysis revealed that the glassy slag was consistent with the blast furnace technology, while the iron-rich slag was characterised as a bloomery smelting slag, with the observation that the slag could also have been produced in a finery forge. A comprehensive survey of the site was then carried out by the Royal Commission for the Historical Monuments of England (Newman 1998), while excavations, quantitative sampling of the assumed ‘bloomery slag deposit’ and geophysical survey were performed by Juleff in 1999 and 2000 and summarised in an interim report (Juleff 2000). The excavated assemblage is the object of the present work. Pottery recovered from the iron-rich slag deposit has been assigned to a date range 1600-1660 (Juleff 2000,15). In 2004 the site was surveyed by English Heritage (Newman 2004) and reports were produced on the geology (Page 2004) and on the historical record associated with it (Phillpotts 2001, 2003).

Thus, the site attracted attention for the following reasons:

- It contained two types of iron slags, one associated with the blast furnace technology and the other with the bloomery technology

- It is the only site in South West England where a blast furnace has been archaeologically identified
- During the iron-working phase, the land of Ausewell Wood belonged to Adrian Gilbert, a wealthy man, deeply involved in the social and political life of 16th century England and in the planning of voyages of explorations for the North-West Passage

1.3 THE AIMS AND RESEARCH QUESTIONS

The site of Ausewell Wood provides a unique opportunity to address questions concerning the technological transitions experienced by the iron industry in the 16th and 17th centuries and to investigate the historical context in which these changes took place. As well as addressing research questions specific to the site, through the investigation of the material evidence excavated at Ausewell Wood, the present work aims to provide a material and historical perspective on some more general themes within the study of post-medieval archaeology.

Archaeological evidence

The first aim was to investigate the macro-morphological features of the metallurgical debris in order to identify the technology that produce them. The following research questions are addressed:

- Does the site contain a bloomery smelting furnace or a finery forge?
- Which macro-morphological features can help us distinguish between the two technologies?

Following this step, through the chemical and microstructural investigation of selected samples, the following research questions are addressed:

- What technology produced the iron-rich slag?
- How does the iron-rich slag deposit relate to the blast furnace located at the opposite end of the site?
- Are the activities producing these different slag deposits connected or do they represent a chronological transition?

General questions include:

- What does the technology at Ausewell Wood tell us about the English iron trade of the period?

- What can we learn in terms of organisation and operational practices more generally?

Historical evidence

Contrary to earlier periods, the archaeology of the post-medieval period is complemented by the use of documentary sources. The interplay between material and historical evidence is advocated by the discipline, however they most often operate independently. The historical documents connecting the activities at Ausewell Wood with Adrian Gilbert present an opportunity to explore the fruitful collaboration between historical analysis and archaeometry. The research questions addressed here are:

- What can the tenancy of Adrian Gilbert, an important figure of 16th century England, tell us about the metal-working activities at Ausewell Wood?
- What additional information on technological change and innovation can be obtained from integrating the two levels of analysis?

Finally, the most significant justification of this project lies in the integration of archaeological and historical perspectives. An integrated approach to the investigation of technological change and innovation improves our understanding of social structures and cultural practices, of which craft and technology represent material expression. The result is a broader view on technology, society and material cultural. Thus, the final objectives of the present work are to explore a material-based approach to the study of metallurgical debris from post-medieval sites and to use scientific analysis alongside documentary sources to gain insight into technological changes of the period.

1.4 THE STRUCTURE OF THIS THESIS

Following this introductory chapter, the history of the iron industry in the post-medieval period is reviewed in chapter 2, with particular reference to the archaeology of England. Thus, Chapter 2 describes the background against which research on post-medieval iron production is undertaken. After describing the properties of iron and iron alloys (section 2.2), the two principal smelting technologies are discussed in a simplified linear perspective that sees first the introduction of water power to the bloomery furnace (section 2.3), and then the

introduction of the blast furnace process. The scholarly debate on the origin of the blast furnace is reviewed in section 2.4, together with current knowledge on the early distribution of the technology in Europe and England. Whenever possible both documentary and archaeological evidence are examined. A detailed reviewed of the history and archaeology of the finery forge is then given in section 2.5. The process is described in the following sub-section 2.5.1, piecing together a range of sources, from historical accounts to more recent literature on the technology. The chapter also briefly deals with the study of metal production within the field of post-medieval archaeology (section 2.6). Finally, some observations about innovation and change in the history of iron technology are presented in section 2.7. Next, chapter 3 presents the case study: Ausewell Wood. Section 3.1 summarises the knowledge prior to this study of the physical details, metallurgical activities and owners of the site, including the new information obtained from the historical research conducted within the scope of this study. The assemblage analysed for this study comes from the excavations of the iron-rich slag deposit conducted in 1999 and 2000, therefore section 3.2 describes the trenches and the quantitative sampling of the excavated assemblage conducted during fieldwork.

The macro-morphological analysis of the assemblage is presented in chapter 4. The first part of the chapter discusses the challenges associated with the creation of typologies using classifications. Standardised materials such as pottery and artefacts render the classification approach suitable for most research questions. Contrary, the classification of slags is a challenging exercise where avoiding subjectivity and prior assumptions appears difficult. This aspect is accentuated when dealing with assemblages for which comparative material is not available and an established terminology does not exist. In the second part of the chapter, the assemblage is described based on identified typologies (section 4.4) and the results are discussed in connection to the archaeological data from the excavations (section 4.5 and 4.6).

The previous step involved the selection of samples for laboratory analysis. The methodology employed and the results of the analytical work are presented in chapter 5. These are presented and discussed in connection with the two main objectives of the scientific investigation, which are to explore the relationship between the blast furnace and the excavated iron-rich deposit and to

characterise the technology that produced the iron-rich slag and related metallurgical debris (sections 5.3 and 5.4). The results are discussed and summarised in section 5.7 and 5.8.

Finally, chapter 6 and 7 present a more general discussion of the site and the material evidence analysed. These chapters bring together all levels of investigation to discuss Ausewell Wood both as a compelling and unique case study and in relation to the wider archaeological and historical context. Finally, in chapter 7 following a review of the present work, observations on the methodology employed are presented and future avenue of research proposed.

CHAPTER 2 MAKING IRON IN THE POST MEDIEVAL PERIOD

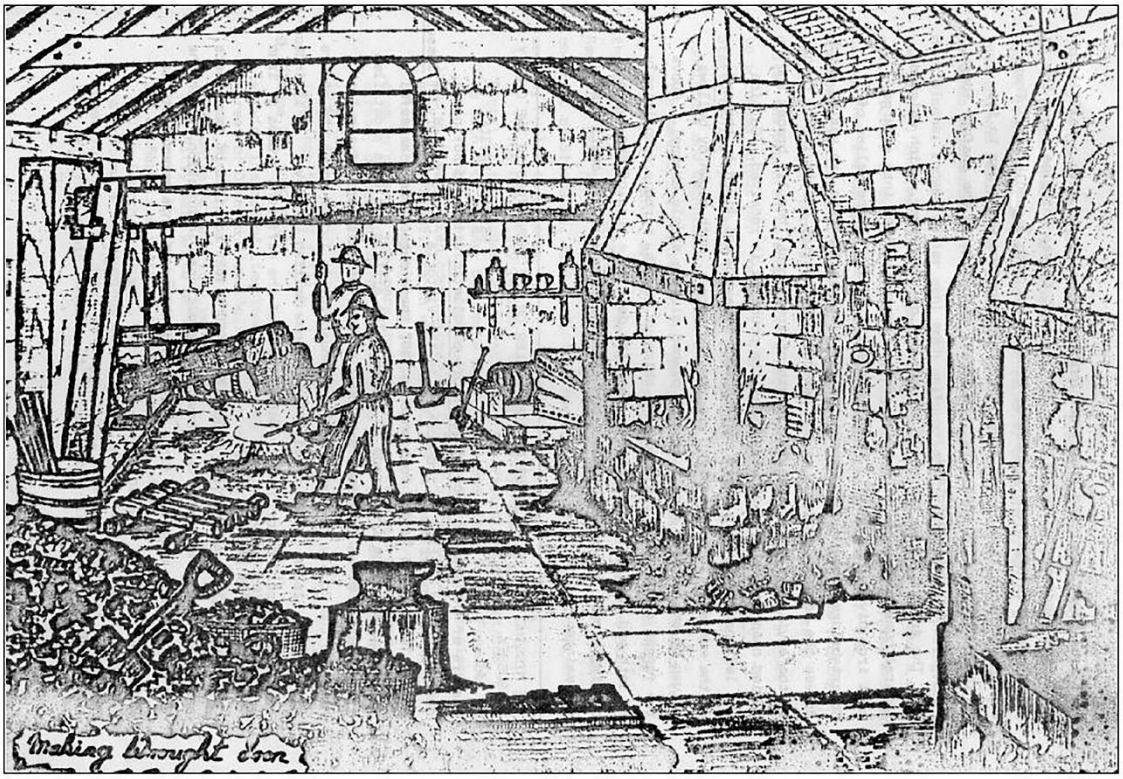

Drawing of a finery forge, Adams, 1979.

2.1 INTRODUCTION

This chapter offers an overview of the history of iron technology in the post-medieval period of Europe, with particular reference to the archaeology of England. The properties of iron, steel and cast iron are presented here (section 2.2), and the technical terminology used in this chapter is elucidated in the glossary. Section 2.3 deals with water-powered bloomeries, while section 2.4 describes smelting by the indirect method using the blast furnace. Section 2.5 deals in more detail with the operation of fining pig iron in the finery forge, offering a documentary and archaeological review of this poorly-understood technology. Section 2.6 briefly discusses the study of metals in post-medieval archaeology. Finally, some observations about innovation and change in the history of iron technology are presented in section 2.7. This chapter therefore represents the background against which research on iron production in the post-medieval period is undertaken.

It is important to note that this overview of the history of iron technology in Europe is inevitably, and necessarily to a degree, an oversimplification. Presented as a linear from bloomery smelting to water-powered bloomery smelting and finally blast furnace smelting allows an explanation of the transition and technological advancement in Western metallurgy. However, the reality is much more complex, and it is now known that liquid iron (steel and cast iron) was produced and probably used long before the blast furnace technology was adopted on the continent, albeit not on a large scale (see Pleiner 2000, Craddock 2003, Kostoglou and Navasaitis 2006, Navasaitis and Selskiene 2007, Crew *et al*. 2011 and references therein). Moreover, outside of Europe, China had started to produce liquid iron already by the 5th century BC (Wagner 1996), while different practices and furnace designs employed in Asia from the first millennium BC resulted in the production of steel and cast iron along with almost pure iron; see for example the Tatara smelting in Japan and the linear box-shaped furnaces of South and South-East Asia (Rostoker and Bronson 1990, 136, Juleff 1996, 2009, Vodyasov *et al.* 2020). Finally, iron smelting in Africa is characterised by a large number of variations of the bloomery smelting and a high degree of experimentation in furnace designs, many of which lead to the production of steel and cast iron (see for example, David *et al.* 1989, Killick 1991, Killick 2015).

2.1.1 Background to post-medieval innovations

The only iron-smelting process known in Europe until medieval times was the bloomery process, also known as the direct method. Only a brief simplified description of the bloomery technology is given here to facilitate the description of iron working by the indirect method. A vast body of literature has been written on bloomery smelting; for an exhaustive description of the process refer to Rostoker and Bronson (1990), Tylecote (1992) and Pleiner (2000).

Bloomery smelting was a solid-state process, where iron was produced in a charcoal-fuelled furnace, equipped with bellows operated by manpower. A variety of furnace types and operational practices characterise bloomery smelting in various parts of the world, but they are all identified by being solid-state processes (Gordon and Killick 1993). Temperatures in the bloomery process were usually below the melting point of iron (1538°C); consequently, the iron did not melt. Instead, the resulting metal was in the form of a solid lump, which was a mixture of metallic iron and slag (i.e. by-products of the smelting operation, usually a mixture of metal oxides and silicon dioxide). This lump, commonly known as bloom (hence the term bloomery), collected at the bottom of the furnace above the molten slag. The iron-rich slag produced during smelting (termed bloomery slag and/or fayalitic slag) pooled at the bottom of the furnace (furnace bottom) or was drained away, or as customarily termed, tapped out (tap slag) of the furnace (or a combination of the two methods) and is characterised by a high iron content. After smelting, the bloom was removed from the furnace, cleaned from the slag and hammered into shape by hot forging. This could be either a billet or an artefact of wrought iron and was obtained during an operation known as smithing. This step also produced slag: smithing slag (‘cakes’ of a characteristic, irregular, plano-convex shape) which formed at the bottom of the smithing hearth during the manufacture of artefacts (Serneels and Perret 2003), and hammerscale that resulted from the detachment and oxidation of hot iron during forging (McDonnell 1991, Dungworth and Wilkes 2007). In England, the bloomery technology was employed from the 8th century BC until the 16th century and later (Historic England 2015, 18). However, over the course of the 12th-15th centuries, Europe and England witnessed the gradual emergence of new metal production technologies. In particular, iron production saw the introduction of water-power

to drive mechanical bellows and hammers (Crossley 1981, Tylecote 1992). The 'traditional' hand-powered bloomery was replaced by higher and bigger furnaces blown by water-powered bellows (section 2.1), paving the way for the blast furnace technology that transformed the scale and nature of production and organisation of ironmaking over succeeding centuries (section 2.6).

A major innovation introduced with the blast furnace technology was the possibility to obtain iron in a liquid state, and consequently to cast it. Only China had developed the technology before the 2nd millennium AD; while the oldest known blast furnace in Europe, found in Sweden at the site of Lapphyttan, dates to the 12th century (Magnusson 1985, Wagner 2008). The conditions necessary to melt the iron were achieved by increasing the fuel/ore ratio, creating more reducing conditions that permitted carburisation of the iron and consequently an alloy with a much lower melting point, called cast iron (with a melting point between 1150°C and 1200°C). Molten slag and metal were both tapped out of the furnaces which were specifically built with two separate tapping arches. The slag in this case is rich in silica and of a glassy nature, very different from bloomery slag. The metal could be cast directly into objects or into iron bars, known as pig iron. The introduction of the blast furnace to England is conventionally dated to the 1490s when French ironworkers migrated to the Sussex area bringing the new technology with them (Awty 1981 and 2007, Crossley 1990). With the advent of the blast furnace, the production of wrought iron became an indirect process, as it required a second step in production to convert cast iron (produced in the blast furnace – section 2.4) back into wrought iron (produced in the finery forge – section 2.5). This was necessary as cast iron is too brittle to be forged into objects and is only suitable for casting. Much of the demand was still for wrought iron, an alloy that could be forged and worked by blacksmiths. With the introduction of the blast furnace more emphasis and resources were put into post-smelting treatments (i.e. fining of pig iron in finery forges), which ultimately defined the nature and properties of the final metal.

2.2 IRON, STEEL AND CAST IRON

Plain or wrought iron is a metal that contains very few impurities (less than 0.1%) and is generally produced in a bloomery furnace. It has a crystal structure comprising grains of a phase known as ferrite (or α-iron), and for this reason is often described as ferritic iron (figure 2.1).

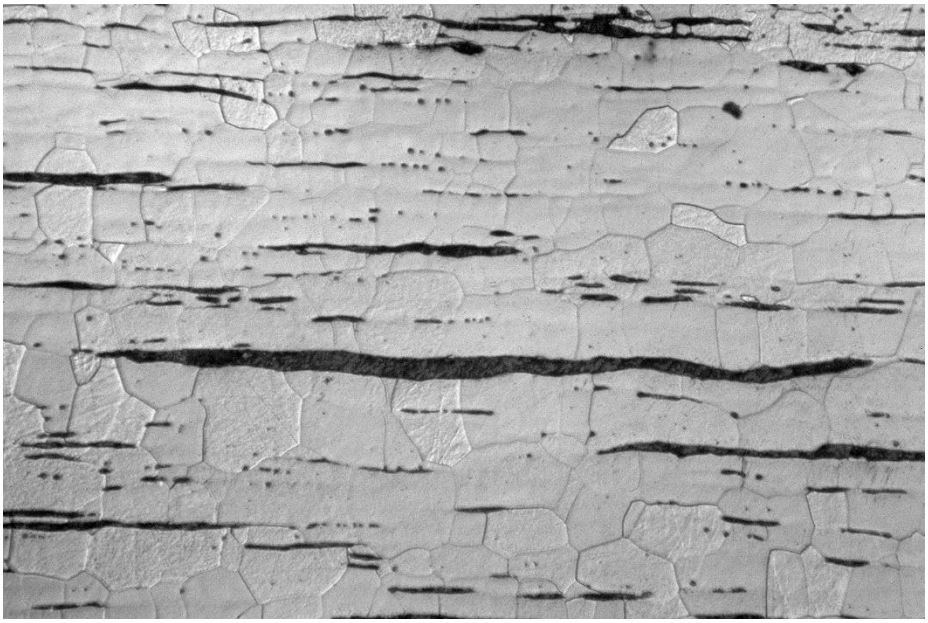

Figure 2.1. Wrought iron with slag inclusions in a ferrite matrix. The elongated shape of the slag inclusions is indicative of the processing direction (commons.wikimedia.org, photo by Mike Meier).

One of the most important characteristics of iron is the fact that its crystalline structure changes depending on a series of conditions, such as temperature, pressure and the presence of alloying elements (Scott and Schwab 2019, 181). The most important alloying element in iron metallurgy is carbon, which drastically changes the microstructure and properties of the metal. When iron is smelted in a furnace with charcoal, carbon acts not only as the fuel for the furnace, but also as reducing agent for the ore. It is the ratio between the gases produced during combustion that determines the condition inside the furnace: CO_2 (not reducing) and CO (reducing). The presence of carbon in the crystalline structure of iron is extremely important, as it determines the melting temperature of the iron alloy. This characteristic had an enormous impact on the technology of iron; since very high temperatures could not be achieved in 'primitive' bloomery furnaces iron was initially produced in a solid state and forged into shape by a blacksmith, hence the term wrought iron. Bloomery iron

contains numerous slag inclusions that are the remnants of the slag produced during smelting and trapped within the iron.

Steel is an iron carbon alloy with a carbon content between 0.1% and about 1.8%. Unlike iron and cast iron, steel was rarely produced by smelting, as control of the ratio CO_2/CO was difficult to obtain. Only in furnaces that were run at higher temperatures than the 'ordinary' bloomery it was possible to obtain blooms with a sufficient amount of carbon to be considered steel (Rostoker and Bronson 1990, 121). The different properties of low-carbon iron and steel were certainly recognised and used from the Iron Age to the early medieval period to make swords and tools. The most common method to obtain steel was to carburise low-carbon iron, either by cementation, where low-carbon iron was exposed to carbon in the form of gas or by putting it in contact with liquid cast iron (Craddock 1995). Steel could also be obtained by decarburisation of cast iron, stopping the process before all carbon was removed (Mack *et al*. 2000). Both methods however produced non-homogeneous steels, as it was difficult to control carbon intake or removal. The most efficient method developed was crucible steel, which originated in South India/Sri Lanka and in Central Asia and enable production of steel in a liquid state and free from impurities (Wayman and Juleff 1999, Rehren and Papakhristu 2000, Feuerbach 2006, Alipour and Rehren 2014). In the West, liquid steel is traditionally associated with the industrial revolution and the work of Benjamin Huntsman in the 1740s in England.

Cast iron is a group of iron carbon alloys with a carbon content between 2% and 5%. It was produced in a blast furnace in a molten state and could either be cast straight into objects or into castings fed by a supplying channel of metal. The name pig iron derives from the resemblance to a sow feeding piglets (figure 2.2).

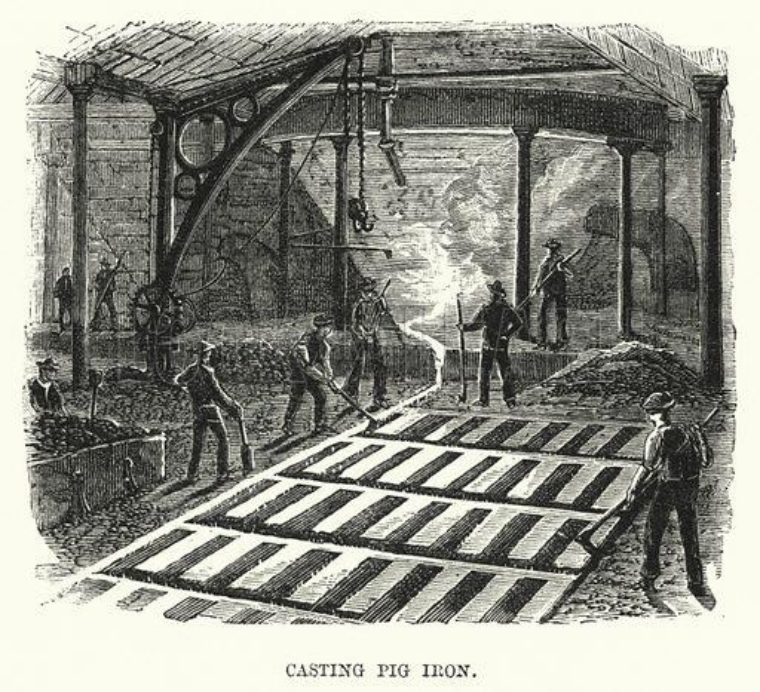

Figure 2.2. Sand moulds for casting pig iron produced at the blast furnace. Illustration for the British Hive and its Working Bees, by Miall (1888). (Downloaded the from the Internet).

Pig iron is therefore an intermediate product – which can either be remelted and cast into objects or converted into wrought iron - while cast iron refers more correctly to a finished product (King 2020). In this thesis, however, the terms cast iron and pig iron are interchangeable as both refer to the product obtained from smelting in the blast furnace; the term cast iron thus refers specifically to a type of iron alloy. There are three types of cast iron: grey, white and mottled (a mixture between grey and white). In grey cast iron, most commonly found in Western metallurgy (Scott and Schwab 2019, 185), free carbon is present in the form of graphite (figure 2.3). In white cast iron, all carbon is combined with iron to form cementite (figure 2.3).

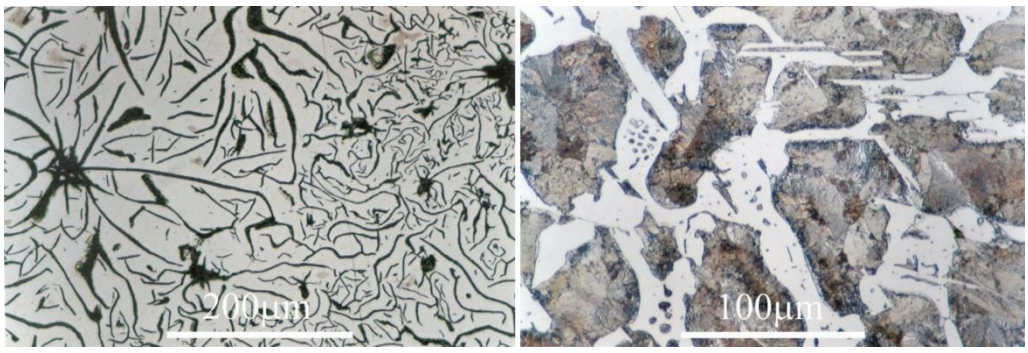

Figure 2.3. Micrographs of grey cast iron (left) and white cast iron (right). Carbon is the form of graphite flakes in grey cast iron, the formation of graphite is promoted by the high silicon content in the alloy. In white cast iron, carbon combine with iron to form cementite (the white phase). The matrix is ferritic (micrographs from doitpoms.ac.uk).

Both microstructures can form with a carbon content higher than 2%, thus their formation will depend on the cooling rates (slower cooling rates favouring the formation of graphite) and on the presence of other alloying elements such as sulphur, manganese, silicon and phosphorus. When phosphorus is present a phase called steadite forms, which is a ternary eutectic between iron, iron phosphide and iron carbide. Steadite is commonly found in grey cast iron in scattered isolated islands in the metal matrix. The microstructure of the matrix, in which graphite or cementite and other constituents precipitate, is generally composed by ferrite (α-iron) and/or pearlite, which is a mixture of ferrite and cementite that forms on slow cooling. With a carbon content of 0.8% the matrix is entirely pearlitic, while above 0.8% the microstructure is characterised by cementite and pearlite, instead of ferrite and pearlite. These changes in the microstructure of iron alloys are shown in the phase diagram in figure 2.4, which provides an indication of the phases that can occur and coexist with a given amount of carbon at various temperatures. The final microstructure is dependent on how fast an alloy solidifies and what impurities are present. In grey cast iron, the presence of silicon will result in graphite flakes in a matrix of ferrite and pearlite.

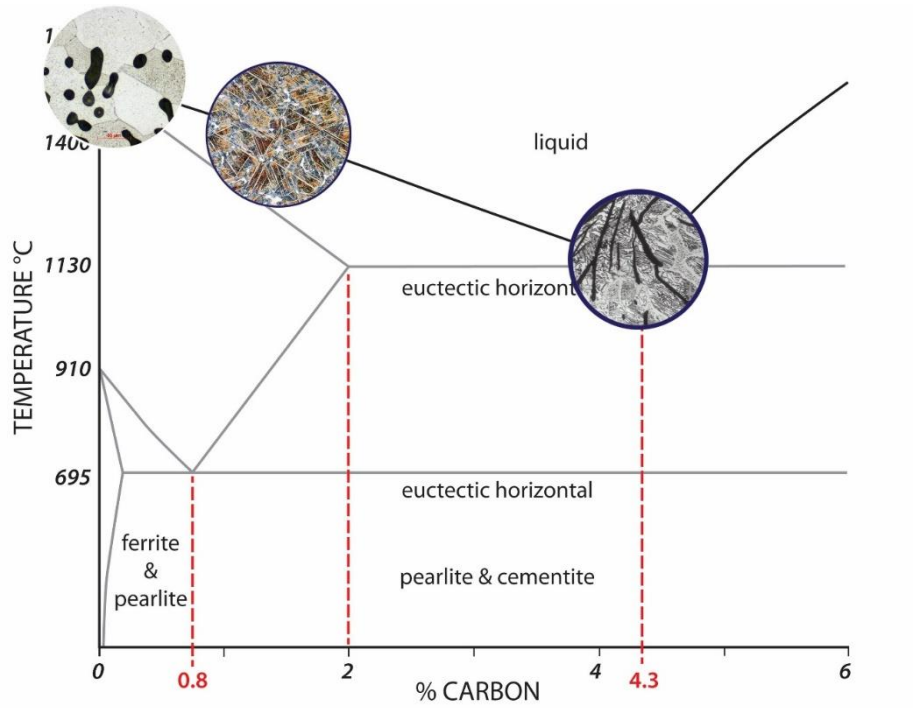

Figure 2.4.Ternary diagram of iron and carbon showing different microstructures with increasing carbon content. Low levels of carbon correspond to ferritic iron, characterised by the presence of slag inclusions. This is the microstructure of both bloomery iron and fined iron. In the middle, the microstructure of steel is shown, with cementite needles in a pearlitic matrix. High contents of carbon correspond to cast iron, the microstructure shown is that of grey cast iron, with carbon as graphite flakes. Many other microstructures are possible based on the level of impurities and cooling rates of the alloy (figure by G. Juleff).

Finally, it remains to explain wrought iron obtained in a finery forge. In order to convert cast iron to wrought iron it is necessary to reduce the carbon content, from the 3-5% of carbon in cast irons to the much lower content usually found in iron (and steel). Microstructures and melting points will thus change according to carbon content. During the conversion process most of the impurities are also removed from the metal, being oxidised in the slag bath in which the process is carried out (see section 2.5). The final product of this operation is the same as in the bloomery process, a solid mixture of iron (or sometimes steel) and slag. This mass, called *loop* (derived from the French *loupe,* meaning mass of metal), then needs to be hammered and forged; an operation that eliminates most of the slag intermixed with the metal, but not all of it. The remaining slag is retained in the metal as inclusions, 'indistinguishable in number and shape from the slag in bloom iron' (Rostoker and Bronson 1990, 140). These slag inclusions are the object of intense study in the field of the archaeometallurgy of iron, as they may provide data to distinguish between bloomery iron and fined iron (see chapter 5).

2.3 THE WATER-POWERED BLOOMERIES

The exact nature of the early use of water-power in European ironworking during the Middle Ages is unknown (Crossley 1990, Historic England 2015. See Lucas 2005 and references therein for the use of water-power in the Roman empire and in other industries in the Middle Ages). Indeed, both from the documentary and archaeological evidence related to the Middle Ages (roughly from the 5th to the 15th century) it is still unclear whether water-power was applied to bellows for smelting or to operate hammers, for ore processing or to consolidate the bloom (Rondelez 2014, 223). In 1086, the Domesday account records a considerable number of iron-smelting sites situated in river valleys and also records two mills in Somerset that were paying rent in blooms, suggesting that water-power was already in use by this time (Tylecote 1992, 76). References to iron mills are also found in France in 1116 and in Spain in 1138 (Cleere and Crossley 1995, 106), but also Sweden (in 1224), Germany and Italy during the 13th and 14th centuries (Lucas 2005, 22). The use of water-power in metallurgy certainly spread over Europe in the second half of the

Middle Ages (Pleiner 2000, 84), and in Central Europe was used for bellows from the middle of the 13th century (Crossley 1981).

Technologically, the introduction of water-power to the bloomery furnace resulted in the production of larger blooms that were cut into pieces and reworked in a second hearth, known in England as the string hearth. However, the information is scarce; water-powered bloomeries are elusive in the archaeological record of Britain. Bayley *et al*. (2008) reported eight excavated 'possible' water-powered bloomeries, including Rockley Smithies in Yorkshire where the good preservation of the archaeological remains allowed identification of a bloomery furnace and two string-hearths (for reheating the bloom for forging) with bellows powered by waterwheels (Crossley and Ashurst 1968). Other possible water-powered bloomeries are identified at Kyrkeknott, Durham (excavated by Tylecote in 1960) and Muncaster Head in Cumbria, although the interpretation as a bloomery furnace is now questioned by Bowden (2000). In most of these sites the archaeological evidence is of difficult interpretation and rarely has the use of water-power for bellows or for hammer been confirmed or unequivocally identified (Girbal 2011). Another emblematic example is Stony Hazel Forge (Cumbria). Originally published as a finery forge by Davies-Shiel (1970), it has since been reinterpreted as a bloomery on the account of traces of hematite ore in the hearth installation excavated, which, however, does not necessarily exclude the use as a finery forge (Bowden 2000, 75, Bayley et al. 2008, 59).

There are a number of reasons that make the identification of these sites a difficult task. Firstly, often the furnaces and hearth installations used in bloomery smelting were subsequently reused in other industries or in later metallurgical activities, such as the finery forge that required similar equipment and layout (Crossley 1981, 37, Cleere and Crossley 1995, 108). In addition, the similarity between the waste residues generated makes the identification of these technologies problematic, especially since excavations of large and complex sites are often, for cost and logistical reasons, very limited in scale (Aldridge, West Midlands – Gould 1969-70) or rely only on geophysical surveys data rather than physical evidence (e.g. Timberholme, North Yorkshire – Vernon *et al*. 1998). Moreover, the scientific analysis of these residues is sparse in comparison to residues from the (unpowered) traditional bloomery sites.

There are, however, a few studies that indicate the very porous nature ('honey-comb texture') of these fayalitic slags as a distinguishing criterion (Tylecote 1960, Tylecote and Cherry 1970, Vernon *et al*. 1998, Photo-Jones and Atkinson 1998, Dungworth 2010, Girbal 2011).

Another very important feature of the bloomery technology of the post-medieval period is the great variety of forms and regional adaptations documented throughout Europe. The most famous are the Catalan forges - which developed in the western Mediterranean and were especially common in the Pyrenees regions of Spain and France, and including a similar process found in Corsica (Tomas 1999, Pleiner 2000), and the Stückofen, the very tall furnaces of Austria (Styria) that spread from there to central European countries and are also found in Scandinavia, Bohemia (present-day Czech Republic), parts of Germany and Hungary.

Thus, the bloomery technology survived in different parts of Europe well beyond the medieval period and the introduction (and use) of the blast furnace. In England, the archaeological evidence suggests that the life of tall (water-powered) bloomeries was shorter when compared to the rest of Europe. In fact, while the technology survived until the middle of the 17th century in many parts of the country serving the needs of small communities (Crossley 1990, 140), it was soon replaced by the blast furnace and the finery forge.

2.4 THE BLAST FURNACE

Gordon and Reynolds in their conference report for 'Medieval Iron in society' held in Sweden in 1985 wrote: 'The origin of iron smelting with the blast furnace is an enigma in the history of Western technology' (1985, 110). This statement appears still true today. What we now know is that blast furnaces were widespread in Sweden, in the Berslagen area, late in the 12th century (Magnusson 1995). The most famous blast furnace is that excavated at Lapphyttan together with eight non-water-powered fineries (Magnusson 1985). Other blast furnaces dating to the 13th and 14th centuries are also known from Switzerland (Guénette-Beck and Serneels 1995) and Germany (Rehren and Ganzelewski 1995, Craddock 1995, Pleiner 2000). There is also evidence of early blast furnaces in Belgium (Tylecote 1962, Den Ouden 1985, Awty 2007), Italy (Rossi and Gattaglia 2015, Cucini *et al*. 2020) and France (Arribet-Deroin 2011). The introduction of the blast furnace to Britain is conventionally dated to

the 1496, with the construction of the ironworks at Newbridge in Sussex, by French ironworkers (Crossley 1990). What is still unclear is the general distribution of early blast furnaces in Europe, as well as the origin of this smelting system, which has generated a long, still unsettled, debate in the history of technology.

There are two main hypotheses concerning the origins of the blast furnace in Europe. One argues that the blast furnace was an independent invention, which developed as a result of using water-power in bloomery furnaces. The variety of shape and size of early furnaces is the main argument in support of an independent origin in various and separate regions of Europe. Here, a slow and long experimentation with water-powered bloomeries developed into the blast furnace, as it happened for example with the *Stückofen*, or tall bloomery furnaces, and the *Flossofen*, the early blast furnaces of Germany and Austria (Pleiner 2000, 139, Craddock 2003, Wagner 2008). The similarity between bloomery furnaces and early blast furnaces seems to further support this argument (Tylecote 1992). Moreover, Craddock (2003, 251) states that absence of early evidence of casting or of 'specifically Chinese heat treatments such as malleabilisation' confirms a European independent origin.

The other theory asserts that the blast furnace technology spread from China, where it was invented by at least the 5th century. This last scenario would see the technology spread to the Arab lands, reach Scandinavia and from there expand into Europe (Killick 2015). Tylecote and Wagner also suggested that the Swedes were among the first Europeans to establish trade with China and noted similarities between the blast furnaces and fineries constructed in Sweden with those used in China (Gordon and Reynolds 1985, 114). Similarly, the furnaces and bellows found in the area of Bergamo and Brescia (Italy) show an oriental influence that suggests that the technology was imported from China, perhaps following the travels of Marco Polo (Den Ouden 1985).

Regardless of the scholarly quest for the origin of the indirect method, it is clear that liquid iron initially produced accidently in high (water-powered) bloomeries slowly became a product that was sought after. This is normally explained by an increase in demand for iron over the course of the 14th – 15th centuries: with the new blast furnaces iron could be produced continuously for days and later in the 18th century, for weeks and even months. This last point introduces some of the

technical novelties that characterise the new technology. As mentioned, the production of liquid iron was possible because by increasing the fuel/ore ratio more reducing conditions were created inside the furnace, which in turn permitted carburisation of the iron and a lower melting point (from 1540°C to about 1200°C). The working temperatures of the furnaces thus had to be at least around 1300°C. It was soon discovered that taller furnaces saved on fuel and kept the iron ore longer under strong reducing conditions at high temperatures. The furnaces were powered by large bellows driven by water wheels, which provided the blast needed for combustion. A large amount of material was charged into the furnaces and a large amount of heat generated, which made working intermittently uneconomical and unnecessary since both metal and slag could be tapped out in liquid form. By contrast, in bloomery smelting, every time that a bloom formed and had to be removed from inside the furnace, smelting was halted (Pleiner 2000). Thus, both slag and pig iron were periodically removed, the pig iron was cast into sand moulds. Both charcoal, ore and limestone (used to promote the formation of slag) were prepared before the smelting campaign began.

Documentary evidence relating to blast furnaces has been collated by Rondelez (2014). The first references to blast furnaces in Belgium, Germany and Sweden are dated to the 12th century AD. Then in the late 14th century references to iron cannon casting are found in Germany, Belgium and France. From the 1480s onwards blast furnaces were built in Normandy, the homeland of the French ironworkers who brought the technology to Britain (Awty 1981). In the 15th century an Italian blast furnace located in Ferriere was described by Filarete (Tylecote 1992, 77) and in 1517 Nicolas Bourbon described a blast furnace probably located in the Forest of Ardennes, a region of extensive forests between Belgium and Luxembourg, extending to Germany and France (Straker 1931, 41). Recent historical research indicates Buxted in Sussex as one of the first blast furnaces built by French immigrants in the south-east of England (Awty 2003:52). In the following decades more furnaces were constructed in the Weald area of Sussex and in Kent (Crossley, 1972, 1975, Bedwin 1980). The iron industry then started to expand outside of the Weald in the mid-16th century, probably motivated by the need to find more woodlands. The technology thus reached the Midlands and northern parts of England with the

construction of Cannock Chase in Staffordshire (in 1561, the first recorded in the Midlands) and Rievaulx Abbey in North Yorkshire (Schubert 1957). Dol-y-Clochydd and Dolgun furnaces in Merioneth, northern Wales, were built in 1597 and in 1719, respectively (Crew 2009).

Archaeological field evidence provides another source of information on the location and construction of blast furnaces. In Sweden the excavation of Lapphyttan in 1970s and 1980s revealed a blast furnace with associated waterwheels, ore storage and roasting pits and a series of non-water-powered finery hearths (Magnusson 1995). The furnace was a square structure built in stones with tap holes for both metal and slag. The excavation of the Dürstel blast furnace in Switzerland brought to light two furnaces; one of which was of a round shape with an external diameter of more than 3 m. Several small fining hearths with a diameter between 50 and 100 cm were found nearby (Guénette-Beck and Serneels 2007, 2). Another furnace excavated in Germany, at the Jubach reservoir, was a rectangular structure whose walls preserved up to 2 metres in height (Rehren and Ganzelewski 1995, 172). Here, a fining and possibly smithing area, were identified by the presence of iron-rich slag. Finally, the blast furnace excavated at Glinet in France was also square and both metal and slag were tapped from the front of the structure. A finery and chafery hearth were also excavated nearby (Arribet-Deroin 2001, Dillmann *et al.* 2003).

Several early blast furnaces have been excavated in England (see also a summary by Blick 1984, which also mentions Ausewell Wood). The ones in the Weald area of Sussex offer information on the blast furnaces of the 15th and 16th century and reflect a phase of experimentation with the new technology. Panningridge was excavated between 1964 and 1970 (Crossley 1972). The walls of the furnace were made in sandstone and survived to a height of about 60 cm. The furnace saw two periods of construction. The second furnace used the layout and much of the debris from the first furnace, which made the identification of the casting area and the hearth difficult. However, their likely position was identified for the second furnace thanks to the layout suggested by the position of the waterwheel, made of oak (Crossley 1972, 54). Some information on the process was obtained by comparing the archaeological evidence with surviving documentary accounts. The main difficulties being associated with the need for a constant supply of wood for charcoal, which

determined the siting of the furnaces (usually located on running rivers in woodlands or forest), and with the long smelting campaigns that not always were achieved as the ironworkers ran into problems and had to either repair or rebuild furnaces. The product of Panningridge was white and mottled pig iron cast in sand beds, which was refined at the finery forge at Robertsbridge located about 10km to the south (Crossley 1975b). Similarly, excavations at the furnace at Batsford (East Sussex), revealed two phases of construction; the furnace was made of sandstone and bricks and built on a terrace cut into the valley (Bedwin 1980). A sandstone charging ramp was also excavated, which was used to charge the furnace from the top, and a gun-casting pit was found in front of the tailrace. Further, a cannonball mould was found that probably belonged to the last period of use before the furnace was abandoned towards the end of the 15th/beginning of the 16th century (Bedwin 1980, 105). The excavations at Chingley in Kent revealed a similar layout, with a square furnace built in stone and bricks with a rubble core. The furnace has two arches, one for the bellows and the other for tapping (Crossley 1975a). The squared hearth was made of sandstone. A finery forge was also excavated at this site (see section 2.2). The layout of Chingley is considered typical of 16th century blast furnaces, which were between 5 and 6 m tall and could produce 250 tonnes of pig iron per year against the 20-25 tonnes obtained in a bloomery furnace (King 2003).

After the 16th century furnaces became taller, increasing from 6 to 9 metres in height, and the output grew considerably (Tylecote 1992, 98). They were usually built against a hill or riverbank to help the feeding of charcoal and ore into the top of the structure. The industry in the Weald doubled in size, going from around 50 furnaces to more than a hundred in the course of 25 years (Cleere and Crossley 1995, 130), and it also expanded geographically to Wales, the Midlands and to the north of England (King 2020). Another important change that was introduced in this period concerned the furnaces themselves. The hearths of the furnaces which had been of a square or pyramidal shape up until 1600, became circular as this minimised wear of the walls and the accumulation of material to the sides (Tylecote 1992, 99).

Finally, the next most important change to the blast furnace was brought about by the change to coke fuel, which started during the 17th century with various experiments – notably Dud Dudley in the Black Country (King 2002). Although

the first successful coke smelting was carried out by Darby at Coalbrookdale in 1709, the adoption of coke-fired blast furnaces was a slow one and furnaces originally built to use charcoal continued to be used for a long time, probably well into the 18th century. But this is yet another chapter in the long history of the iron industry, one that goes well beyond the scope of this thesis.

2.5 THE FINERY FORGE

The pig iron produced in the blast furnace was hard and brittle, useful for large hollow cast objects, such as cannons and cooking pots, but not for tools and objects intended to withstand a range of stresses and had to be forged by the blacksmith. The limitations of pig iron as a new material meant that the blast furnace was only the first half of an indirect smelting process. The second half was represented by the finery forge, where pig iron was converted into malleable iron. This section offers an overview of the documentary and archaeological evidence both in relation to their introduction to England and to the layout and operational practices of finery forges.

The finery forge, together with the blast furnace, was thus introduced to the Weald in *c.*1490 by French ironworkers from the North-East of France (Awty 2007). The fining of cast iron was done in a variety of ways (Percy 1864, Schubert 1951, Starley 1999, Awty 2006, Dillmann *et al.* 2012 and references therein), but can more simply be divided between two main traditions (Tylecote 1992, 102, Awty 2006, 129). In Germany, Austria and Italy, the fining of pig iron was carried out in a single hearth; in Luxembourg, France (before the 19th century) and Britain two hearths were used, termed the finery and the chafery hearths (derived from the French verb chauffer, meaning to heat). This method is known as the Walloon method, from the region where it originated, and it was the only method employed in Great Britain (King 2020, 4).

According to Awty (2006, 2007), who studied the origin and spread of this technology, the earliest Walloon forge so far identified is the one built at Vaux in 1445-6 in the Walloon area. Schubert writing in 1951, indicated the one constructed in 1340 at Marche-les-Dames, near Namur, as one of the first finery forges. Various references to double fineries have also been collected by Awty (2006). From Belgium, the technology spread to north-east and central France, and by the second half of the 15th century it had spread over a great part of France. The finery forge reached Normandy around 1490, and from there it was

introduced to England. From the Weald, it spread to other parts of England, such as the Midlands and Wales during the second half of the 16th century, reaching the north of England at the beginning of the 18th century. The process was introduced to Sweden at the beginning of the 17th century, where it was called the Walloon method to distinguish it from the German process (single hearth), which before the arrival of the Walloon workers had been widely employed (King 2003, 45).

To the author's knowledge, four finery forges located in the Weald have been excavated and published. These are Ardingly Forge (Bedwin 1976), Chingley Forge, Blackwater Green (Crossley 1972, 1975a) and Ifield Forge (Margetts 2021), dated to the 16th and 17th century. Stony Hazel in the Lake District was initially identified as a finery forge but is now interpreted as a water-powered bloomery furnace (Davies-Shiel 1969, Bayley *et al*. 2008, 61). More recently, another excavation in Cumbria has unearthed evidence of a finery forge at Cunsey, Windermere (Schofield and Miller 2017). Archaeological excavations undertaken by Ironbridge Archaeology, revealed an iron forge at Wednesbury, West Midlands. The site was used over five centuries, starting out as finery forge in the late 16th century. The water power system was then adapted and used for the following four centuries for a series of other industries, including nail-making and gun-making in the 17th and 18th century (Belford 2010). A further archaeological project carried out at New Weir Forge in Herefordshire, in the Midlands, suggests the presence of a finery forge dated to the 17th and 18th century (Dorling and Young 2011, Young 2011).

The literature describing the layout of the finery forge and the process is limited. Among the historical sources, a brief description of the Italian forge of Grotta Ferrata, near Rome, is found in the *Treatise on Architecture* by Filarete (1461-1464). The process as described, was conducted in a single hearth, and involved remelting of metal obtained from the furnace. Upon remelting, the metal formed into lumps of various sizes, which were then collected and taken to the hammer (Schubert 1951, 61). The Walloon process is described in the Latin poem *'Ferraria'* written by Nicolas Bourbon in 1517 and translated from French into English by Straker in his *Wealden Iron* (1931, 41). The process is conducted in two hearths: the first with a large chimney where the metal is melted and collected in the form of balls, and a second, where the metal is

reheated and hammered. Further, an early anonymous report on the ironworks of Cannock Chase is described by Jones and Harrison (1978). The report written in 1590 is intended to provide recommendations on how to run the works and provides a complete description of the process, from the procurement of the raw materials to the production of bar iron (Jones and Harrison 1978, 795). The workmen at the forge are described as 'hammerman and finers, besides cariers and colliers' (Jones and Harrison 1978, 805). Carriers transported the raw materials, while colliers were the workers that produced charcoal, of which a great quantity was needed at the finery forge. Interestingly, the writer describing the process says that before the iron arrives to the chafery, the 'bloome' is worked three times in the fire (in the finery hearth) and three times under the hammer. Other early English historical sources are used by Schubert in his *Early refining of pig iron in England* (1951). These are now all available online. They are *A collection of English words not generally used* written by the naturalist Ray in 1674, *An account of the Iron-works in the Forest of Dean* by Powle written in 1678 and *The natural history of Staffordshire* by Plot in 1686. They all describe the forge as having two separated hearths and a hammer built under the same roof. Similarly, the process involves working the metal a few times between the finery hearth and the hammer before it is taken to the chafery. Historical sources dated to the 17th century are also cited in Dillmann *et al.* (2012), where, in addition, there are interesting references to the role of slag and the use of additives to improve the refining process. A detailed description of various methods of converting cast iron into wrought iron is then given by Percy in his *Metallurgy* (1864) and Fell (1908) who described the process in Furness (Cumbria, northwest England) in the 18th century. In the recent literature, the process and its remains are described by Schubert (1957), Morton and Wingrove (1970), Den Ouden (1981 and 1982), Rostoker and Bronson (1990), Tylecote (1992), Mackenzie and Whitman (2006) and Dillmann *et al.* (2012), who also conducted the first, and to the author's knowledge, only experiment on pig iron fining.

2.5.1 The forge and the process

In researching the finery forge, how it was constructed and how it functioned, it is apparent there is no one definitive account and those that have been

published are often incomplete and ambiguous. The following description has been pieced together after a close analysis of a range of sources.

The basic components of a Walloon finery forge are a finery hearth, a water-powered hammer and a chafery hearth, all constructed within the same building. Both hearths were blown with bellows, which were water-powered. Forges were located a considerable distance from the furnace; if the same river was used usually the forge was located downstream from the furnace to regulate the flow of water reaching the various waterwheels (Schubert 1957, 158). The two hearths were normally placed together (one in front of the other), probably to save the heat in the fined metal as it was moved to the chafery hearth for the final operations. The hearths were simple structures of a rectangular shape, with a stone interior lined with cast iron plates and surmounted by a tall chimney. Den Ouden reports the following measurements for the finery hearth: 0.65m long, 0.45m wide and 0.30 deep. The construction of the chafery hearth was similar, but larger, being 0.9m long and 0.6m wide (Den Ouden 1981, 69). According to Fell the fire in the chafery hearth was built with slag and charcoal from previous operations in ‘the shape of a bee-hive, about three feet and a half high, and stood on a hearth or stage of stone with a hollow or saucer-shaped cavity in the centre’ (1908, 251). Figure 2.5 shows a reconstruction drawing by Houghton (1997) showing the layout of a typical Wealden forge. It is reasonable to assume that a similar arrangement is found in other areas of England.

Fining pig iron was an operation that involved several steps. To start the process, the finery hearth was first filled with charcoal and slag. Then, the fire was lit and the blast turned on. The pig, which was inserted into the fire through a hole, was gradually pushed into the hearth where it started to melt, with molten metal falling into the slag bath. At this point, the finer started to stir the molten material, raising the droplets of iron in front of the tuyere.

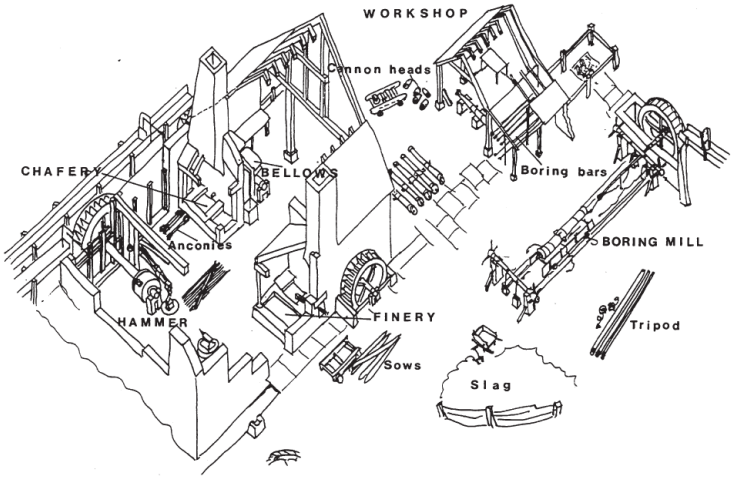

Figure 2.5.Reconstruction drawing by Houghton (1997) showing a finery forge from the Weald. The drawing shows a finery and chafery hearth constructed within the same building. Next to the chafery is a water-powered hammer used to make bar iron.

This operation first caused the oxidisation of the silicon and other impurities contained in the pig iron and started to remove some of the carbon as well. As the stirring and raising of the iron continued, the iron started to solidify as its melting point increased with decreasing carbon content. Fining was usually carried out over a couple of hours, during which the iron was exposed to the heat and oxidising blast, then taken out from the hearth, hammered into a 'half bloom' (Tylecote 1992, 103) and heated again in the finery hearth. Because of the lengthy operation at the finery, often forges contained more than one finery hearth to ensure a regular supply of iron to the chafery hearth (Hyde 1977). At the end of fining, the bloom was forged into the shape of an *ancony*, which is a piece forged in the shape of a bar in the middle but left unworked at the ends (Schubert 1957, 274). At this point, the operation continued in the chafery hearth where the metal was reheated and hammered intermittently until it was shaped into a bar of low carbon iron. Bar iron was then either sold on the market or further processed into objects by other artisans.

As described above, fining took place in a slag bath. The role of the slag in fining needs to be emphasised here. Slag, in fact, not only prevented the iron from further oxidation but it also helped to improve the decarburisation and removal of impurities contained in the pig iron. The importance of the slag was appreciated early on as evidenced by historical sources that mention the need to add slag-forming material (such as hammerscale and sand) as well as

additives such as limestone, which, in removing phosphorus improved the quality of the final metal (see Dillmann *et al.* 2012, 22). It was during this stage (melting of pig iron in the finery hearth) that fayalitic tap slag formed; when the slag had accumulated, excess was let out from the hearth by opening tapping holes positioned on the sides of the hearth. Percy (1861) before and more recently Rostoker and Dvorak (1990), in their valuable study on wrought iron and the various ways to obtain it, describe an important, and rarely mentioned elsewhere, characteristic of the fining process. This is the production of two types of slag, a first rich in silica and then a second 'associated with the finished wrought iron', termed in modern literature, tap slag (Rostoker and Dvorak 1990, 161).

Slag is also produced during reheating of the metal in the chafey hearth and during hammering. Fell (1908, 251) states that the slag that formed in the chafery was let out through a hole at the base of the hearth and formed a type of slag that in English is known as *mosser* or *hambone* (terms used in the Lake District and Midlands respectively). Finally, hammering produced hammerscale and probably smithing slags similar to what happens in smithing operations in bloomery smelting (see McDonnell 1986, Pleiner 2000).

The Walloon method of fining pig iron remained essentially the same until the end of 18th century, when some important changes were gradually introduced, such as the adoption of a water box under the bottom cast iron plate, introduced in the so-called Lancashire forges (Den Ouden 1981, 72). Moreover, the second half of the 18th century witnessed the beginning of a geographical (and then managerial) separation between blast furnace and finery forge, which ultimately lead to the development of a forge sector independent from smelting and which served a separate market (Hyde 1977, Hayman 2003) (section 2.6). Finally, with the introduction of mineral fuel in smelting, the process of converting pig iron also changed. Initially forge masters started to use coal in the chafery hearth, probably around the 1730s (Hyde 1977). Since the iron was only reheated and did not melt, sulphur contamination was minimised during this stage, so by the 1760s using coal in the chafery heart had become a common practice. Then, in a continuous effort to replace charcoal in the entire conversion process, the potting and stamping method was developed by the

Wood brothers (Rostoker and Bronson 1990, 142-143). The process with the use of coal eventually culminated in the puddling furnace developed by Henry Cort, which from the 1790s onwards replaced the Walloon method.

2.6 METALS IN POST-MEDIEVAL ARCHAEOLOGY

The post-medieval period has been traditionally the domain of economic historians, who with the use of documentary sources analysed the changes in society and economy that characterise the period between the end of the 15th century and the 18th century (Bayley and Cranstone 2004, 16). The study of the post-medieval period by historians has focused on economic growth, urbanisation, trade and markets (see for example Hammersley 1973, Hyde 1977, Childs 1981), and technological innovations have been investigated mostly through historical sources, including inventions, patents and early treatises on arts and technologies. Archaeology started to be employed much later, mostly to complement the information obtained from the historical record with the investigation of landscapes and surviving structures (Buchanan 1980, Cranstone 2004b, Photo-Jones *et al.* 2008). Excavations have been rarely used, and even less scientific analysis. Papers by Bayley and Crossley (2004), Bayley and Williams (2005) and Bayley *et al.* (2008) highlight the use of analytical techniques for the study of material remains of earlier periods. On the other hand, the reports that take a scientific approach to waste materials left behind by early industrial sites, emphasise the challenges associated with the study of their material remains as they are often disturbed by the superimposition of material debris and structures from later industries (Belford 2010, Phelps *et al.* 2011, Young 2011).

Indeed, post-medieval (and industrial) archaeology is a multidisciplinary field, which has seen historians, engineers and architects, metallurgists and archaeologists (including amateurs) focus and study different and specific aspects of the period on the basis of their own interests and specialisations. For a long time, the real challenge has been the integration of all inputs into a discipline accepted by the academic world. For archaeometallurgy, itself a multidisciplinary subject, the opportunity is to introduce a material-based approach to the study of metal production in the post-medieval period, which can become part of the historical analysis (Buchanan 1980, 380).

2.7 INNOVATION AND CHANGE IN IRON PRODUCTION

Producing iron by the indirect method introduced many changes in the iron industry. A first important shift was in the scale of production. Bloomery smelting was essentially a small-scale operation that served the need of local communities and, in comparison to the blast furnace, required little in terms of investment. The installation of a blast furnace and forge on the contrary allowed a substantial increase in iron output and required the investment of considerable capital, not only for the construction of the structure itself, but also in the procurement of the raw materials, of which a large stock was needed, and in guaranteeing a reliable supply of water to power the bellows of furnaces and forges. Moreover, while the bloomery 'industry' could move around the landscape when raw materials became scarce, with the blast furnace the location of the installation became permanent and all material had to be brought to the site of the furnace. Thus, also transportation costs needed to be factored into the investment. In addition, the blast furnace also required an organised workforce, who had to work round-the-clock shifts and needed the right operational skills. Consequently, there was an important relationship between ironmaking and the management of these complex installations, both in terms of land and capital investment (Cranstone 2001b).

A shift in this respect had already happened for the installation of water-powered bloomeries, which were associated with monastic bodies that reintroduced the Roman watermills to the industries of the Middle Ages and could afford to invest in the industry (Lucas 2005, 3). The blast furnaces on the other hand were normally constructed by 'major secular landowners and the Crown' (Cranstone 2001b, 187); the first wishing to put into profit their estates, while the latter organised and protected itself as modern states started to emerge and compete in Europe. Indeed, this was a period of growing imperial ambitions for England, and both technologies and inventors working at the service of the Crown, provided the technical basis to expand and assert their power against the other reigns of Europe.

The introduction of the indirect method to England happened under the patronage of the Tudor state, aware of the importance of the blast furnace in the production of heavy artillery (Evans and Rydén 1998, 190). The following spread of the technology from the Weald to the rest of Britain was initiated by

aristocratic landowners who wanted to profit from their reserves of ore and wood. The large-scale adoption of the indirect method placed iron technology within larger systems of production, such as ordnance, navigation and building construction, while at the same time it responded to the need of a growing population with an inevitable metal demand.

In addition, two alloys with different properties were now available. Cast iron that could be used to cast objects directly into moulds, substituting the more expensive bronze alloys; and wrought iron, which could be forged in the same way as bloomery smelted iron. Cast iron was initially used to produce cannons and cannon balls, but by the 18th century a variety of objects were cast, including pots, stoves, anchors and ship fittings. Most of the pig iron produced however, went to the finery forges to be converted in wrought forgeable iron. Wrought iron was used to manufacture many items including nails, wire, chains, horseshoes and locks. A small quantity was employed to make steel by cementation for edged objects such as tools, swords, cutlery and axes.

Consequently, different materials were chosen to manufacture different objects based on material properties, which lead to specialisation of production. For example, the iron industry of the Weald after introducing the indirect method to Britain, started to specialise in castings and in the manufacture of ordnance, and iron mills producing different objects were erected in Wales and other parts of England, with the north specialising in steel production. Indeed, it is argued that the iron industry at this time had a regional character, with the industries exploiting the nearest large markets, which were London, south Wales, the Midlands and the cities in the north of the country (Hyde 1977, 17). The area of Bristol relied on iron imports chiefly from Sweden and Russia, while Cornwall and Devon markets were dominated by Spanish iron (Childs 1981, Evans *et al.* 2002). Both areas also purchased iron transported on the River Severn, which probably came from the Forest of Dean (King 2020, 439). In the meantime, while from the 15th up to the beginning of the 17th century, blast furnace and finery forge were operating together, from the second half of the 17th century they became separated and pig iron started to be traded in the open market (Hayman 2003, 38). The ultimate consequence was a division of labour between smelters and forgemen (Evans 1998).

Returning to the subject of this study, the Walloon method of producing iron (with the blast furnace at one end and the finery forge at the other end of the process) represents in many ways the starting point of modern industrial ironmaking - it was in all respects, an industrial complex where the division of the operation among different installations allowed a continuous process and without delay after the pig iron came from the blast furnace (Jakovļeva *et al.* 2019). Moreover, because fining was a lengthy operation, often forges contained more than one finery hearth so that they could constantly supply the chafery with fined iron ready to be hammered and shaped. However, while the production of bar iron was characterised by a high degree of mechanisation from the outset, fining remained essentially a small-scale operation in the hands of a skilled workforce that had control over the process and its organisation (Evans and Rydén 1998). Many are the historical accounts that tell how the ironmasters resented their dependence on the close-knit group of forgemen (Buchanan 1980, Evans 1999). This reliance on skilled labour dictated the operations at the finery forge, which for a long time remained characterised by strong artisanal practices and a high degree of experimentation.

Therefore, rather than standardised practices, the waste materials generated by fining pig iron, are more likely to represent and record variations in the technology, as the operations were modified to respond to different material properties (different iron ores and consequently different pig iron produced, use of different additions etc.) and strongly depended by the skills and knowledge of the forgemen.

2.8 IN CONTEXT: AUSEWELL WOOD

It is in this context that the study of Ausewell Wood aims to contribute to the understanding of iron production in the post-medieval period. The site belonged to Sir Adrian Gilbert, a gentleman who not only had the means and resources to invest in a large industry but also the knowledge and skills to experiment with new innovative technologies (chapter 3). While we do not know who oversaw the operations on the River Dart, it is reasonable to assume that his involvement in mining and metallurgy played an important role in the establishment of the ironworks in a part of England that is traditionally known for tin and copper production, but much less for iron (chapter 6). Moreover,

although the connection with the search for the North-West Passage is only a fascinating theory for now, the building of ships and development of magnetic compasses to aid navigation fit with the picture of the iron industry in this historical period (see for example Long and Morrall 2019).

The archaeology of the finery forge is a complex one and characterised by a variety of remains often complicated by the superimposition of other industries. This makes the typological approach a challenging task (chapter 4). The lack of archaeometallurgical studies of slag typologies, or indeed of archaeological reports with detailed descriptions of the material excavated, further complicates the investigation of the material remains, as comparison is often impossible. While iron production in this period has been mostly studied from the point of view of the buildings and water-power installations, or even surviving tall blast furnaces, the material remains have often been overlooked, which has inevitably created a lacuna in archaeometallurgical studies of the post-medieval period. A more standard approach combining visual and chemical analysis has been employed for this study, with the aim to provide a reference to future studies.

CHAPTER 3 AUSEWELL WOOD – CURRENT KNOWLEDGE AND UNDERSTANDING

'In a forgotten corner in the lonely backwoods of Ashburton parish…'

(Brown 1997)

3.1 INTRODUCTION

Ausewell Wood lies in the parish of Ashburton and is located near Holne on the south-eastern edge of Dartmoor, in United Kingdom (figure 3.1). The following account of the archaeology and history of the site represents a review of previous studies and of the historical records associated with it, and it summarises knowledge prior to this study of the physical details, metallurgical activities and owners of the site. New information obtained from the historical research carried out for this study is also included here (section 3.1.1). The material analysed for this study comes from the excavations carried out by Juleff and a team of volunteers in 1999 and 2000 (University of Exeter, Dartmoor National Park Authority). Many of the conclusions obtained from the quantitative sampling of the slag heap SH1 (this is termed *bloomery works* in figure 3.2 and SH1 in figure 3.3) form the premise of this research. For this reason, a summary of the observations and results offered in the interim report (Juleff 2000) is reported below in section 3.2.

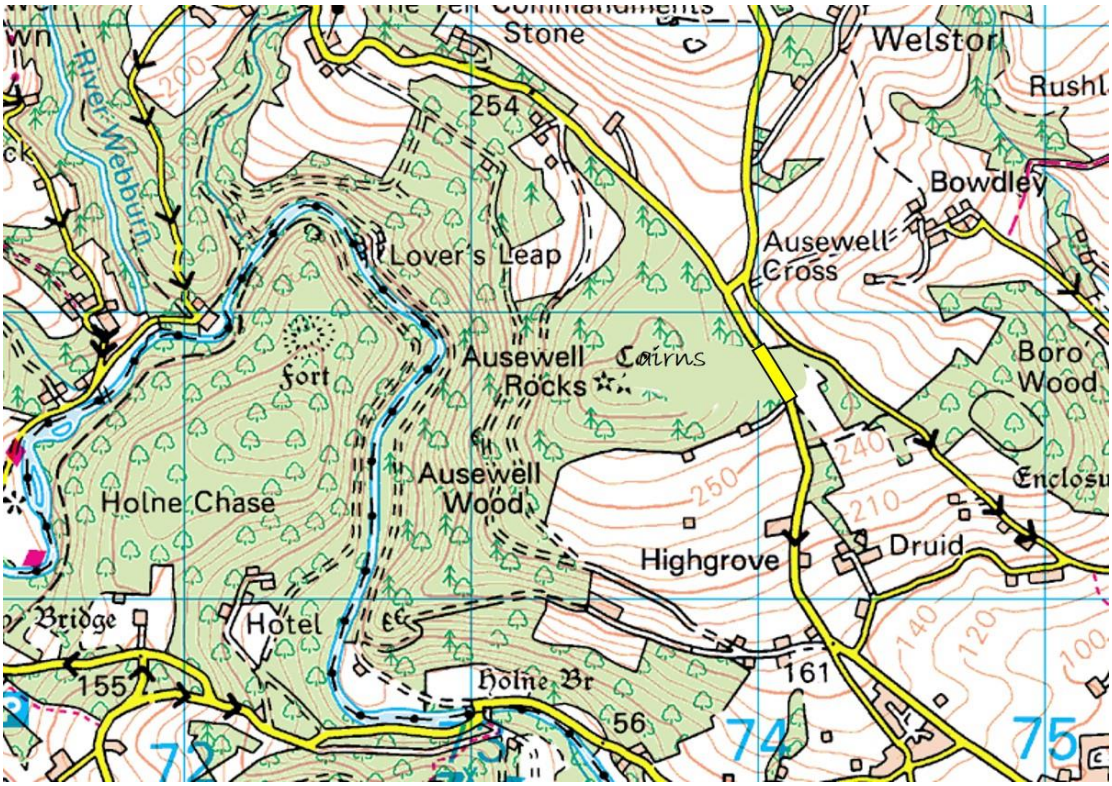

Figure 3.1. Map showing the location of Ausewell Wood within Dartmoor National Park, in Ashburton (devoninfocus.co.uk, Ordnance Survey).

3.1.1 The Archaeology and History of the site

Iron working evidence

The metal-working site occupies a long narrow alluvial floodplain on the east side of the River Dart; it is approximately 600m long and 60m wide (Crombie 1982, Newman 1998, Juleff 2000). The landward side is delimited by the hills of Cleft Rock and Hepstock Rock, all included in a large area of woodland (figure 3.2). A long, stone-lined leat runs from the north of the site along the whole of the east side, serving a series of channels directed east-west that connect the leat with the river (figure 3.3; Newman 1998, Juleff 2000). A survey carried out by Crombie (1982) shows that the leat varies in width as it travels south, being as wide as 4-5 metres on the north side, then decreasing to a 0.75m wide channel to the south. Associated with the east-west channels are wheel pits, probable buildings, dressing floors and ore waste dumps, and at the southern end of the site, the remnants of an iron-smelting blast furnace, or possibly two furnaces (BF, figure 3.3) (Juleff 2000). According to Newman (1998), the leat is quite big in comparison with other water-powered processing sites on Dartmoor. Drawn on the same position on Donne's map of Devon, dated 1605, the leat was modified and possibly enlarged as a consequence of the installation of the 18th century ore dressing floors (see below). In the survey carried out by Newman for the Royal Commission for the Historical Monuments of England (1998), it is proposed that the leat also served as a reservoir to regulate the flow of the river. This is suggested by the presence of a stone wall constructed where the leat meets the artificial channel AC1, which is also marked on the 1605 map (figure 3.4). Indeed, both Crombie (1982) and the RCHME survey (Newman 1998) consider this the likely position of a sluice for regulating the flow of water into channel AC1 and preventing too great a volume of water to reach the working area to the south. There is, however, no archaeological evidence of this remaining on site. Interestingly, Cranstone interprets the artificial channel (AC1) and Building 1 (figure 3.3) as the likely position of a finery forge or of a water-powered bloomery forge, whose layout correspond to that of 'a rectangular mill building with wheel races along both north and south sides' (Cranstone 2004a, 3).

A second leat or channel is found between the iron-rich slag heap (SH1) and the northernmost wheel pit (DF4) (Newman 1998; figure 3.3). It runs parallel to the river and its destination is unclear. Similarly Crombie, in his survey of the site during a rainy day, noticed the shallow channel flowing southwards from the side of the rectangular building (B1) and suggested it could represent a domestic water channel (Crombie 1982, 14). Probably the main leat and the ore dressing floors were built over part of its course. Newman (1998, 10) tentatively connects this second leat with the iron smelting period, but the water supply system and location of the wheel pits supplying water to the blast furnace are not clear due to later disturbance. The evidence for smelting at the site relies mainly on the existence of two heaps of slag. To the north of the artificial channel (AC1) is the heap that appears to consist mainly of iron-rich slag (SH1; termed *bloomery slag heap* or *bloomery works* in previous reports). This would appear to be more of a thick deposit rather than a heap and is associated with structural remains (Newman 1998, Juleff 2000). Moreover, a type of slag displaying features transitional between iron-rich slag (typical of bloomery smelting) and blast furnace slag was identified on the southern edge of the slag spread (Juleff 2000, 4. Chapter 4). This slag is termed ‘intermediate’ in the interim report (see section 3.2). The second heap (SH2) seems to consist exclusively of distinctive glassy blast furnace slag and is situated close to the blast furnace remains, at the south end of the complex. Cranstone (2001a, 5) states that the size of this slag heap indicates substantial and apparently successful smelting campaigns.

Amery (1924) and Crombie (1982) described the remains of the blast furnace. In addition, Amery excavated the interior and produced a drawing showing a plan and section of the furnace (figure 3.4). The west and south walls of the blast furnace are still visible, surviving to a height of 1.5m. They are spaced 0.7m apart and enclose a slightly oval chamber (figure 3.4). It has been suggested that the furnace was up to 6m high, with a conical shaft (Phillpotts 2003). For the furnace lining local slate was used, which displays evidence of heat damage and vitrification. Amery reports that the slate was “converted (by the heat) into a red, stoneware-like, substance” (1924, 96). The evidence on the

ground for the furnace and different constituent parts (for example, Crombie was not able to locate the position of the tapping facilities or where the blast was supplied from) is quite difficult to interpret due to the overgrown nature of the site. Immediately to the north of the first blast furnace, there seem to be the remains of a stone structure that could be a second blast furnace (Juleff 2000, Cranstone 2001a, 5). This appears associated with a second heap of blue blast furnace slag. Cranstone reports that this slag appears different from that in SH2, though still being compatible with interpretation as blast furnace slag (Cranstone 2001a, 5). An investigation of the blast furnace remains was attempted for the present work. Unfortunately, in addition to the difficulty of surveying a site with overgrown tree cover, during a survey in March 2019 a large fallen tree was found lying across the furnace, which was not removed during the time available for this research. Moreover, when this project started the land belonged to a private owner, who granted access to the site through a private road. Then, in January 2020 the Woodland Trust and the National Trust bought the site and due to the following COVID-19 pandemic the author was not able to return to the site.

Three charcoal burning platforms (of which only CBP1 and CBP2 were surveyed and shown in figure 3.3) were recorded to the east of the metal-working complex, indicating that charcoal was produced on site (Newman 1998, 14). They consist of circular platforms, measuring approximately 5m in diameter, and large quantities of charcoal are visible on their surfaces.

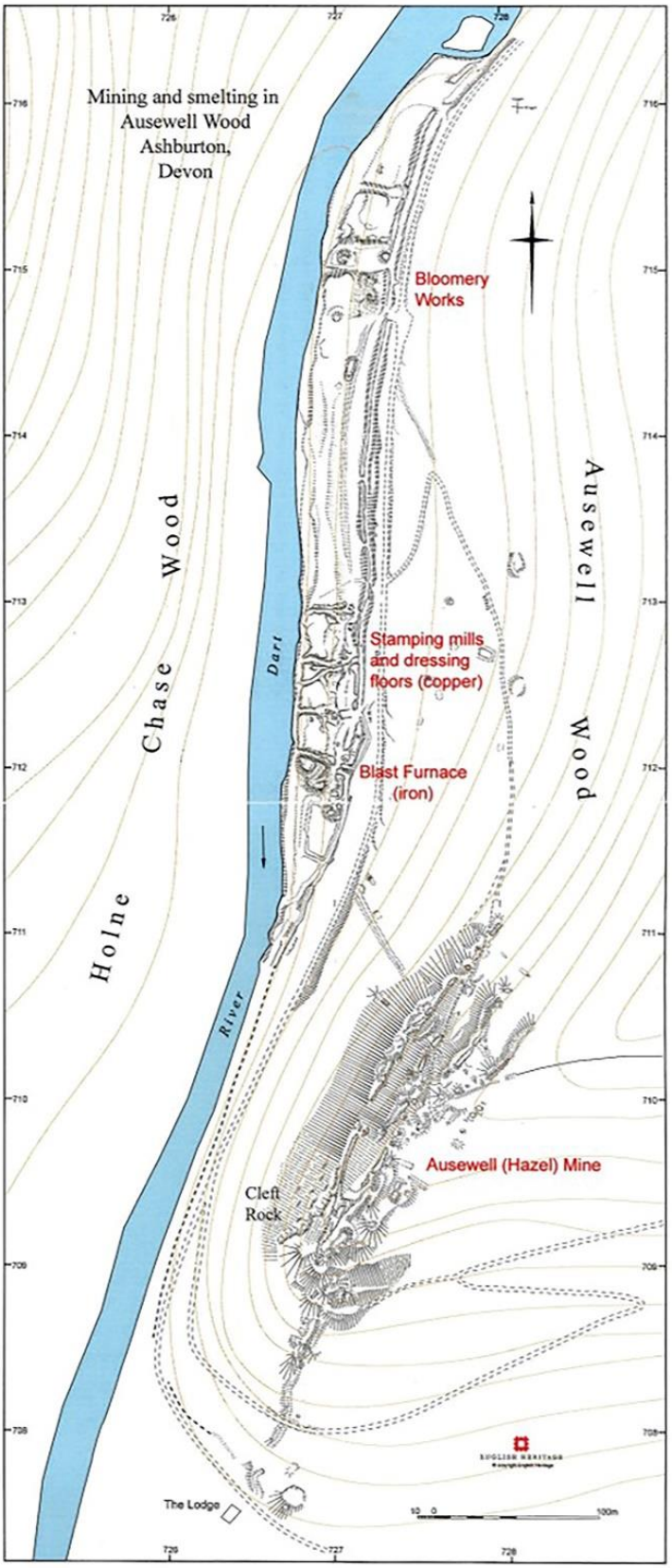

Figure 3.2. Overall plan of the site showing its location, the mines and metal processing areas (Newman 2004, 2). Bloomery works to the north corresponds to slag heap SH1; the excavated material studied here comes from this area.

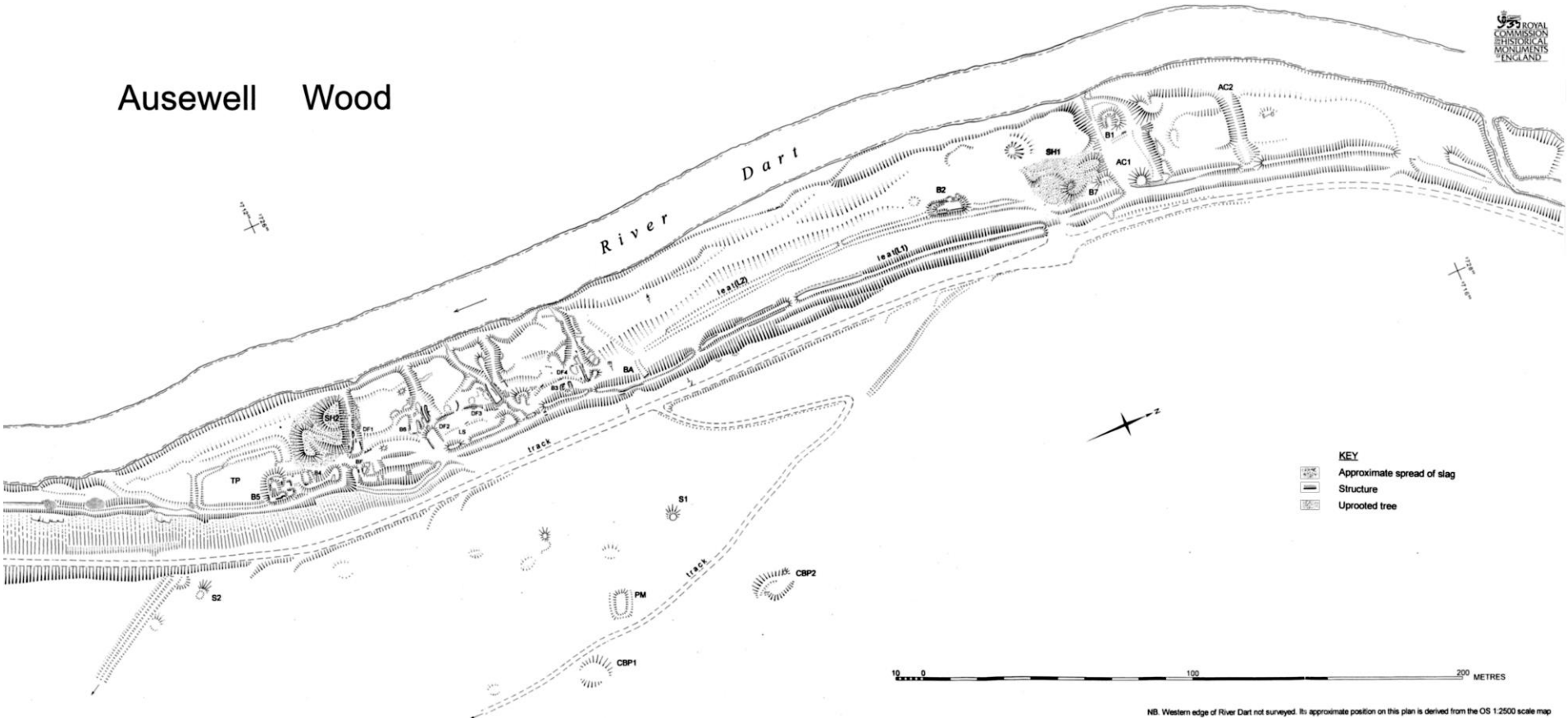

Figure 3.3. Overall plan showing the main features identified after the RCHME survey. The initials are explained in the text. Note the distance between the blast furnace to the south and the excavated slag heap SH1, which corresponds to the location of the finery forge. The river flows north to south in this point, situating the forge upstream from the blast furnace.

Many of the large charcoal fragments recovered during excavation were identified as small diameter roundwood indicating the charcoal was produced from coppice wood (Juleff 2000, 13). The availability of extensive woodlands at Ausewell Wood would have provided the charcoal needed to fuel any smelting process (Page 2004). The remains of five buildings are also present on site; however, there was no evidence to indicate the function of any of them. They could have been buildings for material storage or could have been used for accommodation for the workers who, during the long smelting campaigns in the case of the blast furnace, had to stay on site and pay constant attention to the operation.

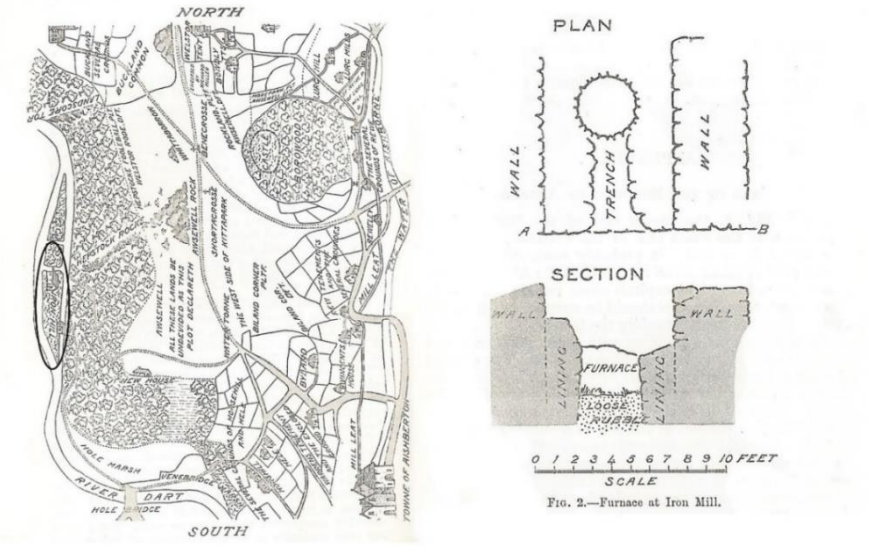

Figure 3.4. Left: map of Ashburton dated to 1605, showing the River Dart, the Hepstock Rocks and a small house accompanied by the words Iron Mills; this is seen on the left by the river circled in black. Right: drawing by Amery showing the plan and section of the blast furnace at Ausewell Wood (Amery 1924, figs.1-2, 94-95).

Ore Dressing Floors and Wheel Pits

The southern area is also occupied by ore dressing floors (DF1-4, figure 3.3) associated with four wheel pits and two possible *buddles* (B1-2, figure 3.3). These ore dressing floors are associated with the 18th century processing of non-ferrous metals, probably copper and tin. Buddles are shallow pits, often of circular form, built in order to wash and separate by sedimentation ore minerals from rock dust, using a flow of water (Salter and Gilmour 2012). The RCHME report gives the most complete description of these features (1998, 6-8) and associates them with a later phase of activity on site, dated to the 18th century.

The construction of the ore dressing floors disturbed the iron-working complex and probably the ore dressing floor 1 (DF1) damaged the blast furnace structure. Spaced approximately 30m from each other, the wheel pits are oriented east to west with *tailraces* bringing the water back to the river. The wheels probably powered stamp devices for crushing copper ores (and only possibly tin). This activity is attested at Ausewell Wood by documentary evidence (Brooke 2001. See below). Stamping mills were employed for mineral extraction by pounding the rock material under heavy vertical beams of wood with iron shoes, operated by waterwheels to lift and drop the stamps (Brewster 1832, 75).

Further evidence for ore processing on site is represented by a large rectangular earthwork situated adjacent to Building 5, which has been interpreted as a *tailings pit* (TP, figure 3.3) (Newman 1998, 13). Tailings are more commonly known as mine dumps, and represent the material left over after separating the valuable minerals from the unwanted fraction of the rock during ore processing (Salter and Gilmour 2012). They are normally produced from crushing mills and are a suspension of fine particles and water.

Evidence for Mining

Evidence for mining at Cleft Rock (figure 3.2) was surveyed by Newman (2004) and a report on the geology was carried out by Page (2004) to test whether the source of iron was local. The results suggested that Cleft Rock has the wrong mineralisation to have been the source of iron ore for the activities at Ausewell Wood and was only used as a copper mine. This still leaves open the question regarding the origin of the iron ore smelted at Ausewell Wood (chapter 5). Phillpotts (2003) who reviewed the surviving documentary evidence for the site offers an intriguing scenario. The land was in the hands of the Elizabethan entrepreneur Adrian Gilbert in 1582, who had an interest in metallurgy and connections to iron mining near South Brent (around 7 kilometres southwest from Ashburton; figure 3.5), silver working at Combe Martin in North Devon, as well as tin mining on Dartmoor (Tyson 1996, Phillpotts 2003, Page 2004).

Figure 3.5. Google Map showing South Brent and the distance from Ashburton. The river to the left of Ashburton is the River Dart.

Documentary evidence of *c.*1593-1598 indicates that Gilbert took iron ore from Brent Hill, South Brent, to "certain iron mills near Ashburton and were found to be very good, both for steel and iron" (Greeves 1987, Phillpotts 2003). Another possibility is that iron was mined more locally, for instance from the Mount Ararat Chert Formation in Holne Chase Woods (Page 2004, 16) (figure 3.2). The Devon historian Thomas Westcote in his *View of Devonshire in 1630 with a pedigree of most of its gentry* mentions iron mines at Ashburton and Brent (Westcote 1845, Phillpotts 2003). Here, there is again a mention to Adrian Gilbert and his involvement in silver working at Combe Martin, which refers of a new silver lode found in town that "first begun to be wrought by Adrian Gilbert, esquire" (Westcote 1845, 65).

Conversely, despite the paucity of records, the presence of copper mining at Ausewell Wood is well known, and references to copper mines are found in Dines (1956) and Hamilton-Jenkins (1981). A further important surviving document is Henric Kalmeter's journal dated 1724-5 (Brooke 2001). Here, he notes that several copper lodes had been worked at Cleft Rock and that in

"Queen Elizabeth's days they were worked for silver ore" (Brooke 2001, 46-47). Kalmeter further states that the copper processing installations were established where "there once stood a blast furnace" and affirms that copper pieces and ingots are found among cinder and slag. From Newman's survey of the Ausewell Mines it would appear that the majority of the extractive evidence dates to the early-mid 18th century, with possibly some earlier activities commencing in the late 17th century (Newman 2004, 15). The copper was worked from open pits, using powder to blast the rock as evidenced by shotholes in the rockface, and possibly also firesetting. This technique continued to be used in the 19th century because it was cheaper than the use of powder (Newman 2004, 14). Copper working continued at Ausewell (Hazel) Mine (figure 3.2) at least until 1810, with some activity in 1833 and then it all ended in 1860 when the lease was surrendered (Page 2004, 13).

Documentary evidence

Besides the documentary evidence in connection with the mining evidence, the most significant reference to Ausewell Wood is the already cited map dated to 1605, which was produced by commissioners investigating evidence of a land dispute (Crombie 1982, 6). The original map is held in the Record Office in London, while a copy was published in the Transaction of the Devonshire Association by the president Amery (1924, 94). He provides various details of the site, including comments on the slag that was analysed by the Vice President of the association, Dr. Satterley, and the Secretary, R.H. Worth, both confirming smelting of iron ores. Describing the map, Amery says, 'we are not left to mere surmise, since the foundations of the buildings yet remain, the bases of the furnaces are there, vitrified by the heat, and large heaps of slag extend from the building towards the river' (Amery 1924, 53). The reference to 'furnaces' in the plural, appears to confirm the field evidence as described by Juleff (2000) and Cranstone (2001). Baring-Gould (1900) also provides another reference to furnaces and slag heaps in the plural. Brown (1997), in his *In search of Ausewell Mine – an examination of the surviving evidence*, highlights the paucity of surviving records on the early metallurgical activities at Ausewell Wood, stating that the reason for the lack of documentary evidence can be

found in the remoteness of the site, ‘in a forgotten corner in the lonely backwoods of Ashburton parish’, and the history of the ownership of the area.

Indeed, in a survey conducted in Devon in 1613/4 by John Norden, a cartographer and surveyor of Crown land, Ausewell Wood (also *spelled* Awsowell and Awsowell Downe) is mentioned twice but is not included in his survey because the land had previously been sold, in the time of Edward VI. The land ‘dismembred’ from the manor of Ashburton, was granted to Hall and Greene and their heirs (figure 3.6). Later in the survey, Norden reports that there was controversy about ownership of some of these lands and left the matter to Prince’s court to decide (Billinge and Martin 2018).

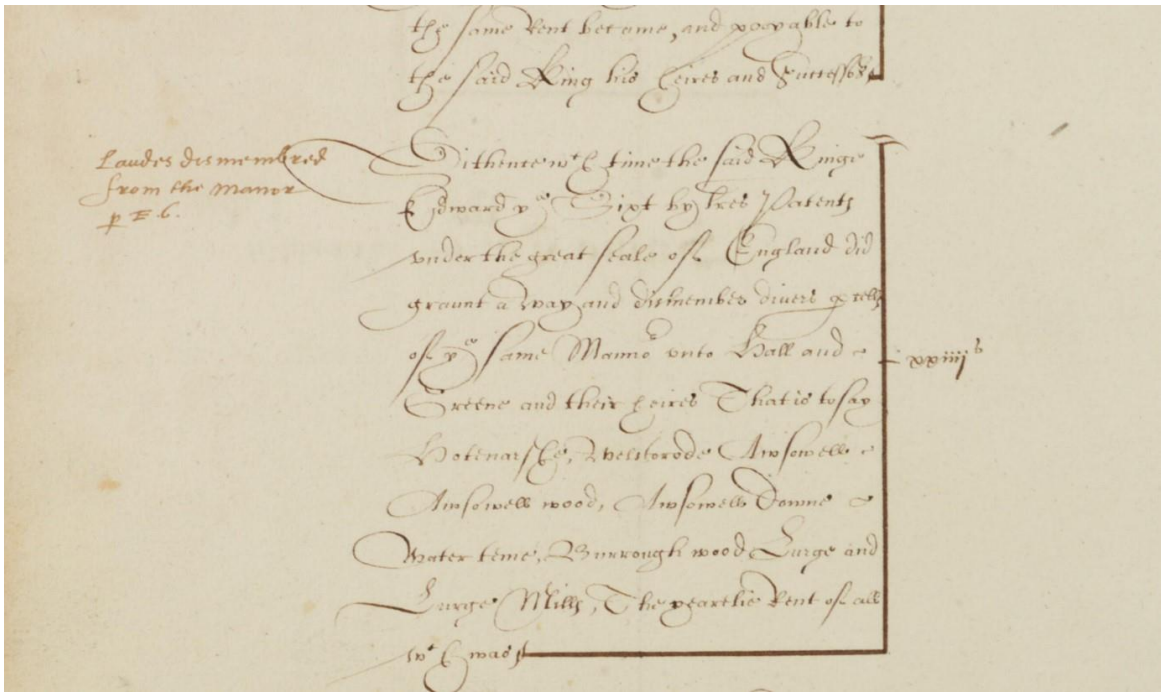

Figure 3.6. Awsowell in Norden’s survey. The marginal note says ‘Landes dismembred from the manor p[er] E[dward] 6’. (After Billinge and Martin, 2018, by the kind permission of London Metropolitan Archive).

When Kalmeter visited Ausewell Wood in 1724 the land belonged to Squire Ford and in 1799 John Pollexfen of the Bastard family purchased Ausewell Manor from the Seymours (Brown 1997). While the tenancy of the land by Adrian Gilbert during the iron working phase appears confirmed by documentary evidence dated to 1593-1598 (Phillpott 2003), we do not know how much he participated in the enterprise, or indeed if the investment was commercial or experimental. He was a tenant of Gregory Sprent by 1582 and it appears that much of his work in Ausewell was clearing the land in the Dart

valley for mining and industry (Phillpott 2003, 14). Similar to the history of Ausewell Wood, little is known of the life of Gilbert, whose undertakings appear overshadowed by the lives of his much more famous brothers. However, the information that we do have is still useful to understand and contextualise the site and ironworking activities of Ausewell Wood.

Gilbert, born in Devon, was the younger brother of the famous Sir Humphrey Gilbert (seaman and explorer) and half-brother to Sir Walter Raleigh, a statesman, writer and explorer who was, at least for a time, Queen Elizabeth's favourite. Adrian was heavily involved in the affairs of Raleigh and was responsible for the construction of his house 'Sherborne Lodge' (in Dorset) and its gardens (Rowe 2012, 40). As well as being known for his interest in gardening and water works, Adrian was a mining and metallurgical entrepreneur, an alchemist, a farmer and a tinner. He was one of the jurats representing Ashburton in the Great Courts or Parliament of Devon Tinners and supported his brother, Raleigh, when in 1585, he became Lord Warden of the Stannaries (Greeves 1987, 157). Moreover, he was a dedicated supporter of the English quest for the North-West Passage, of which his two brothers Humphrey and Walter, the famous English scholar John Dee and the explorer John Davis, were key advocates (Small 2013). The North-West Passage is an historical sea route from the Atlantic Ocean to the Pacific Ocean through the Arctic Archipelago of Canada. The quest for the Passage started in the 15th century, when Europeans became interested in the passage in an attempt to find new trade routes to Asia, after the Ottoman Empire monopolised major land trade routes between Europe and Asia.

Adrian also owned a ship that fought against the Spanish Armada and one of Raleigh's ships was called the *Adrian* after him. When Humphrey Gilbert was lost to sea following the 1583's expedition to Newfoundland, Adrian Gilbert and John Dee were granted a new patent by the Queen to sail 'Northwestward, Northeastward or Northward' (Lemercier-Goddard and Regard 2013). They obtained the financial help from William Sanderson, a wealthy merchant from London who was married to a niece of the Gilbert brothers (Wallis 1964). In his

Diary, Dee recorded numerous meetings between himself, John Davis, Adrian Gilbert and the Queen's Secretary Francis Walsingham to discuss the planning of the expeditions in search of the North-West Passage (Trattner 1964; figure 3.7). Adrian did not sail but funded John Davis on three (unsuccessful) voyages between 1585 and 1587 (Malcolmson 2010).

Following Walter Raleigh's downfall with the Crown (he was accused of treason and beheaded outside of the Palace of Westminster in 1618), Adrian went to live at Wilton House where he became the resident chemist and laboratory technician of Mary Herbert, Countess of Pembroke, with whom shared an interest in alchemy (Malcolmson 2010, 115). He also designed the garden of William Herbert, with elaborate hydraulics and magic symbols inspired by the teachings and influence of John Dee. Scientists, alchemists, mathematicians and explorers of the 16th century England were among Adrian's friends and associates.

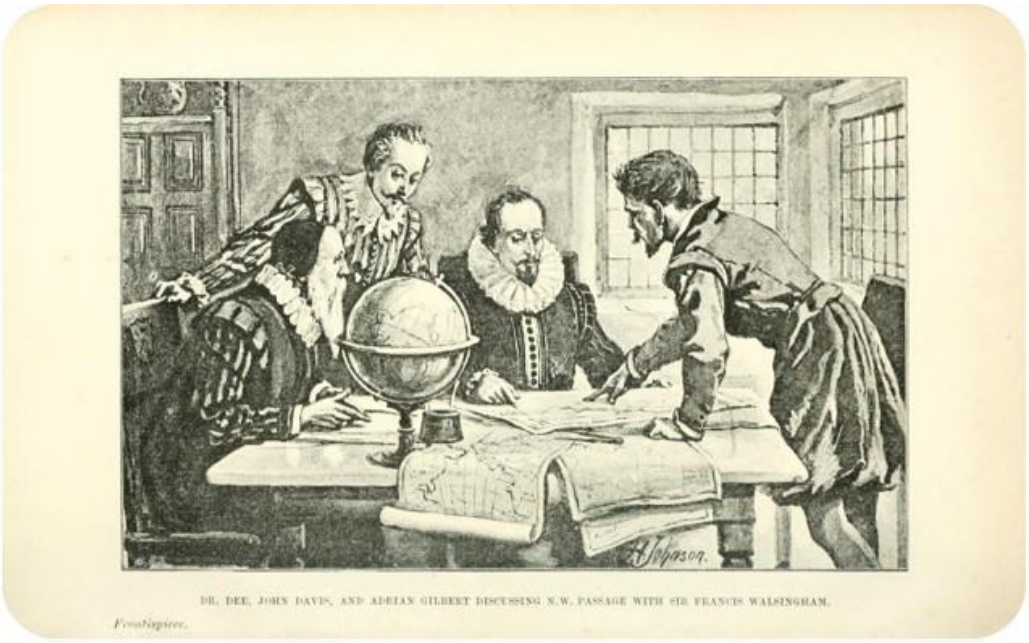

Figure 3.7. Dr Dee, John Davis and Adrian Gilbert discussing the North-West Passage with Sir Francis Walsingham. Frontispiece of the book A life of John Davis the Navigator 1550-1605, discoverer of David Straits by Markham 1889. Available at http://www.archive.org/stream/lifeofjohndavisn00mark#page/n7/mode/2up.

Finally, although fragmented, some interesting references linking Gilbert's interest in iron (and its magnetic properties) to the sea expeditions and development of compasses to aid navigation are found in several studies on

diverse sixteenth century topics. Among these, the most significant is William Gilbert's *De Magnete*. The book appeared in 1600 and gives a full account of his research on magnetism and electricity. William Gilbert (who was not related to Adrian Gilbert) experimented both with natural 'magnets' (loadstones or lodestones) and artificially magnetised iron. Discussing the distribution of iron ores in England, he tells that 'newly' in an English mine, belonging to the gentleman Adrian Gilbert, magnetic iron ore was found (Zilsel 1941, 14). His connection to the North-West Passage expeditions, surely made him interested in the magnetic properties of iron. Unfortunately, the location of the mine is not given in the book, but William Gilbert refers to various mines in Devon that contain deposits of loadstone. Moreover, in his *History of Devonshire* (1797), Polwhele, describing loadstone deposits in England, mentions the following Devon localities: Sotwardstone, South Brent, North Molton, Ashburton and Hennock (Bromehead 1948, 434).

It was the interplay between chemistry, alchemy (and metallurgy), mathematics and navigation that favoured discussion on and experimentation with new technologies, providing a fertile ground for the metallurgical innovations that took place in the 16th century England. As Phillpotts (2003, 13) rightly stated: 'Adrian Gilbert was therefore exactly the type of Elizabethan entrepreneur who might have been experimenting with new iron processes in the south Devon in the late 16th century'.

3.2 THE EXCAVATIONS

Two excavations were carried out on the site of slag heap SH1, in 1999 and 2000.

This section summarises the description of the heap and trenches as detailed in the interim report by Juleff (2000); it only concerns the trenches of the first season of excavation in 1999. The data of the 2000 excavation season, for which no excavation report was generated, is presented in chapter 4, section 4.4.8.

The aim of the excavation and of the quantitative sampling was twofold:

- to characterise and quantify the excavated material

- to gather data on the technological aspects of the iron-working activities

To this end, eleven $1m^2$ trenches were excavated following an east-west baseline, labelled A-B, laid out across the centre and at the highest point of the slag deposit. By offset measurements from this line, trenches could be located on a site grid extending both north and south of the baseline (Juleff 2000, 6). The trenches are thus identified by alphanumeric labels indicating their position relative to the E-W baseline. Trenches to the north of the line are then assigned N, and those to the south S. Finally, the distance from the baseline is indicated in metres. Thus, in order of excavation trenches were labelled: QN1, ZN1, PN1, JN9 and ZS3 for the season 1999 and LS1, MS1, NS1, OS1, RS1 and SS1 for the 2000 season (figure 3.8).

Description of Trenches (season 1999)

Trenches QN1 and PN1 are located side by side and after quantitative sampling in each, they were excavated together as a single trench of 2m x 1m. All trenches were excavated in spits of 0.2m to obtain a total weight of material from a spit of known volume. Each spit was treated as a separate unit, hand sorted, and the slag divided into small, medium, large. The matrix material, which represents soil with fine particles of slags, charcoal, pebbles etc. was sieved through a 1cm sieve. It was then further processed by wet sieving at two size ranges, 1 - 0.5cm and 0.5 - 0.25cm. An interim report on particle count analysis was performed by Chris Carey of the University of Exeter on the 1 - 0.5cm range material in order to explore the variation of material in depth and from trench to trench. The results of this exercise are preliminary, but the data analysed appears to mirror the distribution and variation between trenches and spits observed in the quantitative sampling (Juleff 2000, 11). The total weight of material from the 12 spits was calculated to be 2,846.72kg and the total slag yield (not including the slag at less than 1cm) was 1,709.25kg, meaning that around 60% of the material was slag (see table 4.3 in chapter 4). However, the proportion of slag to non-slag material varies widely from spit to spit. Further, the slag yield for each size category for each trench was calculated (figure 3.9

and Appendix A.2). For the data of the 2000 excavation season see chapter 4, section 4.8.8.

The results showed that in PN1 and QN1 the slag yield drops below the first spit, indicating a surface deposit of slag rather than a heap or thick deposit. Both trenches appear dominated by small slag fragments. A charcoal-rich layer was encountered in trench PN1 (spit 20-40), which contained both macro-size charcoal fragments (up to 3 - 4cm in length) and fine particle charcoal that appeared crushed. Underneath the charcoal-rich layer and the iron-rich tapped slag, was a uniformly 5cm thick layer composed of silica-rich slag, quite different from the typical glassy blast furnace slag (chapter 4). This ‘intermediate’ slag found beneath the tap slag (assumed to be from bloomery smelting at the time of excavation) questioned the technological sequence and stratigraphy of this slag deposit (see section 3.3). No pottery was found here, only one fragment of metal and a large fragment of vitrified clay.

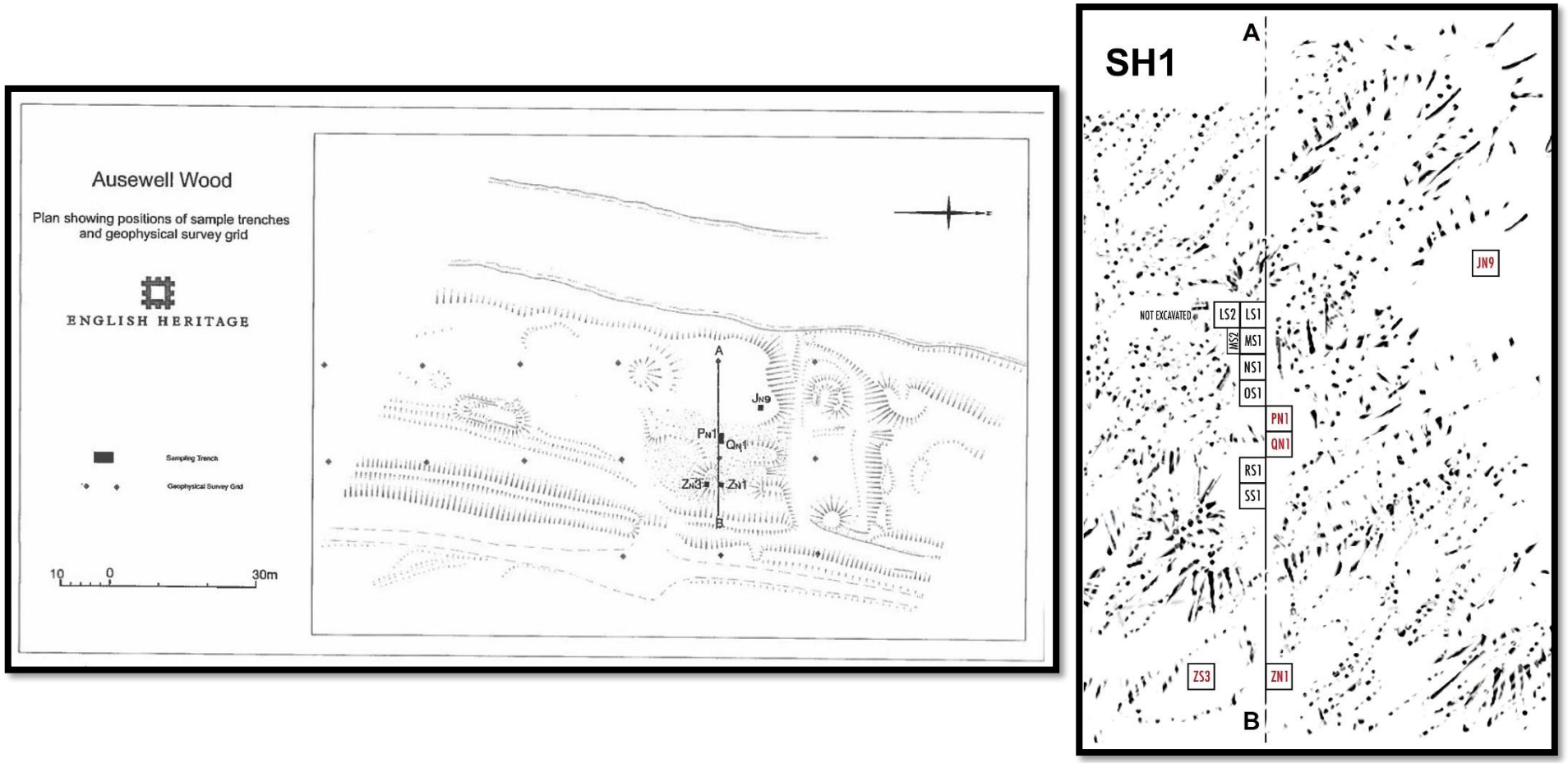

Figure 3.8. To the left: plan of SH1 showing E-W baseline, 1999 sample trenches and geophysical survey grid (Juleff 2000, 21, courtesy of P. Newman RCHME). Drawing from original excavation documentations, showing the baseline A-B and the location of the trenches from both seasons on top of the slag heap SH1. Red trenches are of the 1999 excavation season (digitalised and edited by the author).

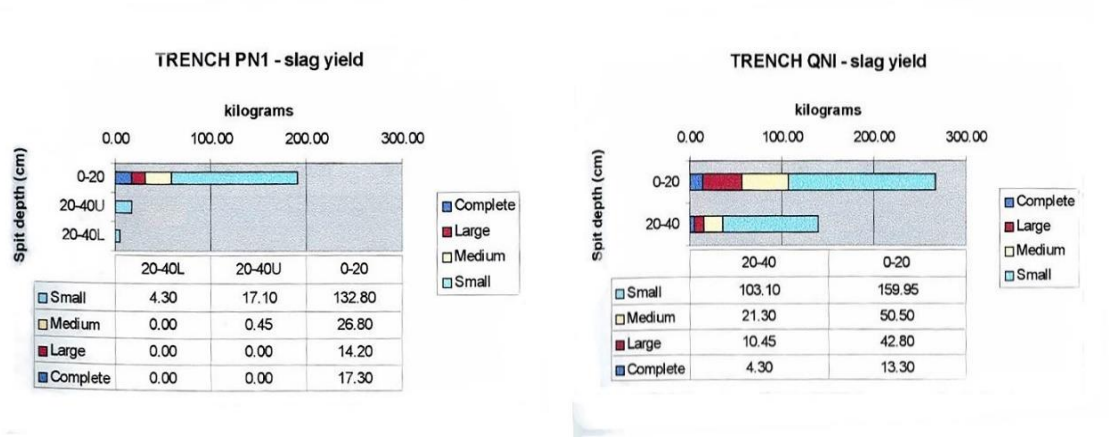

Figure 3.9. Charts showing the slag yield for trenches PN1 and QN1 elaborated for the material excavated during the field season in 1999. Trenches ZN1, ZS3 and JN9 are shown in Appendix A.2. (After Juleff 2000, 24).

Similarly, trench JN9 is dominated by small slag fragments and produced relatively little slag. Several metal fragments, including a possible nail, were recovered from spit level 0-20. Almost no slag pieces were contained in spit 20-40, where a charcoal-rich layer with lenses of clayey-sand was encountered. Quantitative sampling was discontinued for the 20-40 spit, but it was resumed for spit level 40-60. Here, the slag was mostly of the iron-rich tapped slag. Beneath the slag and charcoal deposit of spit 40-60, in the south-eastern corner of the trench, a part of a large feature was revealed; it appeared lined with stones and the fill contained small slag and charcoal fragments (figure 3.10). It was not excavated however, the distinct magnetic signature obtained during the subsequent geophysical survey strengthened the interpretation as a furnace base or hearth structure (see below).

Figure 3.10. Photograph of trench JN9 showing in-situ feature into sandy alluvium below slag and charcoal-rich layers. (Original analogue photograph from the 1999 excavation season, Juleff 2000, plate 6, 28).

Trench ZS3, located at the highest point of the deposit, contained a greater quantity of material and a higher proportion of large slags in comparison with the other trenches, suggesting a primary undisturbed deposit (figure 3.11). The largest piece recorded weighed 25kg. The trench also contained pottery sherds and fragments of metal. It was excavated down to 0.6m, where a continuous layer of sandy alluvium was revealed. This material was encountered in other trenches and is described as ‘natural’.

Figure 3.11. Photograph of trench ZS3 on completion of excavation. The profile of the trench shows a deep deposit of slag on top of a charcoal-rich deposit and natural alluvium. (Original analogue photograph from the 1999 excavation season, Juleff 2000, plate 3, 27).

Trench ZN1 was similar in composition to that of ZS3 and contained the greatest frequency of ‘complete’ slags (the term complete implies examples that conserve all edges intact, including upper and lower surfaces. Chapter 4), however below the first spit the quantity of slag recorded dropped sharply because the remnants of a wall crossed the trench. This feature was not excavated, but it is suggested that the wall could be part of large slate-roofed

structure, whose position was implied in the RCHME survey (Newman 1998). This trench was excavated down to 0.4m. Both spits yielded a high proportion of pottery and other finds such as a clay pipe stem, fragments of iron and roof slate.

Pottery

All pottery sherds were recovered from trenches ZN1 and ZS3. They were analysed by John Allan of the Royal Albert Museum, Exeter, who indicated that the ten sherds from ZN1 derive from the same vessel. This is likely an internally glazed, open bowl of South Somerset yellow slipware, which dates from between *c.*1580-1600 to 1690-1700. Some other sherds from ZS3 belong to South Somerset plain lead-glazed ware which is broadly dated from the late 16th century to the early 18th century. Finally, a single sherd of an imported Frechen ware drinking jug was identified from ZS3 and can be dated to *c.*1550-1650. A date range of 1600-1660 was thus assigned to the deposit from which the pottery was recovered, which is consistent with the recording of an iron mill at Ausewell Wood on the map of 1605 (Amery 1924).

Geophysical and Geochemical Surveys

The geophysical survey performed during excavation in 1999 on SH1 highlights several features beneath the slag deposit. Of these, at least two have magnetic signatures that indicate that they could be 'furnace' bases (Juleff 2000, 12). A further survey was then performed by Substrata in 2000 as a continuation of the previous survey. The report summarises the results of both surveys and describes at least four archaeological features, of which one is more clearly identified as a potential furnace (Dean and Faxon 2000). The feature associated with the furnace displays the maximum magnetic reading recorded during the survey and the interpretation as a possible furnace is supported by the fact that it coincides with the feature encountered in JN9, as well as by the pattern of the slag surrounding it (Juleff 2000, Dean and Faxon 2000). Overall, a group of six features and a potential furnace are identified and considered for further archaeological investigation.

The geochemical survey, conducted as part of the field investigation during the 2000 fieldwork season, was performed by Carey (2000). The aim was to assess the geochemistry of the entire site, thus including the later non-ferrous activities. The transect sampling areas included the tailings pit, dressing floor (DF1), the main leat (L1) and the slag heap (SH1). Although preliminary, the investigation of the non-ferrous activities confirmed the processing of copper ore, but not tin. Finally, the analysis of the samples taken from the excavated spit levels of SH1 revealed elevated levels of lead, manganese, copper, iron, arsenic and very low level of tin. The total level of iron showed a decrease with increasing depth, demonstrating that the higher spit levels had a greater volume of slag, and in accordance with the result of the excavations which characterised SH1 as a surface spread rather than uniform deposit (Juleff 2000, Carey 2000, 69).

3.3 CONCLUSIONS

The stratigraphy revealed by excavation offered a complex sequence of events; in particular in regard to the silica-rich slag found beneath the iron-rich tapped slag. The assumption, prior to the commencement of the excavation, was that the site represented a transition between bloomery and blast furnace smelting, which are represented by the two slag heaps found at the opposite end of the site (SH1 and SH2 in figure 3.2). The following technological explanations are put forward in the conclusions of the interim report:

- Fining of cast iron

This hypothesis considers that the silica-rich slag and the iron-rich slag are the product of the same process. The hypothesis of a finery forge is considered and discarded on the account of the large ‘cakes’ of iron-rich tapped slag, normally associated with bloomery furnaces (chapter 4).

- A bloomery furnace adapted for a blast furnace-type operation, which produced both iron-rich tapped slag and silica-rich slag

This scenario would see the use of a high bloomery furnace for smelting. Employed in many parts of Europe and England before the blast furnace technology was fully developed (chapter 2), these tall furnaces could be operated to produce both bloomery iron and liquid cast iron.

- Bloomery slag imported from elsewhere as feed material for the blast furnace

This last option was considered because in the early stages of smelting in blast furnaces, iron-rich bloomery slag was commonly added to the furnace charge and re-smelted: the strong reducing conditions achieved inside the blast furnaces in fact permitted the extraction of the iron present in bloomery slags in the form of iron silicates.

The technological questions that have arisen from the excavations of this part of the site are addressed in this study. The excavated assemblage was first visually analysed (chapter 4) and consequently, selected samples were subjected to chemical and microstructural analysis (chapter 5).

Ultimately, the site of Ausewell Wood is of value for a couple of reasons. First, because of its connection to Adrian Gilbert. The investigation of the metalworking activities conducted at the site is even more valuable in the light of Gilbert's interest, life experience and involvement in the social, political and cultural life of 16th century England. Second, the site is exceptionally well preserved, albeit disturbed by later non-ferrous metallurgical activities and other forestry activities, the material remains (and to a certain extent the layout of the ironworking phase) are mostly conserved *in situ* and this is a unique opportunity to investigate an early industrial site in this part of England. Indeed, the blast furnace at Ausewell Wood is the only blast furnace archaeologically identified in the region. Finally, in connection with the last point, Devon is not the expected venue for the study of early industrial iron production (chapter 7, section 7.1). Ausewell Wood, located away from later centres of the industrial era, is distinguished by both material and historical evidence, representing a compelling case study, a window into the history and archaeology of the iron industry in the post-medieval period.

CHAPTER 4 MACRO-MORPHOLOGICAL STUDY AND TYPOLOGY

'Multiple voices and silences are represented in any scheme that attempts to sort out the world.'

Bowker and Star, 2002

4 MACRO-MORPHOLOGICAL STUDY AND TYPOLOGY

Before describing the methods employed for the visual analysis of the Ausewell Wood assemblage is necessary to consider some challenges with the methodology encountered during this stage of the research. The first section of this chapter thus consists of two parts: a first where these issues and some observations on methodology and typology are considered and the second part where the methods adopted here are described. This is then followed by the description of the material, divided in types and subtypes, and by the sections on the data obtained from the two excavation seasons (1999 and 2000). The chapter then closes with a discussion of the results and an assessment of the methodology. The work in this chapter is supported by the material presented in Appendix A.

4.1 CHALLENGES TO MACRO-MORPHOLOGICAL ANALYSIS

Dominant terminologies and prior assumptions

The challenges described in this section pertain the methodological approach followed to visually analyse the assemblage. Macro-morphological analyses in archaeology employ and generate classifications in order to organise the material under study. The aim of classification systems for most archaeological material (ceramics and lithics) is to try to achieve objectivity. Standardised materials such as pottery and metal objects make the classification approach suitable for most research questions (Orton 1996). On the contrary, slag classifications according to macroscopic features is a challenging exercise where avoiding prior assumptions and subjectivity appears difficult. Slag, in fact, is the by-product of metal production that forms under an enormous range of conditions; consequently, it displays less ‘standardised’ attributes that can be employed objectively. Moreover, since the material researched is the metal (and the materials employed in its production), the most important information from slag can be obtained only by scientific analysis, making the conclusions that can be drawn from the visual analysis inevitably limited (Hauptmann 2014). Slag classifications within archaeometallurgical studies are largely based on the morphology created by the methods of slag removal and have generated a terminology that often implies technological traits.

In the first stages of this study, the assemblage was approached by the author with the assumption that the slag heap excavated, visually dominated by tap slag – the most recognized and understood type of slag, characterized by a flowing texture that resembles that of lava - was the result of, or related to, iron smelting using a bloomery style technology. A few reports on Ausewell Wood mention the possibility of a finery forge; notably Blick (1984) who analysed a piece of slag from this same deposit (slag heap SH1) and affirmed that the slag was 'a typical bloomery slag which suggests that a bloomery may have preceded the blast furnace, or that the site may also have had a finery' (Blick 1984, 47). The majority of the reports on Ausewell Wood referred to the area under study as 'bloomery work' (Crombie 1982, Newman 1998 and 2004, Cranstone 2001a). Indeed, bloomery smelting is the technology that dominated iron production and was used in many areas (especially those associated in this time period with small scale production) until the 18th century. Mainly on account of the presence of tap slag – the quintessential indicator of smelting – the most accredited theories leaned towards the site representing either a transition between bloomery and blast furnace technology and/or a water-powered bloomery. Although the similarity between finery and bloomery tap slag is acknowledged in archaeometallurgy (Morton and Wingrove 1970, Rostoker and Dvorak 1990, Gordon 1997), the lack of systematic studies and the greater familiarity with waste material from bloomery smelting, seemed to challenge the finery forge hypothesis. In the excavation report, the fining technology is contemplated on account of the presence of silica-rich slag found below the tap slag; however, it is also dismissed because tap slag from bloomery has 'distinctive and diagnostic forms' and because of the spatial distance between the blast furnace and the area of slag heap SH1 (Juleff 2000, 17); a fining hearth is expected to be located much closer to the blast furnace.

Indeed, the assemblage was approached during the visual analysis using tools and methodologies that have been developed to study smelting slag (Appendix A). The classification scheme approach was first used for the study of Sri Lankan smelting slag, produced in furnaces that were powered by wind-pressure (Juleff 1996). It was then developed for the Exmoor Iron Project for the investigation of bloomery smelting waste (Bray 2006). This latest version of the classification scheme was the one employed in this study as a guide for the

classification of the assemblage in material groups that shared morphological features (Appendix A).

Thus, the macro-morphological analysis began by representing the Ausewell Wood material by means of existing typologies. The assemblage was initially described and categorised assuming that tap slag indicated smelting, and consequently, the large slag blocks were classified as furnace slags, i.e. formed inside a furnace. The interpretation of the assemblage was guided by categories established not only by the classification scheme in use but in general by archaeometallurgical studies and typologies on iron waste material, which tend to consider the presence of tap slag as indicative of smelting. For these same reasons, at first the presence of tap slag overshadowed the assemblage and directed the visual analysis, with the rest of the material classified accordingly. Conceptually similar is the case with the Sri Lankan material, where the initial classification of slag types is based on descriptors that 'presupposes a known furnace design' (Juleff 1998, 57) - bowl or shaft design; only to find later in the survey and post-survey data analysis, indications from slag morphology, of a totally different furnace design.

This initial approach thus resulted in discrepancies between the iron-working technologies (and associate materials) and the terminology employed to describe and group the waste material. A fundamental difference behind the terminology employed for the Sri Lankan and Exmoor material is that tap and furnace slag are smelting slag, that is slag produced during the extraction of iron from ores (iron-making process). For the bloomery technology, smelting was carried out in a furnace, an enclosed combustion chamber from which the molten slag could be tapped off. Conversely, the technology documented in Sri Lanka is unique, and it was the specific furnace design and use of strong monsoon winds that permitted to achieve the right conditions (reducing) for smelting and for obtaining a liquid slag that could be tapped (Juleff 1996, 1998).

On the contrary, the waste material analysed in this study was obtained from the conversion of cast iron (smelted in a blast furnace) into malleable iron - an iron-working process that produces slag very similar to that produced in bloomery smelting. Following Percy (1864) and to avoid confusion with bloom refining (in bloomery technology), the term fining is employed here to refer to

the entire process of cast iron conversion. In the present work, refining is used to refer to a stage of the fining process (see glossary and chapter 5). The fining of iron was performed in a hearth, an open installation with a chimney on top and equipped with waterwheels that moved bellows. This technology also produces tap slag, when the surplus slag created in the slag bath within the hearth is removed by opening a tap hole made on the wall of the hearth installation (Schubert 1951). In this context, tap slag is not a smelting slag, but a waste produced during the iron-working phase, more precisely during the oxidation of cast iron to obtain wrought iron.

A related problem is therefore the use of the term bloomery. The earliest iron smelting method is known as bloomery smelting (or direct method). Because the temperatures achieved in the furnace rarely exceeded 1250 °C (i.e. below the melting point of iron), the result of smelting iron-bearing ores with this process is a solid-state reduction of iron, in the form of a porous mass (iron mixed with slag and charcoal) called *bloom*. The furnaces employed in the bloomery process could be of two types; the 'non-slag tapping' furnace, where the slag consolidated into large slag blocks in a pit beneath the furnace and the 'slag-tapping' furnace, which permitted the removal of liquid slag via a hole at ground level that could be opened during the smelt (Cleere and Crossley 1995, Pleiner 2000, Paynter 2011). Slag-tapping furnaces are considered a development in smelting technology; introduced in the Late Iron Age, they became common in the Roman period and lasted until the medieval period, producing great amounts of slag with the typical flowing texture (figure 4.1). Since this process was also the most widespread method for iron production, pre-industrial reduction is often referred to as bloomery process (see also David *et al.* 1989), and the presence of tap slag - which accumulating on the ground (or depressions near the tap hole) formed large 'cakes'- is generally associated with (bloomery) smelting.

Figure 4.1. Comparison between a Roman tap slag produced from bloomery smelting (left) and an example of a tap slag cake from Ausewell Wood. Note the flow pattern on the surface, common to both pieces (photo on the left is after Paynter 2011, figure 3, p.3).

A similar issue was then encountered when describing the dense slag blocks found at Ausewell Wood, a type of slag that can be confused both with furnace slag ‘cakes’ and with large smithing hearth bottoms. The former, also known as furnace bottoms, can be produced during smelting and usually are large accumulation of dense slag that can retain, or partially reflect, the shape of the base of the furnace, forming into bowl-shaped ‘cakes’ with a flat surface (Paynter 2007). They are often characterised by charcoal impressions, a coarse texture and varying degrees of porosity (figure 4.2).

Figure 4.2. Comparison between an example of furnace slag produced from bloomery smelting and excavated from a Late Iron Age site in Kent (left) and an example of hearth slag from Ausewell Wood. Note the coarse texture and small charcoal impressions (photo on the left after Girbal 2013, fig.9, p.96).

The latter, smithing hearth bottoms, are the product of refining and smithing the iron bloom and often are convex-convex - with a depression on the upper surface caused by the air blast - or concave-convex with a sub-circular shape

(figure 4.3). Slag with non-diagnostic shapes can also form during smithing and these are generally known as smithing lumps, but given their amorphous shapes assigning them to smithing or smelting can prove challenging (Selskiené 2007). The larger smithing hearth bottoms can be confused with 'furnace bottoms' and both types were thus considered during the initial slag assessment for this study. The assessment considered consistency and abundance of the material as well as the presence of additional evidence on site to support the interpretation as either furnace bottoms or hearth bottoms (Appendix A).

Figure 4.3. Comparison between a smithing hearth bottom produced during iron smithing and an example of smithing slag recovered from Ausewell Wood. Note the shallow depression on the surface of both pieces. The shape reflects the hearth within which they formed (photo on the left after Paynter 2011, fig. 8, p.6).

The shape, surface texture, density, presence of charcoal and iron are common features among these slag types and only once it was established that the material under study related to post-smelting operations, the interpretation of the dense slag cakes also changed, and their typologies reassessed.

Finery forge assemblages

In contrast to furnace slag 'bottoms' but similar to smithing hearth 'cakes', the slag from Ausewell Wood did not form within a furnace, but in (or around) the hearth installations typical of the finery process. The finery forges in England seem to have used two hearth installations (the Walloon method. See chapter 2): a finery hearth where the oxidation of cast iron was performed, followed by a chafery, where the oxidised mass of iron was reheated prior to being hammered and shaped into iron bars. The process performed in the chafery is the

equivalent of that carried out in the string-hearth in bloomery smelting, where the smelted bloom was purified by a blast of air before being hammered (chapter 2). While the excavations did not reveal if fining was performed in one or two different hearths, if we assume that the Walloon method was indeed the one used at Ausewell Wood, the dense slag retrieved should be representative of the two different stages of fining and classified accordingly.

Finery forges were installations with slag-tapping facilities, so the tap slag can be assigned with a good degree of confidence to this stage of the process. For the chafery installations instead the information on the mechanisms of slag formation is less clear. Chaferies were similar to fineries but did not have slag-tapping facilities (Rondelez 2014, 52). The information available in the literature for this type of installation refers to a hollow hearth built in a bee-hive shape from which the slag ran into a sand floor and collected in the form of ‘mossers’ or rounded mass of slag (Fell 1908, Morton and Wingrove 1970, Tylecote 1992, Phelps *et al.* 2011, Rondelez 2014). Morton and Wingrove (1970) affirmed that the slag was poured in a gassy state, which created a structure in two layers, a denser lower part and porous frothy top layers. This type of slag is described in various studies as ‘saucer-shaped’; thus, mossers are plano-convex cakes of high density, ‘not dissimilar to the larger smithing hearth cakes’ (Rondelez 2014, 52). Tylecote added that those still displaying runners of slag attached have been described as ‘hambones’ (1992, 103). Morton and Wingrove (1970, 28) also report the name hambone, specifying that the term is used in the Midlands (United Kingdom), while mossers is the northern British term for chafery hearth slag, and probably refers to the fact that often moss grows on them.

Clearly, the use of such language-specific terms to indicate chafery hearth slag makes the identification of this poorly understood waste material even more complicated. However, at Glinet (France), a well-documented and studied finery site of the 16th century (Arribet-Deroin 2001, Dillmann *et al.* 2003), together with numerous cast iron artefacts, a large number of what the authors call ‘refining slag cakes’ were found (Dillmann *et al.* 2003, 102). These are similar in appearance to some of the cakes analysed in this study. The authors report two types of refining cakes: a large dense one with a typical plano-convex shape and a less dense one with an almost flat shape. The plano-convex cake once

sectioned revealed a porous structure with large charcoal inclusions, while the plane one displayed a large metallic inclusion with oxidised graphite lamellae (thus oxidised cast iron). Similarly to Ausewell Wood, the excavations at Glinet did not reveal whether fining was performed in one or two hearth installations. The authors suggest that the plano-convex cakes formed in a 'particular stage of refining', while the one with a metallic core, is associated to the 'first stages of refining' where cast iron is oxidised in the finery hearth and decarburised metal droplets are entrapped in the slag bath (Dillmann *et al.* 2003, 103). The description and interpretation of the hearth slag 'cakes' offered in this important study, seem to hint at a differentiation between dense cakes from the finery and those from the chafery hearth, or perhaps at the formation of hearth slag within the finery hearth as a consequence of different operational steps. In fact, even though slag was tapped from the finery hearth, it can be expected that the more viscous slag would solidify within the installation as a dense slag block, and was subsequently removed; similar, to what happens with the bloomery furnace with slag tapping facilities, where part of the slag solidifies within the furnace, either because it falls below the tapping hole or because it is left at the end of the smelt (Pleiner 2000).

Moreover, also in the finery process there is a smithing phase. In bloomery smelting after the bloom was extracted from the furnace, it had to be hammered to clean it from the slag (primary smithing) and subsequently an object could be forged (secondary smithing) (Crew 1996). In finery technology, after the fined iron was heated in the chafery hearth and thus cleaned of slag, it was shaped into bars. These two phases should thus correspond to primary and secondary smithing, respectively, and this stage should again produce similar material waste: the most recognised being smithing hearths bottoms and hammerscale (section 4.4.3 and 4.4.7).

Thus, the similarity in slag morphologies produced by these two different technologies requires the elaboration and the establishment of a 'vocabulary' for the systematic description of the slag, and other waste material, produced in the finery process, with an emphasis on technological aspects alongside the more conventional morphologies. This study is a first attempt to sort waste material produced during the conversion of cast iron.

Evolution of a classification system for Ausewell Wood: context and prior assumptions

Notwithstanding the fact that the point of departure was a classification scheme created for another technology, this also served to highlight differences from a more ‘traditional’ bloomery smelting assemblage; and considering the archaeological context, it offered an insight into the assemblage, whose interpretation slowly moved away from bloomery smelting. Moreover, because the macromorphological characterization of the Ausewell Wood assemblage involved the analysis of the bulk material (which consisted of representative samples for each material type and size, as well as matrix samples) and of on-site selected pieces, a different picture from that seen at the outset started to emerge (section 4.5 and Appendix A.2). Considerations on how tap slag is better understood during sample collection on site and consequently more easily represented in an iron waste assemblage came about only when the assemblage was considered in its entirety and the role of smaller and/or less recognized pieces and features became visible.

In particular, of great importance to understand the assemblage and the technology represented was the presence of small sub-rounded lumps of slaggy conglomerations with fragments of blast furnace slag embedded. Moreover, the shape of this material was suggestive of the stirring operations typical of the fining process. In addition to this, blast furnace slag fragments were also noticed embedded on tap slag cakes and on some of the large dense slags, providing a first link between the remote part of the site where the blast furnace is situated and the excavated slag heap (SH1), and thus strongly hinting at the identification of a site where both smelting and post-smelting operations were performed. Furthermore, the abundance of iron-rich slag and metal scraps pointed to an iron working process. All this was then considered together with the absence of iron ore fragments and vitrified furnace lining, which are normally encountered among iron smelting debris. Finally, the presence (or remnants) of slag channels found in the large slag blocks suggested a different mechanism of formation from that seen for furnace slag bottoms and smithing hearth cakes.

Thus, considering all the above, the visual analysis comprised the following steps:

- The classification scheme in use was adapted to the specifics of the Ausewell Wood assemblage (Appendix A.3). This involved creating entries for the blast furnace slag samples and for the waste material associated with post-smelting processes
- The terminology and descriptors used for tap slag did not change, but the term finery was added to the category name, thus becoming finery tap slag
- Furnace slags were renamed hearth slag, and a differentiation between finery hearth slag and chafery hearth slag was attempted (chapter 2). It was decided not to use the term *mossers* (or *hambones*), as these do not easily permit a comparison with non-British sites. The term hearth slag is thus preferred in this study
- Not all the attributes of the original classification scheme were employed; some of the qualitative features were modified or new attributes added
- To represent the smaller material (and highlight its role in the iron-working process investigated) against the ubiquitous larger and denser tap slag, the samples were counted, and the visual representations (pie and bar charts) produced to support the discussion have been created using the number of pieces (section 4.2.2 and Appendix A.3.2). This was done with the aim of producing figures that reflected the variety of material and forms observed, challenging the idea that the presence of tap slag represents smelting (especially in a late Medieval context) and considering the biases, if any, introduced during sample collection

4.2 METHODOLOGY FOR THE MACRO-MORPHOLOGICAL ANALYSIS

The study and analysis of the material recovered at Ausewell Wood is the main focus of this research and addresses the reconstruction of the technologies present on site. It is particularly important because studies of similar assemblages are scarce in the modern literature and a morphological and chemical characterisation of the ironworking residues related to post-smelting operations is lacking. Moreover, no blast furnaces or forges have yet been

clearly identified archaeologically in the South West of England. A possible explanation for the rarity of blast furnace sites could be the fact that the iron industry at that time was dominated by the well-developed Weald iron industry (South East England), which produced and exported iron to many parts of the country (Hodgkinson 1997, King 2003, 181). Moreover, the iron market in England during this period relied heavily on imports from Spain and Sweden (King 2020) (see chapter 7).

This section will outline the methodology employed to visually analyse the assemblage and how the data obtained was treated and interpreted, once it was established that the material waste under study derives from post-smelting operations (Appendix A.3).

4.2.1 Quantitative sampling during excavation

During excavation, in the course of the quantitative exercise, the assemblage was divided into three main groups: selected samples (and special finds), bulk samples and matrix. The first two groups represent the macroscopic fraction of the assemblage and were further sorted by the excavation team into small, medium and large samples. The matrix represents the smallest fraction that could not be sorted on site. A protocol for the analysis of small matrix samples was elaborated for this assemblage (section 4.3).

Of the total excavated material, together with selected pieces, special finds and matrix samples, representative examples of each class of material and each size category were retained for future study (bulk samples): they represent the premise of this study. The remaining material was used as spoil to back-fill the trenches on completion of the fieldwork.

1. Quantitative bulk sample: in this group is all the excavated material, bagged on site without any particular selection, and thus it might include diagnostic and non-diagnostic samples. This group is comprised of samples representative of the material retrieved from each spit of each trench
2. Selected pieces and special finds: this group comprises pieces with diagnostic features that were deemed to be of particular value during excavation; for example, the piece was intact and/or could be directly linked to a specific stage in iron production, or it displayed traits that

could be used for technological interpretations. Both common types and pieces with unusual features are included here

3. Matrix: this comprises fine mixed residues contained in the excavated soil and obtained after sieving and charcoal flotation

4.2.2 Methodology of Macro-morphological Analysis

The results described here originate from the macro-morphological analysis of all material retained and stored by Dartmoor National Park Headquarters (Bovey Tracey) and the Department of Archaeology at University of Exeter. This amounted to a total of 70 bags of selected samples and size-sorted bulk samples and 29 bags containing matrix samples sieved at two size ranges: approximately 1 – 0.5cm and 0.5 – 0.25cm (Appendix A.1). Sub-samples from each group were selected during this stage for laboratory analysis; the methodology for selection and specimens is described in chapter 5.

The flow diagram in figure 4.4 displays the procedure adopted in this study for the investigation of the assemblage and highlights the actions (circled in yellow), outcomes (in green) and the research project objectives (in blue). The aim is to reconstruct the technological practices, through the macro-morphological characterisation of the selected pieces, and consequently to obtain information on the metal-working technologies documented on site. Moreover, the study of the size-sorted bulk samples permits a holistic overview of the assemblage, offering a characterisation of most of the parts of the waste heap that were excavated, and informs on the social and functional aspects of the technological evidence. This is analysed in connection with the stratigraphic information, with the final aim of understanding the site and its spatial organisation (section 4.5). Finally, the study of small samples drawn from the matrix offers information on activities that are not necessarily reflected at the macroscopic level (i.e. hammerscale from smithing).

During classification of the material, each piece was divided into three different categories based on morphology and features: Discard, Reassessment and Sub-sample. This approach was elaborated by Juleff and her team during the work carried out for the Exmoor Iron Project (University of Exeter, Exmoor National Park), and it proved to be an efficient method for sorting large assemblages.

In particular, material that was deemed of no further interest was discarded. This category thus comprises material of which there were enough examples to keep for further analysis and samples of a highly fragmented nature. In this case, the discarded material was returned to the store at Dartmoor, pending the opportunity to then put it back on site. The material was discarded only after the archaeological data had been extracted and classification completed. Very small fragments with no diagnostic features or original surfaces were recorded as non-diagnostic.

Samples with particular features, specific forms or for which the initial assessment was not certain were assigned to the re-assessment category. After the assemblage was studied in its entirety, the material in this category was reassessed in the light of accumulated experience and what was deemed superfluous was discarded.

Finally, good examples of material with specific and/or singular features, were kept as sub-samples for further analysis. This category also included possible ore samples, special finds and anything that was considered of particular interest for the research project.

As illustrated on the flow chart, this exercise resulted in the creation of a database (figure 4.4 and Appendix A.3.1) and the selection of sub-samples to undergo chemical analyses (chapter 5). On the one hand, the dataset was used and interrogated for the subsequent data analysis; this permitted the creation of figures that illustrate the characteristics of the assemblage and the investigation of the technology in connection to the spatial organisation of the site. The samples selected for laboratory analysis, on the other hand, allowed the reconstruction of the technological practices with an emphasis on the craft and materials employed, but also explored the relationship between the two (apparently distinct) areas of the site, that of the blast furnace (SH2) and that which was subjected to excavations (SH1) (refer to figure 3.2 in chapter 3).

Thus, the interpretation of the technology and of the pattern of activity on site, is achieved by combining three sources of information:

- The visual analysis of the assemblage from which details of the technology employed can be extracted

- The chemical analysis of samples identified during the macro-morphological examination, which offers information on other aspects of the technology, such as materials employed, final products etc.
- The archaeological data, which allows the waste material to be connected to the metallurgical activities and organisation of the same

A first survey of the assemblage was done in order to assess the condition of the polythene bags and labels in which the material had been stored for a number of years. All steps were photographed in order to have a photo archive to refer to at a later stage (Appendix A.1.1).

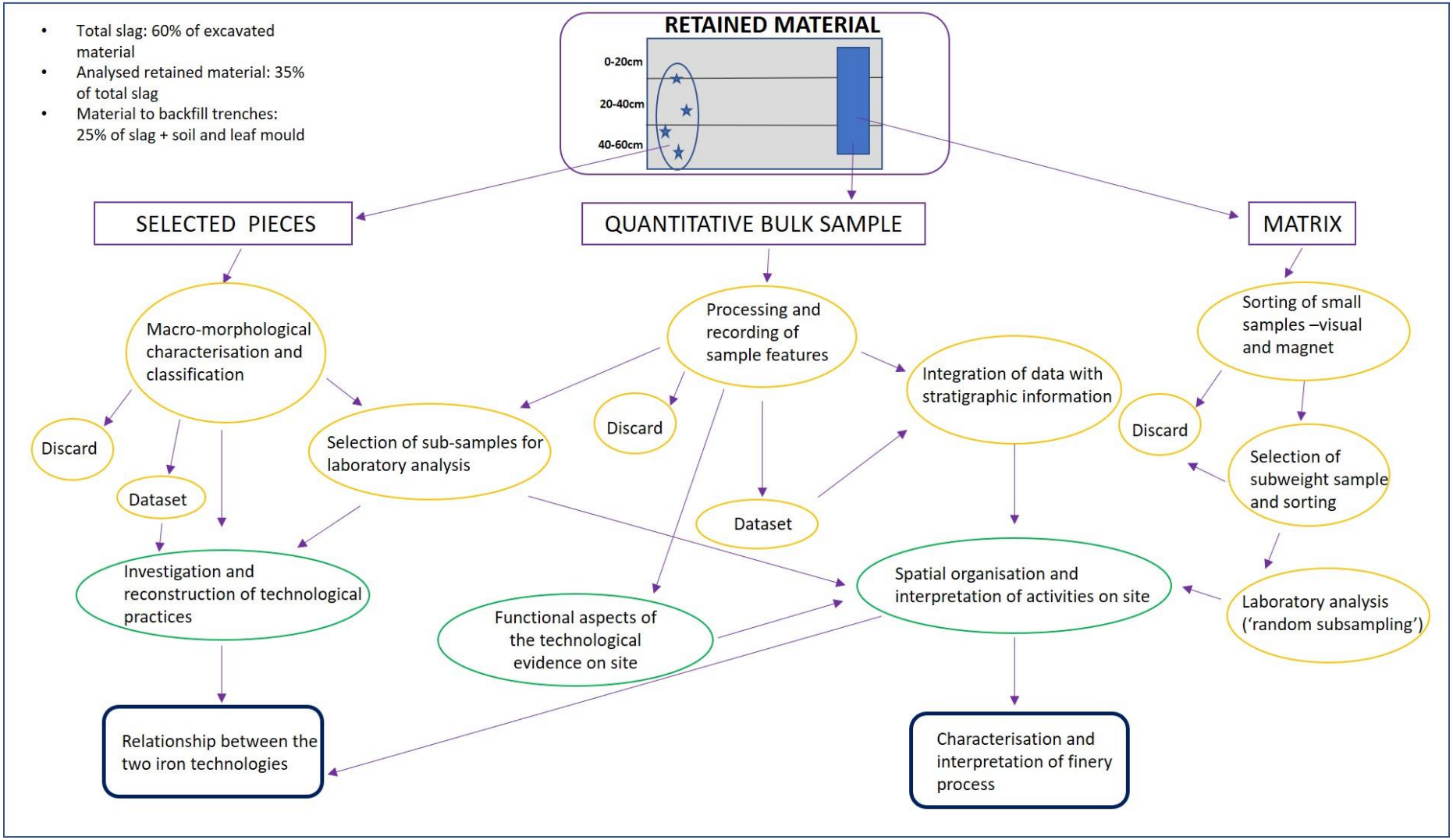

Figure 4.4. Flow chart showing schematically the methodology employed here, with actions and expected results of the macro-morphological analysis. Refer to text for explanation.

The bags and labels were in good condition making possible the retrieval of all information. Due to time constraints, only eight of the ten excavated trenches were surveyed. They were selected following the site grid used during excavation (chapter 3). All trenches from the 1999 excavation season have been analysed (trenches PN1, QN1, ZN1, ZS3 and JN9) as well as trenches LS1, SS1 and RS1 of the 2000 season (refer to figure 3.8 in chapter 3). Both excavations were performed following the same approach and generated quantified data. However, since they represent two different datasets, the data from the two excavation seasons were analysed separately at first and then combined into final observations. The results of the 1999 excavation season were summarised in a preliminary report, which put forward observations on the distribution of the material in the different trenches and illustrated with bar charts the quantified data (Juleff 2000; figure 3.9 in chapter 3 and Appendix A.2.1). A report for the 2000 excavation season was not created, and the quantified data was analysed and illustrated during the data analysis carried out for this research (Appendix A.3); the results are discussed in section 4.8.8. The same material groups were identified in both excavation seasons; there were, however, some differences in the subtypes encountered and the way they occurred in the different trenches. These are described in the sections below.

The second step was to carry out a detailed recording and classification of all the finds. In this stage, the technological debris from all the trenches opened during the 1999 and 2000 excavation seasons were classified into groups on the basis of their morphology and macroscopic features (see for example: Juleff 1998, Chirikure and Rehren 2004, Girbal 2011). The slag size categories created during excavation were retained and only a few samples were reassessed into a smaller or larger category. All visual assessments were made with the naked eye and a magnet. This tested the possible presence of metallic iron and/or magnetite that can inform on the redox conditions existing in the hearth and consequently contribute to the reconstruction of the metallurgical activities (Muralha *et al.* 2011). Only for the matrix samples, which contained small and often difficult to discern fragments of various material, were magnification tools used (section 4.3). All details were recorded into a spreadsheet, where each piece constituted a single entry completed with all the qualitative and contextual information (Appendix A.3). When similar pieces were encountered, these were recorded as group of similar material, noting the number of fragments.

Research into the different conversion processes of the post medieval and industrial era are limited, therefore the assemblage was at first largely divided into morphologically similar groups and described. Once a preliminary database was created, all recorded features for each group were checked against the photographic record. In some cases, this allowed the identification of more specific groups and/or features. The macro-morphological analysis was complete when no further variations in the type of materials present could be identified.

For the macro-morphological characterisation of the assemblage and representation of typologies observed the material was counted rather than weighed. This approach was chosen for two reasons. Firstly, the material was already quantified and to a certain extent sorted on site (the bags containing material representative of small, medium and large samples). See chapter 3 for the results of the assemblage quantification analysis and section 4.8.8 for observations on the results obtained combining quantified data, slag typologies and excavation data.

Secondly and more importantly, because of the nature and size of the material analysed. The assemblage is characterised by a large number of small-sized, low density pieces. During the analysis of the data collected for the visual investigation, it was observed that the small samples would be underrepresented if weighed against the large denser cakes (for example small-sized conglomeration rich in clay coming from inside the hearth compared to tap slag cakes). Using the number of pieces permits their role within the assemblage to be highlighted and each group, even of less dense material, can be proportionally represented. This provides figures that reflect the variety of material observed. Small pieces are generally less understood during sample collection, which is in some ways biased towards larger and more common pieces of slag (i.e. tap slag), but can provide critical insights into the ironworking technology. This approach introduces the issue of over-representing types that tend to break into small fragments; however, this offers the opportunity to make observations on the degree of fragmentation of each class of material, and of the entire assemblage, which in turn can provide information on both the technology, the spatial patterning and deposition.

4.2.3 Classification scheme

The classification of slags is still a matter of debate and many of the proposed classifications schemes and methods are considered too simplistic or not comprehensive enough (McDonnell 2001, Schrüfer-Kolb 2004). Indeed, there is currently no classification of iron working residues associated with the blast furnace and finery process. This study attempts to group the slag and residues in relation to the technological steps from which they derive. To avoid confusion, when necessary, the terminology employed here to describe the various class is referenced to other archaeometallurgical studies available in the literature.

For the Ausewell Wood assemblage, the recording evolved from a general material categorisation, with the identification of types, such as slag, refractory material, geological material and metal, towards a more detailed description. This consisted of noting features such as shape, colour, inclusions, degree of magnetism and degree of fracture, for example. Variations in the morphological features identified were also recorded, as were toolmark impressions. This permitted the material to be grouped under shared morphological properties and to assess the assemblage by groupings which led to assigning types (Girbal 2011, 8). It is important to note here that there was a degree of overlap among these groups, for example between the finery and chafery hearth slag and between hearth slag and smithing slag. The validity of the observations made during this stage are investigated during the analytical work. The final aim of this exercise is the creation of a database, which can be easily accessed and interrogated, highlighting groupings, common and shared features or attributes, and outliers within the assemblage (Appendix A.3.1). This stage requires some basic statistical analysis of the data obtained.

All pieces were photographed alongside a photographic scale and a location label. Large and/or diagnostic samples were photographed individually. The top, bottom and side profiles were photographed when these were recognisable, as well as any important features observed. When the pieces did not show a clear orientation, they were photographed on two opposite sides. Small fragments of slag, stones and charcoal fragments were photographed together in groups of similar material (Appendix A.1.1).

In addition, after this stage, a more narrative approach was employed which allowed for a more in-depth description of the features observed and comparison of material coming from different trenches. This was done for all material types, in each trench and spit, and resulted in the creation of types and subtypes. The morphological features identified for each material type are presented in the next section (see also Appendix A.3).

4.3 PROTOCOL FOR MATRIX SAMPLES

The matrix samples were sorted and analysed with the aim to obtain information from the microscopic material as well as the large fraction. In particular, the investigation of the matrix samples addressed the smithing activities carried out at the site and the spatial organisation of the same. The physical evidence produced by smithing can assist in the interpretation of the entire slag assemblage and provide information on a series of activities that are not necessarily reflected at a macroscopic level.

In total twenty-nine bags of matrix samples collected during the first excavation season (1999) were analysed (Appendix A.3.3). Those of the second excavation season (2000) were not investigated, due to time constraints. Two different sieve sizes were employed on site for particle count characterisation; these are approximately 1 - 0.5cm and 0.5 - 0.25cm (Juleff 2000, 9).

The procedure adopted in this study is described below:

- 250g of material were weighed from matrix material sieved through <1.00cm >0.50cm
- 100g of material were weighed from matrix material sieved through <0.50cm >0.25cm. Floating for charcoal at this stage
- For both sizes: sorting of the material into groups: geological, slag, refractory material etc.
- Each group and each type of slag was then weighed
- Qualitative description/observations
- Photographic documentation of sorted groups – visual documentation of relative proportion of class of material

A dataset was created following a simple classification that included very small fragments of slag, flakes and spheroidal hammerscale, fragments of blast furnace slag, metal scrap, charcoal and geological material. The results obtained during this exercise were elaborated using the dataset alongside the photographic record.

In particular, the study of matrix samples targeted the presence (or absence) of hammerscale, which represent the most characteristic and identifiable products of the smithing process (McDonnell 1984, 1986). The investigation of these residues can reveal the nature of the process. Hammerscale can occur either as small magnetic globules or as magnetic flakes. These two types are produced as a result of, respectively, forge-welding (secondary smithing) and the striking of hot iron/bloom (primary smithing) (Dungworth and Wilkes 2009, Rondelez 2014). The presence of hammerscale is normally interpreted as indicative of smithing (in bloomery technology), but also other metalworking operations have generated morphologically similar material, including the finery process (McDonnell 1986, Historic England 2015).

Finally, anything that went into the furnace and that was discarded or cleaned from the furnace area at the end of the operation, can be identified from the analysis of the matrix. This can shed light on practical aspects of the metalworking activities and provide a more complete reconstruction of the site (Bayley *et al.* 2008).

The results obtained from the visual inspection of the matrix samples are described in section 4.4.7 and more data is presented in Appendix A.3.3.

4.4 MACRO-MORPHOLOGY AND TYPOLOGY

Five main types of slag have been identified, most of them including subtypes (figure 4.5 and table 4.1). These are:

- finery tap slag
- hearth slag
- smithing slag
- blast furnace slag
- iron-rich slag

Other classes of materials were iron scrap, refractory material in the form of small clay fragments, and small pebbles. In the following sections each type and subtype

are discussed and, where possible, the metallurgical activity from which they derive is suggested (table 4.1). Particular features are highlighted where necessary and all photographic documentation is presented in Appendix A.1.1.

As mentioned above, for the macro-morphological analysis the material contained in the bags was counted. The results are illustrated in figure 4.5. The chart represents the proportion of each material type by counts, including their relative subtypes, identified in all investigated trenches of both excavation seasons. The information summarised in the pie chart is qualitatively representative of the material observed and includes all counted pieces regardless of their size. Hearth slag and finery tap slag are the most abundant types, followed by stones and iron-rich slag. The next type for number of fragments is smithing slag and then non-diagnostic pieces, clay fragments, blast furnace slag and metal scraps. Thus, the assemblage is dominated by slag of different types, in accordance with the quantified data from the excavation.

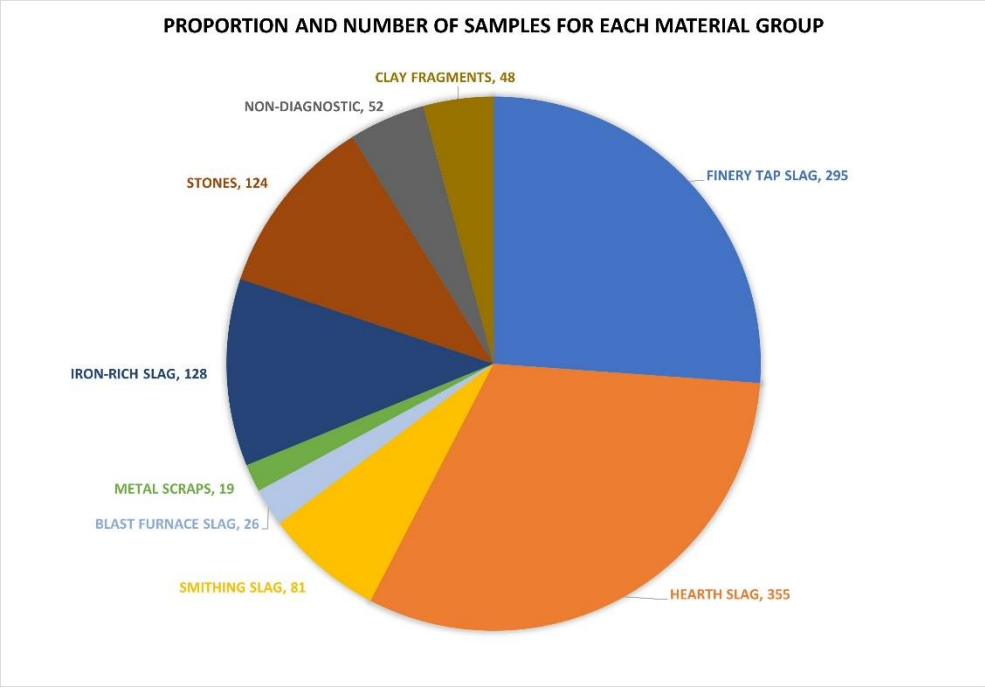

Figure 4.5. Pie chart illustrating the proportion and number of samples for each material group identified during the visual analysis.

Table 4.1. Material groups and relative subtypes identified during the macro-morphological analysis. For each group the possible origin is suggested.

TYPE	SUBTYPE	METALLURGICAL OPERATION
FINERY TAP SLAG	'Cakes'	Probably finery. Fining of cast iron to produce wrought iron produces fayalitic tap slag, very similar in appearance to bloomery tap slag.
	Flowed 'Cakes'	
	Plates	

	Tendrils	
	Non-diagnostic	
HEARTH SLAG	Hearth Slag	Finery/Chafery. Both hearth installations could produce this type of material.
	Conglomerates	
	Hearth 'Cakes'	Chafery. Finery?
	Slag Channels	Finery/Chafery
SMITHING SLAG	Smithing Hearth Bottom (SHB)	Iron working, fined iron bloom consolidation and forging of wrought iron bars
	Double SHB	
	Smithing Flats	
IRON-RICH SLAG and IRON SCRAP		Finery and iron working
BLAST FURNACE SLAG	Glassy	From blast furnace on the south of the site. Probably added to slag bath or attached to pig iron when transported to the finery?
	Vesicular	
Stones, clay fragments and other miscellaneous		Non-diagnostic includes burnt material. Stones and clay fragments also show either adhering slag or sign of burning – coming from hearth installation

4.4.1 Finery Tap Slag

This group comprises all the retrieved slag pieces associated with slag tapping, making this slag group the second most abundant material by total count in the entire assemblage (figure 4.5). All examples exhibit low viscosity and the majority, albeit fragmentary, have well-preserved top and bottom surfaces. Five subtypes have been identified: 'cakes', flowed 'cakes', plates, tendrils and non-diagnostic fragments; the percentages of the total counted samples for each subtype are shown in figure 4.6.

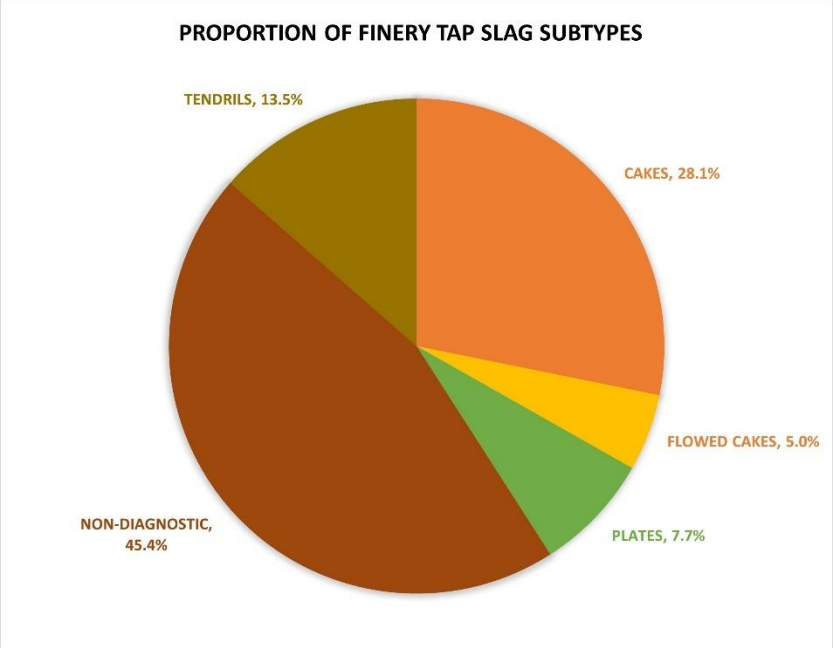

Figure 4.6. Pie chart illustrating the proportion of finery tap slag subtypes by count

'Cakes'

The term 'cake' indicates slag samples that preserve their upper surfaces and bases. This group contains large cakes with the typical flow pattern of tap slag on the top surfaces and undersides showing undulated to rough texture (figure 4.7).

Figure 4.7. Tap slag cakes (QN1 0-20) showing the typical flow pattern on top surfaces (left) and underside with ground debris impressions and rough textures (right). Note the plano-convex shape and rounded edges.

Their undersides are characterised by charcoal and gravel impressions, indicating that the slag ran over small stones, soil and ground debris (figure 4.8).

Incomplete pieces that share similar features with the largest and/or complete cakes are also included in this category. These features are in fact visible also in smaller, broken fragments whose top and bottom surfaces are preserved, enabling their identification (see examples in figure 4.8). All size categories are represented, with samples of small, medium and large size.

Figure 4.8. Left: detail of a fragment of tap slag cake, showing the underside with many charcoal (red arrows) and angular stones impressions. Right: Broken fragments of tap slag cakes, whose top and bottom surfaces are preserved. Note the orange clay adhering to the underside.

Of high density and characterised by low porosity, mostly in the shape of large elongated voids, the slag cakes have plano-convex shapes, sometimes plano-plano, and rounded edges, suggesting they solidified within a depression on the ground (figure 4.7 and figure 4.9). The largest and most complete piece weighing 25kg was encountered in trench ZS3, spit 40-60, and two other large pieces weighing 13.5kg and 7kg were retrieved from QN1 spit 0-20 (figure 4.9). ZS3 and QN1 display most of the large and medium size cakes recovered (Appendix A.3.2), many of which have features of interest that indicate how they formed.

Figure 4.9. Tap slag cake weighing 13.5kg from QN1. Note the plano-convex shape and rounded edges of the fragment to the left. On the right the other fragment displaying in profile multiple flows of slag. Also, note the sandy rough underside. Top and bottom images are shown in Appendix A.1.1.

Multiple flows of slag are visible in profile on some fragments, where the slag ran on top of previous flows (figure 4.9). The average thickness is between 5 and 7cm. Their surface texture is constituted of mostly smooth runs, well-rounded and often flowing in the same direction. Only a few examples exhibit very small ridges on the slag flows, suggesting rapid cooling.

They run horizontally, suggesting that the tapping hole was near ground level. Their width varies between 1 and 2.5cm. Thinner slag runs (0.5 - 1cm) are measured in a cake piece recovered in ZS3 (spit 20-40), indicating lower viscosity. Coming from the same trench and spit is also a piece of tap slag in the form of a plano-convex cake, which displays a flat and smooth profile parallel to the slag flow. The end of this flow is characterised by thin slag runnels flowing downwards (figure 4.10). Another example of slag cake, again found in ZS3, displays a flat side profile, which appear smooth (figure 4.11). This seems to suggest that this slag piece solidified against a wall/surface that was even and clean from soil debris.

Figure 4.10. Example of tap slag cake from ZS3 (20-40) which displays a flat side (left and centre) and slag flowing downwards following the profile of what were presumably the edges of the hearth installation (right). The picture in the centre shows the underside.

Figure 4.11. Example of tap slag cake from ZS3 (20-40) showing a flat smooth profile, which becomes thinner as the slag flow runs perpendicular to the side. Also note the purple patches of iron.

Of interest to understand the origin of these pieces is also a slag from QN1 (0-20), which again shows a flat profile and on top a rope-like texture with an almost globular protrusion of slag attached to one end (figure 4.12). This is characterised by an undulated texture and, as the flow seems to originate from here, could represent the remains of the flow of slag arriving into the slag pit.

Figure 4.12. Broken tap slag cake, with flat profile and globular protrusion on top. This suggests the slag was tapped from the top into a container that was lined with flat stones or iron plates.

Colour

The slags are mainly dark brown with orange and purple patches, present on both upper and lower surfaces. Frequent rusty reddish patches are observed, where the slag was in contact with the metal. Patches of purple colour are quite common in most pieces and in some instances appear as a purple red ‘coating’ with small droplets of ‘weeping’ iron, overlaying the slag flows. The presence of this type of corrosion - ‘brown beads of liquid’- appears influenced by the presence of chloride ions and indicates active corrosion (Selwyn *et al.* 1999, 221). This is probably a post-depositional feature caused by river flooding.

Porosity and Density

Porosity is overall low. Some of the top surfaces are broken, revealing hollow flows and very small (<10mm) spherical voids below the surface. Their profiles, visible on the broken edges, display big spherical/elongated voids, mostly concentrated close to the top surface; small (1 - 2mm) pores are clustered at the bottom. The slags are dense and heavy, some responding to the magnet and thus indicating the possible presence of metallic iron and/or that they are rich in magnetite.

Inclusions

Some pieces show orange clay attached to their surfaces, as well as small pebbles and sand. Areas of vitrified clay indicate it was in contact with hot and molten slag. This suggests that the hearth was lined with clay, or that clay and sand were used as additives during post-smelting operations (Dillmann and L'Héritier 2007, 1815).

Of interest are also examples from trench PN1 (0-20), which display small flakes of material similar to hammerscale attached to the bottom surfaces. Further, the very large cake recovered in QN1 (0-20) displays a metal droplet embedded in the slag (figure 4.13).

Figure 4.13. Details of tapped slag cakes, showing possible hammerscale attached to the bottom surface (left), a prill of metal in the centre of the cake (centre) and fragments with possible blast furnace slag inclusions (right).

Interestingly, no iron ore fragments were observed or retrieved from the bags containing the excavated material. Instead, small fragments of blast furnace slag (green and blue fragments) are found embedded in the slag pieces, as well as with the rest of the assemblage (figure 4.13; see blast furnace slag in section 4.4.5).

Toolmarks

Two fragments from PN1 and ZN1 display features of interest. The piece from trench

PN1, spit 0-20, is a medium-sized cake whose top surface is characterised by the presence of a small shallow depression, most likely produced by a blast of air. The underside also has interesting features in the form of three elongated and parallel shallow depressions, which could be toolmarks (figure 4.14).

Figure 4.14. Examples of tap slag cakes fragments. Top: note the shallow depression on the top surface (left) and linear depressions on the bottom (right). Bottom: fragments displaying clear tool marks on the bottom surfaces (right). Cakes could have been broken during the metal working operation.

Clearer tool marks are also observed on the bottom of a piece from ZN1 (0-20), possibly produced by poking the hearth for the removal and tapping of slag. Two more slag cakes *c.*6cm thick, found in QN1 (0-20), have clear toolmarks; one piece displaying a linear depression on the bottom surface (figure 4.14), the other fragment on one side where, possibly as a consequence of breaking the slag cake with a rod during the operation, flows of slag have run, first to the side and then down to the bottom surface (figure 4.14, bottom).

Surface features

Some differences in the upper surfaces of the slag ‘cakes’ were identified. These are not considered indicative of a different origin, but rather are interpreted as variation from common shapes and surfaces, as a consequence of certain actions performed during the process (for example, covering the slag with soil). Ten pieces display

upper surfaces characterised by the typical flow pattern of tap slag and by areas of rough and agitated textures, globular projections of slag and iron-rich material. Their undersides are similar to the undulated to rough textures described above (figure 4.15).

Figure 4.15. Examples of mixed rough/tap slag. Note the globular protrusions of rough slag on top of the smooth flowing slag. All pieces display iron-rich areas.

One slag piece (ZS3 20-40, figure 4.16) in the form of a small dense cake is an excellent example to illustrate these surface features. The top surface displays a lower portion of smooth flowing slag, the other half is raised of about 1.8cm from this surface and displays a straight smooth side surface, where multiple thin flows of slag are visible. The top surface of this portion has sharp charcoal and soil impressions, thus showing a similar texture to those observed for the undersides. This suggests that some slag was covered with soil and charcoal when still hot and molten. This seems confirmed by another piece from QN1 (0-20), again in the form of a rounded 'cake' of *c.*8cm of diameter. This displays on the upper surface, on top of smooth slag runs, a slag projection with rough texture and charcoal/soil impressions. The profile of this projection shows that it is constituted by multiple overlapping thin flow

of slags, whose smooth texture was probably altered when still hot, by covering it with charcoal and ground debris (figure 4.15, bottom left).

Figure 4.16. Rounded mixed rough/tap slag cake. Note the similarity between the rough texture on top (left) and that of the bottom surface.

Two elongated pieces are also of interest, as they show, on the same piece, surface textures varying from smooth flows of slag to rough and undulated (figure 4.15, top). These rough areas are characterised by the presence of purple patches of iron corrosion products that responded to the magnet. Sand and clay also adhere to these slags; they appear fused with the slag material, indicating they entered the process when the slag was hot and molten. Probably, these slags were channelled away from the hearth and solidified in proximity of a tapping hole.

Flowed 'Cakes'

The slag in this group appears characterised by some degree of fluidity, which suggests that they also relate to slag tapping. However, they display higher viscosity than that observed for the finery tap slag cakes. Although, they probably have a similar origin with the cakes of the previous group, this slag displays some features that deserve special mention and that offer important insights into the mechanisms of formation. Fifteen pieces have been included here, accounting for 5.0% of the total counted samples (figure 4.6).

Figure 4.17. Examples of circular (top) and half-elliptical flowed cakes (bottom). Note the larger slag flows and rough undersides with patches of orange clay.

They all preserve top and bottom surfaces. Their shapes range from circular to half-elliptical, some of the latter appear fractured along the small axis, but the majority are preserved almost intact and fall in the large and medium size category (figure 4.17). The longest diameter measures between 15 and 20cm and the shortest between 13 and 15cm. Their thickness ranges between 5 and 7cm. The top surfaces display both areas of flows of slag, of a rather large size resulting at times in globular slag projections, and areas with a rough texture. The undersides are of a rather coarse texture with charcoal and soil impressions and attached orange clay (figure 4.17, bottom right). No other inclusions are observed. Porosity is high for the slags in

Figure 4.18. Side profile of three examples of flowed cakes from trench ZS3. Larger spherical voids are concentrated on top surfaces, with smaller rounded porosity towards the upper layers. Example on the right is showing at the centre a rectangular cavity left by a slag channel.

this group, at times to the point of frothiness. Large spherical voids are visible on broken edges, making them less dense than finery tap slag and hearth slag (figure 4.18).

On at least four pieces slag channels are still attached, while on two other ‘cakes’ a rectangular cavity where the channel once was is still visible (figure 4.18 and 4.19). This feature suggests that the slag was channelled out from the hearth. The examples in figures 4.18 and 4.19 display cavities of a rectangular section; both are situated at the centre of the cakes, suggesting that the slag was channelled and as it flowed, formed inside a circular feature that contained them.

Admittedly though, it is not entirely clear if these pieces relate to slag tapping in the finery hearth or if the slag runners are connected to the mechanism of slag removal from the chafery hearth. Given that their surface texture recalls that of flowing slag, they were inserted in this category and tentatively interpreted as finery hearth slag. However, their degree of viscosity could situate them both at the end of slag tapping in the finery (higher viscosity than finery tap slag), and at the beginning of the slag produced in the chafery hearth (lower viscosity than hearth slag).

Figure 4.19. Slag cake found in ZS3 (0-20), showing features in between rough and tap slag (top). Note the molten slag on the underside (bottom left). Bottom right: side profile showing a rectangular section of a possible slag channel. Refer to the slag channels described in the text.

This subtype was identified only during the data analysis and after completion of the chemical analysis (chapter 5), so for now it is only possible to make a suggestion on their origins. However, it is very likely that they have a similar chemical and mineralogical composition to that observed for the finery tap slag of the previous group, as well as for bloomery tap slag, since both technologies produce fayalitic slag (Morton and Wingrove 1970, Pleiner 2000). A summary of the studies that attempted to chemically differentiate between finery and bloomery tap slag is given

in chapter 5 and some aspects of this discussion are elaborated in section 5.4 when discussing the results of the chemical analyses carried out for this study.

Slag Plates and Tendrils

The features for these two forms of slag are described together in this section. Slag plates and tendrils represent 7.7% and 13.5% respectively of the total counted slag for this group (figure 4.6). The slag plates display the same features described for the finery tap slag cakes, with flow pattern on top and undulated to rough undersides showing charcoal and ground debris impressions (figure 4.20). They differ in their thickness, which is between 1 and 2.5cm. Like the 'cakes' they are dense, with little porosity, characterised by few elongated voids near the surface.

Figure 4.20. Top: examples of slag plates displaying flow pattern on top and undulated undersides. Bottom: slag tendrils, also including possible slag prills. Their undersides show ground debris impressions (bottom right).

Colour and inclusions are also the same, suggesting both types derive from the same operation and result when molten slag is run out of the furnace. A few fragments display rough and rusty surfaces on both sides, with no clear orientation, but still showing some flowing pattern.

Tendrils of slag (also described as slag prills by some authors: Tylecote 1986, Crew 2000, Girbal 2010) probably represent loose flows that separated from the rest of the slag cakes. Constituted by single or sometimes overlapping ripples of slag, they

have a smooth surface texture and small pebbles impressions on the bottom sides. They all have clear fractures which suggests that they may have been part of bigger pieces.

Non-diagnostic fragments

The non-diagnostic samples included here are highly fragmented pieces with no clear orientation or shape; consequently, they cannot be assigned to a specific step in the process. However, since they display flows of slag and low viscosity it was possible to assign them to this group; they probably represent broken fragments from bigger pieces or drips of slag that did not consolidate into large slag cakes (figure 4.21).

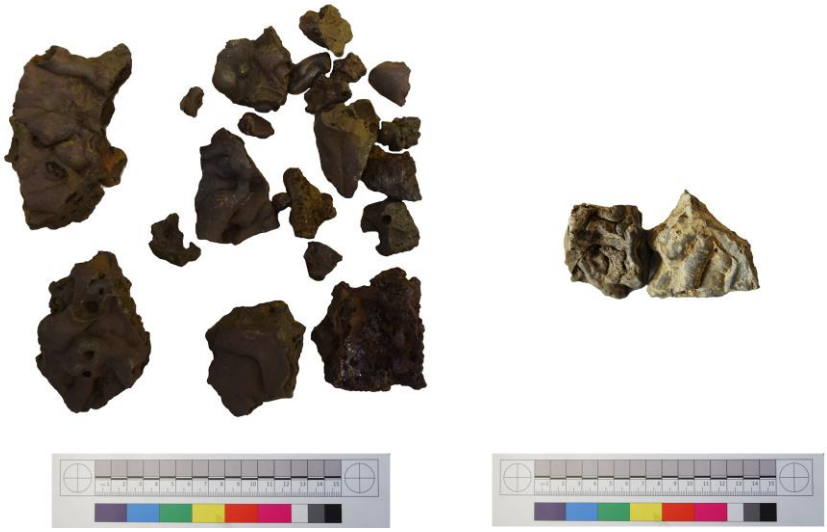

Figure 4.21. Fragments of non-diagnostic finery tap slag. The two fragments on the right, display a different colour from all other fragments, which could indicate that they contain less iron. The clayey concretion is probably post-depositional.

Fragments range in width from 2 to 5cm; thus, they all fall within the small size category. Colour is dark brown, except for two small fragments retrieved from PN1/QN1 that display a light grey colour and are covered by a compacted pale-yellow clay/sand (figure 4.21, right); all samples from the same excavation context show this same crust of material, which is probably post-depositional.

4.4.2 Hearth Slag

The slag pieces in this group are interpreted as material that derives from metallurgical operations performed within or around the hearth installations. Three

hundred and fifty-five pieces were counted, making this the most abundant material in the assemblage (figure 4.6). This group contains a wide variety of shapes and surface features and is the most difficult to interpret. Together with a large number of pieces characterised by a mixture of materials (conglomerates, see below), three types are identified: hearth slag (lumps of 'within-hearth' slag), hearth 'cakes' (a dense type of slag, in the literature normally associated with the chafery hearth) and slag channels (rod and cylindrical slag). Their relative proportions are illustrated in figure 4.22. A common feature is the high viscosity and dense nature of the pieces.

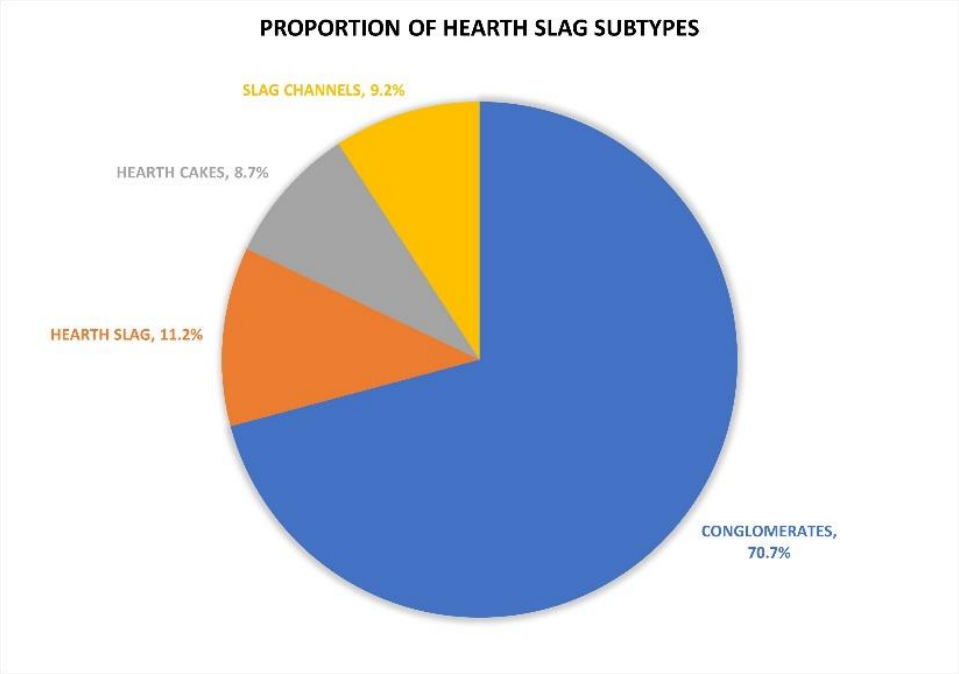

Figure 4.22. Pie chart showing the proportion of hearth slag subtypes by count

Hearth Slag Lumps

The pieces in this group have rough to very rough textures. They are dark brown in colour, with orange vitrified clay adhering to most surfaces and purple patches of iron oxides. The surfaces are characterised by many charcoal voids and impressions. This suggests that these pieces represent conglomeration of molten slag that solidified around the charcoal charge. Dense and characterised by low porosity, their shapes vary from elongated lumps (between 10 and 18cm long) to some fan-shaped pieces and amorphous fragments (figure 4.23).

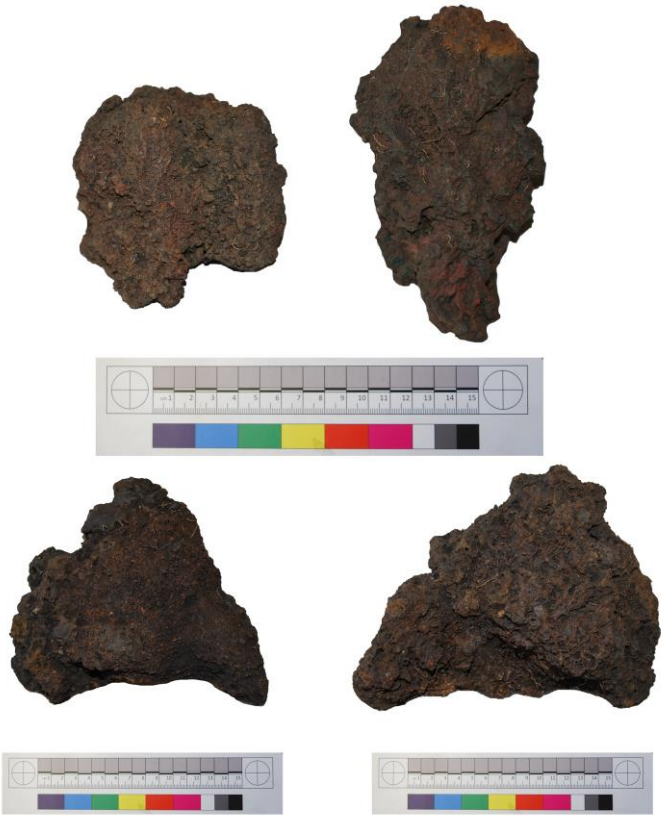

Figure 4.23. Top: lumps of rough slag, showing toolmarks (left) and adhering orange vitrified clay (right). Bottom: examples of fan-shaped slag, note the rough texture and molten slag ends.

Most of the pieces display toolmarks; a variety in the type of impressions observed suggests that more than one type of tool was employed during the metalworking operations. Of interest is a piece recovered in PN1 (0-20; figure 4.24, left). An elongated lump displays adhering orange clay on one end and on the opposite end, a toolmark with two cavities that could indicate the use of tongs and similar tools, while the slag was still hot and molten. Another example from PN1 (0-20) in the form of a rounded lump shows a linear depression possibly created by an iron rod, as well as a series of small linear impressions (figure 4.24, right). Broken edges reveal a solid texture, with few small spherical voids. The fan-shaped pieces and elongated lumps displaying tapering ends suggest these slags are likely to relate to slag tapping; these fragments being part of the slag that remained inside the hearth.

Figure 4.24. Details of toolmarks impressions on two lumps of slag. Left: detail of lump with orange clay attached from PN1 (0-20). Right: sub-rounded lump from same trench and spit, showing linear impressions on the top.

This would seem to find confirmation in the presence of molten slag adhering to the surfaces of the same pieces.

One third of the samples are rich in iron and highly magnetic. Among these, one piece is in the form of a flat plate with some flowing and flat ripples on the top and rough underside with a purple ‘crust’ of iron oxide (figure 4.25). Of interest are also some cone-shaped pieces. Their shape suggests they might have solidified within a conical tap hole. Similar slag pieces were recovered from Stony Hazel, in Cumbria. The excavator suggested the site was a finery forge, while a water-powered bloomery was suggested by other authors (Davies-Shiel 1970, Bowden 2000).

Figure 4.25. Example of iron-rich slag, showing rough purple surfaces. Note the plate and cone-shaped pieces, as well as the presence of adhering orange clay.

Three pieces are of particular interest (figure 4.26). The bigger fragment is a cone shape piece with orange concretion of clay attached to the tip with a small hole. This runs through the body of the slag (figure 4.26, centre), which is rich in iron, charcoal inclusions and of a rather coarse nature. Possibly in association with this slag are two pieces in the form of rings, one of which has broken (figure 4.26, right). They could be pieces of slag that formed around tapping holes. The majority of the slag in this group are of medium size, were selected as diagnostic samples during excavation and probably represent complete pieces.

Figure 4.26. Left: slag with clay attached to one end and hole running through the body of the piece. Centre: detail of the back of the slag showing the length of the cavity. Right: ring of slag, the piece is characterised by a rough texture and feels sandy to the touch.

Conglomerates

A significant proportion of hearth slag (70.7% of the total counted samples) comprises slaggy conglomerations, a mixture of slag, charcoal, clay, sand and small stones (figure 4.27).

Figure 4.27. Slaggy conglomeration of material, showing mostly rounded to sub-rounded pieces.

They are small lumps sub-rounded to rounded in shape and dark brown in colour, with orange patches. Some pieces appear richer in clay, displaying a brighter orange colour and thicker concretions of adhering clay. They are slightly brittle and have a rough texture. Many charcoal and stones inclusions are noticeable, including small pebbles, quartz-rich stones and local schists. Of interest are also fragments of fayalitic slag and of blue and dark grey blast furnace slags found embedded in the mixture (figure 4.28). The material appears fused together and some areas are vitrified, indicating they were subjected to high temperatures.

Figure 4.28. Details of slaggy conglomeration pieces, showing blue and black blast furnace inclusions. Also note the white stone inclusion, the small pebbles and sand particles. All pieces show some degree of vitrification.

The shape, type of inclusions and general appearance suggests that these are ironworking residues related to post-smelting activities and result from operations carried out within the hearth. In particular, the shape could derive from stirring the slag bath during fining to promote oxidation. As such, they also are possibly 'complete' pieces, although some may be fragments of bigger lumps of hearth slag. Admittedly, some fragments could also be smithing waste. Furthermore, the inclusions are consistent with what is reported in the literature as material used to create (and added to) the slag bath (chapter 2, section 2.5). Thus, the slag in this group when considered in relation to the rest of the material, is of significant value to understand the assemblage and offers interesting insights into the process.

Hearth 'Cakes'

This group consists of large, dense cakes and blocks of slag. The majority of them seem to survive complete, allowing some observations on the metalworking structure that contained them.

Shape and Measurement

The shape of the slags in this group is one of the most interesting features. Generally, they are all in the form of ‘cakes’ or blocks, displaying upper and underside surfaces. The principal axis of the complete pieces measure between 15 and 20cm. Some differences in shape were observed that deserve special mention. One piece from SS1 is almost circular in plan; one edge is broken but it is possible to suggest a dish shape (figure 4.29).

It has a flat top surface displaying adhering molten slag, which makes it almost smooth in texture, although underneath this a rough texture is visible. The underside is more disturbed with soil and charcoal impressions. On one side a globular protrusion of slag seems to suggest the presence of a slag channel, now occluded. This same feature is observed on at least six other pieces, of which three have an oval/elliptical shape (Appendix A.1). Another is again dish shaped, with a flat underside and convex top surface; numerous charcoal voids and impressions characterise this piece, which occurs together with two other similar examples in trench ZN1 (figure 4.30, top).

Figure 4.29. Dish-shaped hearth cake, displaying molten slag covering a rough top surface (left) and coarse underside showing debris impression (right). Note the rounded edges and a lateral protrusion, which could be an occluded slag channel.

Of a similar texture, but richer in iron is a piece from JN9 (figure 4.30, bottom left), which also displays a small lateral slag protrusion. Finally, a piece from the same trench with a molten texture has a shape that resembles that of a sheep skull and occurred together with a dense slag block with large charcoal inclusions (figure 4.30, bottom right).

Figure 4.30. Examples of hearth slag cakes and blocks. Numerous charcoal inclusions and impression characterise their surfaces. Note the slag channel visible on the centre of the piece on the top right. Examples that derive from JN9 display some different features. The piece on the bottom left, while of a similar texture, is rich in iron; also note the small slag protrusion on the top left. To the bottom left, two blocks of a smoother texture, with molten slag and charcoal inclusions.

The thicker blocks are between 7 and 10cm deep and have concave and/or convex upper surfaces and flat undersides. Of particular interest are also three blocks that on profile show denser lower parts, with progressively larger voids towards the upper parts (figure 4.31). The top surfaces are characterised by a frothy accumulation of slag, which results in compacted protrusion of slag mixed with small charcoal and clay.

Figure 4.31. Examples of hearth slag cakes on profile. Porosity becomes progressively larger towards the upper layers. Note the bowl shape of the piece in the middle, with an extended rim and slag accumulation on top.

Finally, four pieces display a flat top surface with adhering orange clay, iron-rich areas and a pointy end, giving the pieces a conical shape (figure 4.32 and Appendix A.1). Interestingly, Fell wrote that the chafery hearths were ‘in the shape of a beehive and stood on a hearth with a hollow or saucer-shaped cavity in the centre’, from which the slag flowed out (1908, 251). A similar arrangement may explain the shape and pointy protrusion observed on some of the pieces described here. An example of what appears to be a typical ‘hambone’ (chafery hearth slag), with a slag runner still attached, was recovered in trench ZS3 (figure 4.32).

Figure 4.32. Saucer-shaped example of hearth slag, displaying a pointy slag protrusion on the underside (top). A possible typical example of ‘hambone’ is shown on the bottom. Note the orange clay and iron-rich areas visible on both pieces.

Surface texture and inclusions

Some differences in texture are also observed. Most of them are of a rather coarse nature with large charcoal inclusions and impressions, iron-rich areas and patches of orange clay; while some pieces still display rough surfaces, and do not have inclusions or large impressions. They all have a sandy texture, which appears connected to the orange patches/layer of clay fused to the surfaces. Molten slag adheres to upper and bottom surfaces of some pieces, while others show some vitrification. In one large slag retrieved from ZS3 a small piece of bottle-green blast furnace slag is found embedded in the upper surface. Another block (from RS1)

contains stones, also fused to the surface and covered in slag (Appendix A.1.1). Finally, one piece whose top surface is characterised by a crust of slag, iron oxide and sandy material, displays on the underside a thick layer of pale-yellow clay, with signs of burning and orange colour pointing to an oxidising atmosphere. The slag crust displays the same features of the samples in this group. This appears to be a piece of hearth bottom with adhering slag and iron oxides; it is the biggest (and one of the very few) examples of refractory material encountered, the others being very small fragments of clay (section 4.4.6 and figure 4.48).

Colour

The hearth cakes are all dark brown, with areas of orange and purple coloration. These are observed on both upper and lower surfaces of the pieces, as well as on side profiles. One piece displays a bright red colouration that appears to be more than superficially attached (figure 4.33). A similar piece was also recovered from Cunsey Bloom Forge (Schofield and Miller 2017).

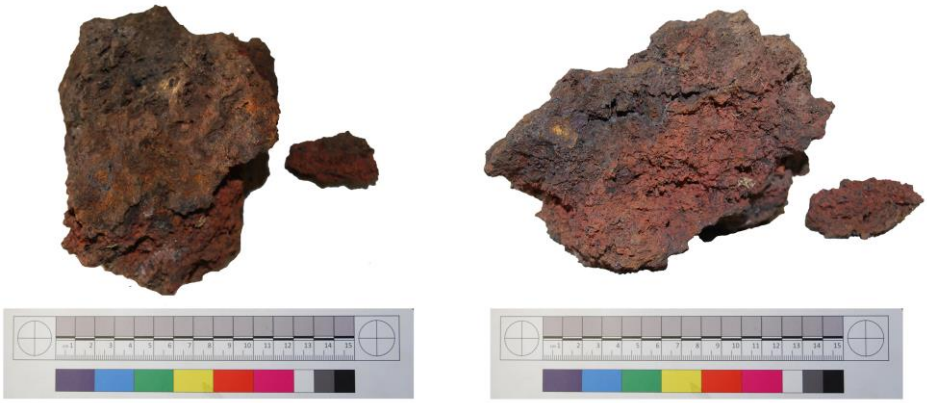

Figure 4.33. Red-coloured piece retrieved from trench RS1. The label 'furnace bottom' refers to the original classification. The piece was noted during the first stages of the visual analysis because of the intense red colouration - no other examples were present in the investigated assemblage - and was sampled for chemical analysis (chapter 5).

Porosity

Porosity is very low, with no visible voids in the pieces with many charcoal impressions. The side profiles of at least four large blocks display a dense mass with few voids towards the bottom and vesicular top layer with larger voids. Morton and Wingrove (1970) describe this same feature for chafery slag, affirming that this "two-layered structure" permitted their identification.

Although, it is not possible to exclude the presence of some large smithing hearth or dense cakes of slag created in the finery hearth, many of the features observed for most of the slag cakes in this group, when compared to the sparse descriptions found in the literature, suggest that these could be slag that formed in the chafery hearth.

Slag Channels

Numerous rod and cylindrical fragments of slag channels have been identified. They constitute the 9.2% of the total counted samples. The majority of this rod-shape slag were found during the second season of excavations, in SS1 and RS1 (figure 4.34). Of the first season trenches only JN9 held this type of slag, around 10 fragments have been identified. This is slag that solidified and 'froze' within a tap hole or channel, taking its shape.

Figure 4.34. Examples of cylindrical rod of slag. Note the hollow cross-section and shape (top). Bottom: example of rod with flat top. Note the rough texture.

They vary from rod shapes of circular or sub-rectangular cross section, whose broken edges reveals a hollow or solid rod, to flat tops, where sometimes material has accumulated. This suggests the flow channels were not filled. Some of them display a fan-shaped or tapering end with small fingers of flowing slag. Dark brown in colour with orange patches, they have rough texture and feel sandy to the touch. Numerous charcoal and stones impressions show the slag run over ground debris.

4.4.3 Smithing Slag

Eighty-one smithing slag pieces have been identified, accounting for approximately 7% of the total counted samples. Three subtypes are identified: smithing hearth bottom, which also includes fragments with features diagnostic of this class of material, 'double' smithing hearth bottom and smithing flats. Their relative proportions are illustrated in figure 4.35.

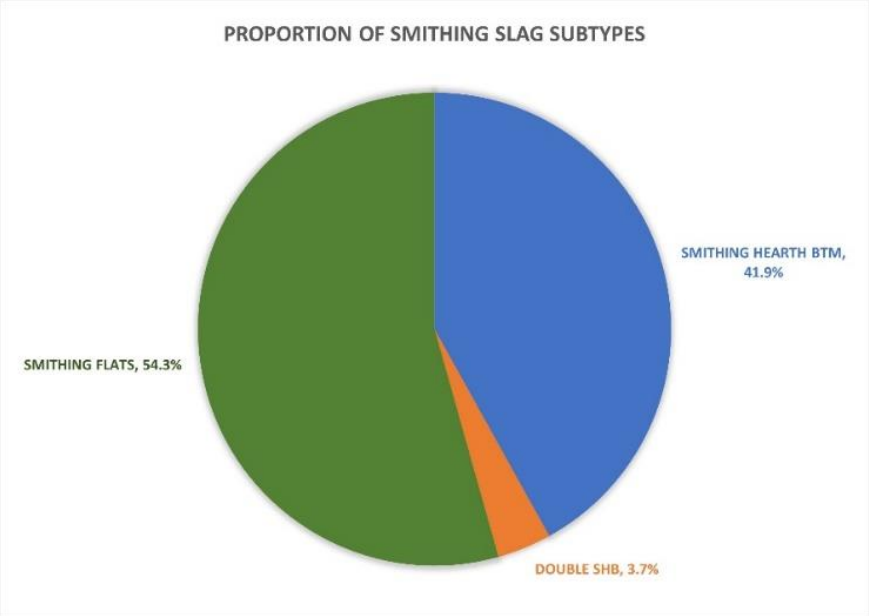

Figure 4.35. Pie chart showing the proportion of smithing slag subtype by count

Smithing Hearth Bottoms

The smithing hearth bottoms consist of both plano-convex and concave-convex pieces (figure 4.36); the majority survives almost complete, falling in the medium size category. One large example was retrieved from RS1, and a few fragmented pieces occurred together with diagnostic samples. The main axis of the largest and most complete example measures approximately 17cm and is 6cm thick.

Another almost complete piece displaying a concave-convex shape measures approximately 13cm; its thickness goes from around 7cm to 2cm as it flattens towards the end (figure 4.36, bottom). They are dark brown to brown in colour, with yellow-orange patches. They are partially magnetic.

Figure 4.36. Examples of smithing hearth bottom retrieved from RS1, showing top surface (left), underside (middle) and profile (right). Note the rounded edges and small depression on the top. Clay and small charcoal inclusions are also noticeable, as well as very low porosity visible on profile.

Broken edges reveal a porosity characterized by small globular voids, sometimes creating a network of bigger dimensions; overall porosity is low contributing to well-compacted dense slags. Rough surfaces and charcoal inclusions are noticeable, as well as sand and quartz-rich stones. Pieces with a flat top display a shallow depression in the centre and more completed examples from RS1, well-defined edges suggesting they solidified within a contained environment, such as the bases of smithing hearths. The shallow depressions are a typical feature of this type of slag, whose top surfaces were subjected to the hot blast from the air inlet (Serneels and Perret 2003).

One example with a less distinctive shape was also inserted in this slag group. It is an elliptical lump of slag, rich in clay that gives it an orange colouration and sandy feel (figure 4.37). Smithing slags without diagnostic shapes are called smithing slag lumps (McDonnell 1989); given that it was only one sample and likely to have a similar origin it was included in this slag group without further distinction. The lump has low density, it is well-compacted and with no visible porosity. Small charcoal inclusions and impressions are visible on all surfaces. This piece possibly represents an example of sandy-clayey slag as described and classified by Serneels and Perret (2003, 475).

Figure 4.37. Possible smithing slag lump: top (left), bottom (middle) and profile (right) surfaces display adhering orange clay and small charcoal impressions. The piece is well-compacted, with no visible porosity.

'Double' smithing hearth bottoms

'Double' smithing hearth bottoms are slag that display a protrusion of slag on the top surface. Three examples were recovered from PN1/QN1, ZN1 and SS1 (figure 4.38). The nature of these protrusions varies from an almost brittle clay and iron-rich (PN1/QN1 and SS1) slag to a denser slaggy material (ZN1). These types of slag would have formed in between smithing episodes, either indicating that the hearth was not cleaned before more smithing was carried out or, in the case of the clay-rich slag protrusions, indicating the use of sand and clay to protect the metal after hot forging (Crew and Rehren 2001, Serneels and Perret 2003). The density varies, with the iron-rich example having higher density. Porosity is low for all three examples.

Figure 4.38. Three examples of 'double' smithing hearth slag, showing a lumpy protrusion of slag of different nature on the top surfaces. Picture on the left is showing the examples from PN1/QN1; the piece occurred together with iron-rich material and another possible small fragment in the form of a small cake, indicated by the arrow.

Although displaying the same shape, their surface textures and features are all different from one another, perhaps indicating different stages in the smithing process. The piece from PN1/QN1, like all samples from this context, is covered by a pale-yellow crust, which covers most of its surface features (figure 4.38, left). It is possible, however, to distinguish some charcoal inclusions and impressions on the underside. This slag is also characterised by areas of brown and purple surface rust, which are flaky and friable, and is highly magnetic. The example from SS1 displays a rough, at times brittle, surface characterised by the presence of orange clay, some purple patches of iron corrosion and small charcoal fragments (figure 4.38, middle). The sample from ZN1 instead has the solid rough texture typical of slag that has formed at the bottom of the hearth, picking up debris such as small stones and charcoal (figure 4.38, right). It occurred together with two non-diagnostic amorphous fragments, which display similar surfaces and colours.

Smithing Flats

Along with the more typical hammerscale flakes and spheroidal hammerscale recovered from the analysis of the matrix material (section 4.4.7), larger flat pieces of material were encountered in the assemblage (figure 4.39). These are interpreted as smithing flats, a type of slag that forms during the first stage of smithing, when the bloom is cleaned from the slag and consolidated by hammering. The resulting slag is flattened on one side, the one that is in contact with the surface on top of which the bloom is hammered (i.e. anvil) and irregular on the side in contact with the bloom (Crew 1996).

Figure 4.39. Smithing flats from trench JN9, which contained the majority of the identified pieces. Note the smooth and rough surfaces and small rusty areas.

All examples fall within the small size category. The majority of the pieces measure between 2 and 5cm and are around 5mm thick. They are slightly curved, displaying one smooth surface and a rough vesicular one. Their colour is dark grey with small patches of reddish iron corrosion products. They are highly magnetic.

Two possible larger smithing flats were recovered from JN9, the trench that yield most of this type of slag (figure 4.40). They have a sort of triangular shape, but are likely broken, and measure between 4 and 6cm across; their thickness is less than 1cm. One surface displays some flowing slag together with areas of rough texture and red purple patches that respond to the magnet. The other side is rough and feels sandy to the touch. On both surfaces small fragments of charcoal are visible as well as some adhering clay.

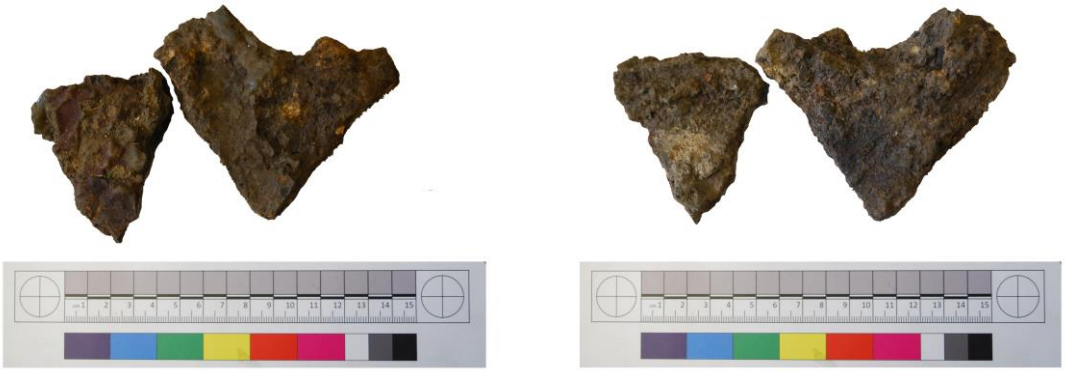

Figure 4.40. Two triangular possible smithing flats were also recovered from trench JN9. Picture on the left is showing molten slag and red patches rich in iron. The other surface instead is rough and displays small charcoal inclusions and adhering clay. Given their size, they are only tentatively inserted in this category; however, is likely that they relate to smithing operations.

4.4.4 Iron-rich Slag and Iron Scrap

A large number of iron-rich slag and metal pieces was identified during the visual analysis and are of great interest for understanding the metal working process. In the process of fining cast iron in the forge a high quantity of iron is lost, resulting in the formation of iron-rich slags (Morton and Wingrove 1969, 55). There is considerable overlap between these two groups, as many of the slag pieces appear to be a mixture of slag, charcoal, ground material and iron (figure 4.41). They are strongly magnetic and rather dense, with no visible porosity.

Most pieces are undiagnostic, with no clear orientation and sub-rounded shapes. A few medium size examples are observed, but the majority are small pieces whose measures range from 10cm to 1cm. Characterised by a dark purple colour, they

have rough and rusty surfaces displaying many inclusions of clay, small stones/sand and charcoal. One piece has a fragment of smooth (tap) slag attached to it (figure 4.41, left) and all pieces have adhering vitrified orange clay. Of interest is also a fragment found in SS1 (spit 20-40). The piece does not have a diagnostic shape, but it displays a clear toolmark on the top characterised by a shallow linear depression (figure 4.41, right). This suggests the use of tools when the slag was still viscous.

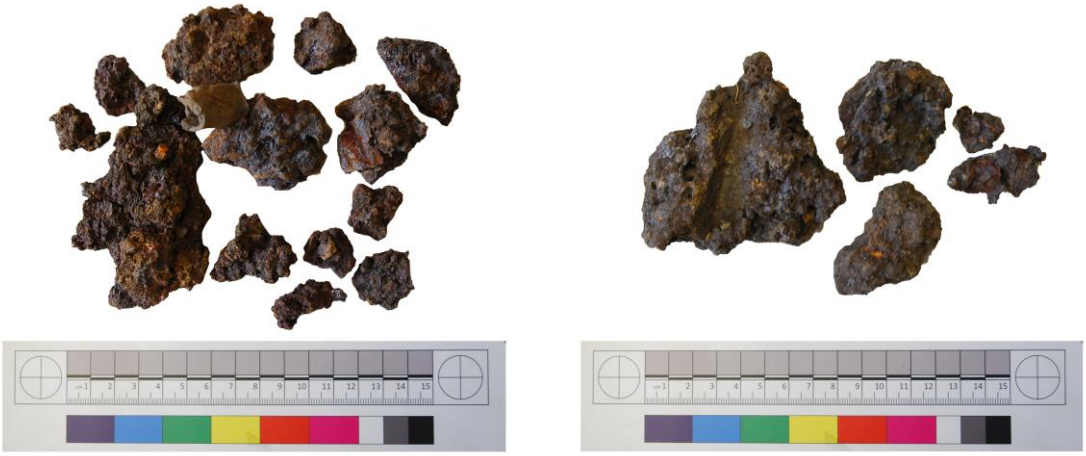

Figure 4.41. Left: Rounded and angular iron-rich slags. Note the fragment of smooth tap slag attached to one of the fragments. Right: Larger pieces of iron-rich slag from trench SS1. Note the elongated shallow depression on the bigger piece. All fragments are strongly magnetic and dense.

Often the iron-rich slags are found together with fragments of metallic iron. These are rounded to sub-rounded, with some pieces displaying a pine-shape (figure 4.42, left; see Eliyahu-Behar *et al.* 2013, 4324). They also show small inclusions of charcoal, small stones, sand and clay. Two small prills (5 - 6mm) have a light green fragment of blast furnace slag partially fused to their surfaces. All pieces are strongly magnetic; many displays surface rusting and corrosion.

Figure 4.42.Top left: pine-shaped iron scrap. Top right: a possible iron artefact with rusty concretion. Bottom: possible fined iron bar from trench RS1.The bar has a metallic core and a layered structure.

A few pieces could be artefacts that were never forged or shaped into objects (figure 4.42, top right). A possible nail was found in PN1 (20-40) and a possible iron bar in RS1 (figure 4.42 bottom); this is of great interest and was selected for chemical analysis. The scientific investigation of the iron scrap and metal artefacts is presented in chapter 5.

4.4.5 Blast Furnace Slag

This class of slag contains two subtypes, totalling to around 30 pieces (Appendix A.3.2). They are all characterized by their vitreous and vesicular texture and low density, due to the low iron content typical of blast furnace slag.

The first subtype is represented by small glassy fragments of various colours, ranging from bright and pale blue, to bottle green and black (figure 4.43). Patches of brown colour are visible on some of them, and a pale blue fragment from QN1 (20-40) has a concretion of material attached to it (figure 4.43, bottom right). Some fragments show possible signs of burning. Although light in weight, they are solid and their porosity is very low (<20%), characterised by few sparse spherical voids.

The majority of the fragments are small (between 1 and 3cm), with few bigger examples of *c.*7cm. The bigger fragments were recovered from PN1/QN1, and again are covered by a yellowish crust of material. The green and black colours of the fragments are still visible underneath this concretion.

One of the black pieces is in the form of a small concave-convex cake and displays multiple flows of slag overlapping each other on the broken edges. The top has a small depression (figure 4.43, top right). This suggests that the slag was very fluid and was tapped outside of the furnace. The green pieces are in the form of fractured blocks and do not show any flowing texture. They also seem characterised by voids and in general appear to be of a more vesicular nature (figure 4.43, top left), though still displaying a solid vitreous texture.

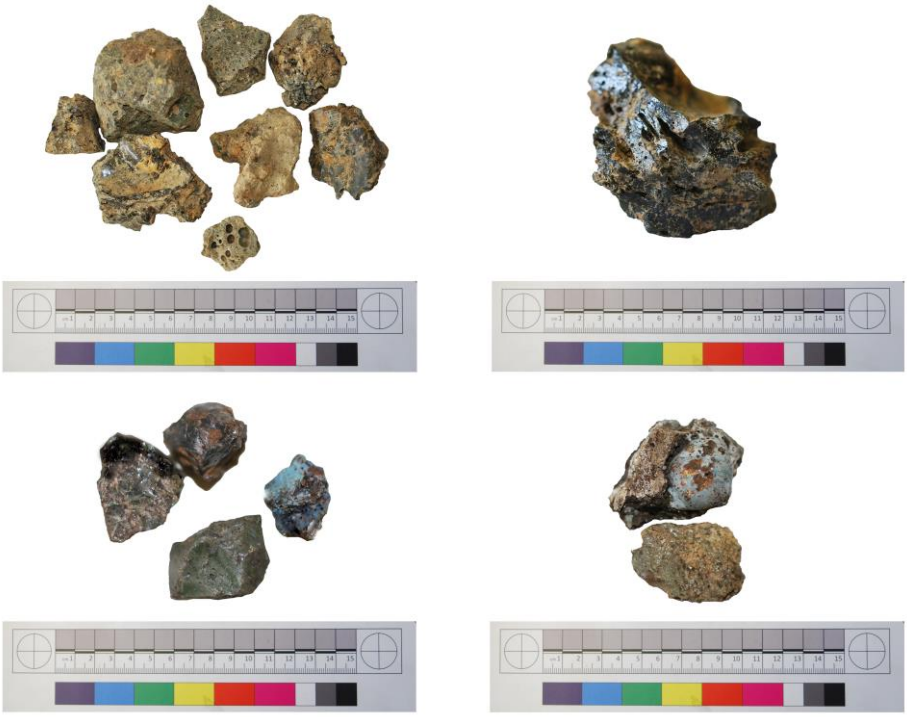

Figure 4.43. Top: glassy blast furnace slag, green vesicular types with yellow material attached (left) and shiny black example (right). Note the multiple flows of slag in cross-section. Bottom: small coloured fragments of glassy blast furnace slag. On the right a pale blue example with white and brownish concretion.

The second subtype is a silica-rich slag, with rough surfaces and vesicular nature (figure 4.44). Only four fragments of this type of slag were recovered. They are in the form of small 'blocks' (*c.*10cm) and their outer surfaces are characterised by a white concretion, which appears to be clay and feels a bit sandy to the touch. Some areas look vitrified, with no clear distinction between the slag and the external white material. It is not entirely clear if this is a superficial concretion of post-depositional

origins. Broken edges reveal a highly vesicular and sand-paper rough texture. Brown-yellow patches and concretions of iron are visible on all four pieces.

Figure 4.44. Examples of subtype II, showing a concrete-like appearance and vesicular interior. Note the brown and orange patches of iron.

Charcoal impressions and small fragments are noticeable on the outer surface but are not present within the slag themselves. These four fragments were noticed and selected during excavation. In the preliminary report they are termed ‘intermediate’ as they are clearly silica-rich material, and thus possibly come from the blast furnace, but do not display the glassy appearance typical of blast furnace slag. They were also analysed during the analytical work conducted for this study. The results are presented in chapter 5.

4.4.6 Stones, clay fragments and other miscellaneous

The other identified material classes included stones, clay fragments and non-diagnostic material. Their proportion as a percentage of the total counted material are illustrated in figure 4.45.

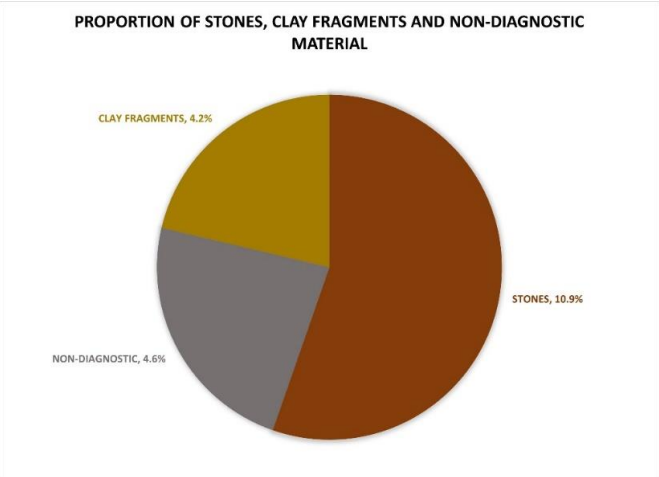

Figure 4.45. Pie chart illustrating the proportion of stones, clay fragments and vitrified non-diagnostic material by count.

Stones

Numerous stones and small river pebbles were retrieved during the excavation seasons (figure 4.46). Fragments of slate, hard angular stones and soft stones (probably sandstone, limestone) are identified. They often display adhering slags and attached vitrified clay. In four examples, large concretions of slaggy material occur together with signs of burning, which is also observed in smaller stones. This suggests they also might have been employed in the metalworking operations.

Figure 4.46. Examples of angular hard stones (top left) and charcoal fragments. Top right: soft-stones and a slate fragment. Bottom pictures display stones with adhering slag, iron-rich concretions and signs of burning.

Also, included here but not in the counted samples, are two possible iron ore samples that were recovered south of the blast furnace installation (figure 4.47). They are surface finds collected during survey prior to the 1999 excavation season. They were analysed to find some possible connection with the iron smelted on site in the blast furnace (chapter 5 and Appendix B.2).

Figure 4.47. Fragments of possible iron ore recovered from south of the blast furnace

Clay Fragments

As previously mentioned, the only refractory material recovered is in the form of small friable clay fragments (figure 4.48, top). The small lumps are sub-rounded in shape and retain no diagnostic forms. The largest piece found in association with the hearth slag cakes displays similar clay (figure 4.48, bottom). Many display signs of burning, with some vitrified areas. The colour varies from some darker orange pieces to pink and yellow examples. Three small light grey fragments are also found in QN1 and ZN1. The same colours are observed in the clay found attached to slag pieces and stones in the rest of the assemblage.

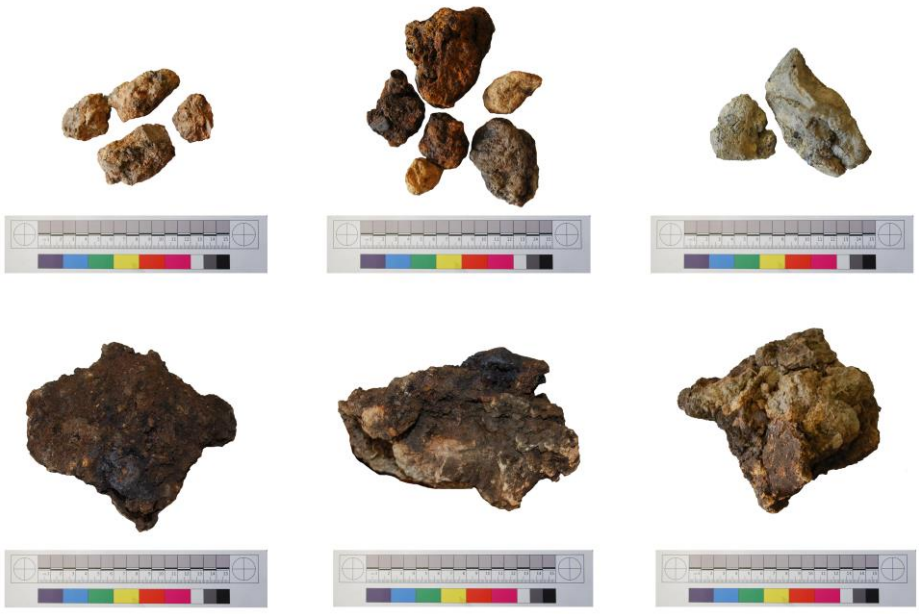

Figure 4.48. Top: small clay fragments showing signs of burning. Colours vary from pink (left) to yellow and dark orange (right) and light grey (left). Bottom: largest piece of hearth bottom displaying a thick layer of slag and iron on the top surface (left), in profile (middle) and on the underside (right) shows the same clay colours observed in the small fragments, some of which may derive from larger hearth lining pieces.

Examples of vitrified refractory material were encountered so infrequently during excavation, that those recovered, even if very small, were recorded and collected as special finds (Juleff 2000, 11). Probably some examples belong to larger hearth lining pieces; however, it also appears likely that the small fragments of clay were added to the slag bath created in the finery hearth during fining (Morton and Wingrove 1970, 27; Schubert 1957, Phelps *et al.* 2011).

Non-diagnostic material

Around 5% of the material observed presents non-diagnostic features. The fragments are all amorphous in shape and quite small (1 to 5cm). Characterised by low-density, they are highly vesicular and with evident signs of burning and vitrification (figure 4.49).

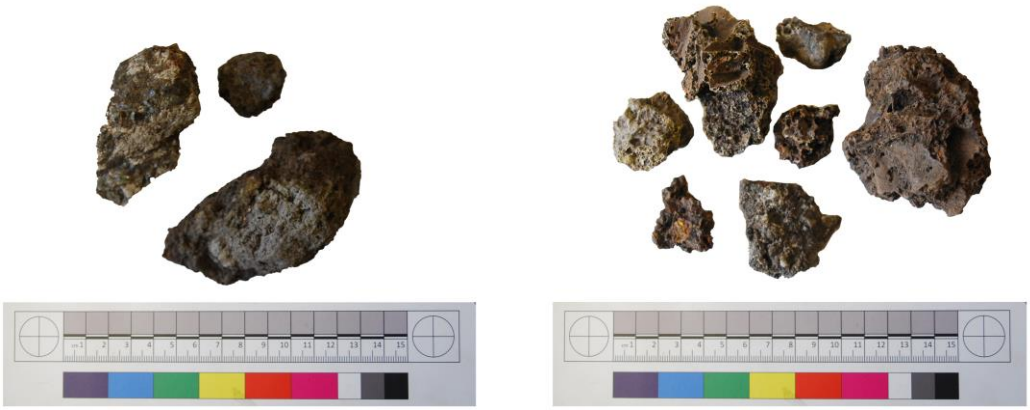

Figure 4.49. Examples of non-diagnostic material, note the vitrification and highly vesicular nature. Some fragments could be fuel ash slag.

On some fragments it is possible to notice some areas of a glassy shiny texture, with black and green hues, typical of blast furnace slags. Some fragments appear to be a mixture of material, with some slag inclusions and/or slaggy concretions and small patches of adhering orange and yellow clay. Some pieces could be fuel ash slag, a material that results from any high temperature activity by the reaction between fuel ash and siliceous material such as clay lining (Crew 1995). The material in this group probably includes broken fragments from bigger pieces as well as burnt material from inside the hearth installations.

4.4.7 Matrix Samples

All matrix bags from the first excavation season were visually analysed following the methodology described above (section 4.3). Eight classes of material were identified. All fragments are between 1 and 0.25cm in size. These are: smooth tap slag, rough iron-rich slag, blast furnace slag, flakes and spheroidal hammerscale, clay pellets, charcoal and stones (figure 4.50 and Appendix A.3.3). A summary of the observations is presented in table 4.2.

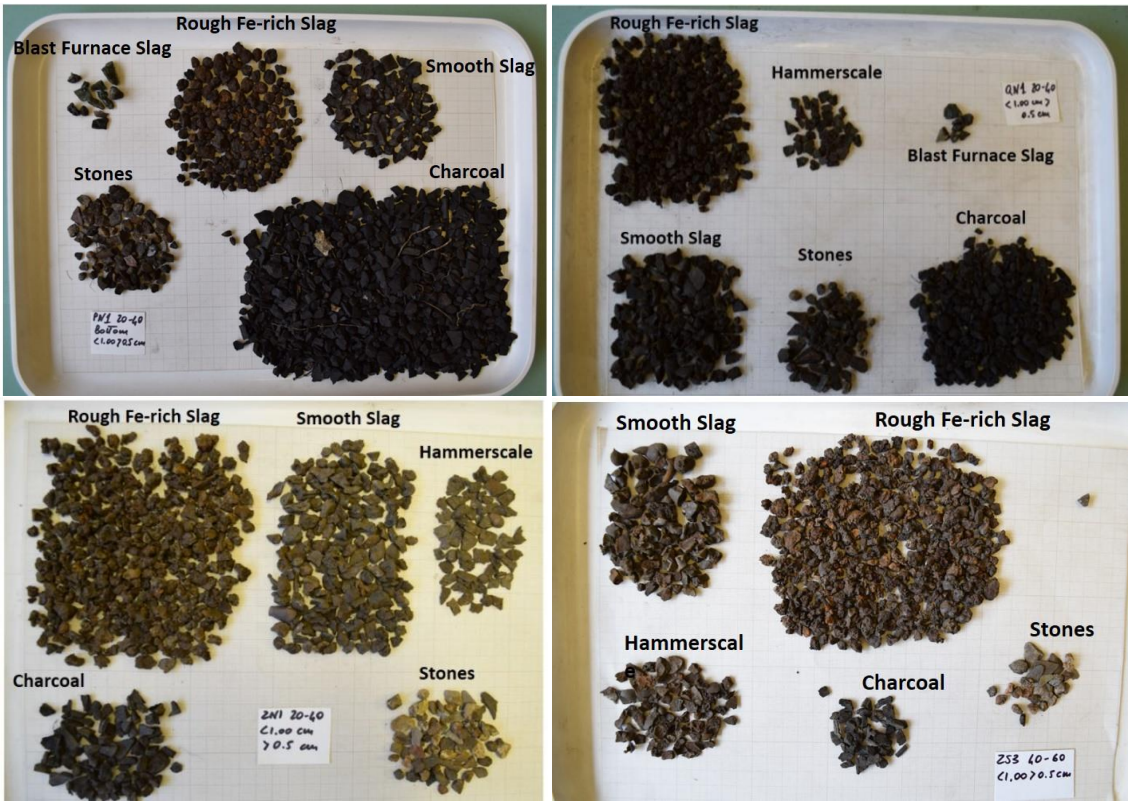

Figure 4.50. Matrix material from trenches PN1 (top left), QN1 (top right), ZN1 (bottom left) and ZS3 (bottom left)

The fragments of smooth and rough slag are probably broken fragments from the larger samples and possibly also small pieces that did not become incorporated into the hearth bottom or tapped slag cakes. The rough slag is rich in iron and highly magnetic. Small magnetic iron balls were also included here, as a real distinction between the two was not possible. They incorporate charcoal and clay as well, which suggests that they formed inside the hearth installation. In bloomery technology this type of slag is known as crown material; it is described as material that forms inside a smelting furnace, remains attached to the iron bloom and is removed during smithing or bloom cleaning process (Chirikure and Rehren 2004). Therefore, crown

material is considered part of smithing slag assemblages. A similar origin is suggested for the iron-rich slag investigated here: its occurrence together with hammerscale seems to corroborate this interpretation.

A small portion of the material is represented by blast furnace slag fragments (PN1 and QN1, figure 4.50, top). These show the blue, green and black colours observed in the bigger fragments and the same glassy texture. Of interest is the presence of flakes and spheroidal hammerscale (figure 4.51). They were all recovered by running a magnet through the material and are dark-grey black in colour. The majority of hammerscale was in the form of flakes: these are less than 1mm thick, display a smooth external surface and a rough interior. They result from the superficial oxidation of iron prior to smithing; when the surface of the iron bloom is hit with the hammer, the oxidised superficial layer becomes detached and is deposited around the anvil (Bayley *et al.* 2001, 35). Many studies have used the distribution of hammerscale around the anvil to reconstruct the spatial use of ironworking workshops (see for example Veldhuijzen and Rehren 2007).

Figure 4.51. Matrix material from trench JN9, which contained the largest amount of this type of slag (left). Right: Hammerscale from the same trench, both flakes and spheroids (red arrow) are present.

The spheroids measure between 2 and 5mm in diameter and some broken ones reveal a hollow structure. They form as a consequence of a series of ironworking activities, including fire-welding (Dungworth and Wilkes 2007), iron smelting (Crew 1988, Bayley *et al.* 2008) and fining of cast iron (Historic England, 2015).

The presence of both flakes and spheroids implies that both smithing and fire-forging were performed. The current interpretation of this type of evidence is that they resulted from the fining of cast iron, an operation that also includes a stage of forging of the lump of decarburised iron (hammering with a hammer) and consolidation of

the same into iron bars with the use of fire. The spatial distribution of these small residues is discussed in section 4.5.

Table 4.2. Summary of the observations derived from the visual analysis of the matrix material excavated during the 1999 excavation season. Data is the sum of the weights (in grams) obtained from the two sieves for each trench and spit, which totalled circa 350g for each spit. QN1 0-20 is circa 500g. Most of the blast furnace slag fragments are found in PN1 and QN1, as also observed on the large material. Overall ZS3 and JN9 yield the majority of hammerscale. Given that less material was excavated from JN9, this trench yields the largest amount of hammerscale of both types. The largest type of slag by weight is represented by the iron-rich slag.

	PN1			**QN1**		**ZN1**		**ZS3**			**JN9**	
	0-20	20-40		0-20	20-40	0-20	20-40	0-20	20-40	40-60	0-20	40-60
		top	btm									
Smooth Slag	180	140	50	290	35	47	60	118	70	50	153	20
Rough/Fe-rich Slag	75	80	90	40	163	251	200	141	220	249	98	100
Hammerscale	21	12	-	27	35	35	29	23	25	34	51	31
Blast Furnace Slag	3 fragments	17 fragments	35 fragments	-	22 fragments	-	-	-	2 fragment	3 fragments	1 fragment	-
Stones	13	29	42	10	30	4	27	24	10	15	13	160
Clay	some	some	some	-	-	-	-	35	-	some	-	-
Charcoal	57	84	167	118	76	11	10	-	23	13	55	26

4.5 ARCHAEOLOGICAL DATA

The focus of this section is to present the macro-morphological observations of the assemblage in relation to the spatial distribution. First, the data from the 1999 excavation season are presented, followed by the data obtained from the second excavation season conducted in 2000. Final observations combining the two datasets are presented in section 4.6 (Appendix A).

Data from Excavation Season 1999

The assemblage from the 1999 excavation season was quantified on site and the results of the quantitative sampling are presented in a preliminary report prepared for the Dartmoor National Park Authority (Juleff 2000). Five trenches and twelve spits were excavated, totalling 2,846.72 kg of material (table 4.3; see chapter 3 for details of excavation). The total slag yield from this material was 1,709.25 kg, the majority of which derived from the first 0-20cm spit, thus indicating a surface spread rather than a slag heap (Juleff 2000, 11). The material was sorted into five groups, represented by slag, stones, matrix samples (smaller than 1cm), charcoal and 'other' - a group which comprises special finds (such as metals and ceramics) and material other than slag. The weight of each material type obtained during the quantitative sampling exercise is illustrated in figure 4.52, which also includes the weight for the matrix fraction to illustrate the total material excavated.

The main focus of the visual analysis of the assemblage as a whole is to understand the spatial organisation of the site in relation to the metal-working technology. This is done by combining the macro-morphological data with the location data from the excavation on two levels. First, by examining the presence and distribution in the trenches of the material types identified, which can offer information about the spatial patterning and the eventual identification of different working areas. Second, the information from the size categories (degree of fragmentation) when put in connection with the spit levels of each trench can inform on the deposition process. This can be used as an indicator of the amount of disturbance of the deposit, but also to obtain information on the arrangement of the materials in their depositional context.

Table 4.3. Summary of gross quantitative sample weights for excavation season 1999 (after Juleff 2000, table 1, p. 10).

	Total material excavated (kg)	**Total Slag > 1.00cm (kg)**	**Slag as % of material excavated**
JN9 0-20	249.45	81.75	32.7
JN9 40-60	219.10	54.45	24.8
PN1 0-20	313.50	191.10	60.5
PN1 20-40U	53.10	17.55	33.0
PN1 20-40L	43.65	4.30	9.8
QN1 0-20	337.58	266.55	78.9
QN1 20-40	229.04	139.15	60.7
ZN1 0-20	390.75	257.55	65.9
ZN1 20-40	55.20	21.00	38.0
ZS3 0-20	319.30	209.80	65.7
ZS3 20-40	317.20	244.35	77.0
ZS3 40-60	318.85	221.70	69.5
TOTAL	2,846.72	**1,709.25**	

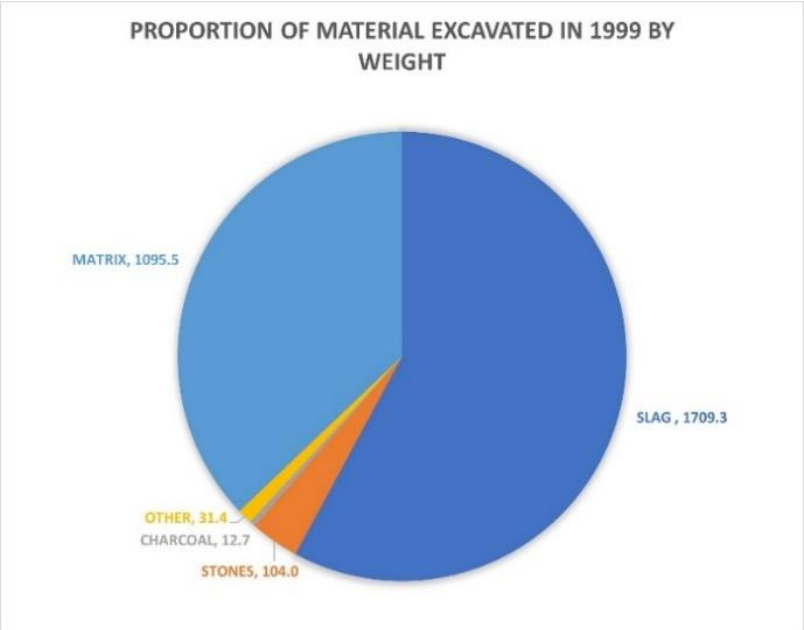

Figure 4.52. Pie chart illustrating the quantitative sample weights for each material group. Data obtained from the 1999 excavation season (Juleff 2000). Figure by author.

The pattern that emerges when looking at the distribution of material types in the different trenches suggests the presence of two different areas: one forming around PN1 and QN1, and one around ZN1, ZS3 and the more distant JN9 (figure 4.53 and figure 4.54). In particular, PN1 and QN1, adjacent to each other and excavated at what appeared to be the centre of the visible slag deposit, are characterised by a large number of finery tap slag, and of lumps of conglomerates in PN1. Most noticeable is then the presence of fragments of blast furnace slag, which is absent from the other trenches. These two trenches were excavated as a single trench (represented in figures by PN1/QN1) down to the natural deposit (at depth of *c.*40cm) and as well as a charcoal-rich layer, displayed a clayey-sand layer that appeared heat affected; this is where the 'intermediate' slag (the vesicular blast furnace subtype, see section 4.4.5) was encountered (Juleff 2000). The majority of the material retrieved from these two trenches comes from the first 0-20 spit level.

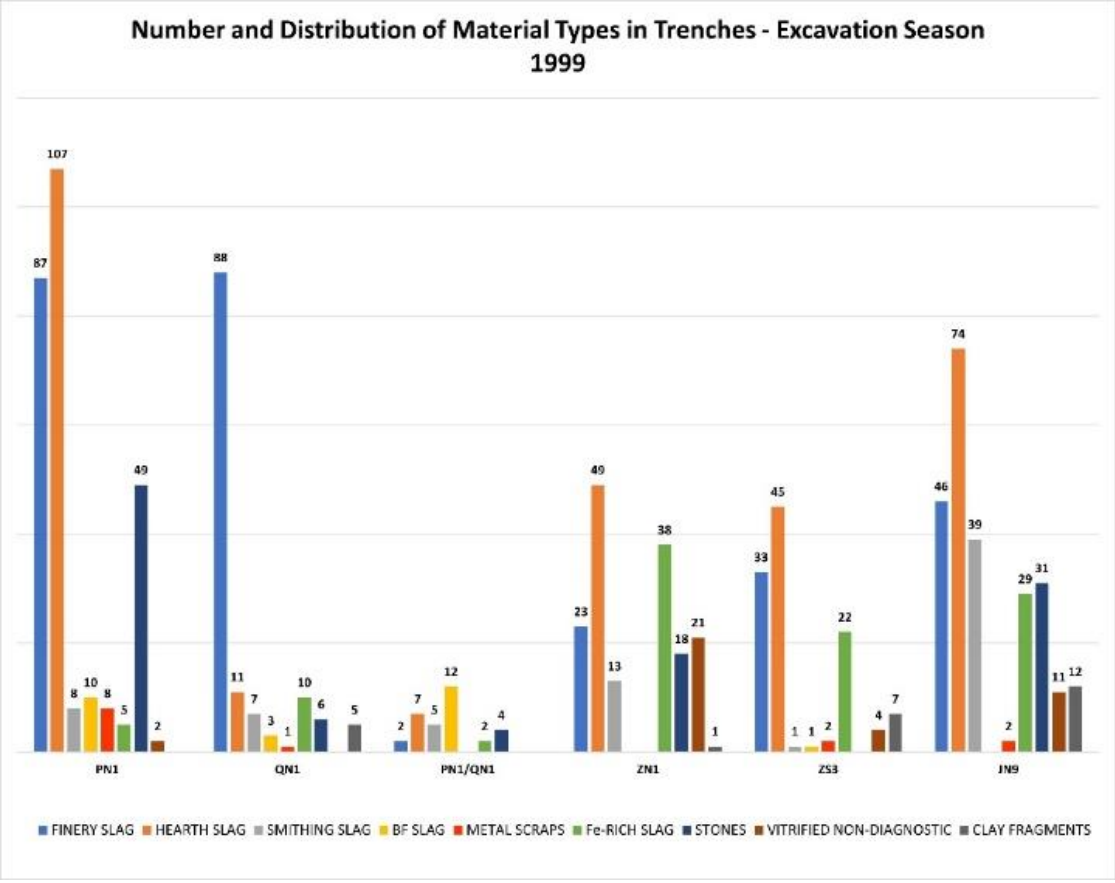

Figure 4.53. Bar chart illustrating number (y axis) and distribution (x axis) of the material types identified during the visual analysis in the trenches of the field season 1999.

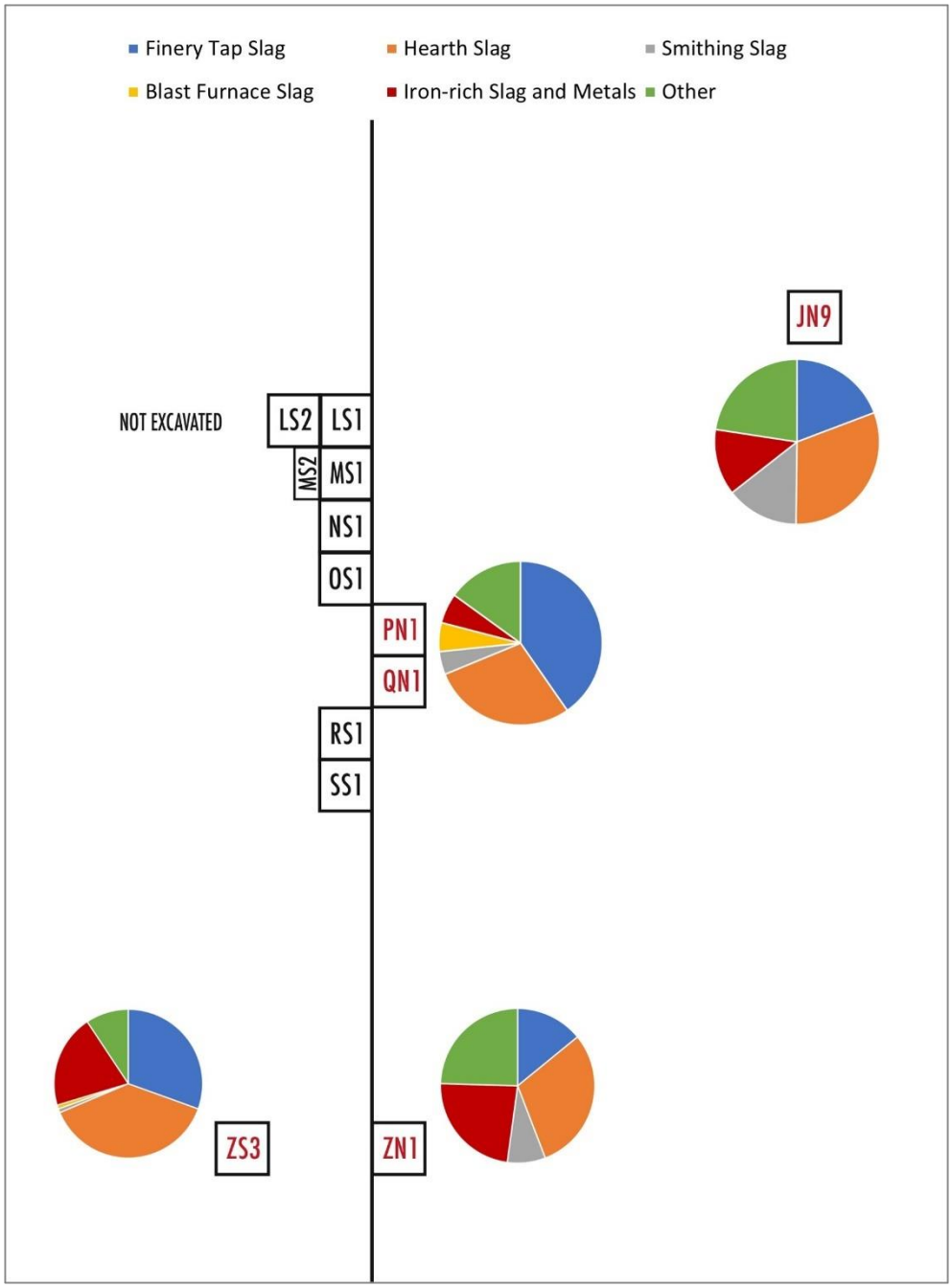

Figure 4.54. Figure illustrating the distribution of material types in trenches of the 1999 excavation season. PN1 and QN1 are represented together and are characterised by the presence of blast furnace slag. The only other trench that yielded some fragments was ZS3. Note the abundance of iron-rich slag and metal scraps in ZS3, ZN1 and JN9.

ZN1, ZS3 and JN9 shows a more similar pattern and as well as by the presence of hearth slag, are marked by the abundance of iron-rich slag and material such as stones, vitrified non-diagnostic and clay fragments. These observations are made more apparent when looking at the subtypes identified for the different slag categories (figure 4.55).

The majority of the non-diagnostic fragments of finery tap slag are found in trenches PN1 and QN1, although a good number of finery tap slag cakes were retrieved from QN1. However, most of the complete examples of finery 'cakes' come from ZS3 and ZN1 (figure 4.56). Of interest is then the presence of flowed cakes mainly in trench ZS3 (figure 4.55, top left). This trench, excavated at a depth of *c.*60 cm of uniform deposit of slag, yielded the greater quantity of material and contained a higher proportion of large slag in comparison with the other trenches (see figure 4.57 below).

A similar pattern is then observed when looking at the distribution of hearth slag subtypes (figure 4.55, top right). PN1 and QN1 are in fact characterised predominantly by conglomerates, while a greater consistency and variety of subtypes is observed in ZN1, ZS3 and JN9 (Appendix A.3.2). Hearth slag lumps, hearth slag cakes and slag channels seem to occur together in these trenches, which in addition are characterised by a large quantity of iron-rich slag and interestingly, also by clay fragments, vitrified non-diagnostic and stones, all materials that appear related to hearth installations (figure 4.55, bottom right).

Regarding the smithing slag, taken together trenches PN1 and QN1 yield the largest number of samples and JN9 displays most of the smithing flats (figure 4.55, bottom left). The examples retrieved from ZN1 were assigned to this category with some uncertainty given their fragmentary nature. The main feature appears the presence of smithing flats in JN9, while the other trenches, except for ZS3, all contain pieces and/or fragments of possible smithing slag.

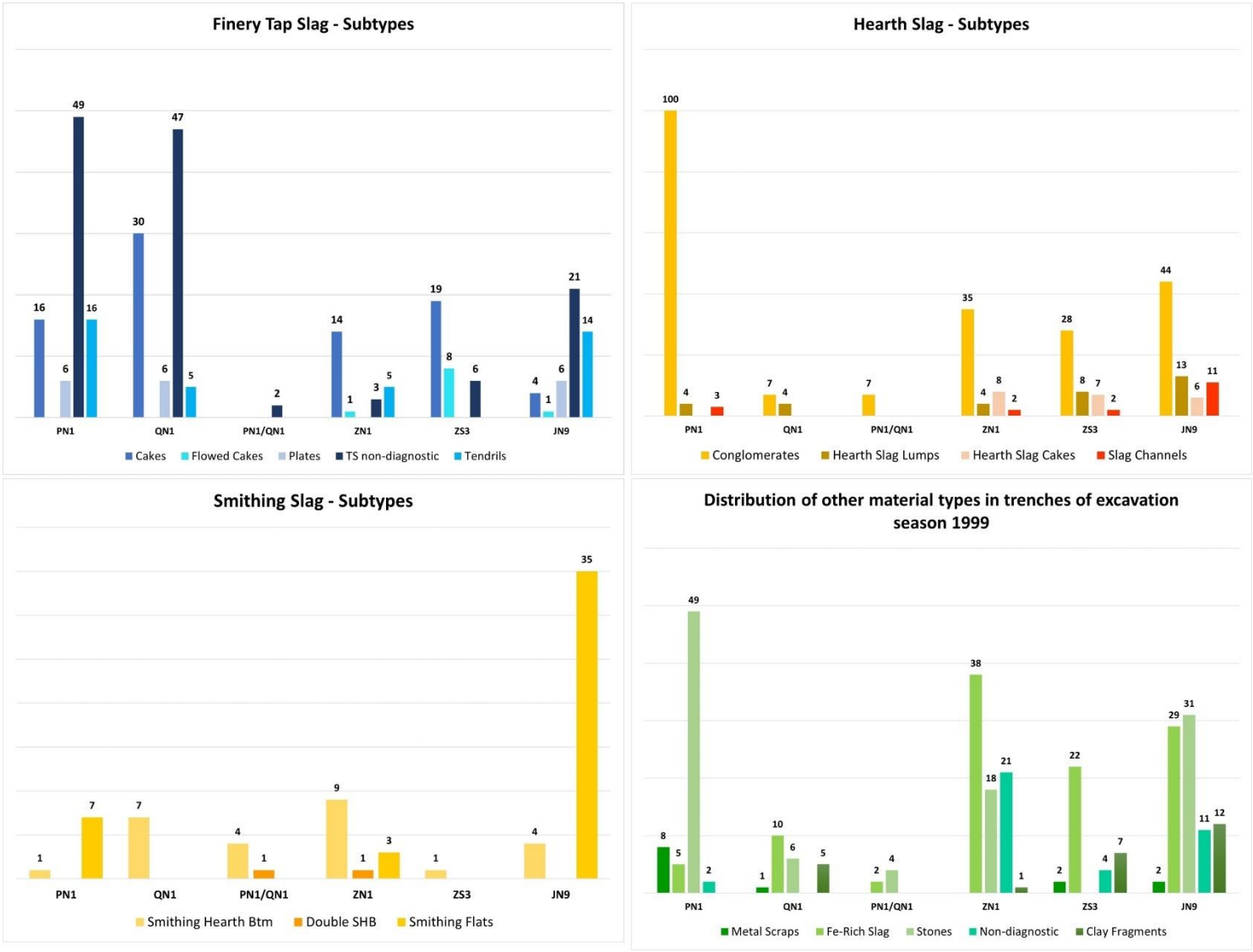

Figure 4.55. Bar charts illustrating number (y axis) and distribution (x axis) of types and subtypes of material from excavation season 1999: finery tap slag (top left), hearth slag (top right), smithing slag (bottom left) and iron-rich slag with other material types (bottom right).

An important parameter in the interpretation of metallurgical waste is the degree of fragmentation of the material present, as it indicates the level of disturbance of a deposit. Moreover, the size of a lump of slag may also be an indicator of the process from which it derives. The assemblage is mainly characterised by samples of small size for all the identified material types. Large samples are only found in finery tap slag and hearth slag. Figure 4.56 shows a high degree of fragmentation that suggests a high level of disturbance, which could indicate movement of material during metal-working operations, clearing of a furnace/hearth or even breakdown of material after deposition. The archaeological survey carried out by the Royal Commission on the historical monuments of England, revealed that the slag heap was cut through by modern vehicle damage (Newman 1998), so the high degree of fragmentation is also attributed to this later disturbance.

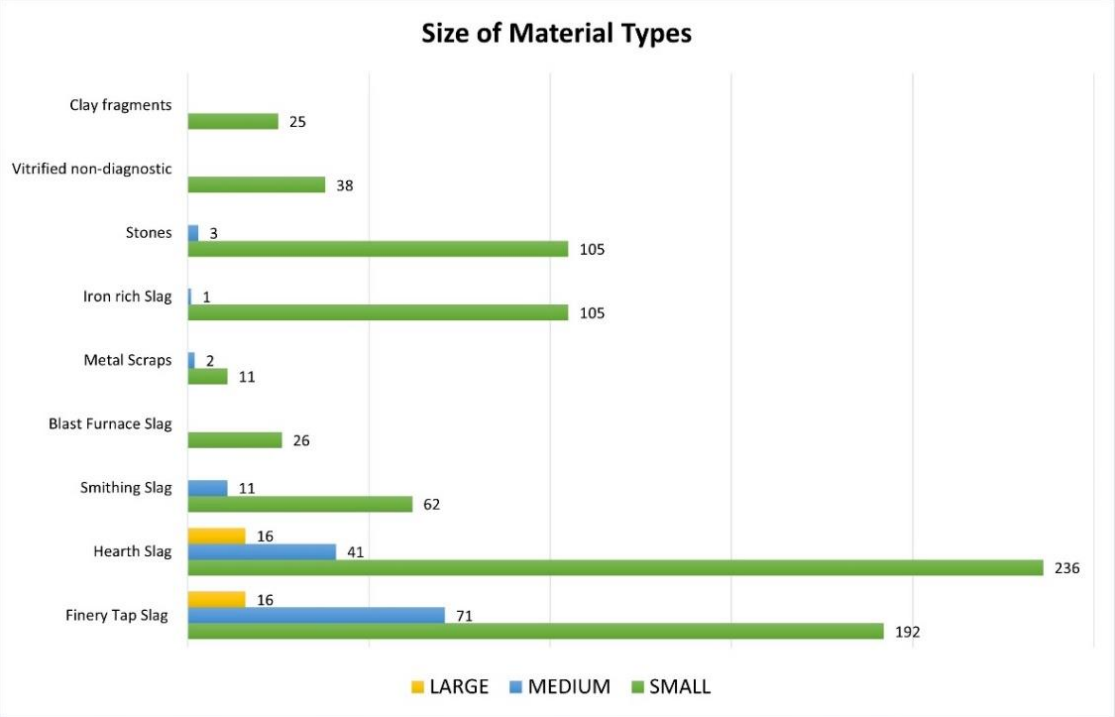

Figure 4.56. The bar chart illustrates the size of the material types identified. The assemblage is characterised by small-sized material for all classes; only finery tap slag and hearth slag contain large examples.

However, it is important to point out, as a general observation for this assemblage, that small does not necessarily mean broken and that some of the small-sized material types might in fact be ‘complete’ pieces. In particular, the small nature of the conglomerates of material and of some of the iron-rich material, appears connected to the technology that produced them, rather than resulting from later movement and disturbance. As mentioned in section 4.4.2, in fact, the subrounded shape of the conglomerates is suggestive of the stirring operations characteristic of the fining process and necessary to promote oxidation. Moreover, when the pig iron was melted in the finery hearth, it fell in the slag bath below in the form of metal droplets, that once oxidised were consolidated into a larger mass of iron. Indeed, the chemical investigation of some of the rounded iron-rich slag and metal scrap confirmed this visual observation, revealing the microstructure of oxidised cast iron (chapter 5).

Focusing in on the distribution within the trenches of finery tap slag and hearth slag - the two slag types that display samples of medium and large size - it is possible to suggest the presence of a primary undisturbed deposit around ZS3, and possibly also ZN1 (figure 4.57 and Appendix A.3.2). Nearly all material from PN1 is of small size, while the assemblage of QN1, marked by the presence of finery tap slag of medium and large size, appears transitional between PN1 and ZN1 and ZS3, pointing to some movement of material or redeposition from a nearby working area. JN9, situated at the north-west edge of the slag deposit, is characterised by the presence of medium and large hearth slag; a feature that is in accordance with the results of the geophysical survey and of the excavation, which revealed the presence of a possible hearth structure (chapter 3).

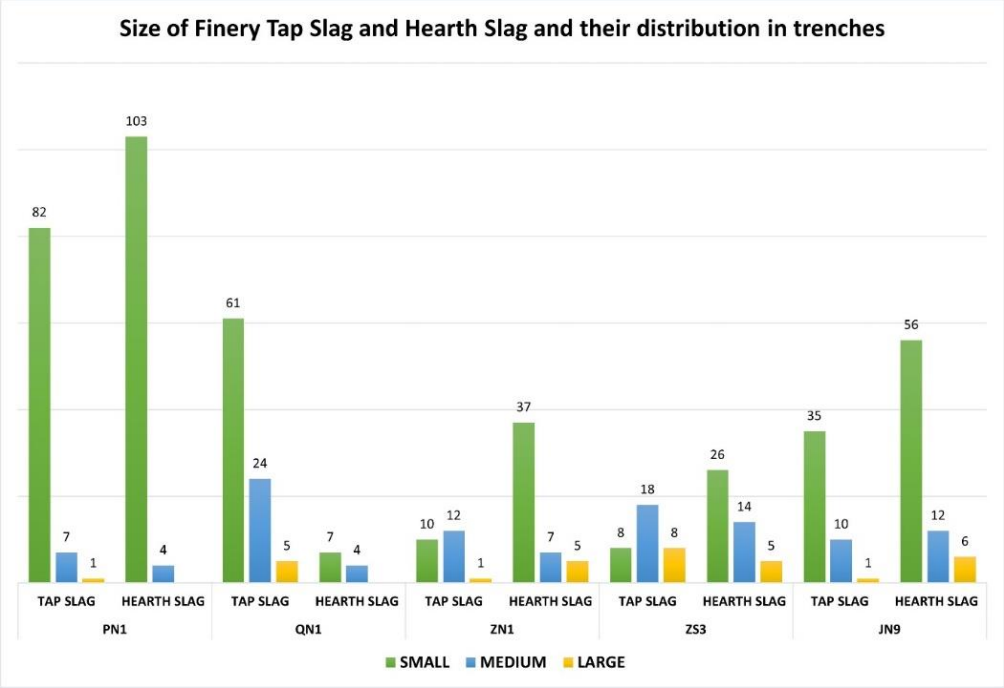

Figure 4.57. Bar chart illustrating the size of finery tap slag and of hearth slag in relation to the distribution in trenches. Y axis is showing the number of pieces.

The observations obtained from the examination of the distribution of the material types are in accordance with the excavation data (figure 4.58 and Appendix A.2). The investigation of the size categories by spits and trenches seems to confirm the presence of a primary deposit around ZS3, where the deeper trenches are characterised by medium and large size material. The high content of material in the small size category may be explained by (post-depositional) movements that caused the small fragments of slag to fall through the voids in the matrix.

The excavation of trench ZN1 was halted because it revealed the presence of a possible structure, also suggested by the RCHME survey (Newman 1998). This explains the small quantity of material coming from the lower spit (20-40) of this trench; yet a relatively large amount of medium and large material was retrieved from the first spit.

PN1 also displayed little and predominantly small material below the first 0-20 spit, the charcoal-rich layer found in spit 20-40 was almost free of slag. The presence of this layer, together with that of the ‘intermediate’ slag at the base of PN1/QN1 suggests the presence of a possible working surface: perhaps, an area where some

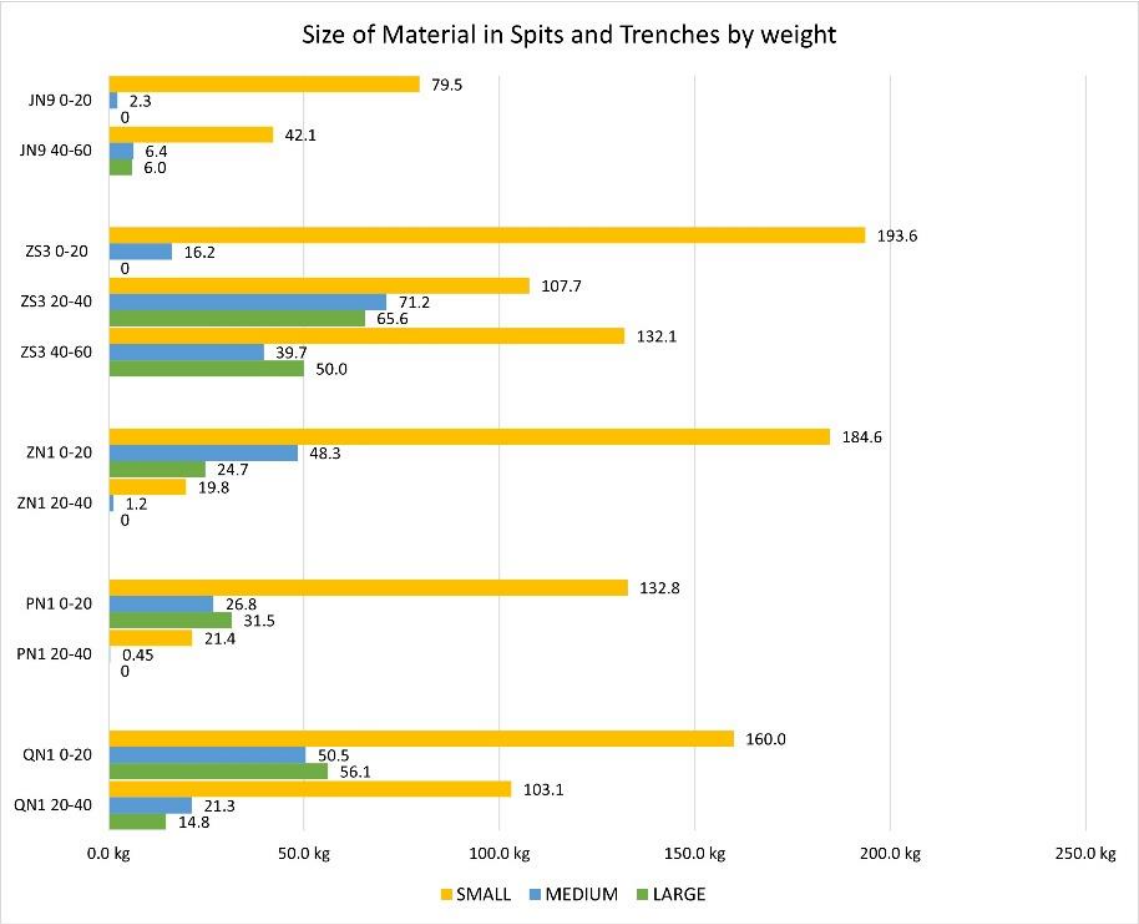

Figure 4.58. The bar chart illustrates, using the weights from the excavation data, the distribution within spits and trenches of small, medium and large material. Figure by author.

operations preliminary to fining were performed but given the limited number of samples this observation is only tentative.

Finally, JN9 is marked mostly by material of small size. A charcoal-rich horizon was also encountered within spit 20-40; this yielded no slag, so sampling was halted but it was restarted for spit 40-60, where a possible hearth structure was found, but not excavated. Interestingly, this level coincides with the presence of hearth slag of medium and large size.

Matrix

Complementary information is obtained from the study of the distribution of the matrix material. The largest number of flakes and spheroid hammerscale derive from trench JN9 (Appendix A.3.3); a feature that seems in accordance with the presence of smithing flats in this trench and could signify the presence of a reheating hearth and anvil.

However, even if in smaller quantity, hammerscale of both types are found in all trenches making difficult the identification of a possible smithing area, or even suggesting the presence of more than one area dedicated to the 'cleaning' and consolidation of the iron *loop* after oxidation – a layout that would be compatible with the complicated fining operations (chapter 2). Another possible explanation for their presence across the slag deposit could be the fact that hammerscale was employed to increase the volume of the slag bath, and so it was collected and moved across the site, from the smithing area where it formed, to the finery hearth.

Blast furnace slag fragments are found in the matrix of PN1, QN1 and ZS3. Their distribution is difficult to interpret since only a small number of larger examples were recovered. However, it is likely that their presence is connected to metal-working operations, such as the addition of blast furnace slag fragments to the slag-bath in the finery hearth (chapter 2) and the movement of smelted pig iron from the blast furnace to the finery forge.

Finally, most of the iron-rich micro residues derive from ZS3 and ZN1, occurring together with vitrified burnt material and small clay pellets, again reflecting the distribution observed for the macroscopic material.

Data from Excavation Season 2000

As mentioned above, no excavation report was generated for this field season, so this section offers an overview of the information obtained from the field notes. The quantified data was organised into tables and figures during the macro-morphological analysis for this study (Appendix A.2.2). A similar quantity of material by weight was retrieved during the second excavation season, in 2000 (table 4.4). The total material excavated was 2,482.1 kg, with 1,041.5 kg being recorded as slag. Six trenches were excavated, three to a depth of 20cm (LS1, MS1 and NS1) and three down to 40cm (OS1, RS1 and SS1). The majority of the material derives from trenches RS1 and SS1. Given their position in relation to the trenches of the first excavation season, some features of their assemblages helped to clarify the spatial patterning of SH1 (figure 4.59).

The assemblage was again sorted into slag (pieces bigger than 1cm), matrix, stones, charcoal, small finds and 'other' (figure 4.60). In this case, the category 'other'

comprises roots, while metal scraps, clay fragments and small diagnostic pieces are included in the category small finds.

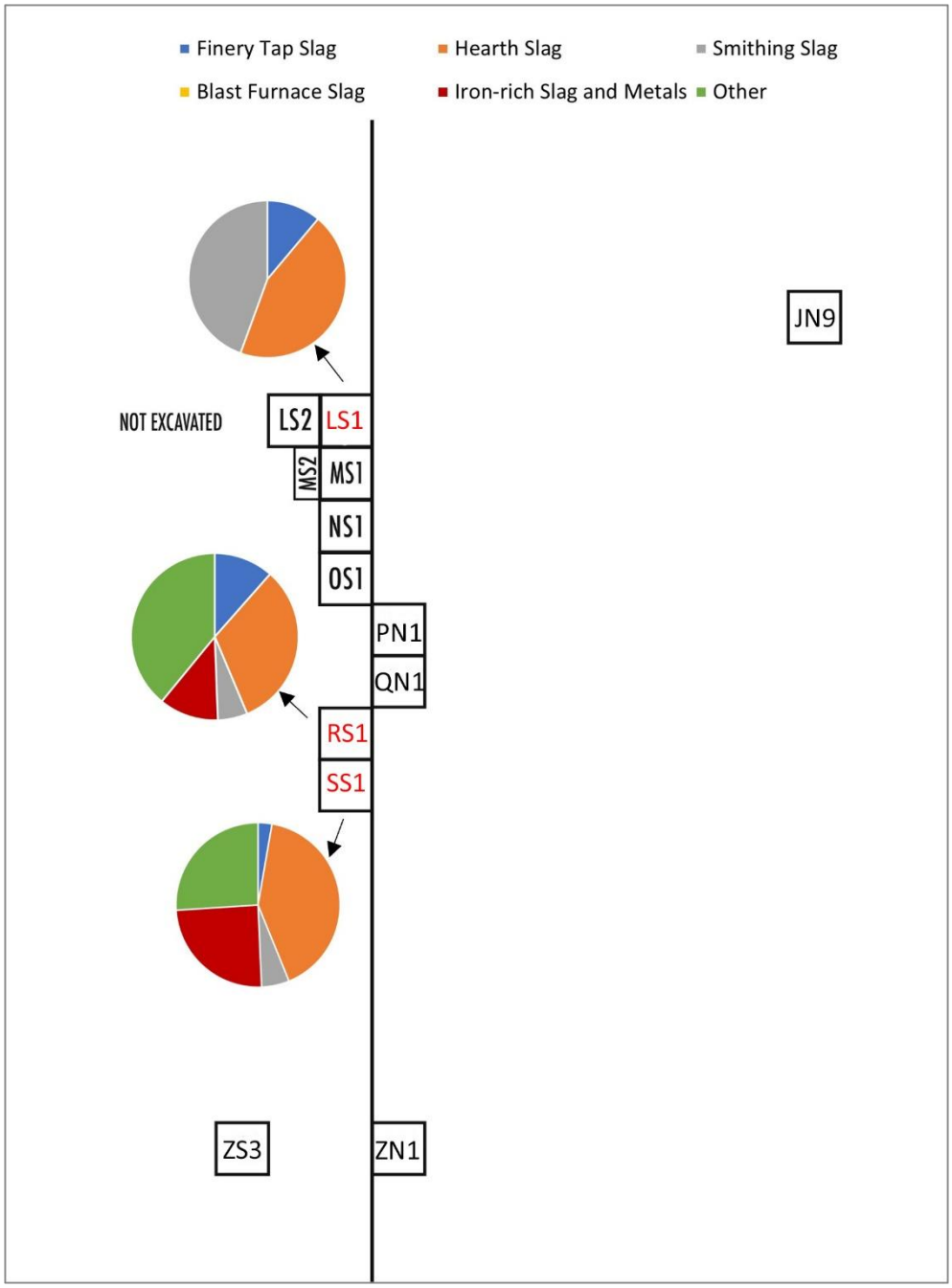

Figure 4.59. Figure illustrating the distribution of material types in trenches of the 2000 excavation season. Note the abundance of hearth slag in trenches RS1 and SS1, while finery tap slag is less abundant and fragmentary. The figures for LS1 are only indicative, as very little material was recovered from this trench and therefore the proportions are not correct. The deposit towards LN1 is thin and disturbed.

Overall, a larger quantity of material classified as small finds, appears to have been recovered during the 2000 excavation season, which suggests that a difference from the assemblage of the first excavation season was observed.

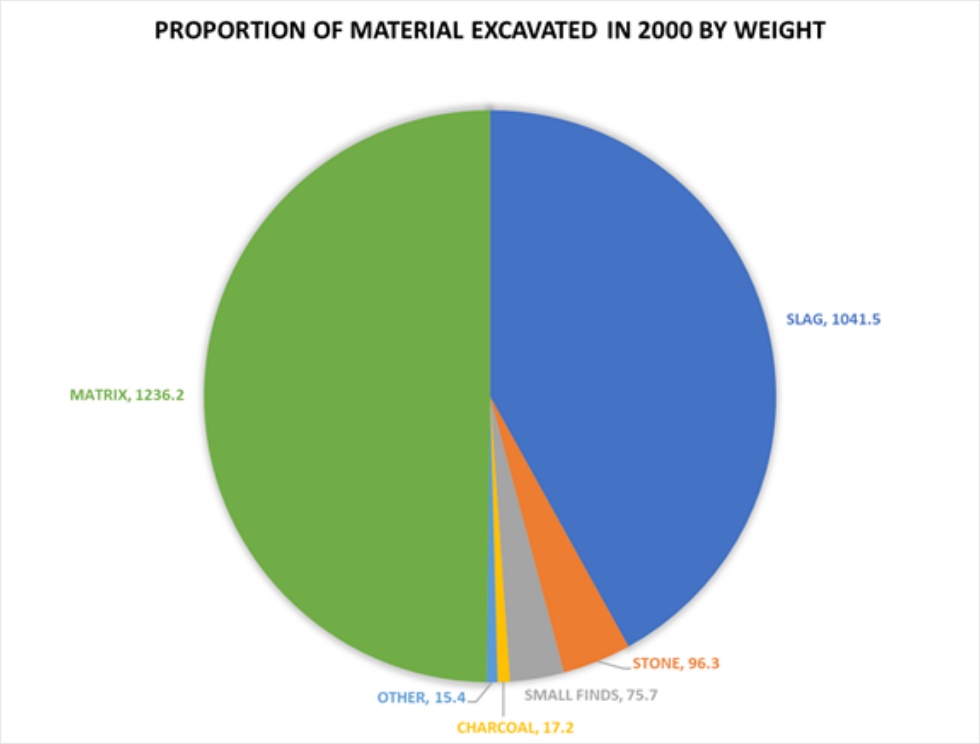

Figure 4.60. Pie chart illustrating the quantitative sample weights for each material group. Data obtained from the 2000 excavation season (Juleff 2000). Figure by author.

The field notes refer to a large quantity of small clay-rich lumps of slag and stones, and overall little occurrence of 'distinctive' tap slag, which is predominantly highly fractured. An abundance of complete 'hearth-bottom slag' is also reported. Moreover, a feature that seems consistent throughout the assemblage is the presence of reddened, heat affected material. Another noted feature is then a difference in the texture/nature of the matrix of trenches MS1, NS1, OS1, which is described as peaty matrix and sandy matrix. Finally, in these same trenches fragments of blast furnace slag are also found.

Table 4.4. Summary of gross quantitative sample weights (data after field notes, table by author)

	Total material excavated (kg)	**Total Slag > 1.00cm (kg)**	**Slag as % of material excavated**
LS1 0-20	212.4	76.95	36.2
MS1 0-20	205.5	43.90	21.3
NS1 0-20	249.8	62.75	25.1
OS1 0-20 OS1 20-40	258.4 206.1	119.10 6.20	46.0 3.0
RS1 0-20 RS1 20-40	370.8 307.0	260.85 138.65	70.3 45.1
SS1 0-20 SS1 20-40	361.2 310.6	197.95 135.10	54.7 43.4
TOTAL	2,482.1	**1,041.5**	

The assemblage was sampled on site and, similarly to the previous field season, representative samples for each size and category were retained and stored between Dartmoor National Park and the department of Archaeology of University of Exeter. The macro-morphological analysis was done on the material retrieved from LS1, RS1 and SS1. LS1 is located towards JN9, on the north-western edge of the slag deposit, while RS1 and SS1 are situated in between PN1 and QN1 and ZS3 and ZN1 (figure 4.59). A total of 43 bags of material were investigated, which only comprised slag bigger than 1cm. The matrix sample of this excavation season were not analysed.

A first feature observed from the inspection of this assemblage, which contrasts with the material excavated and sampled in 1999, is the small amount of finery tap slag (figure 4.61). Only a few small non-diagnostic fragments were retained, probably because of the fragmentary nature of this type of slag observed during excavation.

However, two large samples of what has been classified as flowed cakes are found in trenches LS1 and SS1, indicating that the difference in texture (from a 'standard' finery tap slag) observed during the visual investigation was also noted on site during sampling.

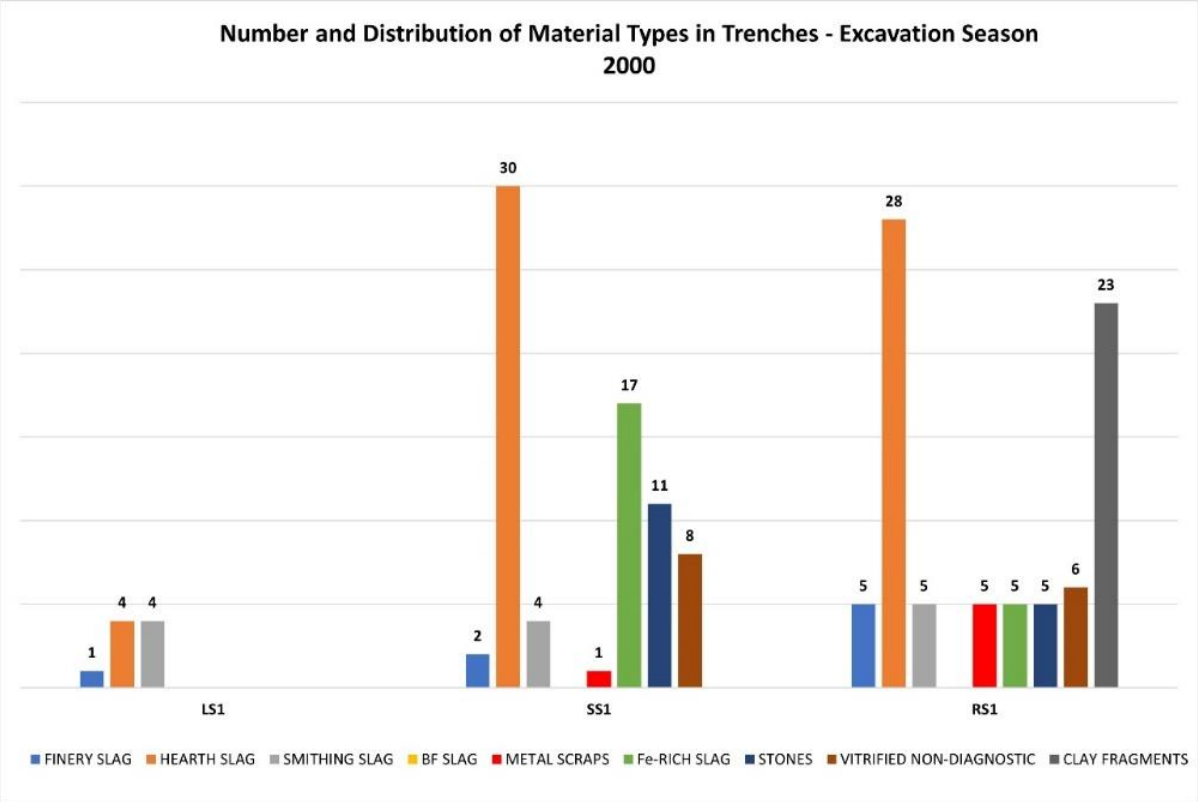

Figure 4.61. Bar chart illustrating number and distribution of the material types identified during the macro-morphological analysis in the trenches of the field season 2000.

Overall, the assemblage is characterised by the presence of hearth slag, iron-rich slag and clay fragments. A small amount of material was excavated (and sampled) from trench LS1, making an interpretation of this area tentative at best. However, as a general observation, its composition appears similar to that observed for JN9, with hearth slag and smithing slag being the predominant types. SS1 and RS1 display similar material types and yield a large amount of hearth slag and of refractory material. Given the scarcity of refractory material overall, the number of examples found in RS1 appears significant for the identification of possible hearth structures. Moreover, a considerable amount of iron-rich material (slag and scrap) was retrieved during the 2000 excavation season, including a possible fined iron bar found in trench RS1, which has been the object of optical and chemical analysis (chapter 5).

The results obtained from the quantified data and illustrated in figure 4.62, confirm that the slag deposit is thicker, and relatively undisturbed, at the south-eastern edge,

becoming progressively thinner and more disturbed towards the northern end. The material yield of trenches LS1, MS1, NS1 and OS1 is dominated by small-sized fractured slag and below spit level 0-20, very little slag was encountered. On the other hand, the stratigraphy of RS1 and SS1 is thicker, with material of medium and large size found in the lower spit levels (20-40).

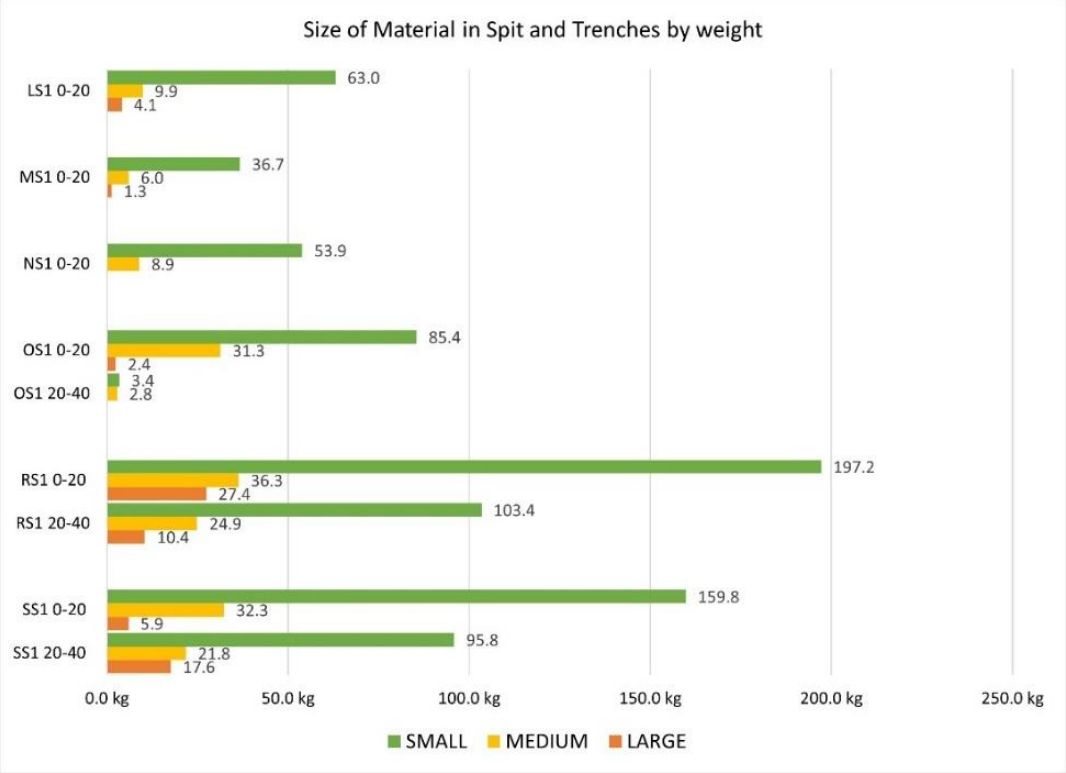

Figure 4.62.The bar chart illustrates, using the weights from the excavation data, the distribution within spits and trenches of small, medium and large material. Figure by author.

4.6 FINAL OBSERVATIONS – COMBINING THE TWO DATASETS

The macro-morphological analysis of the assemblage combined the identification and characterisation of material typologies with the spatial distribution of the same, which allowed some progress in terms of understanding the site layout. The composition of the assemblage is complex, with types occurring together in different areas of the slag deposit. This suggests that different metalworking structures were employed and that different operations produced similar material. This appears especially true for the hearth slag group, whose different types could have been produced both in finery and chafery hearths. It seems likely that the site contained more than one hearth structure. The geophysical investigation performed in 1999

revealed the presence of a number of features with distinctive magnetic signatures; at least four of these are indicated as potential hearth bases (Dean and Faxon, 2000; chapter 3).

The fragmentary nature of the material from PN1-QN1 could be indicative of a passage area, where slag was moved and deposited during the metal-working operations to clear the working hearths. The silica-rich slag ('intermediate') found in the charcoal-rich layer, however, also suggests the presence of some metallurgical activity, whose nature is investigated during the analytical work. The distribution of the finery tap slag suggests the presence of a finery hearth towards ZS3, where the majority of the diagnostic pieces are found.

The material from the 2000 excavation season investigated for the macro-morphological analysis was less than that of 1999, but the information obtained was important to support some of the observation on the slag deposit. The general impression is that in the area of trenches SS1 and RS1 the tap slag encountered was highly fragmented and larger and distinctive hearth slag pieces dominated the assemblage. While it is possible that the small size of tap slag directed the subsequent sampling towards the larger hearth slag examples, it would appear that overall, the composition of the 2000 assemblage (trenches SS1 and RS1) is similar to that of trenches ZN1 and ZS3 indicating a good representative sample of the material types present on site (figure 4.63).

The distribution of these two material groups could reflect the presence of a finery hearth and of a chafery hearth: the former around ZS3 and the latter around RS1/SS1; indeed, the essential core of the material produced in finery forges is concentrated in these trenches. The large number of micro residues and of smithing flats in trench JN9 could indicate the presence of a reheating hearth and anvil.

Another possibility is the presence of two fineries and a chafery hearth, a layout that was employed in the Walloon method to speed up the lengthy fining process (Houghton 1997, Awty 2007). A similar arrangement could correspond to the areas around trenches ZS3 up to PN1/QN1, where the geophysical survey identified two areas with distinctive magnetic signatures, one of which is described as a possible 'double-furnace' (Dean and Faxon, 2000, A21). Indeed, the presence of blast furnace slag in PN1/QN1 and the distribution of smithing slag around the same

trenches, and in ZN1, where the wall of a possible building was encountered, should be further investigated.

The archaeology and material from the finery forge are poorly understood and clearly an industrial site of this complexity, whose traces have been greatly disturbed by later industries and movements, would require substantial excavation in order to clarify the spatial pattern. Moreover, the value of some diagnostic pieces was understood only later in the research, leaving many questions unanswered. The most valuable one to understand the assemblage and the site layout is possibly the distinction between finery and chafery hearth slag. This could have been tackled with the use of chemical analysis to aid the visual analysis.

Notwithstanding this, the visual investigation still produced interesting results that helped to understand the metallurgical activities performed at Ausewell Wood. It is now clear that the two sides of the site are connected and once formed a single large industrial complex, where iron was first smelted in the blast furnace and then converted in the finery forge.

The results obtained from the visual analysis appear corroborated by metallurgical residues excavated more recently at two other forges, New Weir forge in Herefordshire (Dorling and Young 2011), and Cunsey Bloom forge in Windermere (Schofield and Miller 2017). At both sites, the assemblages comprise hearth slag cakes in association with slag channels, tapped/flowed slag and small slag flats (smithing flats in this study). The archaeological report on Cunsey Bloom forge, which includes pictures of same of the most interesting pieces found at the site, shows similar slag pieces, including the red-coloured hearth slag example found at Ausewell Wood. This supported the interpretation of the assemblage under study as finery forge material. The identification of this type of slag could be of significance for the recognition and classification of material coming from similar sites.

Ultimately, the Ausewell Wood assemblage can be considered a typical finery forge material and its analysis has enormous potential to understand and address questions relating to this important but neglected technology of the iron industry.

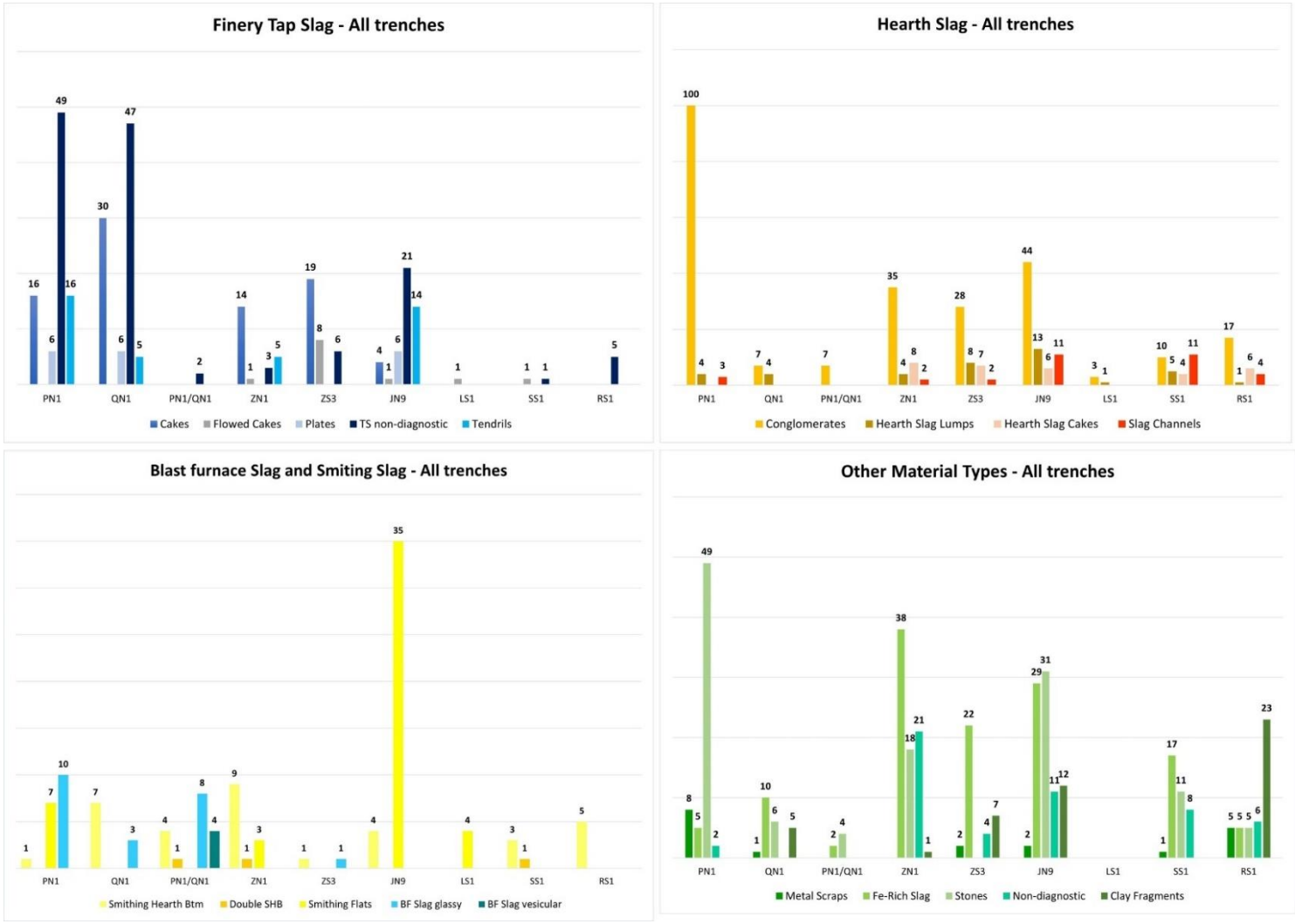

Figure 4.63. Bar charts illustrating the distribution of material types in trenches of both excavation seasons: finery tap slag (left), hearth slag (top right), blast furnace slag and smithing slag (bottom left) and other material types, including iron-rich slag and metal scraps (bottom right).

CHAPTER 5 AUSEWELL WOOD – THE CHEMICAL ANALYSIS

'It should be neither too thin nor too thick, and should run in an uninterrupted and somewhat viscous little stream.'

Percy 1864, 496.

5 AUSEWELL WOOD – THE CHEMICAL ANALYSIS

The archaeology of the finery forge and the scientific study of its material remains have been identified as a research priority by the Historical Metallurgy Society (Bayley *et al.* 2008). The iron industry of the post-medieval and industrial eras features a plethora of iron working processes. After the introduction of the blast furnace and the routine production of cast iron, many different conversion processes were developed and employed in order to obtain iron and/or steel from the high-carbon alloy obtained during smelting (chapter 2). Indeed, for any other use of the pig iron that was not casting, it was necessary to process the metal and reduce its carbon content in order to obtain a (low carbon) alloy, wrought iron, that could be forged and shaped into objects.

To describe these conversion processes Rostoker and Bronson refer to ‘a cluster of related techniques known as fining’ (1990, 139), which appeared in Europe during the 15th century and continued in use, in one form or another, until they were surpassed by the puddling process in the 19th century. Fifteen different methods were reported in 1858 by Tunner the director of the Mining School of Austria (translated in Percy 1864, 580-619), highlighting the high degree of empirical skills and experimentation that characterise them. All this points to great variation in the nature and appearance of the resulting residues, reflecting a variety of furnace designs and operating procedures that are often difficult to distinguish and pinpoint archaeologically. In addition, scientific investigation into the process residues of the various conversion processes has been limited (Phelps *et al.* 2011). In fact, while archaeological studies have extensively employed scientific analysis for the investigation of material record of earlier periods (pre-history, Roman, Medieval), the archaeology of the post-medieval and industrial periods has mainly focused on the recording and surveying of standing structures and visible landscapes, making considerably less use of archaeological science for the study of the material culture (Bayley and Crossley 2004, 15). Furthermore, post-medieval archaeological deposits have often been altered and suffered intense taphonomic processes due to increasing density of occupation and reuse of industrial sites, thus complicating the picture. Often, the sites that survive (with structures and residues) are those situated in rural areas away from urbanisation, as it is the case for Ausewell Wood.

The aim of this chapter is to provide microstructural observations combined with quantitative and qualitative analyses in order to untangle some of the history around the operation of fining cast iron. This chapter is thus divided into three sections. The first describes the results obtained from the microstructural and chemical investigation of ironworking residues selected from the material categories obtained from the macro-morphological analysis (Chapter 4). The second section summarises some of the themes within archaeometallurgical studies of post-medieval ironworking, while in the final section the results are analysed and synthesised into a discussion that references previous research. The work in this chapter is supported by the material presented in Appendix B.

5.1 OBJECTIVES AND METHODOLOGY

5.1.1 Objectives

Following the macro-morphological characterisation of the assemblage (Chapter 4), the next step was the selection of samples for laboratory analysis (Appendix B). The main objectives of this exercise were:

1. To explore the relationship between the blast furnace and the excavated slag heap
2. To understand and characterise the finery process

The first objective entails the characterisation of the site as a whole (not just the excavated areas) and the interpretation of the ironworking activities (table 5.1). As already stated in chapter 3, the presence of the blast furnace and associated glassy smelting slag heaps, and of the iron-rich (*'bloomery'*) slag heap to the northern extremity of the site has been mainly interpreted as evidence of the transition between the two different smelting technologies (Newman 1998). On the contrary, the results of the visual analysis performed for this study indicate a connection between the two sides of the site, whereby the blast furnace to the south represents the beginning of the operating chain, the smelting of iron ore, and the slag heap to the north represents the end of the process, where pig iron was decarburised and worked into bars of malleable iron (figure 5.1). Therefore, in order to verify this visual interpretation, fragments of blast furnace slags (glassy silica-rich waste material) recovered during fieldwork (in 1999) were selected (Appendix B). The analysis of this material was compared to five pieces of blast furnace slag collected near the blast

furnace during a survey of the site carried out for this study (in 2018); these fragments are termed blast furnace surface finds (table 5.1) and were simply collected by hand from immediately below the leaf mould covering the heap. The chemical investigation of these pieces targeted both the composition of the silica-rich glass matrix and mineral phases, and the composition of the metallic prills found embedded in the slags. Moreover, with the aim of establishing what ore(s) were employed in the blast furnace, three possible ore fragments were also prepared and analysed (table 5.1, Appendix B.2). These were collected as surface finds near the blast furnace during the 1999 excavation season (Juleff 2000, 7).

The second objective was to understand and characterise the finery process (table 5.1). This involves the characterisation of the materials employed during the process, the waste material generated and the final products. Consequently, samples were selected from the finery tap slag, the hearth slag (both cakes/lumps and conglomerates) and metal (iron scrap) categories (table 5.1). Five stones and clay samples were also analysed, in order to explore a possible connection with the composition of slags and have an overview of all material types present on site and possibly employed in the process (table 5.1). Furthermore, with the aim of establishing the presence of smithing activities - forging of decarburised iron bar - four samples from the smithing slag group were analysed: a possible smithing hearth bottom and samples from the matrix material that included flakes and spheroidal hammerscale, as well as other small fragments of slag (table 5.1; Appendix B). For the position of cut samples refer to Appendix B.

Finally, one of the problems which persists within archaeometallurgical studies is the difficulty of distinguishing some types of bloomery wastes from those found at finery forges (Bayley *et al.* 2008, 61). In the light of this and taking into account the assumptions discussed in the previous chapter (4.1), the characterisation of the finery technology documented at Ausewell Wood also entailed the identification of diagnostic features (microstructures and mineral phases in slags and microstructures and slag inclusions in metals) that supported the interpretation obtained from the visual analysis. The results obtained from this investigation are compared, when possible, with previous studies of similar materials.

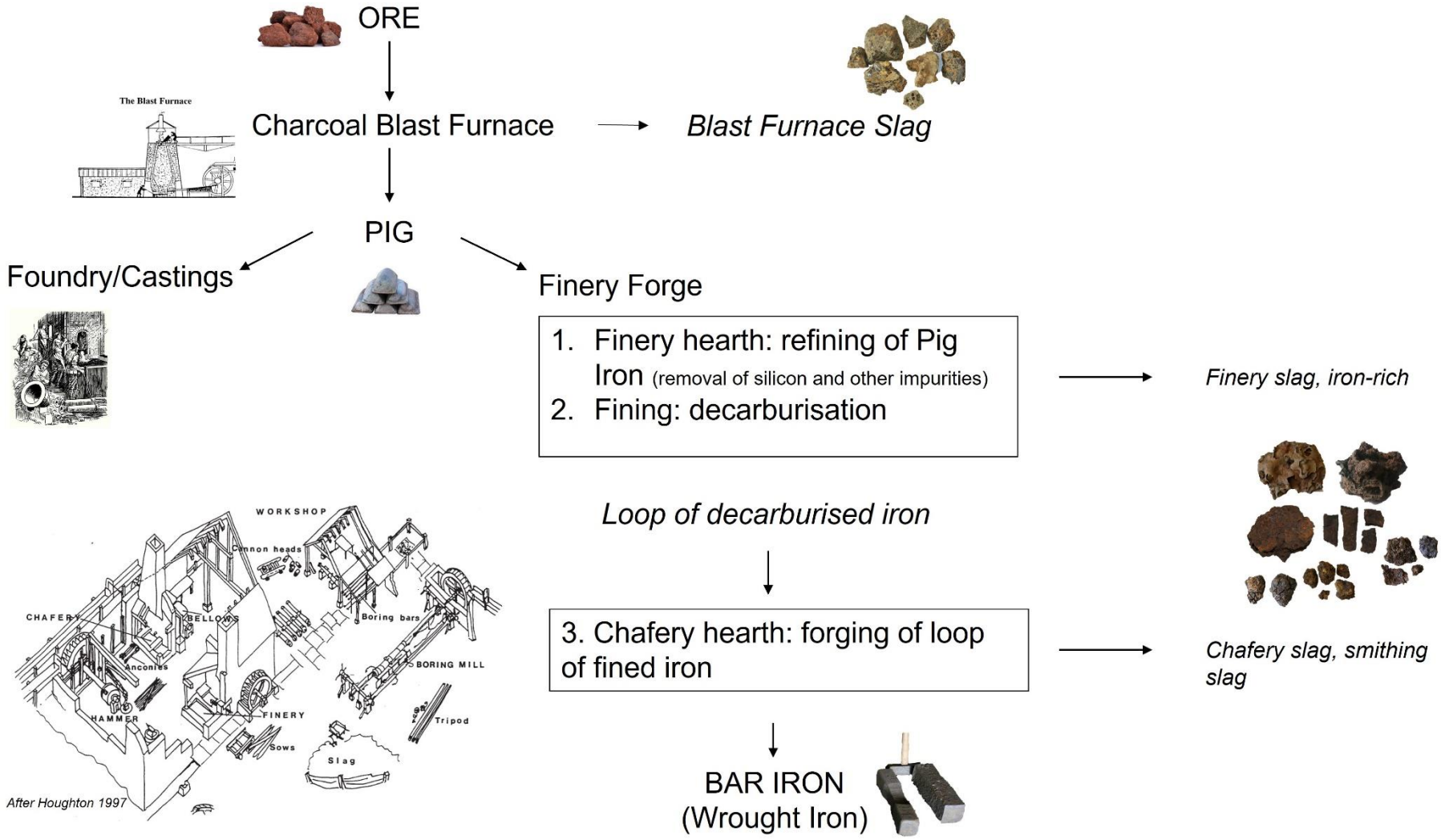

Figure 5.1. Schematic representation of the chaine opératoire of indirect smelting (blast furnace illustration by Chard 1995, drawing of finery workshop by Houghton 1997, cannon foundry illustration by Airne 1935, slags from A.W by the author, bar iron from Saugus irorworks by Markos 2018, iron ore image from shutterstock.com, pig iron from Wikipedia).

Table 5.1. Table showing samples selection for each class of material in relation to the objectives of the chemical analysis

OBJECTIVES	SLAG TYPES		LABELS										N° of samples
1. CONNECTION BETWEEN BLAST FURNACE AND EXCAVATED SLAG HEAP	BF SLAG/SILICA-RICH SLAG		PN1 20-40_2	PN1 20-40_Black 7	PN1 20-40_Blue	PN1 20-40_Green_1	PN1 20-40_Green_2	PN1 20-40_7	PN1 20-40_8	PN1 20-40_blue 8	QN1 20-40_Blue 8		9
			BF Finds_ 1	BF Finds_ 2	BF Finds_3	BF Finds_4	BF Finds_5						5
			PN1-QN1_CXT7_CG-BF-Fe	PN1-QN1_CX7_BF_Green									2
	HEARTH SLAG-CONGLOMERATES (+ objective 2)		QN1 20-40_CGBF	PN1 20-40_CGBFTP_10	PN1 20-40_CGBF_5	PN1 20-40_CGBF_4	JN9 20-40_Fe/Slag	ZS3 40-60_Fe/Slag					6
	ORE SAMPLES		Ore_1	Ore_2	Ore_3								3
2. CHARACTERISATION OF FINERY TECHNOLOGY	bloomery vs finery	FINERY TAP SLAG	ZN1 0-20	QN1 0-20_large	PN1 20-40_13	PN1 20-40_14	PN1 20-40_Run 12	PN1 0-20_Thin Plate					6
		HEARTH SLAG (cakes/lumps)	ZN1 0-20_1	ZN1 0-20_3	RS1 20-40_1	RS1 20-40_2	JN9 20-40_Cyl_3						5
	smithing/forging iron bars	SMITHING SLAG	QN1 0-20_SS_1										1
		MATRIX	PN1 0-20_Mx_1	PN1 20-40_Mx_2	QN1 20-40_Wet_Mx								3 (see text)
	Objectives 1&2	METAL	ZS3 40-60_Flat	RS1 0-20_Bar	JN9 0-20_Iron	PN1 20-40_FeNodule 6	PN1 20-40_FeNodule 11	QN1 20-40_Fe ball (2 samples)	RS1 0-20_Fe1	RS1 0-20_Fe2	RS1 20-40_Fe1	RS1 20-40_Fe2	11
	STONES/CLAY		QN1 20-40_WhiteStone	QN1 20-40_MixClay	PN1-QN1_CXT7_WhiteStone	PN1 20-40_Quartz	PN1 20-40_WhiteStone						5
			TOTAL SAMPLES										56

5.2 SAMPLE PREPARATION AND ANALYTICAL TECHNIQUES

All samples were cut and prepared at the Forensic Institute Analytical Laboratory at Cranfield University (Shrivenham Campus). A total of 56 samples were mounted as polished cross-sections using epoxy resin and following well established procedures (Scott and Schwab 2019). The resin blocks were prepared by manually grinding on successively finer abrasive paper – from P120 to P4000 – before being polished with diamond paste to a 1µm finish. Only the metal samples were polished to a 0.25µm finish.

Optical and electron microscopy

All samples were first observed in their polished state under a reflected light optical microscope equipped with digital camera, the system employed was a Reichert - Jung Polyvar. The optical microscope was used to evaluate carbon content and for the preliminary investigation of microstructures and phases. Etching of archaeological corroded metals could remove corrosion (which itself carries fundamental information on microstructures) and non-slag inclusions; consequently, three metal samples were etched and photographed after the completion of the chemical analysis (one cast iron fragment and two fragments of the low-carbon malleable iron bar found in trench RS1; section 5.4.4).

The next step was the investigation of the samples under a scanning electron microscope with an energy dispersive spectrometer (SEM-EDS). To conduct scanning electron microscope examination, samples have to be electrically conductive to avoid electrostatic charging (Goldstein *et al.* 2003). One of the methods available for applying conductive coating is to cover the surface of the sample with a thin film of a highly conductive material (Goldstein *et al.* 2003, 657). Carbon and gold are frequently employed, as well as silver and other metal alloys; the choice of coating material often depends on the elements of interest or what is available in the laboratory. Carbon is the typical material for coating when chemical analysis is required, especially since early EDS detectors cannot detect carbon and thus its use does not limit the microanalysis (Ul-Hamid 2018). Nowadays, detectors can measure carbon and lighter elements, thus precluding the use of carbon-coating. The solution to avoid charging of the samples is to perform the analysis using scanning electron microscopes without exposing the sample to high vacuum. These microscopes are referred to with different names, such as environmental, low-

vacuum, high-pressure or variable-pressure SEMs (Hanke 1995): they operate at high pressures and introduce gas into the chamber which diminishes the charging of non-conductive samples.

Sample preparation for this study did not involve carbon-coating because this was not available in the laboratory. Consequently, the investigation of the samples was performed without pre-treatment of the resin blocks and using the variable pressure mode. When working at low vacuum, spot analyses of small areas/phases can give results contaminated from the surrounding areas. For this reason, when unsure about the chemical results the analyses are considered qualitative (rather than quantitative), and this is indicated in the relative tables. The SEM-EDS employed was a Hitachi SU3500 fitted with a back-scattered electron (BSE) and a secondary electron (SE) detector for imaging, and an energy-dispersive X rays spectrometer (EDAX) for compositional analysis. The low vacuum mode was operated with a chamber pressure of 80 Pa, accelerating voltage at 20kV and at a working distance of 10mm, with acquisition times of 60 seconds. Compositions were normalised to 100wt% to facilitate comparability and data was rounded to one decimal place. Compositions below the detection limit of the measured element are reported as bdl (i.e. below detection limit, or <0.1wt%). Unless noted otherwise, all results in this thesis are normalised to 100% and given as wt%. All SEM micrographs shown in this thesis are BSE images. To verify the reliability of the chemical data retrieved by SEM-EDS, reference standard material was analysed selecting what was deemed the most appropriate among the certified material available in the laboratory. Three samples of glass (SGT 7, 10, 11) and two samples of steel (16C_ARMI and ZRM 193-1) were analysed to test reliability on blast furnace slag and metal samples respectively. The standard data tables are given in Appendix B.1.

5.3 RESULTS: OBJECTIVE 1 - CONNECTION BETWEEN BLAST FURNACE AND EXCAVATED SLAG HEAP

5.3.1 Silica-rich Slags

The fragments hand-collected from the slag heap nearby the blast furnace (termed blast furnace finds 1-5, table 5.1) are compared with the fragments of blast furnace slag recovered during excavation (Chapter 4, section 4.4.6). A likely connection between the operations performed at the blast furnace site and those represented by the material excavated at SH1 was identified during the visual analysis. In particular,

among the excavated material, there were both individual slag fragments with the typical glassy appearance and fragments embedded both in the iron-rich slags and in conglomerations of material (chapter 4). Many of the embedded slag fragments were identified only during the microscopic analysis, supporting the observations made during the visual analysis, which pointed to the use of lumps of blast furnace slags in the process of fining pig iron (see discussion below).

Therefore, the chemical study performed on silica-rich slag fragments has two main objectives:

1. To confirm that the glassy slag on SH1 was produced from smelting iron ores in the blast furnace located to the south of the site

To this end the chemical composition of slag fragments and inclusions - metallic and non-metallic - is investigated. This analysis in turn can offer information on the smelting system itself: temperatures reached in the furnace, type of ore and fuel employed, use of fluxes and the nature of the metal produced.

2. To verify that fragments of blast furnace slag were employed in the fining operation

The intentional use of blast furnace slags during the fining of iron is only mentioned in a couple of sources in the literature (Mackenzie and Whiteman 2006, Guénette-Beck and Serneels 2007). However, Percy describing the Italian version of fining pig iron (Lombardy process) states that the presence of lime and magnesia in finery slag, in the order of 6wt% and 2wt% respectively, is attributed to the blast furnace slag ‘with which the cavernous pig iron is always impregnated’ (1864, 615). The aim here is thus to investigate whether the fragments of blast furnace slags are intentional additions (i.e. had a role in the oxidation of cast iron) or accidental (see discussion below).

In the following sections, the results of the chemical investigation are described. A discussion and interpretation of the data obtained is presented in section 5.7.1.

Chemical composition of blast furnace slags

Blast furnace slags usually have a glassy appearance and their colour ranges from blue and green to grey and black. The origin of the variations in colour of blast furnace slags is not completely understood; however, it is likely that the different

colours - sometime even observed on the same piece – reflect both the chemistry (presence of chromophore ions, such as Fe^{2+}, Ti^{3+} and S^{2-}) and the physical state and arrangement of these ions (White 1980, Chaouche *et al.* 2016). The colour of the blast furnace fragments studied here was recorded during sample preparation and labelling to enable a check on possible consistent chemical variations; however, no significant link was identified, apart from the expected variations in iron content.

Slags produced in the blast furnace contain four major constituents, which combine together during smelting to form a glassy slag; these are: silica (SiO_2), alumina (Al_2O_3), lime (CaO) and magnesium oxide (MgO) (White 1977). In addition to these oxides, blast furnace slags are formed by other minor but important constituents, such as ferrous oxide, manganese oxide, titanium dioxide and sulphur. Moreover, blast furnace slags produced using charcoal as a fuel, will also contain sodium (Na_2O) and potassium oxide (K_2O). The chemical composition of these slags, that is the mixture of oxides and weight percentage of each compound, can offer indications both of smelting conditions (temperature, efficiency of the furnace) and of the quality and nature of the metal product, cast iron. It might also be possible to identify or obtain some information on the iron ores and fluxes employed during smelting. The study of metallurgical slags thus is a microscopic investigation of their chemistry and mineralogy (Hauptmann 2014). Together with bulk analysis of the glassy matrix, the investigation of slags also tackles mineralogical phases and metal inclusions. The samples analysed here are described, where possible, following this order.

Glassy matrix

Slags produced in a charcoal blast furnace normally have a high silica content, a lime-rich bulk chemistry and low iron content (White 1977, Rehren 2008). All blast furnace slags examined here conform to these features. A comparison with published data on early charcoal blast furnace slag shows similarities confirming that these are ‘typical’ early blast furnace slag (table 5.2). Smelting is an heterogenous process and the chemical variations observed are not unusual: the composition of slags changes from ‘furnace to furnace’ - depending on the proportions and constituents of ores, other materials (fluxes, fuel) and on different operating practices - and to a certain extent also from ‘cast to cast’ in the same furnace (Josephson *et al.* 1949, 55).

Bulk chemical analysis performed on the surface finds (BFF 1-5, table 5.3 and appendix B.3) reveals a low iron content, which ranges from 0wt% in areas away from metallic prills or mineralogical phases, to *c.*10wt% in BFF 5. This indicates highly reducing conditions within the furnace and a good extraction of iron. The composition of BFF 5 is slightly different from the rest of the samples, showing lower calcium oxide levels (16.5wt%) and higher amounts of manganese oxide (10.7wt%) (table 5.3). These differences probably only reflect local variations within the single sample. In order to discuss the main oxides in general terms, the following averaged data is obtained from samples BBF 1, 2, 3 and 4, which show a more homogenous chemical composition. Lime (calcium oxide, CaO) ranges from 26.7wt% to 32.4wt%, with an average content around 29.7wt%; these high values suggest the use of limestone as a fluxing agent (see discussion below). On the contrary, the low concentration of magnesium oxide, with a mean around 1.9wt%, indicates that the limestone used was not dolomitic and that the iron ore employed contained low levels of magnesium. Silica, which also derives from the ore, shows an average content of 47.4wt% and average aluminium content is around 11.1wt%. The low alumina content points to low viscosity for these slags, which suggests a complete or nearly complete separation from the metal. No sulphur was detected in the glassy matrix of all samples; only in BFF 2 was found to be around 1.5wt% in areas adjacent to ‘bands’ of manganese sulphide (see below). Of interest is their manganese levels, which display an average content around 6.3wt%. Manganese minerals often occur together with iron ores. In Europe many limonites and siderites iron ores are manganiferous, with large deposits found in the UK, Germany, Austria, Scandinavian countries and Eastern Europe (Rostoker and Bronson 1990, 20; Iles 2011, 325). High values of manganese are also found in bog ores (Crew *et al.* 2011), while lower concentrations are usually seen in magnetite and hematite iron ores. Moreover, high levels of manganese in blast furnace slag have also been attributed to the re-smelting of old bloomery slags (Starley 1995). Characterised by a high iron content, old bloomery slags were in fact reused in the early stages of smelting with blast furnaces, as the highly reducing conditions achieved in the tall furnaces permitted the extraction of the iron ‘lost’ to the slag (as fayalite) during direct smelting (i.e. bloomery technology; chapter 2).

Table 5.2. Published analysis of blast furnace slags from Europe and North America of the 13th through 19th century. Only charcoal furnaces have been selected.

BF Slags	Na_2O	Mg O	Al_2O_3	SiO_2	P_2O_5	K_2O	CaO	TiO_2	MnO	Fe_2O_3
Guénette-Beck and Serneels, Dürstel 13th century	-	2.5	15.5	38.7	0.6	1.4	35.4	0.8	0.1	4.8
Rehren and Ganzelewski, 1995, Jubach 14th-15th century *(XRF analysis)*	0.2	1.5	20.1	56.6	0.1	4.8	1.2	-	5.1	13.0
Dillmann *et al.* 2003, Glinet, 16th century	0.1	1.0	7.4	60.7	0.08	1.5	14.5	0.5	2.1	11.5
Crossley 1972, Sussex 16th century	-	9.6	19.2	45.5	-	-	20.6	-	4.8	0.05
Rostoker and Bronson, Cannock 16th - 17th century	-	7.2	23.2	49.7	-	-	11.9	-	3.3	4.4
Tylecote 1992, Sharpley Pool 17th century	-	12.0	11.4	49.3	tr.	2.0	22.8	-	0.8	2.7
Tylecote 1992, Coed Ithel, 17th century	-	8.4	7.3	62.8	0.1	-	15.9	0.3	0.4	4.7
Tylecote 1992, Duddon 18th century	-	3.6	12.4	56.4	-	-	14.6	-	9.8	2.6
White (1980), Hopewell 19th century	-	17.3	9.9	51.3	-	-	16.0	-	0.6	4.0
White (1980), Trumbull 19th century	-	3.7	16.0	48.5	-	-	26.5	-	1.7	1.0
Gordon 1997, Mount Riga (USA), 19th century	-	1.5	14.0	53.0	0.15	-	25.0	-	2.3	0.05

Table 5.3. Chemical composition of blast furnace slag finds (collected near the blast furnace). Blick (1984) analysed a fragment of blast furnace slag from the same slag heap near the furnace (chapter 3). His results obtained using a microprobe are shown for comparison. Na_2O was not detected here. Refer to Appendix B.3.

Bulk Compositions BF SLAG FINDS	**MgO**	**Al_2O_3**	**SiO_2**	**SO_3**	**K_2O**	**CaO**	**TiO_2**	**MnO**	**Fe_2O_3**	**N° Analyses**
Glassy matrix (BFF 1)	1.8	11.2	47.8	-	2.3	28.9	0.3	6.7	1.0	(1)
Glassy matrix (BFF 2)	1.8	11.7	47.3	-	2.4	26.7	0.3	5.6	4.0	(3)
Glassy matrix (BFF 3)	1.8	10.9	47.7	-	2.2	30.7	-	6.7	-	(2)
Glassy matrix (BFF 4)	2.0	10.4	46.7	-	1.8	32.4	-	6.2	1.6	(3)
Glassy matrix (BFF 5)	2.0	9.3	48.3	-	2.7	16.5	0.5	10.4	10.7	(3)
Average of BFF 1,2,3,4	1.9	11.1	47.4	-	2.2	29.7	0.3	6.3	2.2	(9)
Blick 1984 (microprobe)	*2.5*	*12.0*	*58.0*	*0.1*	*0.8*	*23.4*	-	*0.2*	*2.9*	*?*

The blast furnace slags recovered at slag heap SH1 are of a similar composition; there are however some differences in the amount of silica, lime and manganese oxides (table 5.4). In particular, the blue and black fragments show higher silica content with a mean value of 54.2wt% and lower lime, which is around 21.9wt%. Manganese is slighter higher, averaging to 7wt%. The green fragments demonstrate a similar pattern of silica and lime content (mean values of 53.8wt% and 26.9wt% respectively), while manganese oxide is as low as 0.7wt%. The chemical results obtained on two samples of the so-called 'intermediate' silica-rich slags recovered in trench PN1/QN1 context 7 show some differences (see chapter 4, section 4.4.5). While the major oxides of silica, lime, alumina and magnesium are consistent with the rest of the analysed samples, no manganese was detected, either in the matrix or in the cast iron prills. Moreover, with the exception of the two samples from context 7, all blast furnace slag examples display a consistent 0.3wt% average content of titanium oxide, another constituent that derives from the mineral ore.

All analysed samples are low in iron, the blue and black slags containing around 1.6wt% and the green pieces 2.8wt%. A mean of around 3wt% is measured in the

two samples from PN1/QN1 context 7 (table 5.4). Similar variations are observed in the blast furnace slag inclusions found embedded in iron-rich conglomerations of material and the fragments selected from the matrix samples (table 5.4). Overall, the results obtained for the blast furnace slags from the blast furnace area and from the slag heap SH1 form a fairly coherent group and were most likely produced using the same materials and operating conditions.

Table 5.4. Chemical compositions of blast furnace slag fragments from trenches PN1 and QN1. The first two rows display the results on green and blue fragments. The following rows show the results from blast furnace slag inclusions found embedded in iron-rich conglomerations and in fragments of blast furnace slag recovered from the matrix sample.

Bulk Composition (SH1)	**Na_2O**	**MgO**	**Al_2O_3**	**SiO_2**	**SO_3**	**K_2O**	**CaO**	**TiO_2**	**MnO**	**Fe_2O_3**	**N° Analyses**
Green BF	0.5	2.2	12.6	53.8	-	1.5	26.9	0.3	0.7	2.8	(7)
Blue/Black BF	0.5	1.4	9.7	54.2	bdl	3.2	21.9	0.4	7.0	1.6	(8)
Intermediate (Si-rich)											
PN1/QN1_CXT7_BFFe	-	2.1	13.9	55.4	-	3.3	22.1	-	-	3.2	(2)
PN1/QN1_CXT7_GREEN	-	1.8	13.3	54.8	-	2.4	25.0	-	-	2.7	(2)
BF in conglomerates											
QN1 CGBF	0.7	3.3	13.2	52.3	-	1.4	22.8	0.4	0.6	5.4	(2)
PN1 CGBF5	0.7	1.7	10.0	51.0	-	3.1	22.5	-	4.7	6.5	(2)
PN CGBFTP10	-	1.4	9.9	51.9	-	2.5	26.2	0.2	6.5	1.4	(2)
PN1 CGBF4	-	1.3	8.5	56.0	-	2.1	24.2	-	8.0	-	(2)
BF in matrix											
QN1 <0.50cm>0.25cm	0.8	1.9	15.2	55.9	-	4.5	16.6	0.4	0.3	4.6	(2)

Mineral phases and inclusions

The mineralogy of blast furnace slags has been little described, including that of modern materials (Young, 2014). The mineralogical phases observed derive from the gangue materials in the ore and are formed by the principal oxides SiO_2, Al_2O_3 and CaO, as well as iron oxides. The mineral phases observed in the glassy matrix of blast furnace slags usually belong to the pyroxene or pyroxenoid mineral group with general formula MeO_xSiO_2 or $Me_xSi_xO_{3x}$ (Mihok *et al.* 2006, Desaulty 2008, 41). Other important mineral phases that form blast furnace slags are part of the olivine groups ($2MeO_xSiO_2$) and of the group of gehlenite and melilite (Mihok *et al.* 2006, 163). Moreover, it is possible sometimes to detect the remnants of the mineral ores that did not melt during reduction, as well as metallic prills and charcoal fragments entrapped in the slag.

Some interesting features are observed in two slag samples analysed in this study (BFF 2 and BFF 3, figure 5.2). The first feature of interest is the presence of rectangular titanium-rich crystals. They appear together with elongated 'bands' of manganese sulphide (MnS), whose appearance suggests that they formed in a liquid, and newly formed cast iron prills (figure 5.2 and table 5.5). Moreover, the surrounding glassy matrix is characterised by the presence of wollastonite crystals ($CaSiO_3$) of various size. The glassy matrix surrounding these features shows an average sulphur content of 1.5wt% (see BFF 2 in Appendix B.2), which suggests that sulphur possibly comes from the ore rather than from the use of mineral fuel such as coke (see discussion below). Possible ore residues have also been analysed, including what appears to be chalcopyrite, which seems to support this observation (figure 5.3). Additionally, inclusions of calcium sulphate ($CaSO_4$, *gypsum*) are also observed in BBF 3 (figure 5.2 bottom left and table 5.5). The addition of limestone or lime-containing materials had two main effects on the smelting system: lowering the melting point of the slag and lowering the sulphur content of the metal produced by solubilisation of calcium sulphate (SO_4) or sulphide (SO_3) (Rostoker and Bronson 1990, 110). The reaction being:

$$S_{ore} + O_2 \rightarrow SO_2$$

$$2SO_2 + O_2 \rightarrow 2SO_3$$

$$2CaCO_3 + SO_2 + SO_3 \rightarrow CaSO_3 + CaSO_4 + 2CO_2$$

Given the appearance of these inclusions (flat crystals of growing gypsum) and their proximity to the MnS bands it is suggested that they formed inside the furnace as solid precipitates. This seems to confirm the addition of limestone to the furnace charge (see discussion below). However, some iron ores contain sulphur in the form of calcium sulphate, which is difficult to remove by roasting (see for example Tylecote on the iron ore employed at Panningridge, Sussex, in Crossley 1972, 67). Such iron ores would therefore produce pig iron with a sulphur content up to 0.20wt%. For the slags of Ausewell Wood, it appears that the addition of limestone and the manganese content of the iron ore, favoured the absorption of sulphur into the slag, producing a pig iron with low levels of sulphur (see section 5.4.4 and discussion in chapter 6, section 6.1).

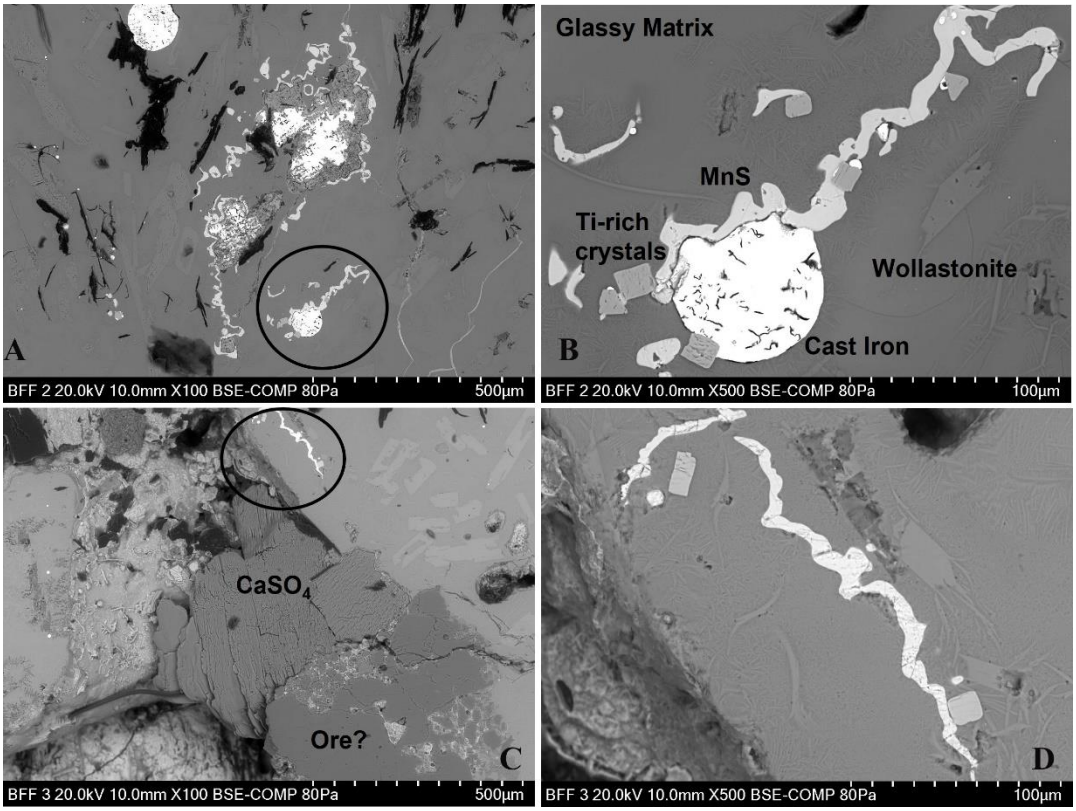

*Figure 5.2. **A** and **B**: BSE images at 100x and at 500x, respectively, showing titanium-rich crystals, MnS bands together with newly formed grey cast iron prills. In the glassy matrix wollastonite or pseudo-wollastonite crystals are also visible. **C**: BSE images at 100x, showing a $CaSO_4$ precipitate, near possible ore residues and iron oxides. The circled area is shown in **D** at higher magnification (500x), focusing on titanium-rich crystals and bands of MnS.*

Table 5.5. Chemical composition of phases and inclusions observed in BFF 2 and BFF 3. The oxygen detected in MnS is almost certainly from the surrounding areas.

Phases/Inclusions	**MgO**	**Al_2O_3**	**SiO_2**	**SO_3**	**K_2O**	**CaO**	**TiO_2**	**MnO**	**Fe_2O_3**	**N° Analyses**	
Wollastonite crystals	1.0	3.4	46.9	1.2	0.7	39.9	0.6	4.2	4.9	(10)	
Ti-rich crystals	0.6	3.0	12.4	1.6	0.6	6.8	68.4	2.8	3.9	(6)	
$CaSO_4$	-	1.0	6.9	49.2	0.3	38.1	-	0.5	4.1	(3)	
MnS	**Mg**	**Al**	**Si**	**S**	**K**	**Ca**	**Ti**	**Mn**	**Fe**	**O**	**N° An.**
	0.5	2.3	7.5	24.8	0.8	6.2	0.4	40.3	3.6	13.9	(6)

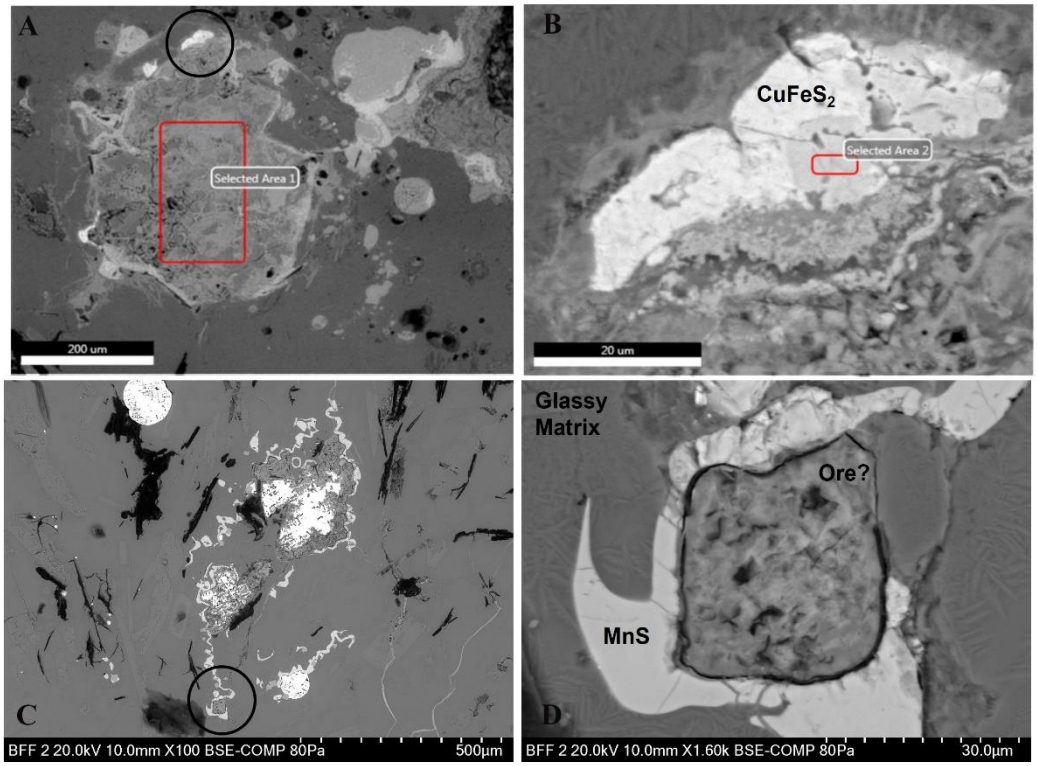

*Figure 5.3. BSE images showing possible ore relict in BFF 2. **A**: micrograph displays an area with mineral ore remnants. The circled area (in black) is shown in **B** at higher magnification (x1.70k): the white/light grey areas have a composition similar to chalcopyrite. **C**: micrograph (at 100x) showing another area of the same sample with possible mineral ore and MnS forming out of the minerals. The black circled area is shown in **D** at higher magnification (x1.60k). The surrounding glassy matrix displays a sulphur content as high as 2.4wt%.*

Of a similar chemical composition are the mineral formations (pyroxenes and pyroxenoids crystals) and mineral ore relics identified in the blast furnace slags excavated at SH1. Indeed, there is a consistency between the elements measured in all slag pieces from both sides of the ironworking complex. This is evident not only in the bulk composition of the glassy matrix (table 5.4) but also in the mineral residues which show high contents of silica and manganese, as well as traces of titanium and vanadium (Appendix B.2). Some copper is also detected, indicating that these are indeed relics of mineral ores. The presence of copper deposits on Dartmoor, including at Ausewell Wood, is well documented (Page 2004, Newman 2010), hence the presence of copper minerals is not surprising (chapter 6).

Metal prills

Metal prills entrapped in slags provide information on the nature and composition of the metal produced. All blast furnace slags analysed for this study (surface finds and excavated examples) contained prills of grey cast iron. The composition of the metal prills in the blast furnace finds (BFF 1-5) are shown in table 5.6. Metallography and chemical analyses revealed the same microstructural features and chemical composition for all samples, including the variety of non-metallic inclusions. These are discussed in more details in the metals section (5.4.4). The microstructure of grey cast iron is characterised by the presence of flake (lamellar) graphite; accordingly, bulk chemical analyses reveal sufficient silicon content to encourage the formation of graphite and suppress the formation of cementite (Higgins 1993). The size, shape and distribution of the flakes is determined by the presence of impurities, as well as by cooling rates (Scott 1991, Hatton *et al.* 2011). The shape and distribution of the graphite in cast iron, as well as the microstructure of the metal matrix are described following the nomenclature and classification established by ASTM International (2019).

The shape and distribution of the flakes observed in prills entrapped in the Ausewell Wood slags vary, exhibiting different types of arrangements identified by standard classification (figure 5.4 and 5.5). This is likely due to the different cooling rates to which these trapped metals are subjected after reduction and after leaving the furnace in a liquid melt, as well as to an incomplete homogenisation of the final melt (figure 5.6). However, the most common microstructure, observed in the ‘final’ metal (section 5.4.4) is of type A (figure 5.5), which corresponds to a uniform distribution and random orientation of the flakes and is the form usually observed in grey cast iron (Radzikowska 2004). The matrix is pearlitic with some ferrite adjacent to the graphite flakes. Numerous islands of steadite are observed (figure 5.7). Steadite is a low-melting binary or ternary eutectic of ferrite and iron phosphide (Fe_3P) or ferrite-Fe_3P and iron carbide (Fe_3C) and is a common characteristic constituent of grey cast iron. The presence of phosphorus in most early cast iron reflects the presence of phosphorus in the mineral ores employed (Percy 1864). The very low phosphorus content analysed in the blast furnace slags indicates the complete reduction of the phosphorus contained in the ore, a feature that is common to cast iron produced in blast furnaces (see for example Dillmann *et al.* 2003). The cast iron prills also

contain inclusions rich in titanium and vanadium (figure 5.7). Their chemical characterisation is hindered by the small size of the inclusions and the consequent contamination from the surrounding matrix. However, the presence of Ti, V, and in at least two inclusions of niobium, Nb, is consistently measured in small cubic crystals observed in the metal matrix, confirming that these are carbide and/or nitride inclusions, commonly found in cast iron. They form when nitrogen and carbon, which are present in high quantities in the air passing through a blast furnace, combine with metals contained in the ore and precipitate as small inclusions during cooling of the melt.

The chemical composition of the entrapped prills show high contents of silicon and manganese, reaching 10wt% in BFF 1 and 4.4wt% in BFF 4 (table 5.6), respectively. A much lower composition is measured in the cast iron fragments identified in SH1 (section 5.4.4, table 5.14), which more securely represent the final product (pig iron) of the smelting operation. This discrepancy could result from an incomplete or different homogenisation of the liquid metal from which these prills separated, which then results in inhomogeneous concentrations in different areas of analysis. Indeed, the reactions that take place in the liquid bath between cast iron and other constituents (slag, fuel, fluxes etc.) is still not completely understood (Arribet-Deroin 2001, 586). Moreover, it is likely that small metallic inclusions react with the surrounding matrix displaying high silicon contents, as in BFF 1 (Girbal 2011). Their compositions therefore do not necessarily represent the ratios of the alloying elements in the final product but can offer some insight into the technology and smelting system that produce them.

Table 5.6. Chemical composition of cast iron prills of different sizes observed in the blast furnace slag finds. Note the high silicon and manganese contents, as well as the presence of phosphorus. Detected oxygen is contamination from the surrounding areas. Data normalised to 100%.

	O	Si	P	Ti	Mn	Fe	N° Analyses
BFF 1	11.0	10.0	0.5	-	3.2	74.5	(2)
BFF 2	3.2	3.5	0.5	bdl	3.7	88.8	(3)
BFF 3	4.1	2.5	0.3	bdl	3.3	89.6	(3)
BFF 4	3.7	5.4	0.4	-	4.4	85.8	(2)
BFF 5	4.8	4.4	0.3	bdl	3.7	86.5	(3)

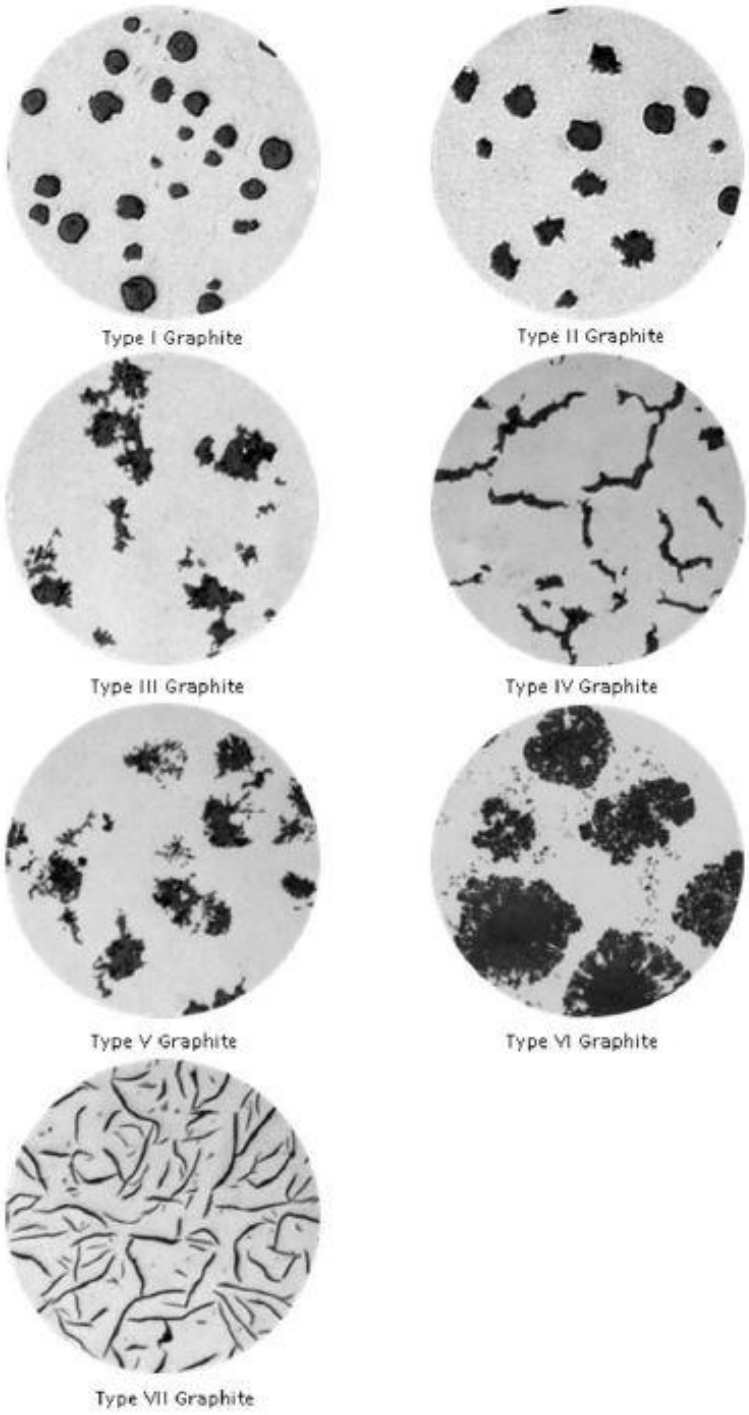

Figure 5.4. Classification of graphite types found in cast iron (after ASTM, A 247-19). Type VII is the form usually found in grey cast iron. Figures are shown for comparison.

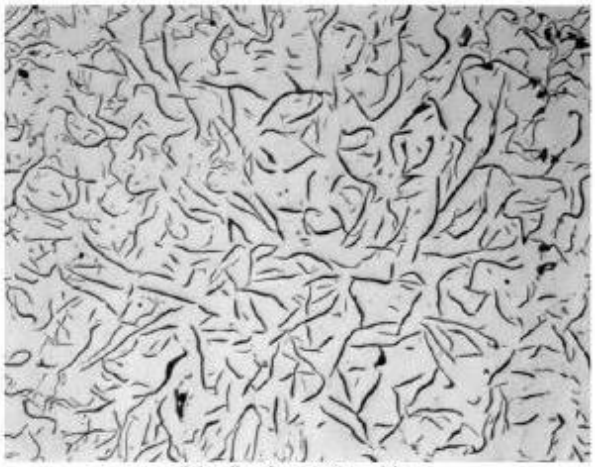
Distribution A Graphite


Distribution B Graphite


Distribution C Graphite

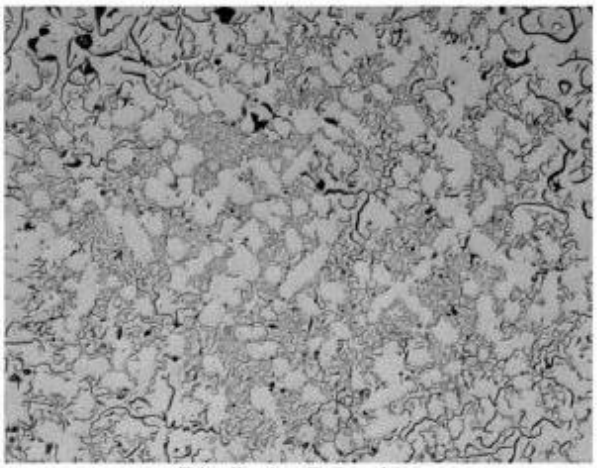
Distribution D Graphite

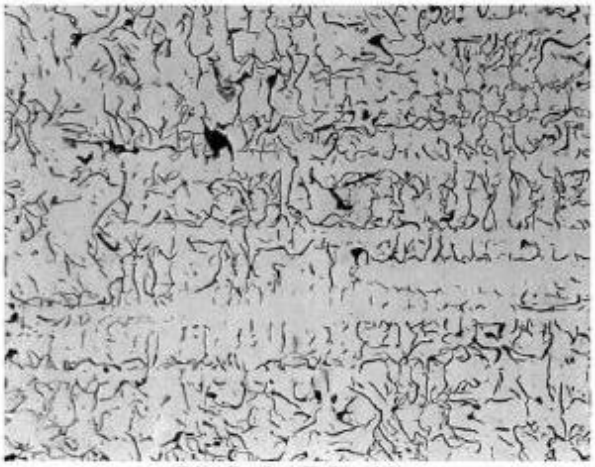
Distribution E Graphite

Figure 5.5. Classification of graphite flakes distribution used to sort type VII graphite flakes in grey cast iron (after ASTM, A 247-19). Figures are shown for comparison.

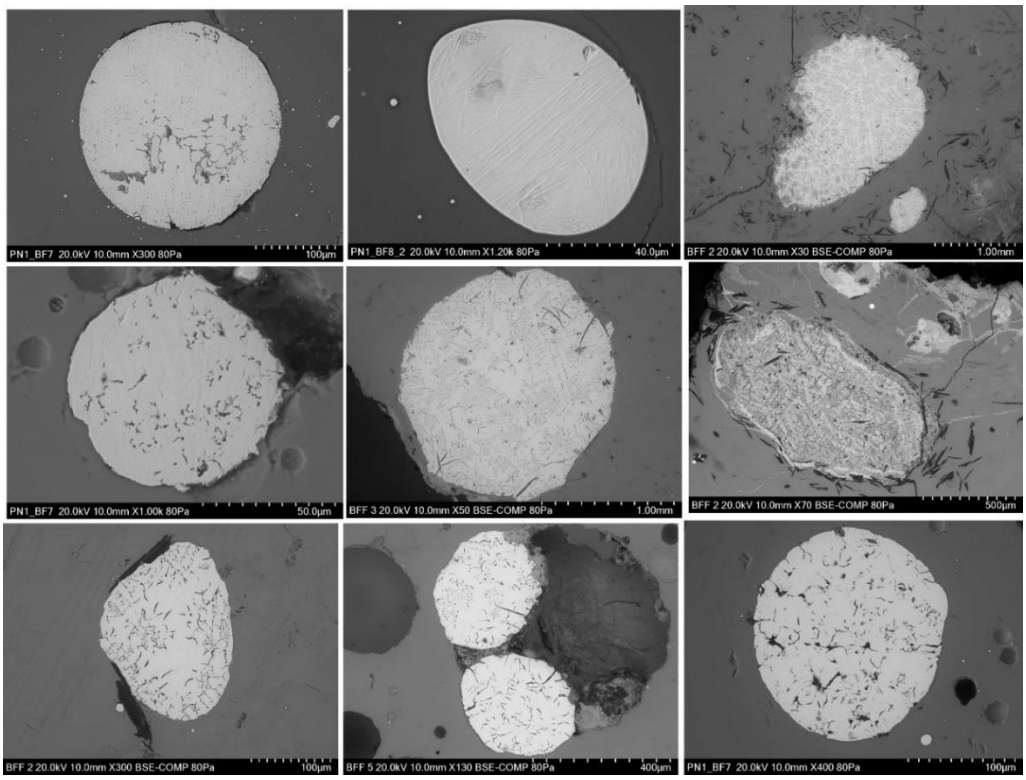

Figure 5.6. BSE micrographs showing trapped cast iron prills in BBF slags in Ausewell Wood samples with increasing carbon and silicon content and different distribution and size of graphite flakes.

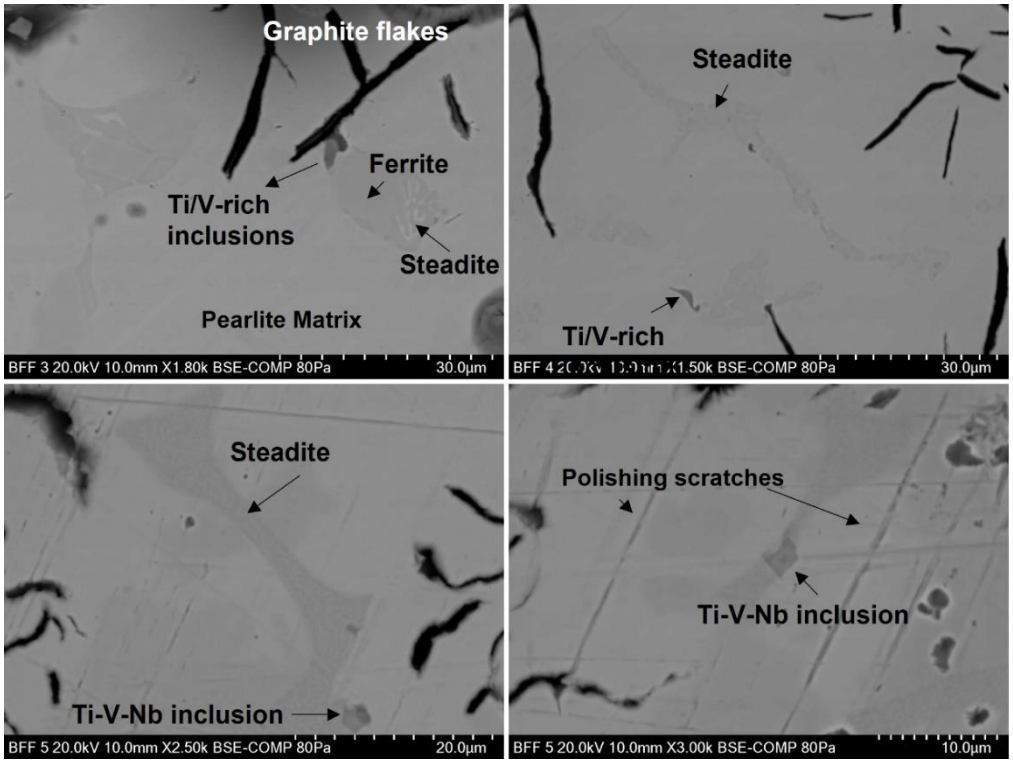

Figure 5.7. BSE micrographs showing the microstructure of cast iron prills in blast furnace slags. Note the ferrite islands near the graphite flakes and the proximity of Ti-V-Nb inclusions with the phosphorus eutectic.

5.3.2 Conglomerates

Another class of material that appeared the most telling in establishing a connection between the blast furnace and the excavated slag heap were the conglomerations of material. These were identified during the visual analysis by their round shape, suggestive of stirring operations, and for the presence of inclusions of fragments of blast furnace slag together with iron-rich slag and metallic inclusions (chapter 4, section 4.4.2). The microstructures reflected this visual interpretation revealing a mixture of materials: fragments of fayalitic slag and blast furnace slag, hammerscale, oxidised cast iron, charcoal and sand embedded in an iron-rich matrix, most of which represents iron corrosion (figure 5.8 and 5.9 at higher magnification). Sometimes samples were initially taken to examine metal scrap and proved to show many different materials under the microscope. The chemical analysis of the blast furnace slags identified is reported in table 5.4 and shows features and compositions similar to the rest of the blast furnace slag examples analysed here. The slaggy conglomerations are currently identified as residues of the slag bath created in the finery hearth to promote the oxidation of pig iron (see discussion 5.7.2). In bloomery smelting, such amalgamations of material are interpreted as smithing waste or remains of working floors (smithing pan) due to the presence of hammerscale and charcoal (see for example Girbal 2011). However, the abundance of oxidised cast iron prills and fayalitic slag suggest that they formed inside the fining hearth (figure 5.9). The chemical composition of the fayalitic slag is consistent with the composition measured on the large pieces of tap slags (see table 5.7 in section 5.4.1 and Appendix B.2). The microstructure is characterised by a high quantity of wüstite and fayalite, with a small quantity of glassy phase. Often wüstite is seen oxidising out of cast iron prills, a clear indication of oxidising conditions (figure 5.9): the metal loses some of its iron which reacts with silica to form slag (see also section 5.4.4 and discussion).

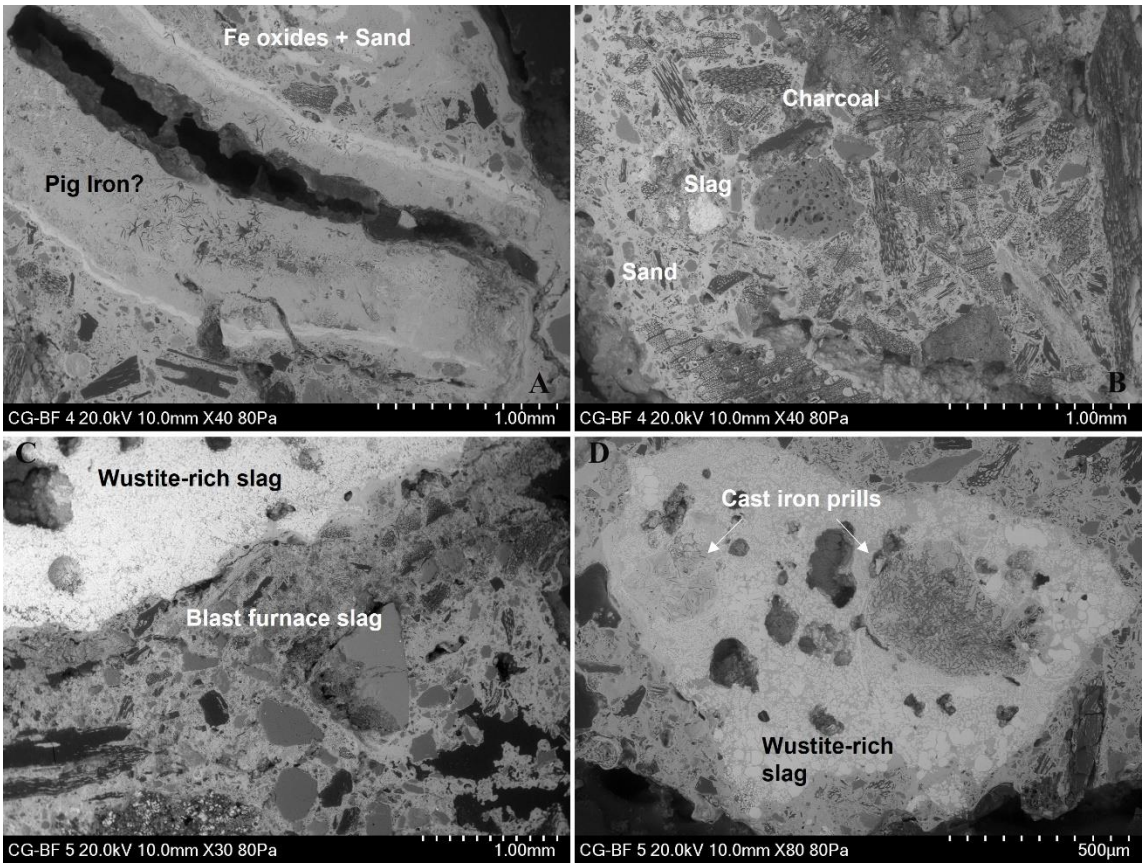

Figure 5.8. BSE micrographs showing the microstructures of examples of conglomerates. A (top left): a possible pig iron fragment, note the rectangular feature, with oxidised graphite flakes and a layer of iron oxide (light grey) highlighting the original surface of the fragment. ***B*** *(top right): the image shows a mixture of sand and charcoal and a small fragment of wüstite-rich slag.* ***C*** *(bottom left): the image shows a fragment of blast furnace slag embedded in iron oxide and sand. A larger fragment of wüstite-rich slag is visible on the top left.* ***D*** *(Bottom right): image shows a wüstite-rich slag with cast iron prills, surrounded by sand. Also refer to figure 5.9 and text for interpretation.*

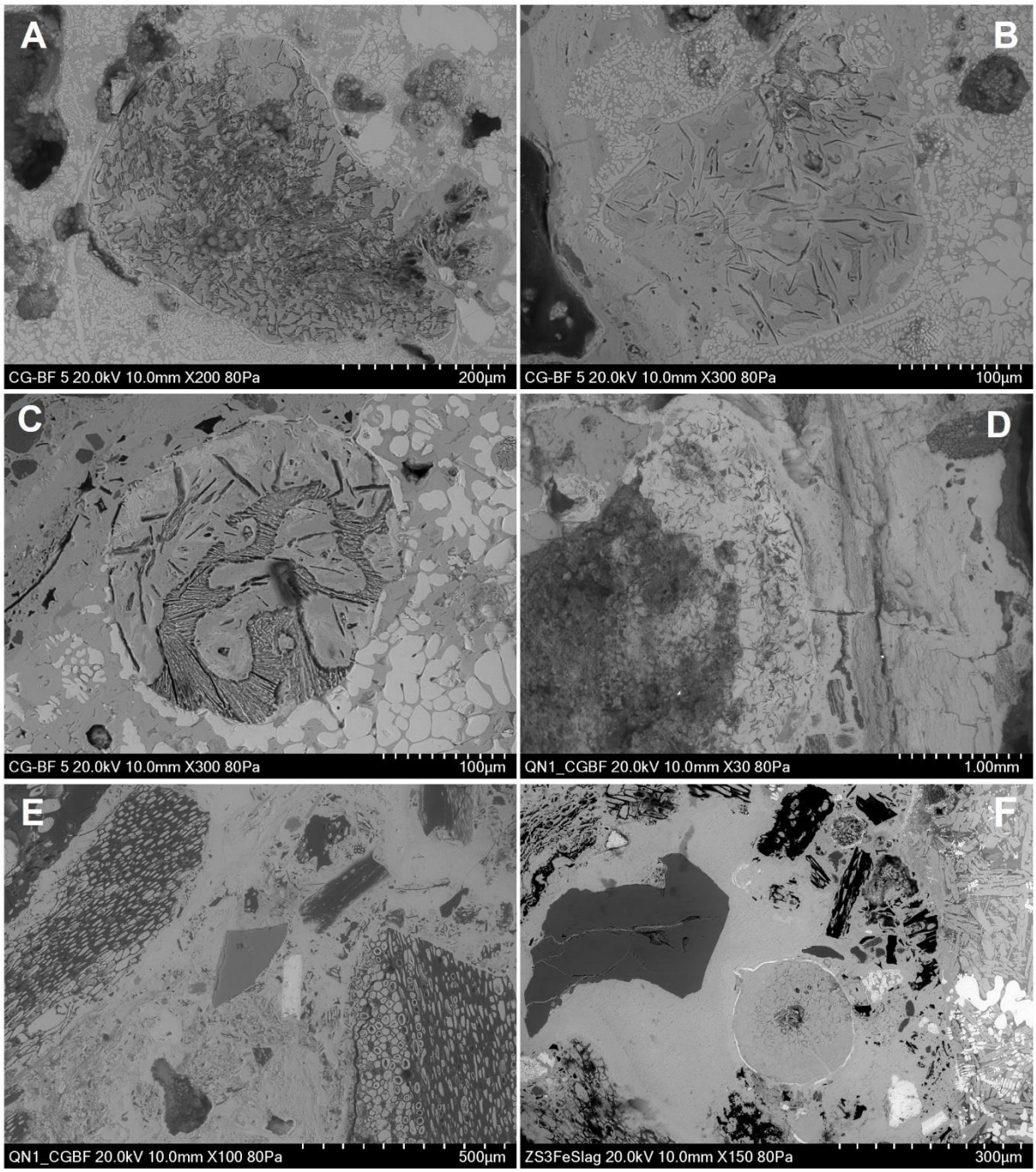

Figure 5.9. BSE micrographs showing the microstructure of conglomerates' samples. ***A***, ***B*** *and* ***C*** *shows wüstite oxidising out from what was probably grey cast iron.* ***D*** *display an inclusion of blast furnace slag (top left corner) with oxidised grey cast iron and iron oxides to the right.* ***E*** *and* ***F*** *show the range of inclusions observed, including spheroid and flake hammerscale, quartz, sand, charcoal and fayalitic slag (right of F).*

5.3.3 Ore samples

The ore samples found near the blast furnace and analysed for this study do not appear related to the iron smelting operations. They are more likely connected to later metallurgical activities performed on site. From historical documentation collected by Brown (1997) it is known that extractive activities were carried out at Ausewell Wood during the 18th and 19th century. In particular, there are references of a lease of 1791 to ore dressing processes and extraction of tin, copper and iron. Moreover, in 1830 tin was extracted at 'the myn ay Hzwell Hazwood' (Brown 1997, 7). The chemical analysis of these fragments displays the presence of silica, iron and tin strongly suggesting that this material come from these more recent activities (Appendix B). Field evidence and geochemistry (Carey 2003) suggest that the ore-dressing works used the main leat of the ironwork complex, overlying and modifying part of it (Cranstone 2004a). One piece (Ore_3) also shows high levels of arsenic, which is consistent with the study performed by Carey (2003) on the dressing floors 1 (DF1, refer to overall plan in figure 3.3, chapter 3) located near the blast furnace, and with the local geology characterised by arsenopyrite and chalcopyrite (Page 2004, 7-8).

Given that these ore samples are not connected to the technologies investigated for this study, they will not be discussed further. Their chemical composition is shown in Appendix B.2.

5.4 RESULTS: OBJECTIVE 2 – CHARACTERISATION OF FINERY TECHNOLOGY

The excavated assemblage from SH1 is characterised by a large quantity of iron-rich waste material, including both tap and hearth slags (chapter 4). This section deals also with the analysis of possible smithing slags and metal scrap (5.4.3 and 5.4.4). Finally, the results of stones and clay fragments are presented in section 5.5.

5.4.1 Finery Tap slags

This section presents the results obtained on the finery tap slags. A total of six samples were analysed: four cakes, one tendril and one plate (see chapter 4 and Appendix B for the position of sample cut). The 'flowed' cakes were not subjected to chemical analysis because some of their features were identified later in the research and only consequently a different slag subtype was created. However, it is likely that their chemical composition and microstructure are similar to the 'standard'

tap slag cakes presented here, and that the dissimilarities identified during the visual analysis do not necessarily correspond to different compositions. Nonetheless, their analysis would be interesting to assess such macromorphological observations and further investigate technological practices (see conclusions and future work in chapter 7).

Because their appearance resembles typical waste material coming from the bloomery process, the original excavation reports suggested that a bloomery process, possibly water-powered, may have produced them (Newman 1998, Juleff 2000; see discussion in previous chapter). The results of the visual analysis however, pointed to the finery technology as the likely origin for this waste material. Therefore, one of the aims of the scientific investigation performed for this study, was to identify the technology that produced these slags. Similarly to the blast furnace slags, the microstructures of the iron-rich slags is characterised by a glassy matrix and a series of crystal phases, as well as metal prills. These constituents can help distinguish between bloomery and finery technology. Discerning between these two processes, however, is not so straightforward. Both technologies in fact produce a fayalitic slag. Fayalite (Fe_2SiO_4) is an important constituent of metallurgical slags, and forms from the reaction between silica and iron oxides contained in the mineral ore. Predictably thus, the bulk chemical compositions of the tapped slags identified during the visual analysis are fayalitic (table 5.7). Between the large fayalite crystals (Fe sometimes partially substituted by *c.*1wt% Mg), a homogenous glassy groundmass is visible (figure 5.10 B, Appendix B.3). The composition of the glassy matrix was characterised chemically whenever large enough areas were observed giving the opportunity to analyse this phase alone. Albeit sometimes very small secondary fayalite crystals formed within the glassy matrix (figure 5.10 D). The average chemical composition is reported in table 5.7 (see also Appendix B.3). It shows an enrichment in alkali metal oxides (Ca, K and Na), alumina and phosphorus. According with observations made during the morphological analysis of the tap slags, many were formed of layers of overlapping slag. This is seen in their microstructures as layers of iron oxide (probably magnetite Fe_3O_4) where the slag had (partially) solidified before being covered by additional runs of slag (figure 5.10 A). In addition, their microstructures are also characterised by an abundance of well-formed dendrites of wüstite (FeO, figure 5.10 C, Appendix B.3). In a smelting

system, this iron oxide forms during reduction of the mineral ore, following the reaction Fe_2O_3 -> Fe_3O_4 -> FeO -> Fe. Its formation is thus a function of the efficiency of the reaction between slag and metal taking place in the furnace, and consequently a slag with little wüstite reflects efficient reduction (Morton and Wingrove 1972). In a finery hearth, on the contrary, wüstite forms because in order to remove the various impurities contained in the cast iron (such as Si, P, Mn and C), it is necessary to create an iron-rich slag that favours the oxidation of these elements. The excess free iron oxide, thus, is necessary to the process. Gordon indicates that “in fining, the slag had to have iron oxide in excess to that needed to form fayalite” (1997, 13) and therefore the abundant presence of wüstite, can be used to discriminate between finery and an efficiently run bloomery smelting process. Moreover, Gordon (1997) analysing bloomery, finery and puddling slag, indicated that finery slag could also be distinguished by the lack of exotic phases (such as leucite, hercynite etc.), which are usually found in bloomery tap slags. Accordingly, no other phases were identified in the tapped slag analysed here and a large quantity of the iron oxide present is in the form of wüstite.

Few metal prills have also been identified (figure 5.10 F); their chemical composition is reported in table 5.8. All metal inclusions are characterised by a high silicon content, going from 2.5wt% to 4.3wt% in larger prills observed in QN1 0-20_Large. A lower silicon content is measured in a few small iron droplets detected in PN1 20-40_small_Tap 14, which averages 1.6wt%.

The only exception to the microstructures described so far is represented by sample PN1 20-40_Tap13 (figure 5.10 E). Visually identical to the other tap slags analysed (see Appendix B, finery tap slag), its microstructure is characterised solely by elongated fayalite crystals in a glassy matrix. This fayalite morphology is typical of rapid cooling, which suggests that the slag solidifies outside the hearth installation. Wüstite is absent and no metal inclusions are observed. The chemical compositions of bulk and glassy matrix are reported in table 5.7 and apart from lower levels of calcium and slightly higher titanium content, do not display particular differences when compared to the other samples (Appendix B.3). Looking at the microstructure alone it is possible to tentatively suggest that this slag formed during the early stages of the fining operations, before the iron-rich slag bath was created.

Table 5.7. Average chemical composition of bulk and glassy matrix of tap slags. Bdl indicates below detection limits; - non detected. Data normalised to 100wt%. Number in () represents the number of analyses on one sample.

Label	Na_2O	MgO	Al_2O_3	SiO_2	P_2O_5	SO_3	K_2O	CaO	TiO_2	V_2O_5	MnO	FeO	
PN1 20-40 TAP 13	-	0.6	3.6	28.6	0.3	-	1.2	0.7	0.2	-	0.2	64.8	**bulk (2)**
	-	-	*9.8*	*35.5*	*0.6*	*bdl*	*3.2*	*1.6*	*0.4*	-	-	*48.8*	*glassy matrix (5)*
PN1 20-40 Run 12	1.2	0.8	2.6	16.7	0.7	bdl	1.1	1.9	0.2	-	0.4	75.4	**bulk (3)**
	1.5	*0.5*	*8.7*	*25.2*	*2.3*	*0.5*	*4.5*	*6.7*	*bdl*	-	*0.2*	*49.8*	*glassy matrix (4)*
PN1 20-40 TAP 14	-	0.7	2.4	12.1	1.1	0.2	0.5	1.7	-	-	0.5	80.9	**bulk (1)**
	1.3	*0.3*	*7.8*	*21.4*	*3.9*	*1.1*	*3.6*	*8.3*	*bdl*	-	*0.5*	*51.8*	*glassy matrix (6)*
QN1 0-20 LTP	1.4	0.7	3.0	19.1	0.7	bdl	0.9	1.2	bdl	bdl	0.3	72.4	**bulk (3)**
	1.8	*0.4*	*11.4*	*26.7*	*2.9*	*0.8*	*5.1*	*4.4*	*bdl*		*0.2*	*46.2*	*glassy matrix (4)*
PN1 0-20 ThinPlate	1.1	0.6	3.7	19.7	0.6	bdl	1.3	1.2	bdl	-	0.3	71.4	**bulk (3)**
	1.6	*0.4*	*11.7*	*25.4*	*2.7*	*0.9*	*4.9*	*4.1*	*0.1*	-	*0.2*	*48.1*	*glassy matrix (6)*
ZN1 0-20 TS	1.3	0.6	4.2	18.6	0.6	bdl	1.3	1.4	0.2	-	0.4	71.6	**bulk (4)**
	1.2	-	*16.0*	*33.0*	*1.4*	*0.7*	*9.5*	*5.1*	-	-	-	*33.1*	*glassy matrix (4)*

Table 5.8. Average chemical composition of iron prills identified in the tap slag samples. Detected oxygen is contamination from the surrounding areas. Data is normalised to 100wt%. Bdl is below detection limits.

	O	Si	P	Ti	Mn	Fe	N° Analyses
PN1 20-40 Run 12	9.9	3.3	bdl	bdl	bdl	86.8	(3)
PN1 20-40 TAP 14	9.6	1.6	bdl	bdl	0.2	88.6	(3)
QN1 0-20 LTP	9.7	4.3	bdl	bdl	bdl	86.0	(4)
PN1 0-20 ThinPlate	10.4	4.0	bdl	bdl	bdl	85.6	(3)
ZN1 0-20 TS	7.4	2.5	bdl	bdl	bdl	90.1	(5)

A similar microstructure is observed in iron slags analysed by Lyalya *et al*. (2012) for a study on the differences between smelting and refining slags. In the African bloomery smelting system described in their study, after reducing and obtaining iron in the form of a slag-rich 'bloom' and before smithing, the bloom was treated further in a small furnace in order to remove impurities and enhance the iron yield (Lyalya *et al*. 2012, 196). This stage in between smelting and smithing produced its own slag, characterised by a flow texture. Notwithstanding the obvious differences between the two technologies (smelting vs. fining, African vs. post-medieval England), a similar origin is conceivable for the microstructure observed here. The aim of fining in fact was not only to reduce the carbon content of the pig iron, but also to clean the metal from the impurities – this operation took place before the proper 'fining' (decarburisation) and likely produced slags of various compositions (see section 5.4.2).

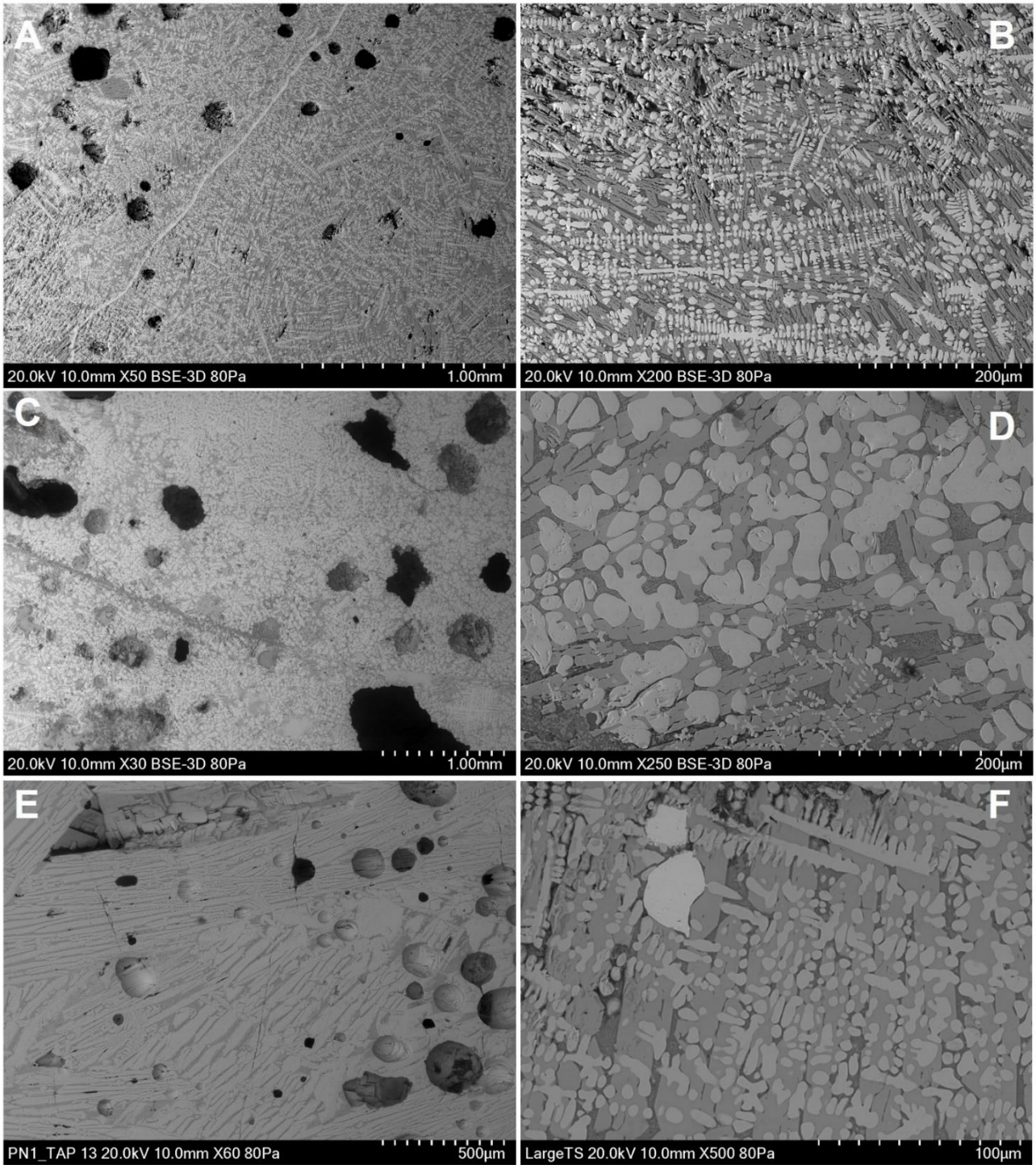

*Figure 5.10. BSE micrographs showing fayalite, glassy matrix and wüstite in finery tap slag samples analysed in this study. Note the high quantity of wüstite and solidification fronts in **A** and **C**. The dark rounded voids are porosity. Images **B** and **D** shows the microstructures at higher magnification, displaying numerous dendritic wüstite (white), fayalite crystals (light grey) and a dark grey glassy matrix in between the crystals. **E** shows the microstructure of the only example of finery tap slag without wüstite crystals; this is possibly a 'refining' slag that solidified outside the hearth and formed in the first stages of fining pig iron. Micrograph **F** shows the microstructure of the large tap slag retrieved from trench QN1 0-20 (Appendix B), displaying the presence of occasional irregular metallic prills.*

5.4.2 Hearth slags

Similar mineral phases are observed in two large samples of hearth slag cakes (ZN1 0-20_1 and ZN1 0-20_3) retrieved from trench ZN1 (figure 5.11, Appendix B). Their microstructures are in fact characterised by fayalite crystals, abundance of dendritic wüstite and a glassy groundmass. Once again, no exotic phases such as leucite and hercynite are observed. Solidification fronts are observed in this slag as well, suggesting that even though this slag was not tapped, it was kept in a liquid state within the hearth (figure 5.11). The results of the chemical analyses of the bulk and glassy matrix are shown in table 5.9 (Appendix B.3). Their composition is similar to the tap slags, including variations in phosphorus, alumina and alkali contents. All these features suggest that both tap and hearth slag result from the same process and installation. As with the tap slags, a few iron inclusions were found in both samples, containing high levels of silicon (between 2.9 and 4.0wt%) and phosphorus around 0.2wt%.

One sample of slag channel retrieved from JN9 was also analysed (figure 5.11). Most of the microstructure is characterised by wüstite, fayalite and glassy matrix. However, here the fayalite crystals are very large, and the interstitial glass is a minor component in comparison to the tap slags. Moreover, wüstite as well as being present as dendrites, is observed in some areas as very fine eutectic concentrated on fayalite laths. The variations in size and forms of these crystals are probably connected to the different cooling and solidification rates that the slag was subjected to as it ran out of the hearth. Its chemical composition shows lower levels of potassium, calcium and alumina oxides in comparison with the hearth cakes analysed, probably indicating less contact with the charcoal fuel and clay (from the hearth) as it likely formed inside a hole for draining the hearth installation from surplus slag. The glassy matrix on the contrary is enriched in these elements and is also characterised by a high phosphorus and sulphur content, with an average content of 8.0wt% and 1.7wt% respectively (Appendix B.3). Even though the slag channels have been visually identified as hearth slag, it is likely that they formed in connection to slag tapping, being fragments that solidified inside slag tapping holes.

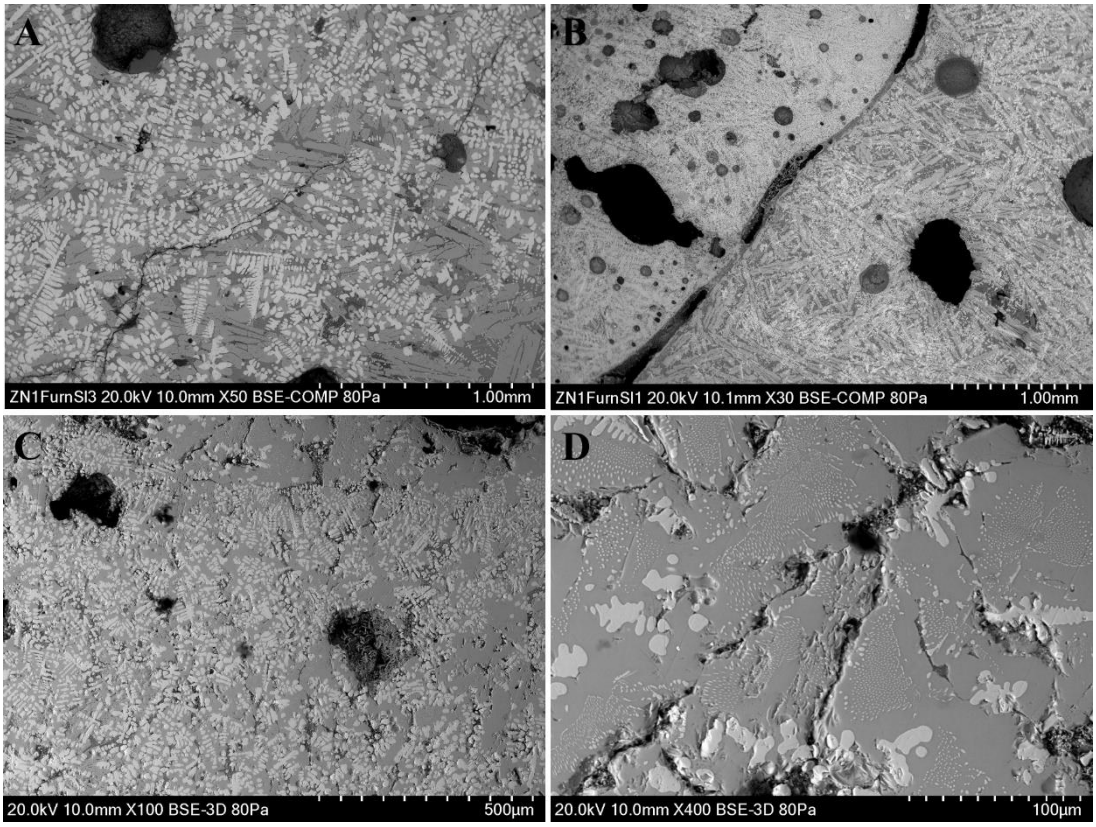

*Figure 5.11. BSE micrographs of hearth slag cakes. **A** and **B** show the microstructure of slags ZN1 1 and 3, characterised by a dark grey glassy groundmass, fayalite crystals (light grey) and dendritic wüstite. Crystals appear smaller than the finery tap slag, suggesting slower cooling rates. **C** shows the microstructure of the slag channel from trench JN9, with large fayalite crystals and abundant wüstite. **D**: micrograph of the same slag channel at higher magnification (400x). Note the eutectic wüstite on the large fayalite crystals.*

Table 5.9. Average chemical composition of hearth slags: ZN1_1 and ZN1_3 are samples from hearth 'cakes', while JN9 is from a slag channel. Data normalised to 100wt%. Number in () is number of analyses on one sample.

Label	Na_2O	MgO	Al_2O_3	SiO_2	P_2O_5	SO_3	K_2O	CaO	TiO_2	MnO	FeO	
ZN1 0-20 HS_1	1.4	0.6	3.9	18.0	0.6	-	2.2	3.2	-	0.3	69.8	**bulk (4)**
	1.3	*-*	*14.7*	*32.7*	*0.4*	*-*	*10.7*	*2.1*	*-*	*-*	*38.1*	*glassy matrix (3)*
ZN1 0-20_HS_3	-	0.8	3.1	16.9	1.2	-	1.2	2.1	-	0.3	74.4	**bulk (1)**
	1.8	*0.4*	*8.0*	*23.8*	*3.8*	*0.6*	*4.7*	*6.9*	*-*	*0.3*	*49.6*	*glassy matrix (4)*
JN9 20-40_Cyl 3	-	0.8	0.5	23.4	0.5	-	0.1	0.6	0.2	0.5	73.6	**bulk (3)**
	1.4	*-*	*5.9*	*19.4*	*8.0*	*1.7*	*4.3*	*5.3*	*0.1*	*0.3*	*53.7*	*glassy matrix (2)*

Rather different are the compositions and microstructure observed in two samples from the hearth slag RS1 20-40 (figure 5.12, Appendix B). Characterised by a red colouration and a rather rough texture this slag cake possibly formed inside the hearth installation. Its upper surface is characterised by an iron-rich concretion, probably a mixture of slag and metal (see figure 4.33 in chapter 4). Unfortunately, it was not possible to sample this area without breaking the entire piece. Given the crumbly consistency, it would have been necessary to consolidate the piece before putting it under the saw. However, this option was not available at the time; hence, it was preferred to preserve the piece for future analysis and sample the bottom of the piece from which it was rather easy to obtain fragments that could be mounted in resin blocks. The results obtained from the analysis of this piece are rather complex but of great interest. Some observations are put forward in the final discussion below. However, being the only piece analysed the validity of these observations are inevitably limited.

The microstructure is characterised by a variety of phases (see also Appendix B.3). Most of the microstructure is characterised by large crystals of fayalite and iron oxides, such as wüstite, and including possible corrosion products (figure 5.12 A and H). There is also some interstitial glass, containing an average 46.0wt% iron content and average silica of around 39.0wt% (Figure 5.12 B and table 5.10). Moreover, together with areas with high levels of calcium and phosphorus (figure 5.12 F and table 5.10), a variety of spinels are observed (figures 5.12 C, E and I). The spinels are characterised by the presence of Ti, V and Cr with possible substitution of these metals in iron aluminium spinels (table 5.10 and 5.13). They have angular shapes and often display an external halo rich in aluminium and a core enriched in Ti, V and Cr (figure 5.14 and table 5.12). Crystals that could be leucite are also observed, the high iron content measured might be contamination from the surrounding iron-rich area (figure 5.12, D and table 5.10). Finally, iron sulphides are observed in multiple-phase areas (figure 5.13 and table 5.11). The analyses obtained on this piece are only qualitative (tables 5.11, 5.12 and 5.13), given the small size of some phases it is likely that there is much contamination from the surrounding areas.

Table 5.10. Average chemical composition of crystals and phases observed in the hearth slag RS1. Refer to text and figure 5.12. Data are qualitative.

Na_2O	MgO	Al_2O_3	SiO_2	P_2O_5	SO_3	K_2O	CaO	TiO_2	V_2O_5	Cr_2O_3	MnO	Fe_2O_3	AREA/FIGURE
-	1.2	2.0	23.7	1.2	0.1	0.5	1.0	0.2	-	-	2.9	67.2	**A Fayalite -Grey crystals**
1.0	0.7	4.1	39.0	2.4	0.2	2.7	1.6	0.1	-	-	2.2	46.0	**B, Glass**
-	0.4	26.1	7.8	0.7	-	0.3	0.8	2.3	2.7	-	1.7	57.2	**C**
-	0.7	25.0	7.7	0.5	0.1	0.2	0.5	2.5	3.8	1.8	1.7	57.6	**E**
1.1	0.6	16.8	36.9	1.3	-	10.8	1.0	0.2	-	-	0.8	31.0	**D (Dark grey round)**
1.8	0.2	4.4	13.9	22.1	bdl	0.8	19.6	0.4	-	-	1.4	35.4	**F**
-	-	1.5	6.7	0.4	-	0.6	0.3	0.1	-	-	0.6	89.9	**H**

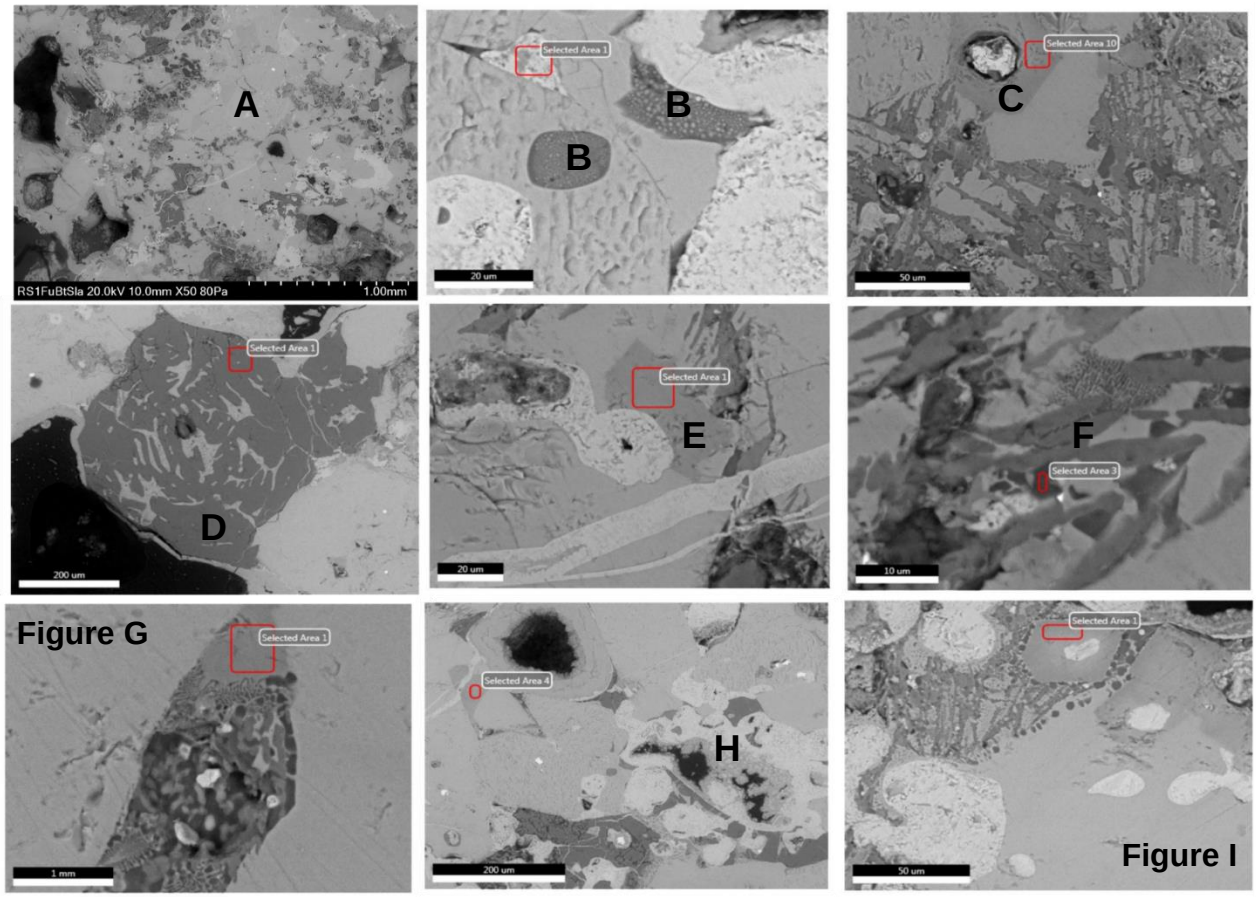

*Figure 5.12. BSE micrographs showing an overview of the microstructure and phases observed in the hearth slag RS1. Refers to table 5.10 above for qualitative data of the areas described. **A**: shows an overview of the microstructure, zooming in in figure **B** small areas of a glassy silica-rich matrix (dark grey) is visible and iron oxides (light grey) filling the voids in between the fayalite crystals (grey). Figure **C** shows areas characterised by high calcium and phosphorus levels (the streaked dark grey area) and spinels (where the letter C is) characterised by high titanium and vanadium levels. Figures **E** and **F** shows similar phases to C, at higher magnification. Note the angular shapes of the spinels in C and E. Figure **D** displays a possible leucite crystal, the iron content measured could be contamination from the surrounding matrix. Figure **G** displays an area with multiple phases: the white specks are iron sulphides. More details are given in figure 5.13 and table 5.11. Figure **H** shows iron oxides and possible corrosion products, while figure **I** shows more spinels, with high levels of titanium, vanadium and chromium (angular cored crystals). Refer to text for more explanation and figures 5.13 and 5.14 with corresponding tables.*

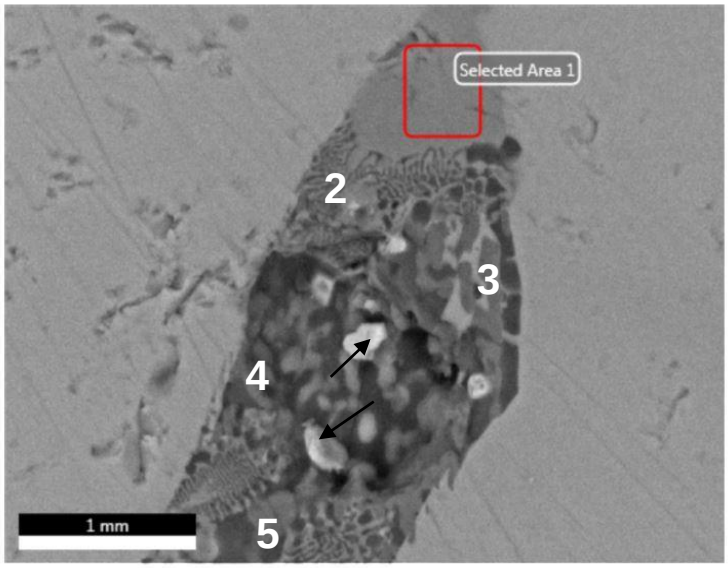

Figure 5.13. BSE image showing the multiphases area of figure G in 5.12. Refer to table 5.11 below for qualitative data of areas described.

Table 5.11. Average chemical analysis of areas in figure 5.13. Data are qualitative.

Na_2O	MgO	Al_2O_3	SiO_2	P_2O_5	SO_3	K_2O	CaO	TiO_2	V_2O_5	MnO	Fe_2O_3	AREA
-	0.7	26.9	8.6	0.4	0.2	0.3	0.6	3.7	1.3	1.8	55.6	**1**
0.8	0.3	20.7	19.3	2.6	0.4	1.7	1.9	2.5	0.5	1.8	47.5	**2**
1.4	0.3	6.1	18.7	15.6	0.7	1.8	14.4	0.2	-	1.8	39.0	**3**
2.4	0.6	7.3	22.0	15.0	0.6	2.2	13.9	0.4	0.2	2.0	33.4	**4**
2.0	0.5	15.1	21.7	10.2	2.1	2.3	7.9	1.5	0.1	1.5	35.2	**5**
O	**Na**	**Mg**	**Al**	**Si**	**P**	**S**	**K**	**Ca**	**Ti**	**Mn**	**Fe**	
18.8	1.4	0.4	1.3	4.3	2.0	21.1	0.4	2.9	0.1	0.8	46.6	**Black**
21.4	1.7	0.4	2.5	5.9	1.5	20.4	0.7	2.1	0.2	0.7	42.6	**Arrows**

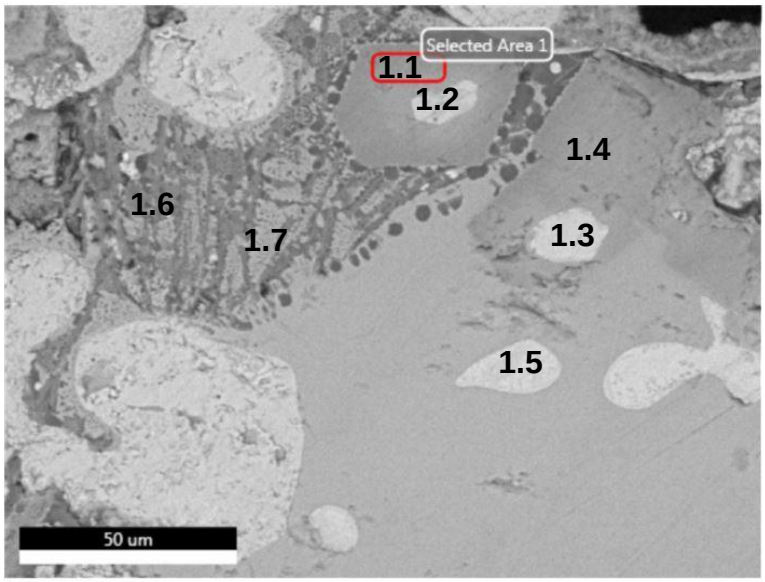

Figure 5.14. BSE image showing figure I in 5.12 of titanium- vanadium- and chromium-rich spinels. Refer to table 5.13 below.

Table 5.12. Average chemical analysis of areas in figure 5.13. Data are qualitative.

Al_2O_3	SiO_2	P_2O_5	SO_3	K_2O	CaO	TiO_2	V_2O_5	Cr_2O_3	MnO	Fe_2O_3	AREA
29.3	5.6	0.9	0.1	0.2	0.9	2.4	3.3	-	1.3	56.2	**1.1**
5.5	5.8	0.7	-	0.2	0.7	1.7	2.3	-	1.3	82.0	**1.2**
4.0	5.2	0.4	-	0.2	0.5	0.8	1.3	-	1.5	86.0	**1.3**
24.8	5.2	0.4	0.1	0.2	0.5	2.5	4.4	2.0	1.3	58.8	**1.4**
2.0	7.2	0.4	-	0.1	0.4	0.9	1.3	-	1.7	86.1	**1.5**
7.9	18.8	12.6	1.2	0.5	10.0	0.4	-	-	1.5	47.2	**1.6**
8.1	21.2	10.7	0.4	0.6	8.3	0.5	-	-	1.7	48.5	**1.7**

5.4.3 Smithing slags

The investigation of smithing activities focused on the analysis of the matrix samples (section 4.4.7, Appendix B). Flakes and spheroid hammerscale generally indicate the hot working of iron or iron alloys. For the technology investigated here, the presence of forging of the metal should be indicative of the presence of a chafery hearth and a hammer. Samples from the matrix material sieved through <0.50cm>0.25cm of trenches PN1 and QN1 were selected, embedding in the same resin block a flake hammerscale, a spheroid and a fragment of blast furnace slag for comparison with the larger samples (figure 5.15). The results are consistent with the larger examples of blast furnace slag and are not further discussed here (see section 5.3.1 and Appendix B.3). Additionally, a possible smithing slag bottom from trench QN1 was also analysed (table 5.13).

Figure 5.15. Selected sample matrix from trench PN1 0-20 (sieved through <0.50cm>0.25cm) including two fragments of flake hammerscale, spheroid hammerscale, a small green fragment of blast furnace (top) and iron-rich slag fragments.

The flake hammerscale examples analysed are composed almost entirely by dendritic wüstite (figure 5.16, A) with a small amount of cementing fayalite, a microstructure that implies rapid cooling rates. The spheroids displayed some porosity (figure 5.16, B). Their microstructures are characterised by less wüstite crystals compared to the flake hammerscale, and lathe-like fayalite crystals in a glassy matrix, where dendrites of wüstite are concentrated. Both types of hammerscale have a similar chemical composition (table 5.13), but the spheroids display higher phosphorus content in the glassy matrix, according to that found by McDonnell (1984).

The smithing slag bottom from QN1 displays an heterogenous microstructure, characterised by large fayalite crystals, glassy matrix with different concentration and shape of iron oxide (wüstite) and a few hercynite crystals (figure 5.16, C). There are also areas that appear vitrified and unaltered quartz inclusions. These features seem to validate the observation made during the visual analysis confirming this piece as a probable smithing slag. The results of the chemical analysis obtained on this sample are shown in table 5.13 (see also Appendix B.3).

Table 5.13. Average chemical composition of smithing slags, including hammerscale flake and spheroid and the smithing slag cake from QN1. Data are normalised to 100wt%. Number in () represents the number of measurements on one piece.

	Na_2O	MgO	Al_2O_3	SiO_2	P_2O_5	SO_3	K_2O	CaO	TiO_2	MnO	Fe_2O_3	N° Analyses
Hammerscale (bulk)	0.3	0.9	11.8	0.3	0.1	-	-	0.6	0.2	0.6	85.2	(3)
Spheroid (bulk)	0.6	0.4	2.1	14.7	0.4	0.1	0.7	0.8	0.3	0.6	79.6	(3)
Spheroid (glassy matrix)	0.2	0.3	1.7	19.1	2.5	0.2	0.2	1.1	0.3	0.4	74.7	(3)
QN1_0-20_SS (bulk)	1.8	0.9	6.4	21.2	0.7	-	1.5	1.1	-	-	67.3	(2)
QN1_0-20_SS (glassy matrix)	2.5	-	19.4	40.5	0.5	-	12.3	0.6	-	-	24.8	(3)

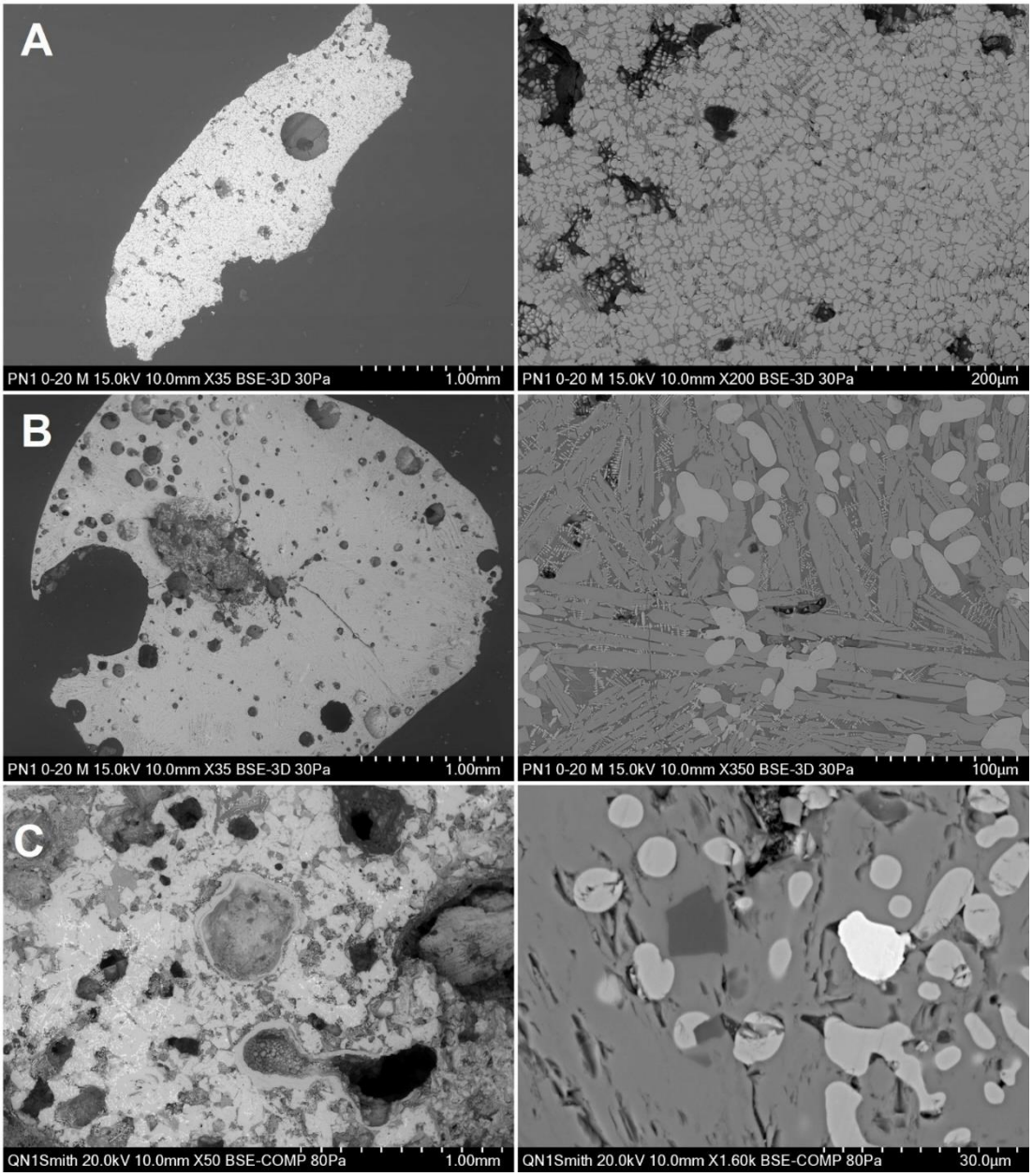

Figure 5.16. BSE micrographs of smithing slags. ***A****: micrographs showing an overview of the hammerscale (left) and to the right the microstructure characterised by dendritic wüstite and cementite fayalite, visible as the dark grey areas. The black voids are porosity.* ***B****: micrographs showing an overview of the spheroid hammerscale with abundant porosity to the left, and to the right the microstructure characterised by elongated fayalite crystals (grey) in a glassy matrix (dark grey). The light grey crystals are wüstite.* ***C****: micrographs showing an overview of the smithing slag from QN1 to the left, and to the right at higher magnification an hercynite crystal (dark grey) in a large fayalite crystal (grey), wüstite (light grey) and an iron prill (white).*

5.4.4 Metal Samples

Ten metal pieces were selected for chemical analysis (table 5.1). Eight samples from trenches PN1, QN1 and RS1 were chosen from the rounded/pine-shaped iron scrap category (section 4.4.4). Further, a flat piece of scrap retrieved from ZS3 and a possible iron bar from RS1 were sampled. For the location of cut samples refer to Appendix B.1 and B.3 for bulk chemical compositions.

The microscopic investigation of the samples from trenches PN1, QN1 and the sub-rounded pieces from RS1 revealed a similar microstructure formed by a mixture of materials, not dissimilar to the conglomerates described in section 5.3.2, but with a higher amount of sound metal preserved. QN1 20-40_FeBall1 and RS1_20-40 Fe1 only contained sound cast iron. The rest of the samples are characterised by areas of both cast iron and ferritic iron, embedded in a mixture of iron-rich slag, iron oxides, sand, charcoal and fragments of blast furnace slag (figure 5.17). This suggests that these residues formed inside the fuel bed of a hearth. Moreover, the presence of both cast and ferritic iron suggests oxidising conditions. The structure of the grey cast iron is that of hypoeutectic cast iron with flake graphite in a pearlitic and ferritic matrix, as seen in the metallic inclusions found embedded in blast furnace slags. Bulk analyses of the cast iron are shown in table 5.14. Numerous steadite islands are observed, confirming that during smelting most phosphorus was reduced to the iron. Two types of non-metallic inclusions are encountered here: iron and manganese sulphides or mixed manganese-iron sulphide inclusions, which also contain small amounts of titanium and vanadium, and titanium-rich inclusions with vanadium ranging from *c.*2 to 6wt% (Appendix B.3).

Moreover, samples PN1 20-40_FeNodule6, RS1 0-20_Fe1 and RS1 20-40_Fe2 show areas of surviving metal inside the oxidised grey cast iron. Here, the microstructure is characterised by cementite needles and ledeburite with a high phosphorus content. Ledeburite is a eutectic between austenite (Fe γ) and cementite (Fe_3C) that forms from liquid iron and is normally found in white cast iron. Microstructures associated with hypereutectoid steel are also observed, where ferritic iron survives at the core of the original cast iron prills. The surrounding matrix is characterised by a network of cementite needles almost entirely corroded in a pearlitic matrix (figure 5.18). These transformations appear thus associated with decarburisation. The microstructures observed suggest a likely sequence whereby

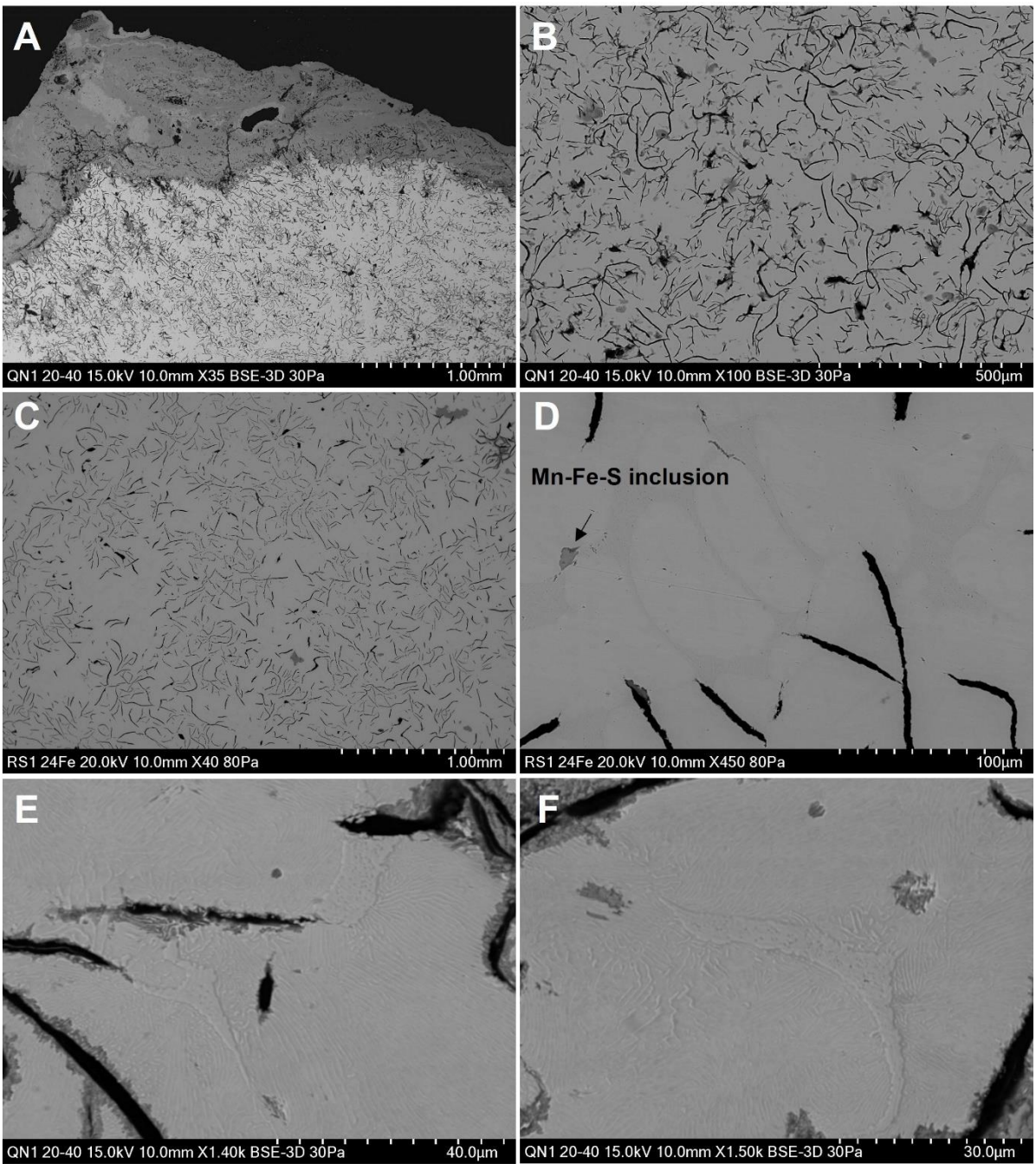

Figure 5.17. BSE micrographs of samples QN1 20-40 Fe 1 and RS1 20-40 Fe 1 showing the microstructure of grey cast iron. ***A*** *is an overview of the microstructure of the sample from QN1, showing external corrosion/oxidation and a sound metal matrix with numerous graphite flakes, shown in* ***B*** *at higher magnification.* ***C*** *is an overview of the microstructure of the sample from RS1, showing numerous graphite flakes.* ***D*** *shows the same microstructure at higher magnification, with a Mn-Fe-S inclusion and graphite flakes (black). The matrix of this sample show islands of ferritic iron and at the grain boundaries a phase that appears to be forming ledeburite with high phosphorus levels (see text).* ***E*** *and* ***F*** *display islands of steadite in a pearlitic matrix.*

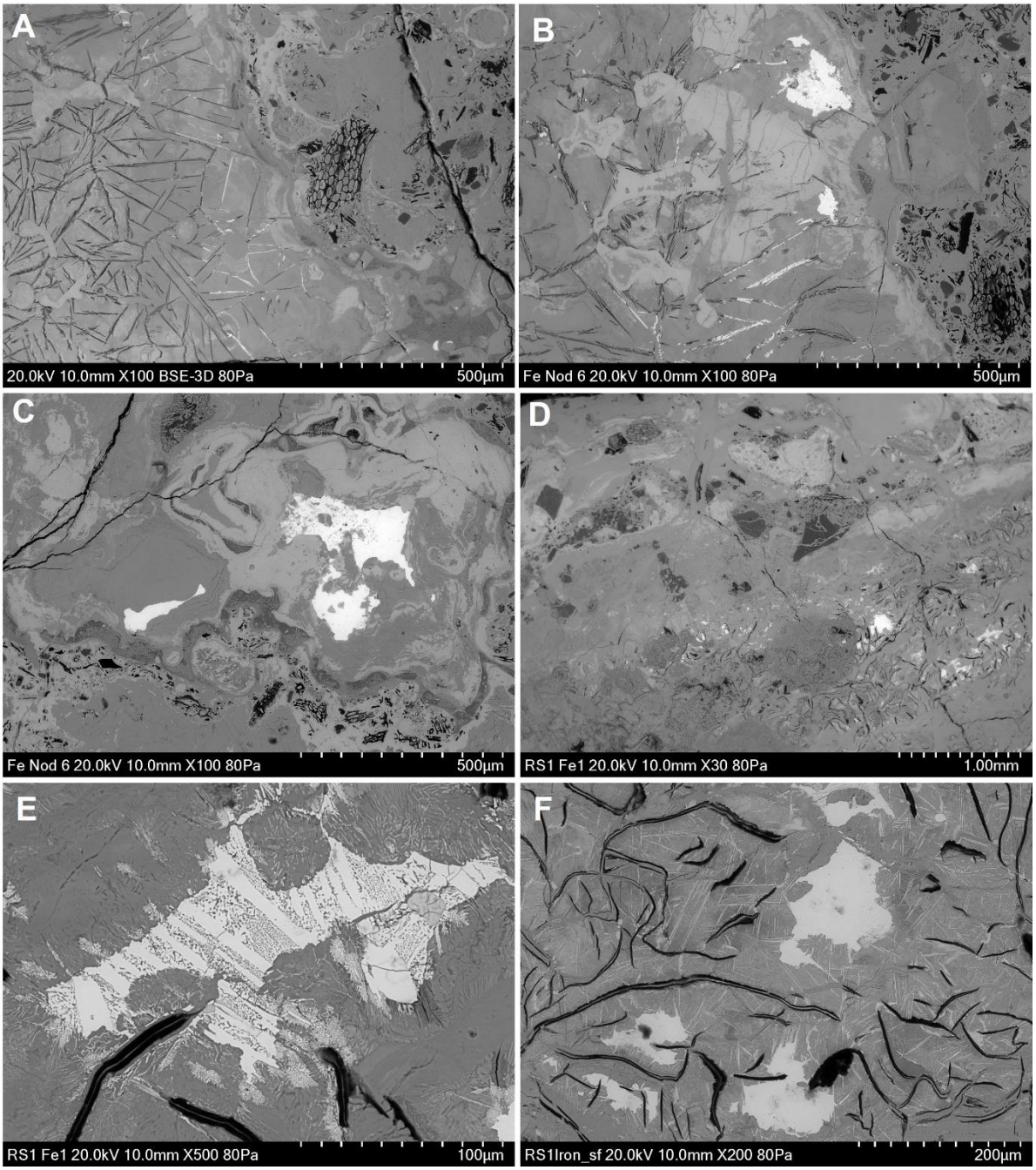

*Figure 5.18. BSE micrographs of samples PN1 20-40_FeNodule6, RS1 0-20_Fe1 and RS1 20-40_Fe2 showing areas of surviving metal in oxidised grey cast iron. **A** and **B** display to the right the interface between oxidised grey cast iron and a layer of sand, iron oxides and charcoal. The needles (both black and white, the latter surviving as sound metal) are cementite. **C** shows islands of ferritic iron surrounded by iron oxides. A similar microstructure is observed in RS1 Fe 1 shown in **D**, the top layers consist of iron oxides, sand and charcoal fragments, while the bottom shows oxidised grey cast iron and surviving sound metal. **E** shows an island of metal of the same sample, at higher magnification. The microstructure display cementite needles and ledeburite, the dotted phase in between the white solid needles of cementite. The matrix is composed of iron oxide and oxidised black graphite flakes are visible on the lower part of the micrograph. An overview of a similar microstructure is shown in **F**, displaying cementite needles and graphite flakes occurring together.*

grey cast iron progressively loses carbon, changing its microstructure into white cast iron, steel and finally iron with a ferritic matrix and a low content of metallic impurities (table 5.14).

Sound ferritic iron is found at the core of samples PN1 20-40_FeNodule6 and QN1 20-40_FeBall 2 (figure 5.19 and 5.20). The silicon and phosphorus content measured in this remaining iron is around 0.2wt%. Moreover, inclusions containing high amounts of phosphorus are detected in the metal matrix (figure 5.19). Their round shape suggests that they formed in a liquid state and probably result from an incomplete dephosphorisation of the metal by the surrounding slag (see discussion below). Their composition is shown in Appendix B.3. These islands of ferritic iron appear either as surviving metal inside former cast iron inclusions or surrounded by fayalitic slag (figure 5.19). A layer of iron oxide seems to separate the metal from the slag. Hence, the metal does not appear to be reducing from the silicates. Rather, the iron oxides formed by exposing cast iron to an oxidising atmosphere, reacted with the silicon present in the metal, as well as in additions such as quartz, sand etc., to form slag. The chemical composition of the fayalitic slag is similar to that analysed in the iron-rich slag, with the glassy matrix enriched in Ca, P, and K. In addition to fayalitic slag, which is also present as small round inclusions and fragments together with sand and charcoal, a less iron-rich slag has formed around the oxidised cast iron. This is seen as small islands or streams of slag that have replaced iron oxides (figure 5.19 and 5.20). Very small spherical iron prills and thin fayalite crystals are dispersed in a mostly glassy matrix.

The investigation of the possible iron artefact with rusty concretion retrieved from ZS3 (40-60) revealed the microstructure of grey cast iron, with a pearlite/ferrite matrix and graphite flakes. After chemical analysis the piece was also etched with Nital (2% solution) and the microstructure appeared uniform across the sample (figure 5.21). The external surfaces are covered by layers of corrosion (figure 5.21). Bulk analysis on the metal matrix shows 0.5wt% silicon, 0.8wt% phosphorus and 0.5wt% manganese (table 5.14). Areas of analysis close to non-metallic inclusions also show about 0.4wt% of sulphur and 0.1wt% of vanadium. The same manganese and iron sulphides and titanium-rich inclusions described above were detected in this piece (Appendix B.3).

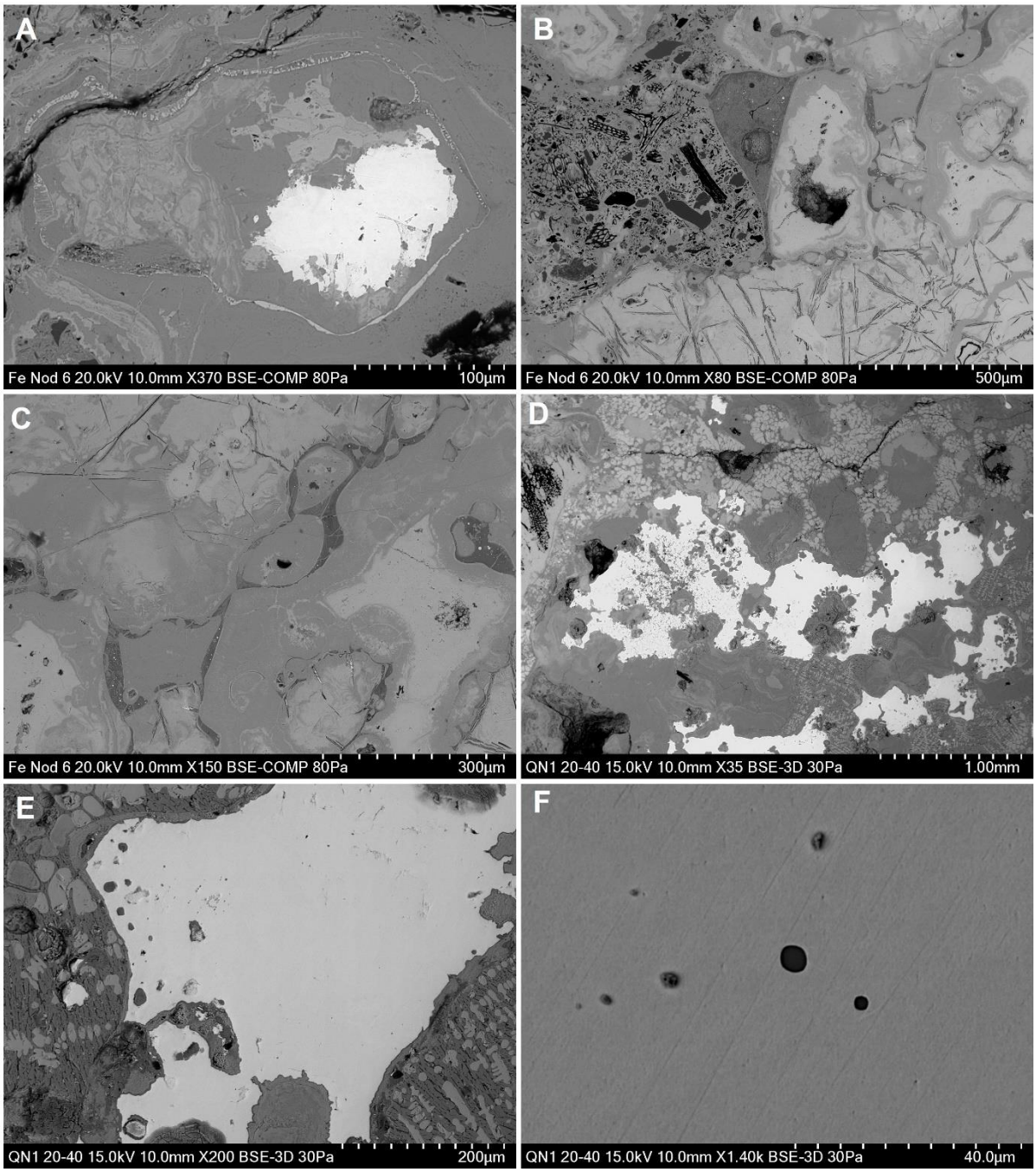

*Figure 5.19. BSE micrographs of samples PN1 20-40_FeNodule6 and QN1 20-40_FeBall 2 showing ferritic iron surrounded by iron oxides and slag (**A**, **D** and **E**). Note the layer of iron oxide surrounding the metal and separating it from the slag. Together with fayalitic, wüstite-rich slag, a glassy slag is seen forming as islands and streams of slag (dark grey in **B** and **C**). **B** also shows oxidised cast iron with some remaining graphite flakes and cementite needles. **E** and **F** shows ferritic iron and at higher magnification rounded phosphorus-rich inclusions.*

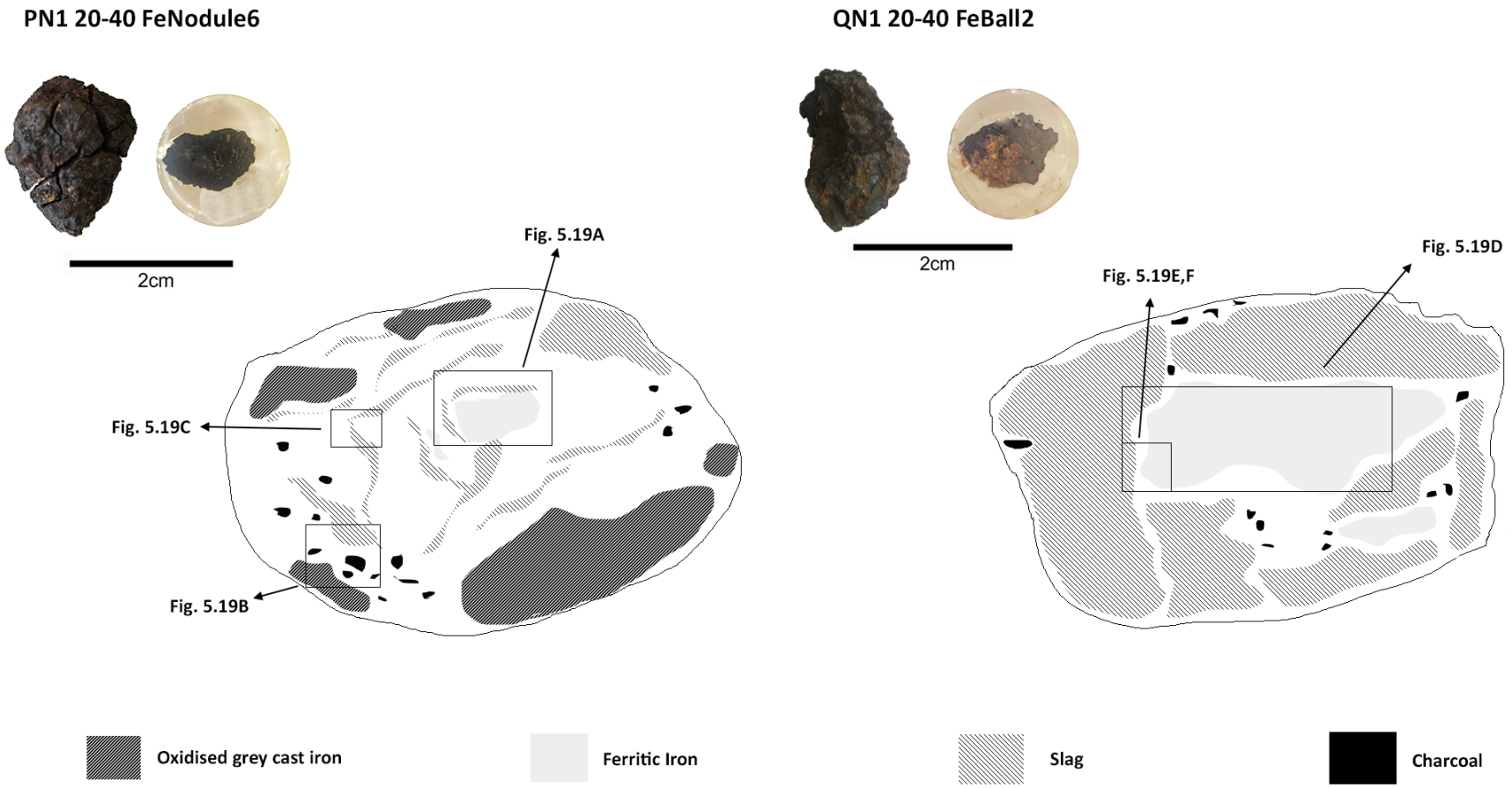

Figure 5.20. Schematic metallographic sections of sample PN1 20-40 FeNodule 6 and QN1 20-40 FeBall 2 (not to scale) locating the BSE micrographs of figure 5.19. The white areas are iron oxides.

The results thus suggest that this is a fragment of pig iron brought from the blast furnace to this side of the site (the finery forge) to be fined but that this was never completed.

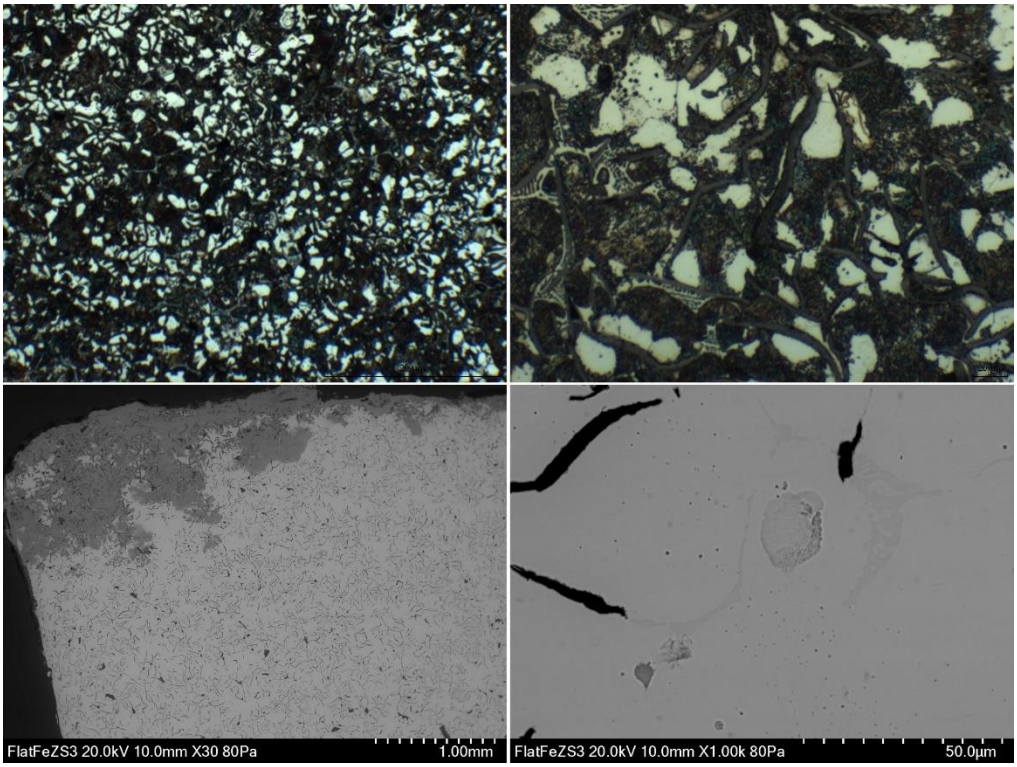

Figure 5.21. Optical microscopy (top) and BSE micrographs (bottom) showing the microstructure of sample ZS3. The matrix is characterised by ferrite and pearlite with steadite islands and graphite flakes. The microstructure is uniform across the sample. Titanium and vanadium rich inclusions are shown in the bottom right image, at the boundaries with steadite.

The last metal piece analysed was a flat piece of metal identified during the visual analysis as a possible iron bar (RS1 0-20_Bar). Two fragments from the same piece were cut and embedded in the same resin block: one displaying sound metal and taken from the core of the piece, while the other almost completely corroded was taken from the surface. Optical microscopy and etching were again performed after the SEM-EDS investigation. Table 5.14 shows the average chemical composition on the metal matrix (Appendix B.3).

Table 5.14. SEM-EDS analysis on metal samples showing the conversion from cast iron (first three rows) to an alloy that is progressively losing carbon and other impurities (four middle rows): the high phosphorus content measured here comes from the ledeburite phase shown in figure 5.18. The oxygen comes from the surrounding areas rich in iron oxides. The last three rows display the results of ferritic iron detected within oxidised cast iron, with the last row showing the average chemical results on the fragment of iron bar from RS1. Totals are shown on the last column. Average analysis of 3 to 4 measurements on each sample. Refer to Appendix B.3.

	O	Si	P	S	Ti	V	Mn	Fe	Totals
ZS3 40-60	1.7	0.5	0.8	0.4	-	0.1	0.5	96.3	100.3
QN1 Fe2	4.2	1.0	0.3	-	-	-	0.6	94.0	99.3
RS1 20-40 Fe1	2.2	0.6	0.3	-	-	-	0.4	96.9	100.0
RS1 20-40 Fe2	12.7	0.3	3.8	0.4	-	0.1	-	82.6	99.9
	16.3	0.4	7.9	0.3	-	0.1	0.1	74.6	99.8
RS1 0-20 Fe1	10.0	0.3	1.1	0.2	0.1	0.2	-	88.1	100.1
	11.6	0.4	4.4	1.2	0.1	-	0.1	82.2	100.1
RS1 20-40 Fe2	5.4	0.4	0.4	0.1	-	-	-	93.7	100.1
QN1 Fe1	3.4	0.3	0.2	-	-	-	0.5	96.0	100.4
PN1 Fe6	10.5	0.4	-	-	-	-	-	89.0	100.0
RS1 Bar	2.3	0.3	0.1	-	-	-	-	97.3	100.0

Micrographs obtained after etching the surface with Nital revealed a ferrite grain structure, which indicates a low carbon content (figure 5.22). The shape and size of the grains appear slightly different observing the piece at the two external surfaces and in the middle of the cross section. For clarity these are described as top, middle and bottom, but there is no indication as to the orientation of the piece. The top appears characterised by equiaxed hexagonal grains, which is the initial structure observed in homogenous alloys (Scott 1991). Somewhat smaller ferrite grains with some (strain?) lines characterise the middle and bottom areas. However, it is not clear if this is caused by corrosion or by (cold) working the iron bar or even by an uneven distribution of carbon content. This last scenario, which appears the most likely, would indicate an uneven decarburisation and the presence of small areas of pearlite at the grain boundaries. This observation appears consistent with the distribution of the non-metallic inclusions across the metal matrix, as explained below. The entire surface is in fact characterised by the presence of numerous non-metallic inclusions (Appendix B.3).

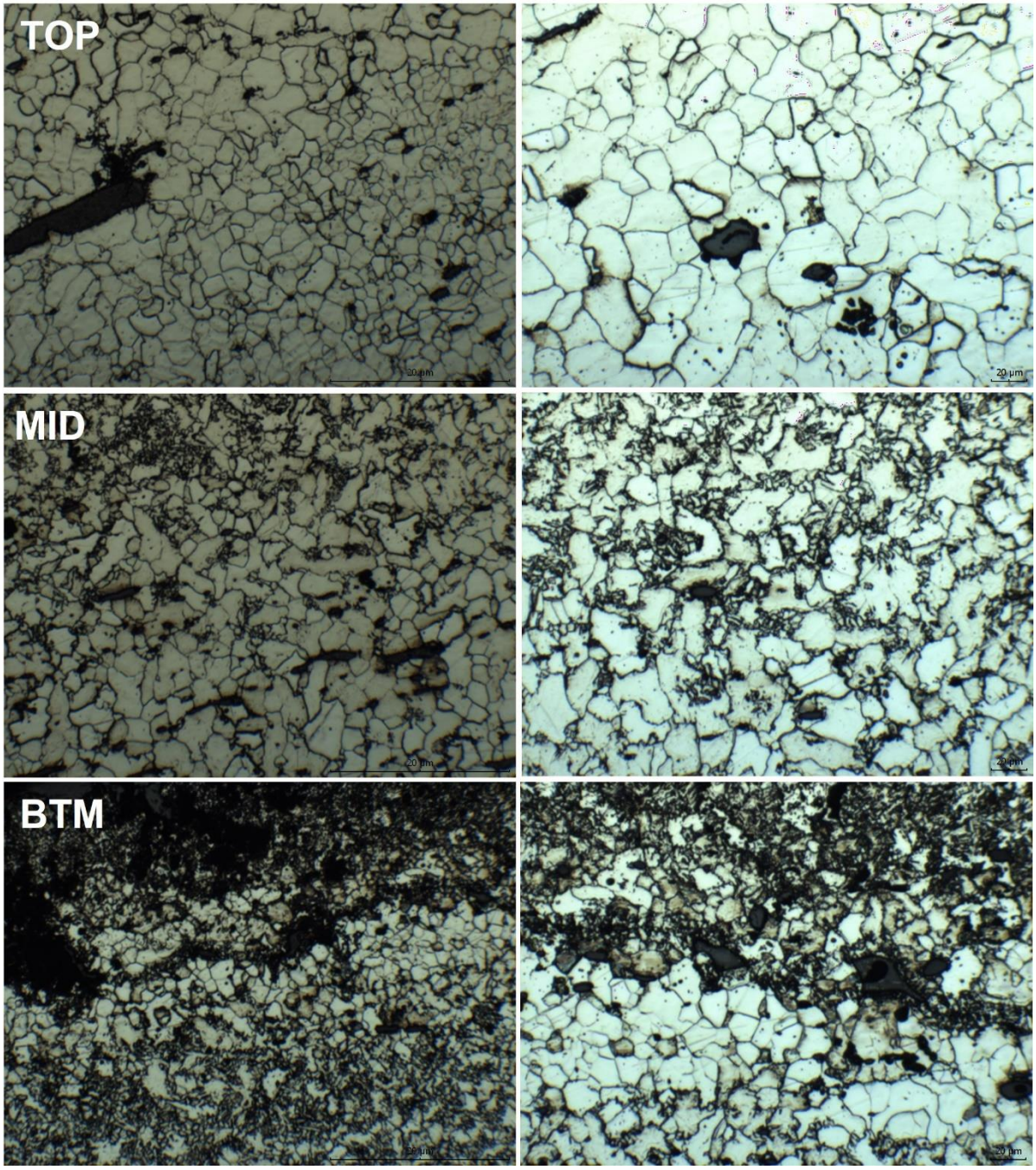

Figure 5.22. Optical microscopy micrographs obtained after etching with Nital (2% solution), taken at x50 (left) and x200 (right) of sample RS1 0-20 Bar. For clarity the sample is described as top, middle and bottom according to the variation in the microstructure observed, there is no indication as to the orientation of the fragment. The microstructure is ferritic and characterised by equiaxed hexagonal grains (top images) and non-metallic inclusions. The grains appear somewhat smaller in the middle of the cross section and the bottom, with some pearlite at the grain boundaries, indicating uneven decarburisation. Some corrosion is also present at the grain boundaries. Refer to text for explanation and to figure 5.22 for the distribution and type of non-metallic inclusions observed.

At least three types of inclusions are identified (figures 5.23):

1. Single phase inclusions, which contained a silica-rich glassy matrix
2. Double phase inclusions, containing wüstite in a fayalitic matrix
3. Three phase inclusions (or sub-double phase inclusions? – see Liu *et al.* 2014)

Among the single-phase inclusions, it was possible to differentiate two further types: one formed by a homogenous matrix and another which features small dark dots of silica (figure 5.23). They display a similar chemical composition, with the dotted ones having a higher silica content. They have spherical and elongated shapes and appear concentrated in the middle and bottom areas of the piece, where the metal matrix shows some pearlite or areas with higher carbon content (Buchwald and Wivel 1998, Mackenzie and Whiteman 2006, 145). The double phase inclusions are larger in comparison to the glassy ones, elongated and generally oriented parallel to the piece. They are characterised by a high iron content (average 81.3wt%) and an average 14wt% silica. They are all located in the ferritic zones at the top of the piece (figure 5.23). Finally, the same ferritic zone also contains some very small spherical inclusions which could contain at least three different phases or constituents. A bigger one was also spotted, displaying a more elongated shape (figure 5.23). The spherical inclusions show a glassy matrix, a central phase (almost like a band in the centre of the sphere) and some dark round spots. In the larger one it is possible to see some regular crystals and a similar dark spot in the glassy phase. These inclusions contain a considerable amount of phosphorus in the glassy matrix.

In archaeometallurgical studies, slag inclusions are employed to differentiate between bloomery and finery technology. An overview of the criteria and methodologies proposed by various researchers is given in section 5.6 and the results obtained on RS1 0-20_Bar are discussed below.

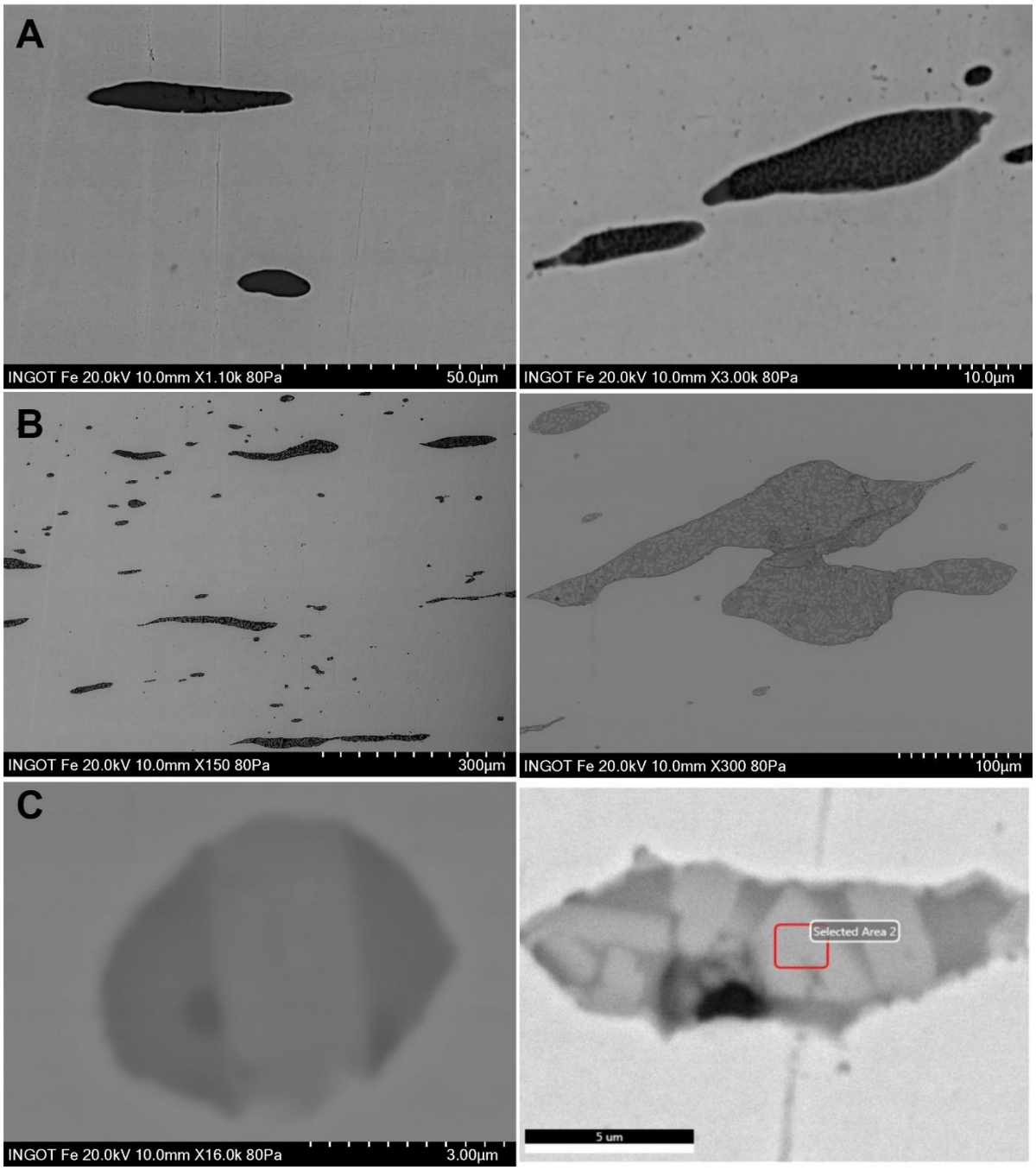

Figure 5.23. BSE micrographs showing three types of non-metallic inclusions observed on the fragment of bar iron retrieved from ZS3. ***A****: shows the single-phase inclusions, to the left a silica-rich inclusion with a homogeneous matrix, to the right an example of slag inclusions with numerous silica dots. They are concentrated on the middle and bottom areas of the piece, where the metal is characterised by higher carbon content.* ***B****: displays examples of elongated double-phase inclusions, containing wüstite in a fayalite matrix. They are located in the ferritic zones, at the top of the fragment. Note the elongated shape in the direction of working.* ***C****: displays examples of very small inclusions containing possibly three phases: a matrix phase (dark grey), light grey crystals and some dark dots. Resolution is hindered by the small size of the inclusions. They contain high levels of phosphorus.*

5.5 STONES AND CLAY

Of the five samples selected for these material types, four turned out to be clay pieces. Their chemical composition is reported in table 5.15. The white/grey soft examples were selected to investigate the presence and use of limestone, but they are in fact fragments of vitrified grey clay, probably coming from the river. The use of grey river clay is also reported at the finery forge at Stony Hazel (Davies-Shiel 1969). Here it was used to coat the cast iron plates that lined the finery hearth (Tylecote 1992, 103).

The only stone analysed (PN1 20-40 Quartz) is a rock fragment similar in composition to the tin-rich ore samples described in section 5.3.3. Tin oxide crystals are observed in a silica and iron matrix, together with some areas rich in arsenic (Appendix B.3).

Table 5.15. Average chemical analysis of clay samples. Fragments show vitrified surfaces indicating they were subjected to high temperatures. Data are normalised to 100wt%. Number in () is number of measurements on one piece.

	Na_2O	MgO	Al_2O_3	SiO_2	K_2O	CaO	TiO_2	Fe_2O_3	N° Analysis
PN1 20-40 white	0.9	2.4	25.3	53.4	4.8	0.5	1.0	11.9	(3)
QN1 20-40 white	1.0	1.9	21.0	60.6	3.8	0.5	0.9	10.6	(3)
QN1 20-40 Mix Clay	0.7	1.9	21.2	61.0	4.6	-	0.9	9.6	(3)
PN1-QN1 Cxt 7 white	0.9	1.5	25.5	53.9	5.2	-	1.0	12.6	(3)

5.6 THEMES IN POST-MEDIEVAL IRONWORKING

Most of the published research into post-medieval iron slags, has focused on two aspects:

1. Identifying criteria to distinguish bloomery smelting from finery technology
2. Distinguishing the residues of different cast iron conversion processes, i.e. finery/chafery technology vs. various puddling processes

Both strands of research have attempted to address these questions by analysing both slags and non-metallic inclusions in metals (either scrap or artefacts). The identification of blast furnace smelting is generally more straightforward because the slags obtained from this technology display a glassy appearance and contain much

less iron; consequently, are more easily distinguished and identified. By contrast, bloomery smelting and the various conversion technologies produce iron-rich wastes, with similar forms and mineralogy. The morphological similarity between bloomery smelting tap slag and finery tap slag has been already discussed in the previous chapter. This section will summarise the research on the mineralogy and microstructures of slags and metals.

Converting pig iron into wrought iron requires the removal of silicon, which reacting with the iron, forms a fayalitic slag with a bulk composition similar to bloomery smelting slag. Consequently, Killick and Gordon (1987) and Gordon (1997), focused on the study of the nature of the minerals present to distinguish bloomery, finery and puddling sites. The former concluded that puddling slags can be distinguished from fayalitic slags produced in bloomery and finery processes by their lower alkali content (sodium and potassium) since metal and slag in the puddling process are never in contact with the fuel. Moreover, they suggested that puddling slags are characterised by magnetite and iron sulphides. Gordon (1997) indicated that the presence of high wüstite and the lack of exotic phases (hercynite, leucite, monticellite-kirschsteinite) are characteristics of finery slags. In addition, Bayley *et al.* (2001, 13) state that finery forge residues can be distinguished from smelting sites by the absence of ore.

More research has been carried out on the non-metallic (slag) inclusions that are always present in wrought iron obtained from bloomery, finery and puddling processes. Hence, both smelting and manufacturing techniques, including forging of iron, introduce non-metallic inclusions in the metal matrix. The rationale here is that these slag inclusions, originating from different processes (smelting and manufacturing processes), should retain elements that are characteristic to each technology and consequently can be used to differentiate them (Rostoker and Dvorak 1990, Buchwald and Wivel 1998, Starley 1999, Dillmann and L'Héritier 2007, Blakelock *et al.* 2009, H. Liu *et al.* 2014, Y. Liu *et al.* 2019). In bloomery smelting, non-metallic inclusions are produced during reduction since slag and metal do not properly separate and a certain amount of slag remains in the metal, in the form of inclusions. These can then be heavily modified during smithing, due to the use of fluxes and reactions with the fuel in the smithing hearth. Dillmann and L'Héritier (2007) demonstrated that for some very manufactured objects (forged), the

inclusions from the smelting stage can be much less abundant compared to those coming from the smithing stage. For semi-finished products however, the inclusions reflect the smelting system that produced them (Dillmann and L'Héritier 2007, Blakelock *et al.* 2009).

For what concerns the indirect method of iron smelting, during reduction the metal is in a liquid state and separated from the slag, therefore the pig iron obtained is virtually slag-free. The slag inclusions observed in wrought iron (from indirect smelting) form during the fining step by oxidation of the elements contained in the pig iron. Thus, elements that are not reduced into the cast iron during the smelting phase, such as Mg, Al, K and Ca, will not be present in high quantities in the non-metallic inclusions of the wrought iron, unlike iron made from the direct process. On the contrary, phosphorus is an element that is completely reduced into the cast iron during smelting; consequently, its concentration is used to distinguish the different processes. During the following fining operation in fact, phosphorus is oxidised, concentrating in the slag and slag inclusions of fined iron.

Similarly, the phosphorus content can also be used to discriminate between different conversion processes, as shown by Y. Liu *et al.* (2019) analysing different decarburisation (solid-state annealing and liquid fining) and manufacturing methods in Chinese iron objects. In addition, the presence of Ca-P phases is considered an indication of fined iron (Vega *et al.* 2003). Adding Ca-rich material (such as limestone) to the finery hearth would facilitate the removal of phosphorus from the metal, forming a stable compound such as calcium phosphate $Ca_3(PO_4)_2$ that would consequently concentrate in the non-metallic inclusions (Dillmann and L'Héritier 2007, 1817*;* Y. Liu *et al.* 2019, 6542). High levels of phosphorus can make iron brittle at low temperatures, and it is known from historical sources that calcareous additions to the slag bath promoted not only decarburisation but also dephosphorisation (Arribet-Derroin 2001, Vega *et al.* 2003, Dillmann *et al.* 2012). Clearly, the presence or absence of high P levels and Ca-P phases will depend both on the process and the materials employed, that is whether calcium-rich material was added during fining, and on the iron ore(s) used – if poor in phosphorus, metal and slag inclusions will not contain this element. In addition, high levels of phosphorus can also be found in bloomery iron obtained smelting P-rich iron ores.

Finally, Chen and Han (2007, as cited in H. Liu *et al.* 2014, 60 and Zhang *et al.* 2021, 111) pointed out that bloomery iron contains large and numerous double-phase inclusions, while fined iron mostly displays single phase (glassy) and sub-double phase inclusions. The latter are described as inclusions that do not display a clear eutectoid phase separation (Liu *et al.* 2014, 60). It is possible that the three phase inclusions identified in sample RS1 0-20_Bar are inclusions where there is not a clear phase separation.

5.7 DISCUSSION

This section will discuss the results obtained from the chemical and microstructural investigation of the selected samples from Ausewell Wood. The samples were selected and analysed with the aim of establishing a connection between the two sides of the site and to characterise the technology represented at SH1 through the chemical investigation of the excavated material. The macro-morphological analysis of the assemblage pointed to post-smelting operations designed to convert pig iron into wrought iron. The identification of both processes characterises Ausewell Wood as a metallurgical complex where iron was first smelted at the blast furnace and then transported to the finery forge, situated along the same river, to be refined into bars of wrought iron. The results are first discussed in connection to the two main objectives of this study and then summarised in a final discussion.

5.7.1 Objective 1: Connection between blast furnace and excavated slag heap (SH1)

In order to establish a connection between the two metallurgical operations represented at Ausewell Wood, blast furnace slags were selected and analysed. Surface samples from the slag heap near the blast furnace were compared to fragments of blast furnace slags excavated at the slag heap SH1 (section 5.3.1). Here, there were both single pieces recovered with the rest of the iron-rich material and fragments embedded in other slags and conglomerations of material.

As confirmed by the analytical description, their identification as blast furnace slags is unequivocal: the glassy appearance of the pieces, the low iron content and the presence of grey cast iron prills are all clear indicators of iron reduction by the indirect method. The presence of charcoal inclusions confirms the use of this material as the fuel for the smelting operations. No major chemical or microstructural differences were revealed between samples from the two metal-working areas,

confirming that they were both smelted at the blast furnace situated at the southern end of the site and transported to the finery forge located to the north. Possible evidence of the use of limestone during smelting of pig iron is offered by the high lime content measured for these slags. In addition, two slag samples display what appear to be newly formed calcium sulphate inclusions, which seems to confirm the use of limestone as fluxing agent. The use of limestone in iron smelting was an established practice by this period (Schubert 1957, 229*).* What is more, the geology surrounding Ausewell Wood is rich in limestone (Page 2004, 4), making the procurement of this raw material an easy task.

Less clear is whether blast furnace slags had a role in the process of fining pig iron and were thus intentionally added to the slag bath in the finery hearth. Given the numerous fragments recovered at SH1 and the fact they were found embedded in iron-rich slag and metal seems to suggest that they were intentionally employed. A possible explanation for their use can be attributed to their lime-rich nature that could have contributed to the removal of phosphorus from the metal. Similarly, the silica contained in these slags could have aided the fluxing of iron oxides produced during fining; silica in the form of quartz or sand was almost always added to the slag bath. However, evidence from other sites would be necessary to confirm this as an operational practice.

The presence of titanium-rich crystals with ‘bands’ of manganese sulphide in two fragments of blast furnace slags from near the furnace (BBF_2 and BFF_3, figure 5.2) offers some indications of the type of ore employed. Moreover, all prills and fragments of cast iron displayed inclusions rich in titanium and vanadium, as well as manganese sulphide inclusions. Finally, possible relics of chalcopyrite were also detected, which is consistent with the geology of Dartmoor, and thus possibly ended up in the furnace charge as accessory minerals. In the light of these results, the historical reference to the use of lodestones (magnetite) mined at South Brent and brought to Ausewell Wood to be smelted appears significant (chapter 3). Magnetite ores often contain titanium and vanadium. However, only the analysis of iron ores from the South Brent mines could clarify this point and confirm them as being the source of the iron smelted at Ausewell Wood.

In order to obtain a rough estimate of smelting temperatures, the blast furnace slags have been plotted in the ternary diagram FeO-Al_2O_3-SiO_2 (figure 5.24, Rehren and

Ganzelewski 1995). Given that manganese has a fluxing effect on the melting point of the slag similar to that of iron, its content has also been plotted together with iron, thus FeO corresponds to the sum of FeO and MnO oxides. The normalised (FeO+MnO)-Al_2O_3-SiO_2 data plotted on the diagram indicate a temperature of about 1400°C. Such temperatures are significantly higher than those achieved in a traditional bloomery furnace and appear corroborated by the evidence for waterwheels that probably powered bellows. Moreover, this temperature points to a free running slag, an important feature of blast furnace slags.

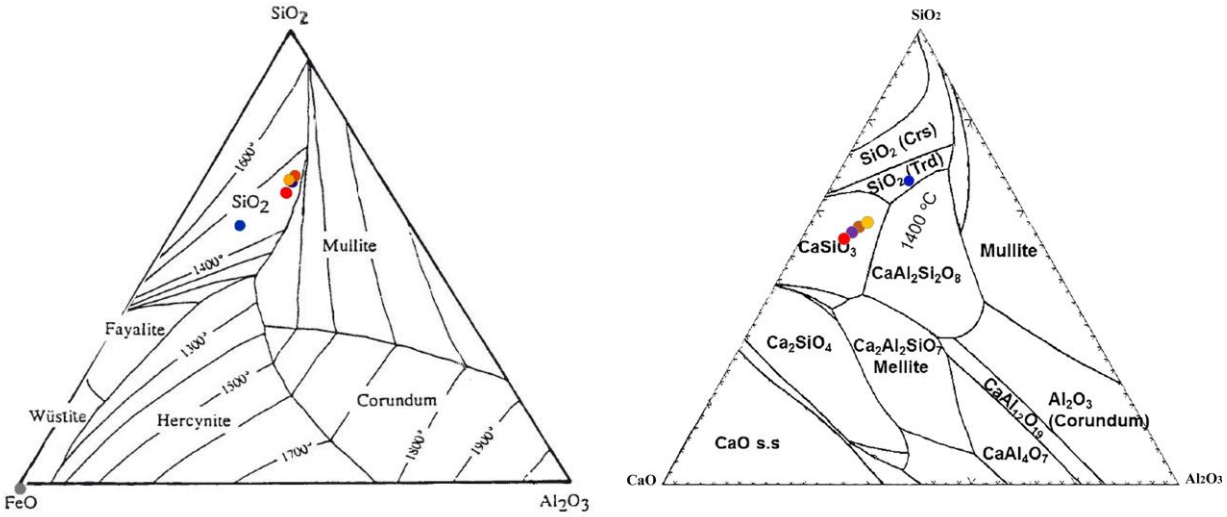

Figure 5.24. Ternary diagram SiO_2-Al_2O_3-(FeO+MnO) plotting the blast furnace samples BFF 1-5, showing a rough estimate of smelting temperatures around 1400°C. The ternary diagram SiO_2-Al_2O_3-CaO shows the samples clustering in the wollastonite area. Sample BFF 5 (blue dot) displays slighter lower temperatures in accordance with the higher manganese and iron content, while the tridymite composition is in accordance with the lower calcium content.

Together with fusibility (slag is liquid at iron-making temperatures) and fluidity (low viscosity), sulphur-removing capacity is another important propriety of blast furnace slags. According to White (1977, 1982 and 1996) the optimal compositional ratio for desulphurisation is a slag with a low SiO_2-Al_2O_3 content and high CaO-MgO content. A desulphurisation index can thus be determined by dividing the combined percentages of CaO and MgO by the combined percentages of SiO_2 and Al_2O_3:

$$\frac{CaO + MgO}{SiO_2 + Al_2O_3}$$

The higher the index the greater is the sulphur-removing capacity (White 1996, 236). Moreover, slags with an optimal composition for desulphurisation also display low viscosity, which is determined by the alumina content as compared to silica and lime

contents. A refractory index can thus be obtained dividing the alumina content by the combined percentages of silica and lime:

$$\frac{Al_2O_3}{SiO_2 + CaO}$$

In this case, a low index indicates a slag of low viscosity. The desulphurisation indexes of the blast furnace slag finds (BFF1-5) are between 0.32 and 0.60 and the refractory indexes range between 0.13 and 0.15 (table 5.16), indicating a low viscosity slag typical of a cold blast furnace (White 1996, 236). Similar values were calculated on the fragments from SH1, as reported in table 5.16. In terms of the sulphur removal capacity the results indicate a poor efficiency and a composition far from the ideal, which should give an ideal desulphurisation index of 1.41 (White 1980, 56). However, this property is particularly important when using coal as fuel, which normally contains high amount of sulphur, but it is less critical in charcoal smelting where the only source of sulphur is the iron ore (White 1996, 236). Moreover, the presence of manganese also contributed to the desulphurisation forming MnS inclusions.

Table 5.16. Table showing desulphurisation and refractory indexes for the blast furnace slag of Ausewell Wood.

	Desulphurisation Index	**Refractory Index**
BFF 1	0.52	0.14
BFF 2	0.48	0.15
BFF 3	0.55	0.13
BFF 4	0.60	0.13
BFF 5	0.32	0.14
SH1		
GREEN	0.43	0.15
BLACK/BLUE	0.36	0.12
CXT 7		
BF Fe	0.34	0.17
GREEN	0.39	0.16

The two silica-rich fragments retrieved from context 7 (termed ‘intermediate’ in the interim report and tentatively identified as products of a technology intermediate between bloomery and blast furnace smelting) characterised by a stony appearance display higher alumina content (around 13wt%) and no manganese but are overall

similar in composition to the glassy samples. The different texture could be related to a slower cooling or could indicate that they formed in hotter zones inside the furnace.

A further observation can be made on the final product obtained, grey cast iron. This microstructure, characterised by carbon in the form of graphite flakes, is favoured by a high content of carbon and silicon and low sulphur content (Scott 1991, 37). Moreover, manganese sulphide inclusions and the phosphorus eutectic steadite also promote the formation of graphite over cementite (chapter 2). Western metallurgy appears to have produced more grey cast iron than white cast iron, which is encountered more often in Chinese metallurgy (Rostoker and Gordon 1990, Wagner 2008, 162). This is due to the nature of the iron ores employed (Williams 2013, 2019). Hence to conclude, the type of cast iron produced at Ausewell Wood can be explained by the chemical composition and observation of the smelting system. In fact, the estimated smelting temperatures (of about 1400°C) reached inside the blast furnace favoured the reduction of silica to elemental silicon, which was rapidly dissolved in the liquid iron. Moreover, the low sulphur content, probably removed in part by the use of limestone and further inhibited by the formation of MnS inclusions, also contributed to the formation of grey cast iron.

5.7.2 Objective 2: Characterisation of finery technology at Ausewell Wood

The first conversion technology in use in England was the so-called Walloon process (Morton and Wingrove 1970, Den Ouden 1981, Awty 2007). This technology employed two hearth installations – finery and chafery – to produce wrought iron by decarburisation of pig iron produced in the blast furnace (chapter 2). The process entailed a series of actions. The pig iron was first ‘refined’ (melted), which caused the removal of silicon and other impurities, then ‘fined’ until most or all carbon was removed from the metal. Following this, a mass containing both slag and metal was obtained (*loop*), which was hammered and forged into bars and/or objects. All these actions produced waste residues. Thus, it is to be expected to find slags from the finery hearth, from the chafery hearth and from the final smithing. For this reason, during sample selection for this study, an attempt was made to investigate material coming from all steps of the process.

Among the iron-rich slag, both tap and hearth slags were selected (section 5.4.1 and 5.4.2). The results show that both are fayalitic slags, with a microstructure characterised by a high abundance of wüstite crystals. Chemically, both groups are reasonably similar, with variations in Al_2O_3, SiO_2, CaO, K_2O and FeO contents that appear related to the mechanism and zone of formation inside the installation and thus to the different contribution of the various materials (charcoal, clay, additions) to the composition of the slags.

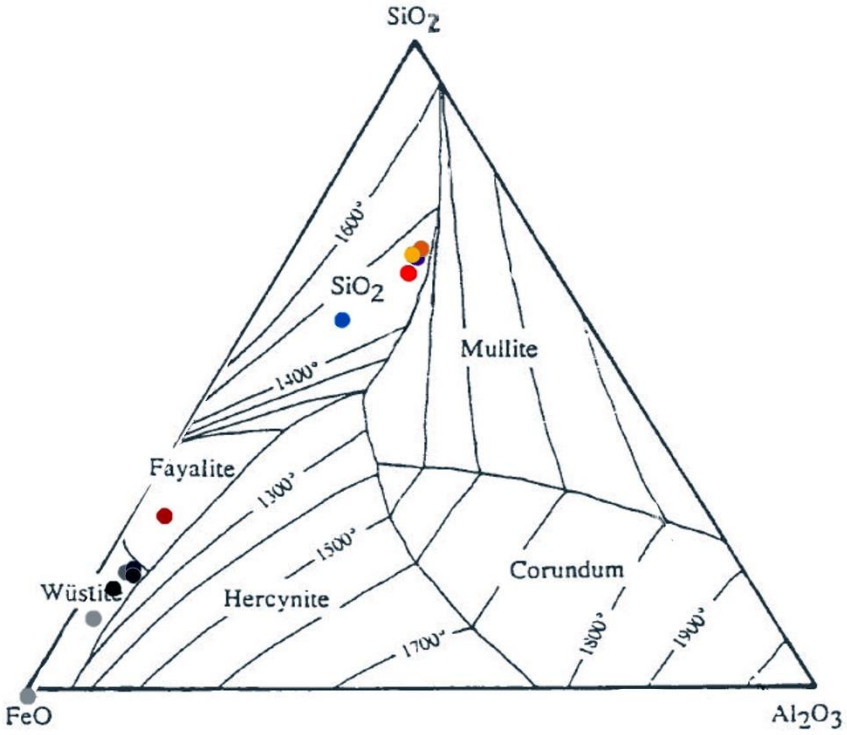

Figure 5.25. Ternary diagram SiO_2-Al_2O_3-(FeO+MnO). The finery tap slags are shown in the plot together with the blast furnace slags for comparison. They plot around the area of formation of wüstite, with temperatures around 1200°C.The red dot in the fayalite area is sample PN1 20-40_Tap13, which does not contain wüstite.

The glassy matrix is enriched in calcium and phosphorus. The phosphorus and sulphur content indicate that both elements have been transferred from the pig iron to the slag, although some phosphorus remained in the metal as indicated by the phosphorus content of slag inclusions in some of the ferritic metal samples (see section 5.4.4 and discussion below. Also, see Dillmann *et al.* 2012, 27-28). A rough estimate of temperatures of formation is obtained by plotting them in the FeO-Al_2O_3-SiO_2 ternary diagram (figure 5.25).

More complex is the interpretation of the hearth slag retrieved from trench RS1 (section 5.4.2). A possible mechanism of formation is suggested, but the interpretation is only tentative, and more analysis would be necessary to validate these observations. Nonetheless, the presence of spinels with titanium, vanadium and chromium strongly suggests a likely connection with the fining of pig iron, as also indicated by the titanium/vanadium-rich inclusions observed in the cast iron analysed. During indirect smelting these elements can in fact be reduced into the pig iron. Then, when exposing the pig iron to oxidising conditions during the first stages of fining, these elements are oxidised and become enriched in the slag. Indeed, in an archaeometallurgical experiment designed to understand the Walloon process, Dillmann *et al.* obtained slag that contained oxide phases containing titanium, vanadium and chromium, 'of formerly angular shapes' (2012, 27). Similarly, Dillmann (1998, as cited in Desaulty 2008, 51) showed that the presence in fined iron of non-metallic inclusions rich in Ti, V and Cr is a feature typical of indirect smelting. The composition of non-metallic inclusions is close to that of the fining slag. Also, the presence of iron sulphides in the multiphase areas identified in RS1 and of iron sulphide inclusions in the fragment of cast iron retrieved from ZS3 appears significant (section 5.4.4). Consequently, this slag is currently interpreted as a finery slag 'cake', which formed at the bottom of the hearth installation during the first stages of refining pig iron before decarburisation was completed.

Another important source of evidence in understanding the practice of fining pig iron at Ausewell Wood is identified in the class of material termed conglomerates (section 5.3.2). In order to promote the decarburisation of pig iron, fining was conducted in a hearth that was filled with charcoal and a layer of slag (chapter 2). Various additions were then made during the process in order to create more slag, while at the same time, once the melting of pig iron commenced, the finer stirred the melted material inside the hearth. It has already been stated how the shape and inclusions observed in this class of material is suggestive of a stirring action. In addition, again during the experiment carried out by Dillmann *et al.* they found at the bottom of the hearth 'several centimetre-sized slag pieces … mixed with charcoal' (2012, 25). It is very likely that the conglomerates recovered at Ausewell Wood derive from a similar operation. Moreover, the similarity between conglomerates and some of the metal examples seem to confirm this observation (section 5.4.4).

The presence of smithing activities is attested by the presence of flake and spheroid hammerscale (section 5.4.3). Generally, the former is produced during hammering of the hot mass of iron and slag and the latter during forge welding. In the finery technology however, the picture appears a little more complex as the *loop* obtained in the finery hearth was heated and hammered at least twice before being transferred to the chafery hearth where it was reheated and forged into a bar (Schubert 1951, Tylecote 1992). It is thus conceivable that these types of slag formed each time that the metal was hammered. Finally, it is likely that the hammer was water-powered as we know that by this time the entire process was mechanised; however, only further excavations could confirm this hypothesis.

Some final observations can be made on the piece of ferritic iron recovered at RS1 and the microstructures observed in samples PN1 20-40_FeNodule6 and QN1 20-40_FeBall, as they most probably represent the final product obtained from fining pig iron at Ausewell Wood. The results obtained from the chemical analysis reveal a low carbon alloy with a low level of phosphorus, between 0.1 and 0.2wt%, and an average silicon content around 0.3wt%. In addition, the number and type of non-metallic inclusions suggest that this is iron obtained by the indirect method. A number of observations support this interpretation:

- there is a significant occurrence of glassy single-phase inclusions
- the double-phase fayalitic inclusions contain high levels of Fe (<80wt%)
- the level of Mg, Al and K are very low, being 0.2, 0.9 and 0.3wt% respectively
- a few inclusions contain high P levels – the highest content is measured in QN1 where it reaches 21.5wt%, in RS1 the highest value measured is around 9.5wt%.

Moreover, the microstructures observed in the metal fragments point to decarburisation, whereby grey cast iron progressively loses its carbon and changes its microstructure into steel and ferritic iron. Finally, in terms of assigning the single pieces or types of slag to a specific step in the process, it is known that the finery hearth produced tap slag as the surplus created in the slag bath was let out probably opening tapping holes situated to the sides of the hearth installation. The slag channels are also probably associated with the finery hearth. The formation of finery and chafery slag cakes (slag that did not leave the hearth) can be expected from

both installations, although the chafery probably produced much less slag in comparison to the finery. Morton and Wingrove (1970, 28) stated that finery and chafery slag are probably best identified by the visual appearance rather than chemical analysis and suggested that in addition to fayalite-wüstite-slag could have other phases such as hercynite from clay additions and magnetite formed on the rapid cooling of these slags. The possible chafery slags visually identified during the macromorphological analysis performed for this study, have not been sampled and analysed within the scope of this study. In the light of the results obtained so far, the microstructural and chemical investigation of the large blocks of hearth slag retrieved from ZS3 and RS1 which show increasing porosity towards the upper layers and of the four pieces with a pointy end and conical shape appears promising.

5.8 SUMMARY AND CONCLUSIONS

Several arguments confirm this assemblage to be material produced by indirect smelting:

- the evidence on site

The blast furnace remains and associated slag heap, together with the waterwheels and water management installations argue for this. Moreover, the lack of iron ore and furnace linings on the excavated slag heap (SH1) points to post-smelting operations.

- the iron content of the blast furnace slags

The low iron content and estimated temperature of formation of these slags strongly points to smelting in a water-powered blast furnace. The level of iron reduction and the silicon content in the cast iron produced cannot be achieved in a bloomery furnace.

- the presence of cast iron and/or wrought iron

The proportion of excavated cast iron is higher than wrought iron. Cast iron in fact is not only found as entrapped inclusions in the blast furnace slags but also as single fragments among the excavated material. They are often in the form of rounded pieces surrounded by slag and sandy material. This strongly points to the operation of exposing pig iron to oxidising conditions and obtaining droplets of molten metal that falls through the slag bath and solidified at the bottom of the hearth. Wrought

iron on the other hand is only found at the core of former cast iron droplets - as shown by the different levels of decarburisation observed in the microstructures of remaining metal – and in the form of an iron bar, the final product of the chaine opératoire of indirect smelting.

- the presence of small conglomerates with blast furnace slag and iron-rich slag

Similarly, to the point discussed above this evidence confirms the practice of melting pig iron and exposing it both to an oxidising atmosphere and iron-rich slag in order to promote and enhance decarburisation. The use of blast furnace slags could have contributed to the fining operations in view of their calcium oxide and silica content.

- the presence of slag with a high content of Ti, V and Cr

This seems to confirm the refining of pig iron in an oxidising atmosphere. While more evidence is needed in support of this interpretation, the presence of similar phases and inclusions in finery forge material identified by other studies suggests that this may be an important distinguishing feature for this technology.

- The type of non-metallic inclusions in RS1_0-20_Bar

As described in the previous section, the chemical composition of non-metallic inclusions characterises this piece of wrought iron as fined iron.

To conclude, while the investigation of large heterogenous assemblages is a complex task, much can be discovered by combining visual macro-morphological analysis with analytical observations. The identification of Ausewell Wood as an indirect smelting site appears unequivocal and is of great interest given the level of preservation of the site.

CHAPTER 6 THE TECHNOLOGY AT AUSEWELL WOOD

'The puddling furnace[1] remained the bottleneck of the industry. Only men of remarkable strength and endurance could stand up to the heat for hours, turn and stir the thick porridge of liquescent metal, and draw off the blobs of pasty wrought iron. The puddlers were the aristocracy of the proletariat, proud, clannish, set apart by sweat and blood. Few of them lived past forty. Numerous efforts were made to mechanise the puddling furnace – in vain. Machines could be made to stir the bath, but only the human eye and touch could separate out the solidifying decarburised metal.'

(Landes, 1996).

[1] Puddling furnace here refers generally to the process of converting cast iron into wrought iron.

6 DISCUSSION OF TECHNOLOGY AT AUSEWELL WOOD – ARCHAEOLOGY AND SCIENTIFIC ANALYSIS

This chapter brings together the results of the macro-morphological and chemical analysis of the assemblage to discuss the technology at Ausewell Wood. Whenever possible the results of this study are discussed in connection with the archaeological data gathered from previous studies. Hence, a reconstruction of the metallurgical operations is offered here. The technology and operations at the blast furnace are discussed first (section 6.1), followed by a discussion of the finery technology represented by the metallurgical debris excavated at SH1 (section 6.2).

6.1 THE BLAST FURNACE (SOUTHERN END OF THE SITE)

Iron ore was first smelted in the blast furnace, located to the southern end of the metallurgical complex (figure 6.1, BF). The presence of another blast furnace nearby appears likely in view of the documentary evidence and of the archaeological surveys performed by Newman (1998) and Juleff (2000) (see chapter 3). Whether they were contemporary, or one was constructed after the other went out use, is a question that can only be answered by excavations in that area of the site.

The Furnace Charge: Charcoal, Ore and Limestone

Charcoal, to be used as fuel, was prepared on site as evidenced by the presence of three charcoal burning platforms (see figure 3.2, CBP1 and CBP2). The small diameter roundwood observed as large charcoal fragments indicated that it was produced from coppice wood. Coppicing is a woodland management technique that comprised rotational cutting of young trees on a cycle of five or more years, allowing the stumps to regrow in order to provide a sustainable supply of wood (nationaltrust.org.uk). The use of charcoal as a fuel for smelting is also confirmed by the occurrence of charcoal inclusions in the blast furnace slags collected as surface finds and analysed for this study (BFF 1-5, chapter 5), as well as by the low sulphur content in the metal matrix of pig iron (see below).

Previous research of Ausewell Wood has focused on the geology of the area (in particular that of the Cleft Rock Mine, situated 250m to the south of the ironworks) to identify the source of the iron ore for smelting (Newman 2004, Page 2004). Page (2004, 9) reports that a large ‘block of very rich, dark slightly reddish-grey hematite’ was recovered adjacent to the blast furnace (the author does not know whether this

block was collected or left on site). Page's geological survey of the district between Holne Chase (tin mine situated on the opposite side of the valley, figure 3.2) and Cleft Rock (Ausewell or Hazel Mine, figure 3.2) revealed that the metalliferous deposits did not contain hematite, which is assumed to be the source needed for iron smelting. The iron mineralisation of the area contains small quantities of siderite (iron carbonate $FeCO_3$, termed 'spathic ore' in old accounts) and limited sulphide mineralisation dominated by pyrite (FeS_2), arsenopyrite (FeAsS) and smaller amounts of chalcopyrite ($CuFeS_2$) (Page 2004, 8).

While the identification of the source of the ore for smelting was beyond the scope of this study, surface samples collected near the blast furnace as possible iron ores, were analysed to establish what type of ore(s) were smelted. The results of this analysis suggest that these samples are more likely related to later tin ore processing activities (section 5.3.3). However, some more information was obtained from the analyses of the blast furnace slag finds (BFF1-5) collected from slag heap SH2 (figure 6.1). The presence of copper iron sulphide, iron sulphide and arsenic in the slag is consistent with the geology of the area, suggesting that local deposits were exploited. Moreover, carbonate ores (siderite) are rich in manganese oxides, which could explain the high levels of manganese measured in the glassy matrix of the blast furnace slags of Ausewell Wood. Page (2004, 14) reports the presence of siderite in dump material in two areas of the site, one to the south of the blast furnace and the other adjacent to the dressing floors, to the north of slag heap SH2. In addition, the identification of titanium and vanadium minerals in slag and in non-metallic inclusions in metal samples, points to the use of magnetite/hematite iron ores.

Hence, it is possible that a local source of iron was exploited and supplemented by other iron ores (magnetite/hematite) brought from another iron mine in the region (e.g., South Brent, according to the historical record). It also possible that the local mine was exhausted, or that iron was not efficiently smelted, and thus more iron ore was imported from richer, larger mines, once the blast furnace had been constructed and established. Indeed, smelting of carbonate ores is more complicated than for iron oxides (such as magnetite and hematite), requiring preheating (an operation called roasting, see glossary) before the ore can be processed in a blast furnace. Moreover, the presence of excessive sulphur might have produced brittle cast iron,

requiring the import of a better iron ore. Overall, it seems likely that ore charge consisted of a mixture of iron ores from more than one source.

Furthermore, the use of limestone was confirmed by the high levels of calcium in the blast furnace slags (CaO 29.7wt%, chapter 5). Limestone would have been sourced locally; the closest limestone deposits are those of Mount Ararat Chert Formation, in the Parish of Ilsington on South Dartmoor. According to Page (2004, 14), Mount Ararat also contains mineral formations more consistent with hematite and magnetite. Thus, Mount Ararat should also be considered as a possible candidate for the source of the smelted iron ore at Ausewell Wood (chapter 7.1).

The Furnace Products: Slag and Pig Iron

The products of the blast furnace were a glassy slag of low viscosity (chapter 5), which was drained from the furnace in a liquid state, and pig iron in the form of grey cast iron. The macro-morphological analysis of some fragments of blast furnace slag indeed shows flows of slag overlapping each other, indicating a fluid slag that was 'tapped' outside of the furnace (chapter 4). Chemically, this is supported by the high manganese content, which increases the fluidity of the slag. Moreover, the slag features a low iron content, indicating a good extraction of metallic iron, and furnace temperatures of about 1400°C, which are consistent with the use of a cold blast typical of early blast furnaces.

The pig iron was probably cast in the form of ingots and transported to the finery forge to be converted into wrought iron. It is not known if pig iron was also used for castings, but grey cast iron is an excellent material for castings – especially of artefacts such as cooking pots and cannons (Wagner 2008, 161).

Finally, some observations are offered here about the quality of the cast iron alloy smelted at Ausewell Wood, as a starting material for the fining process. Williams (2013 and 2019) argues that grey cast iron was more difficult to decarburise than white cast iron, due to the chemical and physical properties of the two iron alloys. From a chemical point of view, the main issue with grey cast iron was the high silicon content; this had to be oxidised before carbon could be removed from iron. The physical issue concerned the fact that grey cast iron, when heated in a charcoal finery, melted to a proper liquid, while white cast iron became a pasty mixture which was easier to manipulate and raise in front of the blast of air, promoting

decarburisation. Therefore, when fining grey cast iron, two technical operations were necessary: the removal of silicon by oxidation and the addition of iron oxide (in the form of iron-rich material, such as finery slag, hammerscale or even iron ore) to the fining process. The decarburisation of grey cast iron produced much more slag than working with white cast iron, as it involved the use of fluxes and required longer operations in the finery hearth.

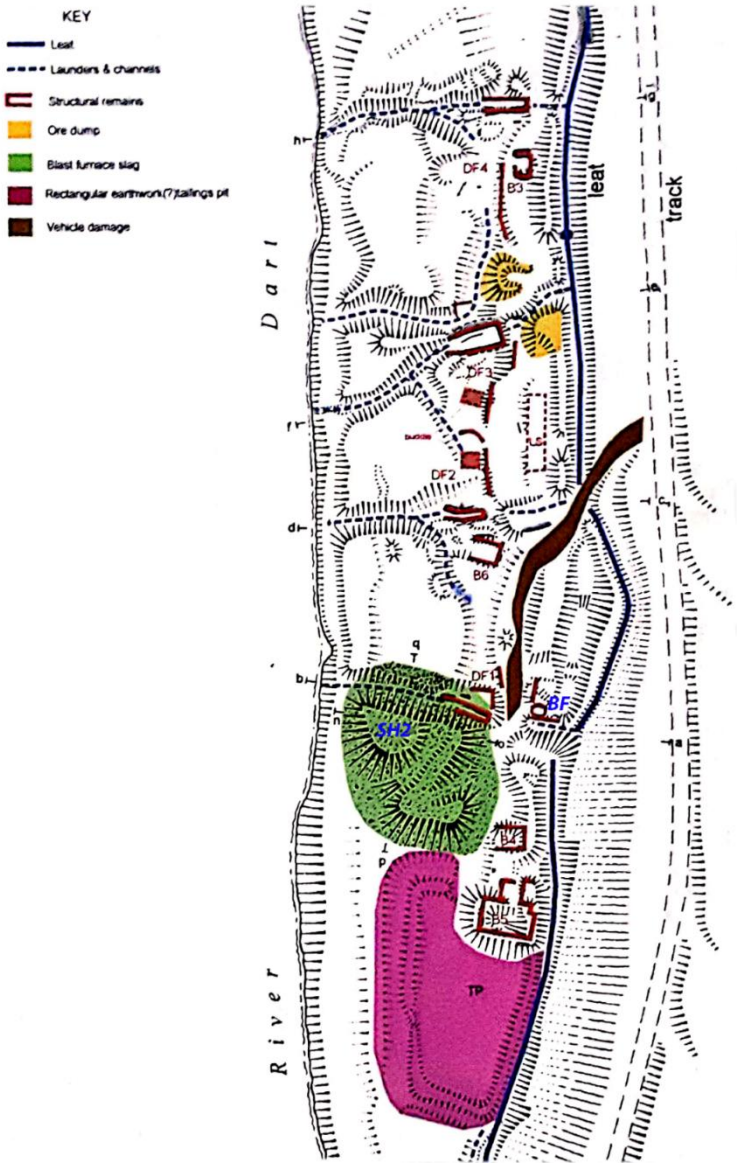

Figure 6.1. Plan showing the southern end of the site, produced by Newman for the Royal Commission on the Historical Monuments of England (1998, 5). The illustration shows the position of the blast furnace and slag heap SH2 (marked in green). Subsequent field walking suggests the slag heap is more extensive, spreading across a similar-sized area to the north. The blast furnace surface samples (BFF1-5) were collected from this slag deposit. The features in red and yellow on the top are in connection with the 18th century non-ferrous activities, including the ore dumps. In blue line, opposite the river, is the main leat which channelled water to a series of water wheels.

In addition, phosphorus and sulphur were the principal cause of ‘cold shortness’ and ‘hot shortness’ (see glossary), respectively, and were thus unwanted elements in the final wrought iron. Sulphur was generally dealt with in the smelting phase, by roasting the iron ore prior to smelting and adding limestone to the furnace charge (chapter 5). Although, the addition of calcium-containing material to finery hearth also contributed to the removal of sulphur (Dillmann *et al.* 2012, 22). Conversely, phosphorus was removed (or rather its content was decreased) during fining, probably in the early stages of the process, in an oxidising atmosphere and in contact with the slag (Neff and Dillmann 2001, Dillmann *et al.* 2012, 28, Williams 2019, 99; see also Young and Hart 2017).

Thus, the grey cast iron smelted at Ausewell Wood was in theory a less than ideal material for fining. The high silicon content, the presence of phosphorus and, although in small amounts, of sulphur, probably made fining a long and complex operation. This appears corroborated by the abundance of iron-rich slags and the numerous cast iron droplets recovered from the excavations. Ultimately, evidence at Ausewell Wood indicates that pig iron was refined (cleaned of impurities) before the actual fining (decarburisation) took place. While it is unlikely that this was a separate step (conducted in a different hearth), refining produced slag with a distinctive chemistry and microstructure, as argued in the section below.

6.2 THE FINERY FORGE (NORTHERN END OF THE SITE)

Slag heap 1 (SH1) is located approximately 475m to the north of the blast furnace. The remains of an unclear rectangular structure and a broad but shallow channel (AC1) have been interpreted as a potential finery forge by Cranstone in 2004 (figure 6.2). The channel is also marked on the 1605 map (chapter 3), confirming its date to be that of the iron smelting phase. The excavation of the slag heap brought to light a possible hearth base in trench JN9 and the remnants of an *in situ* wall in trench ZN1; at present however, the layout of the forge is still unclear. The area has been heavily damaged by vehicle tracks (figure 6.2; Newman 1998).

From the macro-morphological and chemical analysis of the material debris it was possible to obtain some information on the hearth installations where the operations were conducted. Many authors report that the walls and floor of the finery hearth were lined with cast iron plates to protect the brickwork of the structure from the slag

(Bauerman 1868, Schubert 1951, Morton and Wingrove 1970, Rostoker and Bronson 1990, Gordon 1997, Mackenzie and Whiteman 2006).

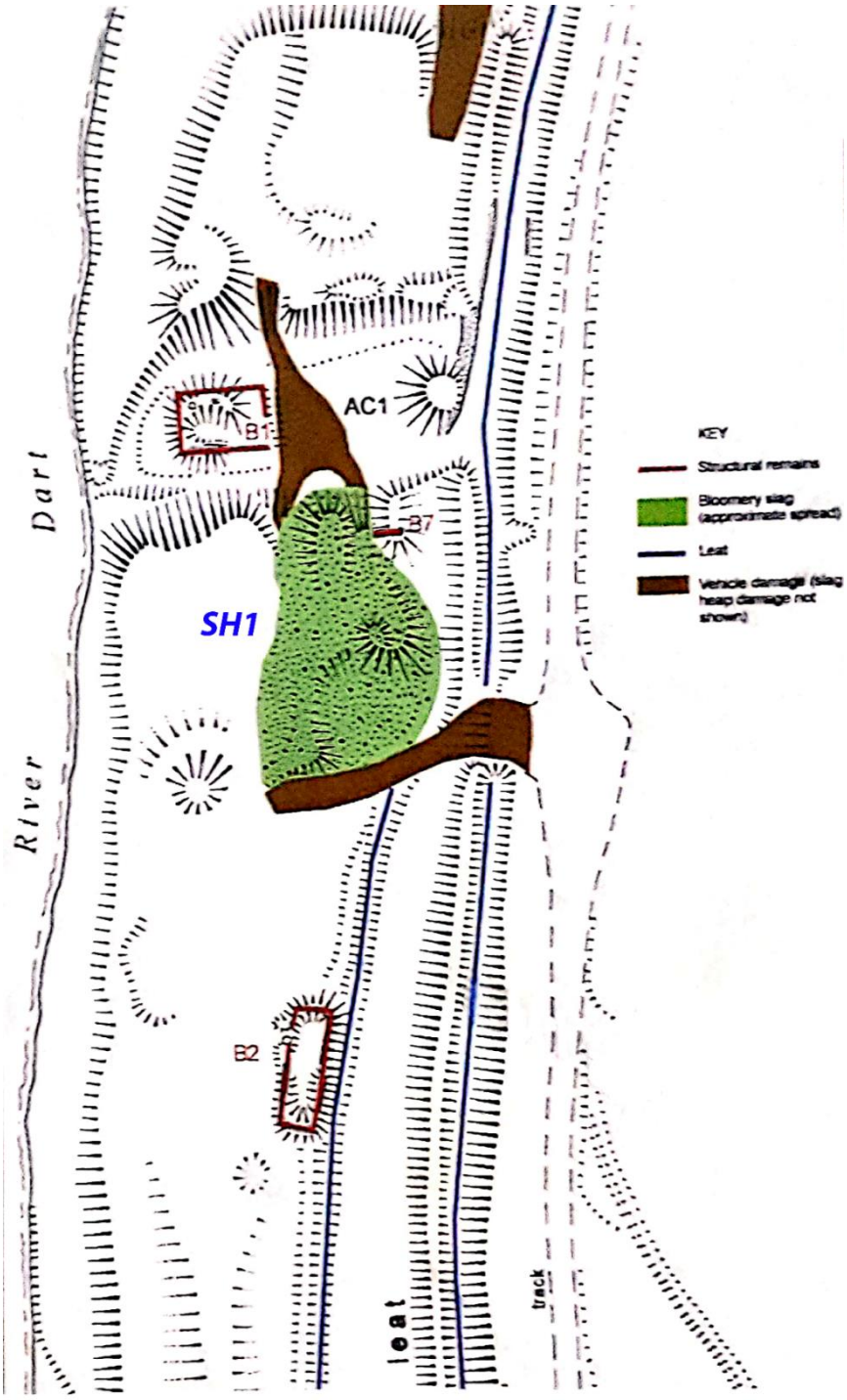

Figure 6.2. Plan showing the northern end of the site, produced by Newman for the Royal Commission on the Historical Monuments of England (1998, 11). The illustration shows the approximate spread of the slag heap SH1 (termed bloomery slag in the report), although subsequent investigations during the excavations of 1999 indicated the spread extending further towards the river, the artificial channel AC1 and building B1, B2 and remains of a possible wall in B7.

While there is no material evidence of this at Ausewell Wood, several slag fragments show flat, smooth profiles, which suggest that they might have solidified against solid even surfaces (see also Landon *et al.* 2001).

Indeed, the scarcity of furnace lining fragments retrieved during the excavations point to a similar arrangement. This is supported by the chemical composition of the finery tap slags, which do not show enrichment in clay minerals such as Al_2O_3, MgO, NaO_2 or K_2O, as there was no interaction between the slag and the hearth structure (see chemical composition of clay fragments in table 5.1.5, section 5.5).

While slag tapping is confirmed by the abundance of slag 'cakes' with molten and rippled textures (finery tap slag, chapter 4), less clear is the origin of the large blocks that show a flat upper surface and a pointy, or lateral, protrusion (section 4.4.2, figure 4.33). It is conceivable that these are slags that formed inside a hearth installation, and that the protrusions represent slag that solidified within a tapping hole or channel, from which the surplus slag was let out of the hearth. Hearth slag that solidified within the installation (and was possibly removed at the end of the operations) probably formed in both finery and chafery hearths. A further observation is that there was more than one system to drain the slag out of the hearths, as demonstrated by the occurrence of slag channels, or rather cavities left by slag channels, in the slags of the subtype 'flowed' cakes (section 4.4.1), and the several slag channel fragments of cylindrical shape (section 4.4.2). Indeed, the variety of slag morphologies observed appears to be a characteristic of the finery technology. This trait might offer a tool for its identification on archaeological sites, especially in relation to the abundance of features indicative of slag tapping. For the smaller material, the other significant evidence is the presence of conglomerates and (sub) rounded pieces which are formed by a mixture of slag, iron and cast iron (chapter 5, sections 5.3.2 and 5.4.4). The schematic representation in figure 6.3 shows a possible mechanism of formation for finery tap slag and hearth slag cakes.

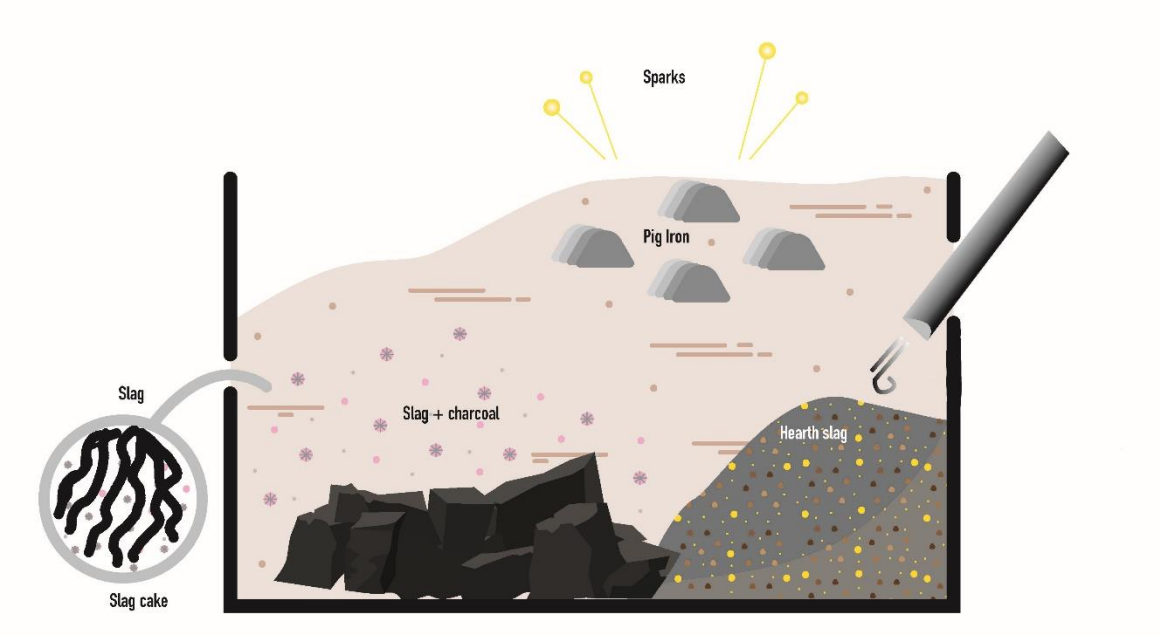

Figure 6.3. Schematic diagram showing a simplified finery forge where pig iron is worked under a blast of air. The hearth is filled with slag and charcoal. More slag is added as the operation progresses. Finery tap slag is let out of the hearth from a tap hole located on the side, while hearth slag forms within the structure. This slag is left inside the hearth for the following fining operations, or removed as large blocks when clearing the hearth (image by the author).

Returning to the technical aspects of the process, fining consisted of two operations:

1. during the first stage, pig iron was refined by melting in front of an oxidising blast of air, which caused the oxidation of silicon and other impurities contained in the pig iron. This operation is essential for the following decarburisation. The resulting slag depends on the nature of the pig iron under treatment, but usually a silicon-rich slag was produced. This slag is what was described by Percy (1864, 619), and later by Bauerman (1868, 255) as *poor* slag, containing around 50wt% of iron oxide and 30wt% of silica.
2. the second operation, is the actual fining, or removal of carbon from iron, which ultimately results in the production of malleable (wrought) iron. The resulting *rich* slag (with more than 60wt% iron oxide) is the ubiquitous tap slag.

The second step thus is clearly recognisable, not only at Ausewell Wood, but at all identified finery forge sites. However, chemical analysis of slags related to the first stage is, to the author's knowledge, almost non-existent in the modern literature. At least for what concerns the charcoal finery technology. In fact, refining, in a separate

purpose-built installation, is mostly associated with later puddling techniques, which dealing with high silicon grey cast iron produced from coke smelting, necessitated to 'pre-treat' pig iron, removing most of the silicon before decarburisation could take place. Refining in charcoal finery is described by Percy (1864), Bauerman (1868), Morton and Wingrove (1970), Rostoker and Dvorak (1990) and by Dillmann *et al.* 2012. Refining essentially produced white cast iron (i.e. grey cast iron was transformed in white cast iron) or hypereutectoid steel, thus an alloy which still contained considerable quantities of carbon, but whose silicon content was greatly reduced. Fining then followed on in the same hearth by stirring and exposing the mass of refined iron to more air blast until a mass of malleable iron was produced. Figure 6.4 shows a simplified overview of the operations in the finery hearth.

In the light of all this, the results obtained from the hearth slag retrieved from RS1 (section 5.4.2) appear significant. The glassy matrix of the slag is characterised by the same composition reported for the *poor* slags, 46.0wt% of iron oxide and 39.0wt% of silica. In addition, the chemistry and microstructure of this piece and slags from refining (for puddling) analysed by Young and Hart (2017) show similarities. These are:

- the occurrence of calcium phosphate and other phosphatic phases
- the presence of hercynitic spinels containing high titanium, chromium and vanadium contents
- manganese (MnO) content between 2-3wt% in the bulk composition
- iron sulphide (FeS) occurring as tiny specks in interstitial areas

Also, Phelps *et al.* (2011, 27-28) tentatively identified refining slag at Downside Mill, in Surrey (South East of England). The site, however, saw the transition from charcoal-fining to puddling; consequently, their identification as slag produced in the finery hearth is hesitant. While more analyses are needed to confirm these observations, it is fair to say that this sample most likely represents a *refining* slag. The study of these slags appears to offer a promising new option for distinguishing between bloomery and finery sites (chapter 7). The identification of this material contributed greatly to the characterisation of the technology at Ausewell Wood. Here, refining and fining were probably carried out in the same finery hearth, before the mass of wrought iron was taken to the chafery hearth.

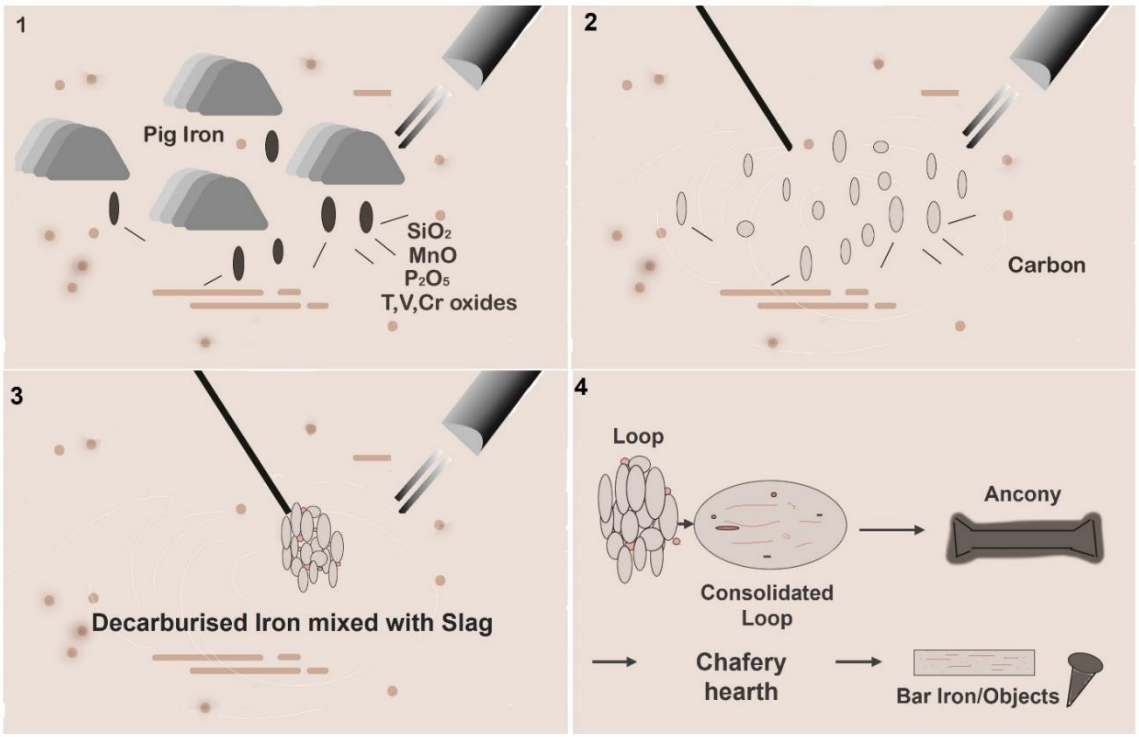

Figure 6.4. Schematic diagram showing a simplified sequence of reactions within the finery hearth. Number 1 illustrates refining, where the pig iron exposed to an oxidising atmosphere first loses silicon and other impurities. Droplets of pig iron thus fall in the slag bath and are stirred and collected with an iron rod (number 2), while progressively losing more and more carbon. The mass of decarburised iron mixed with slag is collected, hammered and exposed more than one time to the oxidising blast (number 3). Then the mass 'comes to nature', meaning that it has a consistency which indicates that decarburisation is complete. The following operations are carried out at the chafery hearth, where roughly shaped pieces of metals (possibly in the form of anconies) where reheated and forged (image by the author).

The presence of a chafery hearth, built for the purpose of reheating the fined *loop*, is assumed rather than confirmed, but it appears likely. Some of the large blocks of hearth slag show features that suggest they are chafery hearth slags. In particular, the presence of pieces with slag runners still attached (*'hambone'*) and the occurrence of slag 'cakes' with large-size porosity on the surface layers and denser lower parts (see for example figure 4.3.2 in chapter 4). Evidence of hammering is then supported by the matrix samples, which contains abundant hammerscale slag. The final working of the metal into bars is confirmed by the iron bar fragment retrieved from trench RS1.

6.3 SOME THOUGHTS ON OUTPUTS AND OPERATIONAL LOGISTICS

Thus, some final considerations on the quality of the wrought iron produced can be made at this point. The low carbon content indicates that the decarburisation of pig

iron was performed successfully, albeit it was non-homogeneous, as shown by the small areas of pearlite at the grain boundaries of the iron bar fragment (chapter 5, section 5.4.4). This however is consistent with iron fined in charcoal fineries (Liu *et al.* 2019). Sulphur and manganese are no longer detectable by SEM-EDS analysis and silicon shows an average content around 0.3wt%. Phosphorus content is lower than that of the pig iron (0.1wt% against 0.8wt%). Overall, the iron obtained contains few impurities. The abundance of non-metallic inclusions is again consistent with the fining technology (Buchwald and Wivel 1998, Mackenzie and Whiteman 2006). The metallic matrix is characterised by equiaxed grains of various size. The elongated shape of the inclusions located at the top of the piece suggests some degree of working (hammering), while the spherical ones at the bottom seem to indicate that no hammering was performed; these however could be inclusions that broke into smaller particles as a result of hot working. Indeed, the flat shape of the piece suggests that the metal was worked into shape, probably alternating annealing (reheating of the metal) to hot working. Ultimately, the iron matrix appears sufficiently ductile to allow some hot working processing. Apart from the retrieval of a possible (completely corroded) nail, there was no indication as to what, if any, objects were produced at Ausewell Wood. The possibility is that iron in the form of bar was sold to other manufacturing workshops. This last scenario however appears less plausible. Given the history and ownership of the site, it is more likely that the industry was experimental, and that production was local in scale, probably responding to the needs of those involved in the enterprise (chapter 3).

A brief consideration of the water management system is due here. The literature suggests that a finery forge, when built on the same river as a blast furnace, was located downstream from the furnace, to regulate the amount of water reaching the water wheels (chapter 3). The finery forge at Ausewell Wood is upstream from the blast furnace. This suggests that behind the construction of the leat and water wheels there was a clear knowledge and understanding of hydraulics, which provides a further link to Adrian Gilbert and his experience with tin works (smelted in blowing houses from the early 14th century) on Dartmoor.

Finally, the establishment of a blast furnace and finery forge in this part of the country, away from large iron mines and large markets, shows considerable effort

and fits with the picture that saw individual entrepreneurs move away from the Weald of South East England, where the technology was first established, in an attempt to experiment with the new technologies and make profit of suitable lands. The fact that the ironworking activities at Ausewell Wood were apparently successful, suggests that experienced iron workers operated on the site. It is impossible to establish whether furnace workers and forgemen were part of the same workforce, or if only skilled forgemen were employed at Ausewell Wood to process the smelted pig iron. However, managing all the necessary activities (organisation and preparation of the raw materials, transport of pig iron to the forge, clearing of the furnaces and forge, water management, repairs etc.) over a large area certainly required considerable organisation and discipline. In all probability, small groups of workers operated on different tasks with some degree of coordination to ensure a successful output.

CHAPTER 7 CONCLUSIONS

Valckenborch Lucas Van, Landscape with Ironworks, 1595 (Museo National del Prado).

7.1. AUSEWELL WOOD IN THE WIDER CONTEXT: A METALLURGICAL 'LABORATORY' IN DEVON

King (2020) in his recently published *A gazetteer of the British Iron industry*, *1490-1815*, provides a history of documentary references to ironworks of the charcoal blast furnace period in England (except the Weald), Scotland and Wales. Devon is included in the Southwestern Peninsula, together with Cornwall and West Somerset. A map of the region marks only two blast furnaces with finery forges; one is West Lee Ironworks, in Molland, a parish in North Devon, located at the foot of Exmoor, the other, in South Devon, is Ausewell Wood (figure 7.1). Schubert (1957) reviewing the history of the iron industry in Britain, makes no mention of Devon.

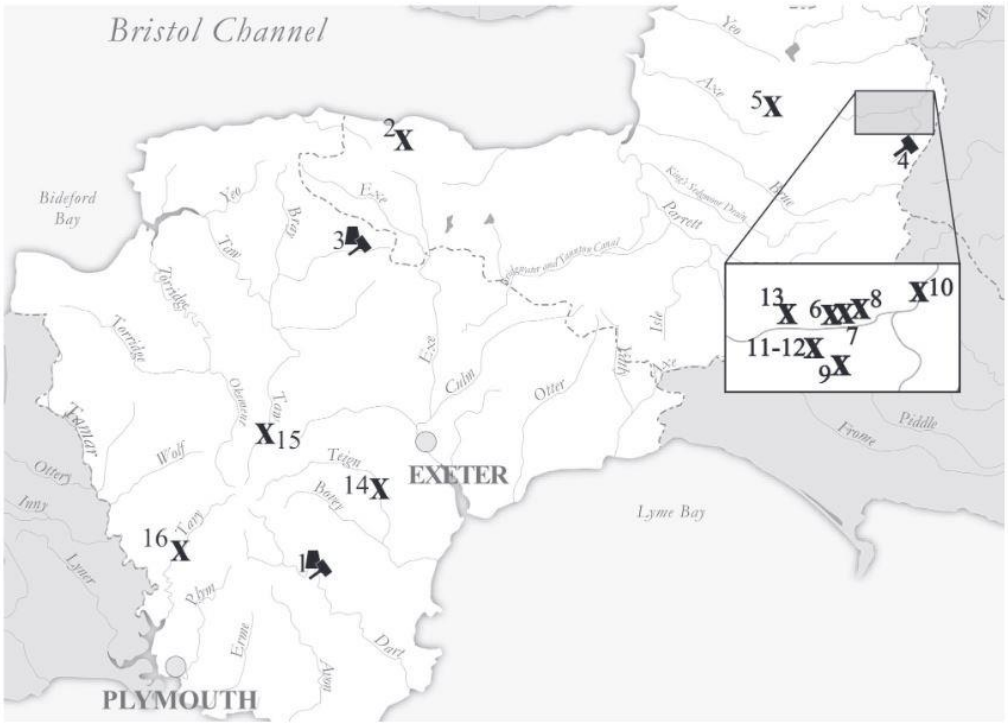

Figure 7.1. Map of the Southwest Peninsula showing the ironworks recorded in the region. The symbols are ▙ for charcoal blast furnace, ➶ for finery forge and **X** *for other ironworks. Ausewell Wood is number 1, marked on the River Dart. The other blast furnace and finery forge is West Lee Ironworks marked as number 3, in North Devon. The only other forge recorded for the period is in South Somerset, number 4, processing pig from the Forest of Dean. (Map after King, 2020, figure 36, 536).*

Only documentary references exist about the West Lee ironworks. In a survey of the parish, dated between 1747 and 1756, the officeholder of Molland reported that 'there is to be seen on the tenement of West Lee some remains of an iron furnace, a forge and a mill, the two latter wrought by water' (King 2020, 536). The land belonged to the Courtenay family of West Molland and according to King (2020), the

ironworks were established sometime in the first half of the 16th century, but no other information is available. It is thus clear how Ausewell Wood and the ironworking enterprise there represents an exception in the region. It has already been mentioned how the British iron industry heavily relied on Swedish, Russian and Spanish imports (chapter 3). The latter, coming from the Basque country, was imported into Cornwall and Devon through the city of Exeter, where merchants traded Spanish iron in exchange for textiles produced by the important woollen trade of Exeter (Uriarte Ayo 1992). Indeed, the regional economy had featured iron imports from Bilbao since the Middle Ages (Evans *et al.* 2002, 650). It was only after the introduction of coke smelting that domestically produced iron reached the levels of, and eventually surpassed imported iron. In the charcoal era, English iron, most of which was produced from phosphoric iron ore, was cold short and only employed in the manufacture of nails or other forgeable artefacts, as it was not suitable for conversion to steel. Imported iron was thus destined for high-quality production, such as the ship building, armament and conversion sectors (Uriarte Ayo 1992, 198), and effectively competed with English iron, hindering the development of a domestic industry, which for centuries retained a regional character (chapter 2).

The history of the medieval iron industry has focused on areas of England where production was considerable and sustained, such as the Weald, south-west Yorkshire and the Forest of Dean (Claughton 2016). In reality, most areas of England exploited small deposits which were sufficient to sustain local production. However, an overall historical account of the history before 1750 does not exist, and it is often down to archaeology to discover new mining areas and identify sustained iron industries. Significant examples are the Exmoor Iron industry (between west Somerset and North Devon), which thrived from the Roman period up to the Medieval period (Juleff 1997), or the discovery of the iron industry of the Blackdown Hills, in East Devon, which mined and smelted iron until at least the second half of the 15th century (Griffith and Weddell 1996). Up until the late 19th century, the iron industry of South West England appears characterised by relatively small, specialised centres of production, which produced iron to supply local workshops and markets, and transported surplus production to other areas of the region.

Devon has small deposits of high-grade ores, most of which were transported and processed in the growing industrial centres of South Wales, subjecting the local

mining industry to heavy transport costs. According to Atkinson *et al.* 1982, the area did not attract smelters because of the lack of large deposits. From the 19th century, the region started to attract attention for the low phosphorus content of its hematite deposits and its manganese-rich carbonate ores, as the metal obtained from smelting these ores could be used in steel production (Claughton 2016, 116). Output from Devon's iron mines reached its peak around the 1860s and 1870s, but after initial fervent activity, the industry declined as it could not satisfy the increasing demand triggered by the introduction of the Bessemer process in 1856 for the production of steel (Atkinson *et al.* 1982, 28, Flinn 1955). England resorted again to the low phosphorus deposits of north Spain.

The Bessemer process was the first attempt towards the mass production of steel. Named after Sir Henry Bessemer of England, the process involved the removal of silicon and other impurities by blowing air through molten pig iron. The process was conducted in a large ovoidal container, termed a converter, which was lined with clay or dolomite, to convert the oxidised pig iron into steel. The process was also aided by other additions, such as ferromanganese alloys. It should not surprise that the principle behind the Bessemer process is very similar to earlier conversion processes, namely charcoal finery but also puddling. It is in fact within this historical context that the study of the charcoal finery technology must be situated. From the introduction of the indirect method to the adoption of coke smelting in 1750, which conventionally marks the beginning of the Industrial Revolution, ironworkers and inventors were trying and experimenting with conversion techniques. They were driven by the need to satisfy an ever increasing demand to produce steel in a non-expensive and efficient way and to exit the industrial bottleneck created by finery and puddling techniques, which were lengthy and largely dependent on artisanal practices (chapter 2).

Returning to Ausewell Wood then, a few considerations can be made here to put into context the ironworks. First, the low phosphorus and high manganese content of pig iron and slags is consistent with the local geology. The fact that the iron ores brought to Ausewell Wood were 'good both for steel and iron' (Phillpotts 2003, 13; chapter 3) suggests that there was already some knowledge of the quality of the iron ores from local deposits. This brief overview of the iron trade in the region highlights the experimental character of the activities conducted at Ausewell Wood. The site,

however, also reflects one of the main features of the Devon iron production, that is the transport of iron ores over long distances. We do not have any information regarding the end of iron working on the River Dart, all the available documentary sources concerns the later non-ferrous metallurgy, but we know that by the time Kalmeter visited the site in 1764, the blast furnace and related operations were a distant memory. This suggests a relatively short working life of the ironworks, which may be related to the exhaustion of local mines or to transport costs which outweighed production. What it is apparent is that the enterprise, similarly to the rest of the Devon iron trade, never developed into a sustained economic activity. Albeit, perhaps, this was not the original intention.

This last point allows us to consider another aspect of Ausewell Wood. The fascinating connection to Adrian Gilbert and his involvement in the cultural and social life of 16th century England (chapter 3) provides a further historical dimension to the discussion of Ausewell Wood. The charcoal blast furnace was usually part of an integrated enterprise (Hyde 1977). Smelting, forging and marketing of the final product was conducted by the same group, which was united either by partnerships or through family links. Examples of this are the Foley family that controlled ironworks in South Wales, the Forest of Dean, Staffordshire and North Wales; the Spencer group which operated several furnaces, forges and a slitting mill in South Yorkshire-Derbyshire region, or again the Knight family in the West Midlands (Johnson 1952, Hyde 1977). The driving force behind these enterprises was surely economic growth, as evidenced by ironworks account books detailing output, expenditure and stock of raw materials. Ausewell Wood offers another perspective on ironworking, reflecting yet another feature of the period under study: the academic interest in nature, which was pursued within laboratories and artisanal workshops (see for example essays in Smith *et al.* 2014).

In the 15th and 16th centuries *laboratorium* indicated a workplace where various ‘chemical’ operations were performed; including alchemical laboratories and artisanal workshops with their furnaces and fires (Dupré 2014). This period saw the rise of what Dupré (2004, xv) describes as a hybrid figure, ‘with one foot in artisanal culture and another in scholarly culture’. Working in laboratories and workshops in this period was not only about transforming base metals into silver or gold – in search of the famous philosopher’s stone, but it implied acquiring knowledge of the

material world through experimentation with new techniques and the art of making. This provided a unique dimension to the manufacture of materials in general, in which production, experimentation and various artisanal practices operated together.

The figure of Adrian Gilbert perfectly fits the definition of a ‘hybrid’ artisan-scholar. As described in chapter 3, he was not only involved in mining and metallurgical activities, which included silver smelting and refining (a metal strictly connected to alchemy), he also worked with plants and water for gardening and to produce ‘medicines’. Lady Johanna, who was an English gardener and herbalist, wrote two recipe books, devoting one and a half pages to Adrian Gilbert’s cordial water, which apparently had curative powers (Leong 2013; figure 7.2). Gilbert was employed by Mary Herbert to work as laboratory assistant for her alchemical experiment, as he was ‘a great chymist in those days’ (Aubrey 1898, 262). Further, he was a friend and associate of John Dee, who spent much of his life reading and practising alchemy (Cavallaro 2006). We know that Adrian Gilbert frequently visited and met with John Dee, not only to prepare for the North-West Passage expeditions, but also to share scientific and magic knowledge. Indeed, it was John Dee who trained explorers in the use of navigation, maps and compasses; he also possessed a large library and taught the Herbert family, and probably the same Adrian Gilbert, about mining and metallurgy (Malcolmson 2010, 118).

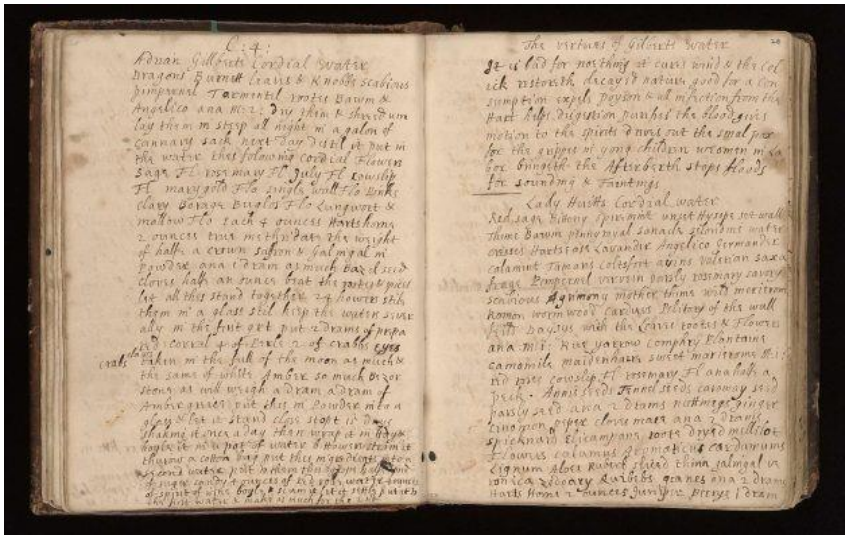

Figure 7.2. Lady Johanna's recipe book, showing the recipe for Adrian Gilbert's cordial water. On the top right page it is written: "It is bad for nothing it cures wind and the colick restoreth decayed nature good for a consumption expels poison & all infection from the Hart helps digestion purifies the blood gives motion to the spirits drives out the smallpox for the grippes in young children weomen in labor bringeth the Afterbirth stops floods for sounding and faintings" (A digitalised copy of the book is available at the Wellcome Library, https://wellcomecollection.org/works/wa8darch/items).

Ultimately, both experimentation and production probably played a significant part in the establishment of the ironworks at Ausewell Wood. Material production, in the world of scientists, scholars and artisans of the period, was not only viewed from a utilitarian perspective, but it also advanced understanding of the natural world and innovations with new materials. It is thus reasonable to assume that the blast furnace and charcoal finery technology at Ausewell Wood, which transformed a liquid metal into a pasty mass with different properties through a series of chemical reactions in boiling molten masses, was perceived and performed in a similar cultural context.

7.2 CONCLUSIONS AND FUTURE WORK

The aim of this thesis is to reconstruct the iron technology at the site of Ausewell Wood on Dartmoor. Characterised by water management structures, the site, which extends along the banks of the River Dart, attracted attention for the presence of two types of iron slag. To the south of the site, near the remains of a blast furnace, the deposit is characterised by light, glassy, silica-rich slags, typical by-products of the indirect method of iron smelting. To the north, at a distance of about 475m, the metallurgical debris features dense, iron-rich slags, of the type normally associated with the direct or bloomery method (chapter 2). The site was thus identified for its potential to shed light on the transition from bloomery iron smelting to blast furnace

production. Documentary evidence and pottery recovered during excavations date the iron-working phase to the early 17th century, a period that saw the indirect method leave the Weald (South East of England), where it had first been imported by French workers, and expand into the rest of the British Isles. The change in iron technology is historically well established, but physical evidence of the first experiments with the new technology is often lacking, as early industrial sites are frequently reused or disturbed by later urbanisation. Ausewell Wood represents a welcome exception; the evidence preserved *in situ*, offered the opportunity to contextualise the technological sequence that characterised the transition to the indirect method. Hence, the primary aim of this study was to investigate and characterise the technology through the analysis of metallurgical debris excavated from the iron-rich slag deposit (slag heap SH1).

The first step towards the reconstruction of the technology was a macro-morphological analysis of the assemblage. This analysis consisted of a number of stages, which entailed the detailed quantification and description of the material, recording of features of interest in a database, such as size and degree of fracture, density, shape, colour, inclusions and location on site, and photographic documentation of the material. The dataset was then analysed with the aim of identifying types of slag and thus create a classification of the assemblage. This step was initially conducted using typologies elaborated for (bloomery) smelting assemblages (chapter 4). The classification approach highlighted prior assumptions within the field of archaeometallurgy that in the first instance affected the results obtained, especially with regard to the presence of tap slag and its association with smelting. However, the investigation of the entire available assemblage pinpointed a series of features that indicated post-smelting activities. This provided a first connection with the blast furnace located to the south and indicated that Ausewell Wood was a single metallurgical complex where both smelting and post-smelting operations were conducted. This interpretation is supported by a series of observations. First, the absence of iron ores and furnace lining, which are commonly found in iron-smelting assemblages. Second, the abundance of iron scrap: iron-working sites (as opposed to smelting sites) are generally characterised by the presence of metal waste. Third, the presence, among the iron-rich slag, of occurrences of glassy blast furnace slag.

Further, the dataset was analysed in connection with the archaeological data to explore the layout of the site and identify possible deposition patterns. The composition of the assemblage is complex with types of slag occurring in the different areas of the slag heap 1 (SH1), which suggests that a series of operations were conducted, probably using different metalworking structures. However, a primary deposit is identified towards the east side of SH1 (landward), while the fragmentary nature of the material retrieved from the centre of the deposit suggests that these may be passage areas, where slag was moved or re-deposited during the metal-working operations.

Hence, the results of the macro-morphological analysis provide a first detailed report (with photographic documentation, too often lacking in archaeological accounts) of an early charcoal finery assemblage. The results summarised below can hence be used for the identification of finery forge sites and assemblages. In addition to the occurrence of fragments of blast furnace slag and abundance of iron-rich material, metallurgical debris from fining are likely to include small slaggy conglomerations of material. The round shape of iron scraps and slag accumulations is an additional identifying feature, as this most likely derives from stirring operations typical of early conversion processes. Finally, elements (such as slag channels and/or protrusions) related to slag tapping and/or removal from hearth installations are to be expected on large masses of slag.

The following step was the chemical and microstructural investigation of selected samples. The sampling strategy adopted targeted representative material of each metallurgical ‘stage’ identified during the macro-morphological analysis; some methodological considerations on this approach are offered below. The main objectives of the analytical study were to confirm the technological connection between the excavated slag heap (SH1) and the area of the blast furnace, and to understand and characterise the finery process. The first objective entailed the characterisation of the site as a whole, whereby the blast furnace, where smelting of iron ores was performed, represented the first half of the operation, while slag heap SH1, represented the second half, where pig iron brought to the finery forge was converted into wrought iron. The analysis of blast furnace slag samples from both sides of the site confirmed that they were produced using the same raw materials and under the same operating conditions. This smelting slag, characterised by a

calcium-alumina-silicate glassy matrix, a low iron content and by the presence of grey cast iron metal inclusions, is unequivocally identified as blast furnace slag produced in the (cold, i.e. not preheated) blast furnace located at the southern end of the metallurgical complex. The fragments of blast furnace smelting slag recovered at the finery forge were either transported with the pig iron, or intentionally added to the finery forge slag bath during conversion. This last aspect needs confirmation from other sites to be identified as an operational practice (see below).

Evidence of the use of both carbonate/sulphide (probably from local mineral deposits) and oxide iron ores (transported from other mines in the county) was identified in the occurrence of titanium and vanadium oxides, as well as in the high manganese content and occurrence of iron copper sulphide. The overall low sulphur content of slags and pig iron confirmed the use of charcoal as a fuel; this was prepared on site from coppicing wood from the surrounding forest. Moreover, the use of limestone is confirmed by the high calcium content of the slags. Thus, the technology is consistent with early experimentations with the new technology, which produced cast iron in a charcoal-fuelled blast structure with the use of fluxes.

For the second objective, the results indicate that the fining process involved at least three steps: refining, which removed silicon and other impurities contained in the pig iron; fining, which converted cast iron into wrought iron by removing (or greatly reducing) the carbon content; and finally heating and consolidating the fined metal mass into iron bars. The first two steps were probably performed inside the finery hearth and produced two different slags: one characterised by a high silicon content and a series of phases formed by other common impurities, such as phosphorus, manganese, but also titanium, vanadium and chromium, and an iron-rich slag of fayalitic composition drained out of the hearth. The former slag formed during the first melting of pig iron, promoting the following decarburisation. Iron oxide, in the form of hammerscale and finery slag (the same iron-rich tap slag by-product of fining), was added to the finery hearth to help with the decarburisation. Other additions, such as silica-rich material in the form of quartz and calcium-rich material in the form of limestone and clay, were also employed. All this formed a slag bath, which also protected the low-carbon iron as it formed from further oxidation. Any surplus slag was drained from the hearth by opening a tap hole located to the side of the installation, thus forming slag cakes with the archetypal flow pattern on the

surface of tap slag. After stirring and raising droplets of metal in front of the blast for a few times, especially when working with grey cast iron, a mass of decarburised iron formed, which was then hammered and consolidated for further work at the chafery hearth. This last step remains somewhat elusive in terms of our understanding of slag formation. Only a specific sampling strategy can fill this gap, and their study in a specially-designed project would provide more information on their mechanism of formation (see below).

Overall, the production of iron at Ausewell Wood using the indirect method appears to have been successful - as demonstrated by the results of the piece of wrought iron – and most likely based on small-scale private production. The lack of documentary evidence detailing costs and operations supports this interpretation. However, this peculiarity makes Ausewell Wood a compelling case study, which offered the opportunity to investigate not only first experiments with the indirect method but also to explore the social and historical context within which this important technological change happened. During the iron-working phase the land was in the possession of the half-brother of Sir Walter Raleigh, Adrian Gilbert, who was heavily involved in the expeditions to find the North-West Passage and also had a keen interest in mining and metallurgy (chapter 3 and section 7.1). The sixteenth and seventeenth centuries were periods of vigorous economic expansion and scientific advancements, which fuelled major technological innovations in important industries. For the iron trade, the driving forces behind the technological developments of the period were the production of ordnance materials and artillery, and oversea explorations and navigation. The construction of a blast furnace and finery forge, with the need for water power and large quantities of raw materials, required considerable capital investments, which only the Crown and aristocratic landowners could afford. As a result, the industry now featured an ironmaster, proprietor of the ironworks, and a dedicated workforce. Skilled forgemen were relocated to sites where wood and water power were available, and employed for their ability to conduct the conversion to wrought iron and/or steel. From here the role of single entrepreneurs and division of labour will become progressively more significant in the iron trade. In the time span of over two hundred years, Henry Cort’s puddling process, introduced a series of technical and organisational changes, which gradually supressed the dependency on artisanal trade, eventually leading to the

mechanised industries of the Industrial Revolution. Indeed, the remainders of the charcoal iron industry documented at Ausewell Wood might be the last remaining traces of iron production still based on artisanal practices and dependent on the skills of the workers.

Considerations on the Methodology employed and Future Work

It remains to comment on the methodology employed for this study and indicate future research directions in the light of the contributions and limitations of this research.

One of the consequences of the methodological challenges encountered during the macro-morphological analysis described in chapter 4, has meant that some features were identified later in the study and consequently, not all slag typologies were sampled for the analytical investigation. Although a methodology is presented as formed by a series of actions that follow each other, working with a large assemblage of material for which there was little comparative material available in the literature (and photographic documentation thereof), meant returning often to the macro-morphological investigation as the study progressed, and more information was obtained from comparing the database created for this study (Appendix A.3) and the sources describing the finery process. This has concerned especially the study of the flowed cakes (section 4.4.1) and of cakes/blocks of hearth slag (section 4.4.2). The former is a type of finery tap slag with remnants of slag channels attached and textures that suggest higher viscosity. While it is likely that these materials present a similar chemical composition to the finery tap slag, their analysis should be included in future analytical projects to investigate mechanisms of formation and operational practices related to slag-tapping.

Even more significant then appears the study of the large masses of hearth slag. Here, the future aim should be the identification of chafery hearth slags, and possible differences with those formed inside a finery hearth. In turn, this will help elucidate the layout and spatial organisation within the forge. The only piece of hearth slag analysed for this study revealed a very distinctive chemistry and microstructure, which offered important insight into the technology practiced at Ausewell Wood. Admittedly, a firm conclusion cannot be drawn without further analysis. However, this is an important avenue for future research identified in this study. Previous studies have focused on the analysis of iron-rich tap slag as a means of distinguishing

between smelting and fining sites (Killick and Gordon 1987, Rostoker and Dvorak 1990, Gordon 1997). However, this approach has proved difficult given the similar chemistry (they are both fayalitic slags) of bloomery tap slag and finery tap slag. The study of slags produced during the refining stage of fining pig iron should be explored further.

Significantly, this study has also highlighted the role of smaller debris, such as the conglomerations of material, often overlooked in favour of large slag examples. This is an aspect that must be first addressed on site when collecting representative pieces of debris for post-excavation processing. The results obtained in this study have been possible because of the quantitative approach adopted during excavations, which required recording of all the excavated material by size and type. The following macro-morphological analysis of the size-sorted assemblage therefore highlighted the role and small nature of these metallurgical debris. The conglomerations were produced through the ironworking technology employed and are representative of the technological operations conducted at Ausewell Wood. This shows the value of macro-morphological analysis of quantified assemblages, also with regard to the selection of samples for chemical and micro-structural analysis.

The sampling strategy adopted for the analytical work sought to reflect the variety of slag types and material observed during the macro-morphological work. The principle behind this choice was that a reconstruction of the technology could only be achieved by obtaining data representative of all (or most) stages of the chaine opératoire of iron production at Ausewell Wood; consequently, most of the size-sorted material groups were sampled (chapter 5). The aim was thus to analyse possible smelting evidence, through ore samples, blast furnace slag samples, but also tap slag; to investigate the evidence of iron fining, through tap slag, silica-rich slags and hearth slags, and of iron working (in a chafery) through matrix samples and smithing slags. Preference was then given to the conglomerations of material and metal samples because of their abundance and the nature of their visible inclusions. While working with a wide range of materials offers an overview of the technology, it also hinders an in-depth investigation of more specific questions. For example, the use and role of the silica and/or lime additions needs further investigation. Were blast furnace slags added to the slag bath? How much did they contribute to the formation of slag and dephosphorisation of pig iron? Further, it is

felt that the study of the non-metallic inclusions of the fragment of iron bar should be further investigated.

The broad scope of this study, reflected in the sampling strategy for the analytical work and in the research questions addressed, was perhaps inevitable, as the archaeometallurgy of the post-medieval period, and of the finery technology especially, is still in its infancy. The main contribution of the present study is first of all to the field of archaeological science, as the main objective was to answer technological questions through a standard archaeometallurgical approach. However, this work also shows that the interplay between archaeology, archaeometry and historical research has enormous potential to shed light on the circumstances of technological innovation and changes of the past. In the present work, the analysis of the physical evidence with other forms of historical evidence, such as the life of Adrian Gilbert or the historical sources on fining, permitted the reconstruction of the technology and - perhaps even more significantly - of the cultural and historical context in which these technological changes happened. The physical evidence is itself documentary evidence and contributes to the wider historical analysis.

The limitations of this broad approach will hopefully result in future studies addressing and identifying aspects that have not been explored in detail in the present work and generate a new set of research questions. For example, the history and archaeology of Dartmoor could be explored in more depth and reveal interesting connections among the figures who were involved in the enterprise. Surely additional avenues of research can be found comparing the analytical results of slags and metals with materials from other known finery assemblages. Finally, the analysis of the materials could be done alongside experimental archaeology and the re-enactment of artisanal practices, which could highlight standard operations and local/regional variations (see Dillmann *et al*. 2012). Researching Ausewell Wood has been a journey into the long history of iron technology. Particularly so as the period and technology investigated still represents a transition phase between the two iron smelting methods. The history of finery technology is compressed between the older bloomery process and the later puddling technology, its material evidence at the crossroad between various technologies, and its structure and organisation at the intersection between artisanal past and industrial future.

Bibliography

Adams R.J. 1979. A reconstruction drawing of a finery forge. *Bullettin of the Wealden Iron Research Group*, 16, 15-17.

Airne C.W. 1935. *The Story of Tudor and Stuart Britain*. Sankey, Hudson.

Amery J.S. 1924. Address of the President. *Transactions of the Devonshire Association for the Advancement of Science, Literature, and Art*. LVI, 43-102.

Arribet-Deroin D. 2001. *Fondre le fer en gueuses au XVIe siècle. Le haut fourneau de Glinet en Pays de Bray (Normandie)*. Unpublished PhD Thesis. Université Paris 1-Panthéon-Sorbonne.

Atkinson M., Waite P. and Burt P. 1982. The iron ore mining industry in Devon. *British Mining*, 19, Northern Mine Research Society, Sheffield, UK, 27-33.

Aubrey, J. 1898. Aubrey's Brief Lives. United States: D.R. Godine, 262.

Awty B.G. 1981. The continental origins of Wealden Ironworkers. *The Economic History Review*, 34:4, 524-539.

Awty B.G. 1989. The Blast Furnace in the Renaissance Period: Haut Fourneau or Fonderie? *Transactions of the Newcomen Society*, 61:1, 65-78.

Awty B.G. 2003. The Queenstock furnace at Buxted, Sussex: the earliest in England? *Historical Metallurgy*, 31:1, 51-52.

Awty B.G. 2006. The elusive Walloon finery forge of Liège. *Historical Metallurgy,* 40:2, 129-137.

Awty B.G. 2007. The development and dissemination of the Walloon method of ironworking. *Technology and Culture*, 48:4, 783-803.

Baring-Gould. 1900. *A book of Dartmoor.* Methuen and Co., London.

Bauerman H. 1868. *A Treatise on the Metallurgy of Iron. Containing outlines of the history of iron manufacture, methods of assay, and analyses of iron ore, processes of manufacture of iron and steel, etc. etc*. Virtue and Co., London, United Kingdom.

Bayley J. and Crossley D. 2004. Archaeological science as an aid to the study of Post-Medieval Industrialization. In Barker D. and Cranstone D. (eds.) *The Archaeology of Industrialization*. Maney, Leeds, 15-23.

Bayley J. and Williams J. 2005. Archaeological Science and Industrial Archaeology: Manufacturing, Landscape and Social Context. *Industrial Archaeology Review*, 27:1, 33-40.

Bayley J., Dungworth, D. and Paynter, S. 2001. *Centre for Archaeology Guidelines: Archaeometallurgy*. London: English Heritage.

Bayley J., Crossley D. and Ponting M. 2008. *Metals and Metalworking: A research framework for archaeometallurgy*. London: Historical Metallurgy Society.

Bedwin O. 1976. The excavation of Ardingly Fulling Mill and Forge, 1975-76. *Post-Medieval Archaeology*, 10:1, 34-64.

Bedwin O. 1980. The excavation of Batsford Mill, Warbleton, East Sussex, 1978. *Medieval Archaeology*, 24:1, 187-201.

Belford P. 2010. Five centuries of iron working: excavations at Wednesbury Forge. *Post-Medieval Archaeology*, 44:1, 1-53.

Bellinge F. and Martin P. 2018. Ausewell Wood Ashburton in John Norden's Survey 1614. Unpublished report *for the author*.

Blakelock E., Martinon-Torres M., Veldhuijzen HA. and Young T. 2009. Slag inclusions in iron objects and the quest for provenance: an experiment and a case study. *Journal of Archaeological Science*, 36:8, 1745-1757.

Blick C. R. 1984. Early Blast Furnaces. *Journal of Historical Metallurgy Society*, 18:1, 44-50.

Bowden M. 2000. *Furness Iron. The Physical Remains of the Iron Industry and Related Woodland Industries of Furness and Southern Lakeland*. English Heritage.

Brady T.A., Oberman H.A. and Tracy J.D. 1994. Introduction: Renaissance and Reformation, Late Middle Ages and Early Modern Era. In Brady T.A., Oberman H.A. and Tracy J.D. (eds.) *Handbook of European History 1400-1600 Late Middle Ages, Renaissance and Reformation. Volume I: Structures and Assertions.* E.J. Brill, Leiden, The Nertherlands, xiii-xxiv.

Bray L.S. 2006. The Archaeology of Iron Production: Romano-British Evidence from the Exmoor Region. Unpublished PhD thesis. University of Exeter.

Brewster D. 1832. *The Edinburgh Encyclopedia*. *Volume XIII.* Joseph and Edward Parker William Brown, printer, Philadelphia. 75-94.

Bromehead, C. 1948. Ships' loadstones. *Mineralogical Magazine and Journal of the Mineralogical Society, 28*(203), 429-437. doi:10.1180/minmag.1948.028.203.04

Brooke J. 2001. *The Kalmeter Journal. The Journal of a Visit to Cornwall, Devon and Somerset in 1724-5*. Twelveheads Press, Truro, 46-47.

Brown M. 1997. In search of Awsewell Mine. An examination of the surviving documentary evidence. Transcripts and Guides for Dartmoor Researchers, vol. 19, Dartmoor Press.

Buchanan R.A. 1980. *Industrial Archaeology in Britain.* Allen Lane, London. Second edition.

Buchwald V.F. and Wivel H. 1998. Slag Analysis as a Method for the Characterisation and Provenancing of Ancient Iron Objects. *Materials Characterisation*, 40, 73-96.

Campbell G. 2019. Introduction. In Campbell G. (ed.) *The Oxford Illustrated History of the Renaissance.* Oxford University Press, Incorporated, 2019. ProQuest Ebook Central, https://ebookcentral.proquest.com/lib/exeter/detail.action?docID=5750067, 1-10.

Carey C. J. 2000. The Application of Geochemical Survey to Sites of Metallurgical Activity: The Ausewell Wood Survey. Unpublished Report.

Cavallaro F. 2006. The alchemical significance of John Dee's Monas Hieroglyphica. In Clucas S. (ed.) *John Dee: Interdisciplinary Studies in English Renaissance Thought*, 159-176.

Chard J. 1971. Historic Ironmaking. *Northeast Historical Archaeology*, 1:1:7, 25-31.

Chaouche M., Gao X.X., Cyr M., Cotte M. and Frouin L. 2016. On the origin of the blue/green color of blast furnace slag-based materials: Sulfur K-edge XANES investigation. *Journal of American Ceramic Society*, 100:4, 1-10.

Childs W.R. 1981. England's Iron Trade in the Fifteenth Century. *The Economic History Review*, 34:1, 25-47.

Chirikure S. and Rehren Th. 2004. Ores, Furnaces, Slags and Prehistoric Societies: Aspects of Iron Working in the Nyanga Agricultural Complex, AD 1300-1900. *African Archaeological Review*, 21:3, 135-152.

Claughton P. 2016. Iron and Ironstone. In Newman P. (ed.) *The Archaeology of Mining and Quarrying in England. A Research Framework for the Archaeology of the Extractive Industries in England.* National Association of Mining History Organisations (NAMHO), Derbyshire, 115-122.

Cleere H. and Crossley D. 1995. *The Iron Industry of the Weald*. Cardiff: Merton Priory Press. 111-165, 219-276.

Craddock P.T. 1995. *Early Metal Mining and Production*. Edinburgh: Edinburgh University Press, 234-275.

Craddock P.T. 2003. Cast iron, fined iron, crucible steel: liquid iron in the ancient world. In Craddock P.T and Lang J. (eds.) *Mining and metal production through the ages.* British Museum Press, London, 231-257.

Cranstone D. 2001a. Ausewell Wood ironworks (Ashburton, Devon): The National Significance. Unpublished report by Cranstone Consultant for Dartmoor National Park Authority. Gateshead.

Cranstone D. 2001b, Industrial archaeology — manufacturing a new society, in R. Newman, Cranstone D. and Howard-Davis C. (eds.) *The Historical Archaeology of Britain, c 1540–1900.* Sutton Publishing Limited: Stroud, 183–210.

Cranstone D. 2004a. Ausewell Wood Mine and Ironworks: Project Design for Further Research. Unpublished report by Cranstone Consultants. Gateshead.

Cranstone D. 2004b. The Archaeology of Industrialization – New Directions. In Barker D. and Cranstone D. (eds.) *The Archaeology of Industrialization*. Maney, Leeds, 313-320.

Crew, P. 1988. Bryn Y Castell hillfort, Gwynedd, North Wales: a preliminary analysis of the iron working debris. In Ellis Jones, J (ed.) *Aspects of Ancient Mining and Metallurgy*. Bangor: University College of North Wales, 129–135.

Crew P. 1995. Bloomery iron smelting slags and other residues. *Historical Metallurgy Society: Archaeology Datasheet 5.*

Crew P. 1996. Bloom refining and smithing slags and other residues. *Historical Metallurgy Society: Archaeology Datasheet 6.*

Crew P. 2000. The influence of clay and charcoal ash on bloomery slags. In Tizzoni C. C. and Tizzoni M. (eds*.) Il ferro nelle Alpi, giacimenti, miniere e metallurgia dell'antichita' al XVI secolo, Atti del convegno*. Commune Di Bienno: Bienno, 38-48.

Crew P. 2009. *Iron working in Merioneth from prehistory to the 18th century.* Darlith Goffa Merfyn Williams Memorial Lecture, Plan Tan y Bwlch, Maentwrog. Snowdonia National Park.

Crew P. and Rehren Th. 2001. High-temperature workshop residues from Tara: iron, bronze and glass. *Discovery Programme Reports*, 6, 83-102.

Crew P., Charlton M., Dillmann P., Fluzin P., Salter C. and Truffaut E. 2011. Cast iron from a bloomery furnace. In Hosek J., Cleere H. and Mihok L. (eds.) *The Archaeometallurgy of Iron. Recent Developments in Archaeological and Scientific Research.* Institute of Archaeology of the ASCR, Prague, 239-262.

Crombie D.S. 1982. Ironworking at Ausewell Wood, East Dartmoor, Devon. A study of an early ironworking site in Devon. Unpublished undergraduate dissertation, University of Exeter.

Crossley D. 1972. A Sixteenth-Century Wealden Blast Furnace: A Report on Excavations at Panningridge, Sussex, 1964-1970. *Post-Medieval Archaeology*, 6:1, 42-68.

Crossley D. 1975a*. The Bewl Valley Ironworks, Kent, C. 1300-1730*. The Royal Archaeological Institute.

Crossley D. (ed.) 1975b. *Sidney Ironworks Accounts 1541-1573.* Royal Historical Society.

Crossley D. 1981. Medieval Iron Smelting. In Crossley D. (ed.) *Medieval Industry*. London: CBA Research Report, 40, 29-41.

Crossley D. 1990. *Post-Medieval Archaeology in Britain*. London: Leicester University Press. Chapter 6-7.

Crossley D. and Ashurt D. 1968. Excavations of Rockley Smithies, a water-powered bloomery of the 16th and 17th centuries. *Post-Medieval Archaeology*, 2:1, 10-54.

Cucini C., Riccardi M.P. and Tizzoni M. 2020. From the bloomery furnace to the blast furnace: The iron working complex of Valle delle Forme at Bienno, Brescia, northern Italy (mid 13th to mid 15th century). *Historical Metallurgy* 53:1, 10-18.

David N., Heimann R., Killick D. And Wayman M. 1989. Between bloomery and blast furnace: Mafa iron-smelting technology in North Cameroon. *The African Archaeological Review*, 7, 183-208.

Davies-Shiel M. 1970. Excavation at Stony Hazel, High Furness, Lake District, 1968-1969: an interim report. *Bulletin of the Historical Metallurgy Group*, 4, 28–32.

Dean R. and Faxon K. 2000. A gradiometer survey over part of Ausewell Wood ore processing and smelting complex, Ashburton, Dartmoor National Park, Devon. A geophysical survey by Substrata Limited.

Den Ouden A. 1981. The production of wrought iron in Finery hearths. Part I. *Historical Metallurgy*, 15:2, 63-87.

Den Ouden A. 1982. The production of wrought iron in Finery hearths. Part II: Survey of remains. *Historical Metallurgy*, 16:1, 29-32.

Den Ouden A. 1985. The introduction and early spread of blast furnace in Europe. *Bulletin of the Wealden Iron Research Group*, 5, Second Series, 21-35.

Desaulty A.M. 2008. Apport des analyses chimiques multi technique à la compréhension du comportement des éléments traces dans les filières sidérurgiques anciennes. Application aux études de provenance et à la distinction des procédés. Le cas du Pays de Bray normand. Sciences de l'Homme et Société. Université de Technologie de Belfort-Montbeliard; Université de Besançon, 2008. Français. (Available at: https://tel.archives-ouvertes.fr/tel-00552060).

Dillmann P., Arribet-Deroin D., Vega E. and Benoit P. 2003. Early modern cast iron and iron at Glinet. In *Proceeding of the Norberg Conference "Norberg-Nora, 700 Years of Iron Production",* Norberg, August 2003, Jernkontorets Bergshistorika Utskott, 99-106.

Dillmann P. and L'Heritier M. 2007. Slag inclusion analyses for studying ferrous alloys employed in French medieval buildings: supply of materials and diffusion of smelting processes, *Journal of Archaeological Science* 34, 1810-1823.

Dillmann P., Perez A., Vega E., Arribet-Deroin D., Aranda R., L'Héritier M., Neff D. and Bellot-Gurlet L. 2012. Understanding the Walloon method of iron refining: archaeological and archeometric experiments, phase 1. *Historical Metallurgy*, 46:1, 19-31.

Dines H.G. 1956. *Memoirs of the Geological Survey of Great Britain: England and Wales. The metalliferous mining region of south-west England. Volume II.* HMSO, London, 795.

Dorling P. and Young T.P. 2011. New Weir Forge, Whitchurch, Herefordshire: A report on Excavations in 2009 and 2010. *Herefordshire Archaeology Report,* 306. (Available at: https://htt.herefordshire.gov.uk/media/1020/ha306_she19111_new_weir_final_excavation_report.pdf).

Dungworth D. 2010. The possible water-powered bloomer at Goscote (Rushall), Walsall, West Midlands. *Historical Metallurgy*, 44:1, 15-20.

Dungworth D. and Wilkes R. 2007. An investigation of hammerscale. Technology Report. *Research Department Report Series* 26-2007, Portsmouth: English Heritage.

Dungworth, D. and Wilkes R. 2009. Understanding hammerscale: the use of high-speed film and electron microscopy. *Historical Metallurgy*, 43, 33–46.

Dupré S. 2014. Introduction. In Dupré S.(ed.) *Laboratories of Art. Alchemy and Art Technology from Antiquity to the 18th century.* Springer, vii-xix.

Eliyahu-Behar A., Yahalom-Mack N., Gadot Y. and Finkelstein I. 2013. Iron smelting and smithing in major urban centers in Israel during the Iron Age. *Journal of Archaeological Science*, 40, 4319-4330.

Evans C. 1998. A skilled workforce during the transition to industrial society: forgemen in the British iron trade, 1500-1850. *Labour History Review*, 63:2, 143-159.

Evans C. 1999. Work and Workloads During Industrialisation: The Experience of Forgemen in the British Iron Industry 1750-1850. *International Review of Social History*, 44:2, 197-215.

Evans C. and Rydén G. 1998. Kinship and the Transmission of Skills: Bar Iron Production in Britain and Sweden, 1500-1860. In M. Berg and K. Bruland (Eds.) *Technological Revolutions in Europe*, Edward Elgar, Cheltenham, 188-206.

Evans C. Jackson O. and Rydén G. 2002. Baltic Iron and the British Iron Industry in the Eighteenth Century. *The Economic History Review*, 55:4, 642-665.

Fell A. 1908. *The Early Iron Industry of Furness and District: an historical and descriptive account from the earliest time to the end of the 18th century with an account of Furness Ironmasters in Scotland, 1726-1800.* Part III, IV and V.

Feuerbach A. 2006. Crucible damascus steel: A fascination for almost 2,000 years. *JOM* 58, 48–50.

Flinn M.W. 1955. British Steel and Spanish Ore: 1871-1914. *The Economic History Review*, 8:1, 84-90.

Geddes J. 1991. Iron. In Blair J. and Ramsay N. (eds.) *English Medieval Industries. Craftsmen, Techniques, Products*. Hambledon Press, London and New York. 167-188.

Girbal B. 2010. Michelmersh, Romsey, Hampshire. Analysis of the slag. Technology Report. Portsmouth: English Heritage Research Department Report Series 78-2010.

Girbal B. 2011. 4 Low Forge, Wortley, South Yorkshire. An investigation of the slags. Technology Report. *Research Department Report Series* 50-2011, Portsmouth: English Heritage.

Girbal B. 2013. Appendix I. Analysis of the Iron Working Waste. A post-excavation assessment following an archaeological investigation on the route of the new water main at Stockbury, near Maidstone, Kent. Kent Archaeological Projects, 85-144.

Goldstein J., Newbury D., Joy D., Lyman C., Echlin P., Lifshin E., Sawyer L. and Michael J. 2003. *Scanning Electron Microscopy and X-Ray Microanalysis.* Springer Science + Business Media New York, third edition.

Gordon R.B. 1997. Process deduced from Ironmaking Wastes and Artefacts. *Journal of Archaeological Science* 24, 9-18.

Gordon R.B. and Reynolds T.S. 1985. Medieval Iron in Society – Norberg, Sweden, May 6-10. *Technology and Culture*, 27:1, 110-117.

Gordon R.B. and Killick D.J. 1993. Adaptation of Technology to Culture and Environment: Bloomery Iron Smelting in America and Africa. *Technology and Culture*, 34:2, 243-270.

Gould J. 1969–70. Excavation of the fifteenth-century iron mill at Bourne Pool, Aldridge, Staffordshire. *Transactions South Staffordshire Archaeological and Historical Society* 11, 58–63.

Greeves T.A.P. 1987. The Great Courts or Parliaments of Devon Tinners 1474-1786. *The Devonshire Association. For the Advancement of Science Literature and Art. Report and Transactions*, 119, 145-167. 63

Griffith F. and Weddell P. 1996. Ironworking in the Blackdown Hills: results of recent survey. In Newman P. (ed.) *The Archaeology of Mining and Metallurgy in South West Britain*. Historic Metallurgy Society, Vol.13, No. 2. 27-34

Guénette-Beck B. and Serneels V. 2007. An early blast furnace at Dürstel, Langenbruck, Baselland, Switzerland. In Archaeometallurgy in Europe, Spring (May-June), Grado and Aquileia, 1-11.

Hamilton-Jenkins A.K. 1981. *Mines of Devon; North and East of Dartmoor.* Devon County Council Library Service, 226.

Hammersley G. 1973. The charcoal iron industry and its fuel, 1540-1750. *The Economic History Review*, 26:4, 593-613.

Hanke, L. 1995. Variable Pressure Scanning Electron Microscopy For Nonconductive and Volatile Samples. *Microscopy Today,* 3:9, 20. doi:10.1017/S1551929500065846.

Hatton A., Engstler M., Leibenguth P. and Mücklich F. 2011. Characterisation of Graphite Crystal Structure and Growth Mechanisms Using FIB and 3D Image Analysis. *Advanced Engineering Materials*, 13:3, 136-144.

Hauptmann A. 2014. The Investigation of Archaeometallurgical Slag. In Roberts B.W. and Thornton C.P. (eds). *Archaeometallurgy in Global Perspective*, New York: Springer, 91-105.

Hauptmann A. 2020. *Archaeometallurgy – Materials Science Aspects*. Chapters 1, 2, 4, 5, 6.6, 7.5., 8.

Hayman R. 2003. *The Shropshire wrought-iron industry c1600-1900. A study of Technological Change.* PhD thesis. The University of Birmingham. (Available at: https://etheses.bham.ac.uk/id/eprint/248).

Higgins R. A. 1993. *Engineering Metallurgy*. Great Britain Edward Arnold. Chapter 15.

Historic England 2015. Archaeometallurgy. Guidelines for Best Practice.

Hodgkinson J. S. 1997. Forges in the late eighteenth century Weald. B*ulletin of the Wealden Iron Research Group*, 17, Second Series, 13-23.

Houghton R.G. 1997. A reconstruction of a Wealden conversion forge and boring mill. B*ulletin of the Wealden Iron Research Group*, 17, Second Series, 23-40.

Humphris J. and Carey C. 2016. New methods for investigating slag heaps: Integrating geoprospection, excavation and quantitative methods at Meroe, Sudan. *Journal of Archaeological Science* 70, 132-144.

Hyde C.K. 1977. *Technological Change and the British Iron Industry, 1700-1870.* Princeton University Press.

Imiolczyk E., Zabiński G., Goryczka T., Aniolek K., Balińska A. and Miśta-Jakubowska E. 2020. An Armour from a finery? – a late medieval couter from Ogrodzieniec Castle in the Kraków-Częstochowa Jura. *Archaeological and Anthropological Sciences* 12:61.

Iles, L. 2011. Reconstructing the Iron Production Technologies of Western Uganda: reconciling archaeometallurgical and ethnoarchaeological approaches. Unpublished PhD thesis. London: UCL (Available at: http://discovery.ucl.ac.uk/1306719/).

JakovĻeva M., AuziŅa D., Brūzis R., Gundersen I.M., Rundberget B., Bebre V., DoniŅa I., KĻava V., Straube G., BĒrziŅš V., VĪksna A., ActiŅš A., Meija R., Popovs K., Upmalis R. and Parfentev A. 2019. Gone to smelt iron in Courland: technology transfer in the development of an early modern industry. *Post-Medieval Archaeology*, 53:1, 102-124.

Johnson B.L.C. 1952. The Foley Partnerships: the iron industry at the end of the charcoal era. *The Economic History Review*, 4:3, 322-340.

Jones A.C. and Harrison C.J. 1978. The Cannock Chase Ironworks. *The English Historical Review*, 93:369, 795-810.

Josephson, G.W., Sillers Jr., F. & Runner, D.G. 1949. *Iron Blast-Furnace Slag*. United States Bureau of Mines, Bulletin 479, Washington, D.C. Chapter III.

Juleff G. 1996. An ancient wind-powered iron smelting technology in Sri Lanka. *Nature*, 379, 60-63.

Juleff G. 1997. Earlier Iron-Working on Exmoor: Preliminary Survey. Exmoor National Park Association and National Trust Survey Report.

Juleff G. 1998. Early Iron and Steel in Sri Lanka. A study of the Samanalawewa Area. Mainz: Verlag Philipp von Zabern.

Juleff G. 2000. Iron smelting in Ausewell Wood. Evaluation excavation and quantitative sampling of slag deposits 1999. Interim Report. Unpublished report for Dartmoor National Park Authority.

Juleff G. 2009. Technology and evolution: a root and branch view of Asian iron from first-millennium bc Sri Lanka to Japanese steel. *World Archaeology*, 41:4, 557-577.

Killick D. 1991. A little-known Extractive Process: Iron Smelting in Natural-draft Furnaces. *JOM: the journal of the Minerals, Metals and Materials Society*, 43:4, 62-64.

Killick D. 2015. Invention and Innovation in African Iron-smelting Technologies. *Cambridge Archaeological Journal* 25:1, 307-319.

Killick D. and Gordon B. G. 1987. Microstructures of puddling slags from Fontley, England and Roxbury. Connecticut, USA. *Journal of Historic Metallurgy Society*, 21:1, 28-36.

King P.W. 2002. Dud Dudley's contribution to metallurgy. *Historical Metallurgy* 36:1, 43-53.

King P.W. 2003. The Iron Trade in England and Wales 1500-1815. The charcoal industry and its transition to coke. PhD thesis. University of Wolverhampton. Chapters 3 and 6. (Available at: https://ethos.bl.uk/OrderDetails.do?uin=uk.bl.ethos.275455).

King P.W. 2020. *A Gazetteer of the British Iron Industry, 1490-1815, Volumes I and II.* Ebook, Oxford, UK: BAR Publishing. Chapters 1 and 36. https://doi-org.uoelibrary.idm.oclc.org/10.30861/9781407315126

Kostoglou M. and Navasaitis J. 2006. Cast iron in ancient Greece: myth or fact? *Mediterranean Archaeology and Archaeometry* 6:2, 55-58.

Lam W., Chen J., Chong J., Lei X. and Tam W.L. 2018. An iron production and exchange system at the center of the Western Han Empire: Scientific study of iron products and manufacturing remains from the Taicheng site complex. *Journal of Archaeological Science*, 100, 88-101.

Lam W., Zhang Q., Chen J. and Wu S.Y. 2020. Provision of iron objects in the southern borderlands of the Han Empire: a metallurgical study of iron objects from Han tombs in Guangzhou. *Archaeological and Anthropological Sciences*, 12, 230.

Landon D., Martin P., Sewell A., White P., Tumberg T. and Menard J. 2001. A Monument to Misguided Enterprise: The Carp River Bloomery Iron Forge. *Industrial Archaeology*, 27:2, 5-22.

Lemercier-Goddard S. and Regard F. 2013. Introduction: The Northwest Passage and the Imperial Project: History, Ideology, Myth. In Regard F. (Ed.) *The quest for the northwest passage: knowledge, nation and empire, 1576-1806*. Routledge Taylor and Francis Group, London and New York, 1-15.

Leong E. 2013. Collecting Knowledge for the Family: Recipes, Gender and Practical Knowledge in the Early Modern English Household. *Centaurus*, 55:2, 81-103.

Leroy S., Simon R., Bertrand L., Foy E., Williams A. and Dillmann P. 2011. First examination of slag inclusions in medieval armours by confocal SR-μ-XRF and LA-ICP-MS. *Journal of Analytical Atomic Spectrometry*, 26:5, 1078-87.

Li Y., Li Y., Yuan H., Juleff G. and Zhang M. 2019. Early iron objects of southwest China: a case study of iron objects excavated from Qiaogoutou cemetery site, Sichuan Province. *Archaeological and Anthropological Sciences*, 11, 1187-1198.

Li. Y., Ma C., Juleff G., Murakami Y., Zhou Z. and Li Y. 2019. Microstructural and elemental analyses of slags excavated from Xuxiebian iron-smelting site, Sichuan, China. *Archaeometry*, 61:6, 1353-1365.

Liu H., Chen J., Mei J., Jia J. and Shi L. 2014. A view of iron and steel making technology in the Yan region during the Warring States period and the Han dynasty: scientific study of iron objects excavated from Dongheishan site, Hebei province, China. *Journal of Archaeological Science*, 47, 53-63.

Liu Y., Martinón-Torres M., Chen J., Sun W. and Chen K. 2019. Iron decarburisation techniques in the eastern Guanzhong Plain, China, during Late Warring States period: an investigation based on slag inclusions analyses. *Archaeological and Anthropological Sciences*, 11, 6537-6549.

Long P.O. and Morrall A. 2014. Craft and Technology in Renaissance Europe. In Campbell G. (ed.) *The Oxford Illustrated History of the Renaissance.* Oxford University Press, Incorporated, 2019. ProQuest Ebook Central, https://ebookcentral.proquest.com/lib/exeter/detail.action?docID=5750067, 338-377.

Lucas A.R. 2005. Industrial Milliing in the Ancient and Medieval Worlds: A survey of the Evidence for an Industrial Revolution in Medieval Europe. *Technology and Culture*, 46:1, 1-30.

Lyaya E.C., Mapunda B.B. and Rehren Th. 2012. The Bloom Refining Technology in Ufipa, Tanzania (1850-1950). BAR International Series 2395, Cambridge

Monographs in African Archaeology 81, *Métallurgie du fer et Sociétés africaines : Bilans et nouveaux paradigmes dans la recherche anthropologique et archéologique.* Archaeopress England, 195-207.

Mack I., McDonnell G., Murphy S., Andrews P. and Wardley K. 2000. Liquid steel in Anglo-Saxon England. *Historical Metallurgy* 34:2, 87-96.

Mackenzie R. J. and Whiteman J. A. 2006. Why pay more? An archaeometallurgical investigation of 19th century Swedish wrought iron and Sheffield blister steel*. Historical Metallurgy*, 40:2, 138-149.

Magnusson G. 1985. Lapphyttan – an example of medieval iron production. In Björkenstam N., Fernheden K., Magnusson G. and Serning I. (eds) *Medieval Iron in Society – Papers Presented at the Symposium in Norberg, Jernkontoret, Stockholm,* 21-57.

Magnusson G. 1995*. The Importance of Ironmaking. Technical Innovation and Social Change*. Papers presented at the Norberg Conference, roMay 8-13, 1995. Jernkontorets Bergshistoriska Utskott H 58, Stockholm.

Malcolmson C. 2010. William Herbert's Gardener: Adrian Gilbert. In Hodgkins C. (Ed.) *George Herbert's Pastoral. New Essays on the Poet and Priest of Bemerton.* Newark: University of Delaware Press, 113-133.

Margetts A. 2021. Medieval and later Wealden iron workings at Ifield Forge and Mill, Crawley, West Sussex. *Sussex Archaeological Collections*, 158, 121-145.

Markham C.R. 1889. *A life of John Davis, the Navigator, 1550-1605, Discoverer of Davis Straits.* London: George Philip and Son, 32 Fleet Street.

McDonnell G. 1984. The study of early iron smithing residues. In Scott B. G. and Cleere H. (eds.) *Crafts of the Blacksmith*. Belfast UISPP, 47-52.

McDonnell G. 1986. The classification of early ironworking slags. Unpublished PhD thesis. (Available at: https://research.aston.ac.uk/en/studentTheses/the-classification-of-early-ironworking-slags).

McDonnell G. 1989. Iron and its alloys in the fifth to eleventh centuries AD in England. *World Archaeology*, 20:3, 373-382.

McDonnell G. 1991. A model for the formation of smithing slags. *Materialy Archeologiczne,* 26, 23-28.

McDonnell G. 2001. Pirotechnology. In Brothwell D.R. and Pollard A.M. (eds.) *Handbook of Archaeological Sciences*. Wiley & Sons, Chichester. Section 6, 493-506.

Miall S.H.C. 1895. *The British Hive and Its Working Bees*. United Kingdom: Isbister.

Mihok L., Demeter P., Baricová D. and Seilerová K. 2006. Utilization of ironmaking and steelmaking slags. *Metalurgija,* 45:3, 163-168.

Morton G.R. and Wingrove J. 1969. Slag, cinder and bear. *Bulletin of the Historical Metallurgy Group*, 3, 55-61. 64

Morton G.R. and Wingrove J. 1970. The charcoal finery and chafery forge. *Bulletin of the Historical Metallurgy Group*, 5:1, 24-28.

Morton G.R. and Wingrove J. 1972. Constitution of Bloomery Slags: Part II: Medieval. *Journal of the Iron and Steel Institute* 210, 478-489.

Muralha V.S.F. Rehren Th. And Clark R.J.H. 2011. Characterization of an iron smelting slag from Zimbabwe by Raman microscopy and electron beam analysis. *Journal of Raman Spectroscopy*, 42, 2077-2084.

Navasaitis J. and Selskienè A. 2007. Metallographic Examination of Cast Iron Lump Produced in the Bloomery Iron Making Process. *Materials Science*, 13:2, 167-173.

Neff D. and Dillmann P. 2001. Phosphorus localisation and quantification in archaeological artefacts by micro-PIXE analyses. *Nuclear Instruments and Methods in Physics Research* B 181, 675-680.

Newman P. 1998. Ausewell Wood ore processing and smelting complex, Ashburton, Devon. An archaeological survey by the Royal Commission on the Historical Monuments of England. RCHME Survey Report.

Newman P. 2004. Ausewell Wood, Ashburton, Devon. Part ii: Ausewell Mine (Wheal Hazel). Survey Report Archaeological Investigation Report Series AI/09/2004. English Heritage.

Newman P. 2010. Environment, antecedent and adventure: tin and copper mining on Dartmoor, Devon, *c.*1700-1914. Unpublished Phd Thesis. University of Leicester. (Available at: https://leicester.figshare.com/articles/thesis/Environment_Antecedent_and_Adventure_Tin_and_Copper_Mining_on_Dartmoor_Devon_C_1700-1914/10104218/1).

Orton C. 1996. Underpinning the discipline. One hundred years (or more) of classification in archaeology. *Archeologia e Calcolatori*, 7, 561-577.

Page K.N. 2004. The geology of the Ausewell Wood mine and mineral processing complex, Holne, Devon. Unpublished Report for Dartmoor National Park Authority.

Paynter S. 2007. Romano-British workshops for iron smelting and smithing at Westhawk Farm, Kent. *Historical Metallurgy* 41:1, 15-31.

Paynter S. 2011. *Introductions to Heritage Assets. Pre-Industrial Ironworks.* English Heritage.

Percy J. 1864. *Metallurgy, Vol 2, Pt 3 Wrought Iron; Steel*. Murray: London.

Phelps M., Paynter S. and Dungworth D. 2011. Downside Mill, Cobham, Surrey. Analysis of metalworking remains. Technology Report. *Research Department Report Series*, 43-2011.

Phillpotts C. 2001. Ausewell, Devon. Documentary Research Assessment. Unpublished Report for Dartmoor National Park Report.

Phillpotts C. 2003. Ausewell Wood, Devon. Documentary Research Report. Unpublished Report for Dartmoor National Park Report.

Photo-Jones E. and Atkinson J.A. 1998. Iron-working in medieval Perth: a case of town and country? *Proceedings of the Society of Antiquaries of Scotland*, 128, 887-904.

Photo-Jones E., Dalglish C., Coulter S., Hall A.J., Ruiz-Nieto R. and Wilson L. 2008. Between archives and the site: the 19th century iron and steel industry in the Monklands, Central Scotland. *Post-Medieval Archaeology*, 42:1, 157-180.

Pleiner R. 2000. *Iron in Archaeology. The European Bloomery Smelters.* Praha: Archeologický ústav AVČR.

Plot R. 1686. *The Natural History of Staffordshire.* Printed at the Theater, Oxford, 163.

Powle H. 1678. An Account of Iron-Works in the Forest of Dean. *Philosophical Transactions (1665-1678)*, 12, 931-935.

Radzikowska J.M. 2004. Metallography and Microstructures of Cast Iron. In Voort G.F.V. (ed.) *ASM Handbook, Volume 9: Metallography and Microstructures.* ASM International, Materials Park, Ohio, USA, 565-587.

Rahil A. and Rehren Th. 2014. Persian Pūlād Production: Chāhak Tradition. *Journal of Islamic Archaeology*, 1.2, 231-261.

Ray J. 1674. *A Collection of English Words Not Generally Used: With Their Significations and Original, in Two Alphabetical Catalogues, the Ones of Such as are Proper to the Northern, the Other the Southern Counties. With Catalogues of English Birds and Fishes, and an Account of Preparing and Refining Such Metals and Minerals as are Gotten in England.* H. Bruges, Princeton University, 127-128. Early English Books Online.

Rehren, Th. 2008 Metals: Primary production studies of. In Pearsall, D, (ed.) *Encyclopedia of Archaeology*. Elsevier: Netherlands, 1616-1620.

Rehren Th. And Ganzelewski M. 1995. Early Blast Furnace and Finery Slags from the Jubach, Germany. In: Magnusson (ed.) *The Importance of Ironmaking.*

Technological Innovation and Social Change, Vol. 1. Norberg Conference, Stockholm, 172-179.

Rehren Th. and Papakhristu O. 2000. Cutting edge technology - the Ferghana Process of medieval crucible steel smelting. *Metalla (Bochum)*, 7:2, 55-69.

Rondelez P. 2014. Ironworking in late medieval Ireland, c. AD. 1200 to 1600. PhD Thesis, University College York. (Available at: https://cora.ucc.ie/handle/10468/1944).

Rossi M. And Gattiglia A. 2015. Il forno di affinazione di Rondolere (1788-1813). *Il Capitale culturale. Studies on the Value of Cultural Heritage*, 12, 149-182.

Rostoker W. and Bronson B. 1990. Pre-industrial iron: its technology and ethnology. *Archaeomaterials Monograph* No. 1, Philadelphia, Pennsylvania: privately published.

Rostoker W. and Dvorak J. 1990. Wrought Irons: Distinguishing Between Processes. *Archaeomaterials*, 4:2, 153-166.

Rowe A. 2012. Hertfordshire's lost water gardens 1500-1750. In Spring D. (ed.) *Hertfordshire Garden History Volume II. Gardens pleasant, groves delicious*. University of Hertfordshire Press, Hatfield, 31-57. 65

Salter C.J. and Gilmour B.J.J. 2012. Glossary of terms used in the study of ancient metalworking and associated processes, Available at: http://hist-met.org/glossary.pdf.

Schofield P. and Miller I. 2017. Cunsey Bloom Forge, Windermere. *Community Archaeology Survey and Excavation Report. Oxford Archaeology North*, 2017-18/1781. Lake District National Park Authority. 1-163.

Schubert H.R. 1951. Early Refining of Pig Iron in England. *Transaction of the Newcomen Society*, 28:1, 59-75.

Schubert H.R. 1957. *History of the British Iron and Steel Industry from c. 450 B.C. to A.D. 1775*. Routledge and Kegan Paul, London, 93-331.

Schrüfer-Kolb I. 2004. *Roman Iron Production in Britain. Technological and socio-economic landscape development along the Jurassic Ridge*. Ebook, Oxford, UK: BAR Publishing. Chapter 3. Available at: https://doi.org/10.30861/978184171669.

Scott D. 1991. *Metallography and Microstructure of Ancient and Historic Metals.* Marina del Rey, CA: Getty Conservation Institute in association with Archetype Books.

Scott D. and Schwab R. 2019. *Metallography in Archaeology and Art.* Springer Nature Switzerland AG, 179-197, 233-240.

Selskiené A. 2007. Examination of smelting and smithing slags formed in bloomery iron-making process. *Chemija* 18:2, 22-28.

Selwin L.S., Sirois P. I. and Argyropoulos V. 1999. The corrosion of excavated archaeological iron with details on weeping and akaganéite. *Studies in Conservation*, 44:4, 217-232.

Serneels V. and Perret S. 2003. Quantification of smithing activities based on the investigation of slag and other material remains. In *Archaeometallurgy in Europe. Proceedings of the International Conference (Milano, 24-26 September)*. Milano: Associazione Italiana di Metallurgia, Vol. 1, 469-478.

Small M. 2013. From Thought to Action: Gilbert, Davis and Dee's Theories behind the Search for the Northwest Passage. *The Sixteenth Century Journal*, 44:4, 1041-1058.

Smith PH, Meyers ARW, Cook HJ (eds). 2014. *Ways of Making and Knowing: The material culture of empirical knowledge*. The University of Michigan Press.

Starley D. 1995. The examination of iron artefacts, raw materials and waste products from Rockley blast furnace, Worsborough, South Yorkshire, 1978-82. *Ancient Monuments Laboratory Report* 40/95.

Starley D. 1999. Determining the Technological Origins of Iron and Steel. *Journal of Archaeological Science*, 26, 1127-1133.

Straker E. 1931. *Wealden Iron*. G. Bell and Sons, Limited. 1-109.

Tomas E. 1999. The Catalan process for the direct production of malleable iron and its spread to Europe and the Americas. *Contributions to Science,* 1:2, 225-232.

Trattner W.I. 1964. God and Expansion in Elizabethan England: John Dee, 1527-1583. *Journal of the History of Ideas*, 25:1, 17-34.

Tylecote R.F. 1960. The location of Byrkeknott: a fifteenth-century iron-smelting site. *Journal of the Iron and Steel Institute* 194, 451–458.

Tylecote R.F. 1986. *The prehistory of metallurgy in the British Isles*. The Institute of Metals, London, 124-226.

Tylecote R.F. 1991. Iron in The Industrial Revolution. In Joan D. and Tylecote R.F. (eds.) *The Industrial Revolution in Metals*. The Institute of Metals, London. 200-260.

Tylecote R.F. 1992. *A History of Metallurgy*. Second Edition. London: The Institute of Materials.

Tylecote R.F. and Cherry J. 1970. The 17th century bloomery at Muncaster Head. *Transaction of the Cumberland and Westmorland Archaeological and Antiquarian Society*, 70, 69-109.

Tyson L.O. 1996. Sir Bevis Bulmer: An Elizabethan Adventurer. *British Mining*, 57, NMRS, 47-69.

Ul-Hamid A. 2018. *A beginners' guide to Scanning Electron Microscopy*. Springer Nature Switzerland. Chapter 5.

Uriarte Ayo R. 1992. Anglo-Spanish Trade through the Port of Bilbao during the Second Half of the Eighteenth Century: Some Preliminary Findings. *International Journal of Maritime History*, IV, 2, 193-217.

Vega, E., P. Dillmann, M. Lheritier, P. Fluzin, P. Crew and P. Benott 2003. Forging of Phosphoric Iron. An Analytical and Experimental Approach. In *Archaeometallurgy in Europe*. Milan, Italy, Associazione Italiana di Metallurgia, 337-346.

Veldhuijzen H.A. and Rehren Th. 2007. Slags and the city: Early iron production at Tell Hammeh, Jordan, and Tel Beth-Shemesh, Israel in La Niece S., Hook D.R. and Craddock P.T. (eds.), *Metals and Mines – Studies in Archaeometallurgy*, Archetype, British Museum, London (2007), pp. 189-201.

Vernon R., McDonnell G. and Schmidt A. 1998. An integrated geophysical and analytical appraisal of early iron-working: three case studies. *Journal of the Historical Metallurgy Society*, 32:2, 67-81.

Vodyasov E.V., Zaitceva O.V., Vavulin M.V. and Pushkarev A.A. 2020. The earliest box-shaped iron smelting furnaces in Asia: New data from Southern Siberia. *Journal of Archaeological Science: Reports*, 31, 102383.

Wagner D.B. 1996. *Iron and steel in ancient China*. Leiden: E.J. Brill (2nd edition with corrections).

Wagner D.B. 2008. *Science and Civilisation in China, Part XI: Ferrous metallurgy. Vol.5*. Cambridge University Press

Wallis H. 1964. England's Search for the Northern Passages in the Sixteenth and Early Seventeenth Centuries. *Artic*, 37:4, 453-472.

Wayman M.L. and Juleff G. 1999. Crucible steelmaking in Sri Lanka. *Journal of the Historical Metallurgy Society*, 33, 26-42.

Williams A. 2009. A Note on Liquid Iron in Medieval Europe. *Ambix* 56:1, 68-75.

Westcote T. 1845. *View of Devonshire in 1630 with a pedigree of most of its gentry*. Oliver G. and Jones P. (eds). W. Roberts, Exeter, 65.

Williams R. 2013. A question of grey or white: Why Abraham Darby I chose to smelt iron with coke. *Historical Metallurgy* 47:2, 125-137.

Williams R. 2019. Grey or white pig? The importance of the starting material whether fining iron in charcoal hearths, clay pots or puddling furnaces. *Historical Metallurgy* 53:2, 84-103.

White J.R. 1977. X-ray Fluorescent analysis of an early Ohio blast furnace slag. *Ohio Journal of Science,* 77:4, 186-188.

White J.R. 1980. Preliminary archaeological examination of Ohio's first blast furnace: the Eaton (Hopewell). *Ohio Journal of Science*, 80:2, 52-58.

White J.R. 1982. Analyses and evaluation of the raw materials used in the Eaton (Hopewell) furnace. *Ohio Journal of Science*, 82:1, 23-27.

White J.R. 1996. The rebirth and demic of Ohio's earliest blast furnace: an archaeological postmortem. *Midcontinental Journal of Archaeology,* 21:2, 217-245.

Young T.P. 2011. Evaluation of metallurgical residues from New Weir Forge, Herefordshire. *GeoArch.* Report 2011/12.

Young T.P. 2014. Archaeometallurgical residues from Ynysfach Ironworks, Merthyr Tydfil. *GeoArch.* Report 2013/29.

Young T.P. and Hart R. 2017. The refining process, part 2: new data from Ynysfach Ironworks, Merthdyr Tydfil. *Historical Metallurgy* 51:1, 34-50.

Zhang M., Ge L., Qiu T., Gan Q., Yang B. and Li Y. 2011. Forging or casting: new evidence of iron production in the Chengdu Plain in the Han dynasty. *Archaeological and Anthropological Sciences* 13: 111, 1-11.

Zilsel E. 1941. The origins of William Gilbert's scientific method. *Journal of the History of Ideas*, 2:1, 1-32.

Technological change and innovation: Ausewell Wood, Dartmoor – an early industrial metallurgical 'laboratory'

Volume 2 of 2

Appendices

Submitted by Carlotta Farci,

To the University of Exeter

as a thesis for the degree of

Doctor of Philosophy in Archaeology,

April 2022.

APPENDIX A

MACRO-MORPHOLOGICAL ANALYSIS

APPENDIX A: INITIAL CLASSIFICATION

This Appendix presents the classification scheme for the visual analysis of ironworking slags and residues as developed for the Exmoor Iron Project and employed for the initial assessment of the Ausewell Wood assemblage. It is followed by the recording sheets with the data collected during the first stages of the macro-morphological analysis. This data is presented in support of the discussion and data illustrated in chapter 4.

Classification Scheme

SLAG

Class		**Type**		**Sub-type**		
Symbol	**Description**	**Symbol**	**Description**	**Symbol**	**Description**	
S	Slag	***i***	Tap slag	***a***	Upper surface and base present (cake)	
				b	Individual tendril	
				c	Fragment – undiagnostic	
		ii	Furnace slag	***d***	Plano-convex base	
				e	Uncertain base	
				f	Fragment – undiagnostic	
		iii	Smithing slag	***g***	Complete	
				h	Hammerscale	***h1*** flakes
						h2 spheroids
				j	Fragment – undiagnostic	
		iv	Blast Furnace Slag	***k***	Glassy	
				l	Vesicular (intermediate)	

		v	Slag Runners	***m***	Rod-shape
		vi	Refining Slag	***n***	Part-cake with basal protrusion
				o	Part of cake
		vii	Furnace residues	***r***	Fragment/lump – undiagnostic but complete
				s	Particulate
				t	Wall? curvature, not clearly base
	Proportion (proportion – visual % of bagged sample in this class)				***Proportion***

VARIANTS AND DESCRIPTORS FOR SLAG

Variant		**Descriptors**		
Symbol	**Description**	**symbol**	**description**	
A	Shape	1	Plano-concave	
		2	Plano	
		3	Plano-convex	
		4	Convex	
		5	Concave-convex	
		6	Amorphous	

		7	Hollow rod	
		8	Single rod	
		9	Multiple rods	
		10	Fine Spheroids	
		11	Elongated	
		12	Flakes	
		13	Spheroids	
B	Overall Size	Record L x W x T if the sample is from a normal bag (not quantitative or others) Measure half of the samples from each size group (max. of 4 from each group)		
C	Thickness			
D	Density	1	High	
		2	Moderate	
		3	Low	
		4	Very low	
E	Porosity proportion	1	Very high (>60%)	
		2	High (40-60%)	

		3	Moderate (20-40%)	
		4	Low (20%)	
		5	Very low (<5%)	
		6	Unclear	
		7	No	
F	Porosity size	1	Large (>10mm)	
		2	Moderate (2-10mm)	
		3	Small (1-2mm)	
		4	Very small (<1mm)	
		5	None	
G	Porosity shape	1	Network	
		2	Elongated	
		3	Spherical	
		4	Broken – random	
		5	Mixed spherical – elongated – all sizes	
		6	None	

H	Surface texture	1	Smooth	
		2	Ropey	
		3	Smooth with broken bubbles	
		4	Small tendrils	
		5	Globular projections	
		6	Rough	
		7	Broken (surface broken/sheered)	
		8	Crystalline/ Glassy	
		11	Abraded	
		12	Rusty	
		13	Undulating (upper surface)	
I	Colour	1	Black	
		2	Grey	
		3	Red	
		4	Brown	
		5	Purple	
		6	Grayish-blue	

		7	Yellow-orange	
		8	Metallic	
		9	Glassy green	
		10	Glassy black	
J	Surface impressions	1	Charcoal	
		2	Soil-geological	
		3	Toolmarks	
		4	Tuyères – furnace wall refractory - clay	
		5	Stone	
		6	None	
		7	Slag	
K	Underside texture	1	Smooth	
		2	Rippled – tendrils	
		3	Rough	
		4	Undulated	
		5	Geological – furnace material	
		6	broken	
		7	Underside not visible	

L	Underside impressions	1	Charcoal	
		2	Soil – geological	
		3	Toolmarks	
		4	Tuyères – furnace wall refractory	
		5	Slag	
		6	none	
		7	metallic iron	
M	Inclusions (all surfaces)	1	Furnace wall – tuyère refractory – clay	
		2	Charcoal	
		3	Geological – soil	
		4	Bloom – iron	
		5	Slag	
		6	none	
N	magnetism	1	High	
		2	Moderate	

		3	Low	
		4	Non-magnetic	
		5	Partially – isolated areas	
O	Viscosity	1	High	
		2	Moderate	
		3	Low	
		4	Unclear	
		5	Not Applicable	
P	Multiple flow episodes	1	Yes	
		2	No	
		3	Unclear	
Q	Degree of fracture	1	Total – all surfaces	
		2	Partial – all edges	
		3	Minor – some old fractures – uncertain	
		4	Complete – edges intact	

		5	Abraded	

REFRACTORY MATERIAL

Class		**Type**		**Sub-type**	
Symbol	**Description**	**Symbol**	**Description**	**Symbol**	**Description**
RF	Refractory material	***i***	Furnace wall	***a***	Straight
				b	Curved
				c	Vitrified deformed
				d	Fragment – undiagnostic - amorphous
		ii	Hearth wall	***e***	Complete circumference
				f	Fragment – furnace wall with surface
		iii	Uncertain		
	Proportion		***Proportion***		***Proportion***
	(proportion – visual % of bagged sample in this class)		(proportion – visual % of class sample of this type)		(proportion – visual % of type sample of this sub-type)

VARIANTS AND DESCRIPTORS FOR REFRACTORY MATERIALS

Variant	**Descriptors**

Symbol	**Description**	**symbol**	**description**	
A	Thickness of wall	1	Thin (<2cm)	
		2	Medium (2-5cm)	
		3	Large (>5cm)	
		4	N/A Unclear	
B	Inner/External diameter	1	Small <20cm	
		2	Medium <50cm	
		3	Large >50cm	
		4	uncertain	
C	Fabric (overall texture)	1	Coarse (>5mm)	
		2	Moderate (2-5mm)	
		3	Fine (<2mm)	

D	Temper, grog inclusions	1	Charcoal	
		2	Organic impressions	
		3	Sand	
		4	Small stones	
		5	Slag	
		6	Furnace wall	
		7	Tuyère	
		8	Quartz	
		9	Bigger stones	
		10	Unclear	
E	Vitrification	1	Minor	
		2	Partial	
		3	Total	
		4	Absent	
F	Oxidation (red/yellow colouration)	1	Heavy	
		2	Moderate	

		3	Light	
		4	none	
G	Reduction (black/grey colouration)	1	Heavy	
	(depth through wall)	2	Moderate	
		3	Light	
		4	none	
H	Oxidation distribution	1	Inside	
		2	Outside	
		3	Both	
		4	Non-specific	
I	Reduction distribution	1	Interior	
		2	Exterior	

		3	Both	
		4	Non-specific	
J	Furnace wall features	1	Internal metallurgical slag	
		2	External metallurgical slag	
		3	Large stone in structure	
		4	Linear impressions	
		5	Tool marks	
		6	Embedded tuyères	
		7	Rim	
		8	Base	
		9	Sheered surface	
		10	Internal magnetic material	
		11	Slag seepage into cracks in wall	
		12	None	
M	Surface inclusion/impressions	1	Charcoal	
		2	Iron rich spheroids	

		3	Possible tool marks	
		4	none	
N	Fragment size	1	Very small, <1cm	
		2	Small, 1-5cm	
		3	Medium, 5-20cm	
		4	Large, >20cm	
O	Fragment abrasion	1	High (edges/breaks smoothed)	
		2	Moderate (some fractures sharp and un-abraded)	
		3	Low (clean un-abraded breaks)	
P	Residue Features	1	Magnetic	
		2	Stones	

		3	Clay Fragment	

GEOLOGICAL MATERIAL

Class		**Type**		**Sub-type**	
Symbol	**Description**	**Symbol**	**Description**	**Symbol**	**Description**
G	Geological material	***i***	Ore	***a***	Magnetic
				b	Non-magnetic
		ii	Worked stone	***c***	Complete artifact
				d	Fragment
		iii	Rock sample	***e***	Quartz
				f	Limestone
				g	Slate
				h	Other
	Proportion		***Proportion***		***proportion***
	(proportion – visual % of bagged sample in this class)		(proportion – visual % of class sample of this type)		(proportion – visual % of type sample of this sub-type)

VARIANTS AND DESCRIPTORS FOR GEOLOGICAL MATERIALS

Variant		**Descriptors**		
Symbol	**Description**	**Symbol**	**description**	
A	Shape	1	Angular	
		2	Sub-angular	
		3	Sub-rounded	
		4	Rounded	
B	Size	1	Large (>15cm)	
		2	Medium (10-15cm)	
		3	Small (5-10cm)	
		4	Very small (<5cm)	
C	Colour	1	Red	
		2	Brown	
		3	Yellow-orange	
		4	White	
		5	Grey	
		6	Metallic	

		7	Black	
		8	Purple	
		9	Green	
		10	Pink	
D	Crystal, grain size/texture	1	Large – coarse (>5mm)	
		2	Moderate (2-5mm)	
		3	Fine (<2mm)	
		4	Homogeneous – e.g. flint	
E	Other features	1	Banding	
		2	Contains ore minerals	
		3	Burning coloration (pink-red)	
		4	Iron staining	
		5	Inter-grown with other minerals/rock	
		6	Porous	
		7	Possible roasting	
		8	From furnace wall	
		9	Adhering slag	

		10	No Other Features	
F	Fracture	1	Total – all surfaces	
		2	Partial – all edges	
		3	Minor – old fractures – uncertain	
		4	Complete – edges intact	
G	Density	1	High	
		2	Medium	
		3	Light	
H	Degree of magnetism	1	High	
		2	Medium	
		3	Low	
		4	None	

METALS

Class		**Type**		**Sub-type**	
Symbol	**Description**	**Symbol**	**Description**	**Symbol**	**Description**
M	Metal	***i***	Bloom	***a***	Complete
				b	Incomplete
				c	Uncertain
		ii	Finished artefact	***g***	Complete
				h	Incomplete
				j	Modern
		iii	Scrap	***k***	Archaeological
				l	Modern
	Proportion		***Proportion***		***Proportion***
	(proportion – visual % of bagged sample in this class)		(proportion – visual % of class sample of this type)		(proportion – visual % of type sample of this sub-type)

VARIANTS AND DESCRIPTORS FOR METALS

Variant		**Descriptors**		
Symbol	**Description**	**symbol**	**description**	

A	Size	1	Large (>10cm)	
		2	Moderate (5-10cm)	
		3	Small (2-5cm)	
		4	Fragment (<2cm)	
B	Magnetism	1	Strong	
		2	Moderate	
		3	Weak	
C	Density	1	High	
		2	Medium	
		3	Low	
D	Colour	1	Black	
		2	Grey	
		3	Yellow – orange	
		4	Brown	
		5	red	

		6	Purple	
		7	Metallic	
		8	Grey Blue	
E	Inclusions	1	Soil – geological	
		2	Charcoal	
		3	Furnace remains	
		4	None	
F	Impressions	1	Charcoal	
		2	Soil – geological	
		3	None	
G	Shape	1	Sub – rounded	
		2	Amorphous	
		3	Sub – angular	
H	Condition	1	Heavily mineralized	

		2	Surface rusting/corrosion	

DATABASE 1999 EXCAVATION SEASON

TRENCH	SPIT	SIZE	DESCRIPTION	SYMBOL	TYPE	SUBTYPE	Shape	Overall Size	Thickness	Density	Porosity	Porosity size	Porosity shape	Surface Texture	Colour	Surface impressions	Underside texture	Underside impressions	Inclusions (all surfaces)	Magnetism	Viscosity	Multiple flow episodes	Degree of fracture
PN1																							
	0-20	Small	**S**	**TS iaP**	**i (5 fragments)**	**a**	A2 (PLATE)	≈ 7x3.5	≈0.5/1.5	D3	E4	F3	G3	H1, H2	I4	J6	K3, K4	L1, L2	M3	N4	O3	P2	Q1
	0-20		**S**	**TS ib**	**i (8 fragments)**	**b**	A8	≈ 5x2.5		D2	E6			H1	I2, I7	J6	K1	L6	M5	N4	O3	P2	Q1
	0-20		**S**	**TS ic**	**i (15 fragments)**	**c**	A6	≈ 5x3		D2/D3	E2/E3	F2	G3	H6	I4	J1, J2, J6	K3, K4	L1, L2	M6	N4	O2	P2	Q1
	0-20		**S**	**FS iif**	**ii (9 fragments)**	**f**	A6			D4	E3	F2	G3	H6	I2, I7	J6	K7	L6	M3	N4	O5	P2	Q1
	0-20		**S**	**TS iaC**	**i (4 pieces)**	**a**	A3, A5	≈ 9x4	≈2/4	D1	E3	F3	G3	H1, H2	I4	J6	K3, K4	L1, L2	M3	N3	O3	P1 ?	Q1
	0-20		**M**	**FeRich Slag**	**FeSlag (5 fragments)**		G1	≈ 3x2		D3					I1 (red stains)	F3			E4	N2			

	0-20		**G**	**G iii**	**iii (8 stones)**	**f, h**	A1, A3	B3						D2							
	0-20	Medium	**S**	**TS iaP**	**i (1 piece)**	**a**	A2 (PLATE)	≈10x 8	≈2.5	D3	E3		G5	H6, H13	I4	J6	K3, K4	L1, L2, L3?, L4	M3	N4	O2	P2	Q1
	0-20		**S**	**TS iaC**	**i (3 pieces)**	**a**	A3			D1	E4	F2	G3	H1, H2	I2	J6	K2, K3, K5	L1, L2, L4	M2, M3, M4	N5	O3	P2	Q1
	0-20		**S**	**FS iie**	**ii (1 piece)**	**e**	A6			D3	E3		G5	H6	I3, I4	J1, J2, J3	K3, K5	L1, L2, L3, L4	M1, M2, M3	N4	O2	P2	Q1
	0-20	Large	**S**	**TS iaC**	**i (1 large cake)**	**a**	A3	≈ 20x1 5	≈ 4	D1	E4	F1	G2	H1, H2	I2, I3	J6	K3	L1, L2, L5	M6	N3	O3	P2	Q1
	0-20	One Slag Complet e																					
	0-20	Medium Selecte d	**S**	**TS iaC**	**i (2 pieces)**	**a**	A2, A3		≈ 5	D1, D2	E3, E4	F2	G2, G3	H1, H2, H6	I2 (red, oran ge stain s)	J6	K3, K5	L1, L2	M1, M3, M5	N3, N5	O2, O3	P3, P2	Q1
	0-20		**S**	**FS iie**	**ii (2 lumps + 1 piece with hole)**	**f**	A6			D2, D3	E6			H6	I3, I4 (red stain s), I5, I7	J2, J4	K3, K7	L1, L2, L3, L4	M1, M2, M3, M4, M5	N4,N 1	O2, O5	P2	Q1
				SS iiig	**iii (1 piece -clay rich)**	**g**	A1	9 x 5cm	~ 4cm	D2	E5	F3	G3	H6	I4, I7	J1	K3	L1, L2	M6	N4	O1	P2	Q3

	20-40 U	Small	**M**	**M iiik**	**iii (6 fragments)**	**k**	G1	A3		C1					D1, D5	F3			E4	B1			
	20-40 U		**S**	**BF slag k**	**iv (6 fragments)**	**k**	A6	≈ 2x1		D4	E5	F4	G3	H8	I6, I9	J6		L6	M5	N4	O2	P2	Q1
	20-40 U		**S**	**Flakes**	**iii (7)**	**h1**	A12	≈ 2x2	0.1/2 ≈	D3	E4	F3	G3	H1	I2	J6	K3	L6	M5	N2	O4	P2	Q1
	20-40 U		**S**	**FS iif**	**ii (30)**	**f**	A6	≈ 2x2		D2	E6			H6, H12	I2, I3	J6	K7	L6	M1, M2	N2	O4	P2	Q1,Q5
	20-40 U		**S**	**TS ib**	**i (8 fragments)**	**b**	A8	≈ 3x2		D2	E4	F2	G3	H1	I2	J6	K1, K2	L6	M5	N4	O3	P2	Q1
	20-40 U		**S**	**SR**	**v (2 piece)**	**m**	A7	≈ 6x3.5	≈ 4	D3	E3	F2	G3	H6	I4	J2 ?	K3	L2 ?	M1, M3	N4	O4	P2	Q1
	20-40 U		**S**	**TS iaC**	**i (8 -5 bigger fragments)**	**a**	A2, A3	≈ 6x4/5		D2	E4	F2	G5	H1, H2	I4 (red stains)	J1	K3, K5	L1, L2	M1, M3	N3	O3	P1	Q1
	20-40 U		**G**	**G iii**	**iii (20)**	**g, h**	A1	B4		G2, G3				D2	C1, C3, C4					H4			
	20-40 U	Medium	**S**	**TS iaC**	**i (1 fragment)**	**a**	A3, A5	10x7 ≈	≈ 3/3.5	D1	E4	F2	G2, G3	H1, H2	I4 (red stains)	J6	K3, K5	L2, L4	M1	N4	N3	P1	Q1

	20-40 L (charcoal rich)	Small	**S**	**TS ic**	**i (≈ 45%) / 34**	**c**	A6			D2	E4		G5	H1, H2	I2 (red stains)	J1, J2, J5	K3, K5, K7	L1, L2	M1, M2, M3	N3	O3	P2	Q1
	20-40 L (charcoal rich)		**S**	**SR**	**v (1 piece)**	**m**	A8	4x2.5x1.5 ≈	1.5 ≈	D2	E3	F3	G3	H6	I4 (a bit red)	J2	K3, K5	L1, L2	M5	N3	O2	P2	Q3
	20-40 L (charcoal rich)		**S**	**BF slag k**	**iv (4 fragments)**	**k**	A6			D4	E5	F4	G3	H8	I9, I10 (+blue)	J6	K7	L6	M5	N4	O2, O1	P2	Q1
	20-40 L (charcoal rich)		**S**	**Undiagnostic**	**(2 fragments)**		A6			D4	E2		G5	H6	I1, I2	J6	K7	L6	M5	N4	O4	P2	Q1
	20-40 L (charcoal rich)		**G**	**G iii**	**iii (≈4% rock samples) / 21**	**g, h**	A2, A3	B3		G2, G3				D2, D3	C1, C3, C5					H4			
	20-40 L (charcoal rich)		**M**	**M iiik**	**iii (2 fragments)**	**k**	G1	A2		C1					D1, D5	F3			E4				
	20-40 L (charcoal rich)		**S**	**FS iif**	**ii (~50%) /61**	**f**	A6			D4	E6			H6	I2, I7	J6	K7	L6	M1, M2, M3, M4, M5	N4	O4	P2	Q1, Q5
QN1																							

	0-20	Small	**S**	**TS iaC**	**i (3 fragments)**	**a**	A6			D2			G5	H7	I1, I3, I5	J1, J2	K3	L1, L2	M2, M3	N5	O2	P2	Q1
	0-20		**S**	**TS ic**	**i (20 fragments)**	**c**	A6			D2	E2	F1, F2	G5	H1, H2	I1, I2	J6	K3	L1, L2	M3	N4	O3	P3	Q1
	0-20		**M**	**M iiik**	**iii (1 little piece)**	**k**	G1	A3		C3					D1, D6					B1			
	0-20		**G**	**G iii**	**iii (1 small stone)**	**f**	A4	B4		G3					C4								
	0-20	Medium +Selected Slag	**S**	**TS iaC**	**i (13 pieces)**	**a**	A1, A3			D1	E4	F2	G3	H1, H2, H6	I2, I4	J2, J3	K3	L1, L2, L3	M2, M3	N5	O2, O3	P1	Q1
	0-20		**S**	**TS iaP**	**i (6 pieces)**	**a**	A2 (PLATE)	≈ 8.5x5x2.5		D1	E4, E5	F2,F3	G3	H1, H2	I1, I4	J6	K3	L1, L2, L3	M3	N4	O2	P3	Q1
	0-20		**S**	**FS iie**	**ii (4 pieces)**	**f**	A6			D1	E4	F2	G2	H6	I4, I5	J3	K3	L1, L3	M6	N3	O3	P2	Q1
	0-20	Large	**S**	**TS iaC**	**i (2 pieces)**	**a**	A3	≈ 5.5x23x6.5		D1	E2, E3	F1,F2	G5	H1, H2	I1, I2 (red stains)	J6	K3	L1, L2	M3	N5	O2, O3	P1	Q2

	0-20		**S**	**BF slag k**	**iv (1 small fragment)**	**k**	A6			D4					I10	J1			M3				
	0-20	Very Large	**S**	**TS iaC**	**i (1 big cake)**	**a**	A3	≈ 12x13x5	≈ 5	D1	E5	F2	G3	H1, H2	I1, I2, I7	J6	K3, K4	L1, L2, L4, L7	M3, M4	N5	O3	P1	Q3
	20-40	Small	**S**	**TS iaC**	**i (4 pieces + 2 fragments)**	**a**	A2, A3	9x5x3 ≈	3-4 ≈	D2	E4	F2	G3	H1, H2	I2 (red stains)	J4 (clay)	K3	L2	M1	N3	O2	P1	Q2 (round edge visible)
	20-40		**S**	**TS ib**	**i (5 pieces)**	**b**	A8, A9	3x1x1.5 ≈	1.5/2 ≈	D3	E4	F4		H1	I2	J6	K3, K5	L2	M5	N3	O3	P2	Q3
	20-40		**S**	**TS ic**	**i (27 small fragments)**	**c**	A6	bigger ≈6x3		D3	E2	F2	G3, G4	H6, H12	I3, I4	J6	K3, K5	L2, L4	M1	N3	O2	P2	Q1
	20-40		**M**	**FeRich Slag**	**FeSlag (4 pieces)**		G1	A3		D1					D1, D5	F3			E4	B1			
	20-40		**S**	**FS iif**	**ii (4 pieces)**	**f**	A6			D4	E6			H6	I4, I7	J1	K7		M1, M2, M5	N4	O5		Q1
	20-40		**G**	**G iii**	**iii (6 small stones)**	**f, h**	A2, A3	B4		G2, G3					C3, C5, C7								

	20-40	Medium	**S**	**TS iaC**	**i (5 pieces)**	**a**	A2, A3	7x4 ≈	4/5 ≈	D1	E4	F2	G3	H1, H2	I2, I4	J6	K3, K5	L1, L2, L5, L7	M1, M4	N3	O3	P1	Q1
	20-40	Large	**S**	**TS iaC**	**i (1 cake)**	**a**	A3	≈17. 5x15	≈5	D1	E3	F1, F2	G2, G3	H2	I4, I5		K3	L1, L2, L5	M2	N3	O1	P1	Q3
	20-40	Small Finds	**S**	**SS iiij**	**iii (6 fragments)**	**j**	A3, A5	≈9x5 x3 / 10x5 ≈	≈3.5/4 / ≈ 5/6	D2	E4	F2	G3	H6, H12	I2, I4, I7	J1, J2,J4, J5, J7	K3, K5	L1, L2, L5, L7	M1, M2, M3, M4	N2	O2	P2	Q2 (round edge visible)
				SS iiig	**iii (1)**	**g**	A3			D1	E6			H6	I2, I7	J6	K3	L1, L5	M5	N5	O1	P2	Q1
	20-40		**S**	**FS iif**	**ii (3 fragments)**	**f**	A6	6x3. 5 ≈		D3	E6			H6	I4, I7				M1, M2, M3,	N4	O5	P2	Q1
	20-40		**S**	**BF slag k**	**iv (2 fragments)**	**k,l**	A6			D4	E6, E2			H8, H6	I6	J6	K7	L6	M1, M3 M5	N4	O1	P2	Q1
	20-40		**M**	**Fe-Rich Slag**	**FeSlag (4 bigger fragments, 2 small)**		G1	A2		C1					D1, D5	F1, F2			E1, E2	B1			
	20-40		**G**	**G iii**	**iii (5 small stones)**	**f, h**	A3, A4	B4		G3				D3	C3, C4					H4			F3

			RF	**RF**	**iii (5)**																
	Spit Unknown	Large	**S**	**TS iaC**	**i (1 big cake)**	**a**	A3	25x6 x7.5		D1	E1, E2		G5	H1, H2	I1, I2, I7	J6	K3	L1, L2, L5	M2, M3	N4, N5	O1	P1	Q2
PN1-QN1																							
		Context 7	**S**	**BF slag l**	**iv (4 pieces)**	**l**	A6			D4	E1	F2	G3	H6	I2 (red stains)	J1	K7		M1	N4	O1	P2	Q1
			S	**BF slag k**	**iv (8 pieces)**	**k**	A6			D4	E2	F2	G2, G3	H8	I1, I9	J1	K7		M2	N4	O1	P1	Q1
			S	**SS iiij**	**iii (3)**	**j**	A1, A6			D2	E6			H6, H12	I4, I7	J1, J2	K3, K5, K7		M1, M2, M3, M4, M5	N2	O4	P2	Q1
			S	**SS iiig**	**iii (2)**	**g**	A3 (+double cake)			D2	E6			H6	I4, I5, I7	J1, J4	K3	L1, L4	M1, M2, M4	N5	O1	P2	Q1
			S	**FS iif**	**ii (7 pieces)**	**f**	A6			D2	E1	F2	G3	H6	I7	J1	K3	L1	M2, M4, M6 ?	N4	O4	P2	Q1
			S	**TS ic**	**i (2 small fragments)**	**c**	A9			D2	E4	F2	G3	H1, H2	I2	J6	K3	L6	M5	N4	O2	P2	Q1

			M	**Fe-Rich Slag**	**FeSlag (2 prills)**		G1			C2					I2, I3	F1, F2			E1, E2, E3, E5	B1			
			G	**G iii**	**iii (4 stones)**	**f, g**	A3	B3		G3				D3						H4			
ZN1																							
	0-20	Small	**S**	**FS iif**	**ii (1 big + 10 fragments)**	**f**	A6			D2	E4	F2	G5	H6, H12	I4	J1, J5	K3	L1, L2	M2, M3	N5	O2	P2	Q1
	0-20		**S**	**SR**	**v (1 piece)**	**m**	A11			D1	E4	F4	G5	H1, H6	I4	J1, J2	K3	L1, L2	M2, M3	N3	O2	P2	Q3
	0-20		**S**	**Undiagnostic**	**7 fragments**	**v**	A6			D4	E1	F2	G3	H6, H12	I2, I4	J1	K3	L1	M5	N4	O2	P2	Q1
	0-20		**M**	**Fe-Rich Slag**	**FeSlag (2 bigger pieces + 5 fragments)**		G1	A2		C1					D1, D6	F3			E4	B1			
	0-20		**S**	**TS iaC**	**i (2 fragments of 'cakes')**	**a**	A2			D2	E2	F1, F2	G5	H3	I4, I5	J6	K3	L1, L2	M3, M4	B5	O2	P3	Q1
	0-20	Medium	**S**	**TS iaC**	**i (5 fragments of 'cakes')**	**a**	A2, A3			D1	E3, E4	F1, F2	G5	H1, H3	I4	J6	K3	L1, L3	M3, M4	N2	O2, O3	P1	Q1

	0-20		**S**	**SS iiij**	**iii (4 fragments, 1 elongated) - ?**	**j**	A6			D2	E3	F1	G5	H6, H12	I4, I7	J6	K3	L1, L3	M2, M3	N3	O1	P2	Q1
	0-20		**M**	**Fe-Rich Slag**	**FeSlag (1 piece)**		G2	A1		C1					D4, D5	E4		F3		B1			
	0-20	Large	**S**	**FS iid**	**ii (1 cake)**	**d**	A2, A3			D2	E4	F2	G5	H1, H13	I4	J5, J7 ?	K3, K5	L1, L2	M2, M3	N4	O3	P1 (some)	Q2
	0-20		**S**	**FS iie**	**ii (1 fan shaped pieces)**	**e**	A3			D2	E2	F2	G4	H6, H12	I4, I7	J1, J2	K3, K5	L1, L2,	M2	N4	O1	P2	Q1
	0-20	Small Finds	**S/ M**	**Fe-Rich Slag**	**FeSlag (4 pieces)**		A6/G1			D2	E7			H6, H12	I4, I5	J1	K7		M1, M2, M3, M4	N2	O5	P2	Q1
	0-20		**S**	**FS iif**	**ii (3 pieces)**	**f**	A6 (subrounded)			D3	E7			H6	I4, I7	J1, J2, J4	K7		M1, M2, M3	N4	O5	P2	Q1
	0-20		**S**	**FS iie**	**ii (1)**	**e**																	
	0-20		**S**	**Undiagnostic**	**(3 pieces)**		A6 (subrounded)			D4	E4	F2	G5	H6	I4, I7	J1	K7		M1, M2	N4	O5	P2	Q1

	0-20		**S**	**FS iid**	**ii (3) - ?**	**d**															
	0-20		**S**	**SS iiij**	**iii (1 pieces)**	**j**	A2,A6			D2	E2	F1, F2	G5	H6	I2, I4	J1, J2	K3, K5	L1, L2	M1, M2	N4	O1	P2	Q1
	0-20	Selected Medium	**S**	**FS iie**	**ii (2 lumps)**	**f**	A3, A6			D2	E2	F1, F2	G5	H6	I3, I4	J1, J2, J5	K3	L1, L2, L3, L5	M2, M3	N4	O1	P2	Q1
			S	**FS iid**	**ii (1)**	**d**																	
			S	**SS iiij**	**iii (1 pieces)**	**j**	A2, A5			D2	E3	F1, F2	G3	H6, H7	I4	J4, J5	K3, K5	L2, L4	M1, M2	N3	O3	P2	Q1
	0-20		**S**	**TS iaC**	**i (2 fragments)**	**a**	A2			D2	E3	F1, F2	G5	H2, H3	I2, I7	J2	K4, K5	L2	M3	N4	O3	P1	Q1
	0-20			**SR**	**v (1 fragment)**	**m**	A2 (PLATE)			D3	E3	F2		H1, H12	I4, I7	J2 (rust)	K3, K5	L1, L2	M5	N4	O3	P1	Q1
	0-20	Furnace Bottom		**FS iid**	**ii (3 big pieces)**	**d**	A3			D2, D3	E1, E2	F1	G5	H6, H12	I2, I4	J1, J3, J4	K3, K5	L1, L2, L3	M2, M3	N4	O1	P2	Q4

	20-40	Small	**S**	**Undiagnostic**	**(8 pieces)**		A6 (subrounded)			D4	E1	F3	G3		I2, I6, I9	J6	K7	L6	M5	N4	O4	P2	Q1
			S-M	**Fe-Rich Slag**	**FeSlag (16 fragments)**		A6/G1			D2	E7			H6, H12	I4, I5	J1	K7		M1, M2, M3, M4	N2	O5	P2	Q1
			S	**TS ic**	**i (3 fragments)**	**c**	A2			D2	E3	F1, F2	G5	H2, H3	I2, I7	J2	K4, K5	L2	M3	N4	O3	P1	Q1
			S	**TS ib**	**i (5)**	**b**				D2	E4	F3	G3	H4	I4, I7	J1, J2	K5	L1, L2	M5	N4	O3	P1	Q1
			S	**FS iif**	**ii (17)**	**f**	A6 (subrounded)			D3	E7			H6	I2, I4, I7	J6	K7	L6	M1, M2, M3	N4	O5	P1	Q1
			S	**SS iiij**	**iii (1) - ?**	**j**	A2			D2	E5				I4	J4, J5	K3, K5	L1, L2	M1, M3	N4	O3	P1	Q1
			S	**Flakes**	**iii (3 pieces)**	**h1**	A12			D3	E4	F3	G3	H1	I2	J6	K3	L6	M5	N2	O4	P2	Q1
			G	**G iii**	**iii (18)**	**h**	A2, A3	B3		G3				D4	C5					H4			F3

		Medium	**S**	**TS iaC**	**i (5 fragments)**	**a**	A2, A6			D2	E3	F1, F2	G4	H1, H2	I4	J6	K3	L1, L2	M1, M2, M3	N4	O3	P1 some	Q1
		Special finds	**S/ M**	**Fe-Rich Slag**	**FeSlag (10 fragments)**		G1			C1, C2					D4, D5, D6	E2		F1		B2			
			S	**SS iiij**	**iii (2)**	**j**	A2, A6			D2	E4	F3	G3	H6	I4, I7	J1, J2, J5	K3	L1, L2	M1, M2, M3	N4	O2	P2	Q1
			S	**SS iiig**	**iii (1)**	**g**	double cake			D1	E6			H6	I4, I7	J1	K3	L1, L5	M1, M2, M5	N5	O1	P2	Q1
			S	**FS iif**	**ii (4 small fragments)**	**f**	A6			D3	E7			H6	I4, I7	INCL	K7	L6	M1, M2, M3, M4	N4	O5	P2	Q1
			S	**Undiagnostic**	**(3 fragments)**		A6			D4	E6			H6, H8 - some glassy bits	I1, I4	J6	K7	L1	M2 ?	N4	O2	P2	Q1
			R F	**RF**	**iii (1 White clay)**																		
	40-60/below 40	One Slag	**S**	**FS iid**	**ii (1)**	**d**	A3			D2	E3	F1,F2	G2,G3	H6	I1, I4	J1, J3, J4	K3	L2	M2, M3	N4	O1	P2	Q2
JN9																							

	0-20	Small	**S**	**SR**	**v (4 fragments)**	**m**	A7			D3	E7 (hollow)			H6, H12	I4, I5	J2, J5	K3	L2	M5	N4	O2	P1	Q1
			S	**Flakes**	**iii (3 flakes)**	**h1**	A12		1 cm~	D3	E3	F4	G3	H1	I2, I4	J6	K5	L6	M5	N4	O2	P1	Q1
			S	**TS ib**	**i (9 fragments)**	**b**	A8, A9			D3	E6			H1	I2, I4	J6	K5	L2	M5	N4	O3	P1	Q1
			S	**FS iif**	**ii (10 fragments)**	**f**	A6			D4	E6			H6	I4, I7	J1, J4	K7		M1, M2	N4	O5	P1	Q1
			S	**Undiagnostic**	**(2 fragments)**		A6			D4	E6			H6, H11 ?	I2				M1, M2, M3	N4	O5	P1	Q1
			S	**TS ic**	**i (4 fragments)**	**c**	A6			D2	E4	F3	G3	H1, H6	I2, I4	J2, J7 ?	K3, K5	L1, L2, L5	M2, M3	N4	O2, O3	P2	Q1
			M	**Fe-Rich Slag**	**FeSlag (6 rounded pieces)**		G1	A3		C1						F1, F2			E1, E3	N1			
			G	**G iii**	**iii (11 stones)**	**f/h**	E2, E3	B3		C3, C5, C10													

		Medium	**S**	**TS iaP**	**i (4)**	**a**	A2 (PLATE)		1.5/2.5 cm~	D2	E2	F1, F2	G3	H2	I2, I4	J6	K5	L1, L2	M3	N4	O1	P2	Q1
			S	**TS iaC**	**i (2 fragments)**	**a**	A1, A6			D3	E2	F2	G3	H2, H6	I4, I5	J2, J7	K3, K5	L1, L2, L5	M3	N4	O2	P1	Q1
			S	**SS iiig**	**iii (1)**	**g**	A5			D2	E5	F3	G3	H6, H12	I4, I5	J1, J2, J5, J7	K3, K5	L1, L2	M2, M3	N4	O1	P1	Q1
		Special Finds	**S**	**SS iiij**	**iii (3 fragments)**	**j**	A2, A3			D2	E2		G5	H6	I4, I7	J1, J2, J4	K3, K5	L1, L2	M1, M2	N4	O3	P1	Q1
			S	**SR**	**v (2 slags)**	**m**	A7			D3	E7			H6, H12	I4, I7	J4	K3, K5	L2	M5	N4	O3	P1	Q1
			S	**Undiagnostic**	**(3 fragments)**		A6			D3, D4	E2, E3	F2, F3	G3	H6, H11	I2, I4	J1, J2	K3	L1, L2	M2, M3	N4	O1	P1	Q1
			S/M	**Fe-Rich Slag**	**FeSlag (9 balls)**		A6/G1			D1/C1	E7			H6, H12	I4, I5, I7	J1, J4, J5	K7		M1, M2, M3, M4	N1, N2	O5	P1	Q1
			G	**G iii**	**iii (1)**	**e**																	
			RF	**RF**	**iii (5)**																		

			S	**TS iaC**	**i (2 elongated pieces)**	**a**	A11			D1	E5	F4	G4	H2, H6, H12	I4, I5	J1, J4, J7	K3, K5	L1, L2	M1, M2, M4	N1	O2	P2	Q1
			S/ R F	**FS iif**	**ii (7 fragments)**	**f**	A6			D3	E7			H6, H12	I4, I5, I7					N4	O5	P1	Q1
			M	**M iiik**	**iii (2 fragments)**	**k**																	
	0-20 Upper	Mixed Slag	**S**	**Undiagnostic**	**(1 fragment)**		A6			D4	E3	F3	G3	H6, H8	I2, I10	J6	K7	L6	M5	N4	O1	P1	Q1
			S	**FS iid**	**ii (2)**	**d**	A2, A3			D1	E4	F2	G3	H6, H12	I4, I5	J1, J7	K3, K5	L1, L5	M2, M3	N5	O1, O2	P1	Q1
	0-20 Lower	Slag Only	**S**	**FS iid**	**ii (4)**	**d, e**	A6	19x16 cm		D1	E2	F2	G3	H1 (Some flow), H6	I4	J6	K4, K5	L1, L2	M2, M3	N4	O2	P1	Q1
			S	**FS iie**	**ii (5)**	**e**	A6			D2	E7			H6, H12	I4, I5	J1, J3			M1, M2, M3, M4	N5	O2	P1	Q1
			S	**TS ib**	**i (3)**	**b**	A9			D3	E2	F2	G3	H2	I4	J5 ?	K5	L2	M5	N4	O3	P1	Q1
			S	**TS ic**	**i (4)**	**c**	A6			D3	E2	F1, F2	G5	H2, H7	I4	J1, J2	K5	L1, L2	M3	N4	O3	P2 (SOME)	Q1

			S	**SR**	**v (2)**	**m**	A7			D2	E3, E4	F3	G3	H6, H12	I4	J6		L2	M3	N4	O2	P1	Q1
			S/ G	**G iii**	**iii (1)**	**h**	A6			D1	E2	F2	G3	H1, H6	I2, I4	J2	K3	L1, L2	M6	N4	O2	P1	Q1
			M	**Fe-Rich Slag**	**FeSlag (1)**		G1			C1					D4, D6					B1			
			S	**SS iiij**	**iii (2)**	**j**	A2 (PLATE)		1 cm ~	D2, D4	E6, E7			H6,H12, H13	I2, I3, I4, I7	J1, J4, J7 (red layer)	K3	L1, L2	M2, M3	N4	O1	P1	Q1
			S	**Undiagn ostic**	**5**																		
	Upper + Lower	Specials	**R F/ MI X**	**FS iif**	**ii (6)**	**f**	A6			D3	E6			H6, H12	I4, I7	J1, J2, J4	K3, K5	L1, L2	M1, M2, M3, M5	N4	O1	P2	Q3
			M/ S	**Fe-Rich Slag**	**FeSlag (3)**		A6			D1				H6, H12	I4, I5, I7					N1			
			R F	**RF**	**iii (1)**																		
	40-60	Small	**S**	**Flakes**	**iii (16)**	**h1**	A12			D2, D3	E3, E5			H1, H6	I2, I4					N2			
			S R		**v (2)**	**m**	A7			D3				H6, H9 ?	I4				M1, M2	N4			

			S	**TS iaP**	**i (5)**	**a**	A2 (PLATE)			D3	E3	F2	G3	H1	I2, I4	J6	K5	L1, L2	M5	N4	O2	P1	Q1
			S/ MI X	**FS iif**	**ii (11 small fragments)**	**f**	A6			D4				H6	I2, I4				M1, M2, M3	N4	O5	P2	Q1
			M	**Fe-Rich Slag**	**FeSlag (10 balls)**		G1			C1					D1, D4				E3	B1			
			S	**TS ic**	**i (5 small fragments)**	**c**	A6			D3	E2		G5	H1	I2				M1	N4	O3	P2	Q1
			R F	**RF**	**iii (5)**																		
			G	**G iii**	**iii (15)**	**h**																	
		Medium	**S**	**TS iaP**	**i (2 plates)**	**a**	A2 (PLATE)		2.5 cm ~	D1	E1	F1, F2	G5	H2, H3	I4, I7	J6	K3, K5	L1, L2	M2, M3	N4	O2	P1	Q1

			S	**FS iie**	**ii (5)**	**e**	A6 (+ one A2)		1.5 cm ~	D1	E6			H6, H12	I4, I5, I7	J1, J4	K3, K5	L1, L2	M2, M3	N1	O3	P1	Q1

		Selected Medium	**S**	**FS iie**	**ii (1 flat underside piece)**	**d**	A1			D2	E4	F4	G3	H6	I4, I5	J1, J3, J4	K4, K5	L1, L2	M1, M2, M3	N1	O3	P1	Q1
		Large	**S**	**FS iie**	**ii (3 pieces, see notes)**	**e**	A6 – cone-shaped			D2	E6			H6, H12	I4, I5	J3			M1, M2, M3, M4	N1	O4	P1	Q1
			S	**FS iid**	**ii (1)**	**d**	A5	~10 x 11 cm	~ 12 cm	D1	E6			H6, H12	I4, I5	J1	K3	L1, L2	M1, M2, M3, M4, M5	N5	O1	P2	Q3
		Special Finds	**S**	**Flakes**	**iii (9)**	**h 1**	A12			D4	E7			H6	I1, I2	J6	K1, K4	L6	M1 (clay attach)	N4	O3	P1	Q1
			S	**FS iif**	**ii (10)**	**f**	A6			D3, D4	E3	F3	G3	H6	I2, I4	J1, J4	K7		M1, M2	N5	O1, O2	P1	Q1
			S	**SR**	**v (1 piece)**	**m**	A11 ?			D2	E6			H6, H12	I4, I5	J1, J2, J4	K3, K5	L1, L4, L5	M1, M2, M3	N5	O2	P1	Q4
			S	**TS ic**	**i (8 fragments)**	**c**	A6, A9			D1	E5	F4	G3	H1, H4	I2, I8	J6	K2	L6	M1 (some clay attach), M2 (one piece charc attach)	N4	O3	P2 (some)	Q1
			S	**TS ib**	**i (2)**	**b**																	

			G-mix	**G iiif**	**iii (3 pieces)**	**f**	A3	B3		G2, G3				D3	C3, C4, C10					H4			
			RF	**RF**	**iii (1)**																		
ZS3																							
	0-20	Small	**S**	**FS iif**	**ii (4 fragments)**	**f**	A6			D2	E3		G5	H1, H6	I4	J6	K3, K5	L1, L2	M2, M3	N4	O2	P1	Q1
			S	**BF Slag k**	**iv (1 small fragment)**	**k**	A6	~ 3cm		D4	E6			H8	I10	J6	K7			N4	O3	P2	Q1
			M	**Fe-Rich Slag**	**FeSlag (6 balls)**		G1	A2		C1					D4, D6	F1, F2			E1, E2, E3	B1			
		Medium	**S**	**FS iid**	**ii (2 lumps)**	**d**	A3			D3	E6			H6	I4, I5	J1, J3, J4	K3, K5	L1, L2	M2, M3	N4	O2	P1	Q1
			S	**TS iaC**	**i (1)**	**a**	A2 (CAKE)			D1	E2	F2	G3	H2, H3	I2, I4	J6	K3, K5	L1, L2	M2, M3	N4	O3	P2	Q1

			S	**FS iid**	**ii (1 piece)**	**d**	A5		7-8cm~	D1	E2		G5	H6, H12	I4, I7	J1, J3, J4	K3, K5	L2	M2, M3	N4	O1	P1	Q1
		Selected Medium	**S**	**TS iaC**	**i (1)**	**a**	A6			D2	E6			H6, H12	I4, I5, I7	J1, J4	K3, K5	L1, L2	M2	N4	O2	P1	Q1
	20-40	Small	**S/MIX**	**FS iif**	**ii (11 fragments)**	**f**	A6			D3	E7			H6, H12	I4, I5, I7	J1, J2, J7	K7		M1, M2, M3, M4	N4	O5	P1	Q1
			S	**TS ic**	**i (3 fragments)**	**c**																	
			S	**Undiagnostic**	**3 fragments**																		
		Medium	**S**	**TS iaC**	**i (6)**	**a**	A2,A3		2 cm ~	D1	E2	F1, F2	G5	H1, H3	I2, I4	J6	K3, K5	L1, L2	M2, M3	N4	O3	P2	Q1
		Large	**S**	**TS iaC**	**i (2 big pieces)**	**a**	A3	21-23 cm by 12-16 cm	3-4 cm ~	D2	E2	F1, F2	G5	H2, H3	I4, I7	J1, J7	K3, K5	L1, L2, L5	M1, M2, M3	N4	O2, O3	P2	Q1
		Special finds																					

		Selected Medium	**S**	**TS iaC**	**i (6 piece)**	**a**	A3		~ 9 cm	D2	E2		G5	H2	I4, I7	J6	K3, K5	L1, L2, L5 ?	M5	N4	O3	P2	Q1
			S	**TS ic**	**i (1)**	**c**	A5 (thin)	~ 14 cm long		D3	E6			H1	I4		K3, K5	L1, L2	M1	N4	O2	P2	Q1
			S	**FS iie**	**ii (3 fragments)**	**e**	A1, A2			D1, D2	E3	F2	G3	H6	I4, I5, I7	J2, J3, J4	K3, K5	L6	M1, M2, M4	N4	O1	P2	Q1
			S	**FS iid**	**ii (1)**	**d**	A3, A5	~ 11x14 (big)	~ 10 cm (big)	D1	E4	F2	G3	H6, H12	I4, I7	J1	K3	L1, L2, L7	M1, M2, M3	N5	O1	P2	Q1
	40-60	Small	**S**	**TS iaC**	**i (3 fragments)**	**a**	A3			D2	E4	F3	G3	H1, H2	I4	J5	K3, K5	L2	M2, M3	N4	O3	P2	Q1
			S	**SR**	**v (2 fragments)**	**m**	A2		0.8-1 cm ~	D3	E4	F3	G3	H6, H12	I4, I7	J6	K3	L6	M5	N4	O3	P1	Q1
			S/M	**Fe-Rich Slag**	**FeSlag (13 fragments)**		A6	A2 (for metals)		D2	E6			H6, H12	I4, I5, I7	J1, J2, J4, J5, J7	K7		M1, M2, M3, M4	N1	O5	P1	Q1
			S	**Undiagnostic**	**(1 small fragment)**		A6	3 cm x 2 cm~		D4	E2	F3	G3	H6	I1, I4	J1	K7		M2	N4	O1	P1	Q1

			S	**FS iif**	**ii (5)**	**f**	A6			D2	E6			H6, H12	I4, I7	J1, J5	K7		M2, M3	N4	O2	P1	Q1
			S	**SS iiij**	**iii (1) - ?**	**j**	A2		~ 1.5 cm	D2	E4	F3	G3	H6	I4, I7	J1	K3, K5	L1	M3	N4	O1	P1	Q1
			RF	**RF**	**iii (7)**		A3	B4		G3				E3	C3, C5, C10					H4			
		Medium	**S**	**TS iaC**	**i (5 fragments)**	**a**	A2, A3			D2	E3		G5	H1, H2, H3	I4, I5	J6	K3, K5	L2	M1, M2, M3, M4	N5	O1	P2 (SOME)	Q1
			S -	**FS iid**	**ii (2 cakes)**	**d**	A3, A6			D1	E6			H6, H12	I4, I5, I7	J1, J2, J3, J7	K3, K5	L1, L2, L3, L5	M1, M2, M3, M4	N5	O2	P2	Q1
			S	**FS iie**	**ii (2 lumps)**	**e**	A6	long lump ~20 cm		D2	E6			H6, H12	I4, I5, I7	J1, J4	K3	L4, L5, L7	M1, M4, M5	N5	O2	P2	Q1
		Selected Medium	**S**	**FS iif**	**ii (4)**	**f**	A6			D2	E4, E6			H6, H12	I4, I5, I7	J1, J4	K7		M1, M2, M3, M4	N5	O4, O5	P1	Q1
			S	**FS iie**	**ii (2)**	**e**	A1 (cake) + fan shaped			D2	E6			H6, H12	I4, I5, I7	J1, J2	K3, K5	L1, L2	M1, M2, M4, M5	N4	O1, O3	P2	Q3

			M	**M iiik**	**iii (2)**	**k**	G2	A1		C1					D3, D6	F1, F2 (a bit on outer surfaces)			E1, E2, E3	B1			
		Special Finds	**S**	**FS iid**	**ii (1)**	**d**	A3	~ 15 x7cm		D1	E4	F2	G3	H6	I1, I4	J1	K3	L2, L5, L7	M1, M5	N5	O2	P2	Q3
			S	**FS iie**	**ii (1 lump)**	**e**	A6			D2	E6			H6, H12	I4, I5	J1, J2	K3, K5	L1, L2	M2, M4	N5	O2	P2	Q3
			S	**FS iif**	**ii (4)**	**f**	A6			D3	E6			H6	I4, I7	J1, J4	K3, K7		M1, M2	N4	O1	P2	Q1
			S	**TS ic**	**i (2)**	**c**	A6			D3	E3	F2	G3	H1	I2	J2, J4	K7		M3	N4	O3	P2	Q1
			S/M	**Fe-Rich Slag**	**FeSlag (3 fragments)**		A6	~3/4cm		D1	E6			H6, H12	I4, I5	J1	K3, K7	L1, L2	M1, M2	N2	O4	P2	Q1
		Large	**S**	**FS iid**	**ii (3 pieces)**	**d**	A3~			D1	E6			H6, H12	I4, I5, I7	J1, J2, J3, J4, J5, J7	K3	L1, L2	M1, M2, M3, M4 + BF slag	N4	O1	P1	Q1

DATABASE 2000 EXCAVATION SEASON

TRENCH	SPIT	SIZE	DESCRIPTION	SYMBOL	TYPE	SUBTYPE	Shape	Overall Size	Thickness	Density	Porosity	Porosity size	Porosity shape	Surface Texture	Colour	Surface impressions	Underside texture	Underside impressions	Inclusions (all surfaces)	Magnetism	Viscosity	Multiple flow episodes	Degree of fracture
LS1																							
	0-20	Large	S	**TS iaC**	ii (1)	d	A3	~ 20 x 13 cm		D1	E4	F2	G2, G3	H3, H6	I4	J6	K3	L1, L2	M1	N5	O2	P2	Q3
	0-20	Small	S	**FS iid**	ii (3)	f	A3, A6			D1	E4	F2	G2, G4	H3, H7	I5	J7	K4	L1, L3	M3 (in section)	N5	O2	P2	Q1
	0-20	Small	S	**Flakes**	iii (4)	h1	A12	~ 2 cm		D4	E5	F4	G3	H1	I4	J6	K7	L6	M6	N3	O5	P2	Q1
SS1																							
	0-20	Small	S	**SS iiig**	iii (1)	g	A5	~ 7 x 8	~ 1cm	D3	E6			H6	I4	J6	K3	L1, L2	M6	N3	O3	P2	Q3
			S	**SR**	v (1)	m	A7	~ 10 long		D3	E4 (hollow)	F2	G5	H6, H12	I4	J1	K3	L1, L2	M6	N4	O2	P2	Q4
			S	**Fe-Rich Slag**	4 fragments		A6			D2	E6			H6, H12	I1, I5	J7	K7	L6	M4, M5	N1	O4	P2	Q1
	20-40	Small	S	**SR**	v (10)	m	A7	~ 5 long		D3	E6 (hollow)			H6	I4	J1	K3	L1, L2	M1	N4	O2	P2	Q1
			S	**TS ic**	i (small fragment)	c	A6			D3	E1	F2	G3	H7	I1			K7	M3	N4	O4	P2	Q1
			S - mix	**FS iif**	ii (10)	f	A6			D3	E6			H6	I4, I7			K7	M1, M2, M5	N4	O5	P2	Q1
			MS	**Fe-Rich Slag**	13 fragments		A6			D2	E6			H6, H12	I1, I5	J3	K3	L6	M6	N1	O3	P2	Q1
				Undiagnostic	8		A6			D4	E6			H6	I6				M5?	N4	O5	P2	Q1
			G	**G iii**	9	e, h	A2, A3	B3		G3				D3, D4	C3, C5, C10	E9				H4			
		Medium	S	**FS iie**	ii (5 pieces)	e	A6			D2	E6			H6	I4, I7	J1, J4, J7	K3	L1, L2	M1, M2, M5	N4	O2, O3	P2	Q3
			S	**SS iiij**	iii (2)	j	A3			D2	E2	F1	G5	H3, H6	I4	J6	K3	L1, L2	M3	N4	O3	P2	Q1
				SS iiig	iii (1)	g	A6			D2	E6			H6	I4, I7	J1, J4, J7	K3	L1, L2, L5	M1, M5	N4	O1	P2	Q3
			S	**FS iid**	ii (1 lumps)	d	A1	~ 15 x 6 (lump)		D1	E5	F4	G3	H3, H12	I3, I4, I7	J1, J2	K3	L1, L2	M1, M2, M5	N4	O3	P2	Q1
			S	**TS iaC**	ii (1)	d																	
			M	**M iiik**	1		G1	~ 9 x 2.5/A2		C1					D4	F2		F2	E4	B1			
			G	**G iii**	iii (2)																		
		Large	S	**FS iid**	ii (3)	d	A3	~ 25 x 10cm		D1	E3	F2	G3	H6, H12	I1, I4, I7	J1, J7	K1, K3	L2, L5	M1, M2, M5	N5	O3	P2	Q4
RS1																							
	0-20	Medium	S	**SR**	v (3)	m	A11			D2	E6 (hollow)			H1, H6	I4	J1, J2	K3	L1, L2	M2, M3	N4	O3	P2	Q3

		Small	S	**TS ic**	i (5)	c	A6			D3	E6			H1, H4	I2	J2	K3, K7	L2	M3	N4	O3	P2	Q1
		Small	RF	**RF iii**	iii (2)	f		N2						C3		E2			M1				
		Small	M	**M iiik**	iii (4)	k	G2, Rectang	A3	~ 3cm rectang piece	C1					D4, D6	F1, F2			E1, E2	B1			
		Small		**Undiagnostic**	2 small fragments																		
	20-40	Large	S	**FS iid**	ii (2)	d	A3, A5	~7 x 11	~ 8 cm	D1	E5	F4	G3	H6	I3, I4	J1	K3	L1, L2	M2	N4	O1	P2	Q3
		Large		**FS iie**	ii (1)	e	A5		~ 8 cm	D2	E6			H6, H12	I4, I5, I7	J4	K5	L4	M1, M2, M5	N4	O1	P2	Q2
	20-40	Small Finds	S	**SS iiij**	iii (3)	j	A2			D2	E2	F1, F2	G3	H6	I4, I7	J1	K3	L1, L2	M1, M2, M3	N4	O1	P2	Q1
		small	S	**Undiagnostic**	4 small fragments																		
		Large	S	**FS iid**	ii (1)	d	A1	~ 15 x6		D2	E6			H6, H12	I4, I5	J1, J2	K3, K5	L1, L2	M2, M3, M5	N4	O1	P2	Q2
		small	S	**FS iif**	ii (13)	f	A6	~ 4/5 cm		D3	E6				I4, I7				M1, M2, M3, M5	N4	O5	P2	Q3
		medium	S	**SR**	v (1)	m	A11	~ 10 long		D3	E6			H1, H6	I4	J2	K3	L1, L2		N4	O2, O3	P2	Q3
		small	RF	**RF iii**	iii (17)			N2															
		small	MS	**Fe-Rich Slag**	5 pieces																		
		small	M	**M iiik**	iii (1)	k	Elongated	A2		C1					D1, D4					B1			
		small	G	**G iiig**	iii (2)	g	A2	B3		G2				D3	C1, C5	E9				H4			F1
Letters given during excavation	**D**	large	S	**FS iid**	ii (1)	d	A5	~ 15 x 9		D1	E4	F2	G3	H6	I4, I7	J2	K3, K5	L1, L2	M1, M2, M3	N4	O1	P2	Q3
	C	large	S	**FS iie**	ii (1)	e	A2	~ 20 x 8		D2	E5	F3	G3	H3, H6	I4, I7	J1, J2, J3	K3	L1, L2	M1, M2, M3	N4	O2	P2	Q3
	J	large	S	**FS iid**	ii (1)	d			~6 cm														
	G+K	large/medium	S	**SS iiig**	iii (2)	g	A5	~ 20 x 8	~ 4/6 cm	D1	E5	F3	G3	H6	I2, I4, I7	J1, J2	K3, K5	L1, L2	M1, M2, M3	N5	O2	P2	Q4
	E + J		S	**FS iif**	ii (4)	f	A6			D2	E6			H6, H12	I1, I3, I4, I7	J1, J2	K3, K5	L1, L2	M1, M2, M3	N5	O1	P2	Q1
	F	small	RF	**RF iii**	iii (4)			N2						C3					D1, D4				
		small	G	**G iii**	iii (3)	e (1), g (2)	A2	B3		G3				D3	C5					H4			

APPENDIX A.1: BAGS SURVEYED FOR VISUAL ANALYSIS

Bags surveyed for macro-morphological analysis of material retrieved from trenches of the 1999 excavation season.

GRID	SPIT	Labels					
PN1	0-20	LARGE	MEDIUM	SMALL	ONE SLAG COMPLETE	SELECTED MEDIUM	
PN1	UPPER 20-40		MEDIUM	SMALL			
PN1	CHARCOAL 20-40			SMALL			
QN1	0-20	LARGE	MEDIUM	SMALL	SELECTED SLAGS		VERY LARGE
QN1	20-40	LARGE	MEDIUM	SMALL	SMALL FINDS		
QN1	0-20 + 20-40	SLAGS SELECTED BY GILL					
QN1	SPIT UNKNOWN	LARGE					
PN1/QN1					CONTEXT 7		
ZN1	0-20	LARGE	MEDIUM	SMALL	SMALL FINDS	SELECTED MEDIUM	FURNACE BOTTOM
ZN1	20-40		MEDIUM	SMALL	SPECIAL FINDS		
ZN1	40-60				ONE SLAG		
ZS3	0-20		MEDIUM	SMALL		SELECTED MEDIUM	
ZS3	20-40	LARGE	MEDIUM	SMALL	SPECIAL FINDS	SELECTED MEDIUM	SELECTED PIECES
ZS3	40-60	LARGE	MEDIUM	SMALL	SPECIAL FINDS	SELECTED MEDIUM	HUGE
JN9	0-20		MEDIUM	SMALL			
JN9	UPPER				MIXED SLAG		
JN9	LOWER				SLAG ONLY		
JN9	UPPER & LOWER				SPECIALS		
JN9	40-60	LARGE	MEDIUM	SMALL	SPECIAL FINDS	SELECTED MEDIUM	

Bags surveyed for investigation of matrix material retrieved from trenches of the 1999 excavation season.

	SPIT	**LABELS/SIEVE**
PN1	0-20	Total Matrix <1
	0-20	<1 >0.5
	0-20	<0.5 >0.28
	20-40 Btm	< 1 >0.5
	20-40 Top	< 1 >0.5
	20-40 Btm	< 0.5 >0.28
	20-40 Top	< 0.5 >0.28
QN1	0-20	Wet Sieved
	0-20	Not sieved
	20-40	<1 >0.5
	20-40	<0.5 >0.28
	20-40	Not sieved
	20-40	Wet sieved
ZN1	0-20	<1 >0.5
	0-20	<0.5 >0.28
	20-40	<1 >0.5
	20-40	<0.5 >0.28
ZS3	0-20	<1 >0.5
	0-20	<0.5 >0.28
	20-40	<1 >0.5
	20-40	<0.5 >0.28
	40-60	<1 >0.5
	40-60	<0.5 >0.28
JN9	0-20	<1 >0.5
	0-20	Wet washed <1 >0.28
	0-20	<0.5 >0.28
	(40-60)	<1 >0.5
	40-60	<1 >0.5
	40-60	<0.5 >0.28

Bags surveyed for the macro-morphological analysis of material excavated during the 2000 excavation season.

GRID	**SPIT**	**Labels**					
LS1	0-20	Slag sample					
SS1	0-20	Slag					
	20-40	Knobby-gritty slag (2 bags)	Slag sample	Context 8			
RS1	0-20	Slag sample	Small finds				
	20-40	In situ' (?) furnace bottom	Slag sample	Grey clay below charcoal	Small finds - furnace lining (?)	Furnace bottom lining (?)	Slag and Clay

APPENDIX A.1.1: PHOTO ARCHIVE OF EXCAVATED TRENCHES

Trench QN1

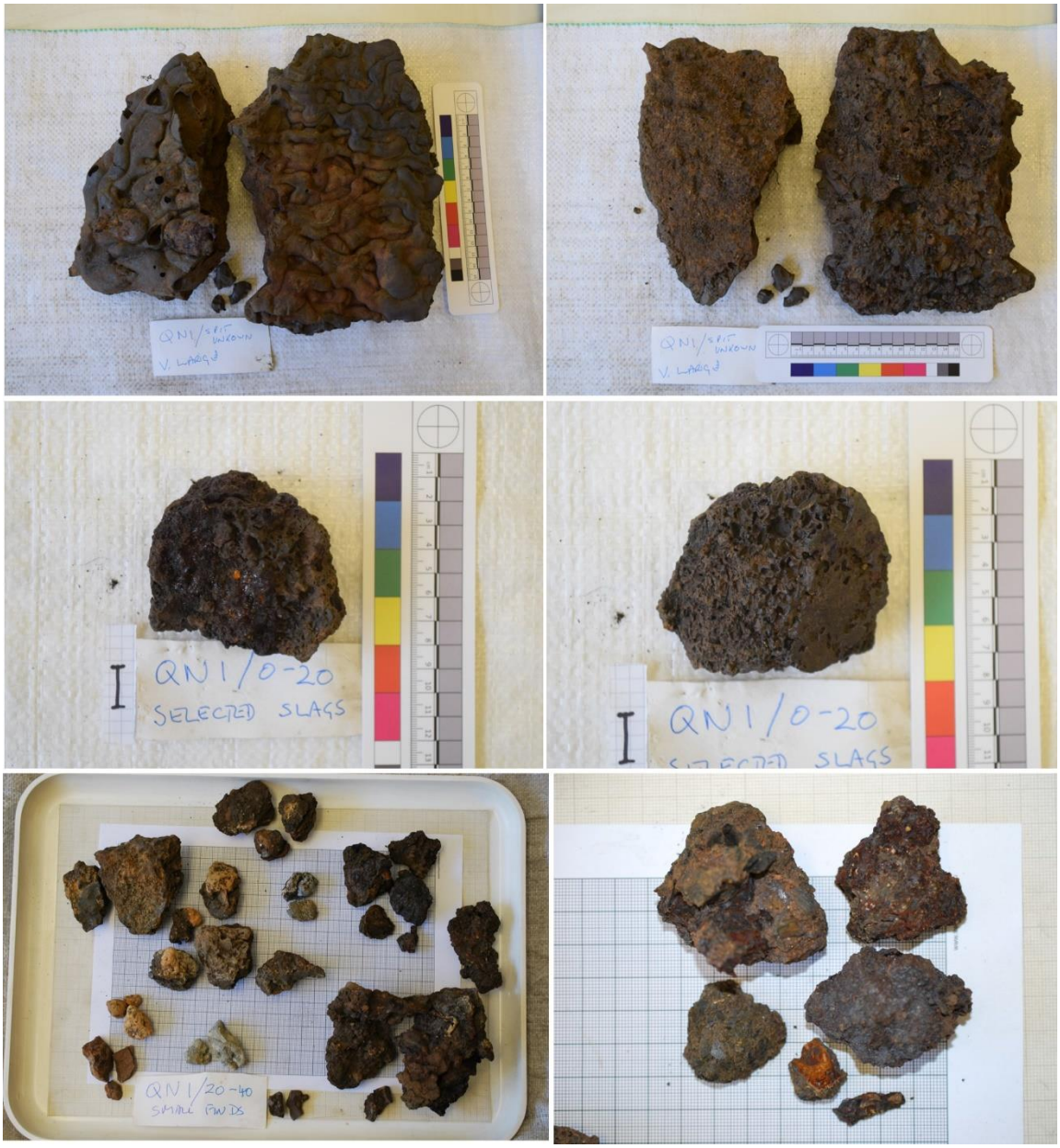

Example of material debris recovered from trench QN1. Dominated by small size samples, the trench also yielded two large finery tap slag cakes.

Trench PN1

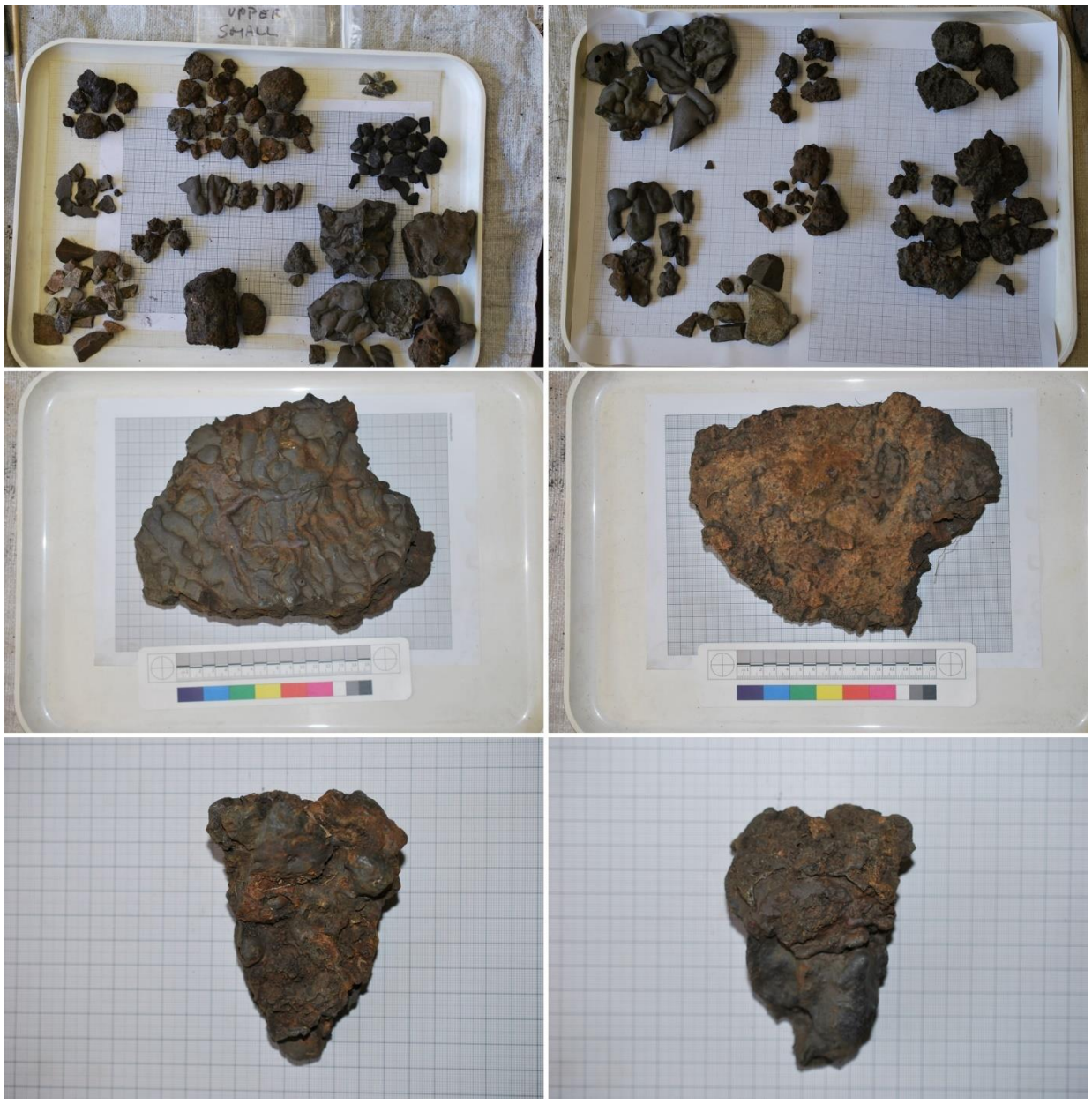

Example of material debris retrieved from trench PN1. Material is mostly small-sized, except for some large finery tap slag cakes. Trench characterised by a large number of conglomerates and several fragments of blast furnace slag (section 4.4.2 and 4.4.5).

Trench ZN1

Example of material debris recovered from trench ZN1. Larger samples characterise this trench, albeit comparatively less material was excavated from here as during excavation the remnants of a wall crossed the trench. Feature not excavated.

Trench ZS3

Example of material debris recovered from trench ZS3. Large and complete pieces were recovered from this trench, suggesting a primary undisturbed deposit. Photos show upper (left) and lower (right) surfaces. Top images: this example has a flat upper surface and a rounded lower part, characterised by charcoal impressions. Note the slag protrusion of the example in the middle and the rectangular channel cavity visible on the example at the bottom.

Trench JN9

Example of material debris recovered from trench JN9. Located 9m away from the baseline excavation, the material in this trench appears characterised by iron-rich fragments and several slag channels fragments (section 4.4.2).

Trench LS1

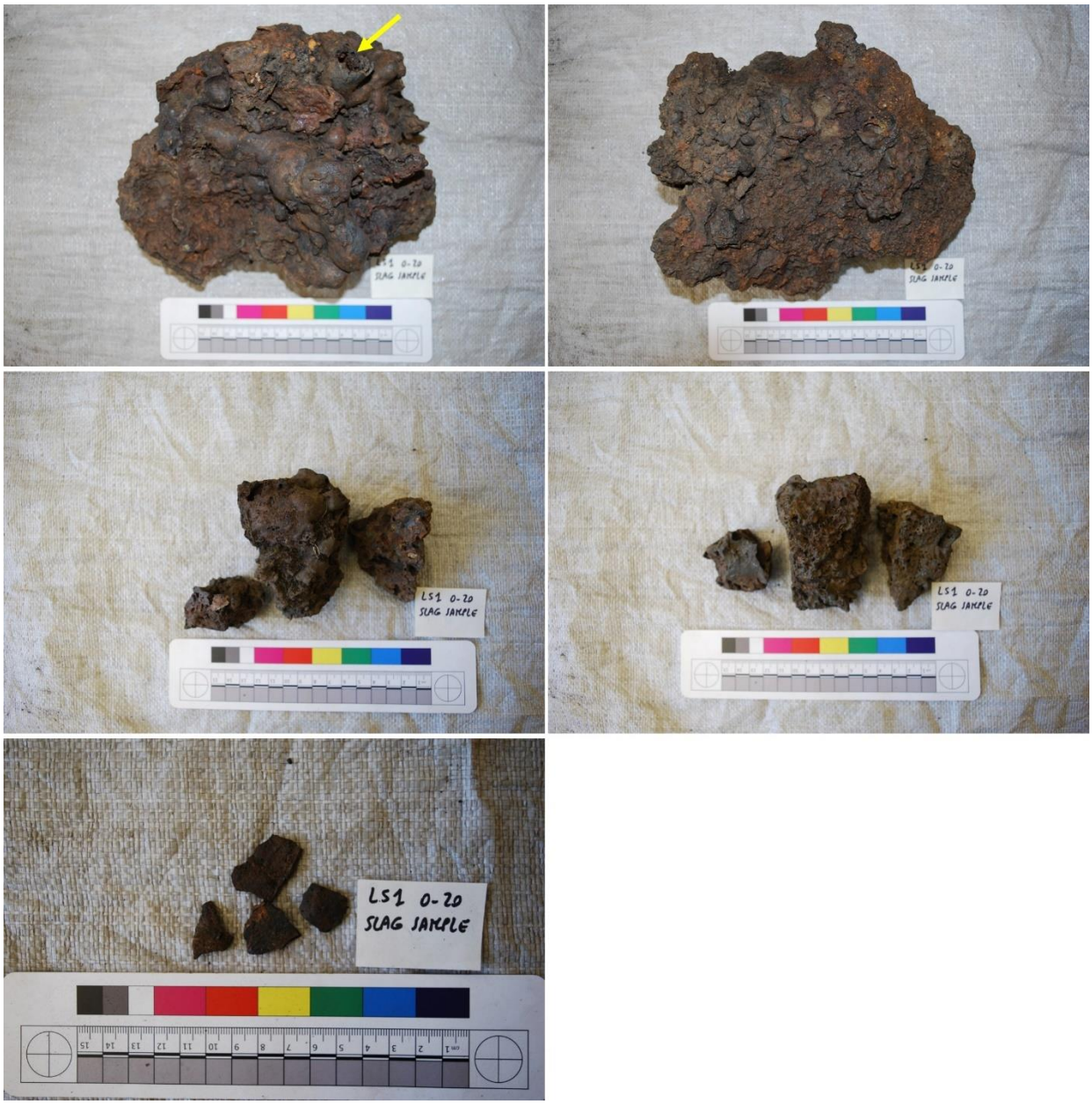

Example of material debris recovered from trench LS1. A small amount of material was excavated from this trench. Top figures show an example of large ‘flowed’ cakes. The arrow is showing a circular hollow slag protrusion, which suggests the presence of a slag channel.

Trench RS1

Example of material debris recovered from trench RS1. Excavated next to QN1 yielded large and complete pieces of slag, as well as slag channels and abundant conglomerates and metal samples, including a fragment of a fined iron bar (section 4.4.4).

Trench SS1

Example of material debris recovered from trench SS1. The slag in this trench is similar to trench RS1. Large hearth cakes with pointy ends are found here and abundant iron-rich slag.

APPENDIX A.2: QUANTIFIED DATA FROM EXCAVATIONS

APPENDIX A.2.1: QUANTIFIED DATA FROM EXCAVATION 1999 AND BAR CHARTS FROM PRELIMINARY REPORT (JULEFF 2000)

PN1	BUCKETS	COMPLETE	LARGE	MEDIUM	SMALL DRY	SMALL WET	STONE	OTHER	MATRIX	PN1	BUCKETS	MEDIUM	SMALL DRY	SMALL WET	STONE	CHARCOAL	OTHER	MATRIX
0-20	7.0	17.3	10.6	11.1	14.0	7.5	3.9	1.0	4.9	**20-40**	7.3	0.5	17.1	8.8	0.5	6.2	0.3	10.1
	7.5		3.6	13.0	9.9	5.5	0.8		8.0		5.0		4.3	1.0	0.8	5.5		7.3
	8.8			2.7	11.0	5.9			8.5		10.6			3.6				11.0
	7.6				10.4	0.9			8.3		1.4							8.8
	15.5				14.8	7.1			7.2		5.7							6.0
	11.3				12.7	10.2			7.9		6.6							5.4
	14.6				9.2				7.7		7.6							5.9
	10.7				9.6				8.7		3.0							4.7
	16.9				11.0				9.6		6.1							7.6
	10.5				15.9				9.4		3.8							5.0
	15.8				14.4				10.0		3.8							4.1
	14.8								10.0		3.4							
	22.6										5.8							
	25.4										6.1							
	14.2										3.6							
	12.3										9.9							
	12.9										7.3							
	14.1																	
	10.0																	
	5.4																	
	12.5																	
	14.7																	
	5.7																	
	17.6																	
	5.7																	
TOTALS	313.5	17.3	14.2	26.8	132.8	36.9	4.7	1.0	100.0	**TOTALS**	96.8	0.5	21.4	13.3	1.3	11.7	0.3	75.6
	TOTAL SLAG	**191.1**									**TOTAL SLAG**	**21.9**						

QN1	BUCKETS	COMPLETE	LARGE	MEDIUM	SMALL DRY	SMALL WET	STONE	OTHER	MATRIX	QN1	BUCKETS	COMPLETE	LARGE	MEDIUM	SMALL DRY	SMALL WET	STONE	MATRIX
0-20	8.7	13.3	12.3	12.0	11.4	5.8	3.0	0.9	50.3	**20-40**	15.4	4.3	8.6	10.4	13.9	8.0	2.0	77.8
	10.3		16.3	13.2	16.8	7.0					12.9		1.9	6.8	9.0		0.9	
	12.4		6.7	8.6	12.0	4.0					10.6			4.1	13.8		1.2	
	14.2		7.5	9.2	14.8						11.8				9.8			
	11.8			7.5	13.0						12.2				13.2			
	13.0				11.4						9.4				5.3			
	10.7				14.2						10.8				9.2			
	8.7				13.8						9.0				9.1			
	13.4				13.8						10.3				11.1			
	16.1				13.8						12.7				6.4			
	9.2				13.3						9.6				2.4			
	8.7				11.7						9.7							
	12.2										10.0							
	13.5										1.7							
	7.0										8.7							
	4.3										8.8							
	4.0										7.6							
	15.4										11.0							
	14.2										7.4							
	15.9										6.0							
	11.0										6.3							
	15.2										10.8							
	6.7										8.6							
	14.2										5.7							
	17.4										2.5							
	3.0																	
	13.7																	

	20.0																	
	13.2																	
TOTALS	337.6	13.3	42.8	50.5	160.0	16.8	3.0	0.9	50.3	**TOTALS**	229.0	4.3	10.5	21.3	103.1	8.0	4.1	77.8
	TOTAL SLAG	**266.6**									**TOTAL SLAG**	**139.2**						

ZN1	BUCKETS	COMPLETE	LARGE	MEDIUM	SMALL DRY	SMALL WET	STONE	OTHER	ZN1	BUCKETS	MEDIUM	SMALL DRY	SMALL WET	STONE	OTHER	MATRIX
0-20	15.2	4.3	10.4	11.1	15.6	3.3	10.2	0.9	**20-40**	11.3	1.2	9.3	1.9	1.0	1.8	6.8
	12.6	1.2	7.8	11.1	9.8	8.2	9.3	4.8		9.6		9.2	1.3	0.4	1.3	3.6
	13.5	1.1		8.6	11.2	8.0	6.9			10.8		1.3				6.0
	13.5			9.1	10.8	11.6				11.4						9.3
	16.4			8.5	9.4					6.6						3.7
	8.8				11.3					5.5						
	17.3				13.1											
	17.8				8.7											
	19.0				10.6											
	12.0				10.3											
	16.3				15.5											
	21.8				11.4											
	14.4				11.5											
	14.6				11.3											
	16.2				10.1											
	14.2				14.2											
	9.8															
	16.0															
	11.4															

	11.0															
	15.5															
	15.7															
	10.4															
	7.4															
	2.1															
	12.2															
	11.9															
	6.0															
	7.2															
	9.8															
	1.2															
TOTALS	390.8	6.6	18.1	48.3	184.6	31.0	26.4	5.7	TOTALS	55.2	1.2	19.8	3.2	1.4	3.1	29.4
	TOTAL SLAG	**257.6**								**TOTAL SLAG**	**21.0**					

ZS3	BUCKETS	MEDIUM	SMALL DRY	SMALL WET	STONE	OTHER	MATRIX	ZS3	BUCKETS	LARGE	MEDIUM	SMALL DRY	SMALL WET	STONE	OTHER	MATRIX	ZS3	BUCKETS	COMPLETE	LARGE	MEDIUM	SMALL DRY	SMALL WET	STONE	OTHER	MATRIX
0-20	10.4	6.7	12.2	8.1	10.9	1.1	11.5	**20-40**	15.7	12.6	11.9	10.8	5.2	3.3	3.9	10.7	**40-60**	9.5	25.0	14.5	6.8	7.5	5.9	3.3	5.0	7.1
	10.2	8.2	14.5	11.0	10.0	1.6	11.2		13.8	10.2	11.0	11.3	3.8			7.8		5.6		5.7	8.9	10.6	4.8			8.7
	7.2	1.3	12.9	4.6	0.5		11.6		13.1	9.1	12.7	9.2	9.1			8.0		10.7		4.8	5.4	7.6	7.5			6.7

	8.6		7.1	3.5			11.1		12.8	3.9	10.3	11.0	8.5			9.5		7.8			10.6	9.6	8.5			12.1
	11.8		8.1	6.7			6.5		4.1	3.2	9.6	9.0				14.0		11.4			8.1	15.3	8.4			9.9
	11.3		12.8	10.0			8.7		11.8	12.0	5.0	10.0						11.2				12.5	6.8			12.6
	13.2		10.5				9.5		9.9	14.6	10.7	10.2						11.6				7.1	2.0			8.4
	9.5		12.2				8.4		4.4			10.2						7.9				11.0				14.1
	12.2		10.4						6.3			7.3						11.9				9.5				
	9.8		13.8						12.8			8.7						3.7				8.0				
	12.3		13.5						5.4			10.2						11.0				8.2				
	18.8		16.0						14.2									9.9				11.5				
	9.6		17.7						11.4									8.8				13.9				
	11.5		19.4						12.0									8.6								
	9.5		12.8						14.2									7.6								
	14.7								14.3									8.4								
	8.0								6.6									25.0								
	11.4								4.6									12.5								
	9.8								13.0									12.7								
	11.9								14.2									12.4								
	8.6								11.8									9.2								
	12.9								8.9									13.4								
	9.3								10.9									13.7								
	11.8								10.5									8.6								
	8.8								6.0									11.8								
	11.7								12.2									7.6								
	12.2								13.4									14.4								
	9.8								12.6									8.2								
	12.5								12.2									5.9								
									4.2									11.6								
																		3.1								
																		2.0								
																		1.2								
TOTALS	319.3	16.2	193.6	43.8	21.3	2.7	78.4	TOTALS	317.2	65.6	71.2	107.7	26.6	3.3	3.9	49.9	TOTALS	318.9	25.0	25.0	39.7	132.1	43.9	3.3	5.0	79.5

	TOTAL SLAG	**209.8**							**TOTAL SLAG**	**244.4**								**TOTAL SLAG**	**221.7**						

JN9	BUCKETS	MEDIUM	SMALL DRY	SMALL WET	STONE	CHARCOAL	OTHER	MATRIX	**JN9**	BUCKETS	LARGE	MEDIUM	SMALL DRY	STONE	CHARCOAL	OTHER	MATRIX
0-20	8.2	1.7	11.9	6.3	5.8	0.8	1.1	7.3	**40-60**	7.3	6.0	4.2	6.1	8.7	0.3	1.3	7.2
	9.0	0.6	13.7	6.7	4.3		6.6	7.6		6.3		2.2	4.0	11.0			6.9
	7.0		11.8	7.1				6.3		8.3			6.5	5.6			8.1
	8.7		9.7	4.9				7.3		8.9			4.0				8.5
	6.9		10.4	6.7				5.7		10.7			11.7				8.6
	6.9		7.0	5.8				6.5		7.7			6.2				11.8
	7.0		4.6	4.4				8.0		9.7			3.8				5.0
	7.6		10.7	2.6				9.6		8.6							4.5
	7.3			3.8				9.8		8.4							9.1
	8.4			6.9				9.9		7.0							7.7
	6.2			5.0				8.5		7.9							9.7
	1.0							3.9		5.6							7.4
	9.3							9.8		9.8							6.0
	9.7							4.6		5.8							8.3
	13.2							6.2		11.4							7.0
	13.5							5.9		7.6							10.0
	14.0							8.5		4.3							8.5
	12.5							9.1		7.3							6.2
	11.4							5.6		5.0							0.9
	11.8									8.8							
	6.2									9.4							
	6.8									10.1							
	8.9									8.0							

	2.4									11.8							
	4.1									4.7							
	4.6									7.4							
	7.7									12.0							
	5.2																
	8.7																
	3.6																
	10.3																
	1.8																
TOTALS	249.5	2.3	79.5	60.0	10.1	0.8	7.7	139.8	TOTALS	219.1	6.0	6.4	42.1	25.2	0.3	1.3	141.1
	TOTAL SLAG	**81.8**								**TOTAL SLAG**	**54.5**						

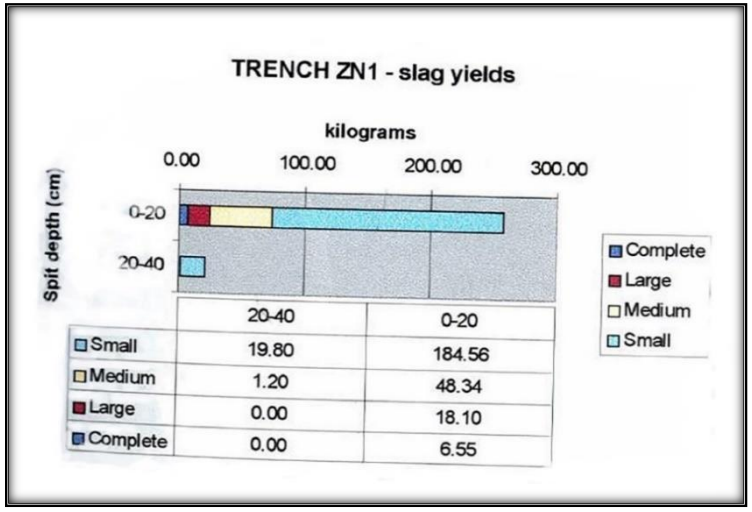

	20-40	0-20
Small	19.80	184.56
Medium	1.20	48.34
Large	0.00	18.10
Complete	0.00	6.55

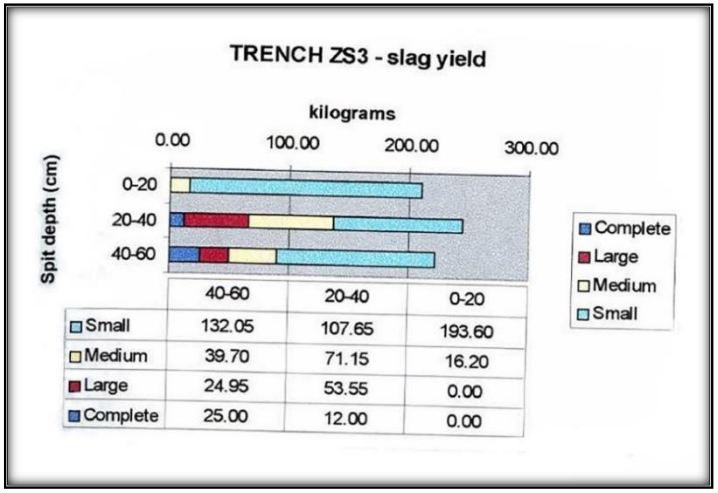

	40-60	20-40	0-20
Small	132.05	107.65	193.60
Medium	39.70	71.15	16.20
Large	24.95	53.55	0.00
Complete	25.00	12.00	0.00

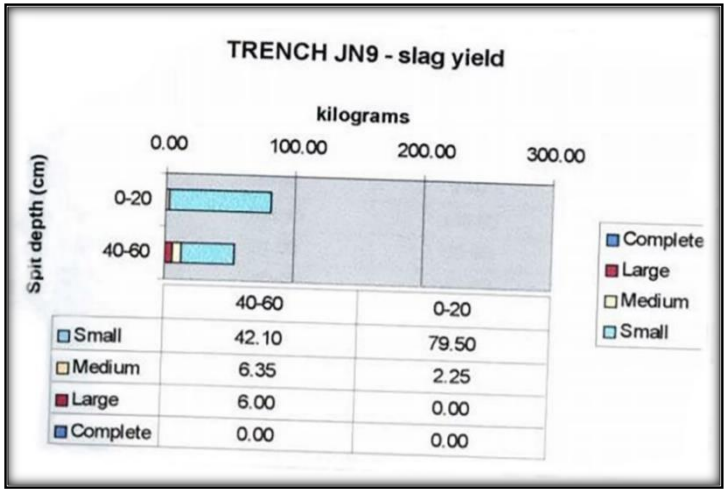

	40-60	0-20
Small	42.10	79.50
Medium	6.35	2.25
Large	6.00	0.00
Complete	0.00	0.00

Charts showing the slag yield for trenches ZN1, ZS3 and JN9 elaborated for the material excavated during the field season in 1999 (*after* Juleff 2000, 23 and 25).

APPENDIX A.2.2: QUANTIFIED DATA 2000 EXCAVATION SEASON

LS1	BUCKETS	COMPLETE	LARGE	MEDIUM	SMALL	STONE	SMALL FINDS	CHARCOAL	OTHER	MATRIX	
0-20	7.1		4.1	8.7	9.8	7.8	0.3	1.4	3.1	7.9	
	11.2			1.2	10.6		1.4		Roots	8.2	
	9.4				9.7					7.4	
	9.1				10.6					7.7	
	8.6				12.7					8.8	
	13.3				5.4					9.7	
	14.6				4.4					7.8	
	15.0									10.5	
	13.8									9.8	
	12.6									9.8	
	14.4									10.8	
	11.0									10.9	
	12.8									8.6	
	18.3									3.9	
	25.8										
TOTALS	197.0		4.1	9.9	63.0	7.8	1.7	1.4	3.1	121.5	TOT MATERIAL
			TOT SLAG	**77.0**							212.4

MS1	BUCKETS	COMPLETE	LARGE	MEDIUM	SMALL	STONE	SMALL FINDS	CHARCOAL	OTHER	MATRIX	
0-20	5.8		1.3	6.0	11.7	6.9	3.5	3.8	5.8	8.2	
Peaty Matrix	9.0				13.4		0.4		Roots	6.6	
	7.4				8.5		4.8			8.3	
	11.4				3.1					9.9	
	12.3									9.8	
	14.4									10.7	
	13.2									7.7	
	6.4									7.8	
	13.0									5.2	
	13.5									8.5	
	10.6									9.9	
	5.4									10.1	
	11.7									0.4	
	19.2									10.1	
	13.6									9.6	
Sandy Matrix	10.6									8.1	
	11.5									6.1	
	9.4										
	3.2										
	5.7										
TOTALS	207.3		1.3	6.0	36.7	6.9	8.6	3.8	5.8	136.7	TOT MATERIAL
			TOTAL SLAG	**43.9**							205.6

NS1	BUCKETS	COMPLETE	LARGE	MEDIUM	SMALL	STONE	SMALL FINDS	CHARCOAL	OTHER	MATRIX	
0-20	10.2			8.9	8.0	14.5	0.9	2.6	3.5	7.9	
Peaty Matrix	8.4				7.2		0.7	2.1	Roots	7.9	
	14.2				12.5		1.8	2.4		8.0	
	13.4				13.4					6.4	
	11.8				6.8					5.2	
	14.1				6.0					7.4	
	16.4									9.5	
	14.6									8.1	
	11.6									7.2	
	13.2									8.5	
	13.4									9.6	
	11.2									10.0	
	8.0									7.6	
	10.8									6.6	
	6.7									8.3	
	12.0									6.8	
Sandy Matrix	6.3									8.0	
	10.6									8.4	
	8.6									8.2	
	11.3									8.4	
	7.0									1.2	
	9.2										
	11.8										
TOTALS	254.8	0	0	8.9	53.9	14.5	3.4	7.1	3.5	158.7	TOT MATERIAL
			TOTAL SLAG	**62.8**							249.8

OS1	BUCKETS	COMPLETE	LARGE	MEDIUM	SMALL	STONE	SMALL FINDS	CHARCOAL	OTHER	MATRIX	OS1	BUCKETS	COMPLETE	LARGE	MEDIUM	SMALL	STONE	SMALL FINDS	CHARCOAL	OTHER	MATRIX	
0-20	8.2		2.4	13.5	9.9	10.1	2.3			6.1	**20-40**	8.1			1.7	3.4	5.6	5.9	2.0		6.1	
Peaty Matrix	12.3			8.9	10.2	9.3				8.1		5.7			1.2			7.2			6.1	
	15.1			2.8	7.1					8.3		10.1									5.6	
	9.5			4.8	10.3					6.5		10.0									3.1	
	13.4			1.4	9.3					7.9		9.0									7.2	
	13.6				11.4					6.8		5.8									7.9	
	11.4				9.3					7.6		13.5									7.7	
	14.8				6.0					7.9		13.2									7.9	
	15.1				12.1					7.9		10.8									8.1	
Sandy Matrix	13.5									8.2		10.7									8.3	
	13.4									7.8		10.9									9.0	
	13.0									7.6		13.2									9.1	
	11.4									7.4		12.8									9.4	
	8.6									8.1		9.6									9.6	
	15.9									5.7		11.2									11.3	
	11.0									6.0		8.2									10.2	
	17.0											8.5									11.3	
	9.8											8.0									10.7	
	10.6											7.8									10.7	
	13.3											11.4									10.8	
	9.0											5.0									9.8	
TOTALS	259.5		2.4	31.3	85.4	19.4	2.3			117.7	**TOTALS**	203.5	0.00	0.00	2.8	3.4	5.6	13.1	2.0		179.3	206.2
			TOTAL	**119.1**										**TOTAL**	**6.2**							

			SLAG										SLAG								

RS1	BUCKETS	COMPLETE	LARGE	MEDIUM	SMALL	STONE	SMALL FINDS	CHARCOAL	OTHER	MATRIX	RS1	BUCKETS	COMPLETE	LARGE	MEDIUM	SMALL	STONE	SMALL FINDS	CHARCOAL	OTHER	MATRIX	
0-20	17.1		10.8	10.8	13.4	2.9	5.0			9.7	**20-40**	11.4		8.1	9.0	11.8	8.0	9.8	0.3	3.0	11.1	
	6.8		4.3	8.9	14.9					8.7		15.3		2.3	5.5	12.8	5.5	1.4	0.8		9.2	
	11.6		12.3	4.0	19.4					9.5		12.8			4.5	11.7		0.1			8.3	
	15.8			12.7	7.6					7.4		11.1			5.1	14.1					11.3	
	16.1				8.4					7.9		14.6			0.9	11.6					11.1	
	12.1				11.0					9.1		12.3				7.8					7.2	
	12.2				12.5					10.2		15.8				8.8					9.6	
	14.7				12.4					5.8		11.5				6.3					9.1	
	15.1				10.8					11.1		14.6				4.7					7.4	
	18.3				12.7					10.7		12.6				6.3					6.7	
	12.4				12.7					12.3		14.6				5.4					5.8	
	17.9				13.1							17.8				2.3					6.8	
	17.3				10.3							13.3									5.6	
	13.2				11.6							2.6									9.2	
	15.8				12.5							13.2									7.5	
	15.6				14.4							13.7									5.3	
	17.1											19.6									6.7	
	15.4											8.0									1.8	
	15.6											10.9										
	15.9											11.6										
	7.9											15.2										
	13.3											11.8										
	15.9											3.8										
	12.8											7.2										

	20.8											2.8										
	10.0											9.2										
												7.9										
TOTALS	376.7		27.4	36.3	197.2	2.9	5.0			102.1	**TOTALS**	315.2		10.4	24.9	103.4	13.5	11.3	1.1	3.0	139.6	307.1
		TOTAL SLAG	260.9										**TOTAL SLAG**	138.7								

SS1	BUCKETS	COMPLETE	LARGE	MEDIUM	SMALL	STONE	SMALL FINDS	CHARCOAL	OTHER	MATRIX	**SS1**	BUCKETS	COMPLETE	LARGE	MEDIUM	SMALL	STONE	SMALL FINDS	CHARCOAL	OTHER	MATRIX	
0-20	16.5		5.9	6.3	12.3	14.2	1.4	0.2		8.6	**20-40**	8.7		7.6	10.4	11.9	9.3	20.3	0.2		13.0	
	16.4			8.5	14.6	2.1	2.8			7.7		8.9		7.4	8.6	18.2	0.2	2.2	0.6		12.0	
	14.0			9.1	10.0		1.6			9.0		7.6		2.6	2.9	16.4		2.3	1.0		11.4	
	16.7			7.5	10.7					7.8		13.2				13.2					13.7	
	16.8			0.9	13.2					5.1		11.4				17.3					12.9	
	20.8				13.7					11.3		10.7				7.9					11.4	
	19.2				11.0					10.0		8.6				11.1					12.5	
	16.8				9.3					9.1		8.8									12.2	
	16.6				9.8					10.1		11.1									9.4	
	15.6				11.8					9.6		15.0									8.8	
	17.2				9.9					10.9		10.9									11.3	
	20.2				10.6					13.0		8.7									11.2	
	18.8				12.8					10.9		10.5										
	16.3				10.4					9.6		13.0										
	15.2									8.7		14.4										
	14.3											13.8										
	18.1											13.5										

	17.3											15.6										
	17.0											18.4										
	15.6											11.9										
	15.6											15.2										
	8.7											13.2										
												9.2										
												4.1										
												17.8										
												9.6										
												9.6										
												0.4										
												1.0										
TOTALS	363.7		5.9	32.3	159.8	16.3	5.7	0.2		141.2	**TOTALS**	314.8		17.6	21.8	95.8	9.5	24.8	1.8	0.0	139.6	310.7
		TOTAL SLAG	198.0										**TOTAL SLAG**	135.1								

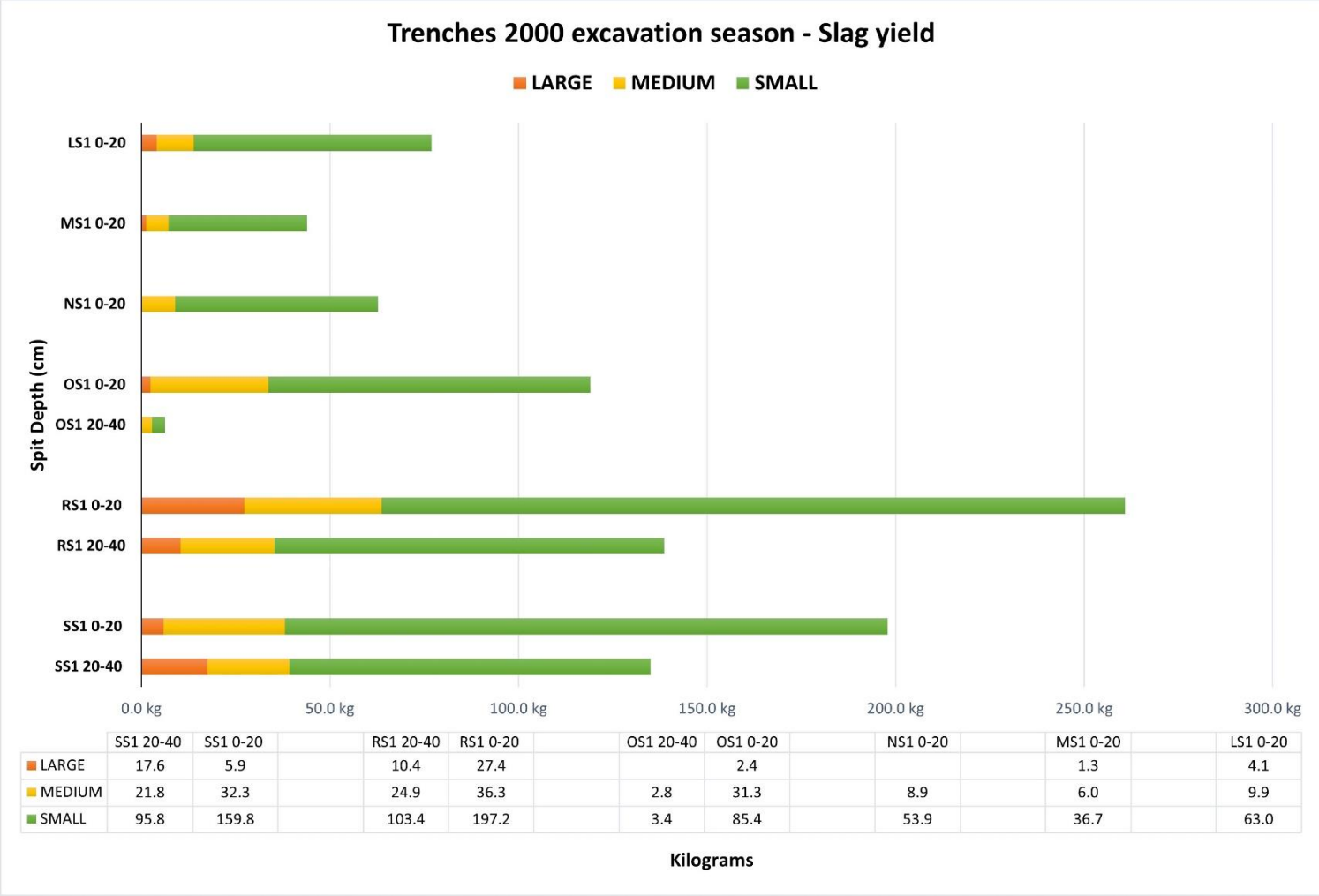

	SS1 20-40	SS1 0-20	RS1 20-40	RS1 0-20	OS1 20-40	OS1 0-20	NS1 0-20	MS1 0-20	LS1 0-20
LARGE	17.6	5.9	10.4	27.4		2.4		1.3	4.1
MEDIUM	21.8	32.3	24.9	36.3	2.8	31.3	8.9	6.0	9.9
SMALL	95.8	159.8	103.4	197.2	3.4	85.4	53.9	36.7	63.0

Slag yield for trenches of the excavation season 2000. Bar chart elaborated for this study and obtained using the quantified data from field notes.

APPENDIX A.3: Classification Scheme for the Ausewell Wood assemblage

Classification scheme elaborated for the Ausewell Wood assemblage.

- Finery tap slag: subtypes a1 and a2 indicating respectively tapped texture and flowed texture, try to introduce and highlight in the proposed classification scheme the difference in texture (H) and viscosity (O) between the two types of finery tap slag cakes, as this could be a feature for the identification of finery forge material
- Hearth slag: subtypes d1 and d2 indicating respectively finery hearth slag and chafery hearth slag are introduced in the proposed classification scheme to indicate that both hearth installation could produce this type of slag. A clear identification was not achieved in this study, and likely a differentiation only by visual analysis is not possible; however, a tentative distinction at the outset of a research on similar assemblages, could then direct the subsequent chemical investigation in this direction

Classification Scheme

SLAG

Class		Type		Sub-type		
Symbol	**Description**	**Symbol**	**Description**	**Symbol**	**Description**	
S	Slag	***FTS***	Finery tap slag	***a***	Upper surface and base present (Cake or Plate)	**a1** Tapped Cake
						a2 Flowed Cake
				b	Individual tendril	
				c	Fragment – non-diagnostic	
		HS	Hearth slag	***d***	Base (cake, block)	**d1** Finery hearth slag
						d2 Chafery hearth slag
				e	Uncertain base - Lumps	
				f	Hearth residues – fragment/lump, non-diagnostic (slaggy conglomeration)	
		SS	Smithing slag	***g***	Complete/smithing hearth bottom	
				j	Fragment – non-diagnostic	
				h	Flats	
				k	Hammerscale	***k1*** flakes
						k2 spheroids
		BFS	Blast Furnace Slag	***l***	Glassy	
				m	Vesicular (Silica-rich)	
		SR	Slag Runners	***n***	Rod-shape	
		FeS	Iron-rich Slag	***o***	Lumps (mixture of metal and slag)	

VARIANTS AND DESCRIPTORS FOR SLAG

Variant		**Descriptors**	
Symbol	**Description**	**symbol**	**description**
A	Shape	1	Plano-concave
		2	Plano (dish/saucer-shaped)
		3	Plano-convex
		4	Convex
		5	Concave-convex
		6	Conical (plano surface, pointy end)
		6	Amorphous
		7	Plate
		8	Hollow rod
		9	Single rod
		10	Elongated
		11	Flakes
		12	Spheroids
B	Overall Size	L x W x T cm	
C	Thickness	cm	
D	Density	1	High
		2	Moderate
		3	Low
		4	Very low
E	Porosity proportion	1	Very high (>60%)
		2	High (40-60%)
		3	Moderate (20-40%)
		4	Low (20%)
		5	Very low (<5%)
		6	Unclear
		7	No
F	Porosity size	1	Large (>10mm)
		2	Moderate (2-10mm)

		3	Small (1-2mm)
		4	Very small (<1mm)
		5	None
G	Porosity shape	1	Network
		2	Elongated
		3	Spherical
		4	Broken – random
		5	Mixed spherical – elongated – all sizes
		6	None
H	Surface texture	1	Smooth
		2	Ropey
		3	Smooth with broken bubbles
		4	Small tendrils
		5	Globular projections
		6	Rough
		7	Broken (surface broken/sheered)
		8	Crystalline/Glassy
		11	Abraded
		12	Rusty
		13	Mixture of flow pattern and rough areas (upper surface)
I	Colour	1	Black
		2	Grey
		3	Red
		4	Brown
		5	Purple
		6	Grayish-blue
		7	Yellow-orange
		8	Metallic
		9	Glassy (green/blue)

		10	Glassy black
J	Surface impressions	1	Charcoal
		2	Soil-geological
		3	Toolmarks
		4	Clay
		5	Stone
		6	None
		7	Slag
		8	Slag Channel
K	Underside texture	1	Smooth
		2	Rippled – tendrils
		3	Rough
		4	Undulated
		5	Geological – hearth material
		6	broken
		7	Underside not visible
L	Underside impressions	1	Charcoal
		2	Soil – geological
		3	Toolmarks
		4	Hearth clay/material
		5	Slag
		6	none
		7	metallic iron
M	Inclusions (all surfaces)	1	Clay
		2	Charcoal
		3	Geological – soil
		4	Metal – iron
		5	Slag
		6	none

N	magnetism	1	High
		2	Moderate
		3	Low
		4	Non-magnetic
		5	Partially – isolated areas
O	Viscosity	1	High
		2	Moderate
		3	Low
		4	Unclear
		5	Not Applicable
P	Multiple flow episodes	1	Yes
		2	No
		3	Unclear
Q	Degree of fracture	1	Total – all surfaces
		2	Partial – all edges
		3	Minor – some old fractures – uncertain
		4	Complete – edges intact
		5	Abraded

REFRACTORY MATERIAL

Class		**Type**		**Sub-type**	
Symbol	**Description**	**Symbol**	**Description**	**Symbol**	**Description**
RF	Refractory material	***RF***	Hearth wall/fragment	***a***	Clay
				b	Cast Iron Plate
				c	Vitrified/Adhering Slag
				d	Fragment – undiagnostic - amorphous
			Uncertain	**e**	Clay Pellets

VARIANTS AND DESCRIPTORS FOR REFRACTORY MATERIALS

Variant		**Descriptors**	
Symbol	**Description**	**symbol**	**description**
A	Thickness of wall/fragment	1	Thin (<2cm)
		2	Medium (2-5cm)
		3	Large (>5cm)
		4	N/A Unclear
B	Inner/External diameter	1	Small <20cm
		2	Medium <50cm
		3	Large >50cm
		4	Uncertain
C	Fabric (overall texture)	1	Coarse (>5mm)
		2	Moderate (2-5mm)
		3	Fine (<2mm)
D	Temper, grog inclusions	1	Charcoal
		2	Organic impressions
		3	Sand
		4	Small stones
		5	Slag
		6	Furnace wall
		7	Tuyère
		8	Quartz
		9	Bigger stones
		10	Unclear
E	Vitrification	1	Minor
		2	Partial
		3	Total
		4	Absent
F	Oxidation (red/yellow colouration)	1	Heavy

		2	Moderate
		3	Light
		4	None
G	Reduction (black/grey colouration)	1	Heavy
	(depth through wall)	2	Moderate
		3	Light
		4	None
H	Oxidation distribution	1	Inside
		2	Outside
		3	Both
		4	Non-specific
I	Reduction distribution	1	Interior
		2	Exterior
		3	Both
		4	Non-specific
J	Hearth wall features	1	Internal metallurgical slag
		2	External metallurgical slag
		3	Large stone in structure
		4	Linear impressions
		5	Tool marks
		6	Embedded tuyères
		7	Rim
		8	Base
		9	Sheered surface
		10	Internal magnetic material
		11	Slag seepage into cracks in wall
		12	None
M	Surface inclusion/impressions	1	Charcoal
		2	Iron rich areas

		3	Possible tool marks
		4	None
N	Fragment size	1	Very small, <1cm
		2	Small, 1-5cm
		3	Medium, 5-20cm
		4	Large, >20cm
O	Fragment abrasion	1	High (edges/breaks smoothed)
		2	Moderate (some fractures sharp and un-abraded)
		3	Low (clean un-abraded breaks)
P	Residue Features	1	Magnetic
		2	Stones
		3	Clay Fragment

GEOLOGICAL MATERIAL

Class		**Type**		**Sub-type**	
Symbol	**Description**	**Symbol**	**Description**	**Symbol**	**Description**
G	Geological material	***O***	Ore	***a***	Magnetic
				b	Non-magnetic
		WS	Worked stone	***c***	Complete artifact
				d	Fragment
		R	Rock	***e***	Quartz
				f	Limestone
				g	Slate
				h	Other

VARIANTS AND DESCRIPTORS FOR GEOLOGICAL MATERIALS

Variant		**Descriptors**	
Symbol	**Description**	**Symbol**	**description**
A	Shape	1	Angular

		2	Sub-angular
		3	Sub-rounded
		4	Rounded
B	Size	1	Large (>15cm)
		2	Medium (10-15cm)
		3	Small (5-10cm)
		4	Very small (<5cm)
C	Colour	1	Red
		2	Brown
		3	Yellow-orange
		4	White
		5	Grey
		6	Metallic
		7	Black
		8	Purple
		9	Green
		10	Pink
D	Crystal, grain size/texture	1	Large – coarse (>5mm)
		2	Moderate (2-5mm)
		3	Fine (<2mm)
		4	Homogeneous – e.g. flint
E	Other features	1	Banding
		2	Contains ore minerals
		3	Burning coloration (pink-red)
		4	Iron staining
		5	Inter-grown with other minerals/rock
		6	Porous
		7	Possible roasting
		8	From hearth wall

		9	Adhering slag
		10	No Other Features
F	Fracture	1	Total – all surfaces
		2	Partial – all edges
		3	Minor – old fractures – uncertain
		4	Complete – edges intact
G	Density	1	High
		2	Medium
		3	Light
H	Degree of magnetism	1	High
		2	Medium
		3	Low
		4	None

METALS

Class		**Type**		**Sub-type**	
Symbol	**Description**	**Symbol**	**Description**	**Symbol**	**Description**
M	Metal	***M***	Metallic lumps	***a***	Sub-rounded/rounded/pine-shaped - complete
				b	Lumps
				c	Uncertain
		A	Finished artefact	***g***	Complete
				h	Incomplete
				j	Modern
		S	Scrap	***k***	Archaeological
				l	Modern

VARIANTS AND DESCRIPTORS FOR METALS

Variant	**Descriptors**

Symbol	Description	symbol	description
A	Size	1	Large (>10cm)
		2	Moderate (5-10cm)
		3	Small (2-5cm)
		4	Fragment (<2cm)
B	Magnetism	1	Strong
		2	Moderate
		3	Weak
C	Density	1	High
		2	Medium
		3	Low
D	Colour	1	Black
		2	Grey
		3	Yellow – orange
		4	Brown
		5	red
		6	Purple
		7	Metallic
		8	Grey Blue
E	Inclusions	1	Soil – geological
		2	Charcoal
		3	Hearth remains/Clay
		4	None
F	Impressions	1	Charcoal
		2	Soil – geological
		3	None
G	Shape	1	Sub – rounded – Pine-shaped
		2	Amorphous
		3	Sub – angular
H	Condition	1	Heavily mineralized
		2	Surface rusting/corrosion

APPENDIX A.3.1: DATABASE FOR AUSEWELL WOOD ASSEMBLAGE

- Database excavation season 1999
- Database excavation season 2000

TRENCH	SPIT	SIZE	DESCRIPTION	SYMBOL	N° FRAGMENTS	SUBTYPE	Shape	Overall Size	Thickness	Density	Porosity	Porosity size	Porosity shape	Surface Texture	Colour	Surface impressions	Underside texture	Underside impressions	Inclusions (all surfaces)	Magnetism	Viscosity	Multiple flow episodes	Degree of fracture
PN1																							
	0-20	Small	S	**FTS aP**	**5 fragments**	**a**	A2 (PLATE)	≈ 7x3.5	≈0.5/1.5	D3	E4	F3	G3	H1, H2	I4	J6	K3, K4	L1, L2	M3	N4	O3	P2	Q1
	0-20		S	**FTS b**	**8 fragments**	**b**	A8	≈ 5x2.5		D2	E6			H1	I2, I7	J6	K1	L6	M5	N4	O3	P2	Q1
	0-20		S	**FTS c**	**15 fragments**	**c**	A6	≈ 5x3		D2/D3	E2/E3	F2	G3	H6	I4	J1, J2, J6	K3, K4	L1, L2	M6	N4	O2	P2	Q1
	0-20		S	**HS f**	**9 fragments**	**f**	A6			D4	E3	F2	G3	H6	I2, I7	J6	K7	L6	M3	N4	O5	P2	Q1
	0-20		S	**FTS aC**	**4 pieces**	**a1**	A3, A5	≈ 9x4	≈2/4	D1	E3	F3	G3	H1, H2	I4	J6	K3, K4	L1, L2	M3	N3	O3	P1 ?	Q1
	0-20		M	**FeS**	**5 fragments**	**o**	G1	≈ 3x2		D3					I1 (red stains)	F3			E4	N2			
	0-20		G	**GR**	**8 stones**	**f, h**	A1, A3	B3						D2									
	0-20	Medium	S	**FTS aP**	**1 piece**	**a**	A2 (PLATE)	≈10x8	≈2.5	D3	E3		G5	H6, H13	I4	J6	K3, K4	L1, L2, L3?, L4	M3	N4	O2	P2	Q1
	0-20		S	**FTS aC**	**3 pieces**	**a1**	A3			D1	E4	F2	G3	H1, H2	I2	J6	K2, K3, K5	L1, L2, L4	M2, M3, M4	N5	O3	P2	Q1
	0-20		S	**HS e**	**1 piece**	**e**	A6			D3	E3		G5	H6	I3, I4	J1, J2, J3	K3, K5	L1, L2, L3, L4	M1, M2, M3	N4	O2	P2	Q1

	0-20	Large	S	**FTS aC**	**1 large cake**	**a1**	A3	≈ 20x15	≈ 4	D1	E4	F1	G2	H1, H2	I2, I3	J6	K3	L1, L2, L5	M6	N3	O3	P2	Q1
	0-20	Medium Selected	S	**FTS aC**	**2 pieces**	**a1**	A2, A3		≈ 5	D1, D2	E3, E4	F2	G2, G3	H1, H2, H6	I2 (red, orange stains)	J6	K3, K5	L1, L2	M1, M3, M5	N3, N5	O2, O3	P3, P2	Q1
	0-20		S	**HS e**	**2 lumps + 1 piece with hole**	**e**	A6			D2, D3	E6			H6	I3, I4 (red stains), I5, I7	J2, J4	K3, K7	L1, L2, L3, L4	M1, M2, M3, M4, M5	N4, N1	O2, O5	P2	Q1
	0-20			**SS g**	**1 piece -clay rich**	**g**	A1	9 x 5cm	~ 4cm	D2	E5	F3	G3	H6	I4, I7	J1	K3	L1, L2	M6	N4	O1	P2	Q3
	20-40 U	Small	M	**MS**	**6 fragments**	**k**	G1	A3		C1					D1, D5	F3			E4	B1			
	20-40 U		S	**BF slag l**	**6 fragments**	**l**	A6	≈ 2x1		D4	E5	F4	G3	H8	I6, I9	J6		L6	M5	N4	O2	P2	Q1
	20-40 U		S	**SS h**	**7 fragments**	**h1**	A12	≈ 2x2	0.1/2 ≈	D3	E4	F3	G3	H1	I2	J6	K3	L6	M5	N2	O4	P2	Q1
	20-40 U		S	**HS f**	**30 pieces**	**f**	A6	≈ 2x2		D2	E6			H6, H12	I2, I3	J6	K7	L6	M1, M2	N2	O4	P2	Q1,Q5
	20-40 U		S	**FTS b**	**8 fragments**	**b**	A8	≈ 3x2		D2	E4	F2	G3	H1	I2	J6	K1, K2	L6	M5	N4	O3	P2	Q1
	20-40 U		S	**SR**	**2 pieces**	**n**	A7	≈ 6x3.5	≈ 4	D3	E3	F2	G3	H6	I4	J2 ?	K3	L2 ?	M1, M3	N4	O4	P2	Q1
	20-40 U		S	**FTS aC**	**8 (5 bigger) fragments**	**a**	A2, A3	≈ 6x4/5		D2	E4	F2	G5	H1, H2	I4 (red stains)	J1	K3, K5	L1, L2	M1, M3	N3	O3	P1	Q1

	20-40 U		G	**GR**	**20 river pebbles**	**g, h**	A1	B4		G2, G3				D2	C1, C3, C4					H4			
	20-40 U	Medium	S	**FTS aC**	**1 fragment**	**a**	A3, A5	10x7 ≈	≈ 3/3.5	D1	E4	F2	G2, G3	H1, H2	I4 (red stains)	J6	K3, K5	L2, L4	M1	N4	N3	P1	Q1
	20-40 L (charcoal rich)	Small	S	**FTS c**	**≈ 45% / 34 pieces**	**c**	A6			D2	E4		G5	H1, H2	I2 (red stains)	J1, J2, J5	K3, K5, K7	L1, L2	M1, M2, M3	N3	O3	P2	Q1
	20-40 L (charcoal rich)		S	**SR**	**1 piece**	**m**	A8	4x2.5 x1.5 ≈	1.5 ≈	D2	E3	F3	G3	H6	I4 (a bit red)	J2	K3, K5	L1, L2	M5	N3	O2	P2	Q3
	20-40 L (charcoal rich)		S	**BF slag l**	**4 fragments**	**l**	A6			D4	E5	F4	G3	H8	I9, I10 (+blue)	J6	K7	L6	M5	N4	O2, O1	P2	Q1
	20-40 L (charcoal rich)		S	**Undiagnostic**	**2 fragments**		A6			D4	E2		G5	H6	I1, I2	J6	K7	L6	M5	N4	O4	P2	Q1
	20-40 L (charcoal rich)		G	**GR**	**≈4% rock samples/ 21 stones**	**g, h**	A2, A3	B3		G2, G3				D2, D3	C1, C3, C5					H4			
	20-40 L (charcoal rich)		M	**MS**	**2 fragments**	**k**	G1	A2		C1					D1, D5	F3			E4				
	20-40 L (charcoal rich)		S	**HS f**	**~50% /61 pieces**	**f**	A6			D4	E6			H6	I2, I7	J6	K7	L6	M1, M2, M3, M4, M5	N4	O4	P2	Q1, Q5
QN1																							
	0-20	Small	S	**FTS aC**	**3 fragments**	**a1**	A6			D2			G5	H7	I1, I3, I5	J1, J2	K3	L1, L2	M2, M3	N5	O2	P2	Q1

	0-20		S	**FTS c**	**20 fragments**	**c**	A6			D2	E2	F1, F2	G5	H1, H2	I1, I2	J6	K3	L1, L2	M3	N4	O3	P3	Q1
	0-20		M	**MS**	**1 little piece**	**k**	G1	A3		C3					D1, D6					B1			
	0-20		G	**GR**	**1 small stone**	**f?**	A4	B4		G3					C4								
	0-20	Medium+ Selected Slag	S	**FTS aC**	**13 pieces**	**a1**	A1, A3			D1	E4	F2	G3	H1, H2, H6	I2, I4	J2, J3	K3	L1, L2, L3	M2, M3	N5	O2, O3	P1	Q1
	0-20		S	**FTS aP**	**6 pieces**	**a**	A2 (PLATE)	≈ 8.5x5 x2.5		D1	E4, E5	F2, F3	G3	H1, H2	I1, I4	J6	K3	L1, L2, L3	M3	N4	O2	P3	Q1
	0-20		S	**HS e**	**4 pieces**	**e**	A6			D1	E4	F2	G2	H6	I4, I5	J3	K3	L1, L3	M6	N3	O3	P2	Q1
	0-20	Large	S	**FTS aC**	**2 pieces**	**a1**	A3	≈ 5.5x2 3x6.5		D1	E2, E3	F1, F2	G5	H1, H2	I1, I2 (red stains)	J6	K3	L1, L2	M3	N5	O2, O3	P1	Q2
	0-20		S	**BF slag l**	**1 small fragment**	**l**	A6			D4					I10	J1			M3				
	0-20	Very Large	S	**FTS aC**	**1 big cake**	**a1**	A3	≈ 12x1 3x5	≈ 5	D1	E5	F2	G3	H1, H2	I1, I2, I7	J6	K3, K4	L1, L2, L4, L7	M3, M4	N5	O3	P1	Q3
	20-40	Small	S	**FTS aC**	**4 pieces + 2 fragments**	**a1**	A2, A3	9x5x 3 ≈	3-4 ≈	D2	E4	F2	G3	H1, H2	I2 (red stains)	J4 (clay)	K3	L2	M1	N3	O2	P1	Q2 (round edge visible)
	20-40		S	**FTS b**	**5 pieces**	**b**	A8, A9	3x1x 1.5 ≈	1.5/2 ≈	D3	E4	F4		H1	I2	J6	K3, K5	L2	M5	N3	O3	P2	Q3

	20-40		S	**FTS c**	**27 small fragments**	**c**	A6	bigger ≈6x3		D3	E2	F2	G3, G4	H6, H12	I3, I4	J6	K3, K5	L2, L4	M1	N3	O2	P2	Q1
	20-40		M	**FeS**	**4 pieces**		G1	A3		D1					D1, D5	F3			E4	B1			
	20-40		S	**HS f**	**4 pieces**	**f**	A6			D4	E6			H6	I4, I7	J1	K7		M1, M2, M5	N4	O5		Q1
	20-40		G	**GR**	**6 small stones**	**f, h**	A2, A3	B4		G2, G3					C3, C5, C7								
	20-40	Medium	S	**FTS aC**	**5 pieces**	**a1**	A2, A3	7x4 ≈	4/5 ≈	D1	E4	F2	G3	H1, H2	I2, I4	J6	K3, K5	L1, L2, L5, L7	M1, M4	N3	O3	P1	Q1
	20-40	Large	S	**FTS aC**	**1 cake**	**a1**	A3	≈17.5 x15	≈5	D1	E3	F1, F2	G2, G3	H2	I4, I5		K3	L1, L2, L5	M2	N3	O1	P1	Q3
	20-40	Small Finds	S	**SS j**	**6 fragments**	**j**	A3, A5	≈9x5 x3 / 10x5 ≈	≈3.5/ 4 / ≈ 5/6	D2	E4	F2	G3	H6, H12	I2, I4, I7	J1, J2,J4, J5, J7	K3, K5	L1, L2, L5, L7	M1, M2, M3, M4	N2	O2	P2	Q2 (round edge visible)
	20-40			**SS g**	**1 piece**	**g**	A3			D1	E6			H6	I2, I7	J6	K3	L1, L5	M5	N5	O1	P2	Q1
	20-40		S	**HS f**	**3 fragments**	**f**	A6	6x3.5 ≈		D3	E6			H6	I4, I7				M1, M2, M3, M5	N4	O5	P2	Q1
	20-40		S	**BF slag l**	**2 fragments**	**l**	A6			D4	E6, E2			H8, H6	I6	J6	K7	L6	M1, M3	N4	O1	P2	Q1
	20-40		M	**FeS**	**4 bigger fragments, 2 small**		G1	A2		C1					D1, D5	F1, F2			E1, E2	B1			

	20-40		G	**GR**	**5 small stones**	**f, h**	A3, A4	B4		G3				D3	C3, C4					H4			F3
	20-40		RF	**RF**	**5 fragments**																		
	Spit Unknow	Large	S	**FTSaC**	**1 big cake**	**a1**	A3	25x6 x7.5		D1	E1, E2		G5	H1, H2	I1, I2, I7	J6	K3	L1, L2, L5	M2, M3	N4, N5	O1	P1	Q2
PN1/ QN1																							
	Context 7		S	**BF slag l**	**8 pieces**	**l**	A6			D4	E1	F2	G3	H6	I2 (red stains)	J1	K7		M1	N4	O1	P2	Q1
			S	**BF slag m**	**4 pieces**	**m**	A6			D4	E2	F2	G2, G3	H8	I1, I9	J1	K7		M2	N4	O1	P1 maybe	Q1
			S	**SS j**	**3 fragments**	**j**	A1, A6			D2	E6			H6, H12	I4, I7	J1, J2	K3, K5, K7		M1, M2, M3, M4, M5	N2	O4	P2	Q1
			S	**SS g**	**2 fragments**	**g**	A3 +double cake			D2	E6			H6	I4, I5, I7	J1, J4	K3	L1, L4	M1, M2, M4	N5	O1	P2	Q1
			S	**HS f**	**7 pieces**	**f**	A6			D2	E1	F2	G3	H6	I7	J1	K3	L1	M2, M4, M6 ?	N4	O4	P2	Q1
			S	**FTSc**	**2 small fragments**	**c**	A9			D2	E4	F2	G3	H1, H2	I2	J6	K3	L6	M5	N4	O2	P2	Q1
			M	**FeS**	**2 prills**		G1			C2					I2, I3	F1, F2			E1, E2, E3, E5	B1			
			G	**GR**	**4 stones**	**f, g**	A3	B3		G3				D3						H4			
ZN1																							

	0-20	Small	S	**HS f**	**1 big + 10 fragments**	**f**	A6			D2	E4	F2	G5	H6, H12	I4	J1, J5	K3	L1, L2	M2, M3	N5	O2	P2	Q1
	0-20		S	**SR**	**1 piece**	**m**	A11			D1	E4	F4	G5	H1, H6	I4	J1, J2	K3	L1, L2	M2, M3	N3	O2	P2	Q3
	0-20		S	**Undiagnostic**	**7 fragments**	**v**	A6			D4	E1	F2	G3	H6, H12	I2, I4	J1	K3	L1	M5	N4	O2	P2	Q1
	0-20		M	**FeS**	**2 bigger pieces + 5 fragments**		G1	A2		C1					D1, D6	F3			E4	B1			
	0-20		S	**FTS aC**	**2 fragments of 'cakes'**	**a1**	A2			D2	E2	F1, F2	G5	H3	I4, I5	J6	K3	L1, L2	M3, M4	B5	O2	P3	Q1
	0-20	Medium	S	**FTS aC**	**5 fragments of 'cakes'**	**a1**	A2, A3			D1	E3, E4	F1, F2	G5	H1, H3	I4	J6	K3	L1, L3	M3, M4	N2	O2, O3	P1	Q1
	0-20		S	**SS j**	**4 fragments, 1 elongated**	**j**	A6			D2	E3	F1	G5	H6, H12	I4, I7	J6	K3	L1, L3	M2, M3	N3	O1	P2	Q1
	0-20		M	**FeSl**	**1 piece**		G2	A1		C1					D4, D5	E4		F3		B1			
	0-20	Large	S	**FTS aC**	**1 cake**	**a2**	A2, A3			D2	E4	F2	G5	H1, H13	I4	J5, J7 ?	K3, K5	L1, L2	M2, M3	N4	O3	P1 (some)	Q2
	0-20		S	**HS e**	**1 fan shaped pieces**	**e**	A3			D2	E2	F2	G4	H6, H12	I4, I7	J1, J2	K3, K5	L1, L2,	M2	N4	O1	P2	Q1
	0-20	Small Finds	S/M	**FeS**	**4 pieces**		A6/G1			D2	E7			H6, H12	I4, I5	J1	K7		M1, M2, M3, M4	N2	O5	P2	Q1

	0-20		S	**HS f**	**3 pieces**	**f**	A6 (subrounded)			D3	E7			H6	I4, I7	J1, J2, J4	K7		M1, M2, M3	N4	O5	P2	Q1
	0-20		S	**HS e**	**1 piece**	**e**																	
	0-20		S	**Undiagnostic**	**3 pieces**		A6 (subrounded)			D4	E4	F2	G5	H6	I4, I7	J1	K7		M1, M2	N4	O5	P2	Q1
	0-20		S	**HS d**	**3 pieces**	**d2?**																	
	0-20		S	**SS j**	**1 pieces**	**j**	A2,A6			D2	E2	F1, F2	G5	H6	I2, I4	J1, J2	K3, K5	L1, L2	M1, M2	N4	O1	P2	Q1
	0-20	Selected Medium	S	**HS e**	**2 lumps**	**e**	A3, A6			D2	E2	F1, F2	G5	H6	I3, I4	J1, J2, J5	K3	L1, L2, L3, L5	M2, M3	N4	O1	P2	Q1
	0-20		S	**HS d**	**1 piece**	**d2?**																	
	0-20		S	**SS j**	**1 pieces**	**j**	A2, A5			D2	E3	F1, F2	G3	H6, H7	I4	J4, J5	K3, K5	L2, L4	M1, M2	N3	O3	P2	Q1
	0-20		S	**FTSaC**	**2 fragments**	**a1**	A2			D2	E3	F1, F2	G5	H2, H3	I2, I7	J2	K4, K5	L2	M3	N4	O3	P1	Q1
	0-20			**SR**	**1 fragment**	**m**	A2 (PLATE)			D3	E3	F2		H1, H12	I4, I7	J2 (rust)	K3, K5	L1, L2	M5	N4	O3	P1	Q1
	0-20	Hearth Bottom	S	**HS d**	**3 big pieces**	**d2?**	A3			D2, D3	E1, E2	F1	G5	H6, H12	I2, I4	J1, J3, J4	K3, K5	L1, L2, L3	M2, M3	N4	O1	P2	Q4
	20-40	Small	S	**Undiagnostic**	**8 pieces**		A6 (subrounded)			D4	E1	F3	G3		I2, I6, I9	J6	K7	L6	M5	N4	O4	P2	Q1
	20-40		S/M	**FeS**	**16 fragments**		A6/G1			D2	E7			H6, H12	I4, I5	J1	K7		M1, M2, M3, M4	N2	O5	P2	Q1

	20-40		S	**FTS c**	**3 fragments**	**c**	A2			D2	E3	F1, F2	G5	H2, H3	I2, I7	J2	K4, K5	L2	M3	N4	O3	P1	Q1
	20-40		S	**FTS b**	**5 pieces**	**b**				D2	E4	F3	G3	H4	I4, I7	J1, J2	K5	L1, L2	M5	N4	O3	P1	Q1
	20-40		S	**HS f**	**17 pieces**	**f**	A6 (subrounded)			D3	E7			H6	I2, I4, I7	J6	K7	L6	M1, M2, M3	N4	O5	P1	Q1
	20-40		S	**SS j**	**1 fragment**	**j**	A2			D2	E5				I4	J4, J5	K3, K5	L1, L2	M1, M3	N4	O3	P1	Q1
	20-40		S	**SS h**	**3 pieces**	**h**	A12			D3	E4	F3	G3	H1	I2	J6	K3	L6	M5	N2	O4	P2	Q1
	20-40		G	**GR**	**18 stones**	**h**	A2, A3	B3		G3				D4	C5					H4			F3
	20-40	Medium	S	**FTS aC**	**5 fragments**	**a1**	A2, A6			D2	E3	F1, F2	G4	H1, H2	I4	J6	K3	L1, L2	M1, M2, M3	N4	O3	P1 (some)	Q1
	20-40	Special finds	S/M	**FeS**	**10 pieces**		G1			C1, C2					D4, D5, D6	E2		F1		B2			
	20-40		S	**SS j**	**2 fragments**	**j**	A2, A6			D2	E4	F3	G3	H6	I4, I7	J1, J2, J5	K3	L1, L2	M1, M2, M3	N4	O2	P2	Q1
	20-40		S	**SS g**	**1 piece**	**g**	double cake			D1	E6			H6	I4, I7	J1	K3	L1, L5	M1, M2, M5	N5	O1	P2	Q1
	20-40		S	**HS f**	**4 small fragments**	**f**	A6			D3	E7			H6	I4, I7	INCL	K7	L6	M1, M2, M3, M4	N4	O5	P2	Q1
	20-40		S	**Undiagnostic**	**3 fragments**		A6			D4	E6			H6, H8 - some glassy bits	I1, I4	J6	K7	L1	M2 ?	N4	O2	P2	Q1
	20-40		RF	**RF**	**1 White clay**																		

	40-60/below 40	Large	S	**HS d**	**1 piece**	**d2?**	A3			D2	E3	F1,F2	G2,G3	H6	I1, I4	J1, J3, J4	K3	L2	M2, M3	N4	O1	P2	Q2
JN9																							
	0-20	Small	S	**SR**	**4 fragments**	**m**	A7			D3	E7 (hollow)			H6, H12	I4, I5	J2, J5	K3	L2	M5	N4	O2	P1	Q1
	0-20		S	**SS h**	**3 flakes**	**h**	A12		1 cm~	D3	E3	F4	G3	H1	I2, I4	J6	K5	L6	M5	N4	O2	P1	Q1
	0-20		S	**FTS b**	**9 fragments**	**b**	A8, A9			D3	E6			H1	I2, I4	J6	K5	L2	M5	N4	O3	P1	Q1
	0-20		S	**HS f**	**10 fragments**	**f**	A6			D4	E6			H6	I4, I7	J1, J4	K7		M1, M2	N4	O5	P1	Q1
	0-20		S	**Undiagnostic**	**2 fragments**		A6			D4	E6			H6, H11 ?	I2				M1, M2, M3	N4	O5	P1	Q1
	0-20		S	**FTS c**	**4 fragments**	**c**	A6			D2	E4	F3	G3	H1, H6	I2, I4	J2, J7 ?	K3, K5	L1, L2, L5	M2, M3	N4	O2, O3	P2 (SOME)	Q1
	0-20		M	**FeS**	**6 rounded pieces**		G1	A3		C1						F1, F2			E1, E3	N1			
	0-20		G	**GR**	**11 stones**	**f/h**	E2, E3	B3		C3, C5, C10													
	0-20	Medium	S	**FTS aP**	**4 pieces**	**a**	A2 (PLATE)		1.5/2.5 cm~	D2	E2	F1, F2	G3	H2	I2, I4	J6	K5	L1, L2	M3	N4	O1	P2 (SOME)	Q1
	0-20		S	**FTS aC**	**2 fragments**	**a1**	A1, A6			D3	E2	F2	G3	H2, H6	I4, I5	J2, J7	K3, K5	L1, L2, L5	M3	N4	O2	P1	Q1
	0-20		S	**SS g**	**1 piece**	**g**	A5			D2	E5	F3	G3	H6, H12	I4, I5	J1, J2, J5, J7	K3, K5	L1, L2	M2, M3	N4	O1	P1	Q1

	0-20	Special Finds	S	**SS j**	**3 fragments**	**j**	A2, A3			D2	E2		G5	H6	I4, I7	J1, J2, J4	K3, K5	L1, L2	M1, M2	N4	O3	P1	Q1
	0-20		S	**SR**	**2 pieces**	**m**	A7			D3	E7			H6, H12	I4, I7	J4	K3, K5	L2	M5	N4	O3	P1	Q1
	0-20		S	**Undiagnostic**	**3 fragments**		A6			D3, D4	E2, E3	F2, F3	G3	H6, H11	I2, I4	J1, J2	K3	L1, L2	M2, M3	N4	O1	P1	Q1
	0-20		S/M	**FeS**	**9 balls**		A6/G1			D1/C1	E7			H6, H12	I4, I5, I7	J1, J4, J5	K7		M1, M2, M3, M4	N1, N2	O5	P1	Q1
	0-20		G	**GR**	**1 stone**	**e**																	
	0-20		RF	**RF**	**5 pieces**																		
	0-20		S	**FTSaC**	**2 elongated pieces**	**a1**	A11			D1	E5	F4	G4	H2, H6, H12	I4, I5	J1, J4, J7	K3, K5	L1, L2	M1, M2, M4	N1	O2	P2	Q1
	0-20		S/RF	**HS f**	**7 fragments**	**f**	A6			D3	E7			H6, H12	I4, I5, I7					N4	O5	P1	Q1
	0-20		M	**MS**	**2 fragments**	**k**																	
	0-20 Upper	Mixed Slag	S	**Undiagnostic**	**1 fragment**		A6			D4	E3	F3	G3	H6, H8	I2, I10	J6	K7	L6	M5	N4	O1	P1	Q1
	0-20 Upper		S	**HS d**	**2 pieces**	**d2?**	A2, A3			D1	E4	F2	G3	H6, H12	I4, I5	J1, J7	K3, K5	L1, L5	M2, M3	N5	O1, O2	P1	Q1
	0-20 Lower	Slag Only	S	**HS d**	**3 pieces**	**d2?**	A6	19x16 cm		D1	E2	F2	G3	H1 (Some flow), H6	I4	J6	K4, K5	L1, L2	M2, M3	N4	O2	P1	Q1
	0-20 Lower		S	**FTSaC**	**1 piece**	**a2**	A6			D2	E7			H6, H12	I4, I5	J1, J3			M1, M2, M3, M4	N5	O2	P1	Q1

	0-20 Lower		S	**HS e**	**5 pieces**	**e**	A9			D3	E2	F2	G3	H2	I4	J5 ?	K5	L2	M5	N4	O3	P1	Q1
	0-20 Lower		S	**FTS b**	**3 fragments**	**b**	A6			D3	E2	F1, F2	G5	H2, H7	I4	J1, J2	K5	L1, L2	M3	N4	O3	P2 (SOME)	Q1
	0-20 Lower		S	**FTS c**	**4 fragments**	**c**	A7			D2	E3, E4	F3	G3	H6, H12	I4	J6	see notes	L2	M3	N4	O2	P1	Q1
	0-20 Lower		S	**SR**	**2 pieces**	**m**	A6			D1	E2	F2	G3	H1, H6	I2, I4	J2	K3	L1, L2	M6	N4	O2	P1	Q1
	0-20 Lower		S/G	**GR**	**1 stone**	**h**	G1			C1					D4, D6					B1			
	0-20 Lower		M	**FeS**	**1 piece**		A2 (PLATE)		1 cm ~	D2, D4	E6, E7			H6,H12, H13	I2, I3, I4, I7	J1, J4, J7 (red layer)	K3	L1, L2	M2, M3	N4	O1	P1	Q1
	0-20 Lower		S	**SS j**	**2 fragments**	**j**																	
	0-20 Lower		S	**Undiagnostic**	**5 fragments**		A6			D3	E6			H6, H12	I4, I7	J1, J2, J4	K3, K5	L1, L2	M1, M2, M3, M5	N4	O1	P2	Q3
	Upper + Lower	Specials	RF/MIX	**HS f**	**6 pieces**	**f**	A6			D1				H6, H12	I4, I5, I7					N1			
	Upper + Lower		M/S	**FeS**	**3 pieces**																		

	Upper + Lower		RF	**RF**	**1 piece**		A12			D2, D3	E3, E5			H1, H6	I2, I4					N2			
	40-60	Small	S	**SS h**	**16 pieces**	**h**	A7			D3	hollow, some big ones			H6, H9 ?	I4				M1, M2	N4			
	40-60		S	**SR**	**2 pieces**	**m**	A2 (PLATE)			D3	E3	F2	G3	H1	I2, I4	J6	K5	L1, L2	M5	N4	O2	P1	Q1
	40-60		S	**FTS aP**	**5 pieces**	**a**	A6			D4				H6	I2, I4	see notes			M1, M2, M3	N4	O5	P2	Q1
	40-60		S/MIX	**HS f**	**11 small fragments**	**f**	G1			C1					D1, D4				E3	B1			
	40-60		M	**FeS**	**10 balls**		A6			D3	E2		G5	H1	I2				M1	N4	O3	P2	Q1
	40-60		S	**FTS c**	**5 small fragments**	**c**																	
	40-60		RF	**RF**	**5 pieces**																		
	40-60		G	**GR**	**15 stones**	**h**	A2 (PLATE)		2.5 cm ~	D1	E1	F1, F2	G5	H2, H3	I4, I7	J6	K3, K5	L1, L2	M2, M3	N4	O2	P1	Q1
	40-60	Medium	S	**FTS aP**	**2 plates**	**a**	A6 (+ one A2)		1.5 cm ~	D1	E6			H6, H12	I4, I5, I7	J1, J4	K3, K5	L1, L2	M2, M3	N1	O3	P1	Q1
	40-60		S	**HS e**	**5 pieces**	**e (+ 1 plate)**	A1			D2	E4	F4	G3	H6	I4, I5	J1, J3, J4	K4, K5	L1, L2	M1, M2, M3	N1	O3	P1	Q1
	40-60	Selected Medium	S	**HS e**	**1 flat underside piece**	**e**	A6 - cone shaped			D2	E6			H6, H12	I4, I5	J3 see notes			M1, M2, M3, M4	N1	O4	P1	Q1

	40-60	Large	S	**HS e**	**3 pieces**	**e**	A5	~10 x 11 cm	~ 12 cm	D1	E6			H6, H12	I4, I5	J1	K3	L1, L2	M1, M2, M3, M4, M5	N5	O1	P2	Q3
	40-60		S	**HS d**	**1 piece**	**d2?**	A12			D4	E7			H6	I1, I2	J6	K1, K4	L6	M1 (clay attach)	N4 (CHECK)	O3	P1	Q1
	40-60	Special Finds	S	**SS h**	**9 pieces**	**h**	A6			D3, D4	E3	F3	G3	H6	I2, I4	J1, J4	K7		M1, M2	N5	O1, O2	P1	Q1
	40-60		S	**HS f**	**10 pieces**	**f**	A11 ?			D2	E6			H6, H12	I4, I5	J1, J2, J4	K3, K5	L1, L4, L5	M1, M2, M3	N5	O2	P1	Q4
	40-60		S	**SR**	**1 piece**	**m**	A6, A9			D1	E5	F4	G3	H1, H4	I2, I8	J6	K2	L6	M1, M2	N4	O3	P2 (some)	Q1
	40-60		S	**FTS c**	**8 fragments**	**c**																	
	40-60		S	**FTS b**	**2 fragments**	**b**	A3	B3		G2, G3				D3	C3, C4, C10					H4			
	40-60		G/mix	**GR**	**3 stones**	**f**																	
	40-60		RF	**RF**	**1 piece**																		
ZS3																							
	0-20	Small	S	**HS f**	**4 fragments**	**f**	A6			D2	E3		G5	H1, H6	I4	J6	K3, K5	L1, L2	M2, M3	N4	O2	P1	Q1
	0-20		S	**BF Slag l**	**1 small fragment**	**l**	A6	~ 3cm		D4	E6			H8	I10	J6	K7			N4	O3	P2	Q1

	0-20		M	**FeS**	**6 balls**		G1	A2		C1					D4, D6	F1, F2			E1, E2, E3	B1			
	0-20	Medium	S	**FTSaC**	**2 pieces**	**a2**	A3			D3	E6			H6	I4, I5	J1, J3, J4	K3, K5	L1, L2	M2, M3	N4	O2	P1	Q1
	0-20		S	**FTSaC**	**1 piece**	**a1**	A2 (CAKE)			D1	E2	F2	G3	H2, H3	I2, I4	J6	K3, K5	L1, L2	M2, M3	N4	O3	P2	Q1
	0-20		S	**HS d**	**1 piece**	**d2?**	A5		7-8cm~	D1	E2		G5	H6, H12	I4, I7	J1, J3, J4	K3, K5	L2	M2, M3	N4	O1	P1	Q1
	0-20	Selected Medium	S	**FTSaC**	**1 piece**	**a2**	A6			D2	E6			H6, H12	I4, I5, I7	J1, J4	K3, K5	L1, L2	M2	N4	O2	P1	Q1
	20-40	Small	S/MIX	**HS f**	**11 fragments**	**f**	A6			D3	E7			H6, H12	I4, I5, I7	J1, J2, J7	K7		M1, M2, M3, M4	N4	O5	P1	Q1
	20-40		S	**FTSc**	**3 fragments**	**c**																	
	20-40		S	**Undiagnostic**	**3 fragments**																		
	20-40	Medium	S	**FTSaC**	**8 pieces**	**a1**	A2, A3		2 cm ~	D1	E2	F1, F2	G5	H1, H3	I2, I4	J6	K3, K5	L1, L2	M2, M3	N4	O3	P2 (SOME)	Q1
	20-40	Large/Selected pieces	S	**FTSaC**	**6 big pieces**	**a1**	A3	21-23 cm by 12-16 cm	3-4 cm ~	D2	E2	F1, F2	G5	H2, H3	I4, I7	J1, J7	K3, K5	L1, L2, L5	M1, M2, M3	N4	O2, O3	P2	Q1
	20-40		S	**FTSaC**	**1 piece**	**a2**																	
	20-40		S	**FTSc**	**1 piece**	**c**	A3		~ 9 cm	D2	E2		G5	H2	I4, I7	J6	K3, K5	L1, L2, L5 ?	M5	N4	O3	P2	Q1
	20-40		S	**HS e**	**3 fragments**	**e**	A5 (thin)	~ 14 cm long		D3	E6			H1	I4		K3, K5	L1, L2	M1	N4	O2	P2	Q1

	20-40		S	**HS d**	**1 piece**	**d2?**	A1, A2			D1, D2	E3	F2	G3	H6	I4, I5, I7	J2, J3, J4	K3, K5	L6	M1, M2, M4	N4	O1	P2	Q1
	40-60	Small	S	**FTS aC**	**3 fragments**	**a**	A3, A5	~ 11x14 (big)	~ 10 cm (big)	D1	E4	F2	G3	H6, H12	I4, I7	J1	K3	L1, L2, L7	M1, M2, M3	N5	O1	P2	Q1
	40-60		S	**SR**	**2 fragments**	**m**	A3			D2	E4	F3	G3	H1, H2	I4	J5	K3, K5	L2	M2, M3	N4	O3	P2	Q1
	40-60		S/M	**FeS**	**13 fragments**		A2		0.8-1 cm ~	D3	E4	F3	G3	H6, H12	I4, I7	J6	K3	L6	M5	N4	O3	P1	Q1
	40-60		S	**Undiagnostic**	**1 small fragment**		A6	A2 (for metals)		D2	E6			H6, H12	I4, I5, I7	J1, J2, J4, J5, J7	K7		M1, M2, M3, M4	N1	O5	P1	Q1
	40-60		S	**HS f**	**5 pieces**	**f**	A6	3 cm x 2 cm~		D4	E2	F3	G3	H6	I1, I4	J1	K7		M2	N4	O1	P1	Q1
	40-60		S	**SS j**	**1 piece**	**j?**	A6			D2	E6			H6, H12	I4, I7	J1, J5	K7		M2, M3	N4	O2	P1	Q1
	40-60		RF	**RF**	**7 pieces**		A2		~ 1.5 cm	D2	E4	F3	G3	H6	I4, I7	J1	K3, K5	L1	M3	N4	O1	P1	Q1
	40-60	Medium	S	**FTS aC**	**5 fragments**	**a1**	A3	B4		G3				E3	C3, C5, C10					H4			
	40-60		S	**HS d**	**2 cakes**	**d2?**	A2, A3			D2	E3		G5	H1, H2, H3	I4, I5	J6	K3, K5	L2	M1, M2, M3, M4	N5	O1	P2 (SOME)	Q1
	40-60		S	**HS e**	**2 lumps**	**e**	A3, A6			D1	E6			H6, H12	I4, I5, I7	J1, J2, J3, J7	K3, K5	L1, L2, L3, L5	M1, M2, M3, M4	N5	O2	P2	Q1
	40-60	Selected Medium	S	**HS f**	**4 pieces**	**f**	A6	long lump ~20 cm		D2	E6			H6, H12	I4, I5, I7	J1, J4	K3	L4, L5, L7	M1, M4, M5	N5	O2	P2	Q1

	40-60		S	**HS e**	**2 pieces**	**e**	A6			D2	E4, E6			H6, H12	I4, I5, I7	J1, J4	K7		M1, M2, M3, M4	N5	O4, O5	P1	Q1
	40-60		M	**MS**	**2 pieces**	**k**	A1 (cake) + fan shaped			D2	E6			H6, H12	I4, I5, I7	J1, J2	K3, K5	L1, L2	M1, M2, M4, M5	N4	O1, O3	P2	Q3
	40-60	Special Finds	S	**HS d**	**1 piece**	**d2?**	G2	A1		C1					D3, D6	F1, F2 (a bit on outer surface)			E1, E2, E3	B1			
	40-60		S	**HS e**	**1 lump**	**e**	A3	~ 15 x7cm		D1	E4	F2	G3	H6	I1, I4	J1	K3	L2, L5, L7	M1, M5	N5	O2	P2	Q3
	40-60		S	**HS f**	**4 pieces**	**f**	A6			D2	E6			H6, H12	I4, I5	J1, J2	K3, K5	L1, L2	M2, M4	N5	O2	P2	Q3
	40-60		S	**FTS c**	**2 pieces**	**c**	A6			D3	E6			H6	I4, I7	J1, J4	K3, K7		M1, M2	N4	O1	P2	Q1
	40-60		S/M	**FeS**	**3 fragments**		A6			D3	E3	F2	G3	H1	I2	J2, J4	K7		M3	N4	O3	P2	Q1
	40-60	Large	S	**HS d**	**2 pieces**	**d2?**	A6	~3/4cm		D1	E6			H6, H12	I4, I5	J1	K3, K7	L1, L2	M1, M2	N2	O4	P2	Q1
	40-60		S	**FTS aC**	**1 piece**	**a2**	A3~			D1	E6			H6, H12	I4, I5, I7	J1, J2, J3, J4, J5, J7	K3	L1, L2	M1, M2, M3, M4 + BF slag	N4	O1	P1	Q1

TRENCH	SPIT	SIZE	DESCRIPTION	SYMBOL	N° FRAGMENTS	SUBTYPE	Shape	Overall Size	Thickness	Density	Porosity	Porosity size	Porosity shape	Surface Texture	Colour	Surface impressions	Underside texture	Underside impressions	Inclusions (all surfaces)	Magnetism	Viscosity	Multiple flow episodes	Degree of fracture
LS1																							
	0-20	Large	S	**FTS aC**	**1 piece**	**a2**	A3	~ 20 x 13 cm		D1	E4	F2	G2, G3	H3, H6	I4	J6	K3	L1, L2	M1	N5	O2	P2	Q3
	0-20	Small	S	**HS d**	**3 fragments**	**d2?**	A3, A6			D1	E4	F2	G2, G4	H3, H7	I5	J7	K4	L1, L3	M3 (in section)	N5	O2	P2	Q1
	0-20	Small	S	**SS h**	**4 pieces**	**h**	A12	~ 2 cm		D4	E5	F4	G3	H1	I4	J6	K7	L6	M6	N3	O5	P2	Q1
SS1																							
	0-20	Small	S	**SS g**	**1 piece**	**g**	A5	~ 7 x 8	~ 1cm	D3	E6			H6	I4	J6	K3	L1, L2	M6	N3	O3	P2	Q3
	0-20		S	**SR**	**1 piece**	**n**	A7	~ 10 long		D3	E4 (hollow)	F2	G5	H6, H12	I4	J1	K3	L1, L2	M6	N4	O2	P2	Q4
	0-20		S	**FeS**	**4 fragments**		A6			D2	E6			H6, H12	I1, I5	J7	K7	L6	M4, M5	N1	O4	P2	Q1
	20-40	Small	S	**SR**	**10 pieces**	**n**	A7	~ 5 long		D3	E6 (hollow)			H6	I4	J1	K3	L1, L2	M1	N4	O2	P2	Q1
	20-40		S	**FTS c**	**1 small fragment**	**c**	A6			D3	E1	F2	G3	H7	I1			K7	M3	N4	O4	P2	Q1
	20-40		S - mix	**HS f**	**10 pieces**	**f**	A6			D3	E6			H6	I4, I7			K7	M1, M2, M5	N4	O5	P2	Q1
	20-40		MS	**FeS**	**13 frag**		A6			D2	E6			H6, H12	I1, I5	J3	K3	L6	M6	N1	O3	P2	Q1

					ments																	
	20-40			**Undiagnostic**	**8 fragments**		A6			D4	E6			H6	I6				M5?	N4	O5	P2	Q1
	20-40		G	**GR**	**9 stones**	**e, h**	A2, A3	B3		G3				D3, D4	C3, C5, C10	E9				H4			
	20-40	Medium	S	**HS e**	**5 pieces**	**e**	A6			D2	E6			H6	I4, I7	J1, J4, J7	K3	L1, L2	M1, M2 , M5	N4	O2, O3	P2	Q3
	20-40		S	**SS j**	**2 pieces**	**j**	A3			D2	E2	F1	G5	H3, H6	I4	J6	K3	L1, L2	M3	N4	O3	P2	Q1
	20-40			**SS g**	**1 piece**	**g**	A6			D2	E6			H6	I4, I7	J1, J4, J7	K3	L1, L2, L5	M1, M5	N4	O1	P2	Q3
	20-40		S	**HS d**	**1 piece**	**d2?**	A1	~ 15 x 6 (lump)		D1	E5	F4	G3	H3, H12	I3, I4, I7	J1, J2	K3	L1, L2	M1, M2 , M5	N4	O3	P2	Q1
	20-40		S	**FTS aC**	**1 piece**	**a2**																	
	20-40		M	**MS**	**1 piece**	**k**	G1	~ 9 x 2.5/A2		C1					D4	F2		F2	E4	B1			
	20-40		G	**GR**	**2 stones**																		
	20-40	Large	S	**HS d**	**3 pieces**	**d2?**	A3	~ 25 x 10cm		D1	E3	F2	G3	H6, H12	I1, I4, I7	J1, J7	K1, K3	L2, L5	M1, M2, M5	N5	O3	P2	Q4
RS1																							
	0-20	Medium	S	**SR**	**3 pieces**	**n**	A11			D2	E6 (hollow)			H1, H6	I4	J1, J2	K3	L1, L2	M2, M3	N4	O3	P2	Q3
	0-20	Small	S	**FTS c**	**5 fragments**	**c**	A6			D3	E6			H1, H4	I2	J2	K3, K7	L2	M3	N4	O3	P2	Q1
	0-20	Small	RF	**RF**	**2 pieces**			N2						C3		E2			M1				
	0-20	Small	M	**MS**	**4 pieces**	**k**	G2, Rectan.	A3	~ 3cm recta	C1					D4, D6	F1, F2			E1, E2	B1			

									ng piece													
	0-20	Small		**Undiagnostic**	**2 small fragments**																	
	20-40	Large	S	**HS d**	**2 pieces**	**d2?**	A3, A5	~7 x 11	~ 8 cm	D1	E5	F4	G3	H6	I3, I4	J1	K3	L1, L2	M2	N4	O1	P2	Q3
	20-40	Large		**HS e**	**1 piece**	**e**	A5		~ 8 cm	D2	E6			H6, H12	I4, I5, I7	J4	K5	L4	M1, M2, M5	N4	O1	P2	Q2
	20-40	Small Finds	S	**SS j**	**3 pieces**	**j**	A2			D2	E2	F1, F2	G3	H6	I4, I7	J1	K3	L1, L2	M1, M2, M3	N4	O1	P2	Q1
	20-40	small	S	**Undiagnostic**	**4 small fragments**																		
	20-40	Large	S	**HS d**	**1 piece**	**d2?**	A1	~ 15 x6		D2	E6			H6, H12	I4, I5	J1, J2	K3, K5	L1, L2	M2, M3, M5	N4	O1	P2	Q2
	20-40	small	S	**HS f**	**13 pieces**	**f**	A6	~ 4/5 cm		D3	E6				I4, I7				M1, M2, M3, M5	N4	O5	P2	Q3
	20-40	medium	S	**SR**	**1 piece**	**n**	A11	~ 10 long		D3	E6			H1, H6	I4	J2	K3	L1, L2		N4	O2, O3	P2	Q3
	20-40	small	RF	**RF**	**17 pieces**			N2															
	20-40	small	MS	**FeS**	**5 pieces**																		
	20-40	small	M	**MS**	**1 piece**	**k**	Elongated	A2		C1					D1, D4					B1			
	20-40	small	G	**GR**	**2 stones**	**g**	A2	B3		G2				D3	C1, C5	E9				H4			F1
	D	large	S	**HS d**	**1 piece**	**d2?**	A5	~ 15 x 9		D1	E4	F2	G3	H6	I4, I7	J2	K3, K5	L1, L2	M1, M2, M3	N4	O1	P2	Q3
Letters given during	**C**	large	S	**HS e**	**1 piece**	**e**	A2	~ 20 x 8		D2	E5	F3	G3	H3, H6	I4, I7	J1, J2, J3	K3	L1, L2	M1, M2, M3	N4	O2	P2	Q3

excavation																						
	J	large	S	**HS d**	**1 piece**	**d2?**			~6 cm													
	G+K	large/ medium	S	**SS g**	**2 pieces**	**g**	A5	~ 20 x 8	~ 4/6 cm	D1	E5	F3	G3	H6	I2, I4, I7	J1, J2	K3, K5	L1, L2	M1, M2, M3	N5	O2	P2	Q4
	E + J	small	S	**HS f**	**4 pieces**	**f**	A6			D2	E6			H6, H12	I1, I3, I4, I7	J1, J2	K3, K5	L1, L2	M1, M2, M3	N5	O1	P2	Q1
	F	**small**	RF	**RF**	**4 pieces**			N2						C3					D1, D4				
		small	G	**GR**	**3 stones**	**e (1), g (2)**	A2	B3		G3				D3	C5					H4			

APPENDIX A.3.2: APPENDIX WITH CHARTS ELABORATED DURING THE MACRO-MORPHOLOGICAL ANALYSIS OF THE ASSEMBLAGE

Trench PN1

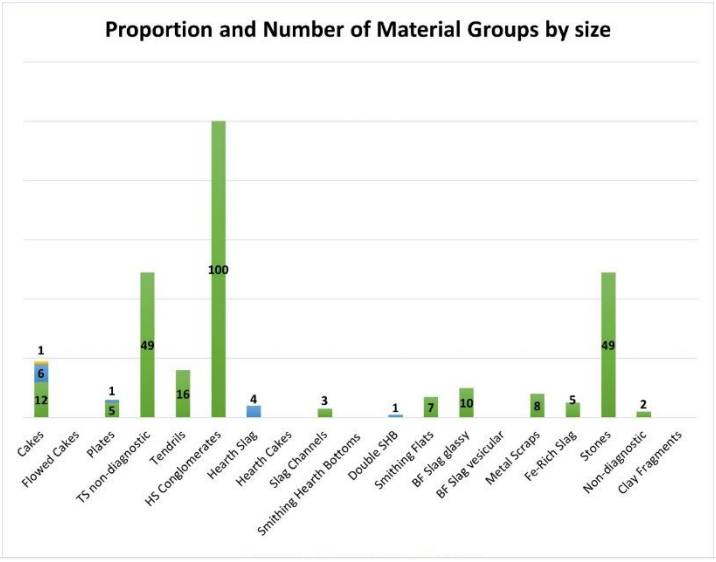

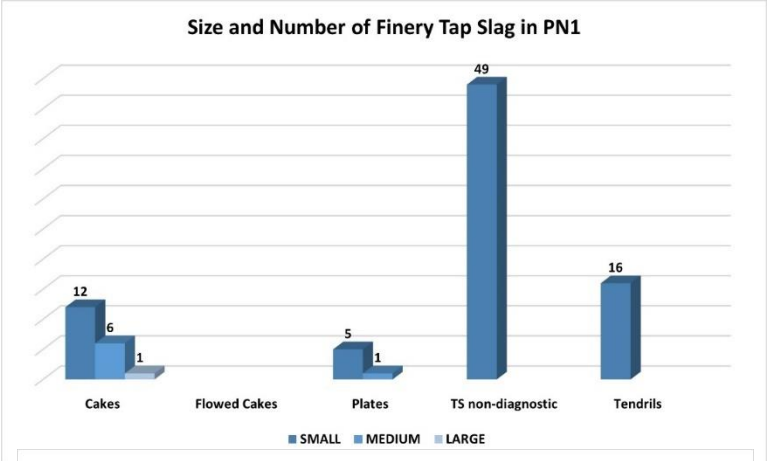

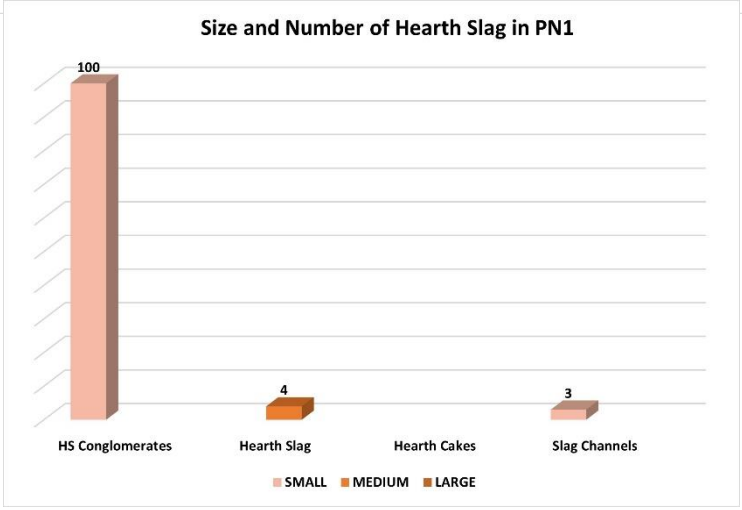

TRENCH QN1

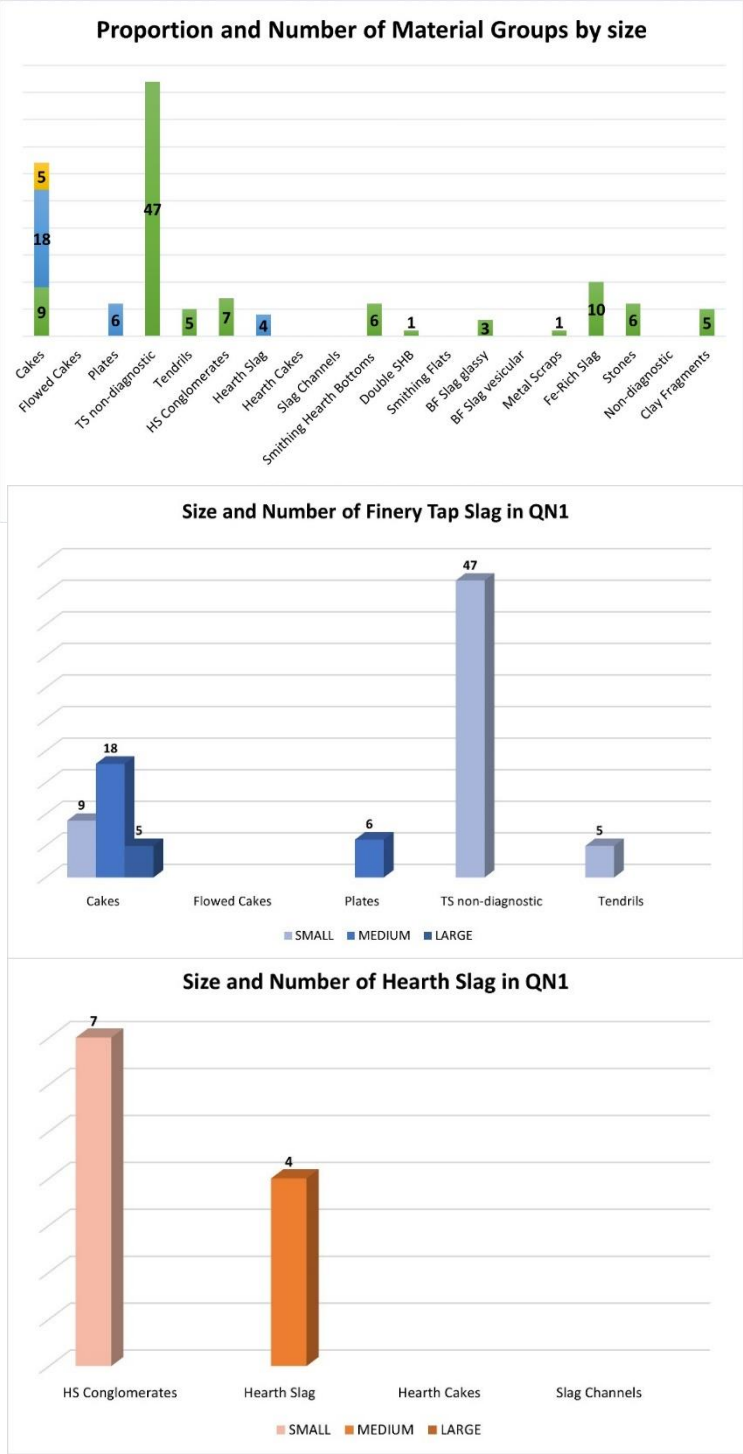
Proportion and Number of Material Groups by size
5
18
9
6
47
5
7
4
6
1
3
1
10
6
5
Cakes
Flowed Cakes
Plates
TS non-diagnostic
Tendrils
HS Conglomerates
Hearth Slag
Hearth Cakes
Slag Channels
Smithing Hearth Bottoms
Double SHB
Smithing Flats
BF Slag glassy
BF Slag vesicular
Metal Scraps
Fe-Rich Slag
Stones
Non-diagnostic
Clay Fragments
Size and Number of Finery Tap Slag in QN1
9
18
5
6
47
5
Cakes
Flowed Cakes
Plates
TS non-diagnostic
Tendrils
SMALL
MEDIUM
LARGE
Size and Number of Hearth Slag in QN1
7
4
HS Conglomerates
Hearth Slag
Hearth Cakes
Slag Channels
SMALL
MEDIUM
LARGE

Trench PN1/QN1

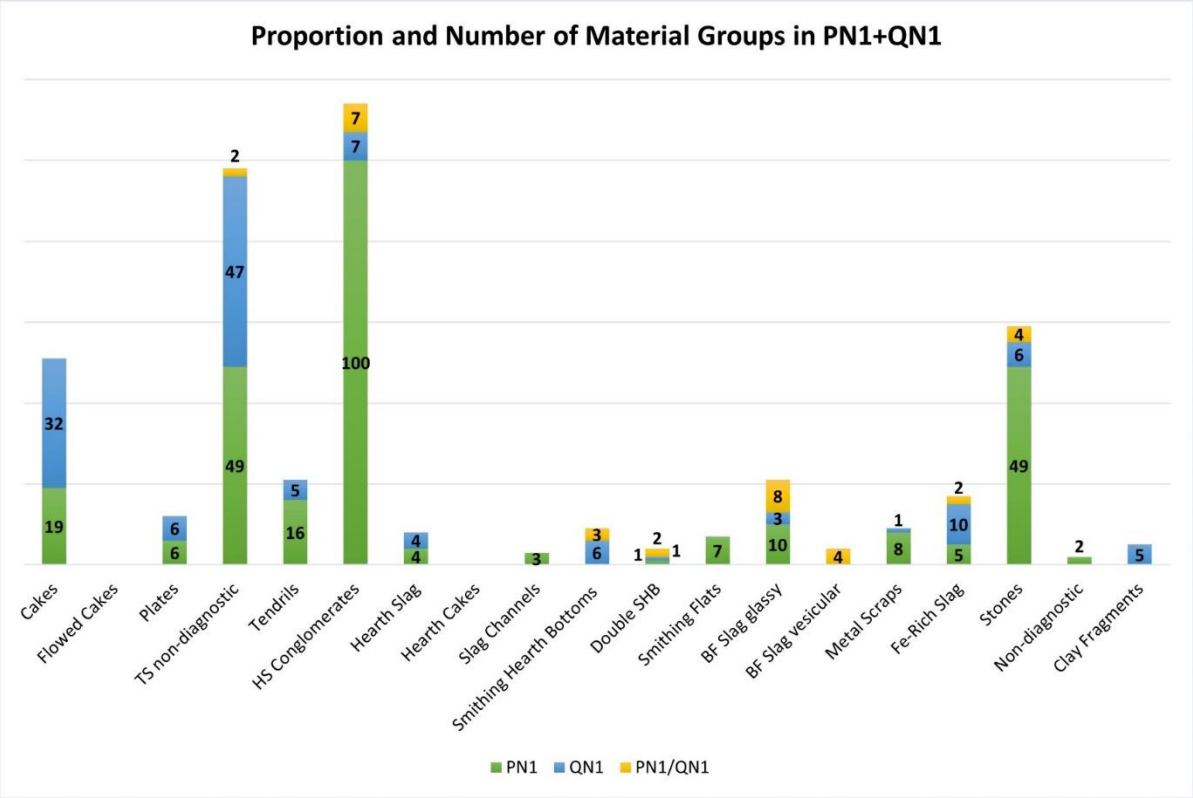

TRENCH ZN1

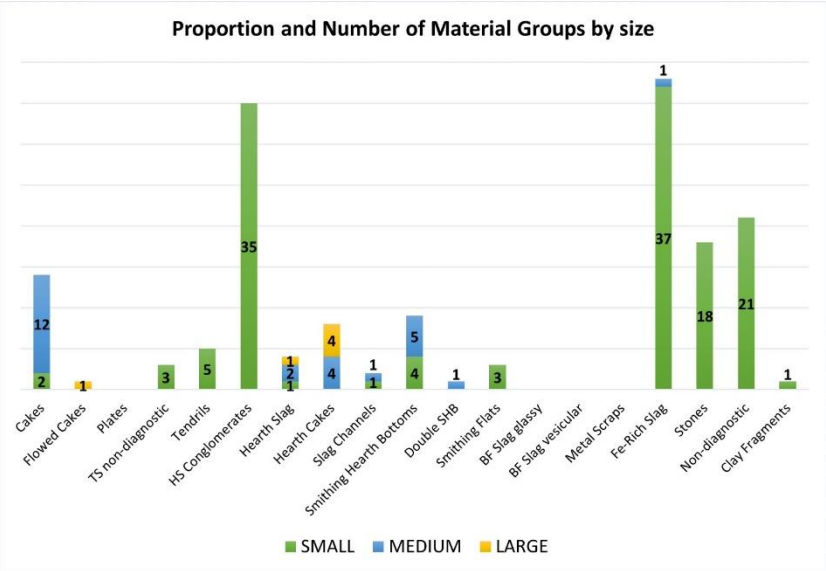
Proportion and Number of Material Groups by size
Cakes
Flowed Cakes
Plates
TS non-diagnostic
Tendrils
HS Conglomerates
Hearth Slag
Hearth Cakes
Slag Channels
Smithing Hearth Bottoms
Double SHB
Smithing Flats
BF Slag glassy
BF Slag vesicular
Metal Scraps
Fe-Rich Slag
Stones
Non-diagnostic
Clay Fragments
SMALL
MEDIUM
LARGE

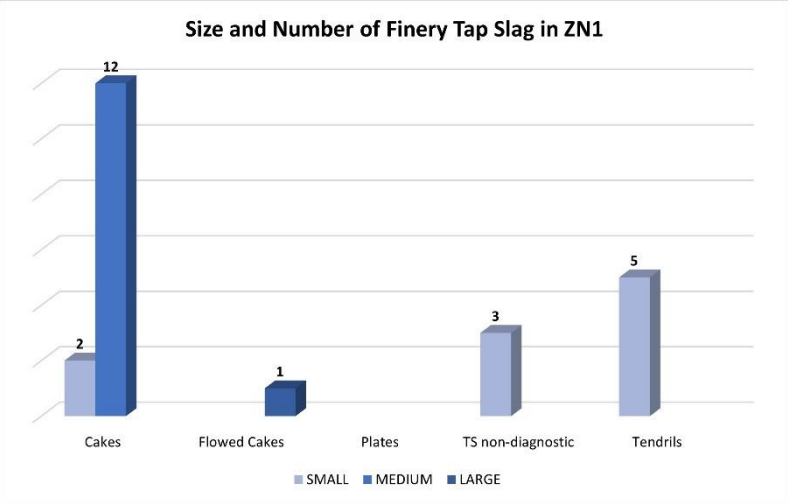
Size and Number of Finery Tap Slag in ZN1
Cakes
Flowed Cakes
Plates
TS non-diagnostic
Tendrils
SMALL
MEDIUM
LARGE

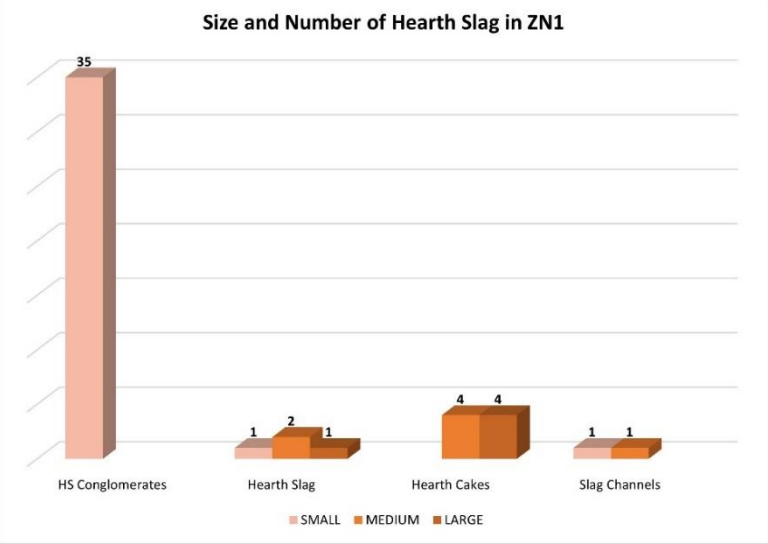
Size and Number of Hearth Slag in ZN1
HS Conglomerates
Hearth Slag
Hearth Cakes
Slag Channels
SMALL
MEDIUM
LARGE

TRENCH ZS3

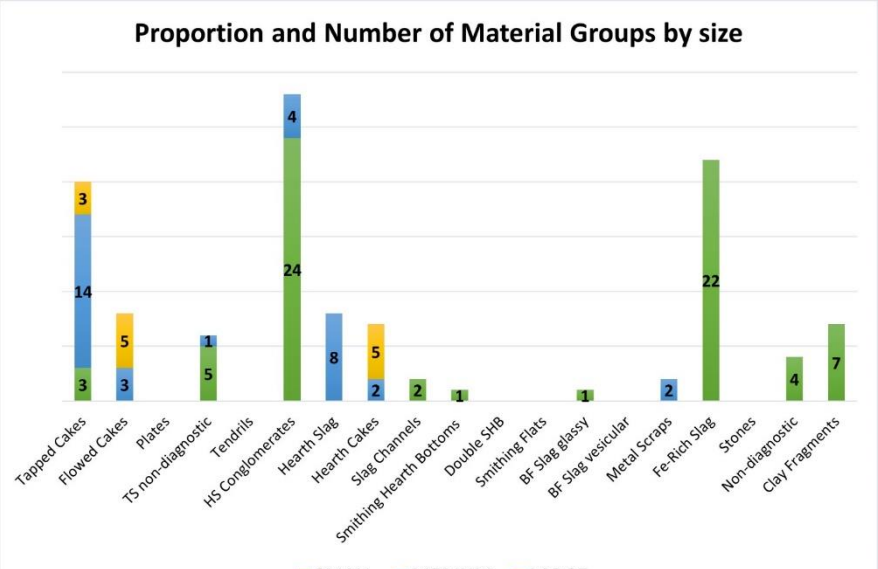
Proportion and Number of Material Groups by size
Tapped Cakes
Flowed Cakes
Plates
TS non-diagnostic
Tendrils
HS Conglomerates
Hearth Slag
Hearth Cakes
Slag Channels
Smithing Hearth Bottoms
Double SHB
Smithing Flats
BF Slag glassy
BF Slag vesicular
Metal Scraps
Fe-Rich Slag
Stones
Non-diagnostic
Clay Fragments

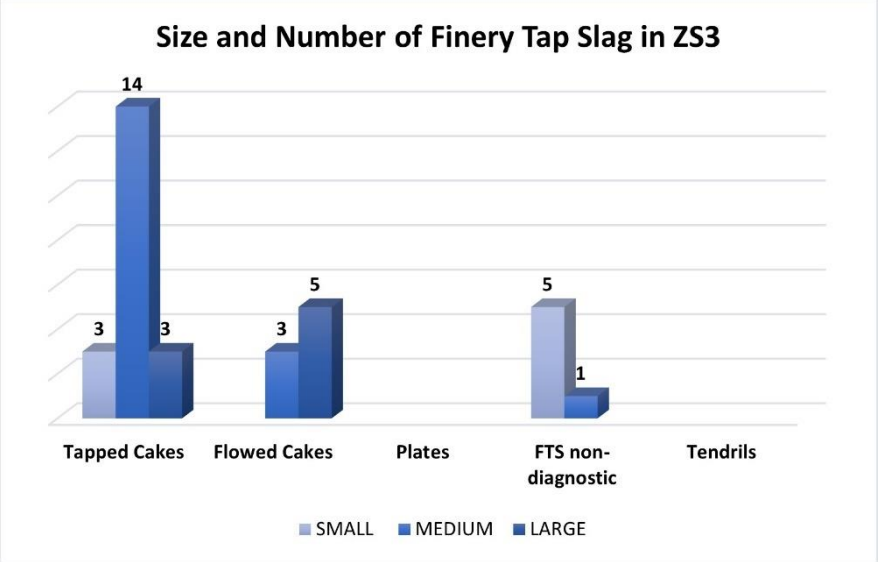
Size and Number of Finery Tap Slag in ZS3
Tapped Cakes
Flowed Cakes
Plates
FTS non-diagnostic
Tendrils
SMALL
MEDIUM
LARGE

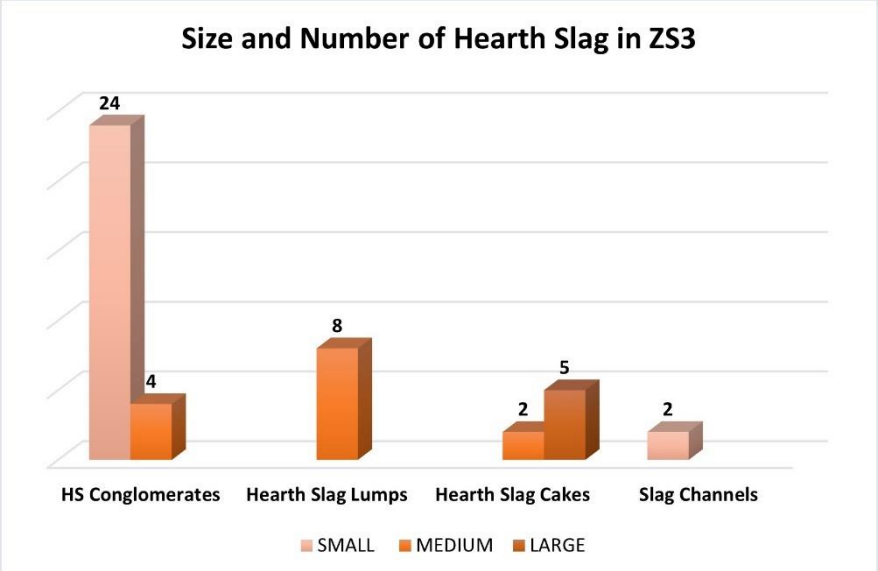
Size and Number of Hearth Slag in ZS3
HS Conglomerates
Hearth Slag Lumps
Hearth Slag Cakes
Slag Channels
SMALL
MEDIUM
LARGE

TRENCH SS1 and RS1 – Charts with all materials by size

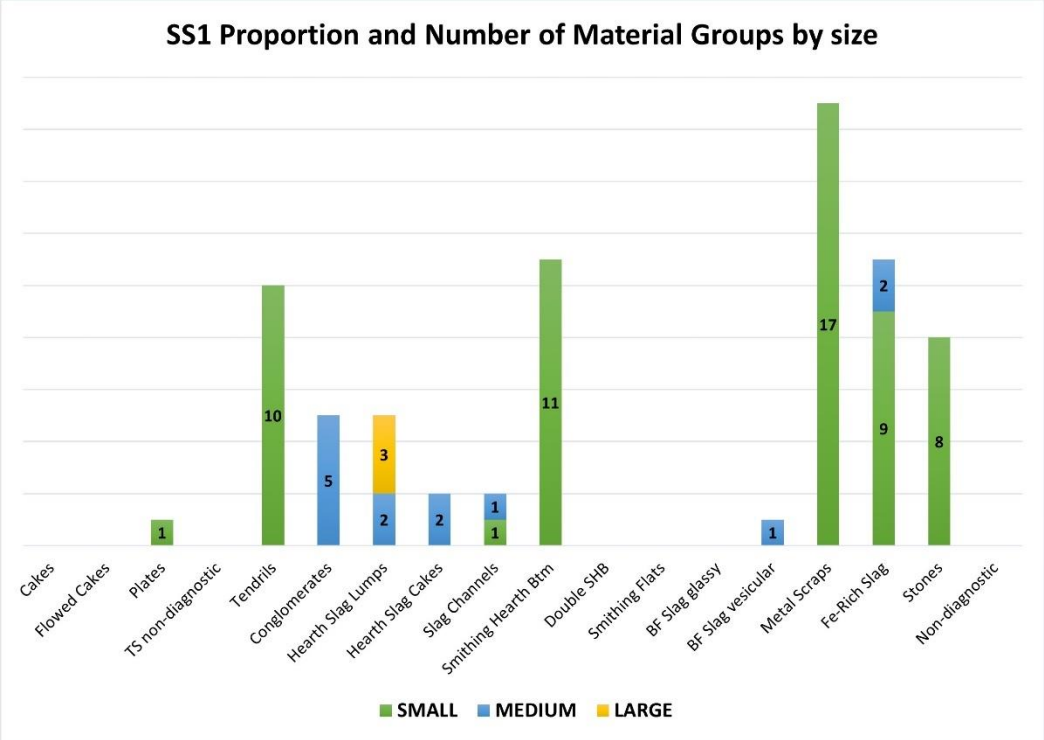

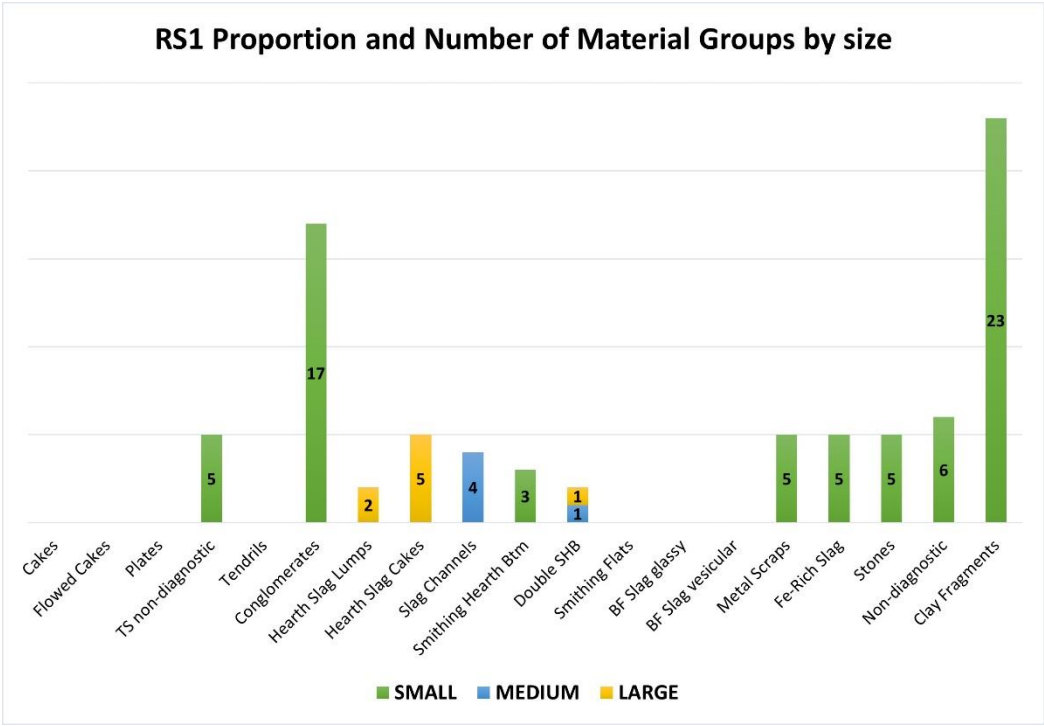

APPENDIX A.3.3: CLASSIFICATION SCHEME FOR MATRIX SAMPLE

The symbols MX stands for Matrix, followed by the initials of the main material group, for example S for slag, RM for refractory material etc. The symbols for the types were created in the same way. Subtypes are represented by lower-case roman numbers.

CLASS		**TYPE**		**SUB-TYPE**	
Symbol	Description	Symbol	Description	Symbol	Description
MXS	SLAG	**SS**	Smooth Slag	i	Fragments of tap slag
				ii	Tendrils
		RS	Rough Slag	iii	Iron-rich slag
		BF	BF Slag	iv	Glassy
				v	High-silica slag
		HS	Hammerscales	vi	Flakes
				vii	Spheroids
MXG	GEOLOGICAL MATERIAL	**IO**	Iron Ore	i	
		L	Limestone	ii	
		S	Slate	iii	
		P/S	Pebbles/Stones	iv	River Gravel
		U	Uncertain	v	
		HW	Hearth Wall	ii	
		O	Others	iv	
MXM	METAL	**A**	Finished Artefact	ii	
		S	Scrap	iii	

PN1	SPIT	SIEVE	Description	Symbol	Symbol	Weight	Notes
	0-20	Total Matrix <1	MXS	SS	i		
				RS	iii	68.8g	soil: 180.4g
				HS	vi		
				HS	vii		
	0-20	<1 >0.5	MXS	SS	i		
				SS	ii	224.4g	
				RS	iii		
				HS	vi		1 spheroid
			MXG	IO	i ?	6.1g	charcoal + veg matter and soil: 19.4g
	0-20	<0.5 >0.28	MXS	SS	i	52.2g (BF incl)	charcoal: 38g
				RS	iii		
				BF	iv		
				HS	vi		
				HS	vii		
			MXG	IO	i ?	6.8g	clay attached
				P/S	iv		
	20-40 Btm	< 1 >0.5	MXS	SS	i	117.6g	No hammerscales in this spit
				RS/Metal S	iii		different from amorphous slag, these are rounded balls, rich in iron and clay (small version of clay-rich material with embedded stones in bulk sample). Majority between 0.5 and 10 mm. Magnetic.
				BF	iv	6.5g	charcoal: 100.5g
			MXG	IO	i ?	32.5g	
				P/S	iv		
	20-40 Top	< 1 >0.5	MXS	SS	i	196.2g	charcoal: 48.6g. Majority is tap slag, similar to previous spit but less "iron balls"
				RS	ii		
				HS	vi		very few
			MXG	P/S	iv	22.8g	some clay attached
				S	iii		
	20-40 Btm	< 0.5 >0.28	MXS	SS	i	23.1g	maybe hammersc in this group + 2 spher. But not clear and not found in BIG sieve either. Charcoal: 67g

				RS	ii + RS/M		again more rounded pieces, like in PN1 20-40 BTM BIG SIEVE.
				BF	iv	1g	
			MXG	IO	i ?		dark stones with red stain and magnetic.
				P/S	iv	10.3g	
				S	iii		
	20-40 Top	< 0.5 >0.28	MXS	SS	i	36.8g	charcoal: 36.2g
				RS	iii		
				BF	iv	0.8g	
				HS	vi		
				HS	vii		
			MXG	P/S	iv	7.2g	

QN1	SPIT	SIEVE	Description	Symbol	Symbol	Weight	Notes
	0-20	Wet Sieved	**MXS**	**SS**	**i**		250g: the rest is charcoal, soil, wood. Round small red/yellow stones, possibly some limestone (burning coloration)
				RS	**iii**	235.7g	
				HS	**vi**		
			MXG	**S**	**iii**	8.9g	
				P/S	**iv**		
	0-20	Not sieved	**MXS**	**SS**	**i**		
				RS	**iii**	128g	soil: 117.6g
				HS	**vi**		
				HS	**vii**		
			MXG	**P/S**	**iv**		
	20-40	<1 >0.5	**MXS**	**SS**	**i**		
				RS	**iii**	185.8g	
				BS	**iv**	2g	
				HS	**vi**		
			MXG	**S**	**iii**	22.1g	charcoal: 36.2g
				P/S	**iv**		
	20-40	<0.5 >0.28	**MXS**	**SS**	**i**		charcoal: 40.3g
				RS	**iii**	48g	
				BF	**iv**	0.4g	
				HS	**vi**		
				HS	**vii**		
			MXG	**IO**	**i ?**		
				S	**iii**	7.9g	
				P/S	**iv**		
	20-40	Not sieved	**MXS**	**SS**	**i**		
				RS	**iii**	104.2g	charcoal: 1.2g
				HS	**vi**		flakes with clay attached
				HS	**vii**		
			MXG	**IO**	**i ?**	2.2g	are these pieces of iron ore?
				P/S	**iv**		

	20-40	Wet sieved	**MXS**	**SS**	**i**		
				SS	**ii**		
				RS	**iii**	237.2g	
				HS	**vi**		
				HS	**vii**		
			MXM	**S**	**iii**	4.9g	
			MXG	**IO**	**i ?**	3.8g	
				L	**ii**		

ZN1	SPIT	SIEVE	Description	Symbol	Symbol	Weight	Notes
	0-20	<1 >0.5	MXS	SS	i		very few stones and fragments of charcoal
				RS	iii	247.1g	some fragments of vesicular material, maybe bones?
				HS	vi		
			MXG	P/S	iv	1.4g	
	0-20	<0.5 >0.28	MXS	SS	i		charcoal: 10.6g
				RS	iii	86.7g	largest group, magnetic
				HS	vi		
				HS	vii		
			MXG	S	iii	2.4g	
				P/S	iv		
	20-40	<1 >0.5	MXS	SS	i	224.6g	charcoal: 6.8g. Limestone burning coloration
				RS	iii		
				HS	vi		
				HS	vii		quite a few
			MXG	IO	i?	18.3g	
				L	ii		
				S	iii		
				P/S	iv		
	20-40	<0.5 >0.28	MXS	SS	i		some fragments of glassy slag too
				RS	iii	69.9g	some fragments of vesicular material, maybe bones?
				HS	vi		charcoal: 4.1g
				HS	vii		quite a few
			MXG	IO	i?		
				L	ii	9g	
				S	iii		
				P/S	iv		

ZS3	SPIT	SIEVE	Description	Symbol	Symbol	Weight	Notes
	0-20	<1 >0.5	MXS	SS	i		little charcoal: 0.6g
				RS	iii	230g	clay attached
				HS	vi		
			MXG	IO	i?		
				S	iii	13.5g	

				P/S	iv		
	0-20	<0.5 >0.28	MXS	SS	i		charcoal+soil: 34.8g
				RS	ii	52.3g	
				HS	vi		
				HS	vii		good amount
			MXG	IO	i?	10.6g	
				S	iii		
				P/S	iv		
	20-40	<1 >0.5	MXS	SS	i		little charcoal: 3.7g
				RS	iii		
				BF	iv	238.8g	1 fragment
				HS	vi		
				HS	vii		
			MXG	L	ii?	7.6g	
				P/S	iv		
	20-40	<0.5 >0.28	MXS	SS	i		charcoal: 19.4g
				RS	iii	76.8g	charcoal impressions, white stones attached
				BF	iv		1 fragment
				HS	vi		
				HS	vii		
			MXG	IO	i?	2.8g	
				S	iii		
				P/S	iv		
	40-60	<1 >0.5	MXS	SS	i		charcoal: 2.5g
				RS	iii	240.4g	biggest group
				BF	iv		1 fragment
				HS	vi		
				HS	vii		
			MXG	S	iii	6.8g	clay too?
				P/S	iv		
	40-60	<0.5 >0.28	MXS	SS	i		charcoal: 11g
				RS	iii		
				BF	iv	83.3g	3 fragments
				HS	vi		
				HS	vii		
			MXG	IO	i?		clay pellets ? Sign of heating
				P/S	iv		

JN9	SPIT	SIEVE	Description	Symbol	Symbol	Weight	Notes
	0-20	<1 >0.5	MXS	SS	i	221.2g	charcoal: 19.9g
				RS	iii		
				HS	vi		magnetic

				HS	vii		not magnetic
			MXG	S	iii	8.4g	
				P/S	iv		
	0-20	Wet washed <1 >0.28	MXS	SS	i	121.5g	charcoal rich layer; charcoal: 108.7 g. This spit and previous one display a high number of hammerscales
				RS	iii		
				HS	vi		
				HS	vii		
			MXG	IO	i ?	19.9g	
				S	iii		
				P/S	iv		
	0-20	<0.5 >0.28	MXS	SS	i	55.3g	charcoal+soil: 35.3g
				RS	iii		
				BF	iv		1 fragment
				HS	vi		
				HS	vii		good amount of spheroids
			MXG	IO	i?	4.6g	
				P/S	iv		
	(40-60)	<1 >0.5	MXS	SS	i		There are two bags for this spit both big sieve. () as in notebook
				RS	iii	164.2g	charcoal: 18.8g. Pieces of pinkish-yellow clay (2.7g) also attached to slag ii and iv
				HS	vi		
			MXG	S	iii	62.6g	
				P/S	iv		
			MXM	S	iii	3g	maybe an object? Two pieces
	40-60	<1 >0.5	MXS	SS	i		Less material overall, more stones and pebbles here
				RS	iii	134.4g	charcoal: 14.4g
				HS	vi		
				HS	vii		
			MXG		iv	94.1g	
	40-60	<0.5 >0.28	MXS	RS	iii		very litte slag, more stone + charcoal (12.2g)
				HS	vi	19.9g	
				HS	vii		
			MXG	S	iii	66.6g	
				P/S	iv		

APPENDIX B

CHEMICAL ANALYSIS

APPENDIX B – SCIENTIFIC ANALYSIS OF THE ASSEMBLAGE

This appendix shows the samples selected for scientific analysis. An overview of the samples based on material typology is given in the table below. This is followed by pictures showing the position of the sample cuts for each material fragment analysed.

FINERY TAP SLAG	HEARTH SLAG	BF SLAG/SILICA-RICH SLAG	HEARTH SLAG/CONGLOMERATES	SMITHING SLAG	METAL	MATRIX	ORE SAMPLES	STONES CLAY
ZN1 0-20	ZN1 0-20_1	PN1 20-40_2	QN1 20-40_CGBF	QN1 0-20_SS_1	ZS3_40-60_Flat	PN1_0-20_Mx_1	Ore_1	QN1 20-40_WhiteStone
QN1 0-20_large	ZN1 0-20_3	PN1 20-40_Black 7	PN1/QN1_CXT7_CG-BF-Fe		RS1_0-20_Bar	JN9_0-20_Mx_2	Ore_2	QN1 20-40_MixClay
PN1 20-40_13	RS1 20-40_1	PN1 20-40_Blue	PN1/QN1_CX7_BF_Green		JN9 0-20_Iron	QN1 20-40_Wet_Mx	Ore_3	PN1/QN1_CXT7_WhiteStn
PN1 20-40_14	RS1 20-40_2	PN1 20-40_Green_1	PN1 20-40_CGBFTP_10		PN1 20-40_FeNodule 6			PN1 20-40_Quartz
PN1 20-40_Run 12	JN9 20-40_Cyl_3	PN1 20-40_Green_2	PN1 20-40_CGBF_5		PN1 20-40_FeNodule 11			PN1 20-40_WhiteStone
PN1 0-20_Thin Plate		PN1 20-40_7	PN1 20-40_CGBF_4		QN1 20-40_Fe ball			
		PN1 20-40_8	JN9 20-40_Fe/Slag		RS1 0-20_Fe1			
		PN1 20-40_blue 8	ZS3_40-60_Fe/Slag		RS1 0-20_Fe2			
		QN1 20-40_Blue 8			RS1 20-40_Fe1			
		BF Finds_ 1, _2, _3, _4, _5			RS1 20-40_Fe2			

FINERY TAP SLAG

ZN1 0-20

QN1 0-20_Large

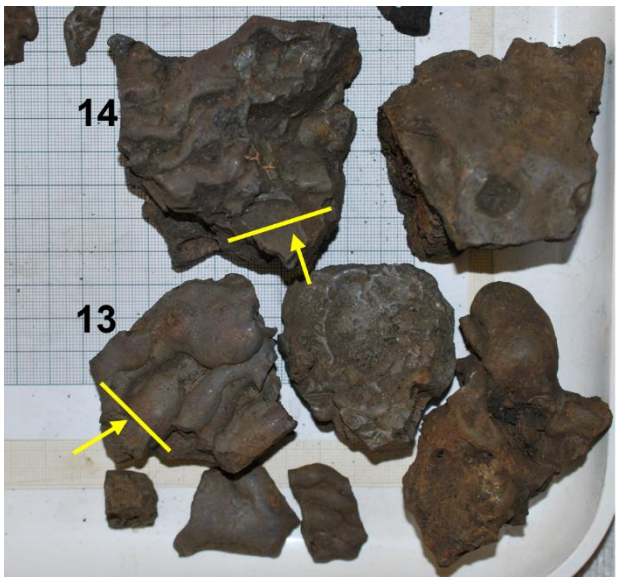

PN1_20-40_13 and 14

PN1 20-40_Run 12

PN1 0-20_Thin Plate

HEARTH SLAG

Cakes/Lumps

ZN1 0-20_1

ZN1 0-20_3

RS1 20-40_1 and 2

JN9 0-20_Cyl 3

Conglomerates

QN1 20-40_CGBF

PN1/QN1_CXT 7_CG-BF-Fe (left) and PN1/QN1_CXT_BF Green (right)

PN1 20-40_CGBFTP_10

PN1 20-40_CGBF_4 and 5

ZS3 40-60_Fe/Slag

JN9 20-40_Fe/Slag

BLAST FURNACE SLAG/SILICA-RICH SLAG

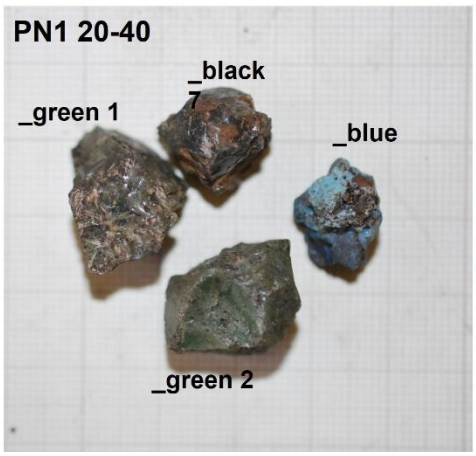

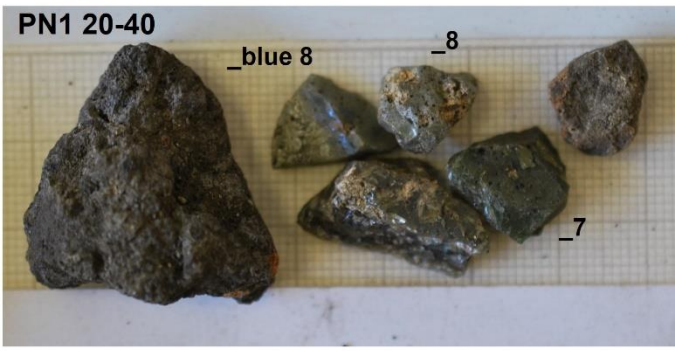

PN1 20-40 samples

QN1 20-40_Blue 8

Samples BFF 1 – 5

SMITHING SLAG AND MATRIX SAMPLES

Smithing slag bottom

QN1 0-20_SS1

Matrix

PN1 0-20_Matrix 1

PN1 20-40_Matrix 2

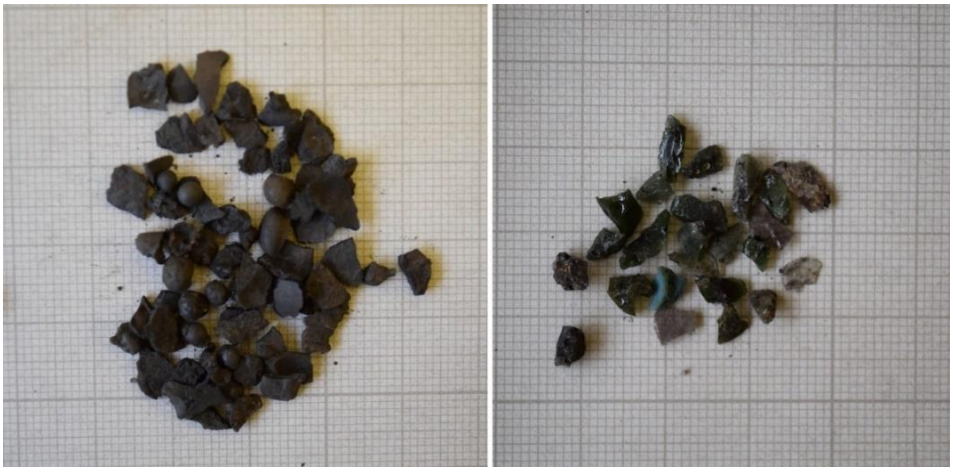

QN1 20-40_Wet Matrix

METAL

ZS3 40-60_Flat

RS1 0-20_Bar

JN9 0-20_Iron and PN1 20-40_Fe nodule 6 and _Fe nodule 11

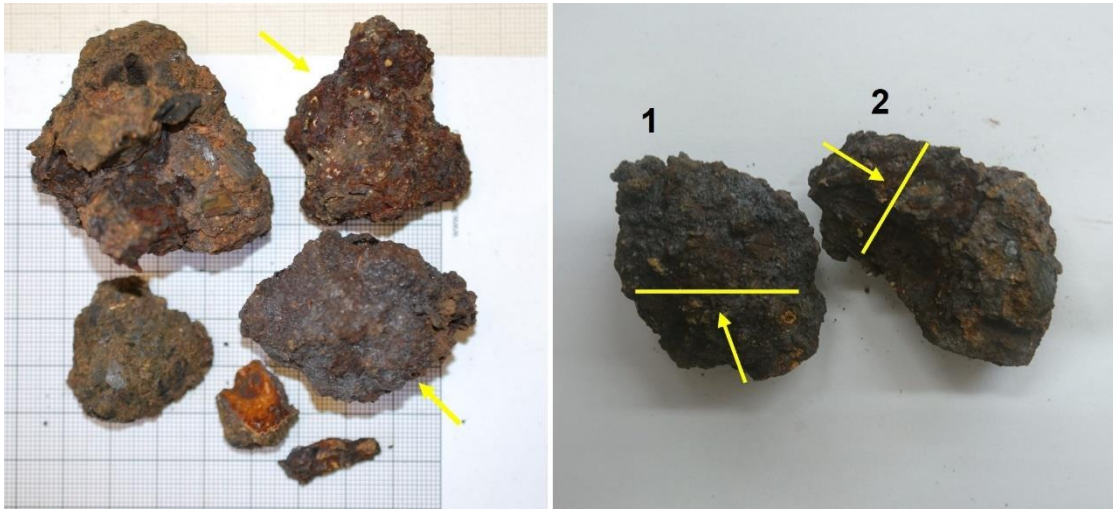

QN1 20-40_Fe nodules 1 and 2

RS1 0-20_Fe1 and Fe2 and RS1 20-40_Fe1 and Fe2

ORE SAMPLES

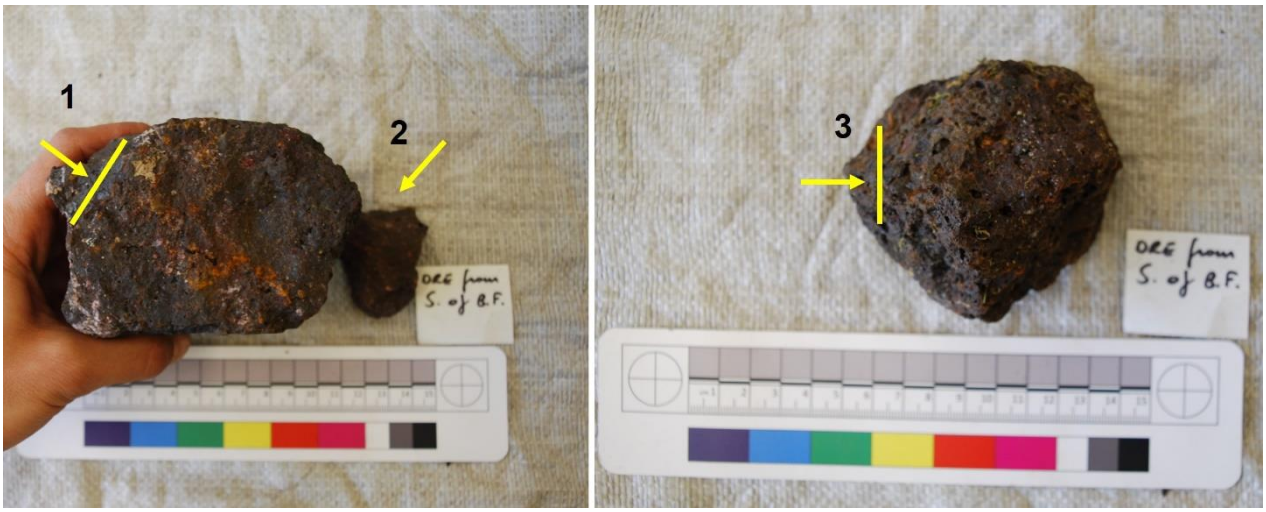

Ore sample 1, 2 and 3

STONES AND CLAY

QN1 20-40_white stone and QN1 20-40_MixClay

PN1/QN1_CXT 7_White Clay, PN1 20-40_White Stone and PN1 20-40_quartz

APPENDIX B.1 – SEM-EDS Analysis of CRM

Five certified reference materials have been analysed by SEM-EDS to assess accuracy and precision. Three samples of glass (SGT 7, SGT 10 and SGT 11) have been analysed to test reliability on blast furnace slag. Two samples of steel (16C-ARMI and ZRM 193-1) have been tested as a comparative material for the metal samples and the metallic prills in the slag samples.

Glass

SGT 7-SLS	**Na_2O**	**MgO**	**Al_2O_3**	**SiO_2**	**SO_3**	**K_2O**	**CaO**	**Fe_2O_3**	**Total**
Measurement 1	16.59	0.45	2.18	68.85	0.12	0.43	11.06	0.32	
Measurement 2	16.64	0.44	2.04	68.83	0.15	0.45	11.12	0.33	
Measurement 3	16.25	0.45	1.99	69.05	0.18	0.43	11.39	0.26	
Average	**16.49**	**0.45**	**2.07**	**68.91**	**0.15**	**0.44**	**11.19**	**0.30**	**100**
Standard deviation	0.21	0.01	0.10	0.12	0.03	0.01	0.18	0.04	
Coefficient of variation (%)	**1.27**	**2.22**	**4.83**	**0.17**	**20.00**	**2.27**	**1.60**	**13.33**	
Reference Values	13.90	0.14	1.50	72.64	0.19	0.43	11.03	0.044	99.87
Normalised Reference Values	**13.93**	**0.14**	**1.50**	**72.73**	**0.19**	**0.43**	**11.04**	**0.044**	**100**
Absolute Error	-2.56	-0.31	-0.57	3.82	0.04	-0.01	-0.15	-0.25	
Relative Error (%)	**-18.37**	**-221.42**	**-38**	**5.25**	**21**	**-2.32**	**-1.35**	**-581.8**	

SGT 10-Amber	**Na_2O**	**MgO**	**Al_2O_3**	**SiO_2**	**SO_3**	**K_2O**	**CaO**	**TiO_2**	**Fe_2O_3**	**Total**
Measurement 1	14.62	2.10	2.23	69.10	0.05	0.35	10.94	0.12	0.50	
Measurement 2	14.98	2.08	2.32	69.05	0.05	0.32	10.80	0.12	0.45	
Measurement 3	15.07	2.17	2.21	69.03	0.05	0.33	10.70	0.12	0.49	
Average	**14.89**	**2.12**	**2.25**	**69.06**	**0.05**	**0.33**	**10.81**	**0.12**	**0.48**	100
Standard deviation	0.24	0.05	0.06	0.04	0.00	0.02	0.12	0.00	0.03	
Coefficient of variation (%)	**1.60**	**2.35**	**2.66**	**0.05**	**0.00**	**6.06**	**1.11**	**0.00**	**6.25**	
Reference Values	12.20	1.80	1.70	72.70	0.05	0.40	10.60	0.09	0.40	99.94
Normalised Reference Values	**12.20**	**1.81**	**1.71**	**72.74**	**0.05**	**0.40**	**10.60**	**0.09**	**0.40**	**100**
Absolute Error	-2.69	-0.31	-0.54	3.68	0.00	0.07	-0.21	0.00	-0.08	
Relative Error (%)	**-22.04**	**-17.12**	**-31.57**	**5.05**	**0.00**	**17.50**	**-1.98**	**0.00**	**-20.00**	

SGT 11-Green	**Na_2O**	**MgO**	**Al_2O3**	**SiO_2**	**SO_3**	**K_2O**	**CaO**	**Cr_2O_3**	**Fe_2O_3**	**Total**

Measurement 1	16.03	2.42	2.53	67.26	0.07	0.68	10.44	0.12	0.44	
Measurement 2	16.01	2.33	2.34	67.44	0.04	0.72	10.45	0.16	0.53	
Measurement 3	16.37	2.45	2.39	67.14	0.06	0.65	10.34	0.11	0.49	
Average	**16.14**	**2.40**	**2.42**	**67.28**	**0.06**	**0.68**	**10.41**	**0.13**	**0.49**	**100**
Standard deviation	0.20	0.06	0.10	0.15	0.02	0.04	0.06	0.03	0.05	
Coefficient of variation (%)	**0.01**	**0.02**	**0.04**	**0.002**	**0.33**	**0.05**	**0.005**	**0.23**	**0.10**	
Reference Values	13.60	2.14	1.83	70.70	0.06	0.69	10.30	0.20	0.34	99.86
Normalised Reference Values	**13.62**	**2.14**	**1.83**	**70.8**	**0.06**	**0.70**	**10.31**	**0.2**	**0.34**	**100**
Absolute Error	2.52	-0.26	-0.59	3.52	0.00	0.02	-0.10	0.07	-0.15	
Relative Error (%)	18.50	-12.15	-32.24	4.97	5.56	2.38	-0.97	35.00	-43.14	

Metal

16C ARMI	**O**	**Al**	**Nb**	**Ti**	**Cr**	**Fe**	**Ni**	**Cu**	**Total**
Measurement 1	1.32	0.08	0.24	1.31	12.54	75.27	7.44	1.80	
Measurement 2	1.39	0.09	0.22	1.26	12.48	75.71	7.40	1.76	
Measurement 3	1.35	0.08	0.25	1.28	12.49	75.57	7.44	1.86	
Average	**1.35**	**0.08**	**0.24**	**1.28**	**12.50**	**75.52**	**7.43**	**1.81**	
Standard deviation	0.04	0.01	0.02	0.03	0.03	0.22	0.02	0.05	
Coefficient of variation (%)	**2.96**	**12.50**	**8.33**	**2.34**	**0.24**	**0.29**	**0.26**	**2.77**	
Reference Values	0.0014	0.07	0.25	1.16	11.34	76.69	8.23	2.08	99.82
Normalised Reference Values	**0.0014**	**0.08**	**0.26**	**1.16**	**11.36**	**76.82**	**8.24**	**2.08**	**100**
Absolute Error	-	0.00	0.02	-0.12	-1.14	1.30	0.81	0.27	
Relative Error (%)	**-**	**0.00**	**7.69**	**-10.34**	**-10.03**	**1.69**	**9.83**	**12.98**	

ZRM 193-1	**Si**	**Mo**	**S**	**Cr**	**Mn**	**Fe**	**Co**	**Ni**	**Cu**	**Total**
Measurement 1	0.29	0.29	0.14	0.27	0.87	96.62	0.18	1.07	0.56	
Measurement 2	0.30	0.30	0.16	0.26	0.92	96.56	0.20	1.06	0.55	
Measurement	0.36	0.29	0.00	0.32	0.95	95.64	0.08	1.19	1.16	
Average	**0.32**	**0.29**	**0.10**	**0.28**	**0.91**	**96.27**	**0.15**	**1.11**	**0.76**	
Standard deviation	0.04	0.01	0.09	0.03	0.04	0.55	0.06	0.07	0.35	
Coefficient of variation (%)	12.0	2.0	87.2	11.3	4.4	0.6	41.9	6.5	46.2	
Reference Values	**0.40**	**0.34**	**0.008**	**0.18**	**0.97**	**-**	**0.007**	**1.17**	**0.59**	**3.665** **Fe 96.33**
Absolute Error	0.08	0.05	-0.09	-0.10	0.06	-	-0.15	0.06	-0.17	
Relative Error (%)	20.83	13.73	-1150.0	-57.41	5.84	-	-2090.5	5.41	-28.25	

APPENDIX B.2 – OBJECTIVE 1: SEM-EDS ANALYSIS AND MICROSTRUCTURES OF SAMPLES

BLAST FURNACE SLAG FINDS

BFF_1

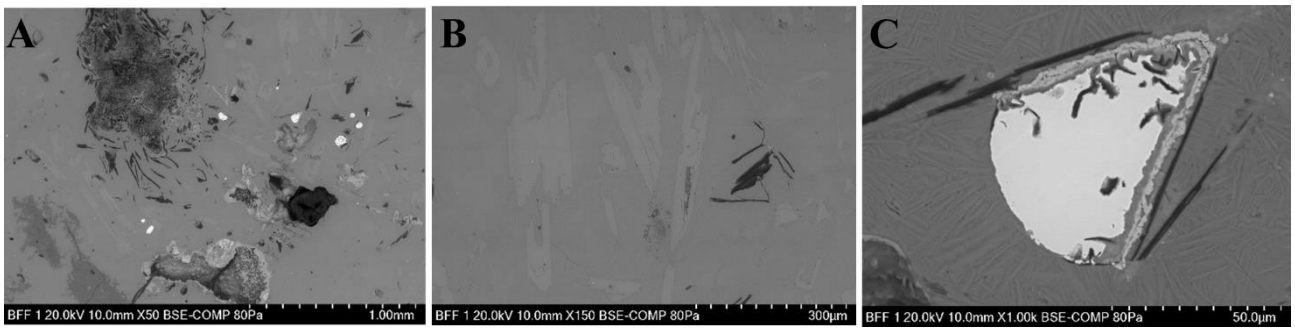

BSE micrographs showing an overview of sample BFF_1 (left) and details of the glassy matrix with wollastonite/pseudowollastonite crystals in the middle. To the right, a forming grey cast iron prill, and fine dendrites fayalite crystals. The table below shows more results on prills, matrix and phases. The iron content measured on the matrix varies based on the area of analysis, higher values are measured near prills or areas of iron oxides.

Prills	**O**	**Mg**	**Al**	**Si**	**P**	**K**	**Ca**	**Mn**	**Fe**
	8.2	0.5	2.4	8.6	0.5	0.6	4.8	3.3	71.2
	12.6	0.7	2.8	9.9	0.6	0.7	5.5	2.8	64.4
Matrix	**Na_2O**	**MgO**	**Al_2O_3**	**SiO_2**	**K_2O**	**CaO**	**TiO_2**	**MnO**	**Fe_2O_3**
	0.6	1.9	12.2	47.3	3.0	24.9	-	4.7	5.5
	-	1.9	12.8	46.8	2.6	22.3	0.5	5.3	7.6
	-	2.8	8.7	49.2	0.3	26.8	-	-	12.2
	-	3.0	9.4	51.7	0.4	26.0	-	-	9.5
	-	1.8	11.2	47.8	2.3	28.9	0.3	6.7	1.0
Phases	**-**	**MgO**	**Al_2O_3**	**SiO_2**	**-**	**K_2O**	**CaO**	**MnO**	**-**
		1.1	2.9	48.7		0.5	43.0	3.8	
		1.2	3.0	48.8		0.6	42.4	3.9	
		1.4	5.3	48.6		1.2	39.3	4.3	

BFF_2

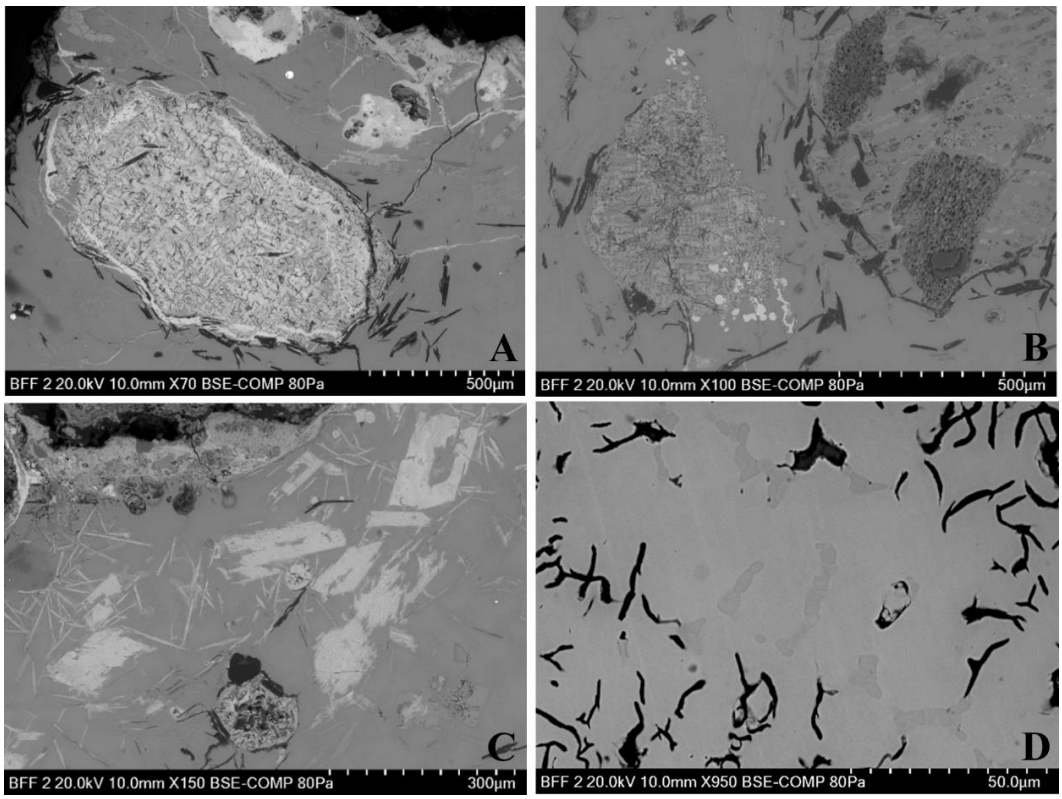

BSE micrographs showing features of sample BFF_2. The matrix is characterised by forming cast iron prills and charcoal inclusions (A and B). Areas rich in iron, see the formation of fayalite crystals (C) and iron oxides, which are likely post-depositional. A detail of the microstructure of a cast iron inclusion is also shown in D. The black flakes are graphite, the matrix is then characterised by numerous dark steadite islands in a light grey pearlitic matrix.

	MgO	Al_2O_3	SiO_2	SO_3	K_2O	CaO	TiO_2	MnO	Fe_2O_3		
Glassy matrix near MnS and titanium-rich inclusions	1.4	11.6	47.1	0.8	2.2	27.2	0.3	6.7	2.8		
	1.6	11.7	47.4	0.6	2.3	26.7		6.6	3.0		
	1.4	11.3	46.3	2.4	2.4	26.0	0.3	7.3	2.5		
	1.5	11.3	46.2	2.3	2.3	26.3	0.3	7.3	2.5		
	O	**Mg**	**Al**	**Si**	**P**	**S**	**K**	**Ca**	**Mn**	**Fe**	**Cu**
Results on mineral ores Chalcopyrite	19.0	0.5	2.0	6.2	0.1	18.9	0.5	2.7	1.4	29.4	19.2
	16.1	0.5	1.9	6.3	bdl	17.7	0.5	2.8	1.1	14.6	38.5
	17.1	0.4	1.6	5.3	bdl	22.3	0.5	2.5	1.6	41.4	7.3
	16.8	0.6	1.9	6.2	bdl	16.8	0.5	2.7	1.1	17.0	36.3
	18.5	0.6	1.9	6.2	bdl	19.1	0.5	2.6	1.3	29.5	19.9
	16.7	0.7	2.0	6.4	bdl	17.3	0.5	2.8	1.1	11.8	40.7

BFF 1	Na_2O	MgO	Al_2O_3	SiO_2	K_2O	CaO	TiO_2	MnO	Fe_2O_3
	0.6	1.9	12.2	47.3	3.0	24.9	-	4.7	5.5
	-	2.0	12.6	49.9	3.1	27.3	-	5.2	-
	-	1.9	12.8	46.8	2.6	22.3	0.5	5.3	7.6
	-	2.8	8.7	49.2	0.3	26.8	-	-	12.2
	-	3.0	9.4	51.7	0.4	26.0	-	-	9.5
Average areas of analysis	**0.6**	**2.3**	**11.1**	**49.0**	**1.9**	**25.5**	**0.5**	**5.1**	**8.7**
stdev	-	0.5	1.9	2.0	1.4	2.0	-	0.3	2.8
min	0.6	1.9	8.7	46.8	0.3	22.3	0.5	4.7	5.5
max	0.6	3.0	12.8	51.7	3.1	27.3	0.5	5.3	12.2

BFF 2	MgO	Al_2O_3	SiO_2	K_2O	CaO	MnO	Fe_2O_3
	1.8	10.9	47.0	2.4	31.3	4.8	1.7
	1.7	11.1	46.7	2.2	27.7	5.0	5.6
	1.9	12.2	47.0	2.6	24.7	4.6	7.0
	2.1	12.6	47.0	2.8	26.1	5.0	4.5
	1.9	12.1	47.8	3.0	24.8	4.8	5.6
	1.8	13.7	47.1	2.6	24.7	4.9	5.2
	2.0	13.5	47.2	2.8	24.4	5.3	4.9
	2.2	12.1	47.8	2.4	23.7	6.7	5.0
Average areas of analysis	**1.9**	**12.3**	**47.2**	**2.6**	**25.9**	**5.1**	**4.9**
stdev	0.2	1.0	0.4	0.2	2.5	0.7	1.5
min	1.7	10.9	46.7	2.2	23.7	4.6	1.7
max	2.2	13.7	47.8	3.0	31.3	6.7	7.0

BFF 3	MgO	Al_2O_3	SiO_2	SO_3	K_2O	CaO	MnO	Fe_2O_3
	1.9	10.5	46.5	-	2.0	32.7	6.5	-
	1.8	10.9	47.4	-	2.2	30.7	7.0	-
	1.8	10.7	46.7	-	2.1	32.1	6.6	-
	1.5	12.3	47.0	2.3	3.0	25.0	4.9	4.0
	1.4	12.4	48.1	0.8	2.7	26.1	5.0	3.6
	1.8	10.9	46.1	-	2.1	28.4	6.7	4.0
Average areas of analysis	**1.7**	**11.3**	**47.0**	**1.5**	**2.4**	**29.2**	**6.1**	**3.8**
stdev	0.2	0.8	0.7	1.1	0.4	3.2	0.9	0.2
min	1.4	10.5	46.1	0.8	2.0	25.0	4.9	3.6
max	1.9	12.4	48.1	2.3	3.0	32.7	7.0	4.0

BFF 4	MgO	Al_2O_3	SiO_2	K_2O	CaO	TiO_2	MnO	Fe_2O_3
	2.0	11.5	44.7	2.3	21.9	-	5.9	11.6
	2.4	12.1	47.6	2.4	25.7	0.5	7.2	2.1
	2.1	12.3	48.4	2.7	25.2	0.5	6.9	1.9
	1.8	10.6	46.1	2.2	30.2	-	5.0	4.1
	1.9	10.7	45.8	2.1	29.3	-	6.1	4.1
Average areas of analysis	2.1	11.4	46.5	2.3	26.5	0.5	6.2	4.8
stdev	0.2	0.8	1.5	0.2	3.4	0.0	0.9	4.0
min	1.8	10.6	44.7	2.1	21.9	0.5	5.0	1.9
max	2.4	12.3	48.4	2.7	30.2	0.5	7.2	11.6

BFF 5	MgO	Al_2O_3	SiO_2	K_2O	CaO	TiO_2	MnO	Fe_2O_3
	2.1	9.4	48.5	2.4	17.4	-	10.4	9.9
	1.9	9.5	49.2	3.1	16.3	0.5	10.8	8.7
	2.1	9.0	47.2	2.5	15.7	-	10.0	13.4
Average areas of analysis	**2.0**	**9.3**	**48.3**	**2.7**	**16.5**	**0.5**	**10.4**	**10.7**
stdev	0.1	0.3	1.0	0.4	0.8	-	0.4	2.4
min	1.9	9.0	47.2	2.4	15.7	0.5	10.0	8.7
max	2.1	9.5	49.2	3.1	17.4	0.5	10.8	13.4

BLAST FURNACE SLAGS FROM SH1

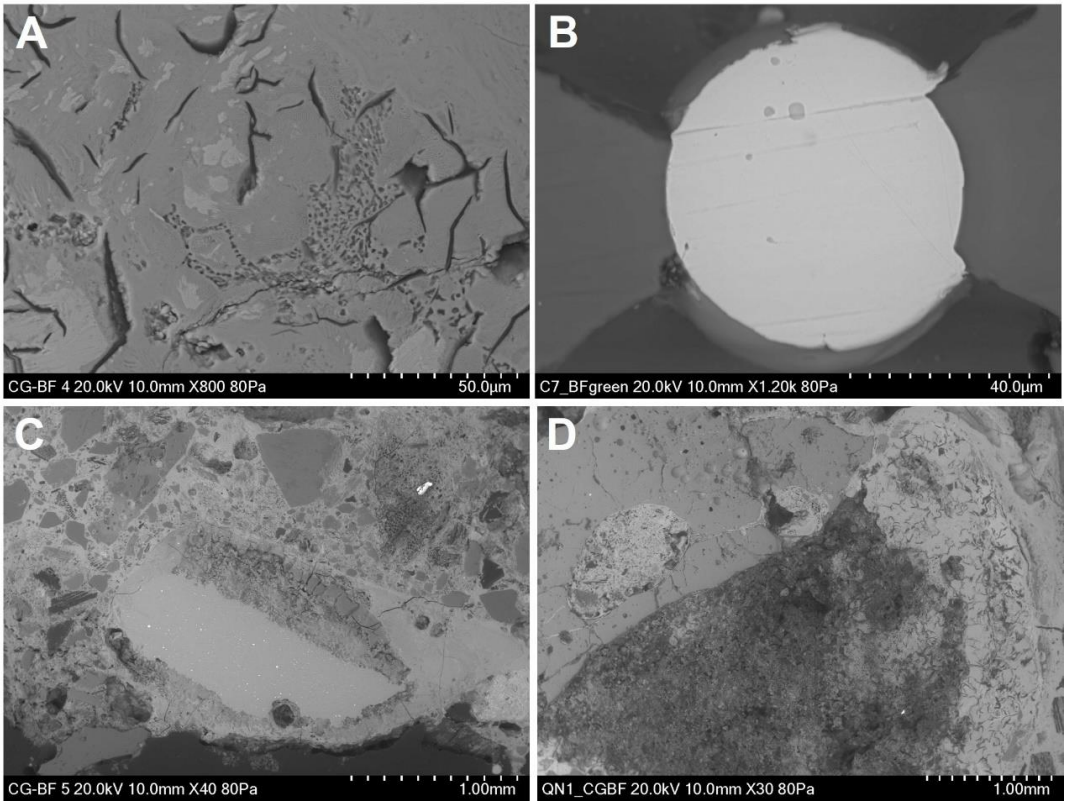

Micrographs A and B show cast iron prills inclusions in blast furnace slags from SH1. The dotted areas in A display arsenic and copper, in accordance with the geology of the area that feature chalcopyrite and arsenopyrite. The dark rounded inclusions in the prill in B are iron sulphide inclusions. Chemical composition of these areas is shown in the table below. Figures C and D show blast furnace inclusions embedded in a mixture of material, the fragment in C is vitrified along the edges. Additional chemical composition of glassy matrix and prills in blast furnace slag from SH1 are displayed in the table below. Figure D shows an oxidised cast iron prill melted to a blast furnace slag fragment.

	O	Mg	Al	Si	S	K	Ca	Fe				
Iron sulphide Inclusions	11.2	0.6	2.4	7.5	20.6	0.6	4.3	52.9				
	10.4	0.4	2.3	7.8	14.0	0.5	4.4	60.3				
	10.9	0.6	2.9	8.9	7.3	0.6	4.7	64.2				
	8.0	0.6	2.7	8.3	-	0.5	4.0	75.8				
	7.7	0.4	2.5	8.0	-	0.4	3.9	77.2				
	MgO	**Al_2O_3**	**SiO_2**	**P_2O_5**	**CaO**	**TiO_2**	**V_2O_5**	**MnO**	**Fe_2O_3**	**CuO**		**As_2O_3**
Arsenic-rich areas in cast iron prills	1.4	-	3.7	0.9	0.3	-	-	0.5	93.2	-		-
	-	0.4	4.9	1.2	1.4	0.3	0.7	1.3	85.4	2.1		2.3
	-	-	4.1	0.7	0.6	-	-	0.5	91.9	0.6		1.6
	-	0.4	5.4	1.5	0.3	-	-	0.8	89.8	0.7		1.4

	Na_2O	**MgO**	**Al_2O_3**	**SiO_2**	**K_2O**	**CaO**	**TiO_2**	**MnO**	**Fe_2O_3**
Glassy matrix of blast furnace slags in SH1	0.7	1.7	10.0	51.0	3.1	22.5	-	4.7	6.5
	-	1.5	9.7	51.0	2.4	25.5	0.2	6.2	3.5
	-	1.3	9.6	50.4	2.4	25.2	0.4	6.3	4.5
	0.6	1.5	9.7	50.5	2.4	24.9	0.2	6.1	4.1
	O	**Mg**	**Al**	**Si**	**P**	**K**	**Ca**	**Mn**	**Fe**
Cast iron prills in blast furnace slags	12.8	0.6	2.3	9.0	0.1	0.8	4.0	1.1	69.3
	16.6	-	0.5	2.5	0.1	--	0.2	1.2	78.9
	21.7	-	0.8	2.9	0.4	0.1	0.3	1.3	72.5
	17.8	-	0.5	1.5	0.2	-	-	0.4	79.6

FAYALITIC SLAG IN CONGLOMERATES

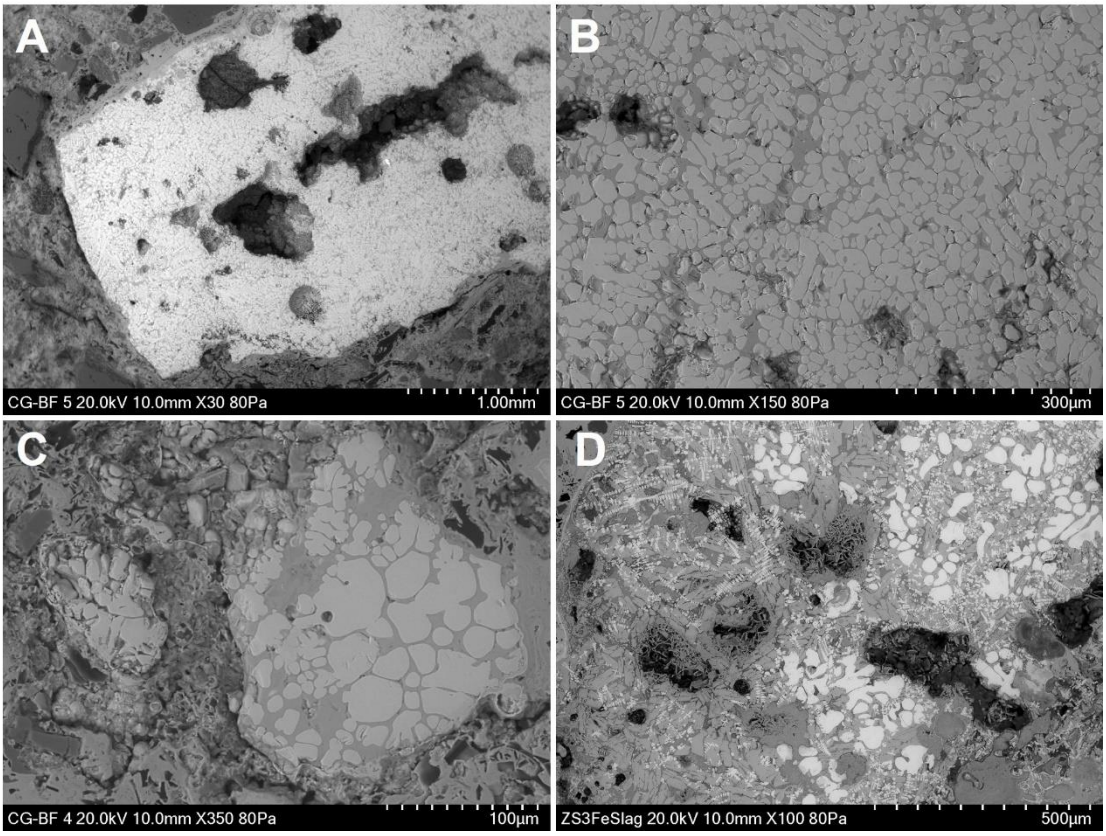

Micrographs show fayalitic wüstite-rich slag fragments in conglomerates. Note the shape of the fragment in A and microstructure in B. Other fragments are seen embedded in a mass of iron oxides and sand material in C and D. Additional chemical composition is shown in the table below.

	MgO	Al_2O_3	SiO_2	P_2O_5	K_2O	CaO	TiO_2	MnO	Fe_2O_3
Bulk composition of wüstite-rich slag inclusions	-	1.4	4.4	0.2	0.2	0.1	0.1	1.8	91.9
	-	1.5	4.8	-	0.2	0.3	-	2.4	90.8
	-	2.0	12.0	1.1	0.2	0.4	0.2	4.1	80.1
	0.5	1.6	9.7	1.1	0.1	0.6	-	4.5	81.9
	0.5	1.4	9.2	1.2	0.2	0.7	0.2	4.4	82.3
	0.6	6.3	0.4	-	-	0.4	0.2	4.6	87.5
Wüstite	-	0.6	2.5	-	-	0.2	-	3.8	92.9
	-	1.1	4.2	0.2	0.2	0.1	-	3.8	90.4
Matrix	0.9	0.8	19.5	1.1	-	0.7	-	7.5	69.4
	0.9	0.8	17.1	1.1	-	1.0	0.1	7.6	71.4
	-	0.4	16.9	0.7	-	0.9	-	7.7	73.3

ORE SAMPLES

	MgO	Al_2O_3	SiO_2	SO_3	K_2O	CaO	SnO_2	Fe_2O_3
Ore sample 1	0.4	0.4	25.8	0.1	-	0.1	0.2	73.1
	-	0.4	40.5	bdl.	0.1	0.2	-	58.8
	-	0.6	52.8	0.1	-	0.2	-	46.4
	O	**Si**	**Sn**	**Fe**				
	20.2	6.7	47.1	26.1				
	20.5	5.7	42.5	31.4				

	Al_2O_3	SiO_2	SnO_2	Fe_2O_3
Ore sample 2	0.7	77.3	0.2	21.8
	0.7	77.3	0.2	21.8
	0.8	90.6	bdl.	8.6
	O	**Si**	**Sn**	**Fe**
	17.3	2.0	50.7	30.0
	20.4	1.9	40.4	37.4
	18.8	7.3	50.6	23.3

	Al_2O_3	SiO_2	P_2O_5	SO_3	CaO	Fe_2O_3	As_2O_3
Ore sample 3	0.4	0.4	0.2	0.1	0.3	90.4	8.3
	0.4	0.4	0.2	-	0.4	90.9	7.7
	0.6	1.0	0.3	0.3	0.3	91.3	6.3
	0.2	0.6	0.1	0.6	0.2	95.3	3.1

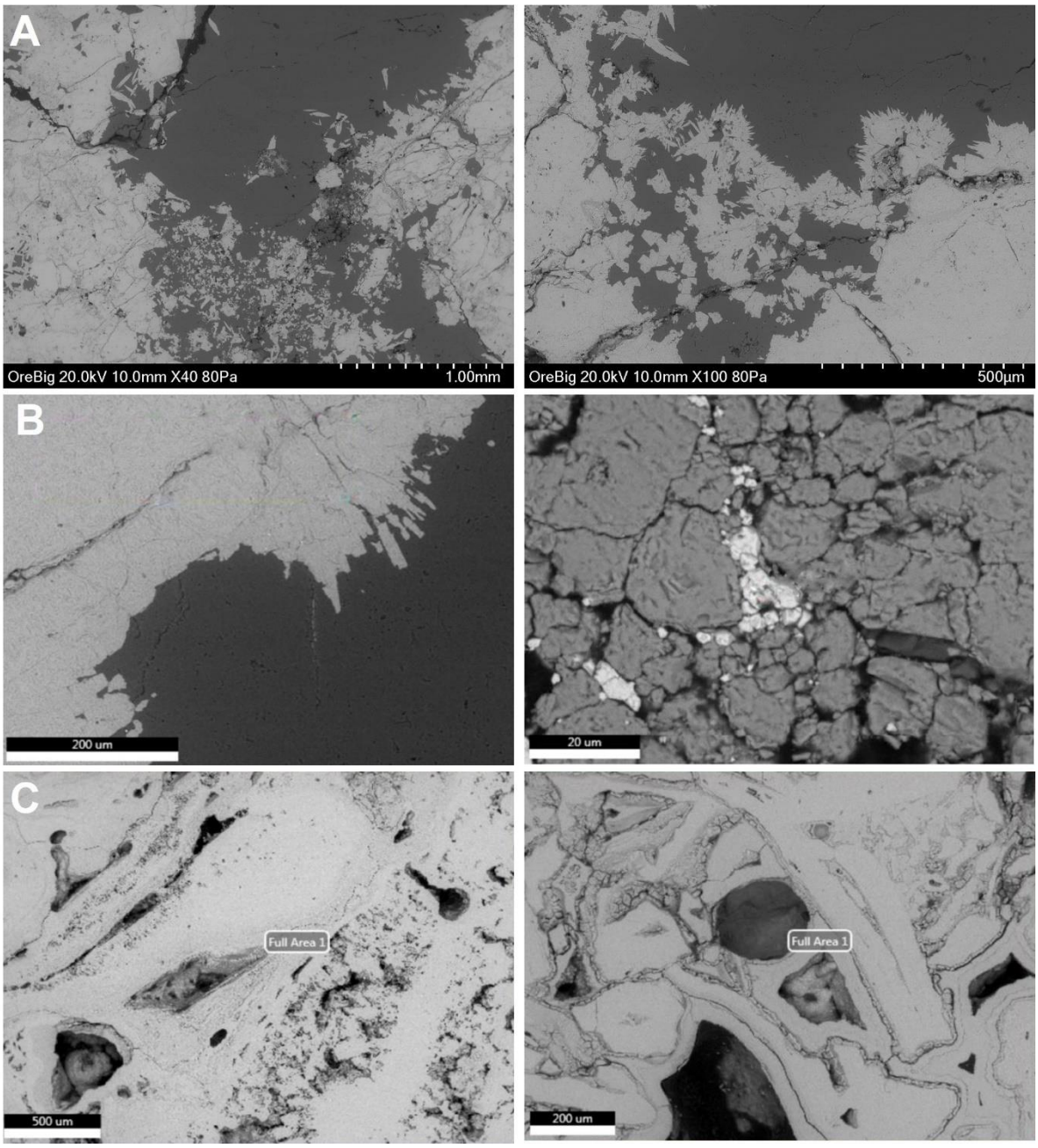

Micrographs of ore samples analysed in the present work. **A**: Sample ore 1 characterised by a matrix of silica and iron oxide and small traces of tin. The results on metallic prills suggest that these mineral rocks probably relate to the 18^{th}/19^{th} century tin ore processing on the site of Ausewell Wood. **B**: Sample ore 2 showing similar microstructure and composition to the ore 1, metallic inclusions in B (right) display high levels of tin. **C**: Sample ore 3 shows a different microstructure and chemical composition. This sample is characterised by high arsenic levels, consistent with the arsenopyrite geology of the mineral deposits from Cleft Rock.

APPENDIX B.3 – OBJECTIVE 2: SEM-EDS ANALYSIS AND MICROSTRUCTURES OF SAMPLES

FINERY TAP SLAG

Average chemical analysis of bulk composition of finery tap slag, including the results of identified phases wüstite and fayalite. Data normalised to 100wt%.

PN1 0-20 Thin Plate	**Na_2O**	**MgO**	**Al_2O_3**	**SiO_2**	**P_2O_5**	**SO_3**	**K_2O**	**CaO**	**TiO_2**	**MnO**	**Fe_2O_3**
wüstite (4)	-	0.4	2.1	8.5	0.2	0.1	0.5	0.5	0.3	0.2	87.3
fayalite (4)	-	1.1	1.7	23.9	0.4	-	0.5	0.8	0.1	0.3	71.2
bulk (3)	**1.1**	**0.6**	**3.7**	**19.7**	**0.6**	**0.1**	**1.3**	**1.2**	**0.1**	**0.3**	**71.4**
Stdev	*0.1*	*0.0*	*0.0*	*0.1*	*0.0*	*0.0*	*0.0*	*0.0*	*0.0*	*0.0*	*0.15*
Min	*1.0*	*0.5*	*3.6*	*19.7*	*0.6*	*0.0*	*1.2*	*1.2*	*0.1*	*0.2*	*71.3*
Max	*1.2*	*0.6*	*3.7*	*19.8*	*0.6*	*0.1*	*1.3*	*1.3*	*0.2*	*0.3*	*71.6*
PN1 20-40 Run 12											
wüstite (3)	-	0.4	1.5	6.3	0.2	0.1	0.6	0.9	0.3	0.3	89.5
fayalite (3)	-	1.1	1.3	21.1	0.4	-	0.6	1.5	0.1	0.3	73.7
bulk (3)	**1.2**	**0.8**	**2.6**	**16.7**	**0.7**	**0.1**	**1.1**	**1.9**	**0.2**	**0.4**	**75.4**
Stdev	*-*	*0.2*	*0.3*	*0.1*	*0.1*	*0.0*	*0.2*	*0.2*	*0.1*	*0.1*	*1.1*
Min	*1.2*	*0.6*	*2.4*	*16.5*	*0.6*	*0.0*	*0.9*	*1.6*	*0.1*	*0.3*	*74.2*
Max	*1.2*	*1.0*	*3.0*	*16.8*	*0.7*	*0.1*	*1.3*	*2.1*	*0.4*	*0.5*	*76.4*
PN1 20-40 Tap 14											
wüstite (3)	-	0.5	1.2	4.4	0.3	-	0.3	0.8	0.2	0.5	91.8
fayalite (3)	-	1.3	1.2	19.4	0.6	0.1	0.3	1.6	0.2	0.8	74.5
bulk (1)	**-**	**0.7**	**2.4**	**12.1**	**1.1**	**0.2**	**0.5**	**1.7**	**-**	**0.5**	**80.9**
PN1 20-40 Tap 13											
fayalite (3)	-	0.9	1.7	27.1	0.2	-	0.5	0.3	-	0.2	69.2
bulk (2)	**-**	**0.6**	**3.6**	**28.6**	**0.3**	**-**	**1.2**	**0.7**	**0.2**	**0.2**	**64.8**
Stdev	*-*	*0.1*	*0.1*	*0.2*	*0.0*	*-*	*0.0*	*0.1*	*-*	*-*	*0.4*
Min	*-*	*0.6*	*3.6*	*28.4*	*0.3*	*-*	*1.2*	*0.7*	*0.2*	*0.2*	*64.5*
Max	*-*	*0.7*	*3.6*	*28.7*	*0.3*	*-*	*1.2*	*0.8*	*0.2*	*0.2*	*65.1*
QN1 0-20 Large											
wüstite (3)	0.4	2.0	8.9	0.3	0.1	0.5	0.5	0.3	0.2	0.2	86.7

fayalite (3)	1.3	1.1	1.5	23.6	0.5	0.1	0.4	0.8	0.1	0.3	71.1
bulk (4)	**1.4**	**0.6**	**3.1**	**20.0**	**0.7**	**0.1**	**1.0**	**1.0**	**0.1**	**0.2**	**71.8**
Stdev	*0.1*	*0.0*	*0.3*	*3.7*	*0.1*	*0.0*	*0.1*	*0.1*	*0.0*	*0.0*	*3.9*
Min	*1.3*	*0.6*	*2.9*	*16.4*	*0.6*	*0.1*	*0.9*	*0.9*	*0.0*	*0.2*	*67.7*
Max	*1.5*	*0.7*	*3.4*	*24.2*	*0.9*	*0.1*	*1.1*	*1.2*	*0.1*	*0.2*	*75.4*
ZN1 0-20											
wüstite (3)	-	-	1.6	5.7	0.3	-	0.5	0.5	0.4	-	91.5
fayalite (3)	-	0.8	1.2	23.5	0.2	-	0.4	0.8	-	0.6	72.9
bulk (4)	**1.3**	**0.6**	**4.2**	**18.6**	**0.6**	**bdl**	**1.3**	**1.4**	**0.2**	**0.4**	**71.6**
Stdev	*0.1*	*0.1*	*0.4*	*0.5*	*0.0*	*0.0*	*0.3*	*0.0*	*0.0*	*0.0*	*0.8*
Min	*1.2*	*0.5*	*3.7*	*18.1*	*0.5*	*0.0*	*1.0*	*1.3*	*0.1*	*0.4*	*70.6*
Max	*1.4*	*0.7*	*4.6*	*19.4*	*0.7*	*0.1*	*1.6*	*1.4*	*0.2*	*0.4*	*72.5*

HEARTH SLAG

Average chemical analysis of bulk composition of hearth slag, including the results of identified phases wüstite and fayalite. Data normalised to 100wt%.

ZN1 0-20_1	**Na_2O**	**MgO**	**Al_2O_3**	**SiO_2**	**P_2O_5**	**K_2O**	**CaO**	**TiO_2**	**MnO**	**Fe_2O_3**
fay (3)	1.3	1.4	2.4	23.1	0.4	1.3	2.7	-	0.4	67.0
wus (2)	1.4	-	2.2	7.4	0.3	1.1	1.2	-	-	86.6
bulk (4)	**1.4**	**0.6**	**3.9**	**18.0**	**0.6**	**2.2**	**3.2**	-	**0.3**	**69.8**
Stdev	*0.2*	*0.1*	*1.3*	*3.4*	*0.3*	*0.5*	*0.6*	-	*0.0*	*6.2*
Min	*1.1*	*0.5*	*2.6*	*14.6*	*0.4*	*1.8*	*2.7*	*0.0*	*0.3*	*63.8*
Max	*1.7*	*0.7*	*5.5*	*21.2*	*1.0*	*3.0*	*3.9*	*0.0*	*0.3*	*76.3*
ZN1 0-20_3										
fay (2)	-	-	1.4	5.7	0.4	0.6	0.8	0.3	0.3	90.8
wus (2)	-	1.6	1.4	22.9	0.6	0.6	1.5	-	0.6	70.9
bulk (1)	**-**	**0.8**	**3.1**	**16.9**	**1.2**	**1.2**	**2.1**	**-**	**0.3**	**74.4**
JN9 Cyl 3										
wus (3)		0.5	0.8	7.5	0.4	0.2	0.4	0.3	0.3	90.1
bulk (3)		**0.8**	**0.5**	**23.4**	**0.5**	**0.1**	**0.6**	**0.2**	**0.5**	**73.6**
Stdev		*0.2*	*0.1*	*0.2*	*0.1*	*0.0*	*0.0*	*0.0*	*0.0*	*0.3*
Min		*0.6*	*0.5*	*23.2*	*0.4*	*0.1*	*0.5*	*0.2*	*0.5*	*73.3*

Max	*0.9*	*0.6*	*23.6*	*0.5*	*0.2*	*0.6*	*0.2*	*0.6*	*74.0*

Average chemical analysis of iron prills in hearth slags. Data normalised to 100wt%. Number in () is number of measurements on one piece.

Prills	O	Al	Si	P	K	Ca	Fe	N° Analysis
ZN1 0-20_1	8.3	1.1	4.0	0.1	0.7	0.7	85.1	(4)
ZN1 0-20_3	8.9	0.6	2.9	0.2	0.5	0.6	86.4	(2)
JN9 Cyl 3	9.9	0.2	2.6	0.1	0.2	0.2	86.9	(3)

RS1 HEARTH SLAG

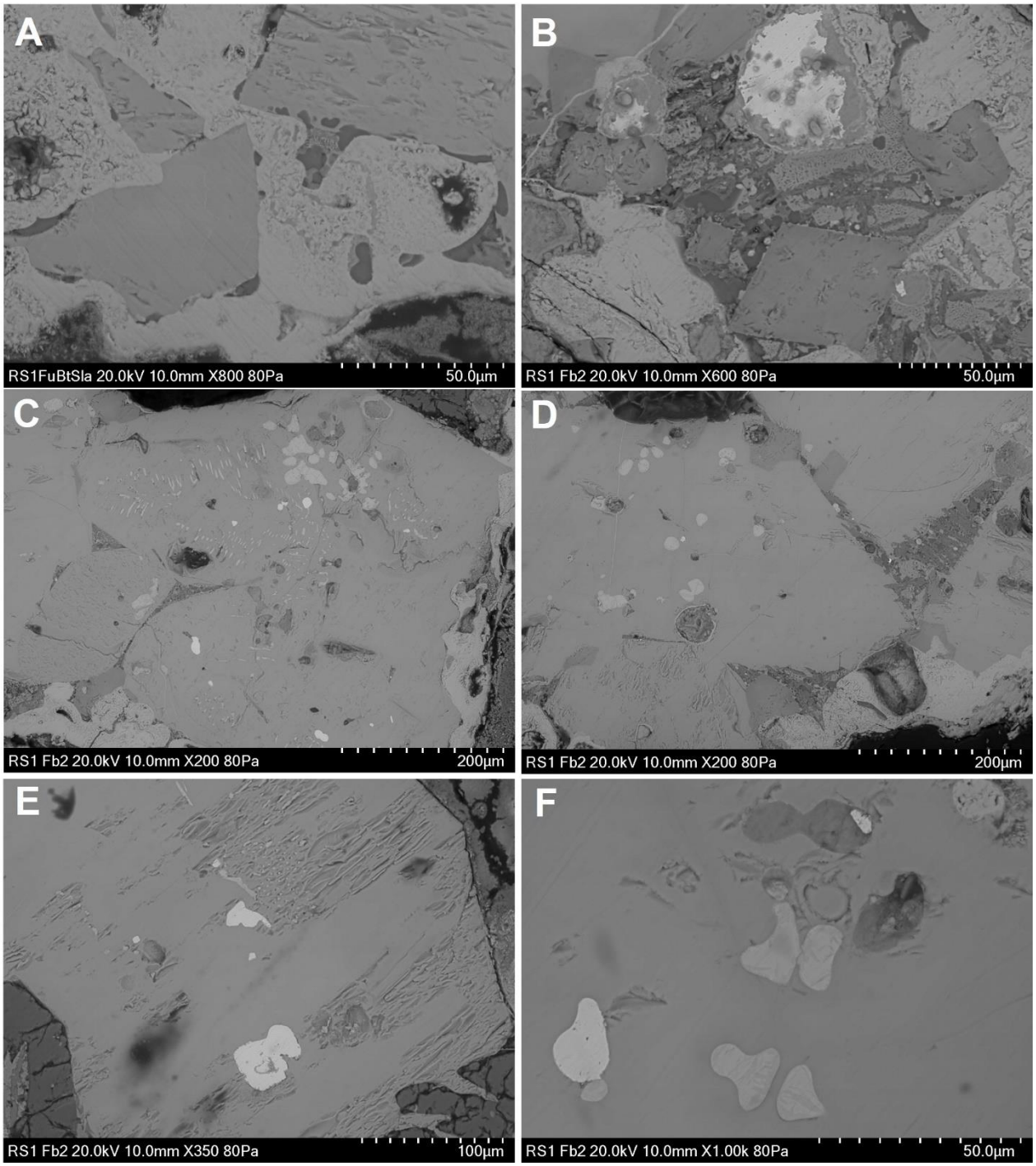

BSE micrographs showing more phases in the hearth slag from trench RS1. **A**: the small dark areas are rich in phosphorus and calcium. Some more spinels rich in titanium, vanadium and chromium are shown in **B**. **C** and **D** display overviews of the sample, with metal-rich phases forming at the boundaries of large fayalite crystals. **E** and **F** show iron prills and wüstite crystals, which are probably former iron prills.

SMITHING SLAGS

Average chemical analysis of matrix samples, including a fragment of blast furnace slag retrieved from the matrix of trench PN1. Data normalised to 100wt%.

BFS 1 (mtx)	**Na_2O**	**MgO**	**Al_2O_3**	**SiO_2**	**K_2O**	**CaO**	**TiO_2**	**MnO**	**Fe_2O_3**		
bulk (3)	**0.6**	**2.0**	**10.7**	**52.8**	**0.9**	**31.0**	**0.3**	**0.3**	**1.5**		
stdev	0.1	0.2	0.2	0.4	0.1	0.1	0.3	0.1	0.4		
min	0.4	1.9	10.5	52.3	0.8	30.9	0.2	0.2	1.0		
max	0.7	2.2	10.9	53.1	1.1	31.1	0.6	0.5	1.8		
Flake Hammerscale	**Na_2O**	**MgO**	**Al_2O_3**	**SiO_2**	**P_2O_5**	**SO_3**	**K_2O**	**CaO**	**TiO_2**	**MnO**	**Fe_2O_3**
wustite (3)	-	-	0.5	3.0	-	-	-	0.2	0.2	0.5	95.8
fayalite (3)	-	0.9	0.6	23.2	0.2	-	0.1	0.7	0.2	0.9	73.2
bulk (3)	**-**	**0.3**	**0.9**	**11.8**	**0.3**	**0.1**	**-**	**0.6**	**0.2**	**0.6**	**85.2**
stdev	-	0.1	0.1	0.3	0.1	-	-	0.0	0.0	0.0	0.4
min	-	0.3	0.8	11.5	0.2	0.1	-	0.6	0.2	0.6	84.8
max	-	0.4	0.9	12.1	0.5	0.1	-	0.6	0.2	0.7	85.5
Spheroid Hammerscale											
wustite (3)	-	1.1	4.0	0.1	-	-	0.4	0.3	0.3	0.4	93.4
fayalite (3)	0.5	0.7	1.3	24.8	0.2	-	0.4	0.8	0.3	0.5	71.1
bulk (3)	**0.5**	**0.4**	**2.9**	**16.6**	**0.5**	**0.2**	**1.0**	**1.0**	**0.2**	**0.5**	**76.6**
stdev	0.3	0.2	1.8	7.2	0.1	0.0	0.7	0.6	0.1	0.1	10.2
min	0.2	0.2	0.9	8.3	0.3	0.1	0.3	0.4	0.1	0.4	70.4
max	0.7	0.5	4.4	21.1	0.6	0.2	1.6	1.5	0.3	0.6	88.4

Average chemical analysis of phases in smithing slag bottom retrieved from QN1. Data normalised to 100wt%.

QN1 0-20 SS	MgO	Al_2O_3	SiO_2	P_2O_5	CaO	TiO_2	Fe_2O_3
fayalite (3)	0.8	1.7	23.8	0.3	0.7	-	72.7
wustite (3)	0.5	1.7	13.2	0.2	0.7	0.6	83.1
hercynite (3)	0.6	32.1	7.3	-	0.4	0.6	59.2

METAL SAMPLES

Average chemical analysis of bulk composition and phases in metal samples. Data normalised to 100wt%. These results are discussed in section 5.4.4 in chapter 5.

ZS3 40-60	O	Si	P	S	V	Mn	Fe
	1.6	0.6	0.6	-	-	0.4	96.8
	1.8	0.7	0.7	-	-	0.2	96.5
	1.8	0.7	0.8	-	-	0.3	96.5
	2.1	0.6	0.6	0.4	0.1	0.9	95.4
	1.9	0.5	0.8	-	-	0.3	96.6
	1.6	0.6	0.7	-	bdl	0.2	96.9
	0.9	0.3	1.3	0.3	0.1	0.9	96.3
	1.9	0.3	0.9	0.4	-	1.0	95.4
Bulk (9)	**1.7**	**0.5**	**0.8**	**0.4**	**0.1**	**0.5**	**96.3**
stdev	*0.4*	*0.2*	*0.2*	*0.1*	*0.0*	*0.3*	*0.6*
min	*0.9*	*0.3*	*0.6*	*0.3*	*0.1*	*0.2*	*95.4*
max	*2.1*	*0.7*	*1.3*	*0.4*	*0.1*	*1.0*	*96.9*

QN1 20-40 Fe2	O	Si	P	Mn	Fe
	6.9	1.3	0.2	0.7	90.8
	2.8	1.1	-	0.4	96.0
	5.9	1.0	0.1	0.6	92.2
	5.8	1.2	0.2	0.6	91.8
	2.8	0.7	0.1	0.6	95.8
	2.7	0.6	0.5	0.7	95.6
	2.4	0.7	0.3	0.5	96.3
	4.4	1.0	0.3	0.6	93.7
	4.5	1.0	0.4	0.5	93.6
Bulk (9)	**4.2**	**1.0**	**0.3**	**0.6**	**94.0**
stdev	*1.7*	*0.2*	*0.1*	*0.1*	*2.1*
min	*2.4*	*0.6*	*0.1*	*0.4*	*90.8*
max	*6.9*	*1.3*	*0.5*	*0.7*	*96.3*

	2.3	0.3	8.5	1.0	87.9
	2.3	0.3	6.8	1.0	89.6
	2.3	0.4	7.0	1.0	89.4
	2.5	0.3	6.3	1.1	89.8
	2.4	0.3	7.2	1.0	89.1
	2.5	0.3	7.0	1.0	89.1
Steadite (6)	**2.4**	**0.3**	**7.1**	**1.0**	**89.1**
stdev	*0.1*	*0.0*	*0.7*	*0.0*	*0.7*
min	*2.3*	*0.3*	*6.3*	*1.0*	*87.9*
max	*2.5*	*0.4*	*8.5*	*1.1*	*89.8*

RS1 20-40 Fe1	**O**	**Si**	**P**	**Mn**	**Fe**
	1.6	0.5	0.3	0.4	97.6
	1.6	0.6	0.3	0.3	97.6
	3.5	0.6	0.3	0.4	95.6
Bulk (3)	**2.2**	**0.6**	**0.3**	**0.4**	**96.9**
stdev	1.1	0.0	0.0	0.1	1.1
min	1.6	0.5	0.3	0.3	95.6
max	3.5	0.6	0.3	0.4	97.6
	O	**Si**	**P**	**S**	**Fe**
	1.2		3.9	0.1	94.8
	1.6	0.1	4.2	0.3	93.6
	1.8	0.2	4.6	0.1	93.2
P-rich areas (3)	**1.5**	**0.2**	**4.2**	**0.2**	**93.8**
stdev	0.3	0.0	0.3	0.1	0.9
min	1.2	0.1	3.9	0.1	93.2
max	1.8	0.2	4.6	0.3	94.8

RS1 20-40 Fe2	**O**	**Si**	**P**	**S**	**Ti**	**V**	**Mn**	**Fe**
	9.2	0.7	1.0	0.1	-	-	-	88.8
	10.7	0.6	0.4	0.1	-	-	-	87.9
	10.7	0.6	0.5	0.1	-	-	-	87.7
	10.4	1.0	0.4	-	-	-	-	87.9
	10.8	0.6	0.6	0.1	-	0.1	-	87.5
	10.9	0.6	1.2	0.1	-	-	-	86.9
ferrite	**10.5**	**0.7**	**0.7**	**0.1**	**-**	**0.1**	**-**	**87.8**
stdev	0.6	0.2	0.3	0.0	-		-	0.6
min	9.2	0.6	0.4	0.1	-	0.1	-	86.9
max	10.9	1.0	1.2	0.1	-	0.1	-	88.8
	O	**Si**	**P**	**S**	**Ti**	**V**	**Mn**	**Fe**
	13.6	0.3	4.5	0.2	bdl	0.1	-	81.0
	13.3	0.3	4.9	0.6	bdl	0.1	-	80.5
	11.1	0.3	2.1	bdl	bdl	0.1	-	86.2

cementite/ledeburite	**12.7**	**0.3**	**3.8**	**0.4**	**-**	**0.1**	**-**	**82.6**
	15.4	0.4	8.4	0.4	-	0.2	0.1	74.9
	17.2	0.5	7.4	0.1	-	0.1	-	74.4
ledeburite	**16.3**	**0.4**	**7.9**	**0.3**	**-**	**0.1**	**0.1**	**74.6**

RS1 0-20 Fe1	**O**	**Si**	**P**	**S**	**Ti**	**V**	**Mn**	**Fe**
Cementite/ledeburite	11.0	0.3	0.5	0.1	0.1	-	-	87.9
	9.0	0.3	1.1	0.3	bdl	0.2	-	88.9
	9.0	0.5	1.1	0.3	-	-	-	89.1
	10.9	0.3	1.9	0.2	0.1	-	-	86.6
	10.0	**0.3**	**1.1**	**0.2**	**0.1**	**0.2**	**-**	**88.1**
Ledeburite	10.6	0.4	2.1	3.0	bdl	-	0.1	83.7
	10.8	0.3	4.8	0.2	0.1	-	-	83.6
	13.6	0.4	6.2	0.4	0.0	-	-	79.3
	11.6	**0.4**	**4.4**	**1.2**	**0.1**	**-**	**0.1**	**82.2**

RS1 0-20 Fe2	**O**	**Si**	**P**	**S**	**Fe**
	1.7	0.6	0.3	-	97.4
	11.3	0.5	0.3	-	87.7
	11.1	0.4	0.2	-	88.3
	1.6	0.4	1.0	-	97.0
	1.3	0.3	0.1	-	98.4
	5.4	0.4	0.4	-	93.7
Bulk (6)	**5.4**	**0.4**	**0.4**	**-**	**93.7**
stdev	*4.7*	*0.1*	*0.3*	-	*4.7*
min	*1.3*	*0.3*	*0.1*	-	*87.7*
max	*11.3*	*0.6*	*1.0*	-	*98.4*
P-rich area	13.9	0.2	6.1	0.4	78.8

QN1 20-40 Fe2	**O**	**Si**	**P**	**Mn**	**Fe**
	2.7	1.0	-	0.5	95.9
	3.6	0.2	0.2	-	96.0
	3.8	0.1	0.1	-	96.0
	3.5	0.2	0.2	-	95.9
	3.3	0.2	0.2	-	96.3
Bulk (5)	**3.4**	**0.3**	**0.2**	**0.5**	**96.0**
stdev	*0.4*	*0.4*	*0.0*	-	*0.2*
min	*2.7*	*0.1*	*0.1*	*0.5*	*95.9*
max	*3.8*	*1.0*	*0.2*	*0.5*	*96.3*

PN1 20-40 Fe6	**O**	**Si**	**Fe**

	9.1	0.2	90.7
	9.4	0.5	90.1
	10.3	0.6	89.1
	11.3	0.4	88.3
	13.9	0.4	85.7
	8.8	0.4	90.8
	8.9	0.5	90.6
	11.0	0.6	88.5
	11.8	0.4	87.8
	10.9	0.4	88.7
Bulk (10)	**10.5**	**0.4**	**89.0**
stdev	*1.6*	*0.1*	*1.6*
min	*8.8*	*0.2*	*85.7*
max	*13.9*	*0.6*	*90.8*

RS1 0-20 Bar	**O**	**Si**	**P**	**S**	**Fe**
	2.3	0.3	0.1	-	97.3
	2.2	0.2	0.1	-	97.5
	2.3	0.3	0.1	-	97.3
	2.1	0.2	0.2	-	97.5
	2.7	0.9	0.1	-	96.3
	2.1	0.4	0.1	-	97.5
	2.1	0.4	0.1	-	97.5
	2.1	0.4	0.1	-	97.4
	2.4	0.1	0.2	0.1	97.1
Bulk (9)	**2.3**	**0.3**	**0.1**	**0.1**	**97.3**
stdev	0.2	0.2	0.1	-	0.4
min	2.1	0.1	0.1	0.1	96.3
max	2.7	0.9	0.2	0.1	97.5

Non-metallic Inclusions

Chemical analysis of a variety of inclusions in cast iron metal samples: these include titanium and vanadium rich inclusions, manganese sulphide inclusions and manganese-iron sulphide inclusions. A selection of BSE micrographs is shown below.

O	**Si**	**P**	**S**	**Ti**	**V**	**Mn**	**Fe**
12.7	0.2	0.7	20.6	0.3	2.3	1.1	61.9
13.3	0.2	0.4	20.5	0.3	2.3	1.1	61.7
15.3	0.4	0.6	21.5	1.0	2.1	1.1	57.8
2.2	-	0.2	19.4	2.8	2.2	0.7	72.6
2.4	0.2	0.4	18.7	2.6	1.9	0.2	73.7
1.5	0.1	0.8	10.7	0.3	2.0	0.9	83.8
1.0	0.2	1.2	14.8	0.0	2.2	0.2	80.6
1.1	0.2	0.6	20.9	0.4	1.9	10.0	65.0

1.2	0.1	0.3	21.7	0.1	0.7	18.7	57.1
1.3	0.2	0.3	20.8	0.1	-	12.9	64.6
1.3		0.2	20.8	0.3	-	15.5	62.0
3.3	0.4	0.3	0.7	34.5	6.1	-	54.7
3.6	0.3	0.3	2.9	36.2	5.3	1.4	50.1
2.0	0.1	0.1	16.7	0.3	-	13.0	67.6
1.8	-	0.6	12.4	0.8	1.7	0.6	81.9
1.3	0.1	-	13.5	0.8	-	13.5	70.9
1.4	-	-	22.1	0.2	-	20.2	56.2

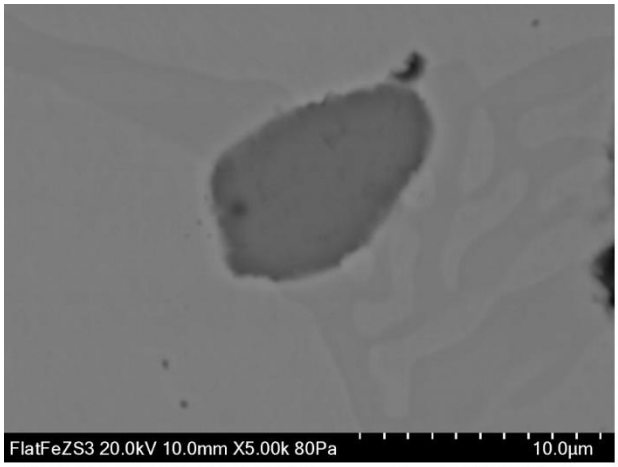
FlatFeZS3 20.0kV 10.0mm X5.00k 80Pa
10.0µm

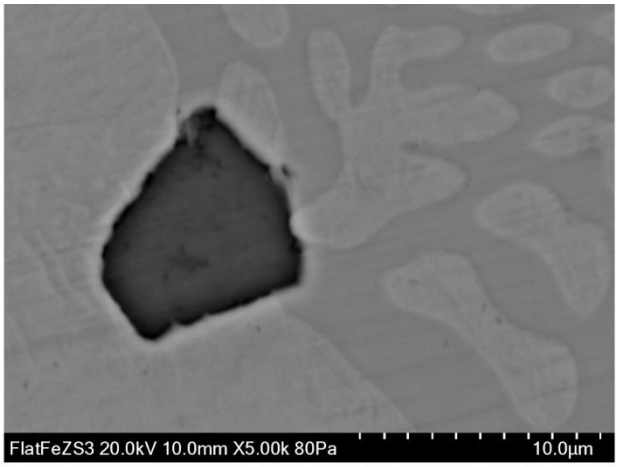
FlatFeZS3 20.0kV 10.0mm X5.00k 80Pa
10.0µm

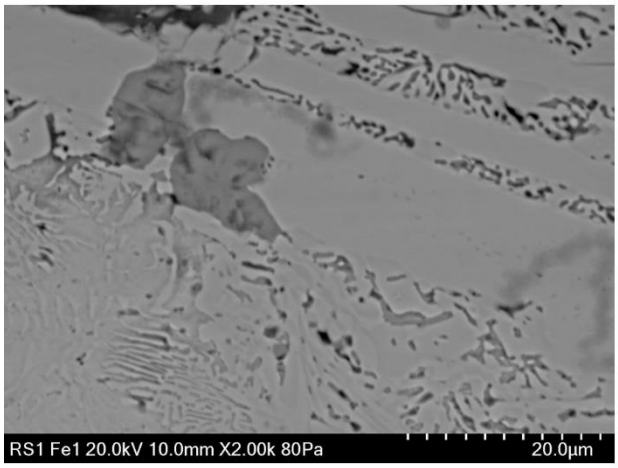
RS1 Fe1 20.0kV 10.0mm X2.00k 80Pa
20.0µm

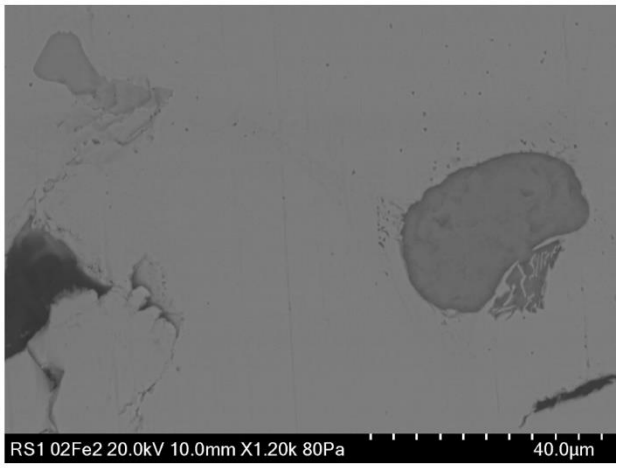
RS1 02Fe2 20.0kV 10.0mm X1.20k 80Pa
40.0µm

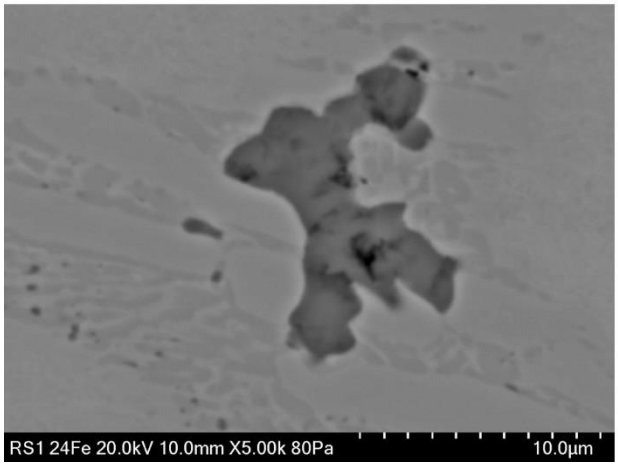
RS1 24Fe 20.0kV 10.0mm X5.00k 80Pa
10.0µm

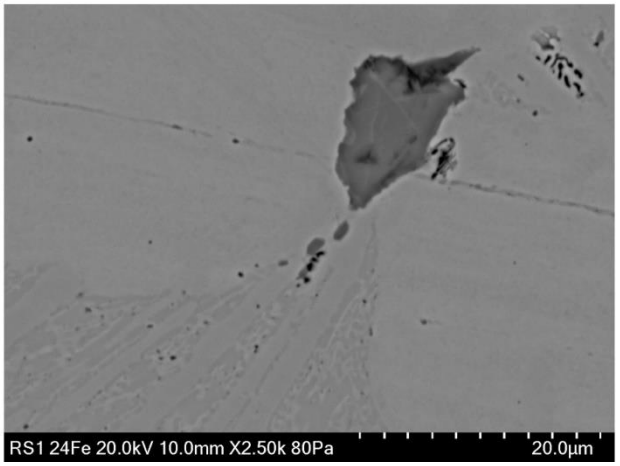
RS1 24Fe 20.0kV 10.0mm X2.50k 80Pa
20.0µm

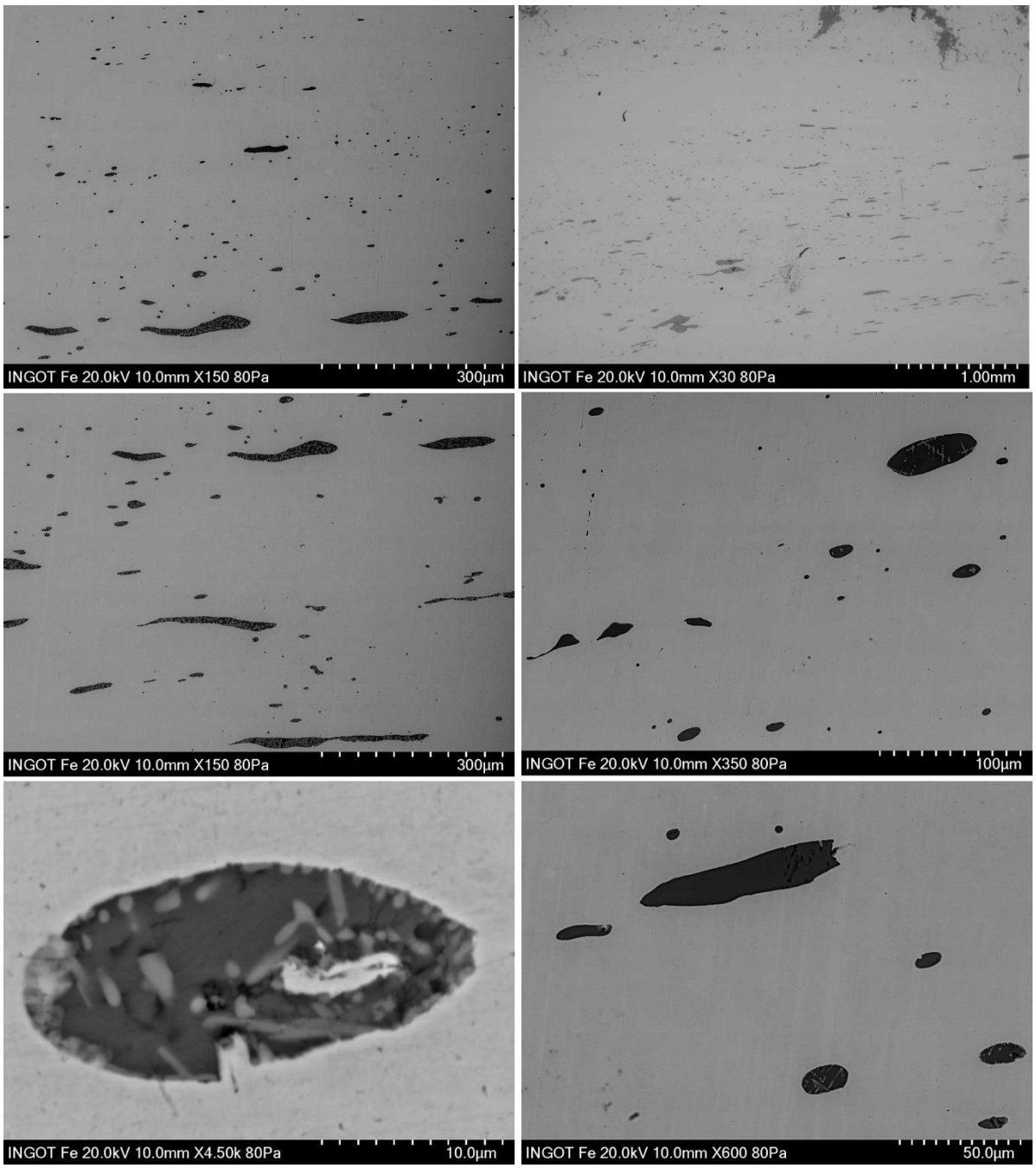

BSE micrographs showing types and distribution of non-metallic inclusions in sample RS1 iron bar. Most of the double inclusions are large and display an elongated shape in the direction of working. Single phase inclusions are generally smaller and rounded, but some elongated ones are also observed (see bottom right).

Average chemical analysis of double phase inclusions in sample RS1 0-20 Bar. Data are normalised to 100wt%.

Double phase inclusions	MgO	Al_2O_3	SiO_2	P_2O_5	SO_3	K_2O	CaO	TiO_2	V_2O_5	MnO	Fe_2O_3
	0.3	0.8	9.0	0.8	0.3	0.3	0.7	0.1	-	0.2	87.5
	0.3	0.8	8.9	0.8	0.2	0.3	0.7	0.1	-	0.2	87.7
	0.2	0.8	9.1	0.8	0.2	0.3	0.7	0.2	-	0.2	87.6
	0.2	0.9	9.0	0.8	0.2	0.3	0.7	0.1	-	0.2	87.5
	0.3	0.9	8.8	0.5	0.2	0.3	0.6	0.1	0.1	0.2	87.9
	0.3	0.7	8.1	0.5	0.2	0.3	0.6	0.1	0.1	0.2	89.1
	0.3	1.1	11.9	0.5	0.2	0.5	0.8	0.1	0.1	0.3	84.3
	0.2	0.7	7.2	0.4	0.1	0.3	0.6	0.1	0.1	0.2	90.2
	0.3	1.1	11.9	0.4	0.2	0.5	0.8	0.2	0.1	0.2	84.3
	0.1	1.2	14.4	0.6	0.5	0.5	1.0	0.2	bdl	0.3	81.2
bulk (10)	**0.2**	**0.9**	**9.8**	**0.6**	**0.2**	**0.3**	**0.7**	**0.1**	**0.1**	**0.2**	**86.7**
stdev	*0.1*	*0.2*	*2.2*	*0.2*	*0.1*	*0.1*	*0.1*	*0.0*	*0.0*	*0.0*	*2.7*
min	*0.1*	*0.7*	*7.2*	*0.4*	*0.1*	*0.3*	*0.6*	*0.1*	*0.1*	*0.2*	*81.2*
max	*0.3*	*1.2*	*14.4*	*0.8*	*0.5*	*0.5*	*1.0*	*0.2*	*0.1*	*0.3*	*90.2*
	0.2	1.2	14.2	1.2	0.4	0.6	1.0	0.1	-	0.2	80.8
	0.2	1.3	14.9	1.3	0.4	0.6	1.0	0.0	-	0.2	80.2
	0.3	1.1	12.6	1.1	0.3	0.5	1.0	0.1	0.1	0.2	82.7
	0.2	1.3	14.7	0.9	0.3	0.6	1.1	0.1	0.1	0.2	80.5
	0.3	1.3	14.0	0.9	0.3	0.5	1.0	0.1	-	0.2	81.5
	0.3	1.3	13.4	0.6	0.2	0.5	0.9	0.1	-	0.2	82.4
	0.3	1.3	13.7	0.5	0.2	0.6	0.9	0.1	0.1	0.3	81.9
	0.3	1.3	13.6	0.5	0.2	0.6	0.9	0.2	-	0.3	82.2
	0.1	1.3	16.1	0.6	0.6	0.5	1.2	0.2	-	0.3	79.1
glassy matrix (9)	**0.2**	**1.3**	**14.1**	**0.9**	**0.3**	**0.5**	**1.0**	**0.1**	**0.1**	**0.2**	**81.3**
stdev	*0.1*	*0.1*	*1.0*	*0.3*	*0.1*	*0.1*	*0.1*	*0.0*	*0.0*	*0.0*	*1.2*

min	*0.1*	*1.1*	*12.6*	*0.5*	*0.2*	*0.5*	*0.9*	*0.0*	*0.1*	*0.2*	*79.1*
max	*0.3*	*1.3*	*16.1*	*1.3*	*0.6*	*0.6*	*1.2*	*0.2*	*0.1*	*0.3*	*82.7*
	-	0.4	2.6	0.2	0.1	0.1	0.2	0.2	0.1	-	96.0
	0.4	0.6	3.5	0.3	0.1	0.2	0.3	0.2	0.1	-	94.4
	0.3	0.4	2.6	0.2	0.1	0.1	0.2	0.1	0.1	-	95.9
	-	0.4	2.0	0.1	-	0.1	0.2	0.2	0.1	0.2	96.7
	-	0.4	2.2	0.1	0.1	0.1	0.2	0.1	0.1	0.1	96.5
	0.6	0.9	7.1	0.3	0.1	0.3	0.5	0.2	0.2	0.2	89.7
	0.5	1.0	8.6	0.3	0.1	0.3	0.6	0.2	0.1	0.2	88.1
	-	0.5	4.1	0.2	0.1	0.1	0.3	0.3	0.4	0.2	93.8
wustite	**0.4**	**0.6**	**4.1**	**0.2**	**0.1**	**0.2**	**0.3**	**0.2**	**0.2**	**0.2**	**93.9**
stdev	*0.1*	*0.2*	*2.5*	*0.1*	*0.0*	*0.1*	*0.1*	*0.1*	*0.1*	*0.0*	*3.3*
min	*0.3*	*0.4*	*2.0*	*0.1*	*0.1*	*0.1*	*0.2*	*0.1*	*0.1*	*0.1*	*88.1*
max	*0.6*	*1.0*	*8.6*	*0.3*	*0.1*	*0.3*	*0.6*	*0.3*	*0.4*	*0.2*	*96.7*

Average chemical composition of single-phase (glassy) inclusions. Data normalised to 100wt%.

Single phase inclusions	**Na_2O**	**MgO**	**Al_2O_3**	**SiO_2**	**P_2O_5**	**SO_3**	**K_2O**	**CaO**	**TiO_2**	**V_2O_5**	**MnO**	**Fe_2O_3**
	-	0.7	2.5	22.1	0.0	0.2	0.8	1.4	0.2	0.2	0.4	71.5
	-	0.3	1.3	13.1	0.2	0.2	0.5	0.9	0.1	0.1	0.3	83.1
	-	0.4	1.5	14.0	0.2	0.2	0.6	1.0	0.2	-	0.3	81.7
	1.2	1.6	5.5	40.0	-	-	1.6	3.4	0.1	-	0.2	46.3
	1.2	1.5	5.3	39.4	-	-	1.5	3.5	0.1	-	0.3	46.9
	-	0.5	2.8	25.5	-	-	1.0	1.3	0.2	0.1	0.4	68.4
	-	0.5	1.5	14.5	0.2	0.2	0.6	1.0	0.2	0.1	0.3	81.0
	-	0.4	1.5	14.4	0.2	0.2	0.6	1.0	0.2	0.1	0.3	81.0
	-	0.4	1.6	15.5	0.6	0.5	0.6	1.2	0.2	0.1	0.3	79.0
Glass (9)	**1.2**	**0.7**	**2.6**	**22.0**	**0.2**	**0.2**	**0.9**	**1.6**	**0.2**	**0.1**	**0.3**	**71.0**

stdev	*0.0*	*0.5*	*1.7*	*10.8*	*0.2*	*0.1*	*0.4*	*1.0*	*0.0*	*0.0*	*0.1*	*14.7*
min	*1.2*	*0.3*	*1.3*	*13.1*	*0.0*	*0.2*	*0.5*	*0.9*	*0.1*	*0.1*	*0.2*	*46.3*
max	*1.2*	*1.6*	*5.5*	*40.0*	*0.6*	*0.5*	*1.6*	*3.5*	*0.2*	*0.2*	*0.4*	*83.1*

Average chemical analysis of small three phase inclusions. The inclusions are very small, so data is considered qualitative, they show however relatively high phosphorus content and are possibly inclusions generated during the smelting phase. Refer to micrographs below.

Micrograph A and B	**MgO**	**Al_2O_3**	**SiO_2**	**P_2O_5**	**SO_3**	**K_2O**	**CaO**	**TiO_2**	**V_2O_5**	**MnO**	**Fe_2O_3**
dark grey area	0.2	0.6	8.4	1.9	0.3	0.6	1.0	0.1	0.1	0.2	86.8
dark grey area	-	0.1	4.2	0.9	0.1	0.3	0.5	0.1	0.2	0.3	93.3
dark grey area	0.2	0.3	8.1	3.0	1.0	0.4	1.1	0.1	-	0.2	85.8
dark grey area	-	0.1	6.3	2.2	0.2	0.2	0.6	0.1	0.1	0.3	90.0
black spots	-	0.8	7.0	1.4	0.1	0.3	0.3	0.1	0.1	0.2	89.6
black spots	-	1.6	11.3	2.3	0.7	0.9	0.8	-	-	0.2	82.2
light grey area in the centre	0.4	0.5	3.0	0.5	-	0.2	0.2	0.3	0.2	0.2	94.5
light grey area in the centre	0.3	0.4	3.4	0.8	0.1	0.1	0.1	0.1	-	-	94.7
Micrograph C											
Bulk	-	0.2	1.6	3.1	0.4	-	0.1	0.1	0.1	0.2	94.2
Light grey crystal	-	-	2.0	9.4	2.9	-	0.3	0.1	0.1	0.4	84.9

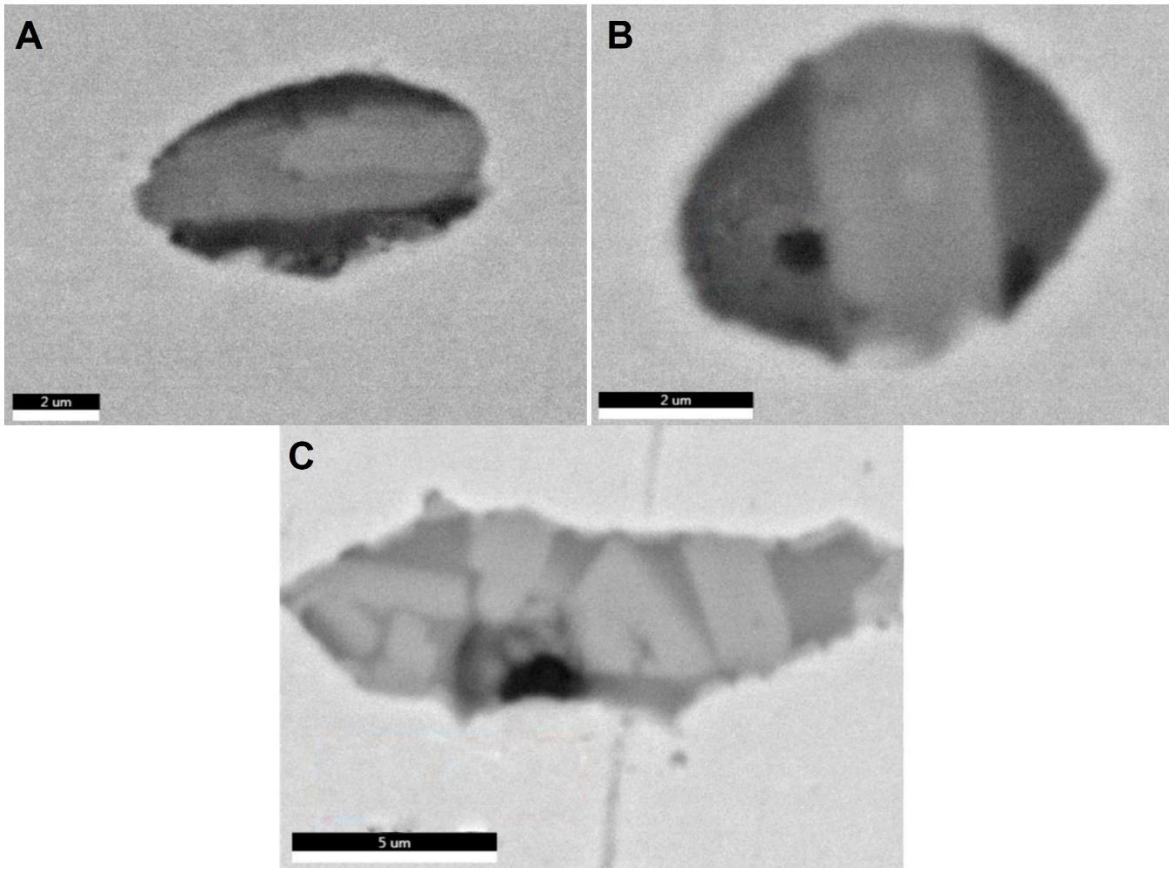
A
2 um
B
2 um
C
5 um

STONES

PN1 20-40 QUARTZ

	Na_2O	MgO	Al_2O_3	SiO_2	K_2O	SnO_2	TiO_2	Fe_2O_3
Bulk	-	0.5	21.3	47.6	5.6	16.0	2.9	6.2
	3.2	3.2	28.4	42.9	-	8.1	0.8	13.5
	-	1.2	25.4	54.4	9.0	3.4	-	6.6
Tin oxide crystals	-	-	1.5	15.8	-	80.1	-	2.6
	-	-	-	19.2	-	78.8	-	2.0
	-	-	-	20.9	-	77.3	-	1.8